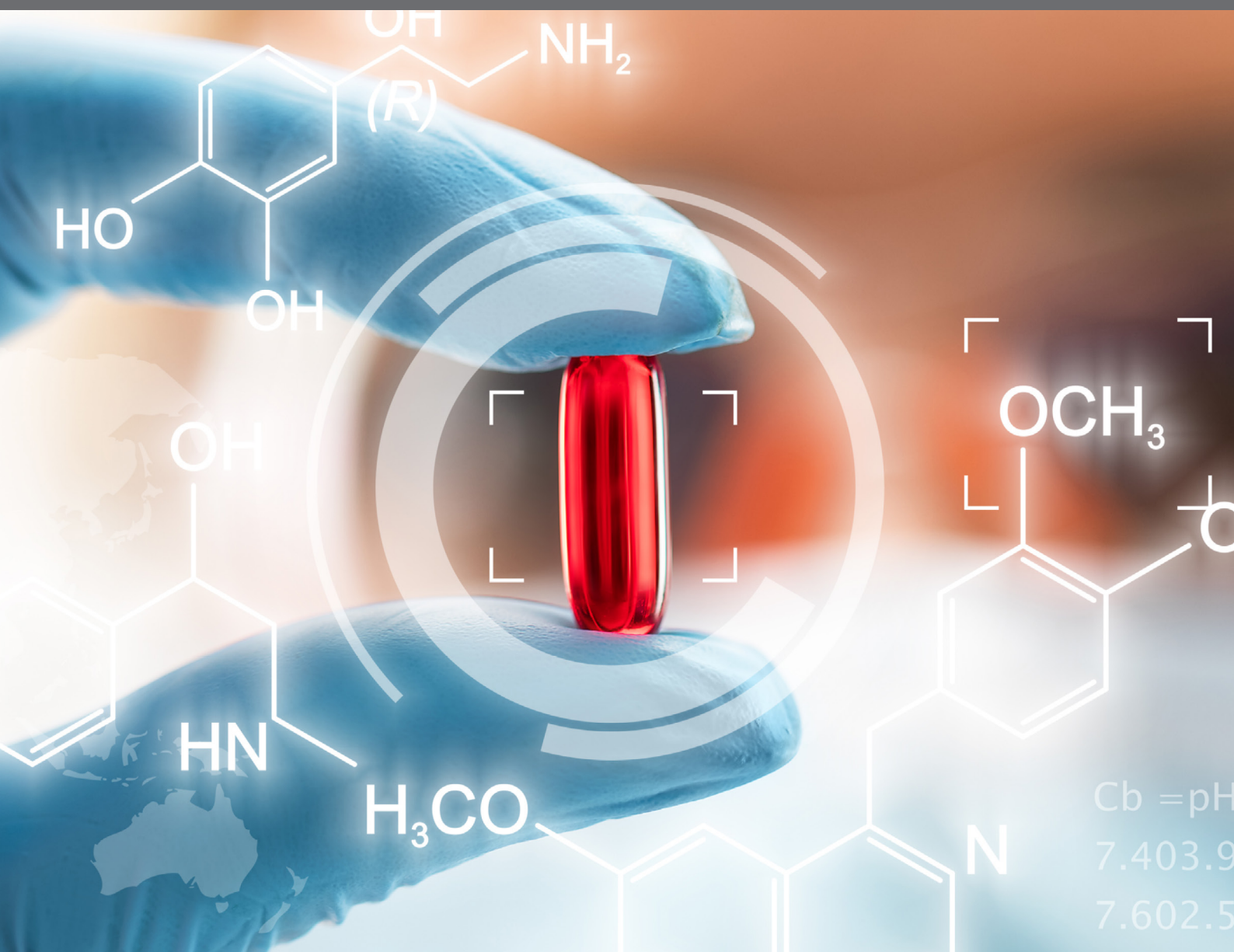


DRUG REPOSITIONING: CURRENT ADVANCES AND FUTURE PERSPECTIVES

EDITED BY: Yuhei Nishimura and Hideaki Hara
PUBLISHED IN: Frontiers in Pharmacology





frontiers

Frontiers Copyright Statement

© Copyright 2007-2019 Frontiers Media SA. All rights reserved.

All content included on this site, such as text, graphics, logos, button icons, images, video/audio clips, downloads, data compilations and software, is the property of or is licensed to Frontiers Media SA ("Frontiers") or its licensees and/or subcontractors. The copyright in the text of individual articles is the property of their respective authors, subject to a license granted to Frontiers.

The compilation of articles constituting this e-book, wherever published, as well as the compilation of all other content on this site, is the exclusive property of Frontiers. For the conditions for downloading and copying of e-books from Frontiers' website, please see the Terms for Website Use. If purchasing Frontiers e-books from other websites or sources, the conditions of the website concerned apply.

Images and graphics not forming part of user-contributed materials may not be downloaded or copied without permission.

Individual articles may be downloaded and reproduced in accordance with the principles of the CC-BY licence subject to any copyright or other notices. They may not be re-sold as an e-book.

As author or other contributor you grant a CC-BY licence to others to reproduce your articles, including any graphics and third-party materials supplied by you, in accordance with the Conditions for Website Use and subject to any copyright notices which you include in connection with your articles and materials.

All copyright, and all rights therein, are protected by national and international copyright laws.

The above represents a summary only. For the full conditions see the Conditions for Authors and the Conditions for Website Use.

ISSN 1664-8714

ISBN 978-2-88945-696-3

DOI 10.3389/978-2-88945-696-3

About Frontiers

Frontiers is more than just an open-access publisher of scholarly articles: it is a pioneering approach to the world of academia, radically improving the way scholarly research is managed. The grand vision of Frontiers is a world where all people have an equal opportunity to seek, share and generate knowledge. Frontiers provides immediate and permanent online open access to all its publications, but this alone is not enough to realize our grand goals.

Frontiers Journal Series

The Frontiers Journal Series is a multi-tier and interdisciplinary set of open-access, online journals, promising a paradigm shift from the current review, selection and dissemination processes in academic publishing. All Frontiers journals are driven by researchers for researchers; therefore, they constitute a service to the scholarly community. At the same time, the Frontiers Journal Series operates on a revolutionary invention, the tiered publishing system, initially addressing specific communities of scholars, and gradually climbing up to broader public understanding, thus serving the interests of the lay society, too.

Dedication to Quality

Each Frontiers article is a landmark of the highest quality, thanks to genuinely collaborative interactions between authors and review editors, who include some of the world's best academicians. Research must be certified by peers before entering a stream of knowledge that may eventually reach the public - and shape society; therefore, Frontiers only applies the most rigorous and unbiased reviews.

Frontiers revolutionizes research publishing by freely delivering the most outstanding research, evaluated with no bias from both the academic and social point of view. By applying the most advanced information technologies, Frontiers is catapulting scholarly publishing into a new generation.

What are Frontiers Research Topics?

Frontiers Research Topics are very popular trademarks of the Frontiers Journals Series: they are collections of at least ten articles, all centered on a particular subject. With their unique mix of varied contributions from Original Research to Review Articles, Frontiers Research Topics unify the most influential researchers, the latest key findings and historical advances in a hot research area! Find out more on how to host your own Frontiers Research Topic or contribute to one as an author by contacting the Frontiers Editorial Office: researchtopics@frontiersin.org

DRUG REPOSITIONING: CURRENT ADVANCES AND FUTURE PERSPECTIVES

Topic Editors:

Yuhei Nishimura, Mie University, Japan

Hideaki Hara, Gifu Pharmaceutical University, Japan



Cover image: Oleksiy Mark/Shutterstock.com

Drug repositioning is the process of identifying new indications for existing drugs. At present, the conventional *de novo* drug discovery process requires an average of about 14 years and US\$2.5 billion to approve and launch a drug. Drug repositioning can reduce the time and cost of this process because it takes advantage of drugs already in clinical use for other indications or drugs that have cleared phase I safety trials but have failed to show efficacy in the intended diseases. Historically, drug repositioning has been realized through serendipitous clinical observations or improved understanding of disease mechanisms. However, recent technological advances have enabled a more systematic approach to drug repositioning. This eBook collects 16 articles from 112 authors, providing readers with current advances and future perspectives of drug repositioning.

Citation: Nishimura, Y., Hara, H., eds. (2019). Drug Repositioning: Current Advances and Future Perspectives. Lausanne: Frontiers Media. doi: 10.3389/978-2-88945-696-3

Table of Contents

- 05 Editorial: Drug Repositioning: Current Advances and Future Perspectives**
Yuhei Nishimura and Hideaki Hara

I. COMPUTATIONAL METHODS

- 08 On the Integration of In Silico Drug Design Methods for Drug Repurposing**
Eric March-Vila, Luca Pinzi, Noé Sturm, Annachiara Tinivella, Ola Engkvist, Hongming Chen and Giulio Rastelli
- 15 Drug Repositioning in Glioblastoma: A Pathway Perspective**
Sze Kiat Tan, Anna Jermakowicz, Adnan K. Mookhtiar, Charles B. Nemeroff, Stephan C. Schürer and Nagi G. Ayad

II. IN SILICO PREDICTION AND IN VITRO AND IN VIVO VALIDATION

- 34 Drug Repurposing of the Anthelmintic Niclosamide to Treat Multidrug-Resistant Leukemia**
Sami Hamdoun, Philipp Jung and Thomas Efferth
- 45 Quantitative and Systems Pharmacology 3. Network-Based Identification of New Targets for Natural Products Enables Potential Uses in Aging-Associated Disorders**
Jiansong Fang, Li Gao, Huili Ma, Qihui Wu, Tian Wu, Jun Wu, Qi Wang and Feixiong Cheng
- 58 Ginkgolide C Alleviates Myocardial Ischemia/Reperfusion-Induced Inflammatory Injury via Inhibition of CD40-NF- κ B Pathway**
Rui Zhang, Dan Han, Zhenyu Li, Chengwu Shen, Yahui Zhang, Jun Li, Genquan Yan, Shasha Li, Bo Hu, Jiangbing Li and Ping Liu
- 73 Halofuginone Attenuates Osteoarthritis by Rescuing Bone Remodeling in Subchondral Bone Through Oral Gavage**
Wenbo Mu, Boyong Xu, Hairong Ma, Jiao Li, Baochao Ji, Zhendong Zhang, Abdusami Amat and Li Cao
- 83 Nardosinone Suppresses RANKL-Induced Osteoclastogenesis and Attenuates Lipopolysaccharide-Induced Alveolar Bone Resorption**
Chenguang Niu, Fei Xiao, Keyong Yuan, XuChen Hu, Wenzhen Lin, Rui Ma, Xiaoling Zhang and Zhengwei Huang
- 96 Synergistic Effect of Pleuromutilins With Other Antimicrobial Agents Against *Staphylococcus aureus* In Vitro and in an Experimental *Galleria mellonella* Model**
Chun-Liu Dong, Lin-Xiong Li, Ze-Hua Cui, Shu-Wen Chen, Yan Q. Xiong, Jia-Qi Lu, Xiao-Ping Liao, Yuan Gao, Jian Sun and Ya-Hong Liu
- 104 Chymase Inhibitor as a Novel Therapeutic Agent for Non-alcoholic Steatohepatitis**
Shinji Takai and Denan Jin

III. USING CLINICAL DATABASES

- 110** *Drug Repositioning of Proton Pump Inhibitors for Enhanced Efficacy and Safety of Cancer Chemotherapy*

Kenji Ikemura, Shunichi Hiramatsu and Masahiro Okuda

- 115** *Simvastatin Therapy for Drug Repositioning to Reduce the Risk of Prostate Cancer Mortality in Patients With Hyperlipidemia*

Yu-An Chen, Ying-Ju Lin, Cheng-Li Lin, Hwai-Jeng Lin, Hua-Shan Wu, Hui-Ying Hsu, Yu-Chen Sun, Hui-Yu Wu, Chih-Ho Lai and Chia-Hung Kao

IV. NOVEL TOOLS AND CONCEPTS

- 122** *Three-Dimensional in Vitro Cell Culture Models in Drug Discovery and Drug Repositioning*

Sigrid A. Langhans

- 136** *Is There an Opportunity for Current Chemotherapeutics to Up-regulate MIC-A/B Ligands?*

Kendel Quirk and Shanmugasundaram Ganapathy-Kanniappan

V. PATENTS AND APPROVALS

- 143** *Drug Repositioning in the Mirror of Patenting: Surveying and Mining Uncharted Territory*

Hermann A. M. Mucke

- 146** *Overcoming Obstacles to Drug Repositioning in Japan*

Yuhei Nishimura, Masaaki Tagawa, Hideki Ito, Kazuhiro Tsuruma and Hideaki Hara



Editorial: Drug Repositioning: Current Advances and Future Perspectives

Yuhei Nishimura^{1*} and Hideaki Hara²

¹ Department of Integrative Pharmacology, Mie University Graduate School of Medicine, Tsu, Japan, ² Molecular Pharmacology, Department of Biofunctional Evaluation, Gifu Pharmaceutical University, Gifu, Japan

Keywords: computational drug repositioning, integrative strategies, clinical database, data sharing, patenting

Editorial on the Research Topic

Drug Repositioning: Current Advances and Future Perspectives

Drug repositioning (DR) is the process of identifying new indications for existing drugs. At present, the conventional *de novo* drug discovery process requires an average of about 14 years and US\$2.5 billion to approve and launch a drug (Nosengo, 2016). DR can reduce the time and cost of this process because it takes advantage of drugs already in clinical use for other indications or drugs that have cleared phase I safety trials but have failed to show efficacy for the intended diseases. Historically, DR has been realized through serendipitous clinical observations or improved understanding of disease mechanisms. However, recent technological advances have enabled more systematic approaches to DR.

It has been widely recognized that most small-molecule drugs interact with more than one target protein (Paolini et al., 2006; Mestres et al., 2008). Understanding of the polypharmacology is a crucial aspect of DR (Lavecchia and Cerchia, 2016). Various *in silico* methods have been developed to apply the polypharmacology for DR, including omics based (Nagaraj et al., 2018) and molecular docking based (Xu et al., 2018) approaches. March-Vila et al. and Tan et al. present overviews about the computational methods for DR (March-Vila et al.; Tan et al.). Various *in vitro* assays have been performed to systematically assess the biological function of drugs. These drugs' bioactivities, combined with their chemical structure, physical properties, and clinical indications, have been recorded in various public databases, such as PubChem (Kim et al., 2016), ChEMBL (Gaulton et al., 2017), DrugBank (Wishart et al., 2018), and DrugCentral (Ursu et al., 2017). The concept that similar drugs (in terms of their functions and/or structures) may have similar clinical indications has been widely used in DR. If drug A has bioactivities similar to those of drug B, which has been approved to treat disease X, it is plausible that drug A may also treat disease X. Transcriptional responses induced by drugs and diseases can also be used in DR. If the transcriptional signature of drug C is inversely correlated to that of disease Y and/or positively correlated to that of drug D, which has been used to treat disease Y, it is likely that drug C may be used to treat disease Y. Representative resources for this approach are the Connectivity Map (Lamb et al., 2006) and the Library of Integrated Network-based Cellular Signatures (LINCS; Subramanian et al., 2017; Keenan et al., 2018; Koleti et al., 2018). Additionally, similarity of protein structures, especially for the ligand binding site, can be useful information in DR. If protein A, a key molecule of disease Z (for which no therapeutics exist), has a local structure similar to that of protein B, which is known as a therapeutic target of drug E, one can predict that drug E may be used to treat disease Z. Various databases are useful for this approach, including Protein Data Bank (PDB; Rose et al., 2017), Protein Binding Sites (ProBis; Konc and Janezic, 2014), and Protein-Ligand Interaction Profiler (PLIP; Salentin et al., 2015). Integrating these approaches can extend the domain of applicability of each method and provide novel information. Representative databases for these integrative approaches are the Drug Repurposing Hub (Corsello et al., 2017), Drug Target Commons

OPEN ACCESS

Edited and reviewed by:

Filippo Caraci,
Università degli Studi di Catania, Italy

Reviewed by:

Xianjin Xu,
University of Missouri, United States

*Correspondence:

Yuhei Nishimura
yuhei@doc.medic.mie-u.ac.jp

Specialty section:

This article was submitted to
Experimental Pharmacology and Drug
Discovery,
a section of the journal
Frontiers in Pharmacology

Received: 10 August 2018

Accepted: 03 September 2018

Published: 20 September 2018

Citation:

Nishimura Y and Hara H (2018)
Editorial: Drug Repositioning: Current
Advances and Future Perspectives.
Front. Pharmacol. 9:1068.
doi: 10.3389/fphar.2018.01068

(Tang et al., 2018), and Open Targets (Koscielny et al., 2017). Databases that have information about clinical results of DR have also been developed, including repoDB (Brown and Patel, 2017) and repurposeDB (Shameer et al., 2018).

Combining *in silico* prediction and *in vitro* validation, Hamdoun et al. found that anthelmintic niclosamide can be used to treat multidrug-resistant leukemia (Hamdoun et al.). Fang et al. developed an integrated systems pharmacology approach for DR of natural products targeting aging-associated disorders (Fang et al.). DR of natural products have also been reported, including ginkgolide C for myocardial ischemia/reperfusion-induced inflammatory injury (Zhang et al.), halofuginone for osteoarthritis (Mu et al.), nardosinone for alveolar bone resorption (Niu et al.), and pleuromutilins for infections due to *Staphylococcus aureus* (Dong et al.). Takai and Jin reviewed the possibility of chymase inhibitors as a novel therapeutic agent for non-alcoholic steatohepatitis (Takai and Jin).

Retrospective analysis of clinical records can be used to confirm the validity of DR. Proton pump inhibitors, H⁺/K⁺-ATPase inhibitors, have been reported to protect cisplatin-induced nephrotoxicity through inhibition of renal basolateral organic cation transporter 2 and to enhance the sensitivities of anticancer agents by inhibiting V-ATPase in tumor cells (Ikemura et al., 2017). These off-target effects of proton pump inhibitors have been successfully validated by retrospective analysis of electronic health records (Ikemura et al.; Wang et al., 2017). The inhibitory effects of statin for carcinogenesis in various tissues, including prostate, have been demonstrated in a number of experimental studies (Thurnher et al., 2012; Yu et al., 2014). Chen et al. demonstrated that simvastatin reduced the risk of prostate cancer mortality in patients with hyperlipidemia using a health insurance research database (Chen et al.). Sharing clinical records such as electronic health records, health insurance records, and clinical trial data, can be effective for determining DR.

High throughput screening of chemicals using *in vitro* and/or *in vivo* systems can also strongly drive DR (Nishimura and Hara, 2016). However, most *in vitro* systems currently used for high throughput screening are two-dimensional monolayer cultures that differ from physiological conditions. Langhans reviewed the three-dimensional *in vitro* cell culture models that may recapitulate microenvironmental factors that resemble *in vivo* tissue and disease pathology and discussed the significance and challenges of the system in DR (Langhans).

REFERENCES

- Brown, A. S., and Patel, C. J. (2017). A standard database for drug repositioning. *Sci. Data* 4:170029. doi: 10.1038/sdata.2017.29
- Corsello, S. M., Bittker, J. A., Liu, Z., Gould, J., Mccarren, P., Hirschman, J. E., et al. (2017). The Drug Repurposing Hub: a next-generation drug library and information resource. *Nat. Med.* 23, 405–408. doi: 10.1038/nm.4306
- Gaulton, A., Hersey, A., Nowotka, M., Bento, A. P., Chambers, J., Mendez, D., et al. (2017). The ChEMBL database in 2017. *Nucleic Acids Res.* 45, D945–D954. doi: 10.1093/nar/gkw1074
- Hashimoto, K., Man, S., Xu, P., Cruz-Munoz, W., Tang, T., Kumar, R., et al. (2010). Potent preclinical impact of metronomic low-dose oral topotecan combined

Low-dose metronomic chemotherapy has emerged as a regimen that can alter the tumor environment and suppress innate features supporting tumor growth by targeting not only tumor cells but also endothelial and immune cells (Loven et al., 2013). The concept of low-dose metronomic chemotherapy has been successfully used in DR (Hashimoto et al., 2010; Pasquier et al., 2011). Quirk and Ganapathy-Kanniappan hypothesized that current chemotherapeutics at sub-lethal, non-toxic doses might up-regulate MHC-class I chain related protein A or B and enhance the efficacy of immunotherapy mediated by natural killer cells that recognize these proteins (Quirk and Ganapathy-Kanniappan). Detailed investigation is necessary to further validate this hypothesis.

Patenting in DR can be challenging, especially if the novel indications have already been claimed by competitors within the same drug class (Sternitzke, 2014). Mucke provided useful strategies for patenting in DR, suggesting the importance of systematic collections of DR patent documents and the expert systems that assist researchers in extracting relevant patent information (Mucke).

The regulatory system for approval can also significantly affect the stream of DR. Nishimura et al. provided perspectives and future directions for DR, including an approval system suitable for DR (Nishimura et al.).

This research topic will maximize knowledge of DR, with the hope of identifying drugs that can be exploited to prevent and/or treat diseases for which effective medications are currently lacking.

AUTHOR CONTRIBUTIONS

YN drafted the editorial. Both authors revised and approved it.

FUNDING

This work was supported in part by the Japan Society for the Promotion of Science KAKENHI (16K08547) and Takeda Science Foundation.

ACKNOWLEDGMENTS

We would like to thank all the authors and reviewers who have participated in the success of this research topic.

with the antiangiogenic drug pazopanib for the treatment of ovarian cancer. *Mol. Cancer Ther.* 9, 996–1006. doi: 10.1158/1535-7163.MCT-09-0960

- Ikemura, K., Hiramatsu, S., and Okuda, M. (2017). Drug repositioning of proton pump inhibitors for enhanced efficacy and safety of cancer chemotherapy. *Front. Pharmacol.* 8:911. doi: 10.3389/fphar.2017.00911
- Keenan, A. B., Jenkins, S. L., Jagodnik, K. M., Koplev, S., He, E., Torre, D., et al. (2018). The library of integrated network-based cellular signatures NIH program: system-level cataloging of human cells response to perturbations. *Cell Syst.* 6, 13–24. doi: 10.1016/j.cels.2017.11.001
- Kim, S., Thiessen, P. A., Bolton, E. E., Chen, J., Fu, G., Gindulyte, A., et al. (2016). PubChem substance and compound databases. *Nucleic Acids Res.* 44, D1202–D1213. doi: 10.1093/nar/gkv951

- Koleti, A., Terryn, R., Stathias, V., Chung, C., Cooper, D. J., Turner, J. P., et al. (2018). Data Portal for the Library of Integrated Network-based Cellular Signatures (LINCS) program: integrated access to diverse large-scale cellular perturbation response data. *Nucleic Acids Res.* 46, D558–D566. doi: 10.1093/nar/gkx1063
- Konc, J., and Janezic, D. (2014). ProBiS-ligands: a web server for prediction of ligands by examination of protein binding sites. *Nucleic Acids Res.* 42, W215–W220. doi: 10.1093/nar/gku460
- Koscielny, G., An, P., Carvalho-Silva, D., Cham, J. A., Fumis, L., Gasparyan, R., et al. (2017). Open Targets: a platform for therapeutic target identification and validation. *Nucleic Acids Res.* 45, D985–D994. doi: 10.1093/nar/gkw1055
- Lamb, J., Crawford, E. D., Peck, D., Modell, J. W., Blat, I. C., Wrobel, M. J., et al. (2006). The Connectivity Map: using gene-expression signatures to connect small molecules, genes, and disease. *Science* 313, 1929–1935. doi: 10.1126/science.1132939
- Lavecchia, A., and Cerchia, C. (2016). *In silico* methods to address polypharmacology: current status, applications and future perspectives. *Drug Discov. Today* 21, 288–298. doi: 10.1016/j.drudis.2015.12.007
- Loven, D., Hasnis, E., Bertolini, F., and Shaked, Y. (2013). Low-dose metronomic chemotherapy: from past experience to new paradigms in the treatment of cancer. *Drug Discov. Today* 18, 193–201. doi: 10.1016/j.drudis.2012.07.015
- Mestres, J., Gregori-Puigjane, E., Valverde, S., and Sole, R. V. (2008). Data completeness—the Achilles heel of drug-target networks. *Nat. Biotechnol.* 26, 983–984. doi: 10.1038/nbt0908-983
- Nagaraj, A. B., Wang, Q. Q., Joseph, P., Zheng, C., Chen, Y., Kovalenko, O., et al. (2018). Using a novel computational drug-repositioning approach (DrugPredict) to rapidly identify potent drug candidates for cancer treatment. *Oncogene* 37, 403–414. doi: 10.1038/onc.2017.328
- Nishimura, Y., and Hara, H. (2016). Integrated approaches to drug discovery for oxidative stress-related retinal diseases. *Oxid. Med. Cell Longev.* 2016:2370252. doi: 10.1155/2016/2370252
- Nosengo, N. (2016). Can you teach old drugs new tricks? *Nature* 534, 314–316. doi: 10.1038/534314a
- Paolini, G. V., Shapland, R. H., Van Hoorn, W. P., Mason, J. S., and Hopkins, A. L. (2006). Global mapping of pharmacological space. *Nat. Biotechnol.* 24, 805–815. doi: 10.1038/nbt1228
- Pasquier, E., Ciccolini, J., Carre, M., Giacometti, S., Fanciullino, R., Pouchy, C., et al. (2011). Propranolol potentiates the anti-angiogenic effects and anti-tumor efficacy of chemotherapy agents: implication in breast cancer treatment. *Oncotarget* 2, 797–809. doi: 10.18632/oncotarget.343
- Rose, P. W., Prlic, A., Altunkaya, A., Bi, C., Bradley, A. R., Christie, C. H., et al. (2017). The RCSB protein data bank: integrative view of protein, gene and 3D structural information. *Nucleic Acids Res.* 45, D271–D281. doi: 10.1093/nar/gkw1000
- Salentin, S., Schreiber, S., Haupt, V. J., Adasme, M. F., and Schroeder, M. (2015). PLIP: fully automated protein-ligand interaction profiler. *Nucleic Acids Res.* 43, W443–W447. doi: 10.1093/nar/gkv315
- Shameer, K., Glicksberg, B. S., Hodos, R., Johnson, K. W., Badgeley, M. A., Readhead, B., et al. (2018). Systematic analyses of drugs and disease indications in RepurposeDB reveal pharmacological, biological and epidemiological factors influencing drug repositioning. *Brief Bioinform.* 19, 656–678. doi: 10.1093/bib/bbw136
- Sternitzke, C. (2014). Drug repurposing and the prior art patents of competitors. *Drug Discov. Today* 19, 1841–1847. doi: 10.1016/j.drudis.2014.09.016
- Subramanian, A., Narayan, R., Corsello, S. M., Peck, D. D., Natoli, T. E., Lu, X., et al. (2017). A next generation connectivity map: L1000 platform and the first 1,000,000 profiles. *Cell* 171, 1437–1452.e17. doi: 10.1016/j.cell.2017.10.049
- Tang, J., Tanoli, Z. U., Ravikumar, B., Alam, Z., Rebane, A., Vaha-Koskela, M., et al. (2018). Drug target commons: a community effort to build a consensus knowledge base for drug-target interactions. *Cell Chem. Biol.* 25, 224–229.e2. doi: 10.1016/j.chembiol.2017.11.009
- Thurnher, M., Nussbaumer, O., and Gruenbacher, G. (2012). Novel aspects of mevalonate pathway inhibitors as antitumor agents. *Clin. Cancer Res.* 18, 3524–3531. doi: 10.1158/1078-0432.CCR-12-0489
- Ursu, O., Holmes, J., Knockel, J., Bologna, C. G., Yang, J. J., Mathias, S. L., et al. (2017). DrugCentral: online drug compendium. *Nucleic Acids Res.* 45, D932–D939. doi: 10.1093/nar/gkw993
- Wang, X., Liu, C., Wang, J., Fan, Y., Wang, Z., and Wang, Y. (2017). Proton pump inhibitors increase the chemosensitivity of patients with advanced colorectal cancer. *Oncotarget* 8, 58801–58808. doi: 10.18632/oncotarget.18522
- Wishart, D. S., Feunang, Y. D., Guo, A. C., Lo, E. J., Marcu, A., Grant, J. R., et al. (2018). DrugBank 5.0: a major update to the DrugBank database for 2018. *Nucleic Acids Res.* 46, D1074–d1082. doi: 10.1093/nar/gkx1037
- Xu, X., Huang, M., and Zou, X. (2018). Docking-based inverse virtual screening: methods, applications, and challenges. *Biophys. Rep.* 4, 1–16. doi: 10.1007/s41048-017-0045-8
- Yu, O., Eberg, M., Benayoun, S., Aprikian, A., Batist, G., Suissa, S., et al. (2014). Use of statins and the risk of death in patients with prostate cancer. *J. Clin. Oncol.* 32, 5–11. doi: 10.1200/JCO.2013.49.4757

Conflict of Interest Statement: The authors declare that the research was conducted in the absence of any commercial or financial relationships that could be construed as a potential conflict of interest.

Copyright © 2018 Nishimura and Hara. This is an open-access article distributed under the terms of the Creative Commons Attribution License (CC BY). The use, distribution or reproduction in other forums is permitted, provided the original author(s) and the copyright owner(s) are credited and that the original publication in this journal is cited, in accordance with accepted academic practice. No use, distribution or reproduction is permitted which does not comply with these terms.



On the Integration of *In Silico* Drug Design Methods for Drug Repurposing

Eric March-Vila¹, Luca Pinzi¹, Noé Sturm¹, Annachiara Tinivella¹, Ola Engkvist², Hongming Chen² and Giulio Rastelli^{1*}

¹ Molecular Modelling & Drug Design Lab, Department of Life Sciences, University of Modena and Reggio Emilia, Modena, Italy, ² Discovery Sciences, Innovative Medicines and Early Development Biotech Unit, AstraZeneca R&D Gothenburg, Mölndal, Sweden

Drug repurposing has become an important branch of drug discovery. Several computational approaches that help to uncover new repurposing opportunities and aid the discovery process have been put forward, or adapted from previous applications. A number of successful examples are now available. Overall, future developments will greatly benefit from integration of different methods, approaches and disciplines. Steps forward in this direction are expected to help to clarify, and therefore to rationally predict, new drug–target, target–disease, and ultimately drug–disease associations.

OPEN ACCESS

Edited by:

Yuhei Nishimura,
Mie University, Japan

Reviewed by:

Antonio Macchiarulo,
University of Perugia, Italy
Yoshito Zamami,
Tokushima University Graduate
School of Medical Sciences, Japan

*Correspondence:

Giulio Rastelli
giulio.rastelli@unimore.it

Specialty section:

This article was submitted to
Experimental Pharmacology and Drug
Discovery,
a section of the journal
Frontiers in Pharmacology

Received: 07 April 2017

Accepted: 10 May 2017

Published: 23 May 2017

Citation:

March-Vila E, Pinzi L, Sturm N,
Tinivella A, Engkvist O, Chen H and
Rastelli G (2017) On the Integration
of *In Silico* Drug Design Methods
for Drug Repurposing.
Front. Pharmacol. 8:298.
doi: 10.3389/fphar.2017.00298

Keywords: drug repurposing, drug discovery, molecular modeling, chemogenomics, structure-based drug design, ligand-based drug design, machine learning, transcriptomics

INTRODUCTION

Drug repurposing (also known as drug repositioning) aims at identifying new uses for already existing drugs (Novac, 2013). In drug discovery, drug repurposing has gained an increasingly important role, because it helps to circumvent preclinical development and optimization issues, hence reducing time efforts, expenses and failures typically associated with the drug discovery process.

Over the years, biological and chemical information has been generated at an ever-increasing pace, marking the entrance in the so-called “big data” era (Costa, 2014). This offers the scientific community new opportunities to link drugs to diseases, although this relationship is indirect and relies on complex mechanisms of action. Therefore, a better understanding of the relationships between drugs and their targets, and between targets and diseases, is a key for drug repurposing. Unfortunately, we are still far from understanding the overall picture, partly due to the heterogeneity and incompleteness of the available data. However, computational methods offer valuable opportunities to create such links, as it will be illustrated below.

In this perspective, different computational methods and approaches are briefly presented, and their ability to complement and integrate each other in drug repurposing is discussed, which will certainly gain a foothold in the future.

COMPUTATIONAL DRUG REPURPOSING STRATEGY BASED ON TRANSCRIPTIONAL SIGNATURES

Transcriptomic data can provide a list of over- and under-expressed genes in a biological system treated by a pharmacologically active compound. The perturbation of a biological system

can be measured from genome wide transcriptional responses, and the drug induced transcriptional responses represent the signature of the compound activity on biological systems. These molecular transcriptional signatures can then be compared to establish therapeutic relationships between known drugs and new disease indications.

One of the most comprehensive and systematic approaches toward leveraging the transcriptional signature approach for drug repositioning is the Connectivity Map project (Lamb et al., 2006). The publicly funded CMap database¹ initially contained profiles of 164 drugs and was later expanded to 1309 FDA-approved small molecules. These compounds are tested in five human cell lines, generating over 7000 gene expression profiles in the database. The cell perturbation profile of each drug in the reference collection contains, for each gene measured, a rank-based measure of the change in transcriptional activity after exposure to the drug compound, i.e., gene signatures. These signatures form the basis of comparing drugs mechanism of action at transcriptional level and have been successfully applied for drug repurposing in many examples. Chang et al. (2010) used CMap to identify new analgesic and antinociceptive properties of phenoxybenzamine, originally an anti-hypertensive drug. Subsequent testing using a rat inflammatory model validated the analgesic activity. In contrast with CMap gene signatures, biclustering methods were applied to CMap to group coregulated genes with the drugs they respond to Iskar et al. (2013). This led to the identification of vinburnine, a vasodilator, and sulconazole, a topical antifungal, as interesting cell cycle blockers for cancer therapy.

NETWORK-BASED DRUG REPURPOSING

In recent years, network-based computational biology has attracted increasing attention. It aims at organizing the relationships among biological molecules in the form of networks to find newly emerged properties at a network level, and to investigate how cellular systems induce different biological phenotypes under different conditions. In the network pharmacology framework, a network can be depicted as a connected graph, where each node can represent either an individual molecular entity (e.g., a drug), its biological target, a modifier molecule within a biological process, or a target pathway, while an edge represents either a direct or indirect interaction between two connected nodes. Ultimately, both the efficacy and the toxicity of a drug are a consequence of the complex interplay among different cellular components. A system-scale perspective is therefore needed to aid modern drug discovery, especially for complex diseases, which are known to be caused by perturbation of biological networks.

Network-based analysis has become a widely used strategy for computational drug repositioning. Hu and Agarwal (2009) created a disease-similarity network using publicly available gene expression profiles from NCBI Gene Expression Omnibus

(GEO)² and integrated this network with molecular profiles and knowledge of drugs and drug targets to infer drug repositioning opportunities and suggest molecular targets and mechanisms underlying drug effects. Jin et al. (2012) developed a novel method to repurpose drugs for cancer therapeutics by leveraging off-target effects that may affect important cancer cell signaling pathways. The off-target effects of drugs on signaling proteins were identified by using a hybrid model composed of a network component called cancer-signaling bridges and Bayesian factor regression model.

LIGAND-BASED APPROACHES IN DRUG REPURPOSING

Ligand-based approaches are based on the concept that similar compounds tend to have similar biological properties. In drug repurposing, these methods have been extensively used to analyze and predict the activity of ligands for new targets. Public databases of bioactive molecules, such as PubChem, ChEMBL, and DrugBank contain information retrieved and manually curated from literature data (Wishart et al., 2006; Gaulton et al., 2017; Wang et al., 2017). These databases represent a huge and ever-growing reservoir of chemical and biological information such as binding affinity, cellular activity, functional and ADMET data. Recent advances in drug repurposing include the release of databases focused on repurposed drugs, failed drugs, their therapeutic indications, and bioactivity data (Brown and Patel, 2017; Shameer et al., 2017).

One advantage of applying these approaches to drug repurposing is that the number of publicly accessible compound records (more than hundred millions provided only by PubChem) is far greater than the number of deposited protein crystal structures (as of today, less than 150,000 in the Protein Data Bank) (Berman et al., 2000; Wang et al., 2017). On the other hand, ligand-based methods obviously depend on the chemical space coverage of already known molecules. Moreover, a high overall similarity does not necessarily guarantee activity on a secondary target, since local structural divergences in chemical scaffolds can lead to “activity cliffs” (Stumpfe and Bajorath, 2012). This limitation, however, will eventually be overcome by the increase of structural diversity in bioactivity databases (Hu and Bajorath, 2013).

Recently, a 2D ligand-based similarity analysis of ChEMBL combined with support vector machine models and analysis of 3D structural information of protein–ligand complexes, identified a promising set of target combinations and associated ligands within the Hsp90 interactome, which are particularly suitable for multitarget drug design (Anighoro et al., 2015). Another ligand-based method correctly predicted 23 new drug–target associations using the similarity ensemble approach (Keiser et al., 2009). Pharmacophore screening has also been a

¹<http://www.broadinstitute.org/cmap>

²<http://www.ncbi.nlm.nih.gov/geo/>

valuable strategy for drug repurposing (Liu et al., 2010). In this approach, a drug can be represented as a set of pharmacophoric features which can subsequently be used to interrogate chemical compound databases to provide compounds with different scaffolds.

Complementing different levels of ligand description increases the chances of identifying new repurposing possibilities. For example, Vasudevan et al. (2012) used 3D shape-based descriptors to compare approved drugs with a set of H1 receptor antagonists. Thirteen of the 23 tested drugs selectively inhibited histamine-induced calcium release by acting at the H1 receptor level. Interestingly, these drugs would not have been detected with 2D similarity searching (Vasudevan et al., 2012). Furthermore, Mervin et al. (2015) demonstrated how the inclusion of inactive data improved early recognition abilities in statistical prediction models. On different grounds, predictive models built upon disease feature descriptors, large-scale drug–target and target–disease associations showed performance improvements in predicting new drug–disease links (Iwata et al., 2015; Sawada et al., 2015). In particular, it was shown that chemical similarity and phenotypic similarity are complementary to each other, and that integrating predictions from both methods is beneficial (Sawada et al., 2015).

LIGAND-BASED CHEMOGENOMICS AND MACHINE LEARNING IN DRUG REPURPOSING

A variety of *in silico* approaches have been applied in ligand-based chemogenomic campaigns (Mestres et al., 2006; Bender et al., 2007; Gregori-Puigjané and Mestres, 2008). During the last years, machine learning algorithms, which span from the older but still attractive Bayesian classifiers to the more advanced support vector machines, have become increasingly popular to assist the drug repositioning process (Bender et al., 2007). Methods such as deep learning and multi-task learning have been successfully used in chemogenomic benchmark studies (Unterthiner et al., 2014). Moreover, matrix factorization methods offer the opportunity to combine bioactivity data with other information, such as disease information, in one framework (Zhang et al., 2014). On a different line, other techniques inspired by e-commerce websites have shown interesting results in identifying new drug–target associations (Alaimo et al., 2016). In the study, the technique relies on a network-based inference algorithm and a drug–target bipartite graph extracted from DrugBank. It was shown that the algorithm performed better in predicting new drug–target associations when target and drug similarities are considered.

Given the versatility in their use and their computational efficiency, machine-learning approaches will likely continue to play a prominent role in *in silico* chemogenomics. Despite many papers have described test cases and various types of method development, there is still a lack of published success stories that employed ligand-based chemogenomics modeling in drug repurposing.

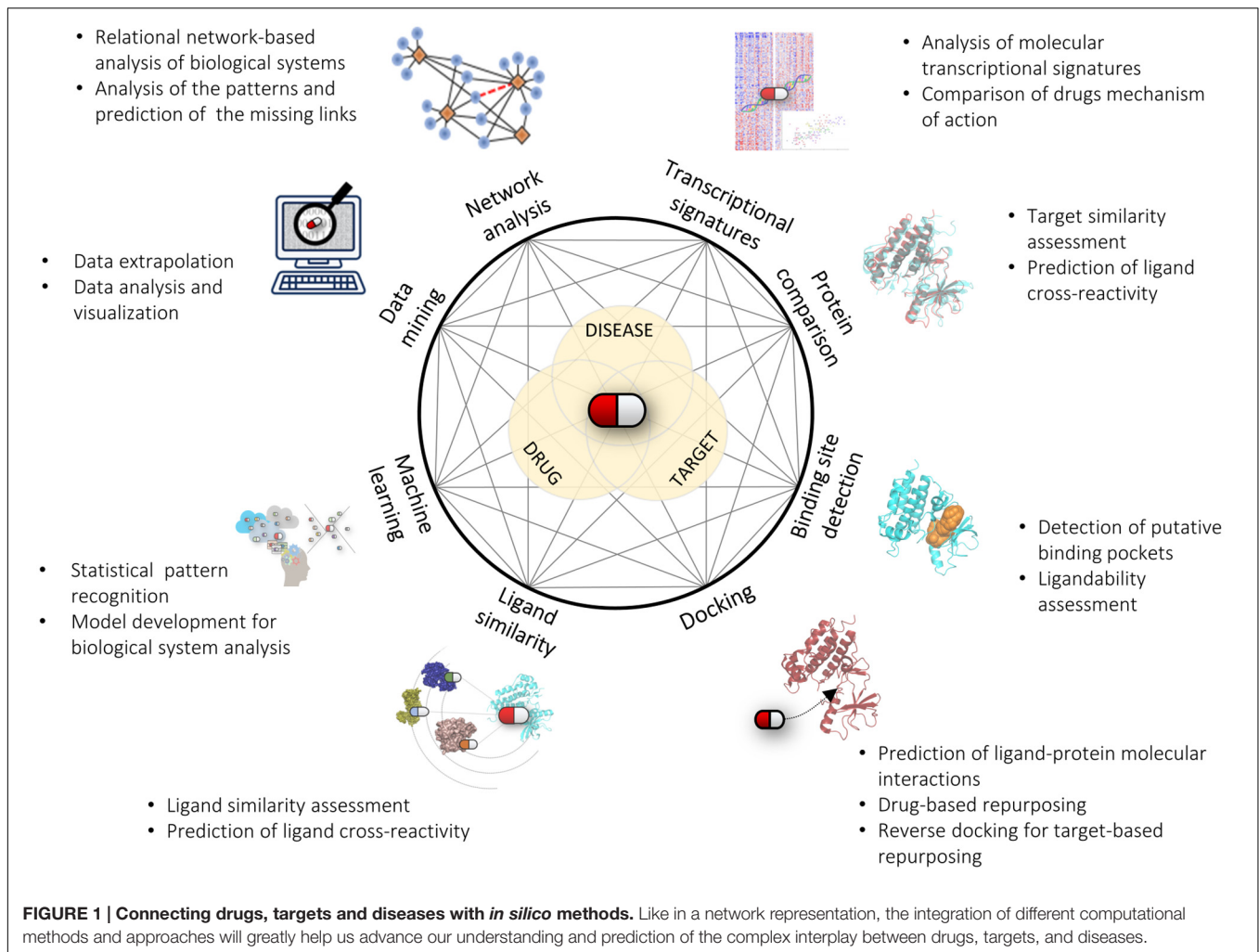
STRUCTURE-BASED APPROACHES IN DRUG REPURPOSING

It is established that the similarity principle observed for ligands applies also to proteins. Proteins with similar structures are likely to have similar functions and to recognize similar ligands. In the field of drug repurposing, protein comparison is used as a method to identify secondary targets of an approved drug (Ehrt et al., 2016).

From a global point of view, proteins can be compared by sequence similarity. Protein sequences have been used to build phylogenetic trees, the most popular of which is represented by the kinome (Manning et al., 2002). In this tree, proteins of the same family are prone to have related functions and also to recognize related substrates or ligands, such as for example dual inhibitors of epidermal growth factor receptor (EGFR) and epidermal growth factor receptor B2 (ErbB2) (Zhang et al., 2004). Modern methods to perform multiple-sequence alignments, such as BLAST, are nowadays widely used and available through web-servers. It is important to note that small differences localized at key positions, such as those occurring in correspondence of the gatekeeper residue of protein kinases or of other oncogenic mutations, may have a huge impact on ligand binding (Huang and Fu, 2015). Hence, local differences in globally conserved protein sequences should be given careful consideration. Moreover, a study based on the similarity ensemble approach showed that similar ligands were able to bind proteins with distantly related sequences (Keiser et al., 2007). Overall, local binding site similarities can be more important than global similarities to determine polypharmacology and drug repurposing (Jalencas and Mestres, 2013b; Anighoro et al., 2015).

In identifying unknown targets of known ligands, sequence alignments perform well when proteins share a high degree of sequence identity, whereas local protein comparison performs better when proteins share low sequence identity (Chen et al., 2016). Detecting local similarities by comparing protein binding sites has become increasingly important (Ehrt et al., 2016). Binding site identification and comparison are commonly performed by scanning the protein surface in order to identify cavities (Laurie and Jackson, 2006) and then by calculating descriptors of different nature useful to derive a similarity score.

It is important to note that several approaches and algorithms for binding site comparison have been put forward, but none of them appears to be devoid of failures or limitations (Ehrt et al., 2016). Notwithstanding, binding site similarity has proven a valuable tool in a number of studies. For example, a study carried out by Defranchi et al. (2010) used a binding site comparison method to predict the cross-reactivity of four protein kinase inhibitors with Synapsin I. These discoveries were supported by sub-micromolar affinities of the kinase inhibitors for Synapsin I. Interestingly, binding site similarity and other molecular modeling techniques were used in combination to uncover new targets of the drugs entacapone and tolcapone (Kinnings et al., 2009). The study started from a large set of similar binding sites, which was further



finalized by simulating the binding mode of entacapone and tolcapone using docking. Proteins for which ligands gave the best docking scores were prioritized and further experimentally validated.

It is worth mentioning that ligand binding modes, when available, are a strong asset in the process of identifying new targets. One way to model the molecular recognition is to focus on target–ligand interactions. This can be achieved with various methods, such as structure-based pharmacophores or interaction fingerprints. When the structure of a protein–ligand complex is not available, one can use computational methods to predict hot spots in the binding site (Hall et al., 2015). Another approach joining ligand information to protein environments uses the concept of chemoisosterism (Jalencas and Mestres, 2013a). Chemoisosterism can be defined as the property of two protein environments to bind the same molecular fragment, and can shed light into the inherent cross-pharmacology between protein targets. The degree of chemoisosterism was found to be related to the polypharmacology of chemical fragments (Jalencas and Mestres, 2013b). This approach allows the creation of interaction

networks connecting chemical fragments to chemoisosteric protein environments. These networks, complemented with target–disease associations, constitute attractive starting points for drug repurposing efforts.

Based on similar concepts, a method for interrogating large data sets of proteins (as large as the PDB) with highly customizable geometric patterns as searching templates was recently described (Inhester et al., 2017). This method was able to identify chemoisosteric protein environments binding the uracil moiety of uridine diphosphate from a query built with deoxythymidine.

Structure-based methods are obviously dependent on the availability of crystallographic structures of protein–ligand complexes. Resolution and sensitivity to atomic coordinates impact the level of details that one can use to model a binding site. While crystallographic structures represent a static model of a protein, other pockets may appear upon conformational changes. Detecting those cryptic sites has become an emerging field of research, because it may provide additional options in drug repurposing. In fact, cryptic allosteric sites may be useful to gain selectivity, explore new chemical spaces for

drug design, and establish drug–target associations beyond the more commonly explored orthosteric site. For instance, Markov models have been applied in combination with experimental assays using a chemical probe to uncover cryptic allosteric sites of TEM-1 β -lactamase (Bowman et al., 2015). Overall, uncovering new allosteric sites in proteins may provide far more opportunities to repurpose drugs than is currently recognized.

MOLECULAR DOCKING

Molecular docking is a versatile tool used to predict the geometry and to score the interaction of a protein in complex with a small-molecule ligand (Kitchen et al., 2004). Therefore, these methods can be used to predict if a given drug is potentially able to bind other targets. Docking studies have been successfully exploited in drug repurposing, as reported in many recent studies (Kinnings et al., 2009; Li et al., 2011; Dakshanamurthy et al., 2012). In this context, virtual screenings can be performed either by docking a known drug into a large set of different target structures, or by docking a database of approved drugs into one intended specific target. Molecular docking is in fact a convenient and fast method to screen large libraries of both ligands and targets, with a full range of sampling options (Kitchen et al., 2004), and is obviously restricted to studies in which a 3D structure of the target is available through crystallography, nuclear magnetic resonance (NMR), or comparative models. It should be noted that docking methods still have drawbacks and limitations, mainly arising from the use of approximate scoring functions and imperfect binding mode placement algorithms. Often these problems can be overcome by post-processing docking results with more accurate scoring functions and/or other criteria (Sgobba et al., 2012).

In the study of Li et al. (2011), docking methods have been successfully exploited as a stand-alone method in drug repurposing, by docking the drugs of the DrugBank database into 35 crystal structures of MAPK14. The study identified the chronic myeloid leukemia drug nilotinib as a potential anti-inflammatory drug with an *in vitro* IC₅₀ of 40 nM (Li et al., 2011).

Docking is notably well suited for either drug-based and target-based drug repurposing, as reported in the results of the work of Dakshanamurthy et al. (2012), where an anti-parasitic drug was successfully tested as an anti-angiogenic vascular endothelial growth factor receptor 2 (VEGFR2) inhibitor, and a new connection was discovered between previously untargeted Cadherin-11, implied in rheumatoid arthritis, and cyclooxygenase-2 (COX-2) inhibitor celecoxib.

It is important to note that docking, despite its limitations, is a well-established and experimentally validated approach for predicting new drug–target associations. Once integrated with ligand-based methods and other available information about target–disease associations, it constitutes a powerful approach to repurpose (newly) targeted drugs for a specific disease.

INTEGRATING DIFFERENT APPROACHES AND FUTURE DIRECTIONS

The goal of drug repurposing is to uncover new links between drugs and diseases, most commonly *via* targets. As illustrated in the previous sections, computational predictions followed by experimental assessment have been successfully used to identify new drug repurposing possibilities. As always, each computational method has its own field of applicability, drawbacks and limitations. One should be aware of the fact that none of these methods alone will be sufficiently able to disclose (or even model) the complex interplay between drugs, targets and diseases. Therefore, we are left with the possibility of using one or more computational approaches to “navigate” through the wealth of available information and hopefully find “clues” solid enough to justify a repurposing hypothesis worth of experimental investigation. The choice of the most appropriate method(s) will basically depend on the nature of the problem to solve and on the type, quality, and quantity of information available on that problem in the literature or in public or proprietary databases. Unfortunately, information is often fragmented, and generally reflects only a single or few aspects of a much more complicated story. Future efforts should be more thoroughly directed toward disclosing hubs and links of the complex network that relates drugs, targets and diseases. Integrating the huge and heterogeneous amount of available data (chemical, biological, structural, clinical) into a unified workflow is obviously a challenging task. In this respect, the integration and use of different computational methods as shown above will provide valuable opportunities to extend the domain of applicability of each method and more thoroughly exploit information coming from different sources (Figure 1). Likewise, this will greatly benefit from better integration of multidisciplinary work. A network-based approach built upon these considerations will likely provide new routes to navigate through all the potential links between drugs and diseases, thus creating new opportunities for drug repurposing and drug discovery in general.

AUTHOR CONTRIBUTIONS

All authors contributed in writing and editing the manuscript. EM-V, LP, NS and AT contributed equally. GR conceived the study and coordinated the writing.

FUNDING

The project leading to this article has received funding (for EM-V, OE, HC, and GR) from the European Union’s Horizon 2020 research and innovation program under the Marie Skłodowska-Curie grant agreement No 676434, “Big Data in Chemistry” (“BIGCHEM”, <http://bigchem.eu>). The article reflects only the authors’ view and neither the European Commission nor the Research Executive Agency are responsible for any use that may be made of the information it contains.

REFERENCES

- Alaimo, S., Giugno, R., and Pulvirenti, A. (2016). Recommendation techniques for drug-target interaction prediction and drug repositioning. *Methods Mol. Biol.* 1415, 441–462. doi: 10.1007/978-1-4939-3572-7-23
- Anighoro, A., Stumpfe, D., Heikamp, K., Beebe, K., Neckers, L. M., Bajorath, J., et al. (2015). Computational polypharmacology analysis of the heat shock protein 90 interactome. *J. Chem. Inf. Model.* 55, 676–686. doi: 10.1021/ci5006959
- Bender, A., Scheiber, J., Glick, M., Davies, J. W., Azzaoui, K., and Hamon, J. (2007). Analysis of pharmacology data and the prediction of adverse drug reactions and off-target effects from chemical structure. *ChemMedChem* 2, 861–873. doi: 10.1002/cmdc.200700026
- Berman, H. M., Westbrook, J., Feng, Z., Gilliland, G., Bhat, T. N., Weissig, H., et al. (2000). The protein data bank. *Nucleic Acids Res.* 28, 235–242. doi: 10.1093/nar/28.1.235
- Bowman, G. R., Bolin, E. R., Hart, K. M., Maguire, B. C., and Marqusee, S. (2015). Discovery of multiple hidden allosteric sites by combining Markov state models and experiments. *Proc. Natl. Acad. Sci. U. S. A.* 112, 2734–2739. doi: 10.1073/pnas.1417811112
- Brown, A. S., and Patel, C. J. (2017). A standard database for drug repositioning. *Sci. Data* 4, 170029. doi: 10.1038/sdata.2017.29
- Chang, M., Smith, S., Thorpe, A., Barratt, M. J., and Karim, F. (2010). Evaluation of phenoxybenzamine in the CFA model of pain following gene expression studies and connectivity mapping. *Mol. Pain* 6:56. doi: 10.1186/1744-8069-6-56
- Chen, Y.-C., Tolbert, R., Aronov, A. M., McGaughey, G., Walters, W. P., and Meireles, L. (2016). Prediction of protein pairs sharing common active ligands using protein sequence, structure, and ligand similarity. *J. Chem. Inf. Model.* 56, 1734–1745. doi: 10.1021/acs.jcim.6b00118
- Costa, F. F. (2014). Big data in biomedicine. *Drug Discov. Today* 19, 433–440. doi: 10.1016/j.drudis.2013.10.012
- Dakshnamurthy, S., Issa, N. T., Assefnia, S., Seshasayee, A., Peters, O. J., Madhavan, S., et al. (2012). Predicting new indications for approved drugs using a proteo-chemometric method. *J. Med. Chem.* 55, 6832–6848. doi: 10.1021/jm300576q
- Defranchi, E., De Franchi, E., Schalon, C., Messa, M., Onofri, F., Benfenati, F., et al. (2010). Binding of protein kinase inhibitors to synapsin I inferred from pairwise binding site similarity measurements. *PLoS ONE* 5:e12214. doi: 10.1371/journal.pone.0012214
- Ehrt, C., Brinkjost, T., and Koch, O. (2016). Impact of binding site comparisons on medicinal chemistry and rational molecular design. *J. Med. Chem.* 59, 4121–4151. doi: 10.1021/acs.jmedchem.6b00078
- Gaulton, A., Hersey, A., Nowotka, M., Bento, A. P., Chambers, J., Mendez, D., et al. (2017). The ChEMBL database in 2017. *Nucleic Acids Res.* 45, D945–D954. doi: 10.1093/nar/gkw1074
- Gregori-Puigjané, E., and Mestres, J. (2008). A ligand-based approach to mining the chemogenomic space of drugs. *Comb. Chem. High Throughput Screen.* 11, 669–676.
- Hall, D. R., Kozakov, D., Whitty, A., and Vajda, S. (2015). Lessons from hot spot analysis for fragment-based drug discovery. *Trends Pharmacol. Sci.* 36, 724–736. doi: 10.1016/j.tips.2015.08.003
- Hu, G., and Agarwal, P. (2009). Human disease-drug network based on genomic expression profiles. *PLoS ONE* 4:e6536. doi: 10.1371/journal.pone.0006536
- Hu, Y., and Bajorath, J. (2013). Compound promiscuity: what can we learn from current data? *Drug Discov. Today* 18, 644–650. doi: 10.1016/j.drudis.2013.03.002
- Huang, L., and Fu, L. (2015). Mechanisms of resistance to EGFR tyrosine kinase inhibitors. *Acta Pharm. Sin. B* 5, 390–401. doi: 10.1016/j.apsb.2015.07.001
- Inhester, T., Bietz, S., Hilbig, M., Schmidt, R., and Rarey, M. (2017). Index-based searching of interaction patterns in large collections of protein-ligand interfaces. *J. Chem. Inf. Model.* 57, 148–158. doi: 10.1021/acs.jcim.6b00561
- Iskar, M., Zeller, G., Blattmann, P., Campillos, M., Kuhn, M., Kaminska, K. H., et al. (2013). Characterization of drug-induced transcriptional modules: towards drug repositioning and functional understanding. *Mol. Syst. Biol.* 9, 662. doi: 10.1038/msb.2013.20
- Iwata, H., Sawada, R., Mizutani, S., and Yamanishi, Y. (2015). Systematic drug repositioning for a wide range of diseases with integrative analyses of phenotypic and molecular data. *J. Chem. Inf. Model.* 55, 446–459. doi: 10.1021/ci500670q
- Jalencas, X., and Mestres, J. (2013a). Chemoisosterism in the proteome. *J. Chem. Inf. Model.* 53, 279–292. doi: 10.1021/ci3002974
- Jalencas, X., and Mestres, J. (2013b). Identification of similar binding sites to detect distant polypharmacology. *Mol. Inform.* 32, 976–990. doi: 10.1002/minf.201300082
- Jin, G., Fu, C., Zhao, H., Cui, K., Chang, J., and Wong, S. T. C. (2012). A novel method of transcriptional response analysis to facilitate drug repositioning for cancer therapy. *Cancer Res.* 72, 33–44. doi: 10.1158/0008-5472.CAN-11-2333
- Keiser, M. J., Roth, B. L., Armbruster, B. N., Ernsberger, P., Irwin, J. J., and Shoichet, B. K. (2007). Relating protein pharmacology by ligand chemistry. *Nat. Biotechnol.* 25, 197–206. doi: 10.1038/nbt1284
- Keiser, M. J., Setola, V., Irwin, J. J., Laggner, C., Abbas, A. I., Hufeisen, S. J., et al. (2009). Predicting new molecular targets for known drugs. *Nature* 462, 175–181. doi: 10.1038/nature08506
- Kinnings, S. L., Liu, N., Buchmeier, N., Tonge, P. J., Xie, L., and Bourne, P. E. (2009). Drug discovery using chemical systems biology: repositioning the safe medicine Comtan to treat multi-drug and extensively drug resistant tuberculosis. *PLoS Comput. Biol.* 5:e1000423. doi: 10.1371/journal.pcbi.1000423
- Kitchen, D. B., Decornez, H., Furr, J. R., and Bajorath, J. (2004). Docking and scoring in virtual screening for drug discovery: methods and applications. *Nat. Rev. Drug Discov.* 3, 935–949. doi: 10.1038/nrd1549
- Lamb, J., Crawford, E. D., Peck, D., Modell, J. W., Blat, I. C., Wrobel, M. J., et al. (2006). The connectivity map: using gene-expression signatures to connect small molecules, genes, and disease. *Science* 313, 1929–1935. doi: 10.1126/science.1132939
- Laurie, A. T. R., and Jackson, R. M. (2006). Methods for the prediction of protein-ligand binding sites for structure-based drug design and virtual ligand screening. *Curr. Protein Pept. Sci.* 7, 395–406.
- Li, Y. Y., An, J., and Jones, S. J. M. (2011). A computational approach to finding novel targets for existing drugs. *PLoS Comput. Biol.* 7:e1002139. doi: 10.1371/journal.pcbi.1002139
- Liu, X., Ouyang, S., Yu, B., Liu, Y., Huang, K., Gong, J., et al. (2010). PharmMapper server: a web server for potential drug target identification using pharmacophore mapping approach. *Nucleic Acids Res.* 38, W609–W614. doi: 10.1093/nar/gkq300
- Manning, G., Whyte, D. B., Martinez, R., Hunter, T., and Sudarsanam, S. (2002). The protein kinase complement of the human genome. *Science* 298, 1912–1934. doi: 10.1126/science.1075762
- Mervin, L. H., Afzal, A. M., Drakakis, G., Lewis, R., Engkvist, O., and Bender, A. (2015). Target prediction utilising negative bioactivity data covering large chemical space. *J. Cheminformatics* 7, 51. doi: 10.1186/s13321-015-0098-y
- Mestres, J., Martín-Couce, L., Gregori-Puigjané, E., Cases, M., and Boyer, S. (2006). Ligand-based approach to in silico pharmacology: nuclear receptor profiling. *J. Chem. Inf. Model.* 46, 2725–2736. doi: 10.1021/ci600300k
- Novac, N. (2013). Challenges and opportunities of drug repositioning. *Trends Pharmacol. Sci.* 34, 267–272. doi: 10.1016/j.tips.2013.03.004
- Sawada, R., Iwata, H., Mizutani, S., and Yamanishi, Y. (2015). Target-based drug repositioning using large-scale chemical-protein interactome data. *J. Chem. Inf. Model.* 55, 2717–2730. doi: 10.1021/acs.jcim.5b00330
- Sgobba, M., Caporuscio, F., Anighoro, A., Portioli, C., and Rastelli, G. (2012). Application of a post-docking procedure based on MM-PBSA and MM-GBSA on single and multiple protein conformations. *Eur. J. Med. Chem.* 58, 431–440. doi: 10.1016/j.ejmech.2012.10.024
- Shameer, K., Glicksberg, B. S., Hodos, R., Johnson, K. W., Badgeley, M. A., Readhead, B., et al. (2017). Systematic analyses of drugs and disease indications in RepurposeDB reveal pharmacological, biological and epidemiological factors influencing drug repositioning. *Brief. Bioinform.* doi: 10.1093/bib/bbw136 [Epub ahead of print].
- Stumpfe, D., and Bajorath, J. (2012). Exploring activity cliffs in medicinal chemistry. *J. Med. Chem.* 55, 2932–2942. doi: 10.1021/jm201706b
- Unterthiner, T., Mayr, A., Klambauer, G., Steijaert, M., Wegner, J. K., Ceulemans, H., et al. (2014). *Deep Learning as an Opportunity in Virtual Screening*. Available at: <http://www.datascienceassn.org/sites/default/files/Deep%20Learning%20as%20an%20Opportunity%20in%20Virtual%20Screening.pdf> [accessed March 20, 2017].

- Vasudevan, S. R., Moore, J. B., Schymura, Y., and Churchill, G. C. (2012). Shape-based reprofiling of FDA-approved drugs for the H1 histamine receptor. *J. Med. Chem.* 55, 7054–7060. doi: 10.1021/jm300671m
- Wang, Y., Bryant, S. H., Cheng, T., Wang, J., Gindulyte, A., Shoemaker, B. A., et al. (2017). PubChem BioAssay: 2017 update. *Nucleic Acids Res.* 45, D955–D963. doi: 10.1093/nar/gkw1118
- Wishart, D. S., Knox, C., Guo, A. C., Shrivastava, S., Hassanali, M., Stothard, P., et al. (2006). DrugBank: a comprehensive resource for in silico drug discovery and exploration. *Nucleic Acids Res.* 34, D668–D672. doi: 10.1093/nar/gkj067
- Zhang, P., Wang, F., and Hu, J. (2014). Towards drug repositioning: a unified computational framework for integrating multiple aspects of drug similarity and disease similarity. *AMIA Annu. Symp. Proc. AMIA Symp.* 2014, 1258–1267.
- Zhang, Y.-M., Cockerill, S., Guntrip, S. B., Rusnak, D., Smith, K., Vanderwall, D., et al. (2004). Synthesis and SAR of potent EGFR/erbB2 dual inhibitors. *Bioorg. Med. Chem. Lett.* 14, 111–114.

Conflict of Interest Statement: The authors declare that the research was conducted in the absence of any commercial or financial relationships that could be construed as a potential conflict of interest.

Copyright © 2017 March-Vila, Pinzi, Sturm, Tinivella, Engkvist, Chen and Rastelli. This is an open-access article distributed under the terms of the Creative Commons Attribution License (CC BY). The use, distribution or reproduction in other forums is permitted, provided the original author(s) or licensor are credited and that the original publication in this journal is cited, in accordance with accepted academic practice. No use, distribution or reproduction is permitted which does not comply with these terms.



Drug Repositioning in Glioblastoma: A Pathway Perspective

Sze Kiat Tan¹, Anna Jermakowicz¹, Adnan K. Mookhtiar¹, Charles B. Nemeroff²,
Stephan C. Schürer³ and Nagi G. Ayad^{1*}

¹ Department of Psychiatry and Behavioral Sciences, Center for Therapeutic Innovation, Miami Project to Cure Paralysis, Sylvester Comprehensive Cancer Center, University of Miami Brain Tumor Initiative, University of Miami Miller School of Medicine, Miami, FL, United States, ² Department of Psychiatry and Behavioral Sciences and Center on Aging, University of Miami Miller School of Medicine, Miami, FL, United States, ³ Department of Molecular Pharmacology, Center for Computational Sciences, Sylvester Comprehensive Cancer Center, University of Miami Miller School of Medicine, Miami, FL, United States

OPEN ACCESS

Edited by:

Yuhei Nishimura,
Mie University Graduate School of
Medicine, Japan

Reviewed by:

Alexander A. Mongin,
Albany Medical College, United States
Alessandro Poggi,
Ospedale Policlinico San Martino, Italy

*Correspondence:

Nagi G. Ayad
nayad@med.miami.edu

Specialty section:

This article was submitted to
Experimental Pharmacology and Drug
Discovery,
a section of the journal
Frontiers in Pharmacology

Received: 10 January 2018

Accepted: 27 February 2018

Published: 16 March 2018

Citation:

Tan SK, Jermakowicz A,
Mookhtiar AK, Nemeroff CB,
Schürer SC and Ayad NG (2018) Drug
Repositioning in Glioblastoma: A
Pathway Perspective.
Front. Pharmacol. 9:218.
doi: 10.3389/fphar.2018.00218

Glioblastoma multiforme (GBM) is the most malignant primary adult brain tumor. The current standard of care is surgical resection, radiation, and chemotherapy treatment, which extends life in most cases. Unfortunately, tumor recurrence is nearly universal and patients with recurrent glioblastoma typically survive <1 year. Therefore, new therapies and therapeutic combinations need to be developed that can be quickly approved for use in patients. However, in order to gain approval, therapies need to be safe as well as effective. One possible means of attaining rapid approval is repurposing FDA approved compounds for GBM therapy. However, candidate compounds must be able to penetrate the blood-brain barrier (BBB) and therefore a selection process has to be implemented to identify such compounds that can eliminate GBM tumor expansion. We review here psychiatric and non-psychiatric compounds that may be effective in GBM, as well as potential drugs targeting cell death pathways. We also discuss the potential of data-driven computational approaches to identify compounds that induce cell death in GBM cells, enabled by large reference databases such as the Library of Integrated Network Cell Signatures (LINCS). Finally, we argue that identifying pathways dysregulated in GBM in a patient specific manner is essential for effective repurposing in GBM and other gliomas.

Keywords: glioblastoma, drug repurposing, blood-brain barrier, Library of Integrated Network Based Cell Signatures, LINCS

INTRODUCTION

Glioblastoma multiforme (GBM) is the most common and aggressive adult primary brain tumor. Despite decades of research and clinical trials, the median survival remains at approximately 14 months. This is in part due to the highly invasive nature of GBM cells, which makes complete surgical resection difficult. In addition, GBM cells develop resistance against the current multimodal treatment regimen that includes the alkylating agent temozolomide (TMZ) and radiation. Furthermore, tumors expressing the DNA repair protein O6-methylguanine methyltransferase (MGMT) are resistant to TMZ. Finally, many targeted therapies fail in clinical trials because they do not effectively cross the blood-brain barrier (BBB). Collectively, these findings necessitate the discovery of novel therapeutic avenues for treating GBM. Impressive technological

advances have enabled us to decipher the genetic and cellular makeup of GBM tumors (Verhaak et al., 2010; Clarke et al., 2013). However, the lengthy time required to develop new small molecules and to demonstrate their efficacy and safety in preclinical models is a major impediment for uncovering novel treatments for this devastating disorder.

Drug repositioning may be one means of expediting therapeutic drug development for GBM. Drug repositioning, or drug repurposing, is the method of expanding the therapeutic range of an established Food and Drug Administration (FDA)-approved drug to another disease by identifying a novel use for the drug. One of the reasons drug repositioning may be more advantageous over novel drug discovery is that the pharmacokinetic and safety profiles of that drug are already known. In addition, drug repurposing is considerably less costly and less time intensive than novel small molecule discovery.

The rationale of drug repositioning lies, in part, in the ability of small molecules to target distinct proteins in cells. Different pathways involved in cancer initiation or progression that are considered unrelated to each other can thus be targeted by the same molecule. This concept is also known as “polypharmacology.” This is in contrast to the traditional mindset in drug discovery where the goal is to identify one drug solely for one target, with the hope that this high selectivity can enhance efficacy of the drug and reduce off-target toxicities. In this review, we focus on drug repositioning in glioblastoma, with emphasis on novel uses of psychiatric and non-psychiatric drugs, which are known to cross the BBB. In addition, we highlight recent efforts to utilize systems approaches for identifying repurposing agents in cancer that can be applied to glioblastoma.

One of the most challenging parts of GBM treatment is the complete elimination of the glioblastoma stem cell (GSC) population (Clarke et al., 2013). Among the heterogeneous cellular mass of gliomas, a small subpopulation of cells that are responsible for brain tumor initiation, termed GSCs, have been described to be primarily responsible for the recurrence of malignant glioma, due to their self-renewal ability, and multi-lineage differentiation potential (Jiang et al., 2016; Lubanska and Porter, 2017). These cells recapitulate the parental tumor cells in their complex biological nature. Chemotherapies usually kill the proliferating cells by inducing DNA damage, but do not affect stem cells, which remain at the original site after resection and eventually lead to tumor infiltration and recurrence, as well as GBM resistance to TMZ (Lubanska and Porter, 2017). Hence, many of the recent studies focus on this subpopulation of stem cells. Therefore, in considering repurposing drugs for GBM, it is essential that we consider their efficacy in eliminating GSCs.

PSYCHIATRIC DRUGS FOR TREATING GLIOBLASTOMA

Several studies have investigated the ability of FDA-approved psychotropic agents to inhibit GBM cell proliferation and migration (**Table 1**) (Triscott et al., 2012; Lee J. K. et al., 2016). Screens that yielded compounds previously shown to be brain penetrant were considered especially promising

because this is an obvious prerequisite for reducing GBM growth in humans. An intact BBB only allows diffusion of lipid-soluble molecules smaller than 400 Da, and molecules which are naturally transported by the existing carrier proteins (Gan et al., 2017). There is also an active efflux mechanism for compounds that enter the brain, mainly due to transporters located at the BBB. Organic anion-transporting polypeptide 1A2 (OATP1A2/SLCO1A2), organic anion transporter 3 (OAT3/SLC22A8), P-glycoprotein (P-gp), multidrug-resistance-associated protein 4 (MRP4/ABCC4), and monocarboxylate transporter 1 (MCT1/SLC16A1) are examples of transporters, which are present at the BBB (Urquhart and Kim, 2009). The restriction of the BBB, which causes low distribution of therapeutic agents in the brain, remains a challenge. Therefore, compounds that have been previously shown to be equally distributed throughout the whole brain are especially attractive for treating GBM patients.

Importantly, many GBM patients are treated with psychopharmacological agents because they suffer from comorbid psychiatric disorders such as anxiety, depression with suicidal ideation, psychosis, and acute confusional status (Lee J. K. et al., 2016). Interestingly, the incidence of cancer occurrence is inversely proportional to antipsychotic drug treatment in patients with schizophrenia, perhaps suggesting that there is a benefit to treatment with antipsychotic drugs for cancer patients (Barak et al., 2005; Tran et al., 2009). Whether this is due to a direct effect on tumor growth or indirectly due to the psychological benefits for the medications remains to be determined. Although many of the primary targets of these drugs are present in GBM cells, most reports discuss the off-targets effects of these drugs and favor polypharmacology. Below we discuss some drugs commonly used in psychiatry that have potent anti-proliferative properties *in vitro* and *in vivo*.

Typical Antipsychotics (Neuroleptics)

Antipsychotic drugs, also known as neuroleptics or major tranquilizers, are primarily used in the treatment of psychosis, schizophrenia, acute mania, bipolar disorder, and Tourette syndrome. Haloperidol, trifluoperazine, fluphenazine, thioridazine, perphenazine, and chlorpromazine (CPZ) are some of the commonly used antipsychotics. All typical antipsychotics block dopamine D₂ receptors.

Antipsychotics suppress proliferation, invasion, and anchorage-independent growth of GBM cells (Oliva et al., 2017; Pinheiro T. et al., 2017). Dopamine receptor subtype 2 is present in GBM cells and is responsible for the mitogenic signaling (Bartek and Hodny, 2014). There have been several mechanisms of action proposed for their potential anti-tumor effect (**Table 1**). For example, a recent publication by Kang et al. showed that trifluoperazine binds to a Ca²⁺-binding protein, calmodulin subtype 2 (CaM2), de-represses the Ca²⁺ release channel inositol 1,4,5-triphosphate receptor (IP₃R) subtype 3, and subsequently stimulates the irreversible mass release of Ca²⁺ in GBM cells (Kang et al., 2017) (**Figure 1**). Ca²⁺ is essential for numerous functions in cells such as regulating gene expression and metabolism (Kang et al., 2017). Intracellular Ca²⁺ homeostasis is tightly regulated in a biological system

TABLE 1 | Summary of primary indications, primary mechanism of actions, antineoplastic mechanism in GBM, and BBB penetrance of different psychiatric and non-psychiatric drugs.

Drug	Mechanism of action	Primary indications	Mechanism of action in GBM	References	BBB penetrant
PSYCHIATRIC DRUGS					
Typical antipsychotics (Haloperidol, trifluoperazine, fluphenazine, thioridazine, perphenazine, chlorpromazine)					
	Block D ₂ receptors	Psychosis, schizophrenia (mostly positive symptoms), acute mania, bipolar disorders, Tourette syndrome	Suppress proliferation, invasion, and anchorage-independent growth: – de-repressing the IP ₃ R, stimulates mass release of Ca ²⁺ – inhibiting mitochondrial CoO – inhibiting GPCR σ -receptors – increasing AMPK activity	Kang et al. Oliva et al. Cheng et al. Lee et al.	Yes
Atypical antipsychotics (Olanzapine, clozapine, asenapine, lurasidone, quetiapine, risperidone, aripiprazole)					
	Inhibit 5-HT _{2A} , D ₂ , H ₁ , α ₁ , and α ₂ receptors	Schizophrenia bipolar disorder, major depressive disorder, generalized anxiety disorder, Huntington's disease	Reduce cell proliferation, anchorage-independent growth, migration, promote apoptosis and necrosis by: – inhibiting the Wnt/ β -catenin signaling pathway – downregulating AMPK, c-Jun – cell cycle arrest at G2/M phase – promoting the differentiation into OL-like cells – reducing expression of PIK3CD	Karpeel-Massler et al. Guo et al. Ferno et al. Wang et al. Karbownik et al.	Yes
Tricyclic antidepressants (Amitriptyline, imipramine, doxipramine, doxepin, amoxepine)					
	Prevent reuptake of norepinephrine and serotonin at the presynaptic receptors	Major depression, neuropathic pain, migraine prophylaxis, anorexia, anxiety disorders	Reduce cell proliferation, cell stemness, limit invasion, induce autophagy, and regulate GSC plasticity and cancer immunity by: – downregulating Sox1, Sox2, Nestin, Ki67, CD44 – inhibiting PI3K/Akt/mTOR signaling pathway – increasing phospho-c-Jun and cytochrome c – regulating NADPH oxidase-mediated ROS generation	Higgins and Pilkington et al. Tzadok et al. Lawrence et al. Bielecka-Wajdman et al. Jeon et al. Levkovitz et al. Munson et al.	Yes
Selective serotonin receptor inhibitors (Sertaline, citalopram, fluoxetine, fluvoxamine, escitalopram, paroxetine)					
	Inhibit reuptake of serotonin into neurons	Major depression, bipolar disorder, anxiety disorder	Inhibit GBM invasion, proliferation, increase apoptosis by: – inhibiting actin polymerization – lamellipodia suppression – decreasing FAK, Akt and mTOR phosphorylation – activating AMPA receptors, increases Ca ²⁺ influx into mitochondria – releasing cytochrome c, caspase-9, caspase-3, and PARP, triggering apoptosis	Leykovich et al. Hayashi et al. Munson et al. Tzadok et al. Liu et al.	Yes
Sedative hypnotics (Benzodiazepines: Diazepam, lorazepam, triazolam, temazepam, oxazepam, midazolam)					
	Facilitate GABA _A receptor complex action in CNS by increasing the frequency of Cl ⁻ channel opening	Anxiety disorders, spasticity, status epilepticus, detoxification, night terrors, sleepwalking	Inhibit cell proliferation, sensitize GBM cells to chemotherapy by: – inactivating Rb protein at G1/S transition (cell cycle arrest) – facilitating hypericin-induced and etoposide-induced cytotoxicity	Chen et al. Saritsky et al.	Yes
Antiepileptics (Sodium valproate, carbamazepine, levetiracetam)					
	Prolong Na ⁺ channel inactivation and inhibits GABA transaminase	Myoclonic seizures, migraines, bipolar disorders	Reduce cell proliferation, increase autophagy, increase GBM sensitivity to TMZ and radiosensitivity by: – inhibiting HDAC – downregulating MGMT – enhancing p53 expression – increasing binding of HDAC1/mSin3A complex to the MGMT promoter – binding to SV2A, enhance GABA release	Zhang et al. Chinnaiyan et al. Tseng et al. Bobustuc et al. Lee et al. Pinheiro et al. Knudson-Baas et al. Peddi et al.	Yes
Disulfiram					
	Inhibits ALDH enzyme	Alcohol abuse	Inhibits proliferation, self-renewal, increases sensitivity by: – inhibiting ALDH – inhibiting proteasome and NF- κ B pathways by chelation – inhibiting p97 pathway – decreasing MGMT expression, PLK1 protein and mRNA	Triscott et al. Chen et al. Choi et al. Paranjpe et al. Lun et al. Skrott et al.	Yes

(Continued)

TABLE 1 | Continued

Drug	Mechanism of action	Primary indications	Mechanism of action in GBM	References	BBB penetrant
NON-PSYCHIATRIC DRUGS					
Mebendazole	Microtubule inhibitor	Anthelmintic drug	<ul style="list-style-type: none"> - Inhibiting microtubule polymerization - Inhibiting protein kinase - Inducing metaphase arrest 	De Witt et al.	Polymorph A – No; Polymorph B and C - Yes
Vincristine	Microtubule inhibitor	Chemotherapy in various cancers	Prevents mitotic spindle formation and M-phase arrest	De Witt et al.	No
Clomifene	Antagonist at estrogen receptors in the hypothalamus	Women infertility due to anovulation, PCOS	<ul style="list-style-type: none"> - Inhibiting mutant IDH1, reduces D-2HG - Increasing apoptosis 	Kipper et al. Zheng et al. Yaz et al.	Unknown
Biguanides (Metformin, phenformin)	Inhibit gluconeogenesis, increase glycolysis, and increase insulin sensitivity by promoting peripheral glucose uptake	Type II diabetes mellitus	<ul style="list-style-type: none"> Inhibit cell proliferation, migration, angiogenesis, TMZ resistance, self-renewal, stemness of GSC and induce apoptosis by: - inhibiting complex I of the ETC and mTORC1 - inhibiting AMPK and STAT3 pathways - increases of miR-124 and let-7 - inhibiting glutamate dehydrogenase, reduces D-2HG - inhibiting CLIC1, leads to G1 arrest 	Jiang et al. Molenaar et al. Feria et al. Uzbek et al. Yang et al. Elmaci et al. Kast et al. Aldea et al. Lee et al. Gritti et al.	Yes
Repaglinides	Insulin secretagogue	Type II diabetes mellitus	<ul style="list-style-type: none"> Inhibit proliferation, migration, and increase immune cytotoxicity by: - inducing apoptosis - suppressing autophagy - downregulating Bcl-2, Beclin-1 and PD-L1 	Xiao et al.	Modest
Cyclin-Dependent Kinases (First generations: Flavopiridol; Second generation: Palbociclib, dinaciclib, roscovitine, milciclib, purvalanol A)	Cell cycle checkpoint regulators	Anti-cancer drugs	<ul style="list-style-type: none"> Cytotoxic to cells, reduce cell proliferation by: - inhibiting DNA repair activity at G2M transition - inactivating Rb 1 phosphorylation 	Jane et al.	Varies (Yes for abemaciclib and pablociclib)
EGFR inhibitors (TKI: erlotinib, gefitinib; mAbs: nimotuzumab, cetuximab)	Prevent ligand binding, and tyrosine kinase activation	Anti-cancer drugs (NSCLC, HNSCC)	Tyrosine kinase inhibitors	Miranda et al.	Varies (Low)
Statins (Lovastatin, pravastatin, rosuvastatin, simvastatin)	HMG-CoA reductase inhibitors	Lipid lowering agents	<ul style="list-style-type: none"> Cytotoxic to GBM cells by: - TRAIL-sensitizing effect - increasing Bim - reducing MAPKs-dependent pathway activations with GTPase activation; - suppression of ERK1/2 and Ras/P13K/AKT pathway - Activation of JNK1/2 	Yanae et al. Tapia-Perez et al.	Varies

*ALDH, acetaldehyde dehydrogenase; AMPA, α -amino-3-hydroxy-5-methyl-4-isoxazolepropionic acid; AMPK, 5'-AMP-activated protein kinase; BBB, blood brain barrier; Bcl-2, B-cell lymphoma 2; CcO, cytochrome c oxidase; CLIC1, chloride intracellular channel-1; CNS, central nervous system; D₂, dopamine 2; D-2HG, D-2-hydroxyglutaric acid; ERK1/2, extracellular regulated kinase 1/2; ETC, electron transport chain; FAK, focal adhesion kinase; GABA_A, γ -aminobutyric acid A; GBM, glioblastoma multiforme; GPCR, G-protein coupled receptor; GSC, glioma stem cell; HDAC, histone deacetylase; HMG-CoA, β -hydroxy- β -methylglutaryl coenzyme A; HNSCC, squamous cell carcinoma of head and neck; IDH, isocitrate dehydrogenase; I β -R, inositol 1,4,5-triphosphate receptor; JNK1/2, c-Jun N-terminal kinase 1/2; mAbs, monoclonal antibodies; MAPKs, mitogen-activated protein kinases; MGMT, O⁶-methylguanine-DNA methyltransferase; mTORC1, mammalian target of rapamycin complex 1; NSCLC, non-small-cell lung carcinoma; OL, oligodendrocyte; PARR, poly (ADP-ribose) polymerase; PCOS, polycystic ovarian syndrome; PD-L1, programmed death-ligand 1; PIK3CD, phosphatidylinositol-4,5-bisphosphate 3-kinase catalytic subunit delta; PLK1, serine/threonine-protein kinase; Rb, retinoblastoma; ROS, reactive oxygen species; STAT3, signal transducer and activator of transcription 3; SV2A, synaptic vesicle glycoprotein 2A; TKI, tyrosine kinase inhibitors; TMZ, temozolamide; TRAIL, TNF-related apoptosis-inducing ligand.

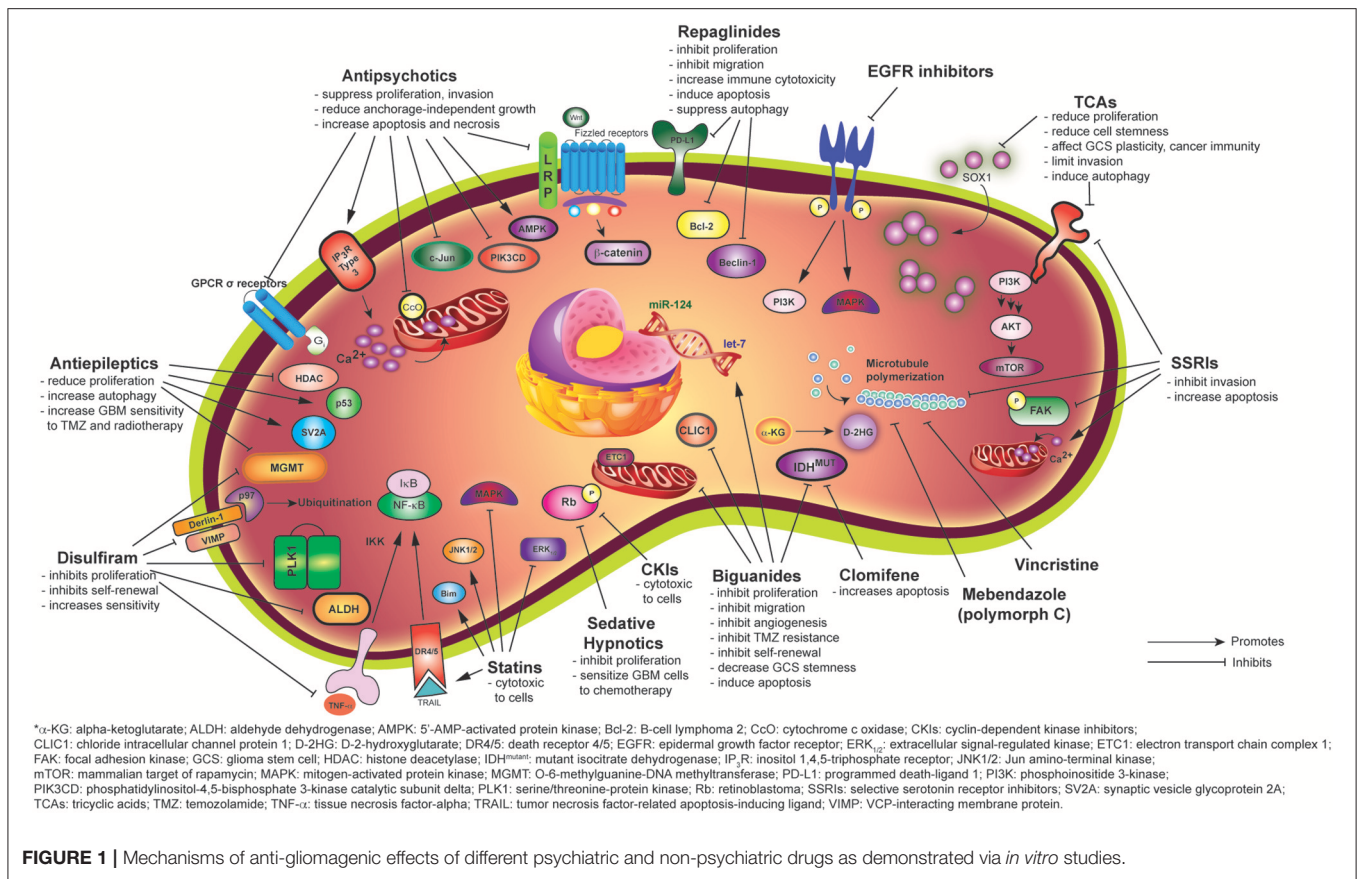


FIGURE 1 | Mechanisms of anti-gliomagenic effects of different psychiatric and non-psychiatric drugs as demonstrated via *in vitro* studies.

and an alteration in Ca²⁺ levels can result in cell death (Kang et al., 2017). A phenothiazine, CPZ, was demonstrated by Oliva et al. to inhibit mitochondrial cytochrome c oxidase (CcO) in chemoresistant glioma cells and GSCs when CcO subunit 4 isoform 1 (COX4-1) is present, but not COX4-2 (Oliva et al., 2017). However, this was only true for TMZ-resistant cells as TMZ-sensitive cells were not affected by CPZ. Attenuated CcO reduces the efficacy of mitochondrial OxPhos dependent ATP-linked respiration and lowers reactive oxygen species production, thereby lowering glioma progression (Oliva et al., 2017). COX4 affects the sensitivity of GBM cells to CPZ (Oliva et al., 2017). Increased CcO activity and increased COX4-1 expression were observed to be associated with worse prognosis in GBM (Oliva et al., 2017). Oliva et al. also demonstrated the beneficial effect of CPZ in prolonging survival in an *in vivo* preclinical study (Oliva et al., 2017). Importantly, there were no adverse behavioral effects noticed with CPZ use in this model, suggesting that similar use in GBM patients could be well-tolerated.

Another potential means for reducing GBM growth is via inhibiting G-protein coupled receptors (GPCRs) that regulate GBM cell proliferation. For instance, pimozide inhibits σ-receptors, one of the atypical GPCRs expressed, and thus attenuates GBM proliferation (Lee J. K. et al., 2016) (Figure 1). Another antipsychotic, thioridazine, has been shown to be cytotoxic to GBM cells by increasing 5'-AMP-activated protein kinase (AMPK) activity, which is downstream of GPCR signaling

(Cheng et al., 2015). Given the substantial literature associated with GPCR signaling, it will be important to correlate clinical efficacy of drugs affecting GBM progression in clinical trials with the signaling pathway the drug affects.

Atypical Antipsychotics

Although the exact molecular mechanisms underlying the therapeutic actions of atypical antipsychotics remain obscure, they have multiple effects on dopamine, 5-HT₂, α-, and H₁-receptors. Their low-risk profiles make them especially attractive for repurposing in GBM. Olanzapine, clozapine, asenapine, lurasidone, quetiapine, risperidone, aripiprazole, brexpiprazole, and ziprasidone are some examples of second-generation atypical antipsychotics (Table 1).

Olanzapine is used in the treatment of schizophrenia, bipolar disorder, and neurological conditions such as Huntington's disease. Olanzapine is an antagonist of the serotonin (5-HT_{2A}) and dopamine (D₂) receptors. In the cancer field, olanzapine has been used to control pain and chemotherapy associated nausea. Olanzapine has emerged as an attractive therapeutic candidate for repurposing in brain cancer as it reduced glioblastoma cell expansion *in vitro* and *in vivo* (Karpel-Massler et al., 2015; Karbownik et al., 2016). Karpel-Massler et al. reported that olanzapine has antineoplastic capability and its cytotoxicity effect *in vitro* is enhanced when combined with TMZ (Karpel-Massler et al., 2015). Furthermore, olanzapine

reduces GBM cancer cell proliferation, decreases anchorage-independent colony formation, inhibits migration, and induces mixed apoptosis and necrosis in GBM cells (Karpel-Massler et al., 2015). The mechanism of action includes downregulation of the Wnt/ β -catenin pathway and c-Jun and is also thought to be dependent on the extracellular concentration of phospholipase D and other factors (Karpel-Massler et al., 2015) (**Figure 1**). However, the efficacy of olanzapine likely varies among different GBM cell lines given the heterogeneous nature of GBM as another study found that treatment of glioma cells with olanzapine did not affect viability (Ferno et al., 2006). The increase in AMPK thought to promote cell death in the Karpel-Masler study was not observed in this study (Karpel-Massler et al., 2015). Another possibility to account for the differential effects is that the concentrations used were vastly different. Indeed, the concentrations used in the Karpel-Massler study were very high and not likely to be attained in the clinical setting.

Another atypical antipsychotic, quetiapine, acts as an antagonist at serotonin (5-HT_{1A} and 5-HT_{2A}), dopamine (D₁ and D₂), histamine (H₁), and adrenergic (α_1 and α_2) receptors. It is an FDA-approved drug for the treatment of schizophrenia, bipolar disorder, and often used in major depressive disorder (MDD) as well as generalized anxiety disorder. In a recent publication, Wang et al., demonstrated that quetiapine suppresses GBM cell growth *in vitro* and *in vivo* (Wang et al., 2017b). High doses of quetiapine suppress GSC proliferation by arresting cells at the G2/M phases of the cell cycle. Importantly, quetiapine improves survival of mice bearing glioma. The proposed mechanism of action involves promoting the differentiation of GSCs into oligodendrocyte (OL)-like cells by inhibiting the Wnt/ β -catenin signaling pathway (Wang et al., 2017b) (**Figure 1**). This anti-gliomagenic property is attributed to the finding that well-differentiated cells are more sensitive to chemotherapy than less differentiated ones (Persson et al., 2010). This is significant in demonstrating that quetiapine may inhibit TMZ-resistant glioma (Wang et al., 2017b).

Another mechanism through which quetiapine controls cell growth is via downregulation of the phosphoinositide 3-kinase (PI3K) pathway, a major driver of GBM cell proliferation (**Figure 1**). Karbownik et al. in 2016 demonstrated that quetiapine reduces mRNA expression of the PI3K component PIK3CD in GBM cells (Karbownik et al., 2016).

Tricyclic Antidepressants

Approximately 90% of GBM patients are reported to have significant depressive symptoms and neurological disturbances (Bielecka-Wajdman et al., 2017). One can easily foresee that the severe stress associated with GBM patients both from the poor prognosis and the consequences of therapy contribute to depression. Furthermore, oncologists often also prescribe these antidepressants to control chronic and neuropathic pain, migraines, anorexia, anxiety disorders, and circadian rhythms. Tricyclic antidepressants (TCAs) such as amitriptyline, imipramine, clopiramine, doxepin, and amoxapine act primarily by preventing the reuptake of norepinephrine and serotonin at presynaptic terminals (Higgins and Pilkington, 2010).

Although the antidepressant effects of TCAs are well established, the anticancer effect remains a big question due to many conflicting reports discussing whether antidepressants can induce or reduce tumorigenesis. TCAs reduce cell proliferation in rat C6 glioma, human neuroblastoma, and human astrocytoma cells (Higgins and Pilkington, 2010; Tzadok et al., 2010; Lawrence et al., 2016). Bielecka-Wajdman et al. also demonstrated that antidepressants, especially amitriptyline and imipramine, can reduce the “stemness” of the GSCs at a rate dependent on the oxygen content of the hypoxic microenvironment in which the tumor resides. The low oxygen content in tumors is a common issue for most cancers and it is responsible for GBM invasion (Monteiro et al., 2017). Bielecka-Wajdman et al. observed a downregulation of the “stemness genes” Sox1, Sox2, Nestin, Ki67, and CD44 after TCA treatment (Bielecka-Wajdman et al., 2017). They also hypothesized that TCAs can affect GCS plasticity and cancer immunity by regulating pro- and anti-inflammatory cytokines, immune cells, and reactive oxygen species (Bielecka-Wajdman et al., 2017). Hence, it is possible that TCA can trigger the host immune response.

In addition, imipramine, as demonstrated by Jeon et al., reduces U-87MG glioma cell growth by inhibiting the PI3K/Akt/mTOR signaling pathway and inducing autophagy, but not apoptosis (Jeon et al., 2011) (**Figure 1**). This is in response to the report from Levkovitz et al. where they demonstrated that some TCAs but not imipramine, increase apoptosis (Levkovitz et al., 2005). They observed a rapid rise in phospho-c-Jun levels and increased mitochondrial cytochrome c release in glioma cells after TCA treatment (Levkovitz et al., 2005). Munson et al. in 2012 also demonstrated that imipramine blue is able to limit the invasion of GBM cells and this “containment” helps to enhance the effect of chemotherapy at the tumor field. This is suggested to be modulated by NADPH oxidase-mediated reactive oxygen species generation (Munson et al., 2012). These off-targets effects seen with TCA use are likely to inhibit GBM cells survival.

A recent nation-wide study conducted by Pottegard et al. in Denmark investigated the protective effects of TCAs against gliomas. In a sample of 75,340 control patients and 3,767 patients with glioma, long term (>3 years) use of TCAs was inversely correlated with glioma risk, with an odds ratio of 0.72 (Pottegard et al., 2016). This is contrary to the observation reported by Walker in 2012 in the United Kingdom that exposure to TCA post-diagnosis of glioma does not improve survival (Walker et al., 2012). However, patients in this study were not receiving TCAs previously, so the experimental designs in these two studies are quite different.

Selective Serotonin Reuptake Inhibitors

Selective serotonin reuptake inhibitors (SSRIs), the most commonly used antidepressants, increase serotonin concentrations at the synapses and activate the postsynaptic neurons (**Table 1**). Commonly used SSRIs are sertraline, citalopram, fluoxetine, fluvoxamine, escitalopram, and paroxetine. A report from the Glioma Outcomes Project has shown that patients who are depressed, either during the surgery or post-operative management period, are more likely to suffer from more comorbidities and have an increased rate of

death (Caudill et al., 2011). Although Caudill in 2010 concluded that the use of SSRIs is safe in GBM patients, there is still a debate as they are associated with a higher risk of seizures (Caudill et al., 2011). Compared to citalopram and sertraline, fluoxetine, and paroxetine can inhibit the CYP450 2D6 isoenzyme and lead to drug-drug interactions that may account for the higher toxicity of these medications in GBM patients (Rooney and Grant, 2012).

SSRIs have recently gained much attention for potential anti-GBM property due to their BBB penetration properties and favorable safety profile. Fluvoxamine, which is able to be selectively transported into the brain at higher concentration without causing peripheral side effects, is safe to be used in treating depression in GBM patients. In addition to reducing cell proliferation, SSRIs can induce apoptosis in GBM (Levkovitz et al., 2005). Fluvoxamine has been demonstrated to reduce actin polymerization through inhibition of actin polymerization-related proteins, thereby reducing GBM cell invasion via lamellipodia suppression (Hayashi et al., 2016) (**Figure 1**). Hayashi et al. demonstrated that fluvoxamine decreases FAK phosphorylation at Y397, Akt phosphorylation at T308 and S473, as well as mTOR phosphorylation at S2448 and S2481 (Hayashi et al., 2016) (**Figure 1**). Although fluvoxamine does not affect GBM cell proliferation, a reduction in proliferating cells was seen in fluvoxamine treated tumors, and fluvoxamine was shown to reduce tumor burden in mice bearing tumors from human glioma-initiating cells, suggesting that the positive effects of fluvoxamine in preclinical glioma models is achieved via reducing the invasive capacity of tumor cells. In their model, fluvoxamine maleate is administered at 50 mg/kg/day, which is higher than the daily human equivalent dose that is usually given to patients in the clinic. (Hayashi et al., 2016).

In contrast to fluvoxamine, fluoxetine induces glioma cell death. Importantly, fluoxetine is not toxic to primary astrocytes and neurons (Liu et al., 2015). Fluoxetine directly binds to GluR1, activates AMPA receptors and increases Ca^{2+} influx into the mitochondria (Liu et al., 2015). This Ca^{2+} influx subsequently induces mitochondrial membrane damage and releases cytochrome c, as well as activating caspase-9, caspase-3, and poly (ADP-ribose) polymerase (PARP), thereby triggering apoptosis (Liu et al., 2015). Interestingly, fluoxetine is similar to TMZ in reducing GBM growth *in vivo* (Munson et al., 2012). Tzadok et al. in 2010 also demonstrated the synergistic effect of fluoxetine, sertraline, or perphenazine with the tyrosine kinase inhibitor imatinib in reducing GBM cell proliferation, suggesting a potential use for GBM therapy (Tzadok et al., 2010).

Sedative Hypnotics

Benzodiazepines are often used as a general anesthetic and are also indicated for patients suffering from several anxiety disorders, spasticity, status epilepticus, detoxification, night terrors, and sleepwalking. Diazepam, lorazepam, triazolam, temazepam, oxazepam, and midazolam are the most widely available benzodiazepines (**Table 1**). They facilitate γ aminobutyric acid A ($GABA_A$) receptor complex action in the central nervous system by increasing the frequency of Cl^- channel opening (Chen et al., 2013). In GBM patients, diazepam can help alleviate post-cancer therapy anxiety and

inhibit chemotherapy-associated delayed emesis. Even though benzodiazepines easily cross the BBB, the need for a higher dose to achieve efficacy in anticancer therapy remains a safety concern.

In 2013, Chen et al. investigated the anti-proliferative property of diazepam in human glioblastoma (Chen et al., 2013). They demonstrated that by inactivating the cell cycle protein Rb, diazepam can cause a cell cycle arrest at the G0/G1 phase in human GBM cells in a dose-dependent manner (**Figure 1**). This result adds on to an earlier study, which showed that diazepam facilitates hypericin-induced and etoposide-induced cytotoxicity in GBM cells (Sarissky et al., 2005). Altogether, this demonstrates that diazepam not only sensitizes GBM cells to chemotherapy, but also kills tumor cells.

Antiepileptics/Anticonvulsants

Nearly 22–60% of GBM patients exhibit epileptic seizures as an initial clinical complication (Van Nifterik et al., 2012). Sodium valproate or valproic acid (VPA) is one of the most commonly prescribed antiepileptic drugs (AEDs) that has been used for decades. The prescription is usually justified after a first and single seizure in a GBM patient. VPA is also utilized for the treatment of myoclonic seizures, migraines and bipolar disorder. Sodium valproate prolongs Na^+ channel inactivation and inhibits gamma-butyric acid (GABA) transaminase, hence increasing the concentration of GABA (**Table 1**).

Sodium valproate or VPA is also a histone deacetylases (HDACs) inhibitor that has been proposed as a potential adjuvant in cancer treatment. Histone lysine residue acetylation and deacetylation are among the most widely characterized posttranslational modifications in epigenetics. Histone deacetylases promote neoplasia by condensing chromatin and repressing transcription of tumor suppressor genes, and these HDACs are often overexpressed in GBM (Rundle-Thiele et al., 2016). As epigenetic modifiers, HDAC inhibitors can increase the cancer cell's sensitivity to ionizing radiation, while preventing normal cells from being killed by radiotherapy (Zhang et al., 2016). Sodium valproate exposure increases histone hyperacetylation in glioma cells, inhibits cell growth, and increases cell radiosensitivity (Chinnaiyan et al., 2008; Van Nifterik et al., 2012; Lee C. Y. et al., 2016; Zhang et al., 2016; Tseng et al., 2017). Sodium valproate has also been used in combination with other chemotherapies such as TMZ, topoisomerase inhibitors, and carboplatin in medulloblastoma and glioma studies (Felix et al., 2011). By contrast, Lee et al. demonstrated that at a therapeutic dose, sodium valproate alone inhibits <20% of cell proliferation (Lee C. Y. et al., 2016). However, when combined with TMZ, VPA shows a significant antineoplastic impact in TMZ-resistant glioma cells via downregulating MGMT expression (**Figure 1**). This combination therapy also showed promising results in a Phase II clinical trial of newly diagnosed GBM patients. Interestingly, a hybrid compound of TMZ and an HDAC inhibitor named HYBCOM was developed in order to minimize resistance (Pinheiro R. et al., 2017). The authors were able to demonstrate the efficacy of this compound in reducing glioma cell proliferation through selective autophagy in tumor cells and reduced multi-drug resistance, as compared

to TMZ alone. However, VPA can inhibit several enzymes, such as CYP2C coenzymes, epoxide hydroxylase, and uridine diphosphate-glucuronosyltransferase, which may be linked to its unfavorable side effects. Killick-Cole et al. also proposed repurposing VPA for the treatment of diffuse intrinsic pontine glioma (DIPG), a deadly pediatric brain tumor (Killick-Cole et al., 2017). In DIPG, sodium valproate reduced survival of *ex vivo* DIPG cells, induced apoptosis, and showed minimal toxicity to rat hippocampal neuronal and glial cells. In addition, pre-conditioning of DIPG cells by sodium valproate is synergistic with carboplatin in inducing cytotoxicity in these cells (Killick-Cole et al., 2017). However, there is no report on targeting Na⁺ in GBM by an antiepileptic.

Importantly, some of the drugs or drug combination can influence the recognition of GBM cells by the immune system. Hence it is possible that these drugs can also activate a host immune response. For instance, the alkylating agent administered to GBM patients, TMZ, can stimulate the expression of stress-induced antigens such as NKG2D ligands (MICA and ULBPs) on GBM cells (Chitadze et al., 2016). This sensitizes them to be killed by anti-tumor effector cells. Interestingly, the same effect is also seen in GBM cells when treated with HDAC inhibitors (Adamopoulou and Naumann, 2013).

Recently, nation-wide based data from 1,263 GBM patients in Norway from 2004 to 2010 showed that the choice of AED does not affect survival of GBM patients (Knudsen-Baas et al., 2016). Hapold and colleagues in 2016 prospectively analyzed a pooled dataset of 1,869 newly diagnosed GBM patients recruited from four different clinical trials and showed that the use of sodium valproate does not correlate with survival (Hapold et al., 2016).

By contrast, carbamazepine was the most frequently prescribed AED for GBM patients from 2004 to 2006 in Norway. However, this shifted toward levetiracetam (LEV) at a later period, namely from 2009 to 2010. LEV, another commonly used anticonvulsant, is effective in treating and preventing focal seizures, which are common in patients with intracranial tumors. It binds to the vesicular protein SV2A and enhances the release of GABA. It also penetrates the BBB rapidly and has a high therapeutic index, as compared to other AEDs (Knudsen-Baas et al., 2016). Importantly, this drug may be especially promising in treating GBM because of its lack of interaction with chemotherapy agents.

Peddi et al. in 2016 reported the first possible case of glioblastoma regression after combination treatment of dexamethasone and LEV intended for seizure prophylaxis (Peddi et al., 2016). This opens up many questions regarding the cause of this remarkable finding. LEV, as demonstrated by Bobustuc et al., has the ability to abrogate glioma cell proliferation and increase GBM cellular sensitivity to TMZ (Bobustuc et al., 2010). LEV enhances the expression of the tumor suppressor protein p53 and increases binding of the HDAC1/mSin3A complex to the MGMT promoter (Bobustuc et al., 2010). This survival benefit is further validated in a prospective randomized study by Kim et al. in 2015, showing that the median progression-free survival (PFS), and overall survival (OS) for GBM patients taking LEV

in combination with TMZ is significantly longer than those receiving TMZ alone (Kim et al., 2015).

Disulfiram

Disulfiram (tetraethylthiuram disulfide), which is currently used to treat alcoholism, is one of the most promising FDA-approved drugs for repurposing in GBM. Disulfiram was initially discovered in the rubber manufacturing industry in 1937, where it was observed that rubber workers who were exposed to disulfiram developed flu-like symptoms whenever they imbibed alcohol (Triscott et al., 2015). Based on this serendipitous finding, disulfiram has been utilized for the treatment of alcohol abuse and has been used for more than 60 years. The mechanism of action for disulfiram is that it inhibits the liver acetaldehyde dehydrogenase (ALDH) enzyme, which normally catalyzes the oxidation of acetaldehyde to acetate with the aid of the NAD⁺ cofactor (Triscott et al., 2012). After ALDH inhibition, acetaldehyde accumulates, which contributes to flushing, sweating, headache, nausea, and other hangover symptoms.

Multiple *in vitro* and *in vivo* studies have indicated that disulfiram may be effective for the treatment of brain tumors. Triscott et al. in 2012 demonstrated that even low-dose disulfiram inhibits proliferation and self-renewal of GBM cells that are resistant to TMZ, without affecting normal human astrocytes (Triscott et al., 2012). However, the dose of disulfiram used in their study is higher than the 250 mg/day dose given to patients, and therefore the potential utility is questionable (Triscott et al., 2012). In 2015, the same group also demonstrated that GBM cells are sensitive to disulfiram, but not TMZ (Triscott et al., 2015). Choi et al. showed that disulfiram crosses the BBB in mice and inhibits atypical teratoid rhabdoid tumors (Choi et al., 2015). Paranjpe et al. reported that disulfiram can increase cell killing by decreasing MGMT expression in xenograft models (Paranjpe et al., 2014). Collectively, these studies suggest that disulfiram should be considered for the treatment of GBM.

The antineoplastic property of disulfiram may be due to several mechanisms. As the most established pathway affected by disulfiram is the ALDH enzyme, ALDH has been shown to be upregulated in tumor cells with enhanced tumor growth in xenografts as well as resistance to chemotherapies (Triscott et al., 2015) (**Figure 1**). Furthermore, disulfiram inhibits the proteasome and NF- κ B pathways (Triscott et al., 2015). Disulfiram is pharmacokinetically converted into a smaller metabolite called diethyldithiocarbamate (DTC), which chelates with copper or zinc ions (Chen et al., 2006; Lun et al., 2016). The complexes formed can suppress proteasome activity and increase oxygen free radicals. Indeed, some studies have shown that combining disulfiram with copper can increase cytotoxicity in cancer cells *in vitro* and *in vivo*. A very recent study demonstrated reduction of tumor volume in mice treated with disulfiram with copper gluconate as compared to disulfiram alone. The chelation product after disulfiram ingestion, the DTC-copper complex, was hypothesized to bind NPL4, and subsequently inhibit the p97 pathway, thus resulting in cell death (Skrott et al., 2017) (**Figure 1**). However, a similar effect was observed in normal cells, suggesting that identifying a therapeutic window

is essential when using disulfiram. In addition, Choi et al. cautioned that there are potential side-effects when ingesting too much copper and zinc, again suggesting that a careful dosing strategy is needed when using disulfiram and copper and zinc (Choi et al., 2015).

Disulfiram inhibits cancer stem cells in lung cancer, breast cancer, ovarian cancer, pancreatic cancer, and blood cancers. Importantly, disulfiram is able to penetrate the BBB, favoring its use in treating brain tumors. Despite having an already established safe therapeutic index, many ongoing studies are investigating a dosing schedule and chemotherapy combination that will deliver the maximum effects in tumor cells (Triscott et al., 2012). These findings suggest the potential role of disulfiram to be repurposed for use in GBM, and potentially in pediatric brain tumors in the future.

NON-PSYCHIATRIC DRUGS

In addition to drugs used in psychiatry, which have favorable brain exposures for treating GBM and other brain cancers, several groups have focused on repurposing FDA approved compounds not used in psychiatry. However, the challenge here is to determine the efficacy of these compounds in reducing tumor growth in the brain. For many of these compounds, the brain exposure profiles and the pharmacokinetics properties have not been determined. Therefore, considerable efforts are needed to determine whether combination therapies of these repurposed compounds with the current standard-of-care will either facilitate or inhibit BBB penetrance of these compounds.

Mebendazole

A microtubule inhibitor, mebendazole is an FDA-approved antihelmintic drug. The ability of mebendazole to form different polymorphs (A, B, and C) depends on the crystallization conditions. Polymorph A does not penetrate the BBB as efficiently as polymorphs B and C (**Table 1**) (Bai et al., 2015). Mebendazole generally has a benign safety profile, although it has been shown to cause bone marrow suppression and liver toxicity at higher doses (De Witt et al., 2017).

Mebendazole can exhibit anti-tumor effects by inhibiting protein kinases. It is unknown whether the cell death observed in tumor cells treated with mebendazole is also mediated by the microtubule destabilizing effect. It was demonstrated by De Witt et al. that mebendazole inhibits microtubule polymerization and induces metaphase arrest, very similar to the mechanism of action of another microtubule inhibitor, vincristine (De Witt et al., 2017) (**Figure 1**). Furthermore, mebendazole polymorph C shows a survival benefit in a model of C57BL/6 mice bearing GL261 cells (Bai et al., 2011, 2015; De Witt et al., 2017). Although the authors observed increased survival with 100 mg/kg of administered mebendazole as compared to 50 mg/kg, it is close to the maximum tolerated dose and may not be achievable in humans. However, due to the efficacy of mebendazole in tumor suppression, it was recommended that mebendazole replaces vincristine in neuro-oncology management.

Vincristine

From the family of vinca alkaloids, vincristine binds to β -tubulin, and inhibits microtubule polymerization, thereby inhibiting the formation of the mitotic spindle during cell division (M-phase arrest) (De Witt et al., 2017) (**Figure 1**).

In contrast to mebendazole, vincristine cannot penetrate the BBB well due to its large molecular size (825 Da) and its tendency to be transported (De Witt et al., 2017). Vincristine is currently used in the treatment of 1p/19q co-deleted anaplastic oligodendroglioma and low-grade glioma when combined with procarbazine and lomustine (CCNU) (De Witt et al., 2017). Although vincristine has been used in brain tumor management, the poor BBB penetrance and its significant side effects remain the biggest concern. Importantly, De Witt et al. demonstrated that at the same dose as mebendazole, vincristine failed to improve survival *in vivo* (De Witt et al., 2017).

The beneficial effect of a combination of two microtubule inhibitors in patients is questionable. Although the combination of vinblastine and mebendazole was shown to improve the sensitivity of resistant glioma cells to TMZ (Kipper et al., 2017), mebendazole and vincristine co-administration exacerbates peripheral neuropathy side effects *in vivo*. Hence, more research needs to be done to determine how to utilize similar combination therapies while minimizing toxicities.

Clomifene

Clomifene is commonly used as a selective estrogen receptor modulator in the treatment of female infertility due to anovulation, such as polycystic ovarian syndrome (PCOS) (Zheng et al., 2017). It is also used off-label for treating hypogonadism in men (Zheng et al., 2017). It acts as an antagonist at estrogen receptors in the hypothalamus and thus prevents normal feedback inhibition, which subsequently increases release of Luteinizing Hormone (LH) and Follicle-Stimulating Hormone (FSH) from the anterior pituitary gland, leading to ovulation.

By utilizing structure-based virtual ligand screening, Zheng et al. identified clomifene as an inhibitor of mutant isocitrate dehydrogenases (IDH) 1, which is essential for tumorigenesis in multiple cancers (Zheng et al., 2017). They demonstrated that mutant IDH1 was selectively inhibited by clomifene, thus reducing the accumulation of downstream D-2-hydroxyglutaric acid (D-2HG) (Zheng et al., 2017) (**Figure 1**). D-2HG drives carcinogenesis by inhibiting histone demethylases and this increases global methylation of histones and DNA (Zheng et al., 2017). The administration of clomifene also increases apoptosis of glioma cancer cells with IDH1 mutations *in vitro* and *in vivo*, without causing any side effects of hepatotoxicity or nephrotoxicity (Zheng et al., 2017). An earlier study by Yaz et al. also showed the cytotoxic effect of clomifene on glioma cells *in vitro* (Yaz et al., 2004). Furthermore, mutant IDH1-mediated H3K9me3 levels were decreased in mouse xenografts after treatment of clomifene.

Biguanides (Metformin and Phenformin)

Metformin is an oral drug belonging to the cationic biguanide class, which is a first-line medication in the treatment of Type II

diabetes mellitus (TIIDM). It is a readily available, inexpensive, and safe drug (Molenaar et al., 2017). Phenformin is a lipophilic analog of metformin, which is also used in TIIDM management. However, phenformin was withdrawn from TIIDM treatment by the FDA and European Medicines Agency (EMA) in the 1970s because of its lactic acidosis side effect (Molenaar et al., 2017). Although the exact mechanism is unknown, metformin is believed to inhibit gluconeogenesis, increase glycolysis, and increase insulin sensitivity by promoting peripheral glucose uptake. Interestingly, metformin was correlated to cancer prevention and thus is of interest in drug repositioning for cancer treatment (Adeberg et al., 2015; Seliger et al., 2016).

Biguanides were shown to demonstrate anti-gliomagenic properties by inhibiting GBM cell proliferation, decreasing migration, inducing apoptosis, decreasing angiogenesis, reducing TMZ resistance, reducing self-renewal, and inhibiting stemness of GSCs (Ferla et al., 2012; Ucbek et al., 2014; Elmaci and Altinoz, 2016; Jiang et al., 2016; Yang et al., 2016).

Biguanides also induce tumor regression and prolong survival in xenograft models. Several mechanisms have been postulated as to why biguanides exhibit anti-tumor characteristics. Biguanides inhibit complex I of the electron transport chain in the mitochondria of cells and cause accumulation of AMP levels (Figure 1). This in turn upregulates LKB1-5'-AMP-activated protein kinase (LKB1-AMPK) and subsequently inhibits the mammalian target of rapamycin complex 1 (mTORC1) (Kast et al., 2011; Aldea et al., 2014). As mTORC1, a key signal for tumorigenesis, is reduced, cancer cell growth also decreases. Intracellular mitochondrial-dependent ATP production is switched to glycolytic ATP production with more lactate production (Sesen et al., 2015). AMPK activation also directly reduces insulin and insulin-like growth factor-1 (IGF-1), which normally stimulate cell growth (Elmaci and Altinoz, 2016). In addition, biguanides also inhibit AMPK and signal transducer and activator of transcription 3 (STAT3) pathways (Ferla et al., 2012).

Interestingly, biguanides modulate microRNAs (miRNAs) that regulate the posttranslational gene expression of cells (Jiang et al., 2016). These miRNAs are critical for energy metabolic pathways, cell cycle, and stemness. For instance, phenformin increases expression of miR-124 and let-7, which are essential for self-renewal of GSC (Jiang et al., 2016) (Figure 1). Biguanides can increase the bioavailability of let-7 when its binding partner H19 is downregulated, and thus enhancing the inhibitory effect of let-7 on the oncogene HMGA2 (Lee and Dutta, 2007; Jiang et al., 2016). Biguanides inhibit glutamate dehydrogenase and reduce glutaminolysis and the production of oncometabolite D-2-HG in IDH1/2 mutated glioma (Molenaar et al., 2017). Finally, Gritti et al. demonstrated that metformin can selectively target chloride intracellular channel-1 (CLIC1) in GBM and this inhibition leads to G1 arrest of GSCs. Importantly, the multiple pathways targeted by biguanides make them especially promising candidates for repurposing for the treatment of heterogeneous tumors such as GBM.

Similar to clomifene, metformin when combined with chloroquine can also reduce IDH1-mutated glioma tumors in clinical trials. *In vivo* studies have demonstrated that metformin

and chloroquine can pass through the BBB appreciably. However, high levels of metformin efflux transporters have been reported in glioma and this raises concerns regarding the intratumoral bioavailability of metformin (Molenaar et al., 2017). Molenaar et al. thus proposed to use phenformin instead because phenformin is lipid-soluble and does not depend on transporters to enter cells.

Repaglinide

Repaglinide is a non-sulfonylurea insulin secretagogue belonging to the family of meglitinide that was invented in 1983. It is an oral medication used in addition to diet and exercise to control postprandial glucose excursions for the treatment of TIIDM. It promotes the early release of insulin from the pancreas beta-islet cells by closing ATP-dependent potassium channels in the membrane of beta cells (Xiao et al., 2017). This results in depolarization and calcium influx to induce insulin secretion.

Repaglinide has been reported to kill hepatic, breast, and cervical carcinoma cells (Xiao et al., 2017). Xiao et al. first identified repaglinide as a potential candidate in GBM and verified that *in vitro* and *in vivo*. Other than its ability to inhibit proliferation and migration of GBM cells *in vitro*, GBM-bearing mice treated with repaglinide also survive longer (Xiao et al., 2017). The authors postulated the effects seen were via inducing apoptosis, repressing autophagy, or immune-activation. This was thought to be achieved via downregulation of the mitochondria-mediated anti-apoptotic protein Bcl-2, as well as engagement of the Beclin-1 and PD-1/PD-L1 immune pathway (Figure 1).

Cyclin-Dependent Kinase Inhibitors (CKIs)

Cyclin-dependent kinases (CDKs) are important checkpoint regulators in the cell cycle. In GBM cells as in most proliferating cells, CKIs arrest cells in S phase and at the G2/M transition. Importantly, CDK4/6 inhibitors have been approved for the treatment of breast cancer and thus there is considerable potential to repurpose this class of drugs (de Groot et al., 2017).

Flavopiridol, a first generation CKI, has cytotoxic effects on GBM cells (Cobanoglu et al., 2016). It also enhances the anti-tumorigenesis effect of TMZ in GBM cells by inhibiting DNA repair activity at the G2M transition. However, first generation CKIs are disfavored because of their low specificity. Roscovitine, milciclib, palbociclib, purvalanol A, and dinaciclib are some of the examples of second-generation CKIs developed later (Table 1). Jane et al. demonstrated that dinaciclib, which selectively inhibits CDK1, CDK2, CDK5, and CDK9, can reduce GBM cell proliferation independent of p53 status (Jane et al., 2016). Palbociclib, a CDK4/6 inhibitor, can also inhibit the cell cycle in GBM by inhibiting Rb1 phosphorylation (Lubanska and Porter, 2017). When combined with TMZ and radiotherapy, the brain penetrant CKIs abemaciclib and pablociclib show a GBM tumor suppressing effect. Although these CKIs show promising results in pre-clinical studies, most of them fail to make it into clinical trials, possibly due to their limited therapeutic window.

Interestingly, recent studies have looked into the non-canonical binding partners of CDKs which are usually not inhibited by CKIs. It is hypothesized that these non-canonical binding partners can continue activating CDKs in the presence of CKIs. Some of the binding partners described are Spy1A1, p35, and p39 protein (Lubanska and Porter, 2017). Lubanska and his team investigated the inhibition of Spy1A1 protein in brain tumor initiating cells as a potential target in GBM (Lubanska and Porter, 2017). Pre-clinical studies using BTICs have shown that Spy1 inhibition reduces cell proliferation and regulates stemness of cells (Lubanska et al., 2014).

EGFR Inhibitors

EGFR is a transmembrane glycoprotein with a molecular weight of 170 kDa. When EGFR is bound to a ligand, it can activate downstream pathways such as PI3K/Akt, mTOR, or Ras/Raf/MAPK, and stimulate GBM progression, angiogenesis, and invasion.

EGFR is overexpressed, amplified, or mutated in GBM (Clarke et al., 2013; Miranda et al., 2017). EGFR variant III (EGFRvIII), which is a truncated yet constitutively active form of EGFR, is present in 20–30% of glioblastoma tumors. This variant is the result of deletion of 267 amino acids in its extracellular domain. EGFRvIII is thought to stimulate proliferation of GBM by PKA-dependent phosphorylation of Dock180 (Miranda et al., 2017). However, multiple attempts to inhibit this pathway in glioblastoma using EGFR tyrosine-kinase inhibitors (TKIs) and naked monoclonal antibodies (mAbs) have not been successful. Some of the TKIs that are used in glioma studies are erlotinib and gefitinib; and the mAbs utilized are nimotuzumab and cetuximab. However, whether this is a pharmacodynamic failure (the drug is not effective against glioblastoma cells) or a pharmacokinetic failure (the drug is unable to achieve a therapeutic level in the tumor due to the BBB) is still unclear. Immunotoxins, a group of antibody-drug conjugates (ADCs) have been generated to overcome drug delivery issues. An antibody targeting EGFR is conjugated to a linker and a cytotoxic payload (this can be drug, bacterial toxin, or radioactive isotope). ADCs recognize cell surface receptors, get internalized into the cytoplasm, transported to lysosomes for degradation, and subsequently release their payload. Studies have shown that ADCs can deliver higher concentrations of drugs to the tumor tissues, as compared to systemic administration of drug alone. ADCs have been shown to be effective in inhibiting glioblastoma growth *in vivo*.

In the past 3 years, ADCs have been used in clinical trials for glioma, namely ABT-414 and AMG-595 (Gan et al., 2017). ABT-414 is an ADC that is comprised of an anti-EGFR antibody conjugated to monomethyl auristatin F (MMAF), an inhibitor of tubulin assembly. Although it only penetrates BBB partially, it is hypothesized that this ADC can overcome resistance of GBM cells. A Phase 1 study showed that ABT-414 is safe and pharmacokinetically acceptable in newly diagnosed and recurrent GBM patients. Although most patients developed ocular toxicity, they are treated with corticosteroids and respond well to this treatment (Gan et al., 2017). Therefore, ADC therapy is an exciting promising avenue for the treatment of GBM and other gliomas.

Statins

HMG-CoA (β -hydroxy- β -methylglutaryl coenzyme A) reductase inhibitors, or statins, are the most widely used lipid-lowering agents in the clinic. Among the commonly used statins are lovastatin, pravastatin, rosuvastatin, and simvastatin. These inhibit the conversion of HMG-CoA to mevalonate, a cholesterol precursor, and reduce mortality of a large number of patients with cardiovascular diseases (Table 1). The reduction of mevalonate also reduces farnesyl pyrophosphate (FPP) or geranylgeranyl pyrophosphate (GGPP), and the subsequent post-translational isoprenylation of GTP-binding protein including Ras, Rac, and Rho. These proteins are important for cell proliferation and are often mutated or amplified in several cancers including glioma.

Gais et al. in 2014 and Bhavsar et al. in 2016 have epidemiologically studied the pleiotropic effect of pre-operative use of statins on the prognosis of GBM patients (Gaist et al., 2014; Bhavsar et al., 2016). Possibly due to the differences in study design, they have generated mixed results (Lu and McDonald, 2017). Nevertheless, several experimental studies have shown the considerable cytotoxic activities of statins in GBM in time- and dose-dependent manners (Yanae et al., 2011). Multiple mechanisms of these statins in inhibiting GBM are: 1. TNF-related apoptosis-inducing ligand (TRAIL)-sensitizing effect; 2. an increase in expression of pro-apoptotic protein Bim; 3. reduction of the MAPK-dependent pathway and GTPase activation; 4. suppression of extracellular regulated kinase 1/2 (ERK1/2) and Ras/PI3K/Akt pathway; and 5. activation of c-Jun N-terminal kinase 1/2 (JNK1/2) (Tapia-Perez et al., 2011; Yanae et al., 2011) (Figure 1). However, a higher dose of statins is usually needed to achieve a therapeutic benefit, which may be accompanied with increased toxicity.

TARGETING CELL DEATH PATHWAYS IN GLIOBLASTOMA

A major goal of repurposing FDA approved compounds for GBM is to identify drugs that are cytotoxic rather than cytostatic in GBM as the ultimate goal of therapy is to eliminate remaining cancer cells after standard treatment. However, the molecular pathways controlling cell death in GBM are not completely understood. Apoptosis is a well-studied programmed cell death (PCD) pathway (Valdes-Rives et al., 2017). This intricate, tightly regulated, cellular process is widely considered to be a fundamental component of numerous processes including turnover in normal cells. Many anti-GBM therapies take advantage of PCD pathways, for instance to induce apoptosis in GBM cells, by the employment of drug treatments, chemotherapeutic agents and radiotherapy strategies. Most of the drugs repurposed for GBM treatment as discussed earlier can induce apoptosis in GBM cells. Escape from apoptosis is also one of the hallmarks of carcinogenesis, including the progression of GBM (Wong, 2011).

One of the major causes for GBM tumor expansion is the inability of the treated cells to undergo apoptosis. Nonetheless many players of the apoptotic cascades are present in GBM cells and can be modulated therapeutically. Furthermore, if GBM

cells can regain susceptibility to apoptosis through effective intervening therapies, a significant improvement in treatment success will be achieved. Further elucidating the oncogenic forces that are driving resistance to apoptosis and how to target them in GBM could provide interesting insights and open doors to future investigations on how to overcome cell death resistance.

Numerous components are part of apoptosis signaling but a family of conserved cysteine-dependent aspartate-directed proteases known as caspases, are the central module initiating and facilitating the apoptosis-signaling cascade (Elmore, 2007). There are two distinct functional groups of caspases that are essential for carrying out apoptosis: initiator caspases (caspase 2, 8, 9, and 10) and executioner caspases (caspase 3, 6, and 7) (Elmore, 2007). Initially, caspases are expressed in the inactive form, but are rapidly cleaved and sequentially activated in the presence of extrinsic death receptor activation and other intrinsic apoptotic stimuli (Elmore, 2007). Canonically, initiator caspases are subjected to auto-proteolytic cleavage whereas executioner caspases are cleaved by initiator caspases (Howley and Fearnhead, 2008). The cleavage and activation of initiator caspases results in the stimulation of the cleavage and activation of several executioner caspases. Executioner caspases have been implicated in the degradation of over 600 cellular components that are necessary to induce the morphological changes that underlie apoptosis (Sollberger et al., 2014). This highly ordered proteolysis allows for an amplifying cascade for the degradation of cellular components and a minimization of immune response during apoptosis.

Several apoptotic pathway components are dysregulated in GBM. Prominent examples of these include inactivating mutations or altered expression of specific proteins or their downstream signals. These include p53, inhibitor of apoptosis proteins (IAPs), and the B-cell lymphoma (BCL-2) family of proteins (Fels et al., 2000; Lytle et al., 2005; Nagpal et al., 2006; Ziegler et al., 2008; Berger et al., 2010; Liwak et al., 2013; Yang et al., 2014; Daniele et al., 2015; Wang et al., 2016).

The tumor suppressing gene, p53, plays a critical role in regulating the response mechanisms of DNA damage through apoptosis and cell cycle signaling. Likewise, p53 alteration has an effect in a vast number of cancers, including GBM (Nagpal et al., 2006). p53 is regulated by murine double minute (MDM) 2 and 4, which inhibit p53 stability or activity. Following DNA damage, p53 is activated and induces the transcription of response genes such as p21^{Cip1}, a negative regulator of the cell cycle, or BCL-2-like protein 4 (BAX), a mediator of apoptosis (Essmann and Schulze-Osthoﬀ, 2012). In addition to its regulation through transcriptional activity, p53 also can promote apoptosis through transcription-independent mechanisms and direct interactions with members of the BCL-2 and the caspase family of proteins (Essmann and Schulze-Osthoﬀ, 2012). In a comprehensive genomic study by The Cancer Genome Atlas (TCGA) Research Network, human GBM genes and associated pathways were characterized. This study revealed that p53 signaling was altered in 87% of all GBM patients by mutations in at least one component of the pathway (Biasoli et al., 2014). Some examples of drugs

that target p53 reactivation are Nutlins, benzodiazepinediones, spiro-oxindoles, RITA (Reactivation of p53 and induction of tumor cell apoptosis), and Serdemetan (Yu et al., 2014). Given the importance of the p53 pathway in the regulation of apoptosis in human GBM and many other cancers, several efforts have been made to develop both pharmacological and biological therapeutics targeting this pathway. However, due to delivery, selectivity, and toxicity problems, many of these therapies fail in development and clinical trials. Hence, repurposing FDA approved drugs that target p53 directly or indirectly for use in GBM treatment may have therapeutic potential.

IAPs are cellular checkpoints that can inhibit pro-apoptotic caspase signaling. Additionally, IAPs have been found to modulate cell invasion and metastasis in GBM and several cancers. All IAPs contain a Baculovirus Inhibitor of apoptosis protein Repeat (BIR) domain and are commonly termed BIRCs. The IAP family consists of six primary members: NLR family Apoptosis Inhibitory Protein (NAIP or BIRC1), Cellular IAP (CIAP 1 and 2 or BIRC2 and 3), X-linked IAP (XIAP or BIRC4), Survivin (BIRC5), and BIR repeat-containing ubiquitin-conjugating enzyme (BRUCE or BIRC6) (Hunter et al., 2007; Owens et al., 2013). BIRC4 is the only IAP that directly associates with caspases. It has been shown to bind with high affinity to executioner caspase 3 and 7, in addition to initiator caspase 9, in turn inhibiting apoptotic function. All other IAPs do not bind to caspases directly. A leading model suggests that apoptosis inhibition is achieved by forming complexes with other partners such as BIRC4 (Silke and Meier, 2013). Several compounds have been shown to cause degradation of IAPs including the Smac mimetic, SM-164, small molecule inhibitors of BIRC4, Arylsulfonamides and Embelin, and a small molecule inhibitor of BIRC5, YM155 (Owens et al., 2013). A comprehensive list of IAP inhibitors can be found in Owens et al. (2013). Inhibition of IAPs has been implicated in both inducing apoptosis directly but also sensitizing cells to radiation and chemotherapy treatment (Rathore et al., 2017). Repurposing drugs that target this family of proteins may be a promising strategy in treating GBM but may also have synergistic potential when used in combination with other treatments.

The BCL-2 protein family has a key role in tightly regulating the mitochondrial pathway of apoptosis. Members in this family functionally promote or inhibit apoptosis. All proteins in this family share at least one of four BCL-2 homology (BH) domains (Wang et al., 1996). The proteins that have anti-apoptotic functions contain both BH1 and BH2 domains (BCL-2 and BCL-X) while the proteins that exhibit pro-apoptotic functions widely lack sequence homology to the family, but contain the BH3 domain only (BAX, BAK, BID, BAD) (Wang et al., 1996). Anti-apoptotic signaling is achieved either by sequestering caspases or by preventing the release of mitochondrial apoptosis driving factors that activate caspases, such as cytochrome c and apoptosis-inducing factor (AIF), into the cytoplasm. By contrast, pro-apoptotic BCL-2 members, trigger the release of caspases from death antagonists and act on the mitochondrial permeability transition pore to induce

the release of pro-apoptotic mitochondrial factors into the cytoplasm. In patients with GBM, expression of anti-apoptotic BCL-2 proteins is increased, which may contribute to apoptotic resistance and relapse that is commonly observed (Fels et al., 2000; Martin et al., 2001). A few examples of drugs that inhibit BCL-2 family of proteins that have been used in cancer treatment are Venetoclax, Servier-1, and Disarib. Regulating the homeostasis of anti and pro-apoptotic BCL-2 family proteins may be a worthwhile strategy in combatting GBM. Repurposing drugs that target activation of BH3 domain only BCL-2 proteins could be used to induce apoptosis in GBM. Importantly, repositioning drugs inhibiting the function of anti-apoptotic BCL-2 proteins could restore sensitivity of some apoptotic-inducing treatments of GBM.

Necroptosis is a caspase-independent, pro-inflammatory form of PCD that can also be pharmacologically targeted in GBM (Jiang et al., 2011). Morphologically, necroptosis shares similar features to necrosis such as loss of plasma membrane integrity. However, cellular membrane permeabilization induced by necroptosis signaling is tightly regulated. Necroptosis induction begins with activation of the tumor necrosis factor (TNF) family of cytokines or TRAIL (Vanden Berghe et al., 2010). These stimuli are known to also regulate cell survival and apoptosis induction. The activated receptor then interacts with Receptor-interacting serine/threonine-protein kinase (RIPK) 1 and recruits IAPs such as BIRC2 and 3 (Christofferson and Yuan, 2010). This results in the formation of a membrane associated complex that leads to cell survival through NF- κ B and mitogen-activated protein kinases (MAPKs) pathways. When IAPs are inhibited, RIPK1 is rapidly deubiquitinated by cylindromatosis lysine 63 deubiquitinase (CYLD) and disassociated from the membrane bound complex (Christofferson and Yuan, 2010). The free RIPK1 binds to the adaptor protein Fas-associated protein with death domain (FADD) and caspase 8, which in turn activates caspase 8 and induces apoptosis. In addition, active caspase 8 dynamically inhibits necroptosis by cleaving its core regulators, RIPK1 and RIPK3. In the event that caspase activity is inhibited, necroptosis is executed. RIPK1 binds with RIPK3 to form an insoluble amyloid complex known as the necrosome. The formation of the necrosome promotes autophosphorylation of RIPK3, which then recruits and phosphorylates the pseudo-kinase, mixed lineage like kinase (MLKL). Phosphorylated MLKL oligomerizes and is inserted in to the membrane to form a pore, leading to necroptosis by the loss of plasma and intracellular membrane integrity (Christofferson and Yuan, 2010; Vanden Berghe et al., 2010; Geng et al., 2017). Necroptosis initiation is often viewed as a backup mode to ensure cell death execution, but emerging evidence suggest that necroptosis may act as a primary cell death mode under certain pathological conditions. Recent reports suggest that under conditions where apoptosis is inhibited, apoptosis inducing drugs, such as IAP and BCL-2 inhibitors, can induce necroptosis in cancer cells (Su et al., 2016). Targeting this novel cell death pathway may have therapeutic potential in apoptosis-resistant GBM cells (Jiang et al., 2011). Repurposing drugs that activate necroptosis may not only be used as an effective primary treatment but could also be

used in combination with other therapies after drug-resistance develops.

Autophagy is a catabolic process in which cells induce lysosomal degradation of cellular components. It is a highly-conserved pathway that has a pivotal role in cell stress response such as nutrient starvation, DNA damage, and organelle damage (Glick et al., 2010). Autophagy is regulated primarily by a large number of proteins, from a family identified in yeast known as autophagy related genes (ATGs) (Glick et al., 2010). mTOR signaling is also a central regulator of autophagy (Dunlop and Tee, 2014). Activation of mTOR by AKT and MAPK signaling suppresses autophagy signaling, while mTOR inhibition by the negative regulators AMPK and p53 drives the process forward (Jung et al., 2010). Mammalian kinase orthologs of ATG1, UNC-51-like kinase (ULK) 1, 2, and 3 initiate autophagy downstream of mTOR. ULK 1 and 2 form a large complex with mATG13, FIP200, and a PI3K Class III complex, which contains the proteins Beclin-1, hVps34, p150, and ATG14 (Itakura and Mizushima, 2010). This complex eventually promotes invagination of the membrane, which leads to the formation of the autophagosome and subsequent execution of autophagy by fusion of the autophagosome with the lysosome by the Atg5-Atg12 and the microtubule-associated protein 1 light chain 3 (LC3) pathway (Jiang and Mizushima, 2014).

Autophagy has garnered much attention in the cancer field and is widely being evaluated for its potential in GBM therapy. Lefranc et al. demonstrated that glioma therapies are more likely to be successful by inducing autophagy rather than apoptosis, as two potent cytotoxic drugs, TMZ and rapamycin, induce autophagy (Lefranc and Kiss, 2006). Furthermore, several reports indicated that Atg5 and LC3 loss of function promotes glioblastoma progression (Lefranc and Kiss, 2006). Autophagy certainly plays a role in inhibiting tumor growth progression and metastasis. Yet the role of autophagy causing cell death directly in contrast to occurring in parallel to PCD needs to be further elucidated. It has been shown to function as a tumor suppressor as well as to play a role in tumor cell survival (Yonekawa and Thorburn, 2013). It is important to note that cells undergoing autophagy are found in high numbers under certain conditions such as nutrient starvation induced PCD, but autophagy in this context is not considered to be a PCD pathway because inhibition of autophagy attenuates cell death rather than inhibiting it (Tsujiimoto and Shimizu, 2005; Gozuacik and Kimchi, 2007). In parallel, it has been shown that hyper-activation of autophagy can indeed lead to PCD that is morphologically distinct from other PCD pathways, termed autophagic cell death (Tsujiimoto and Shimizu, 2005). Autophagy and apoptotic pathways substantially interact; the two processes both negatively and positively regulate each other (Ryter et al., 2014). For example, many apoptosis inducing signals, such as TNF, TRAIL, and FADD, also induce autophagy (Das et al., 2012).

Therefore, identifying FDA approved compounds that modulate these components in GBM may be especially attractive since this will increase the chances of eliminating GBM cells within tumor cells.

COMPUTATIONAL AND DATA-DRIVEN APPROACHES TO IDENTIFY DRUGS WITH EFFICACY IN GLIOBLASTOMA

Various computational and data-driven methods are applicable for the systematic identification and prioritization of candidate drugs for repurposing in glioblastoma. Such *in-silico* methods can be based on known GBM targets or pathways or entirely data-driven without requiring knowledge on the mechanism of action. In the former case, the goal is to identify drugs that target specific pathways or proteins relevant in GBM or, inversely, identify such targets among approved drugs. Computational target prediction can broadly be classified into ligand- and structure-based methods. Ligand-based *in silico* target screening aims to predict biological targets based on the chemical structure of the drug (Jenkins et al., 2007). This approach leverages large bioactivity databases including public resources such as ChEMBL (Bento et al., 2014) and PubChem (Wang et al., 2017a) or licensed databases such as the KKB (Sharma et al., 2016) in combination with machine learning (Nidhi et al., 2006; Schurer and Muskal, 2013; Bento et al., 2014) or statistical scoring (Keiser et al., 2009). As in many other areas deep learning has recently received a lot of attention (Gawehn et al., 2016). Structure-based approaches make use of the ever-increasing corpus of experimentally determined protein structures or computational protein structure models using docking (Lauro et al., 2011) or binding site similarity predictions at the genome-wide scale (Hwang et al., 2017). Cheminformatics ligand- and structure-based repositioning approaches are well established and have also been extensively reviewed for drug repositioning, for example recently by March-Vila et al. (2017). Importantly, several well annotated databases of approved drugs and compounds in clinical trials are publicly available including ChEMBL (Bento et al., 2014), DrugBank (Wishart et al., 2006), and DrugCentral (Ursu et al., 2017).

In contrast to mechanism- or target-based drug repurposing, system-wide perturbation response signatures can be used to identify repurposing opportunities without bias for specific targets or pathways. One of the most systematic and comprehensive of such data-driven approaches is the Connectivity Map (CMap) project, which is based on gene expression signatures (Lamb et al., 2006). Initially covering 164 drugs and a few cell lines, it has recently been scaled by more than 1,000-fold using the L1000 reduced representation high throughput gene expression profiling platform (Subramanian et al., 2017). These data have been generated as part of the Library of Integrated Network-based Cellular Signatures (LINCS) project along with several other cellular perturbation response signatures and computational tools (Keenan et al., 2017). LINCS has been developing a larger-scale integrated approach to data curation, with baseline gene expression signatures for 99 cell lines and transcriptional profile responses to over 30,000 perturbations and many other datasets. To ensure validity and consistency, as well as to allow comparison across cell lines and perturbations for different datasets, the data in the LINCS database were collected and processed in a highly standardized and coordinated manner enabling integrated analysis of drug action (Vempati et al., 2014; Vidovic et al., 2014). LINCS datasets are available in

different data-type specific repositories and via the LINCS Data Portal (Koleti et al., 2017).

Using LINCS data in a recent study, the ability to predict novel drug repositioning candidates based on several perturbational features was assessed in four cancer types, including glioblastoma. Reference expression profiles for GBM tissue and controls were downloaded from TCGA and a list of known drugs in glioblastoma was compiled from public databases. For these compounds, different signature types were generated based on chemical structure, targets, and gene-expression data. Classifiers were constructed for each signature type as well as combinations and evaluated by cross validation, comparison against data NCI-60 data, and cell viability screening. The gene expression-based signatures gave the best predictions for anti-cancer hits (Lee H. et al., 2016). This study highlights the utility of data-driven approaches to identify potential drugs based on transcriptional responses to drug treatments.

To address the considerable variability in efficacy of targeted cancer drugs for individual patients, Artemov et al. used gene expression signatures of individual tumor samples and predicted a drug score based on signaling pathway activation analysis (OncoFinder algorithm). They tested the approach for five drugs in seven cancer types and reported significant correlation of responders to drug treatment and the percent of tumors showing high drug scores (Artemov et al., 2015).

Beyond the use of individual approaches for drug repositioning, such as gene expression, target predictions, or pathway analyses, integrative “multi-scale” methods in computational pharmacology that integrate multiple resources and data types can enable the discovery of novel associations of drugs and diseases; such data types can include drug target interaction data, gene expression data, phenotypic drug screening data, drug side effects, and electronic health records (Hodos et al., 2016).

Recently, researchers at the Broad Institute have established the Drug Repurposing Hub, which is a database of 4,707 compounds, including 1,988 launched drugs and 1,348 compounds that have reached clinical trial Phase 1–3 (Corsello et al., 2017). It is a highly curated resource, integrating various information including detailed target annotations, mode of action, disease indications, and commercial availability for a very comprehensive list of approved drugs and clinical compounds. The compounds were carefully curated and annotated including chemical structures, purity, mechanisms of action based on several databases and literature curation, their approved indications and clinical trial status, as well as supplier IDs for commercial sources. A well designed graphical user interface allows querying this information (<https://clue.io/repurposing>).

The interactions among fundamental molecular entities and processes involving genes, transcripts, proteins, metabolites are tightly regulated to sustain a healthy biological system. In a diseased state, this normally interconnected network is disrupted by stressors and the aim of the therapy is to restore the system to its normal state. As discussed in Lee et al., gene expression data can be an excellent predictor of drug repositioning efficacy (Lee H. et al., 2016). As sequencing techniques improve and the availability of genomic data increases, combined transcriptomes and multi-scale integrative

methods in computational pharmacology improve predictions of drug-disease associations and enable computational drugs repurposing. One integrated effort to relate genes to diseases is the Illuminating the Druggable Genome (IDG) project (<https://commonfund.nih.gov/idg/>). A specific priority for IDG is to identify understudied disease relevant targets. All IDG data and a query interface are available via the Pharos Data Portal (Nguyen et al., 2017).

Although these databases are important resources for identifying single repurposed compounds in GBM, it is likely essential to identify combinations of drugs for the treatment of GBM. Advances in single cell sequencing allow the characterization of sub-populations in individual GBM tumors based on gene expression to identify small molecules that have the greatest probability of affecting pathways common in all malignant cells within a tumor (Patel et al., 2014). In addition to intratumoral heterogeneity in GBM, there is also intertumoral heterogeneity. Combinations of drugs with different mechanisms of action are one approach to increase the success rate in drug repurposing (Sun et al., 2016). This is particularly relevant in heterogeneous cancers where clinical duration is often limited due to emerging resistance. Computational approaches as described above can be used to prioritize combination therapies; either rationally based on known mechanism of action or data-driven, for example using gene expression signatures. With the knowledge of targets, it is also possible to rationally design single-agent poly-pharmacology compounds (Allen et al., 2015).

To help identify patient-specific therapies we have previously described a bioinformatics pipeline to identify genes and pathways that are dysregulated in a particular GBM tumor (Stathias et al., 2014). This was accomplished by first performing RNA-sequencing of each GBM tumor and then using the significant sequencing information in TCGA to increase statistical power of the analyses. We found that by using both a hypergeometric test and Pearson correlation, we can identify networks dysregulated in each GBM tumor. Importantly, we are currently integrating this approach with the LINCS perturbation response gene expression signatures to identify therapeutic combinations in GBM and other gliomas. Although these computational approaches have not been validated in a clinical setting, it is our ultimate hope that our *in vitro* and *in vivo* studies will lead to patient specific drug combinations for the treatment of GBM.

CONCLUSION

GBM is a deadly primary parenchymal central nervous system neoplasm disease with very dismal prognosis. By bypassing

time-consuming chemical optimization and toxicology testing in drug development steps, repositioning of existing FDA-approved drugs can help to better manage GBM. As compounds need to be brain penetrant to have maximum efficacy in GBM, it is ideal to select compounds that are known to pass the blood brain barrier and are not substrates of efflux transporters. Many antipsychotic compounds are known to cross the blood brain barrier and can be directly utilized for treating GBM if they are shown to be effective in reducing GBM growth *in vivo*. In addition, non-antipsychotic compounds can also be utilized after demonstrating efficacy in GBM animal models and robust brain penetrance. Thousands of compounds have been approved for human use or are in advanced clinical testing. In addition to the rational selection of antipsychotics and non-antipsychotic drugs with likely efficacy in GBM, advanced computational tools are now available to prioritize prospective drugs and drug combinations for GBM. We propose that uncovering pathways controlled by each drug is essential for identifying therapeutic combinations for treating GBM. Identifying such combinations is essential for treating GBM tumors that exhibit both intertumoral and intratumoral heterogeneity. Future studies are needed to identify drug sensitive cell types within tumors without affecting normal brain cells.

AUTHOR CONTRIBUTIONS

SKT and NGA conceived the concept and idea of the present review. SKT and NGA designed the strategy and selected the topics to be discussed. SKT did literature searches, read the references, and wrote the first outline of the review. AJ and AKM reviewed and contributed a section into final manuscript. CBN, SCS, and NGA reviewed the manuscript and helped with the final writing. The content of figures was conceived and prepared by SKT and NGA.

ACKNOWLEDGMENTS

We acknowledge funding from the NIH via grants R56102590 to NGA, U54CA189205, and U24TR002278 (Illuminating the Druggable Genome Knowledge Management Center, IDG-KMC, and Resource Dissemination and Outreach Center, IDG-RDOC) and U54HL127624 (BD2K LINCS Data Coordination and Integration Center, DCIC) to SCS. We also acknowledge support from the Sylvester Comprehensive Cancer Center to NGA. The IDG, LINCS, and Big Data to Knowledge (BD2K) programs are funded by the trans-NIH Common Fund. IDG-KMC, IDG-RDOC, and BD2K-LINCS DCIC are administered by the NCI, NCATS, and NHLBI, respectively.

REFERENCES

- Adamopoulou, E., and Naumann, U. (2013). HDAC inhibitors and their potential applications to glioblastoma therapy. *Oncoimmunology* 2:e25219. doi: 10.4161/onci.25219
- Adeberg, S., Bernhardt, D., Ben Harrabi, S., Bostel, T., Mohr, A., Koelsche, C., et al. (2015). Metformin influences progression in diabetic glioblastoma patients. *Strahlenther. Onkol.* 191, 928–935. doi: 10.1007/s00066-015-0884-5
- Aldea, M. D., Petrushev, B., Soritau, O., Tomuleasa, C. I., Berindan-Neagoe, I., Filip, A. G., et al. (2014). Metformin plus sorafenib highly impacts temozolomide resistant glioblastoma stem-like cells. *J. BUON* 19, 502–511.
- Allen, B. K., Mehta, S., Ember, S. W., Schonbrunn, E., Ayad, N., and Schurer, S. C. (2015). Large-scale computational screening identifies first in class multitarget inhibitor of EGFR kinase and BRD4. *Sci. Rep.* 5:6924. doi: 10.1038/srep16924
- Artemov, A., Aliper, A., Korzinkin, M., Lezhnina, K., Jellen, L., Zhukov, N., et al. (2015). A method for predicting target drug efficiency in cancer based

- on the analysis of signaling pathway activation. *Oncotarget* 6, 29347–29356. doi: 10.18632/oncotarget.5119
- Bai, R. Y., Staedtke, V., Aprhys, C. M., Gallia, G. L., and Riggins, G. J. (2011). Antiparasitic mebendazole shows survival benefit in 2 preclinical models of glioblastoma multiforme. *Neurooncology* 13, 974–982. doi: 10.1093/neuonc/nor077
- Bai, R. Y., Staedtke, V., Wanjiku, T., Rudek, M. A., Joshi, A., Gallia, G. L., et al. (2015). Brain penetration and efficacy of different mebendazole polymorphs in a mouse brain tumor model. *Clin. Cancer Res.* 21, 3462–3470. doi: 10.1158/1078-0432.CCR-14-2681
- Barak, Y., Achiron, A., Mandel, M., Mirecki, I., and Aizenberg, D. (2005). Reduced cancer incidence among patients with schizophrenia. *Cancer* 104, 2817–2821. doi: 10.1002/cncr.21574
- Bartek, J., and Hodny, Z. (2014). Dopamine signaling: target in glioblastoma. *Oncotarget* 5, 1116–1117. doi: 10.18632/oncotarget.1835
- Bento, A. P., Gaulton, A., Hersey, A., Bellis, L. J., Chambers, J., Davies, M., et al. (2014). The ChEMBL bioactivity database: an update. *Nucleic Acids Res.* 42, D1083–D1090. doi: 10.1093/nar/gkt1031
- Berger, B., Capper, D., Lemke, D., Pfennig, P. N., Platten, M., Weller, M., et al. (2010). Defective p53 antiangiogenic signaling in glioblastoma. *Neurooncology* 12, 894–907. doi: 10.1093/neuonc/noq051
- Bhavsar, S., Hagan, K., Arunkumar, R., Potylchansky, Y., Grasu, R., Dang, A., et al. (2016). Preoperative statin use is not associated with improvement in survival after glioblastoma surgery. *J. Clin. Neurosci.* 31, 176–180. doi: 10.1016/j.jocn.2016.03.010
- Biasoli, D., Sobrinho, M. F., da Fonseca, A. C., de Matos, D. G., Romao, L., de Moraes Maciel, R., et al. (2014). Glioblastoma cells inhibit astrocytic p53-expression favoring cancer malignancy. *Oncogenesis* 3:e123. doi: 10.1038/oncsis.2014.36
- Bielecka-Wajdman, A. M., Lesiak, M., Ludyga, T., Sieron, A., and Obuchowicz, E. (2017). Reversing glioma malignancy: a new look at the role of antidepressant drugs as adjuvant therapy for glioblastoma multiforme. *Cancer Chemother. Pharmacol.* 79, 1249–1256. doi: 10.1007/s00280-017-3329-2
- Bobustic, G. C., Baker, C. H., Limaye, A., Jenkins, W. D., Pearl, G., Avgeropoulos, N. G., et al. (2010). Levetiracetam enhances p53-mediated MGMT inhibition and sensitizes glioblastoma cells to temozolomide. *Neurooncology* 12, 917–927. doi: 10.1093/neuonc/noq044
- Caudill, J. S., Brown, P. D., Cerhan, J. H., and Rummans, T. A. (2011). Selective serotonin reuptake inhibitors, glioblastoma multiforme, and impact on toxicities and overall survival: the mayo clinic experience. *Am. J. Clin. Oncol.* 34, 385–387. doi: 10.1097/COC.0b013e3181e8461a
- Chen, D., Cui, Q. C., Yang, H., and Dou, Q. P. (2006). Disulfiram, a clinically used anti-alcoholism drug and copper-binding agent, induces apoptotic cell death in breast cancer cultures and xenografts via inhibition of the proteasome activity. *Cancer Res.* 66, 10425–10433. doi: 10.1158/0008-5472.CAN-06-2126
- Chen, J., Ouyang, Y., Cao, L., Zhu, W., Zhou, Y., Zhou, Y., et al. (2013). Diazepam inhibits proliferation of human glioblastoma cells through triggering a G0/G1 cell cycle arrest. *J. Neurosurg. Anesthesiol.* 25, 285–291. doi: 10.1097/ANA.0b013e31828bac6a
- Cheng, H. W., Liang, Y. H., Kuo, Y. L., Chuu, C. P., Lin, C. Y., Lee, M. H., et al. (2015). Identification of thioridazine, an antipsychotic drug, as an anti-glioblastoma and anticancer stem cell agent using public gene expression data. *Cell Death Dis.* 6:e1753. doi: 10.1038/cddis.2015.77
- Chinnaiyan, P., Cerna, D., Burgan, W. E., Beam, K., Williams, E. S., Camphausen, K., et al. (2008). Postirradiation sensitization of the histone deacetylase inhibitor valproic acid. *Clin. Cancer Res.* 14, 5410–5415. doi: 10.1158/1078-0432.CCR-08-0643
- Chitadze, G., Lettau, M., Luecke, S., Wang, T., Janssen, O., Furst, D., et al. (2016). NKG2D- and T-cell receptor-dependent lysis of malignant glioma cell lines by human gamma delta T cells: modulation by temozolomide and A disintegrin and metalloproteases 10 and 17 inhibitors. *Oncoimmunology* 5:e1093276. doi: 10.1080/2162402X.2015.1093276
- Choi, S. A., Choi, J. W., Wang, K. C., Phi, J. H., Lee, J. Y., Park, K. D., et al. (2015). Disulfiram modulates stemness and metabolism of brain tumor initiating cells in atypical teratoid/rhabdoid tumors. *Neurooncology* 17, 810–821. doi: 10.1093/neuonc/nou305
- Christofferson, D. E., and Yuan, J. (2010). Necroptosis as an alternative form of programmed cell death. *Curr. Opin. Cell Biol.* 22, 263–268. doi: 10.1016/j.ceb.2009.12.003
- Clarke, J., Penas, C., Pastori, C., Komotar, R. J., Bregy, A., Shah, A. H., et al. (2013). Epigenetic pathways and glioblastoma treatment. *Epigenetics* 8, 785–795. doi: 10.4161/epi.25440
- Cobanoglu, G., Turacli, I. D., Ozkan, A. C., and Ekmekci, A. (2016). Flavopiridol's antiproliferative effects in glioblastoma multiforme. *J. Cancer Res. Ther.* 12, 811–817. doi: 10.4103/0973-1482.172132
- Corsello, S. M., Bittker, J. A., Liu, Z., Gould, J., McCarren, P., Hirschman, J. E., et al. (2017). The Drug repurposing hub: a next-generation drug library and information resource. *Nat. Med.* 23, 405–408. doi: 10.1038/nm.4306
- Daniele, S., Costa, B., Zappelli, E., Da Pozzo, E., Sestito, S., Nesi, G., et al. (2015). Combined inhibition of AKT/mTOR and MDM2 enhances glioblastoma multiforme cell apoptosis and differentiation of cancer stem cells. *Sci. Rep.* 5:9956. doi: 10.1038/srep09956
- Das, G., Shrivage, B. V., and Baehrecke, E. H. (2012). Regulation and function of autophagy during cell survival and cell death. *Cold Spring Harb. Perspect. Biol.* 4:a008813. doi: 10.1101/cshperspect.a008813
- de Groot, A. F., Kuijpers, C. J., and Kroep, J. R. (2017). CDK4/6 inhibition in early and metastatic breast cancer: a review. *Cancer Treat. Rev.* 60, 130–138. doi: 10.1016/j.ctrv.2017.09.003
- De Witt, M., Gamble, A., Hanson, D., Markowitz, D., Powell, C., Al Dimassi, S., et al. (2017). Repurposing mebendazole as a replacement for vincristine for the treatment of brain tumors. *Mol. Med.* 23, 50–56. doi: 10.2119/molmed.2017.00011
- Dunlop, E. A., and Tee, A. R. (2014). mTOR and autophagy: a dynamic relationship governed by nutrients and energy. *Semin. Cell Dev. Biol.* 36, 121–129. doi: 10.1016/j.semcdb.2014.08.006
- Elmaci, I., and Altinoz, M. A. (2016). A metabolic inhibitory cocktail for grave cancers: metformin, pioglitazone and lithium combination in treatment of pancreatic cancer and glioblastoma multiforme. *Biochem. Genet.* 54, 573–618. doi: 10.1007/s10528-016-9754-9
- Elmore, S. (2007). Apoptosis: a review of programmed cell death. *Toxicol. Pathol.* 35, 495–516. doi: 10.1080/01926230701320337
- Essmann, F., and Schulze-Osthoff, K. (2012). Translational approaches targeting the p53 pathway for anti-cancer therapy. *Br. J. Pharmacol.* 165, 328–344. doi: 10.1111/j.1476-5381.2011.01570.x
- Felix, F. H., Trompieri, N. M., de Araujo, O. L., da Trindade, K. M., and Fontenele, J. B. (2011). Potential role for valproate in the treatment of high-risk brain tumors of childhood—results from a retrospective observational cohort study. *Pediatr. Hematol. Oncol.* 28, 556–570. doi: 10.3109/08880018.2011.563774
- Fels, C., Schafer, C., Huppe, B., Bahn, H., Heidecke, V., Kramm, C. M., et al. (2000). Bcl-2 expression in higher-grade human glioma: a clinical and experimental study. *J. Neurooncol.* 48, 207–216. doi: 10.1023/A:1006484801654
- Ferla, R., Haspinger, E., and Surmacz, E. (2012). Metformin inhibits leptin-induced growth and migration of glioblastoma cells. *Oncol. Lett.* 4, 1077–1081. doi: 10.3892/ol.2012.843
- Ferno, J., Skrede, S., Vik-Mo, A. O., Havik, B., and Steen, V. M. (2006). Drug-induced activation of SREBP-controlled lipogenic gene expression in CNS-related cell lines: marked differences between various antipsychotic drugs. *BMC Neurosci.* 7:69. doi: 10.1186/1471-2202-7-69
- Gaist, D., Hallas, J., Friis, S., Hansen, S., and Sorensen, H. T. (2014). Statin use and survival following glioblastoma multiforme. *Cancer Epidemiol.* 38, 722–727. doi: 10.1016/j.canep.2014.09.010
- Gan, H. K., van den Bent, M., Lassman, A. B., Reardon, D. A., and Scott, A. M. (2017). Antibody-drug conjugates in glioblastoma therapy: the right drugs to the right cells. *Nat. Rev. Clin. Oncol.* 14, 695–707. doi: 10.1038/nrclinonc.2017.95
- Gawehn, E., Hiss, J. A., and Schneider, G. (2016). Deep learning in drug discovery. *Mol. Inform.* 35, 3–14. doi: 10.1002/minf.201501008
- Geng, J., Ito, Y., Shi, L., Amin, P., Chu, J., Ouchida, A. T., et al. (2017). Regulation of RIPK1 activation by TAK1-mediated phosphorylation dictates apoptosis and necroptosis. *Nat. Commun.* 8:359. doi: 10.1038/s41467-017-00406-w
- Glick, D., Barth, S., and Macleod, K. F. (2010). Autophagy: cellular and molecular mechanisms. *J. Pathol.* 221, 3–12. doi: 10.1002/path.2697
- Gozuacik, D., and Kimchi, A. (2007). Autophagy and cell death. *Curr. Top. Dev. Biol.* 78, 217–245. doi: 10.1016/S0070-2153(06)78006-1

- Happold, C., Gorlia, T., Chinot, O., Gilbert, M. R., Nabors, L. B., Wick, W., et al. (2016). Does valproic acid or levetiracetam improve survival in glioblastoma? A pooled analysis of prospective clinical trials in newly diagnosed glioblastoma. *J. Clin. Oncol.* 34, 731–739. doi: 10.1200/JCO.2015.63.6563
- Hayashi, K., Michiue, H., Yamada, H., Takata, K., Nakayama, H., Wei, F. Y., et al. (2016). Fluvoxamine, an anti-depressant, inhibits human glioblastoma invasion by disrupting actin polymerization. *Sci. Rep.* 6:23372. doi: 10.1038/srep23372
- Higgins, S. C., and Pilkington, G. J. (2010). The *in vitro* effects of tricyclic drugs and dexamethasone on cellular respiration of malignant glioma. *Anticancer Res.* 30, 391–397.
- Hodos, R. A., Kidd, B. A., Shameer, K., Readhead, B. P., and Dudley, J. T. (2016). *In silico* methods for drug repurposing and pharmacology. *Wiley Interdiscip. Rev. Syst. Biol. Med.* 8, 186–210. doi: 10.1002/wsbm.1337
- Howley, B., and Fearhead, H. O. (2008). Caspases as therapeutic targets. *J. Cell. Mol. Med.* 12, 1502–1516. doi: 10.1111/j.1582-4934.2008.00292.x
- Hunter, A. M., LaCasse, E. C., and Korneluk, R. G. (2007). The inhibitors of apoptosis (IAPs) as cancer targets. *Apoptosis* 12, 1543–1568. doi: 10.1007/s10495-007-0087-3
- Hwang, H., Dey, F., Petrey, D., and Honig, B. (2017). Structure-based prediction of ligand-protein interactions on a genome-wide scale. *Proc. Natl. Acad. Sci. U.S.A.* 114, 13685–13690. doi: 10.1073/pnas.1705381114
- Itakura, E., and Mizushima, N. (2010). Characterization of autophagosome formation site by a hierarchical analysis of mammalian Atg proteins. *Autophagy* 6, 764–776. doi: 10.4161/auto.6.6.12709
- Jane, E. P., Premkumar, D. R., Cavaleri, J. M., Sutera, P. A., Rajasekar, T., and Pollack, I. F. (2016). Dinaciclib, a cyclin-dependent kinase inhibitor promotes proteasomal degradation of Mcl-1 and enhances ABT-737-mediated cell death in malignant human glioma cell lines. *J. Pharmacol. Exp. Ther.* 356, 354–365. doi: 10.1124/jpet.115.230052
- Jenkins, J. L., Bender, A., and Davies, J. W. (2007). *In silico* target fishing: predicting biological targets from chemical structure. *Drug Discov. Today* 3, 413–421. doi: 10.1016/j.ddtec.2006.12.008
- Jeon, S. H., Kim, S. H., Kim, Y., Kim, Y. S., Lim, Y., Lee, Y. H., et al. (2011). The tricyclic antidepressant imipramine induces autophagic cell death in U-87MG glioma cells. *Biochem. Biophys. Res. Commun.* 413, 311–317. doi: 10.1016/j.bbrc.2011.08.093
- Jiang, P., and Mizushima, N. (2014). Autophagy and human diseases. *Cell Res.* 24, 69–79. doi: 10.1038/cr.2013.161
- Jiang, W., Finniss, S., Cazacu, S., Xiang, C., Brodie, Z., Mikkelsen, T., et al. (2016). Repurposing phenformin for the targeting of glioma stem cells and the treatment of glioblastoma. *Oncotarget* 7, 56456–56470. doi: 10.18632/oncotarget.10919
- Jiang, Y. G., Peng, Y., and Koussougbo, K. S. (2011). Necroptosis: a novel therapeutic target for glioblastoma. *Med. Hypotheses* 76, 350–352. doi: 10.1016/j.mehy.2010.10.037
- Jung, C. H., Ro, S. H., Cao, J., Otto, N. M., and Kim, D. H. (2010). mTOR regulation of autophagy. *FEBS Lett.* 584, 1287–1295. doi: 10.1016/j.febslet.2010.01.017
- Kang, S., Hong, J., Lee, J. M., Moon, H. E., Jeon, B., Choi, J., et al. (2017). Trifluoperazine, a well-known antipsychotic, inhibits glioblastoma invasion by binding to calmodulin and disinhibiting calcium release channel IP3R. *Mol. Cancer Ther.* 16, 217–227. doi: 10.1158/1535-7163.MCT-16-0169-T
- Karbownik, M. S., Szemraj, J., Wieteska, L., Antczak, A., Gorski, P., Kowalczyk, E., et al. (2016). Antipsychotic drugs differentially affect mRNA expression of genes encoding the neuregulin 1-downstream ErbB4-PI3K pathway. *Pharmacology* 98, 4–12. doi: 10.1159/000444534
- Karpel-Massler, G., Kast, R. E., Westhoff, M. A., Dwucet, A., Welscher, N., Nonnenmacher, L., et al. (2015). Olanzapine inhibits proliferation, migration and anchorage-independent growth in human glioblastoma cell lines and enhances temozolomide's antiproliferative effect. *J. Neurooncol.* 122, 21–33. doi: 10.1007/s11060-014-1688-7
- Kast, R. E., Karpel-Massler, G., and Halatsch, M. E. (2011). Can the therapeutic effects of temozolomide be potentiated by stimulating AMP-activated protein kinase with olanzapine and metformin? *Br. J. Pharmacol.* 164, 1393–1396. doi: 10.1111/j.1476-5381.2011.01320.x
- Keenan, A. B., Jenkins, S. L., Jagodnik, K. M., Koplev, S., He, E., Torre, D., et al. (2017). The library of integrated network-based cellular signatures NIH program: system-level cataloging of human cells response to perturbations. *Cell Syst.* 6, 13–24. doi: 10.1016/j.cels.2017.11.001
- Keiser, M. J., Setola, V., Irwin, J. J., Laggner, C., Abbas, A. I., Hufeisen, S. J., et al. (2009). Predicting new molecular targets for known drugs. *Nature* 462, 175–181. doi: 10.1038/nature08506
- Killick-Cole, C. L., Singleton, W. G. B., Bienemann, A. S., Asby, D. J., Wyatt, M. J., Boulter, L. J., et al. (2017). Repurposing the anti-epileptic drug sodium valproate as an adjuvant treatment for diffuse intrinsic pontine glioma. *PLoS ONE* 12:e0176855. doi: 10.1371/journal.pone.0176855
- Kim, Y. H., Kim, T., Joo, J. D., Han, J. H., Kim, Y. J., Kim, I. A., et al. (2015). Survival benefit of levetiracetam in patients treated with concomitant chemoradiotherapy and adjuvant chemotherapy with temozolomide for glioblastoma multiforme. *Cancer* 121, 2926–2932. doi: 10.1002/cncr.29439
- Kipper, F. C., Silva, A. O., Marc, A. L., Confortin, G., Junqueira, A. V., Neto, E. P., et al. (2017). Vinblastine and antihelminthic mebendazole potentiate temozolomide in resistant gliomas. *Invest. New Drugs.* doi: 10.1007/s10637-017-0503-7. [Epub ahead of print].
- Knudsen-Baas, K. M., Engeland, A., Gilhus, N. E., Storstein, A. M., and Owe, J. F. (2016). Does the choice of antiepileptic drug affect survival in glioblastoma patients? *J. Neurooncol.* 129, 461–469. doi: 10.1007/s11060-016-2191-0
- Koleti, A., Terryn, R., Stathias, V., Chung, C., Cooper, D. J., Turner, J. P., et al. (2017). Data portal for the Library of Integrated Network-based Cellular Signatures (LINCS) program: integrated access to diverse large-scale cellular perturbation response data. *Nucleic Acids Res.* 46, D558–D566. doi: 10.1093/nar/gkx1063
- Lamb, J., Crawford, E. D., Peck, D., Modell, J. W., Blat, I. C., Wrobel, M. J., et al. (2006). The connectivity map: using gene-expression signatures to connect small molecules, genes, and disease. *Science* 313, 1929–1935. doi: 10.1126/science.1132939
- Lauro, G., Romano, A., Riccio, R., and Bifulco, G. (2011). Inverse virtual screening of antitumor targets: pilot study on a small database of natural bioactive compounds. *J. Nat. Prod.* 74, 1401–1407. doi: 10.1021/np100935s
- Lawrence, J. E., Steele, C. J., Rovin, R. A., Belton, R. J. Jr., and Winn, R. J. (2016). Dexamethasone alone and in combination with desipramine, phenytoin, valproic acid or levetiracetam interferes with 5-ALA-mediated PpIX production and cellular retention in glioblastoma cells. *J. Neurooncol.* 127, 15–21. doi: 10.1007/s11060-015-2012-x
- Lee, C. Y., Lai, H. Y., Chiu, A., Chan, S. H., Hsiao, L. P., and Lee, S. T. (2016). The effects of antiepileptic drugs on the growth of glioblastoma cell lines. *J. Neurooncol.* 127, 445–453. doi: 10.1007/s11060-016-2056-6
- Lee, H., Kang, S., and Kim, W. (2016). Drug repositioning for cancer therapy based on large-scale drug-induced transcriptional signatures. *PLoS ONE* 11:e0150460. doi: 10.1371/journal.pone.0150460
- Lee, J. K., Nam, D. H., and Lee, J. (2016). Repurposing antipsychotics as glioblastoma therapeutics: potentials and challenges. *Oncol. Lett.* 11, 1281–1286. doi: 10.3892/ol.2016.4074
- Lee, Y. S., and Dutta, A. (2007). The tumor suppressor microRNA let-7 represses the HMGA2 oncogene. *Genes Dev.* 21, 1025–1030. doi: 10.1101/gad.1540407
- Lefranc, F., and Kiss, R. (2006). Autophagy, the Trojan horse to combat glioblastomas. *Neurosurg. Focus* 20:E7. doi: 10.3171/foc.2006.20.4.4
- Levkovitz, Y., Gil-Ad, I., Zeldich, E., Dayag, M., and Weizman, A. (2005). Differential induction of apoptosis by antidepressants in glioma and neuroblastoma cell lines: evidence for p-c-Jun, cytochrome c, and caspase-3 involvement. *J. Mol. Neurosci.* 27, 29–42. doi: 10.1385/JMN:27:1:029
- Liu, K. H., Yang, S. T., Lin, Y. K., Lin, J. W., Lee, Y. H., Wang, J. Y., et al. (2015). Fluoxetine, an antidepressant, suppresses glioblastoma by evoking AMPAR-mediated calcium-dependent apoptosis. *Oncotarget* 6, 5088–5101. doi: 10.18632/oncotarget.3243
- Liwak, U., Jordan, L. E., Von-Holt, S. D., Singh, P., Hanson, J. E., Lorimer, I. A., et al. (2013). Loss of PDCD4 contributes to enhanced chemoresistance in Glioblastoma multiforme through de-repression of Bcl-xL translation. *Oncotarget* 4, 1365–1372. doi: 10.18632/oncotarget.1154
- Lu, V. M., and McDonald, K. L. (2017). The current evidence of statin use affecting glioblastoma prognosis. *J. Clin. Neurosci.* 42, 196–197. doi: 10.1016/j.jocn.2017.04.036
- Lubanska, D., and Porter, L. (2017). Revisiting CDK inhibitors for treatment of glioblastoma multiforme. *Drugs R D* 17, 255–263. doi: 10.1007/s40268-017-0180-1
- Lubanska, D., Market-Velker, B. A., deCarvalho, A. C., Mikkelsen, T., Fidalgo da Silva, E., and Porter, L. A. (2014). The cyclin-like protein Spyl1 regulates growth

- and division characteristics of the CD133+ population in human glioma. *Cancer Cell* 25, 64–76. doi: 10.1016/j.ccr.2013.12.006
- Lun, X., Wells, J. C., Grinshtein, N., King, J. C., Hao, X., Dang, N. H., et al. (2016). Disulfiram when combined with copper enhances the therapeutic effects of temozolomide for the treatment of glioblastoma. *Clin. Cancer Res.* 22, 3860–3875. doi: 10.1158/1078-0432.CCR-15-1798
- Lytle, R. A., Jiang, Z., Zheng, X., Higashikubo, R., and Rich, K. M. (2005). Retinamide-induced apoptosis in glioblastomas is associated with down-regulation of Bcl-xL and Bcl-2 proteins. *J. Neurooncol.* 74, 225–232. doi: 10.1007/s11060-005-7305-z
- March-Vila, E., Pinzi, L., Sturm, N., Tinivella, A., Engkvist, O., Chen, H., et al. (2017). On the integration of *in silico* drug design methods for drug repurposing. *Front. Pharmacol.* 8:298. doi: 10.3389/fphar.2017.00298
- Martin, S., Toquet, C., Oliver, L., Cartron, P. F., Perrin, P., Meflah, K., et al. (2001). Expression of bcl-2, bax and bcl-xl in human gliomas: a re-appraisal. *J. Neurooncol.* 52, 129–139. doi: 10.1023/A:1010689121904
- Miranda, A., Blanco-Prieto, M., Sousa, J., Pais, A., and Vitorino, C. (2017). Breaching barriers in glioblastoma. part I: molecular pathways and novel treatment approaches. *Int. J. Pharm.* 531, 372–388. doi: 10.1016/j.ijpharm.2017.07.056
- Molenaar, R. J., Coelen, R. J., Khurshed, M., Roos, E., Caan, M. W., van Linde, M. E., et al. (2017). Study protocol of a phase IB/II clinical trial of metformin and chloroquine in patients with IDH1-mutated or IDH2-mutated solid tumours. *BMJ Open* 7:e014961. doi: 10.1136/bmjopen-2016-014961
- Monteiro, A. R., Hill, R., Pilkington, G. J., and Madureira, P. A. (2017). The role of hypoxia in glioblastoma invasion. *Cells* 6:45. doi: 10.3390/cells6040045
- Munson, J. M., Fried, L., Rowson, S. A., Bonner, M. Y., Karumbaiah, L., Diaz, B., et al. (2012). Anti-invasive adjuvant therapy with imipramine blue enhances chemotherapeutic efficacy against glioma. *Sci. Transl. Med.* 4:127ra136. doi: 10.1126/scitranslmed.3003016
- Nagpal, J., Jamoona, A., Gulati, N. D., Mohan, A., Braun, A., Murali, R., et al. (2006). Revisiting the role of p53 in primary and secondary glioblastomas. *Anticancer Res.* 26, 4633–4639.
- Nguyen, D. T., Mathias, S., Bologa, C., Brunak, S., Fernandez, N., Gaulton, A., et al. (2017). Pharos: collating protein information to shed light on the druggable genome. *Nucleic Acids Res.* 45, D995–D1002. doi: 10.1093/nar/gkw1072
- Nidhi, Glick, M., Davies, J. W., and Jenkins, J. L. (2006). Prediction of biological targets for compounds using multiple-category Bayesian models trained on chemogenomics databases. *J. Chem. Inf. Model.* 46, 1124–1133. doi: 10.1021/ci060003g
- Oliva, C. R., Zhang, W., Langford, C., Suto, M. J., and Griguer, C. E. (2017). Repositioning chlorpromazine for treating chemoresistant glioma through the inhibition of cytochrome c oxidase bearing the COX4-1 regulatory subunit. *Oncotarget* 8, 37568–37583. doi: 10.18632/oncotarget.17247
- Owens, T. W., Gilmore, A. P., Streuli, C. H., and Foster, F. M. (2013). Inhibitor of apoptosis proteins: promising targets for cancer therapy. *J. Carcinog. Mutagen.* 14(Suppl. 14), S14–S004. doi: 10.4172/2157-2518.S14-004
- Paranjpe, A., Zhang, R., Ali-Osman, F., Bobustuc, G. C., and Srivenugopal, K. S. (2014). Disulfiram is a direct and potent inhibitor of human O-methylguanine-DNA methyltransferase (MGMT) in brain tumor cells and mouse brain and markedly increases the alkylating DNA damage. *Carcinogenesis* 35, 692–702. doi: 10.1093/carcin/bgt366
- Patel, A. P., Tirosh, I., Trombetta, J. J., Shalek, A. K., Gillespie, S. M., Wakimoto, H., et al. (2014). Single-cell RNA-seq highlights intratumoral heterogeneity in primary glioblastoma. *Science* 344, 1396–1401. doi: 10.1126/science.1254257
- Peddi, P., Ajit, N. E., Burton, G. V., and El-Osta, H. (2016). Regression of a glioblastoma multiforme: spontaneous versus a potential antineoplastic effect of dexamethasone and levetiracetam. *BMJ Case Rep.* 2016:bcr2016217393. doi: 10.1136/bcr-2016-217393
- Persson, A. I., Petritsch, C., Swartling, F. J., Itsara, M., Sim, F. J., Auvergne, R., et al. (2010). Non-stem cell origin for oligodendroglioma. *Cancer Cell* 18, 669–682. doi: 10.1016/j.ccr.2010.10.033
- Pinheiro, R., Braga, C., Santos, G., Bronze, M. R., Perry, M. J., Moreira, R., et al. (2017). Targeting gliomas: can a new alkylating hybrid compound make a difference? *ACS Chem. Neurosci.* 8, 50–59. doi: 10.1021/acschemneuro.6b00169
- Pinheiro, T., Otrocka, M., Seashore-Ludlow, B., Rrakli, V., Holmberg, J., Forsberg-Nilsson, K., et al. (2017). A chemical screen identifies trifluoperazine as an inhibitor of glioblastoma growth. *Biochem. Biophys. Res. Commun.* 494, 477–483. doi: 10.1016/j.bbrc.2017.10.106
- Pottgard, A., Garcia Rodriguez, L. A., Rasmussen, L., Damkier, P., Friis, S., and Gaist, D. (2016). Use of tricyclic antidepressants and risk of glioma: a nationwide case-control study. *Br. J. Cancer* 114, 1265–1268. doi: 10.1038/bjc.2016.109
- Rathore, R., McCallum, J. E., Varghese, E., Florea, A. M., and Busselberg, D. (2017). Overcoming chemotherapy drug resistance by targeting inhibitors of apoptosis proteins (IAPs). *Apoptosis* 22, 898–919. doi: 10.1007/s10495-017-1375-1
- Rooney, A., and Grant, R. (2012). SSRIs may (or may not) be a safe treatment for depression in GBM. *Am. J. Clin. Oncol.* 35:100. doi: 10.1097/COC.0b013e31820dbdef
- Rundle-Thiele, D., Head, R., Cosgrove, L., and Martin, J. H. (2016). Repurposing some older drugs that cross the blood-brain barrier and have potential anticancer activity to provide new treatment options for glioblastoma. *Br. J. Clin. Pharmacol.* 81, 199–209. doi: 10.1111/bcp.12785
- Ryter, S. W., Mizumura, K., and Choi, A. M. (2014). The impact of autophagy on cell death modalities. *Int. J. Cell Biol.* 2014:502676. doi: 10.1155/2014/502676
- Sarissky, M., Lavicka, J., Kocanova, S., Sulla, I., Mirossay, A., Miskovsky, P., et al. (2005). Diazepam enhances hypericin-induced photocytotoxicity and apoptosis in human glioblastoma cells. *Neoplasma* 52, 352–359.
- Schurer, S. C., and Muskal, S. M. (2013). Kinome-wide activity modeling from diverse public high-quality data sets. *J. Chem. Inf. Model.* 53, 27–38. doi: 10.1021/ci300403k
- Seliger, C., Ricci, C., Meier, C. R., Bodmer, M., Jick, S. S., Bogdahn, U., et al. (2016). Diabetes, use of antidiabetic drugs, and the risk of glioma. *Neurooncology* 18, 340–349. doi: 10.1093/neuonc/nov100
- Sesen, J., Dahan, P., Scotland, S. J., Saland, E., Dang, V. T., Lemarie, A., et al. (2015). Metformin inhibits growth of human glioblastoma cells and enhances therapeutic response. *PLoS ONE* 10:e0123721. doi: 10.1371/journal.pone.0123721
- Sharma, R., Schurer, S. C., and Muskal, S. M. (2016). High quality, small molecule-activity datasets for kinase research. *F1000Res* 5:1366. doi: 10.12688/f1000research.8950.3
- Silke, J., and Meier, P. (2013). Inhibitor of apoptosis (IAP) proteins-modulators of cell death and inflammation. *Cold Spring Harb. Perspect. Biol.* 5:a008730. doi: 10.1101/cshperspect.a008730
- Skrott, Z., Mistrik, M., Andersen, K. K., Friis, S., Majera, D., Gursky, J., et al. (2017). Alcohol-abuse drug disulfiram targets cancer via p97 segregase adaptor NPL4. *Nature* 552, 194–199. doi: 10.1038/nature25016
- Sollberger, G., Strittmatter, G. E., Garstkiewicz, M., Sand, J., and Beer, H. D. (2014). Caspase-1: the inflammasome and beyond. *Innate Immun.* 20, 115–125. doi: 10.1177/1753425913484374
- Stathias, V., Pastori, C., Griffin, T. Z., Komotar, R., Clarke, J., Zhang, M., et al. (2014). Identifying glioblastoma gene networks based on hypergeometric test analysis. *PLoS ONE* 9:e115842. doi: 10.1371/journal.pone.0115842
- Su, Z., Yang, Z., Xie, L., DeWitt, J. P., and Chen, Y. (2016). Cancer therapy in the necroptosis era. *Cell Death Differ.* 23, 748–756. doi: 10.1038/cdd.2016.8
- Subramanian, A., Narayan, R., Corsello, S. M., Peck, D. D., Natoli, T. E., Lu, X., et al. (2017). A next generation connectivity map: L1000 platform and the first 1,000,000 profiles. *bioRxiv*. doi: 10.1016/j.cell.2017.10.049
- Sun, W., Sanderson, P. E., and Zheng, W. (2016). Drug combination therapy increases successful drug repositioning. *Drug Discov. Today* 21, 1189–1195. doi: 10.1016/j.drudis.2016.05.015
- Tapia-Perez, J. H., Kirches, E., Mawrin, C., Firsching, R., and Schneider, T. (2011). Cytotoxic effect of different statins and thiazolidinediones on malignant glioma cells. *Cancer Chemother. Pharmacol.* 67, 1193–1201. doi: 10.1007/s00280-010-1535-2
- Tran, E., Rouillon, F., Loze, J. Y., Casadebaig, F., Philippe, A., Vitry, F., et al. (2009). Cancer mortality in patients with schizophrenia: an 11-year prospective cohort study. *Cancer* 115, 3555–3562. doi: 10.1002/cncr.24383
- Triscott, J., Lee, C., Hu, K., Fotovati, A., Berns, R., Pambid, M., et al. (2012). Disulfiram, a drug widely used to control alcoholism, suppresses the self-renewal of glioblastoma and over-rides resistance to temozolomide. *Oncotarget* 3, 1112–1123. doi: 10.18632/oncotarget.604
- Triscott, J., Rose Pambid, M., and Dunn, S. E. (2015). Concise review: bullseye: targeting cancer stem cells to improve the treatment of gliomas by repurposing disulfiram. *Stem Cells* 33, 1042–1046. doi: 10.1002/stem.1956

- Tseng, J. H., Chen, C. Y., Chen, P. C., Hsiao, S. H., Fan, C. C., Liang, Y. C., et al. (2017). Valproic acid inhibits glioblastoma multiforme cell growth via paraoxonase 2 expression. *Oncotarget* 8, 14666–14679. doi: 10.18632/oncotarget.14716
- Tsujimoto, Y., and Shimizu, S. (2005). Another way to die: autophagic programmed cell death. *Cell Death Differ* 12(Suppl. 2), 1528–1534. doi: 10.1038/sj.cdd.4401777
- Tzadok, S., Beery, E., Israeli, M., Uziel, O., Lahav, M., Fenig, E., et al. (2010). *In vitro* novel combinations of psychotropics and anti-cancer modalities in U87 human glioblastoma cells. *Int. J. Oncol.* 37, 1043–1051. doi: 10.3892/ijo.00000756
- Ucbek, A., Ozunal, Z. G., Uzun, O., and Gepdiremen, A. (2014). Effect of metformin on the human T98G glioblastoma multiforme cell line. *Exp. Ther. Med.* 7, 1285–1290. doi: 10.3892/etm.2014.1597
- Urquhart, B. L., and Kim, R. B. (2009). Blood-brain barrier transporters and response to CNS-active drugs. *Eur. J. Clin. Pharmacol.* 65, 1063–1070. doi: 10.1007/s00228-009-0714-8
- Ursu, O., Holmes, J., Knockel, J., Bologna, C. G., Yang, J. J., Mathias, S. L., et al. (2017). DrugCentral: online drug compendium. *Nucleic Acids Res.* 45, D932–D939. doi: 10.1093/nar/gkw993
- Valdes-Rives, S. A., Casique-Aguirre, D., German-Castelan, L., Velasco-Velazquez, M. A., and Gonzalez-Arenas, A. (2017). Apoptotic signaling pathways in glioblastoma and therapeutic implications. *Biomed Res. Int.* 2017:7403747. doi: 10.1155/2017/7403747
- Van Niftrik, K. A., Van den Berg, J., Slotman, B. J., Lafleur, M. V., Sminia, P., and Stalpers, L. J. (2012). Valproic acid sensitizes human glioma cells for temozolomide and gamma-radiation. *J. Neurooncol.* 107, 61–67. doi: 10.1007/s11060-011-0725-z
- Vanden Berghe, T., Vanlangenakker, N., Parthoens, E., Deckers, W., Devos, M., Festjens, N., et al. (2010). Necroptosis, necrosis and secondary necrosis converge on similar cellular disintegration features. *Cell Death Differ.* 17, 922–930. doi: 10.1038/cdd.2009.184
- Vempati, U. D., Chung, C., Mader, C., Koleti, A., Datar, N., Vidovic, D., et al. (2014). Metadata standard and data exchange specifications to describe, model, and integrate complex and diverse high-throughput screening data from the Library of Integrated Network-based Cellular Signatures (LINCS). *J. Biomol. Screen.* 19, 803–816. doi: 10.1177/1087057114522514
- Verhaak, R. G., Hoadley, K. A., Purdom, E., Wang, V., Qi, Y., Wilkerson, M. D., et al. (2010). Integrated genomic analysis identifies clinically relevant subtypes of glioblastoma characterized by abnormalities in PDGFRA, IDH1, EGFR, and NF1. *Cancer Cell* 17, 98–110. doi: 10.1016/j.ccr.2009.12.020
- Vidovic, D., Koleti, A., and Schurer, S. C. (2014). Large-scale integration of small molecule-induced genome-wide transcriptional responses, Kinome-wide binding affinities and cell-growth inhibition profiles reveal global trends characterizing systems-level drug action. *Front. Genet.* 5:342. doi: 10.3389/fgene.2014.00342
- Walker, A. J., Grainge, M., Bates, T. E., and Card, T. R. (2012). Survival of glioma and colorectal cancer patients using tricyclic antidepressants post-diagnosis. *Cancer Causes Control* 23, 1959–1964. doi: 10.1007/s10552-012-0073-0
- Wang, D., Berglund, A., Kenchappa, R. S., Forsyth, P. A., Mule, J. J., and Etame, A. B. (2016). BIRC3 is a novel driver of therapeutic resistance in Glioblastoma. *Sci. Rep.* 6:21710. doi: 10.1038/srep21710
- Wang, K., Yin, X. M., Chao, D. T., Milliman, C. L., and Korsmeyer, S. J. (1996). BID: a novel BH3 domain-only death agonist. *Genes Dev.* 10, 2859–2869. doi: 10.1101/gad.10.22.2859
- Wang, Y., Bryant, S. H., Cheng, T., Wang, J., Gindulyte, A., Shoemaker, B. A., et al. (2017a). PubChem BioAssay: 2017 update. *Nucleic Acids Res.* 45, D955–D963. doi: 10.1093/nar/gkw118
- Wang, Y., Huang, N., Li, H., Liu, S., Chen, X., Yu, S., et al. (2017b). Promoting oligodendroglial-oriented differentiation of glioma stem cell: a repurposing of quetiapine for the treatment of malignant glioma. *Oncotarget* 8, 37511–37524. doi: 10.18632/oncotarget.16400
- Wishart, D. S., Knox, C., Guo, A. C., Shrivastava, S., Hassanali, M., Stothard, P., et al. (2006). DrugBank: a comprehensive resource for *in silico* drug discovery and exploration. *Nucleic Acids Res.* 34, D668–D672. doi: 10.1093/nar/gkj067
- Wong, R. S. (2011). Apoptosis in cancer: from pathogenesis to treatment. *J. Exp. Clin. Cancer Res.* 30:87. doi: 10.1186/1756-9966-30-87
- Xiao, Z. X., Chen, R. Q., Hu, D. X., Xie, X. Q., Yu, S. B., and Chen, X. Q. (2017). Identification of repaglinide as a therapeutic drug for glioblastoma multiforme. *Biochem. Biophys. Res. Commun.* 488, 33–39. doi: 10.1016/j.bbrc.2017.04.157
- Yanae, M., Tsubaki, M., Satou, T., Itoh, T., Imano, M., Yamazoe, Y., et al. (2011). Statin-induced apoptosis via the suppression of ERK1/2 and Akt activation by inhibition of the geranylgeranyl-pyrophosphate biosynthesis in glioblastoma. *J. Exp. Clin. Cancer Res.* 30:74. doi: 10.1186/1756-9966-30-74
- Yang, S. H., Li, S., Lu, G., Xue, H., Kim, D. H., Zhu, J. J., et al. (2016). Metformin treatment reduces temozolomide resistance of glioblastoma cells. *Oncotarget* 7, 78787–78803. doi: 10.18632/oncotarget.12859
- Yang, W., Cooke, M., Duckett, C. S., Yang, X., and Dorsey, J. F. (2014). Distinctive effects of the cellular inhibitor of apoptosis protein c-IAP2 through stabilization by XIAP in glioblastoma multiforme cells. *Cell Cycle* 13, 992–1005. doi: 10.4161/cc.27880
- Yaz, G., Kabadere, S., Oztocpu, P., Durmaz, R., and Uyar, R. (2004). Comparison of the antiproliferative properties of antiestrogenic drugs (nafoxidine and clomiphene) on glioma cells *in vitro*. *Am. J. Clin. Oncol.* 27, 384–388. doi: 10.1097/01.COC.0000071945.15623.C6
- Yonekawa, T., and Thorburn, A. (2013). Autophagy and cell death. *Essays Biochem.* 55, 105–117. doi: 10.1042/bse0550105
- Yu, X., Narayanan, S., Vazquez, A., and Carpizo, D. R. (2014). Small molecule compounds targeting the p53 pathway: are we finally making progress? *Apoptosis* 19, 1055–1068. doi: 10.1007/s10495-014-0990-3
- Zhang, C., Liu, S., Yuan, X., Hu, Z., Li, H., Wu, M., et al. (2016). Valproic acid promotes human glioma U87 cells apoptosis and inhibits glycogen synthase kinase-3beta through ERK/Akt signaling. *Cell. Physiol. Biochem.* 39, 2173–2185. doi: 10.1159/000447912
- Zheng, M., Sun, W., Gao, S., Luan, S., Li, D., Chen, R., et al. (2017). Structure based discovery of clomifene as a potent inhibitor of cancer-associated mutant IDH1. *Oncotarget* 8, 44255–44265. doi: 10.18632/oncotarget.17464
- Ziegler, D. S., Wright, R. D., Kesari, S., Lemieux, M. E., Tran, M. A., Jain, M., et al. (2008). Resistance of human glioblastoma multiforme cells to growth factor inhibitors is overcome by blockade of inhibitor of apoptosis proteins. *J. Clin. Invest.* 118, 3109–3122. doi: 10.1172/JCI31410

Conflict of Interest Statement: CBN has been funded by National Institutes of Health (NIH), Stanley Medical Research Institute. For last three years, he has consulted for Xhale, Takeda, Taisho Pharmaceutical Inc., Prismic Pharmaceuticals, Bracket (Clintara), Total Pain Solutions (TPS), Gerson Lehrman Group (GLG) Healthcare & Biomedical Council, Fortress Biotech, Sunovion Pharmaceuticals Inc., Sumitomo Dainippon Pharma, Janssen Research & Development LLC, Magstim, Inc., Navitor Pharmaceuticals, Inc., TC MSO, Inc., Intra-Cellular Therapies, Inc. He is also a stockholder in Xhale, Celgene, Seattle Genetics, Abbvie, OPKO Health, Inc., Network Life Sciences Inc., Antares, BI Gen Holdings, Inc. He serves as member of the scientific advisory boards for American Foundation for Suicide Prevention (AFSP), Brain and Behavior Research Foundation (BBRF) [formerly named National Alliance for Research on Schizophrenia and Depression (NARSAD)], Xhale, Anxiety Disorders Association of America (ADAA), Skyland Trail, Bracket (Clintara), RiverMend Health LLC, Laureate Institute for Brain Research, Inc. He is a member of Board of Directors for AFSP, Gratitude America, ADAA. His income sources or equity of \$10,000 or more are from American Psychiatric Publishing, Xhale, Bracket (Clintara), CME Outfitters, Takeda. He holds the patents for: Method and devices for transdermal delivery of lithium (US 6,375,990B1); Method of assessing antidepressant drug therapy via transport inhibition of monoamine neurotransmitters by *ex vivo* assay (US 7,148,027B2). SKT, AJ, AKM, and SCS declare that the research was conducted in the absence of any commercial or financial relationships that could be construed as a potential conflict of interest. NGA is a shareholder of Epigenetix, Inc.

Copyright © 2018 Tan, Jermakowicz, Mookhtiar, Nemeroff, Schürer and Ayad. This is an open-access article distributed under the terms of the Creative Commons Attribution License (CC BY). The use, distribution or reproduction in other forums is permitted, provided the original author(s) and the copyright owner are credited and that the original publication in this journal is cited, in accordance with accepted academic practice. No use, distribution or reproduction is permitted which does not comply with these terms.



Drug Repurposing of the Anthelmintic Niclosamide to Treat Multidrug-Resistant Leukemia

Sami Hamdoun, Philipp Jung and Thomas Efferth*

Department of Pharmaceutical Biology, Institute of Pharmacy and Biochemistry, Johannes Gutenberg University, Mainz, Germany

OPEN ACCESS

Edited by:

Yuhei Nishimura,
Mie University, Japan

Reviewed by:

Antonio Macchiarulo,
University of Perugia, Italy
Toshiyuki Matsunaga,
Gifu Pharmaceutical University, Japan

*Correspondence:

Thomas Efferth
efferth@uni-mainz.de

Specialty section:

This article was submitted to
Experimental Pharmacology and Drug
Discovery,
a section of the journal
Frontiers in Pharmacology

Received: 05 December 2016

Accepted: 22 February 2017

Published: 10 March 2017

Citation:

Hamdoun S, Jung P and Efferth T
(2017) Drug Repurposing of the
Anthelmintic Niclosamide to Treat
Multidrug-Resistant Leukemia.
Front. Pharmacol. 8:110.
doi: 10.3389/fphar.2017.00110

Multidrug resistance, a major problem that leads to failure of anticancer chemotherapy, requires the development of new drugs. Repurposing of established drugs is a promising approach for overcoming this problem. An example of such drugs is niclosamide, a known anthelmintic that is now known to be cytotoxic and cytostatic against cancer cells. In this study, niclosamide showed varying activity against different cancer cell lines. It revealed better activity against hematological cancer cell lines CCRF-CEM, CEM/ADR5000, and RPMI-8226 compared to the solid tumor cell lines MDA-MB-231, A549, and HT-29. The multidrug resistant CEM/ADR5000 cells were similar sensitive as their sensitive counterpart CCRF-CEM (resistance ration: 1.24). Furthermore, niclosamide caused elevations in reactive oxygen species and glutathione (GSH) levels in leukemia cells. GSH synthetase (GS) was predicted as a target of niclosamide. Molecular docking showed that niclosamide probably binds to the ATP-binding site of GS with a binding energy of -9.40 kcal/mol. Using microscale thermophoresis, the binding affinity between niclosamide and recombinant human GS was measured (binding constant: $5.64 \mu\text{M}$). COMPARE analyses of the NCI microarray database for 60 cell lines showed that several genes, including those involved in lipid metabolism, correlated with cellular responsiveness to niclosamide. Hierarchical cluster analysis showed five major branches with significant differences between sensitive and resistant cell lines ($p = 8.66 \times 10^5$). Niclosamide significantly decreased nuclear factor of activated T-cells (NFAT) activity as predicted by promoter binding motif analysis. In conclusion, niclosamide was more active against hematological malignancies compared to solid tumors. The drug was particularly active against the multidrug-resistant CEM/ADR5000 leukemia cells. Inhibition of GSH synthesis and NFAT signaling were identified as relevant mechanisms for the anticancer activity of niclosamide. Gene expression profiling predicted the sensitivity or resistance of cancer cells to niclosamide.

Keywords: chemotherapy, pharmacogenomics, drug resistance, transcription factors, oxidative stress

Abbreviations: ABC, ATP-binding cassette; GS, glutathione synthetase; GSH, glutathione; MDR, multidrug resistance; NFAT, nuclear factor of activated T-cells; Pgp, P-glycoprotein; ROS, reactive oxygen species.

INTRODUCTION

Niclosamide, an anthelmintic drug that has been used for about 50 years, is known to be safe and well tolerated. Niclosamide has been identified as a potential anticancer agent that exerts cytotoxic and cytostatic activity against a wide range of cancer types, including leukemia, breast cancer, prostate cancer, hepatocellular carcinoma, and glioblastoma. Additionally it has shown anti-invasive and anti-migratory effects. Several signaling pathways are inhibited by niclosamide in cancer cells including the Wnt/ β -catenin, mechanistic target of rapamycin complex 1 (mTORC1), signal transducer and activator of transcription 3 (STAT3), nuclear factor kappa-light-chain-enhancer of activated B cells (NF- κ B), and Notch pathways (Li et al., 2014).

Multidrug resistance (MDR) is a major problem in cancer patients that leads to failure of chemotherapy. It affects most cancers and is characterized by cross-resistance to a wide range of commonly used chemotherapeutic drugs (Bartsevich and Juliano, 2000). Most cancers consist of a mixture of heterogeneous malignant cells. Some of them are drug-sensitive and others are drug-resistant. As a result, chemotherapeutic agents mostly kill sensitive cells, but leave out a great proportion of resistant cell populations. Therefore, recurrent tumors are frequently resistant with fatal consequences for the patients (Housman et al., 2014). Of the various mechanisms that contribute to MDR in cancer, the increased efflux of drugs by the ATP-binding cassette (ABC) transporters is the most encountered. The most important of these transporters is P-glycoprotein (Pgp; Bellamy, 1996).

Elevated levels of reactive oxygen species (ROS) occur in almost all types of cancer. They are involved in the promotion of tumor development and progression (Storz, 2005). Cancer cells also express increased levels of antioxidants to detoxify ROS. The process of ROS detoxification is facilitated either through antioxidant enzymes, which scavenge different types of ROS, or by non-enzymatic molecules. Antioxidant enzymes include catalase, superoxide dismutase, and peroxiredoxins. Non-enzymatic antioxidants include glutathione (GSH), flavonoids, vitamins A, C, and E (Liou and Storz, 2010). Treatment of cancer cells with vitamin E and vitamin C (ROS scavengers) increased the expression of Pgp. This suggests that Pgp-mediated MDR can be circumvented under conditions of elevated ROS levels. One of the compounds that elevate ROS levels in cancer cells is niclosamide. ROS generation plays an important role in the anticancer activity of niclosamide in acute myeloid leukemia and lung cancer cells (Wartenberg et al., 2005; Jin et al., 2010; Lee et al., 2014).

The ultimate goal of drug development is to identify molecules with the desired effect in the human body and to establish its quality, safety, and efficacy for treating patients (Kraljevic et al., 2004). Drug development, starting with the initial discovery of a promising target to the final marketed medication, is an expensive, lengthy, and incremental process (Hoelder et al., 2012). An alternative approach is drug repositioning or repurposing, in which new indications are found for existing drugs. The advantages of this approach is that the pharmacokinetics, pharmacodynamics, and toxicity profiles of the investigated drugs are already known. If successful, this leads

to a great reduction in time and money expenditures for the evaluation of drugs during preclinical and clinical development (Ashburn and Thor, 2004; Tada et al., 2006).

In order to evaluate the usefulness of niclosamide for MDR, we investigated its activity on the sensitive CCRF-CEM and the MDR (Pgp overexpressing) CEM/ADR5000 leukemia cells. As niclosamide is known to elevate ROS levels in cancer cells, we also tested its effect on ROS generation in both cell lines. Furthermore, we have attempted to identify the molecular mechanisms of action of niclosamide, by microarray-based analyses.

MATERIALS AND METHODS

Cell-Lines

CCRF-CEM and CEM/ADR5000 leukemia, RPMI-8226 multiple myeloma, and HT-29 colorectal cancer cells were grown in RPMI 1640 medium supplemented with 10% fetal bovine serum (FBS), penicillin (100 U/ml)/streptomycin (100 μ g/ml) in a 5% CO₂ atmosphere at 37°C. MDA-MB-231 breast cancer and A549 lung cancer cells were grown in Dulbecco's Modified Eagle's Medium supplemented with 10% FBS, penicillin (100 U/ml)/streptomycin (100 μ g/ml) in a 5% CO₂ atmosphere at 37°C. Cells were passaged twice weekly. Resistance of CEM/ADR5000 was maintained by treatment with 5000 ng/ml doxorubicin for 24 h every 2 weeks. All experiments were performed with cells in the logarithmic growth phase.

Cytotoxicity Assay

Cells obtained from exponential phase cultures were counted and seeded into 96-well plates. The seeding density was 10⁴ cells per well for both cell lines. Cells were then exposed to niclosamide (Sigma-Aldrich, Taufkirchen, Germany) using 0.001, 0.01, 0.1, 1, 10, and 100 μ M, in all cell lines. After a 72 h incubation period, 20 μ l of resazurin 0.01% w/v was added to each well and the plates were incubated at 37°C for 4 h. Fluorescence was measured using an Infinite M2000 Pro plate reader (Tecan, Crailsheim, Germany). Dose-response curves were generated by plotting the mean cell viability (%) against the concentration of the compound (μ M). IC₅₀ values were calculated from a calibration curve by linear regression using Microsoft Excel. The resistance ratio for sensitive CCRF-CEM and resistant CEM/ADR5000 cells was calculated by: IC₅₀ resistant/IC₅₀ sensitive. Experiments were repeated three times.

ROS Assay

For each sample 2 \times 10⁶ cells were seeded in each well of a six-well plate. Each well was treated with 1.5 μ M of niclosamide or dimethyl sulfoxide (DMSO). After 24 h incubation, cells were centrifuged and resuspended in RPMI-1640 culture medium and incubated with 10 μ M 2',7'-dichlorodihydrofluorescein-diacetate (H₂DCFH-DA) for 20 min in the dark. Subsequently, cells were centrifuged, washed with phosphate buffered saline (PBS), resuspended in culture medium and measured in a BD-C6 flow cytometer (Becton-Dickinson, Heidelberg, Germany). Cells were also treated with H₂O₂ for 15 min as a positive control. For each sample, 1 \times 10⁴ cells were counted. 2',7'-dichlorofluorescein

(DCF) was measured at 488 nm excitation and detected using a 530/30 nm bandpass filter. The experiment was repeated three times.

Target Prediction

The structure of niclosamide was obtained from ChemSpider¹ and saved as a mol file. The compound was then submitted to the DRAR-CPI software². The protein targets showing the highest docking scores were obtained.

Glutathione Assay

The levels of GSH were determined after the treatment of cells with 0.75, 1.5, 3, 6, and 12 μM niclosamide, and incubated for 24 h at 37°C. The cells were then centrifuged and suspended in PBS supplemented with 5% FBS. The cells were stained with 40 μM monochlorobimane and incubated for 20 min. Fluorescence was read using an LSR-Fortessa flow cytometer (Becton-Dickinson, Heidelberg, Germany) using a 405 nm laser. The experiment was repeated three times.

Molecular Docking

The PDB file for the crystal structure of GSH synthetase (GS) (PDB ID: 2HGS) was downloaded from the protein data bank³. To perform molecular docking, the protein structure of GS were first processed with AutodockTools-1.5.6rc316 to overcome problems of incomplete structures due to missing atoms or water and the presence of multimers or interaction partners of the receptor molecule. The output file after preparation was set in PDBQT format, where information about atomic partial charges, torsion degrees of freedom and different atom types were added, e.g., aliphatic and aromatic carbon atoms or polar atoms forming hydrogen bonds. A grid box was then constructed to define docking spaces. The dimensions of the grid box were set around the entire protein molecule in a manner that the ligand could freely move and rotate in the docking space. The grid box consisted of 126 grid points in all three dimensions (X, Y, and Z) separated by a distance of 1 Å between each one. Energies at each grid point were evaluated for each atom type present in the ligand, and the values were used to predict the energy of a particular ligand configuration. Docking parameters were set to 250 runs and 2,500,000 energy evaluations for each cycle. Docking was performed for niclosamide on GS using Autodock4 by means of a Lamarckian algorithm. The corresponding binding energies and the number of conformations in each cluster were attained from the docking log files (dlg). The process was repeated in a triplicate. The mean and standard deviation were calculated.

Microscale Thermophoresis

The interaction between recombinant human GS (Abcam, Cambridge, UK) and niclosamide was studied using microscale thermophoresis as previously described (Seo and Efferth, 2016). Protein was labeled according to the MonolithTM NT.115 Protein Labeling Kit BLUE-NHS (Amine reactive; NanoTemper

Technologies GmbH, Munich, Germany). The labeled human GS was titrated with niclosamide. The final concentrations of niclosamide were 200, 100, 50, 25, and 3.125 μM in analysis buffer (50 mM Tris buffer pH 7.6 containing 150 mM NaCl, 10 mM MgCl_2 , and 0.05% Tween-20). Samples were analyzed using hydrophilic capillaries in NanoTemper MonolithTM NT (NanoTemper Technologies GmbH, Munich, Germany) for blue dye fluorescence.

COMPARE Analyses

The mRNA microarray data of the NCI tumor cell line panel available at the NCI website⁴ was used (Scherf et al., 2000; Staunton et al., 2001). COMPARE analyses were performed to produce rank-ordered lists of genes expressed in the NCI cell lines as previously described (Paull et al., 1989; Wosikowski et al., 1997). Briefly, every gene of the NCI microarray database was ranked for similarity of its mRNA expression to the $\log_{10}\text{IC}_{50}$ values for niclosamide. To derive COMPARE rankings, a scale index of correlation coefficients (*R*-values) was created.

Hierarchical Cluster Analysis

Hierarchical cluster analysis was performed, in order to create a cluster model for the different cell lines. This was done by classifying objects into dendrograms. The distances were calculated according to the closeness of between-individual distances. Cluster models have previously been validated for gene expression profiling and for approaching molecular pharmacology of anticancer agents (Efferth et al., 1997; Scherf et al., 2000).

Promoter Binding Motif Analysis

Binding motifs for transcription factors in the promoter sequences of genes were analyzed by Cistrome analysis software (Liu et al., 2011). Briefly, genes of interest were retrieved in BED format from <https://genome.ucsc.edu/cgi-bin/hgTables>. SeqPos⁵ was used to screen for enriched transcription factor binding motifs in gene promoter sequences. The screening was performed for motifs deposited in the Transfac, JASPAR, UniPROBE, and PDI databases. Moreover, *de novo* motifs were identified by using MDscan algorithm.

Nuclear Factor of Activated T-Cells Reporter Assay

HEK293 cell lines were transfected with nuclear factor of activated T-cells (NFAT)-luciferase reporter construct (Qiagen, Germantown, MD, USA). The cells were cultured, according to the manufacturer's recommendations. The cells were treated with varying concentrations of niclosamide for 24 h. NFAT promoter activity was quantified with Dual-Luciferase Reporter Assay System (Promega, Madison, WI, USA) by measuring the firefly and renilla luciferase luminescences on an Infinite M2000 ProTM plate reader (Tecan). The ratio of firefly luciferase intensity to renilla luciferase intensity yielded a measure for NFAT activity.

¹<http://www.chemspider.com>

²<https://cpi.bio-x.cn/drar>

³<http://www.rcsb.org/pdb>

⁴<https://ntp.cancer.gov>

⁵<http://cistrome.org>

The relative luminance for each sample was calculated as: firefly luciferase luminescence/renilla luciferase luminescence. DMSO treatment served as control. Normalized NFAT activity was calculated by the formula: relative luciferase of sample/relative luciferase of the DMSO control. The experiment was repeated three times.

Statistical Analysis

Data were expressed as mean \pm SD of three independent tests. Statistical significance was determined using the Student's *t*-test. A *p*-value of less than 0.05 denoted significance in all cases. Hierarchical cluster analysis was performed using the Ward's method (WinSTAT program, Kalmia, Cambridge, MA, USA).

RESULTS

Cytotoxicity Assay

The cytotoxic activity of niclosamide was tested on CCRF-CEM and CEM/ADR5000 leukemia, RPMI-8226 multiple myeloma, HT-29 colorectal cancer, MDA-MB-231 breast cancer, and A549 lung cancer cells, using resazurin assay. Niclosamide showed varying activity towards the tested cell lines as shown in **Figure 1**. It was most active against the hematological cancer cell lines CCRF-CEM, CEM/ADR5000, and RPMI-8226, compared to the solid tumor cell lines HT-29, MDA-MB-231, and A549. The resistance ratio between the sensitive CCRF-CEM and multidrug resistant CEM/ADR5000 cells was 1.24, indicating that CEM/ADR5000 were sensitive to niclosamide.

ROS Assay

Cellular ROS levels were analyzed after niclosamide treatment by H₂DCFH-DA staining and flow cytometry. A clear dose-dependent increase in cellular ROS levels was observed after 24 h incubation with niclosamide (**Figure 2**). Thus, niclosamide can be regarded as a ROS inducer in acute lymphoblastic leukemia cells.

Target Prediction

A total of 391 biological targets were identified for niclosamide by the DRAR-CPI algorithm. Interestingly, GS, which is directly involved in ROS metabolism, was among the predicted targets. Niclosamide showed a docking score of -47.8 and a *Z'*-score of -0.788 for GS. We therefore hypothesized that the binding of niclosamide to GS and the subsequent inhibition of GSH production played an important role in the increase of ROS after treatment of cells.

Glutathione Assay

In order to test whether niclosamide affected GSH levels in the sensitive and resistant cell lines, GSH assays were performed after treatment of leukemia cells with different concentrations of niclosamide. The cells were stained with monochlorobimane and fluorescence was measured using flow cytometry. As shown in **Figure 3**, niclosamide significantly reduced the intracellular GSH levels in a dose-dependent manner in both

cell lines. However, the effect on sensitive CCRF-CEM cells was slightly higher than the effect on the resistant CEM/ADR5000 cells, which is consistent with the results from the ROS assay.

Molecular Docking

To predict the binding affinity of niclosamide to GS and propose its binding site, we performed molecular docking. The protein structure of GS was downloaded in PDB format, processed using Autodock Tools and finally converted to PDBQT format. A grid box was then constructed. Energies at each grid point were then evaluated for each atom type present in the ligand. The values were used to predict the energy of a particular ligand configuration. Docking was performed for niclosamide on GS with Autodock4 using the Lamarckian Algorithm. The corresponding binding energies and the number of conformations in each cluster were attained from the docking log files (dlg). As shown in **Figure 4**, the lowest binding energy for niclosamide on GS was predicted to be -9.40 ± 0.01 kcal/mol, which is a considerably low value. The amino acids involved in the interaction included Ile143, Asn373, Tyr375, Met398, Glu399, Ile401, Arg450, Lys452, and Ala457. Two of the amino acids (Arg450 and Ala457) showed interactions with hydrogen bonding.

Microscale Thermophoresis

Microscale thermophoresis was used to analyze the direct interaction between GS and niclosamide (**Figure 5**). This method is used to determine the binding affinity between a fluorescently labeled protein and a non-labeled compound. Labeled GS was titrated with different concentrations of niclosamide. An equilibrium binding constant of $5.64 \mu\text{M}$ was obtained providing evidence for direct binding of GS to niclosamide.

Microarray Analysis

To correlate the cellular responses of niclosamide with the expression of the deregulated genes, we performed COMPARE analyses. Using the NCI database, we correlated the microarray-based transcriptome-wide mRNA expression of 60 tumor cell lines with the log₁₀IC₅₀ values for niclosamide. We ran a standard COMPARE, which correlated the lowest IC₅₀ values with the lowest mRNA expression levels of genes. We then ran a reverse COMPARE which correlated the lowest IC₅₀ values with the highest gene expression level. The threshold for correlation coefficients were $R > 0.55$ for standard COMPARE and $R < -0.55$ for reverse COMPARE (Supplementary Table S1). The genes that showed good correlation with sensitivity to niclosamide included those involved in signal transduction (*TP53INP2*, *LAMTOP5*, *PDE6G*), lipid metabolism (*SOAT*, *GMA2*), regulation of cell growth and development (*MAP6*, *TANC2*) and others. On the other hand, genes that correlated with resistance included those involved in signal transduction (*MUC13*, *S100P*, *ARHGFE5*, *LMO7*), lipid metabolism and transport (*PLA2G2A*, *CYP3A4*, *APOM*), protein synthesis (*RPS16*, *E1F2S2*) and others. The mRNA expression values of these genes were used to perform a hierarchical cluster analysis. The dendrogram of this cluster analysis could be divided into five main cluster branches

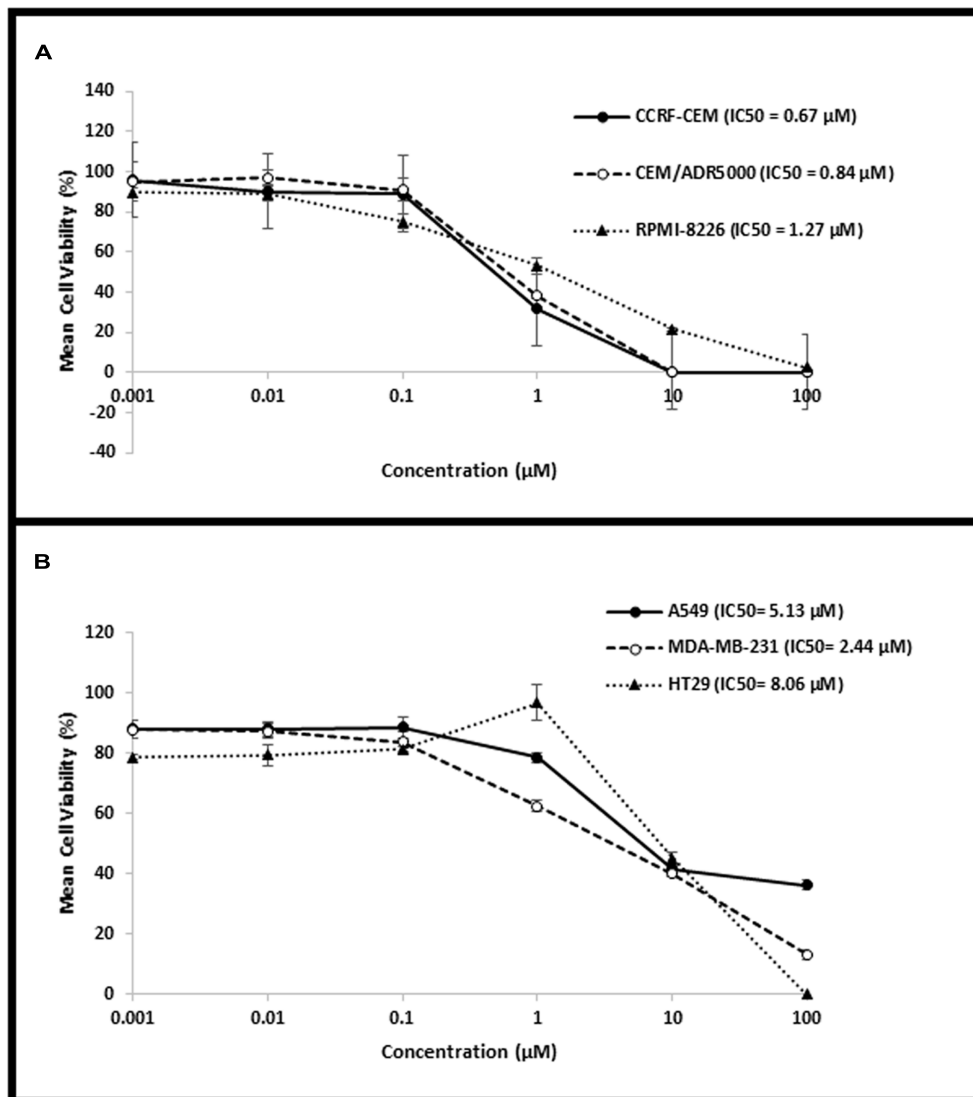


FIGURE 1 | Dose–response curves from the cytotoxicity assays of (A) hematological cancer cell lines (CCRF-CEM, CEM/ADR5000, and RPMI-8226) and (B) solid tumor cell lines (HT-29, MDA-MB-231, and A549).

(Figure 6). Sensitivity or resistance to niclosamide and its derivative were predicted by the distribution of cell lines in the dendrogram according to their gene expression profiles. We found a significant difference in the distribution of sensitive and resistant cell lines between the branches of the dendrogram ($p = 8.66 \times 10^{-5}$). The response of this cell line panel to niclosamide and its derivative can therefore be determined by the gene expression profile.

Promotor Binding Motif Analysis

To further determine the transcription factors and the signaling pathways involved in the anticancer activity of niclosamide, we performed promotor binding motif analysis. To accomplish that, a set of 30 deregulated genes from the microarray data were selected. As shown in Table 1, several

transcription factors might be involved in the cellular response of cancer cells to niclosamide. Among them were *CEBPA* and *CEBPB* (cell cycle regulation), *RELA* and *CREL* (NF- κ B pathway), *TCF7L1* (Wnt/ β -catenin signaling pathway), *SMAD3* [transforming growth factor beta (TGF- β) signaling], *FOXO1* and *NFAT*, all of which are involved in cancer initiation and progression.

NFAT Reporter Assay

The NFAT was among the transcription factors that may potentially bind to the gene promoters of deregulated genes from the microarray data. In order to confirm this finding, we performed an NFAT reporter assay. As shown in Figure 7, niclosamide indeed caused a significant decrease in NFAT activity in a dose dependent manner.

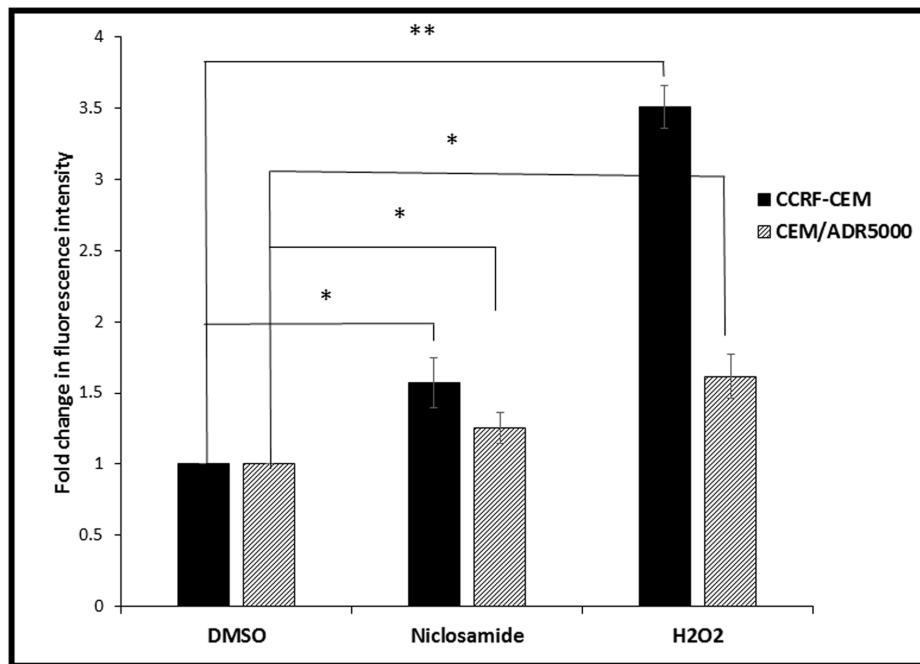


FIGURE 2 | Effect of 24 h treatment with niclosamide (1.5 μM) on ROS levels in CCRF-CEM and CEM/ADR5000 cells. H_2O_2 (50 μM) was used as a positive control (* $p < 0.05$, ** $p < 0.01$, compared to DMSO-treated control cells).

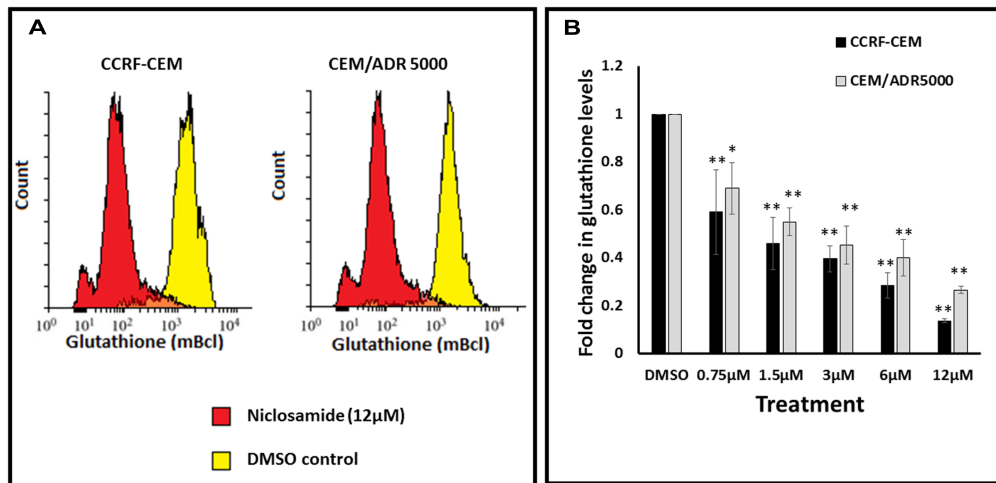


FIGURE 3 | Effect of niclosamide on glutathione levels in CCRF-CEM and CEM/ADR5000 cells. **(A)** Flow cytometric analysis of glutathione levels after treatment with niclosamide (12 μM) for 24 h. **(B)** Statistical quantification of glutathione levels after treatment with different concentrations of niclosamide (* $p < 0.05$, ** $p < 0.01$, compared to DMSO-treated control cells).

DISCUSSION

A major problem of anticancer therapy is the development of MDR. Pgp, an energy dependent efflux pump, plays an important role in the development of MDR. Clinical studies have shown that the overexpression of Pgp in cancer cells is associated with poor prognosis (Bellamy, 1996). This protein transports chemotherapeutic drugs that are central to many anticancer

regimens (Allen et al., 2000). Niclosamide showed cytotoxic effects against various types of cancer (Li et al., 2014). Our cytotoxicity assay results on the hematological, breast, lung, and colorectal cancer cell lines, showed that niclosamide is more active against the three hematological cell lines, compared to the solid tumor cell lines cell lines, which were more resistant. However, to the best of our knowledge, the effect of niclosamide on MDR cancer has never been investigated, as of

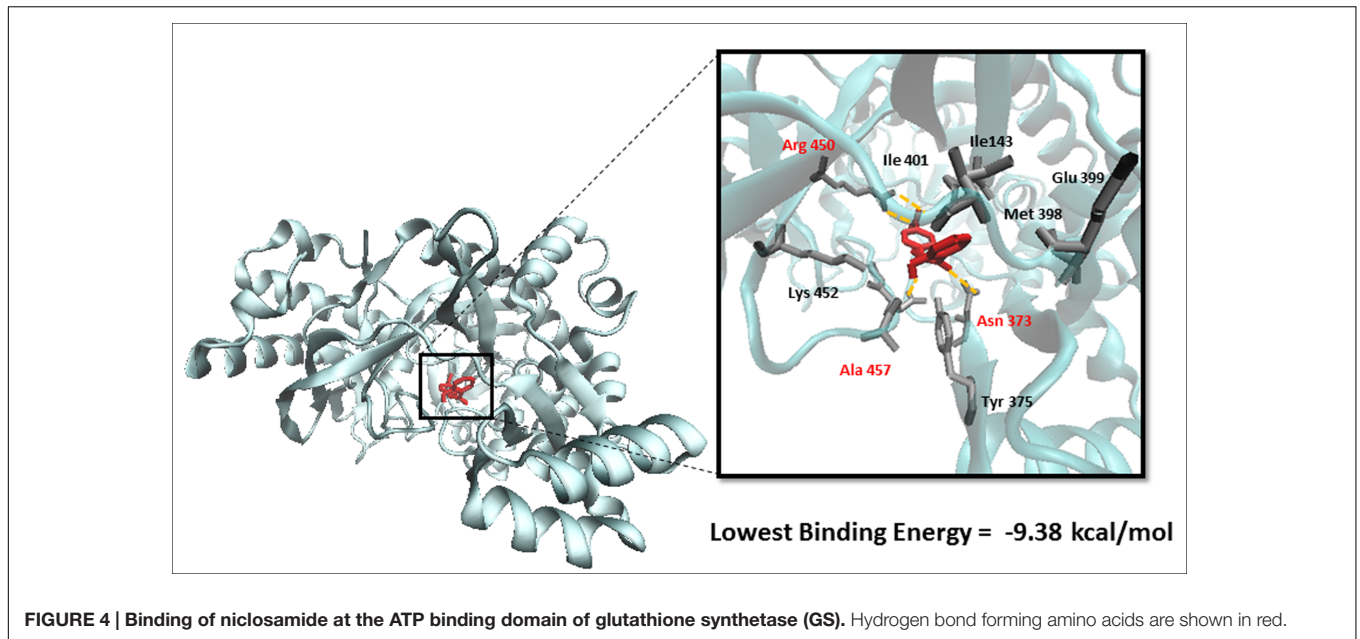


FIGURE 4 | Binding of niclosamide at the ATP binding domain of glutathione synthetase (GS). Hydrogen bond forming amino acids are shown in red.

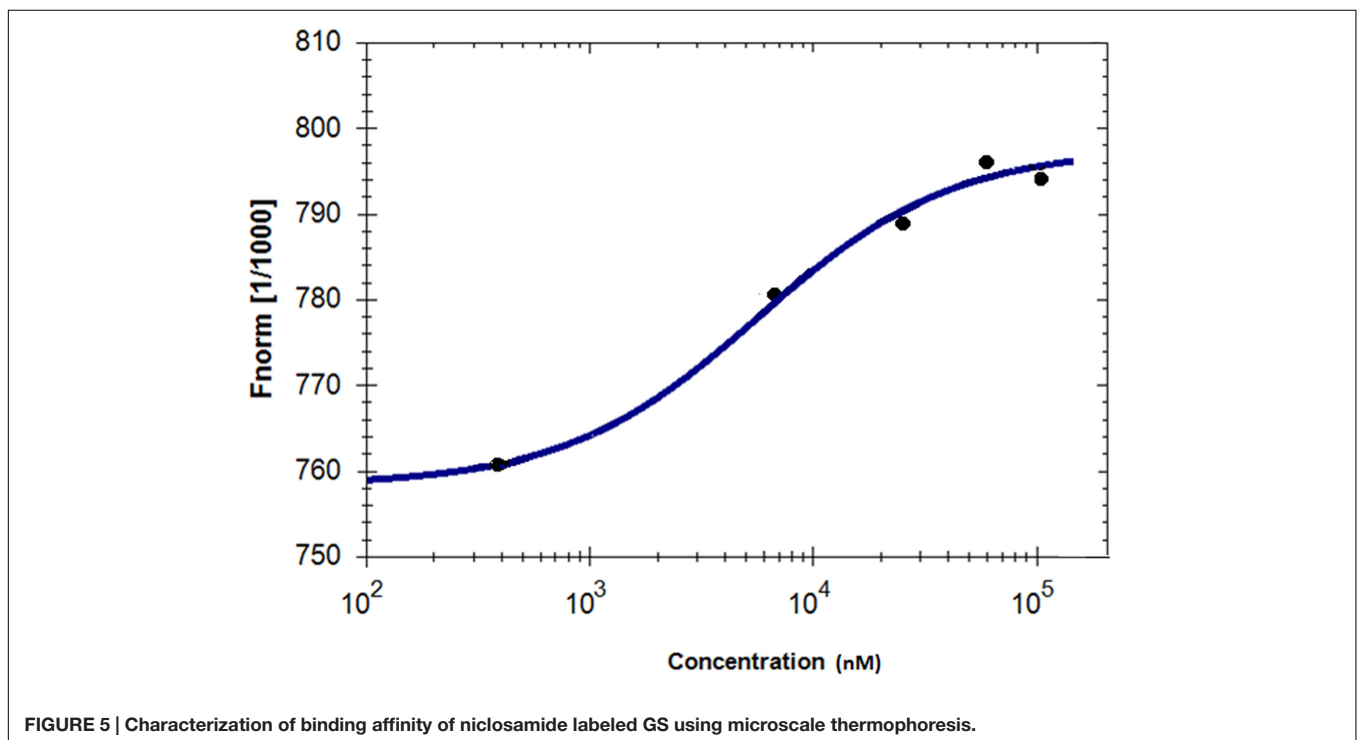


FIGURE 5 | Characterization of binding affinity of niclosamide labeled GS using microscale thermophoresis.

yet. Interestingly we have found niclosamide to be active against both the sensitive and MDR (Pgp-overexpressing) leukemia cells. The resistance ratio was found to be 1.24, indicating that niclosamide shows significant cytotoxic activity against leukemia cells that display the MDR phenotype. The reason may be due to its rapid uptake and the effective bypassing of Pgp, leading to its higher intracellular accumulation and effectiveness. To the best of our knowledge, we report for the first time that niclosamide is active against MDR cancer cells.

ROS are highly reactive chemical entities including radicals, ions or molecules that have a single unpaired electron in their outermost shell of electrons (Liou and Storz, 2010). The use of agents that significantly increase ROS represents an effective strategy to kill cancer cells. Thus, a common approach to treat cancer represents the application of agents with strong pro-oxidant properties. Such agents would either directly generate ROS or inhibit the antioxidant systems in the cell. This will lead to an increase of ROS levels above the threshold, with

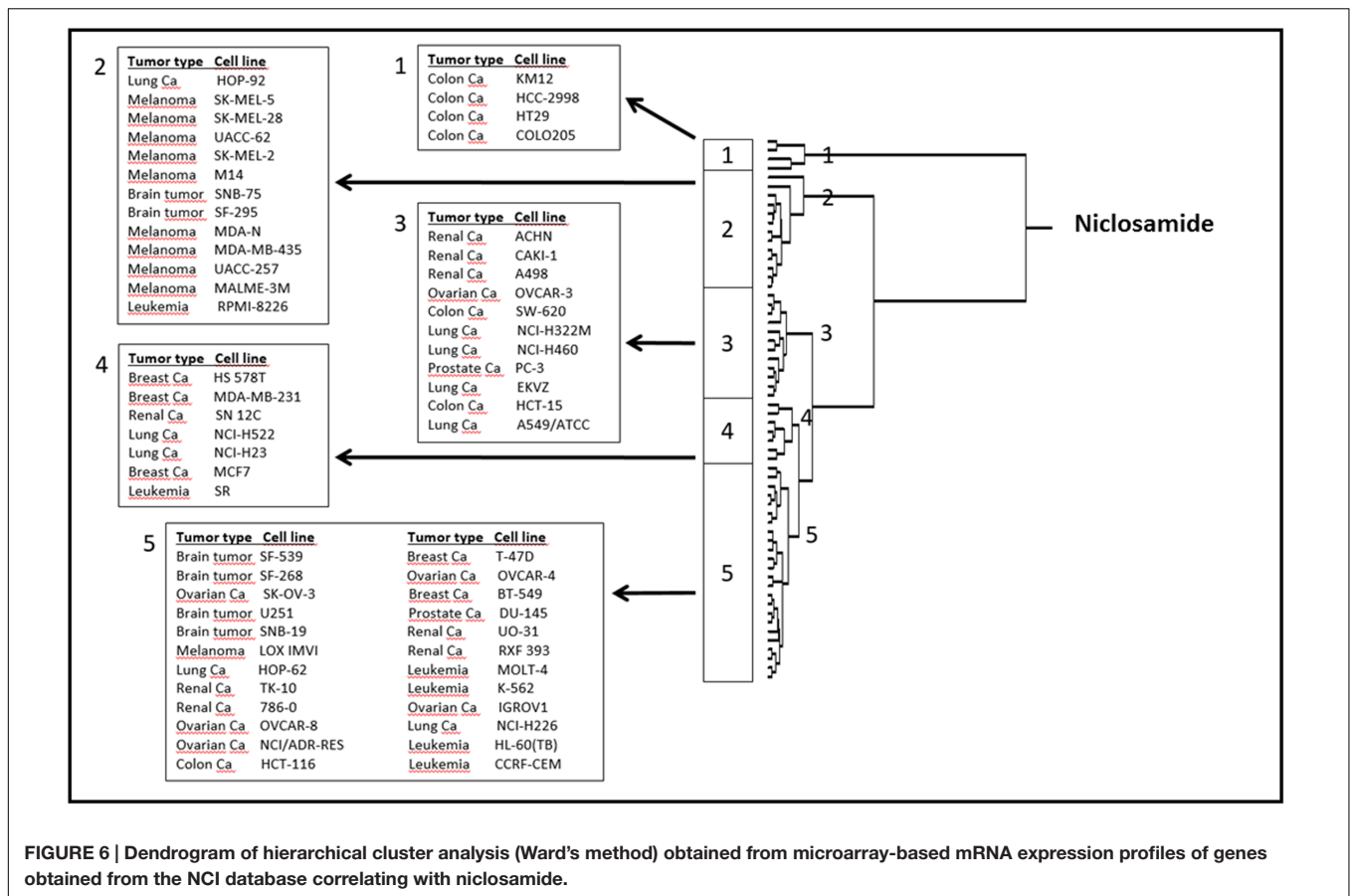


FIGURE 6 | Dendrogram of hierarchical cluster analysis (Ward's method) obtained from microarray-based mRNA expression profiles of genes obtained from the NCI database correlating with nicosamide.

the subsequent induction of apoptosis and cell death (Ivanova et al., 2013). Nicosamide is known to increase ROS levels in cancer cells, including acute myeloid leukemia and lung cancer cells (Wartenberg et al., 2005; Jin et al., 2010; Lee et al., 2014;

Liao et al., 2015). However, the mechanism behind this effect has not been previously investigated. Our results showed that nicosamide also caused the elevation of ROS levels in both the sensitive and MDR leukemia cells. In an effort to elucidate

TABLE 1 | Transcription factors for which promoter motifs are found in the genes identified by COMPARE analysis.

Clusters	Factor	Z-score	-10*log (p-value)	Clusters	Factor	Z-score	-10*log (p-value)
1.	EmBP-1b	-4.81	140.979	18.	Pax-4	-3.543	85.274
	Opaque-2	-3.995	103.405	19.	MAF	-3.523	84.535
2.	ZNF766	-4.459	123.985	20.	RFX1	-3.496	83.506
3.	GCR1	-4.445	123.338	21.	THRAP6	-3.443	81.539
4.	CEBPB	-4.158	110.418	22.	bZIP911	-3.374	79.016
5.	REL	-4.09	107.455	23.	Smad3	-3.35	78.123
	c-Rel	-3.438	81.363	24.	NAC69-1	-3.347	78.039
6.	Gat4	-4.083	107.159	25.	FOXO1	-3.337	77.664
7.	TCF7L1	-4.025	104.642	26.	E2A TCF3	-3.292	76.045
8.	Zfp105	-3.969	102.289	27.	PBF1	-3.288	75.932
9.	Tcfap2e	-3.95	101.515	28.	POU6F1	-3.253	74.699
10.	CEBPA	-3.808	95.674	29.	NF-AT	-3.246	74.44
11.	IRF-2	-3.789	94.879		ESE1 ELF3	-3.177	72.038
12.	ATF6	-3.688	90.89	30.	Elk1	-3.201	72.867
	ROM	-3.482	82.969	31.	PTF1-beta	-3.196	72.707
13.	CPRF-1	-3.367	78.765	32.	Zic2	-3.164	71.599
14.	CPRF-3	-3.204	72.955	33.	GCR1	-3.119	70.039

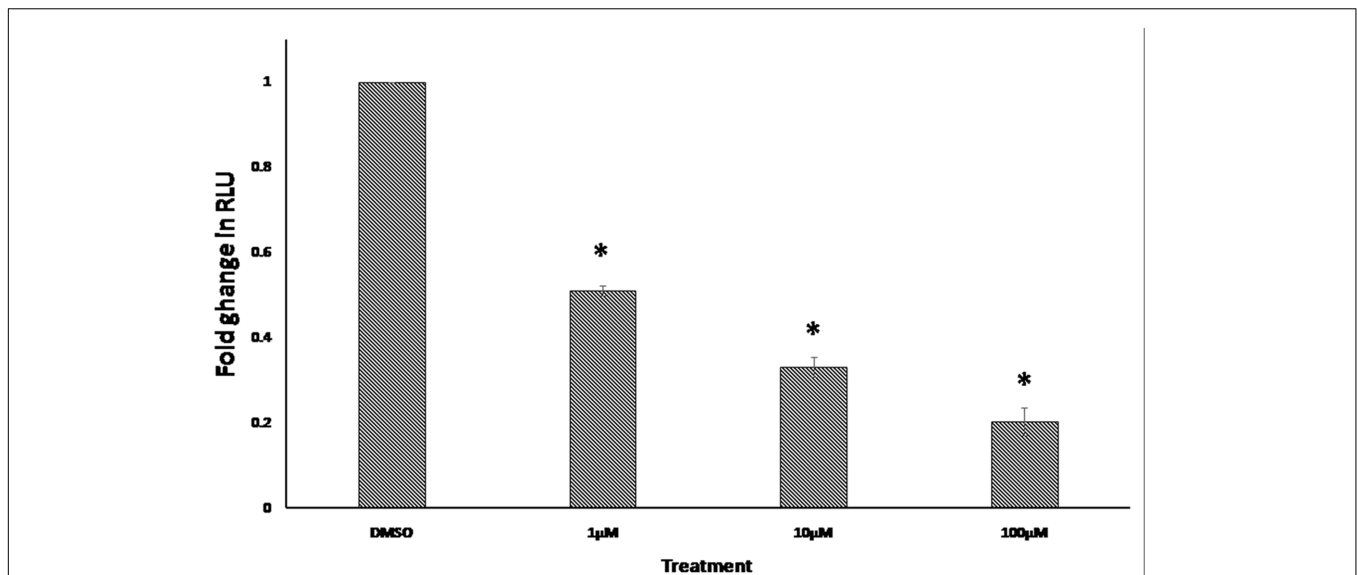


FIGURE 7 | Effect of 24 h treatment with various concentrations of niclosamide on NFAT signaling activity. Results shown are the mean values \pm SD of three independent experiments (* $p < 0.01$, compared to DMSO-treated control cells).

the mechanism by which niclosamide elevated ROS levels, we identified GS as a possible target of niclosamide. GS is a key role player in GSH synthesis, as it catalyzes the formation of GSH from γ -glutamylcysteine and glycine, and therefore determines the overall GSH synthetic capacity in certain tissues, especially under stressful conditions (Lu, 2013). GSH is one of the most important antioxidants in the cell. It plays several vital roles including the maintenance of the redox state, drug detoxification, and cellular protection from damage by free radicals, peroxides, and toxins (Singh et al., 2012). It is involved in DNA repair and apoptosis (Ichijo et al., 1997; Izbicka et al., 1997; Harwaldt et al., 2002), and is clearly associated with cancer resistance to chemotherapeutic agents (Capron et al., 2001; Harwaldt et al., 2002). Niclosamide should therefore reduce the GSH levels in cancer cells. Accordingly, we measured GSH levels in leukemia cells after treatment with different concentrations of niclosamide. The significant reduction in GSH levels indicates an inhibition of GSH synthesis. As GSH is known to be involved in the development of drug resistance (Townsend and Tew, 2003), the inhibition of its synthesis probably plays a role in the activity of niclosamide on MDR cells.

Molecular docking was used to confirm and clarify the inhibitory effect of niclosamide on GS. This bioinformatical tool is considered essential and valuable in drug discovery and development. It gains its value from its ability to predict the conformation of small-molecule ligands within the appropriate target-binding site. It also estimates the ligand receptor binding free energy involved in the molecular interaction (Meng et al., 2011). Niclosamide gave a low binding energy indicating a high affinity to GS. In order to validate the molecular docking result, we studied the real interaction between GS and niclosamide, using microscale thermophoresis. The results showed good binding affinity, confirming our findings. We can

therefore postulate that niclosamide is a possible inhibitor of GS. Niclosamide is therefore expected to inhibit the synthesis of GSH in cancer cells causing a reduction of GSH levels shown by the GSH assays. This then leads to the reduction in the ROS scavenging effects of GSH, causing the increased accumulation of ROS in cancer cells. A crystallographic study of the interaction of GS with ATP revealed that Ile143, Tyr375, Met398, Glu399, Ile401, and Lys452 contribute to the interaction between GS and ATP (Polekhina et al., 1999; Dinescu et al., 2004). Accordingly, niclosamide inhibits GS activity by competitively binding to the ATP binding site, and therefore blocks the interaction with ATP. Interestingly GS inhibitors have not been described in previous studies. Niclosamide is therefore the first compound reported to cause inhibition of GS.

The genes identified by the microarray-based COMPARE analyses that showed good correlation with the cellular response of niclosamide included those involved in lipid metabolism, signal transduction, regulation of cell growth and development, protein synthesis, and others. The result of the hierarchical cluster analysis showed a significant difference in the distribution of sensitive and resistant cell lines between the branches of the dendrogram. The response of this cell line panel to niclosamide can therefore be determined by the gene expression profile. Inhibitors of lipogenic enzymes are quite active and efficient anticancer agents. Several other compounds that target lipid and cholesterol metabolism and homeostasis have shown relevant anticancer activity (Beloribi-Djefaflija et al., 2016). According to our findings from the microarray data analysis, lipid metabolism might play a central role in the cytotoxic activity of niclosamide against cancer cells. Further studies are required to confirm this mechanism of action. These would include the determination of the effect of niclosamide on the levels of lipogenic enzymes and on the amounts of total lipid, total cholesterol and triglyceride in

cancer cells. It is worth noting that none of the ABC transporters was found to be associated with resistance to niclosamide. This is consistent with our finding that overexpression of Pgp is not involved in the resistance to niclosamide. The promoter binding motif analysis of the microarray data of niclosamide showed that a number of transcription factors might potentially bind to these gene promoters. Those that are related to cancer include *CEBPA*, *CEBPB*, *RELA*, *CREL*, *TCF7L1*, *NFAT*, and *SMAD3*. Thus, several signaling pathways would be involved in the anticancer activity of niclosamide. These pathways include the NF- κ B, Wnt, NFAT, TGF- β , and forkhead box protein O (FOXO) signaling pathways. In addition, the CCAAT/enhancer-binding protein (CEBP) transcription factors, involved in cell cycle regulation, might also play a role in the activity of niclosamide. In accordance with our findings, niclosamide is known to exert anticancer activity through inhibition of NF- κ B and Wnt signaling pathways (Li et al., 2014). Niclosamide is also known to inhibit mechanistic target of rapamycin (mTOR) signaling (Fonseca et al., 2012). The mTOR signaling pathway regulates FOXO activity as well as TGF- β signaling (Mori et al., 2014; Yu et al., 2015). Furthermore, it controls the ratio of CEBP isoform expression. It is therefore possible that the effect of niclosamide on the expression of FOXO, TGF- β , and CEBP regulated genes is through the inhibition of mTOR signaling.

Previously, the effect of niclosamide on several signaling pathways has been investigated (Li et al., 2014). Even though, its effect on NFAT activity has not been studied yet. The NFAT signaling pathway has an important role in the development and function of the immune system. It is also involved in the development of cardiac, skeletal muscle, and nervous systems. This pathway is activated by increased calcium levels, resulting from its release from the endoplasmic reticulum or its influx through activated channels in the cell membrane. Recent findings have shown that NFAT contributes to cancer development and progression, including solid tumors and hematological malignancies. NFAT signaling is also known to be persistently active in mouse models of human leukemia (Medyouf and Ghysdael, 2008). Inhibition of NFAT signaling pathway in leukemia cells caused cell growth arrest and induction of apoptosis *in vitro* and *in vivo* (Mancini and Toker, 2009). Due to the importance of NFAT signaling in the progression of leukemia and our finding from the promoter binding motif

analysis, we further investigated the effect of niclosamide on NFAT signaling using a reporter cell line. We found for the first time that niclosamide significantly inhibited NFAT signaling in a dose-dependent manner. The inhibition of NFAT activity may therefore lead to growth arrest and induction of apoptosis, participating in the anticancer activity of niclosamide.

We conclude that niclosamide exhibits a great potential as an anticancer agent. In this study niclosamide showed excellent activity against MDR leukemia. Niclosamide may therefore have the potential to solve the problem of MDR in cancer patients. The findings of the present study indicate that the cytotoxic activity of niclosamide is due to its targeting of several signaling pathways in cancer cells. We identified the inhibition of GSH synthesis and NFAT signaling as novel mechanisms for the anticancer activity of niclosamide. The microarray data analyses showed that the cellular response of a cancer type can be predicted by its gene expression profile. These data also suggest the involvement of lipid metabolism in the anticancer activity of niclosamide. It is therefore reasonable to consider niclosamide as a clinical candidate for the treatment of refractory MDR cancers.

AUTHOR CONTRIBUTIONS

SH performed the cytotoxicity, reactive oxygen species, glutathione and NFAT reporter assays, promoter binding motif analysis, and wrote the paper. PJ performed the microarray analysis and molecular docking. TE supervised the project and wrote the paper.

FUNDING

The authors are grateful for the Ph.D. stipend of the German Academic Exchange Service (DAAD) to SH.

SUPPLEMENTARY MATERIAL

The Supplementary Material for this article can be found online at: <http://journal.frontiersin.org/article/10.3389/fphar.2017.00110/full#supplementary-material>

REFERENCES

- Allen, J. D., Brinkhuis, R. F., van Deemter, L., Wijnholds, J., and Schinkel, A. H. (2000). Extensive contribution of the multidrug transporters P-glycoprotein and Mrp1 to basal drug resistance. *Cancer Res.* 60, 5761–5766.
- Ashburn, T. T., and Thor, K. B. (2004). Drug repositioning: identifying and developing new uses for existing drugs. *Nat. Rev. Drug Discov.* 3, 673–683. doi: 10.1038/nrd1468
- Bartsevich, V. V., and Juliano, R. L. (2000). Regulation of the MDR1 gene by transcriptional repressors selected using peptide combinatorial libraries. *Mol. Pharmacol.* 58, 1–10.
- Bellamy, W. T. (1996). P-glycoproteins and multidrug resistance. *Annu. Rev. Pharmacol. Toxicol.* 36, 161–183. doi: 10.1146/annurev.pa.36.040196.001113
- Beloribi-Djefafli, S., Vasseur, S., and Guillaumond, F. (2016). Lipid metabolic reprogramming in cancer cells. *Oncogenesis* 5, e189. doi: 10.1038/oncsis.2015.49
- Capron, A., Capron, M., Dombrowicz, D., and Riveau, G. (2001). Vaccine strategies against schistosomiasis: from concepts to clinical trials. *Int. Arch. Allergy Immunol.* 124, 9–15. doi: 10.1159/000053656
- Dinescu, A., Cundari, T. R., Bhansali, V. S., Luo, J. L., and Anderson, M. E. (2004). Function of conserved residues of human glutathione synthetase: implications for the ATP-grasp enzymes. *J. Biol. Chem.* 279, 22412–22421. doi: 10.1074/jbc.M401334200
- Efferth, T., Fabry, U., and Osieka, R. (1997). Apoptosis and resistance to daunorubicin in human leukemic cells. *Leukemia* 11, 1180–1186. doi: 10.1038/sj.leu.2400669
- Fonseca, B. D., Diering, G. H., Bidinosti, M. A., Dalal, K., Alain, T., Balgi, A. D., et al. (2012). Structure-activity analysis of niclosamide reveals potential role for cytoplasmic pH in control of mammalian target of rapamycin complex 1 (mTORC1) signaling. *J. Biol. Chem.* 287, 17530–17545. doi: 10.1074/jbc.M112.359638

- Harwaldt, P., Rahlfs, S., and Becker, K. (2002). Glutathione S-transferase of the malarial parasite *Plasmodium falciparum*: characterization of a potential drug target. *Biol. Chem.* 383, 821–830. doi: 10.1515/bc.2002.086
- Hoelder, S., Clarke, P. A., and Workman, P. (2012). Discovery of small molecule cancer drugs: successes, challenges and opportunities. *Mol. Oncol.* 6, 155–176. doi: 10.1016/j.molonc.2012.02.004
- Housman, G., Byler, S., Heerboth, S., Lapinska, K., Longacre, M., Snyder, N., et al. (2014). Drug resistance in cancer: an overview. *Cancers* 6, 1769–1792. doi: 10.3390/cancers6031769
- Ichijo, H., Nishida, E., Irie, K., ten Dijke, P., Saitoh, M., Moriguchi, T., et al. (1997). Induction of apoptosis by ASK1, a mammalian MAPKKK that activates SAPK/JNK and p38 signaling pathways. *Science* 275, 90–94. doi: 10.1126/science.275.5296.90
- Ivanova, D., Bakalova, R., Lazarova, D., Gadjeva, V., and Zhelev, Z. (2013). The impact of reactive oxygen species on anticancer therapeutic strategies. *Adv. Clin. Exp. Med.* 22, 899–908.
- Izbicka, E., Lawrence, R., Cerna, C., Von Hoff, D. D., and Sanderson, P. E. (1997). Activity of TER286 against human tumor colony-forming units. *Anticancer. Drugs* 8, 345–348. doi: 10.1097/00001813-199704000-00006
- Jin, Y., Lu, Z., Ding, K., Li, J., Du, X., Chen, C., et al. (2010). Antineoplastic mechanisms of niclosamide in acute myelogenous leukemia stem cells: inactivation of the NF- κ B pathway and generation of reactive oxygen species. *Cancer Res.* 70, 2516–2527. doi: 10.1158/0008-5472.can-093950
- Kraljevic, S., Stambrook, P. J., and Pavelic, K. (2004). Accelerating drug discovery. *EMBO Rep.* 5, 837–842. doi: 10.1038/sj.embor.7400236
- Lee, S. L., Son, A. R., Ahn, J., and Song, J. Y. (2014). Niclosamide enhances ROS-mediated cell death through c-Jun activation. *Biomed. Pharmacother.* 68, 619–624. doi: 10.1016/j.biopha.2014.03.018
- Li, Y., Li, P. K., Roberts, M. J., Arend, R. C., Samant, R. S., and Buchsbaum, D. J. (2014). Multi-targeted therapy of cancer by niclosamide: a new application for an old drug. *Cancer Lett.* 349, 8–14. doi: 10.1016/j.canlet.2014.04.003
- Liao, Z., Nan, G., Yan, Z., Zeng, L., Deng, Y., Ye, J., et al. (2015). The anthelmintic drug niclosamide inhibits the proliferative activity of human osteosarcoma cells by targeting multiple signal pathways. *Curr. Cancer Drug. Targets* 15, 726–738. doi: 10.2174/1568009615666150629132157
- Liou, G. Y., and Storz, P. (2010). Reactive oxygen species in cancer. *Free Radic. Res.* 44, 479–496. doi: 10.3109/10715761003667554
- Liu, T., Ortiz, J. A., Taing, L., Meyer, C. A., Lee, B., Zhang, Y., et al. (2011). Cistrome: an integrative platform for transcriptional regulation studies. *Genome Biol.* 12:R83. doi: 10.1186/gb-2011-12-8-r83
- Lu, S. C. (2013). Glutathione synthesis. *Biochim. Biophys. Acta* 1830, 3143–3153. doi: 10.1016/j.bbagen.2012.09.008
- Mancini, M., and Toker, A. (2009). NFAT proteins: emerging roles in cancer progression. *Nat. Rev. Cancer* 9, 810–820. doi: 10.1038/nrc2735
- Medyouf, H., and Ghysdael, J. (2008). The calcineurin/NFAT signaling pathway: a novel therapeutic target in leukemia and solid tumors. *Cell Cycle* 7, 297–303. doi: 10.4161/cc.7.3.5357
- Meng, X. Y., Zhang, H. X., Mezei, M., and Cui, M. (2011). Molecular docking: a powerful approach for structure-based drug discovery. *Curr. Comput. Aided Drug Des.* 7, 146–157. doi: 10.2174/157340911795677602
- Mori, S., Nada, S., Kimura, H., Tajima, S., Takahashi, Y., Kitamura, A., et al. (2014). The mTOR pathway controls cell proliferation by regulating the FoxO3a transcription factor via SGK1 kinase. *PLoS ONE* 9:e88891. doi: 10.1371/journal.pone.0088891
- Paull, K. D., Shoemaker, R. H., Hodes, L., Monks, A., Scudiero, D. A., Rubinstein, L., et al. (1989). Display and analysis of patterns of differential activity of drugs against human tumor cell lines: development of mean graph and COMPARE algorithm. *J. Natl. Cancer Inst.* 81, 1088–1092. doi: 10.1093/jnci/81.14.1088
- Polekhina, G., Board, P. G., Gali, R. R., Rossjohn, J., and Parker, M. W. (1999). Molecular basis of glutathione synthetase deficiency and a rare gene permutation event. *EMBO J.* 18, 3204–3213. doi: 10.1093/emboj/18.12.3204
- Scherf, U., Ross, D. T., Waltham, M., Smith, L. H., Lee, J. K., Tanabe, L., et al. (2000). A gene expression database for the molecular pharmacology of cancer. *Nat. Genet.* 24, 236–244. doi: 10.1038/73439
- Seo, E. J., and Efferth, T. (2016). Interaction of antihistaminic drugs with human translationally controlled tumor protein (TCTP) as novel approach for differentiation therapy. *Oncotarget* 7, 16818–16839. doi: 10.18632/oncotarget.7605
- Singh, S., Khan, A. R., and Gupta, A. K. (2012). Role of glutathione in cancer pathophysiology and therapeutic interventions. *J. Exp. Ther. Oncol.* 9, 303–316.
- Staunton, J. E., Slonim, D. K., Collier, H. A., Tamayo, P., Angelo, M. J., Park, J., et al. (2001). Chemosensitivity prediction by transcriptional profiling. *Proc. Natl. Acad. Sci. U.S.A.* 98, 10787–10792. doi: 10.1073/pnas.191368598
- Storz, P. (2005). Reactive oxygen species in tumor progression. *Front. Biosci.* 10, 1881–1896. doi: 10.2741/1667
- Tada, Y., Brena, R. M., Hackanson, B., Morrison, C., Otterson, G. A., and Plass, C. (2006). Epigenetic modulation of tumor suppressor CCAAT/enhancer binding protein alpha activity in lung cancer. *J. Natl. Cancer Inst.* 98, 396–406. doi: 10.1093/jnci/djj093
- Townsend, D. M., and Tew, K. D. (2003). The role of glutathione-S-transferase in anti-cancer drug resistance. *Oncogene* 22, 7369–7375. doi: 10.1038/sj.onc.1206940
- Wartenberg, M., Hoffmann, E., Schwindt, H., Grunheck, F., Petros, J., Arnold, J. R., et al. (2005). Reactive oxygen species-linked regulation of the multidrug resistance transporter P-glycoprotein in Nox-1 overexpressing prostate tumor spheroids. *FEBS Lett.* 579, 4541–4549. doi: 10.1016/j.febslet.2005.06.078
- Wosikowski, K., Schuurhuis, D., Johnson, K., Paull, K. D., Myers, T. G., Weinstein, J. N., et al. (1997). Identification of epidermal growth factor receptor and c-erbB2 pathway inhibitors by correlation with gene expression patterns. *J. Natl. Cancer Inst.* 89, 1505–1515. doi: 10.1093/jnci/89.20.1505
- Yu, J. S., Ramasamy, T. S., Murphy, N., Holt, M. K., Czapiewski, R., Wei, S. K., et al. (2015). PI3K/mTORC2 regulates TGF-beta/Activin signalling by modulating Smad2/3 activity via linker phosphorylation. *Nat. Commun.* 6, 7212. doi: 10.1038/ncomms8212

Conflict of Interest Statement: The authors declare that the research was conducted in the absence of any commercial or financial relationships that could be construed as a potential conflict of interest.

Copyright © 2017 Hamdoun, Jung and Efferth. This is an open-access article distributed under the terms of the Creative Commons Attribution License (CC BY). The use, distribution or reproduction in other forums is permitted, provided the original author(s) or licensor are credited and that the original publication in this journal is cited, in accordance with accepted academic practice. No use, distribution or reproduction is permitted which does not comply with these terms.



Quantitative and Systems Pharmacology 3. Network-Based Identification of New Targets for Natural Products Enables Potential Uses in Aging-Associated Disorders

Jiansong Fang^{1*}, Li Gao², Huili Ma¹, Qihui Wu¹, Tian Wu¹, Jun Wu¹, Qi Wang^{1*} and Feixiong Cheng^{3,4*}

¹ Institute of Clinical Pharmacology, Guangzhou University of Chinese Medicine, Guangzhou, China, ² Modern Research Center for Traditional Chinese Medicine, Shanxi University, Taiyuan, China, ³ Department of Cancer Biology, Center for Cancer Systems Biology, Harvard Medical School, Dana-Farber Cancer Institute, Boston, MA, United States, ⁴ Center for Complex Networks Research, Northeastern University, Boston, MA, United States

OPEN ACCESS

Edited by:

Yuhei Nishimura,
Mie University Graduate School of
Medicine, Japan

Reviewed by:

Huixiao Hong,
United States Food and Drug
Administration, United States
Yoshihiro Uesawa,
Meiji Pharmaceutical University, Japan

*Correspondence:

Jiansong Fang
fangjs@gzucm.edu.cn
Qi Wang
wangqi@gzucm.edu.cn
Feixiong Cheng
fxcheng1985@gmail.com

Specialty section:

This article was submitted to
Experimental Pharmacology and Drug
Discovery,
a section of the journal
Frontiers in Pharmacology

Received: 24 August 2017

Accepted: 03 October 2017

Published: 18 October 2017

Citation:

Fang J, Gao L, Ma H, Wu Q, Wu T,
Wu J, Wang Q and Cheng F (2017)
Quantitative and Systems
Pharmacology 3. Network-Based
Identification of New Targets for
Natural Products Enables Potential
Uses in Aging-Associated Disorders.
Front. Pharmacol. 8:747.
doi: 10.3389/fphar.2017.00747

Aging that refers the accumulation of genetic and physiology changes in cells and tissues over a lifetime has been shown a high risk of developing various complex diseases, such as neurodegenerative disease, cardiovascular disease and cancer. Over the past several decades, natural products have been demonstrated as anti-aging interveners via extending lifespan and preventing aging-associated disorders. In this study, we developed an integrated systems pharmacology infrastructure to uncover new indications for aging-associated disorders by natural products. Specifically, we incorporated 411 high-quality aging-associated human genes or human-orthologous genes from *mus musculus* (MM), *saccharomyces cerevisiae* (SC), *caenorhabditis elegans* (CE), and *drosophila melanogaster* (DM). We constructed a global drug-target network of natural products by integrating both experimental and computationally predicted drug-target interactions (DTI). We further built the statistical network models for identification of new anti-aging indications of natural products through integration of the curated aging-associated genes and drug-target network of natural products. High accuracy was achieved on the network models. We showcased several network-predicted anti-aging indications of four typical natural products (caffeic acid, metformin, myricetin, and resveratrol) with new mechanism-of-actions. In summary, this study offers a powerful systems pharmacology infrastructure to identify natural products for treatment of aging-associated disorders.

Keywords: quantitative and systems pharmacology, natural products, target identification, aging, network-based

INTRODUCTION

Aging is a complex biological process accompanied by accumulation of degenerative damages as well as the decline of various physiological function, leading to the death of an organism ultimately (Fontana et al., 2010; Lopez-Otin et al., 2013; Vaiserman et al., 2016). As an inevitable outcome of life, aging is a primary risk factor for various complex diseases, including cancer, cardiovascular

diseases, and neurodegenerative disease (Kaeberlein et al., 2015; Vaiserman and Marotta, 2016). Thus, development of novel agents for delaying or preventing aging-associated disorders plays essential roles during drug discovery and development.

Natural products have been demonstrated preclinical or clinical efficiency for developing anti-aging interveners with few side effects (Ding et al., 2017). Over the past few decades, several natural products have been reported as anti-aging agents to extend lifespan and prevent aging-associated diseases in various organism and animal models (Pan et al., 2012; Correa et al., 2016). Currently, over 300,000 natural products have been available for drug discovery and development (Banerjee et al., 2015). Among of them, 547 natural products and derivatives have been approved by U.S. Food and Drug Administration (FDA) for treating or preventing various disorders by the end of 2013 (Patridge et al., 2016). There is pressing need of novel approaches or tools for systematic identification of natural products with novel pharmacotherapeutic mechanism-of-action for treatment of aging-associated disorders.

Traditional drug target identification includes ligand-based and structure-based approaches, such as machine learning and molecular docking (Fang et al., 2013, 2017b). However, machine learning is limited by high quality of negative samples as well as overfitting issues on small training sets, while molecular docking is constrained by lack of available crystallographic three-dimensional (3D) structures of proteins. To overcome the pitfalls of traditional approaches, several network-based approaches for prediction of drug-target interaction (DTI) have been proposed recently (Cheng et al., 2012a,b; Wu et al., 2016, 2017). These approaches have showed a great promise in drug discovery and development, since they do not rely on either 3D structures of proteins or negative DTIs.

Quantitative and systems pharmacology refers to a multidisciplinary approach for the emerging development of efficacious drugs with novel mechanisms via integration of experimental assays and computational strategies (Vicini and van der Graaf, 2013; Fang et al., 2017b,c). In the past decade, systems pharmacology-based approaches have demonstrated advance in drug discovery and development (Lu et al., 2015; Cheng et al., 2016; Fang et al., 2017a). For example, a recent study has reported a systems pharmacology approach for identifying new anticancer indications via integrating drug-gene signatures from the connectivity map into the cancer driver genes derived from tumor-normal matched whole-exome sequencing data (Cheng et al., 2016). They identified several new anticancer indications of resveratrol with new molecular mechanisms. Recently, the same group further proposed a system pharmacology approach that facilitated to identify new anticancer indications of natural products through integration of known DTI network into significantly mutated genes in cancer (Fang et al., 2017a). The high-confidence anticancer indications were identified computationally and further validated by various literatures on four natural products, including resveratrol, quercetin, fisetin, and genistein. They showed that integration of the computationally predicted DTIs could significantly enhance the success rate of identifying new anticancer indications of natural products via reducing the incompleteness of known drug-target

networks. The aforementioned examples have shed light on the systems pharmacology-based approaches for drug discovery through exploiting the polypharmacology of natural products with pleiotropic effects for treatment of various complex diseases (Fang et al., 2017b).

In this study, we further proposed an integrated systems pharmacology framework (**Figure 1**) to identify new targets of natural products for potential treatment of aging-associated disorders. Specifically, we manually collected high-quality aging-associated human genes or human-orthologous genes covering four species: *caenorhabditis elegans* (CE), *drosophila melanogaster* (DM), *mus musculus* (MM), and *saccharomyces cerevisiae* (SC). We reconstructed a global DTI network of natural products by integrating both experimentally reported and computationally predicted DTIs from our previous predictive network models (Wu et al., 2016; Fang et al., 2017c). Finally, we built the statistical network models with high accuracy to prioritize new anti-aging indications of natural products through integration of the curated aging-associated genes and drug-target network of natural products. We computationally identified anti-aging indications of multiple natural products with novel molecular mechanisms, providing potential promising candidates for further treatment of aging-associated diseases. Taken together, this study offers a powerful systems pharmacology infrastructure for identification of natural products with new mechanism-of-action for potential treatment of aging-associated disorders.

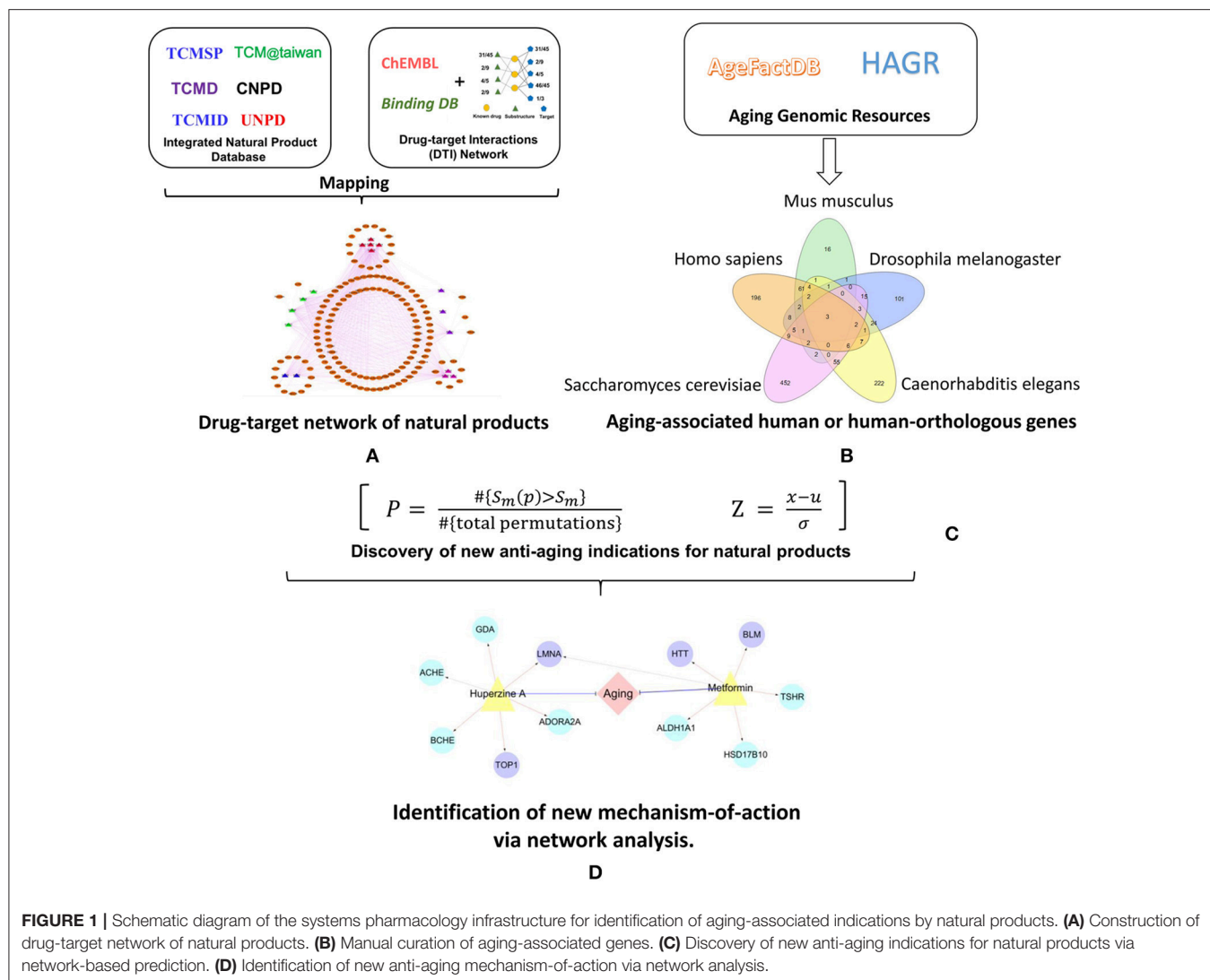
MATERIALS AND METHODS

Manual Curation of Aging-Associated Genes

Aging-associated genes (AAGs) were collected from two comprehensive databases: the JenAge Ageing Factor Database (AgeFactDB) (Huhne et al., 2014) and Human Ageing Genomic Resources database (HAGR) (Tacutu et al., 2013). AgeFactDB collects and integrates aging phenotype data with both experimental and computational evidence, while HAGR only contains AAGs from experiments. In this study, we only extracted AAGs from AgeFactDB and HAGR with well-known experimental evidences across five organisms: *Homo sapiens* (HS), CE, DM, MM, and SC. After removing the duplicated genes between two databases, we obtained 309 (HS), 194 (DM), 1,012 (SC), 1,149 (CE), and 143 (MM) AAGs, respectively. We then obtained high-quality human-orthologous AAGs via mapping human-orthologous genes across four species (CE, DM, MM, and SC) from ensemble database (<http://www.ensembl.org/index.html>). Finally, 169 (DM), 555 (SC), 331 (CE), and 96 (MM) human-orthologous AAGs were collected (**Table S1**).

Construction of a Known Drug-Target Network of Natural Products

We firstly integrated comprehensive natural products from six publically available natural product-related data sources: traditional Chinese medicine database (TCMDb) (He et al., 2001), Chinese natural product database (CNPD) (Shen et al., 2003), traditional Chinese medicine integrated database



(TCMID) (Xue et al., 2013), traditional Chinese medicine systems pharmacology (TCMSP) (Ru et al., 2014), traditional Chinese medicine database@Taiwan (TCM@Taiwan) (Chen, 2011), and universal natural product database (UNPD) (Gu et al., 2013). For each data source, we converted its initial structure format (e.g., mol2) into unified SDF format. Secondly, we merged the unified SDF files from the six data sources into single SDF file, and removed the duplicated natural products according to InChIKey by Open Babel (v2.3.2) (O'Boyle et al., 2011). Finally, 259,547 unique natural products were collected. The details are provided in our previous study (Fang et al., 2017a,c).

To construct a global drug-target network of natural products, we pooled DTIs from two commonly used databases: ChEMBL (v21) (Bento et al., 2014) and BindingDB (v19, accessed in June 2016) (Gilson et al., 2016). All chemical structures were carefully standardized via removing salt ions and standardizing dative bonds using Open Babel toolkit (v2.3.2). We further filtered DTIs with the following five criteria: (i) K_i , K_d , IC_{50} , or $EC_{50} \leq 10 \mu M$; (ii) the target organism should be homo sapiens;

(iii) the target has a unique UniProt accession number; (iv) compound can be transformed to canonical SMILES format; and (v) compound has at least one carbon atom. Subsequently, we extracted experimentally validated DTIs for 2,349 natural products after mapping 259,547 unique natural products into the global DTIs using the "InChIKey."

Prediction of New Drug-Target Interactions of Natural Products

In a recent study, we have developed predictive network models to predict targets of natural products via a balanced substructure-drug-target network-based inference (bSDTNBI) (Fang et al., 2017c; Wu et al., 2017) approach. The bSDTNBI utilizes resource-diffusion processes to prioritize potential targets for both known drugs and new chemical entities (NCEs) via substructure-drug-target network (Wu et al., 2016). The substructure-drug (or NCE)-target network was built via integrating the known DTI network, drug-substructure associations and NCE-substructure associations. Two parameters

were introduced to balance the initial resource allocation of different node types (α) and the weighted values of different edge types (β), respectively. The third parameter γ was imported to balance the influence of hub nodes in resource-diffusion processes. The fourth parameter k denotes for the number of resource diffusion processes. Herein, four parameters ($\alpha = \beta = 0.1$, $\gamma = -0.5$, and $k = 2$) in bSDTNBI were adopted based on our previous study (Wu et al., 2016). Here, the predictive model based on KR molecular fingerprint (bSDTNBI_KR) with the best performance was used to predict the new targets of natural products and top 20 predicted candidates were used (Wu et al., 2016, 2017).

Identification of New Anti-aging Indications for Natural Products

Here, we further proposed an integrated statistical network model to prioritize new anti-aging indications of natural products by incorporating DTI network of natural products and the manually curated AAGs. We asserted that a natural product with polypharmacological profiles exhibits a high possibility to treat an aging-associated disorder if its targets are more likely to be aging-associated proteins (AAPs). Then we utilized a permutation testing to estimate the statistical significance of a natural product to be prioritized for anti-aging indications. The null hypothesis asserts that targets of a natural product randomly locate at AAPs across the human proteome. The permutation testing was performed as below:

$$P = \frac{\# \{S_m(p) > S_m\}}{\# \{\text{total permutations}\}} \quad (1)$$

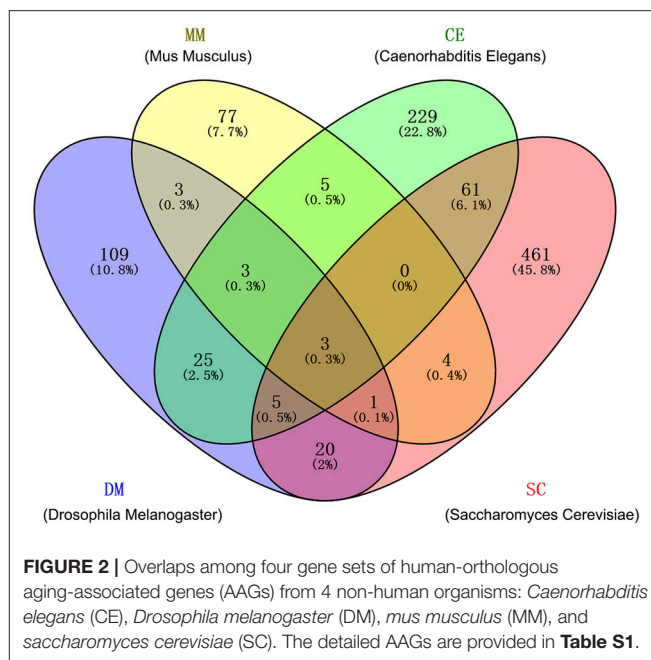
A nominal P was computed for each natural product by counting the number of observed AAPs greater [$S_m(p)$] than the permutations (S_m). Here we repeated 100,000 permutations by randomly selecting 441 proteins (the same number of AAPs) from protein products at the genome-wide scale, 20,462 human protein-coding genes from the National Center for Biotechnology Information (NCBI) database (Coordinators, 2017; Table S2). Subsequently, the nominal P -values from the permutation tests were corrected as adjusted P -values (q) based on Benjamini-Hochberg approach (Benjamini and Hochberg, 1995) using R package (v3.01). In addition, a Z -score was calculated for each natural product to be prioritized for anti-aging indications during permutation testing:

$$Z = \frac{x - \mu}{\sigma} \quad (2)$$

where x is the real number of AAPs targeted by a given natural product, μ is the mean number of AAPs targeted by a given natural product during 100,000 permutations, and σ is the standard deviation.

Network and Statistical Analysis

The statistical analysis in this study was carried out using the Python (v3.2, <http://www.python.org/>) and R platforms (v3.01, <http://www.r-project.org/>). Networks were visualized by Cytoscape (v3.2.0, <http://www.cytoscape.org/>).



RESULTS

A Catalogue of Aging-Associated Genes

We collected the high-quality human-orthologous AAGs from four species: CE, DM, MM, and SC. In total, 1,006 human-orthologous AAGs identified in at least one species with literature-reported experimental evidences were collected after removing the duplicated AAGs (Figure 2). Among 1,006 genes, 130 human-orthologous AAGs are reported in at least two non-human organisms (CE, DM, MM and SC) simultaneously. Meanwhile, 12 human-orthologous AAGs (e.g., *AKT1*, *CAT*, *GABARAP*, *MAPK8*, *MAPK9*, *MAPK10*, *MTOR*, *PRDX1*, *PRDX2*, *RPS6KBI*, *SIRT1*, and *SOD2*) were included in at least three non-human organisms. To improve the quality of gene set, we only selected the 130 human-orthologous AAGs identified in at least two non-human organisms. We found that 130 human-orthologous AAGs are significantly enriched with 309 human AAGs (28 overlapping genes, $P = 1.7 \times 10^{-24}$, Fisher's exact test). Finally, we pooled 130 human-orthologous AAGs and 309 human AAGs and generated 411 AAGs (Table S3) for building the statistical network models.

Reconstruction of Anti-aging Drug-Target Network for Natural Products

We constructed a global drug-target network of natural products by integrating 7,314 high-quality experimental DTIs as well as 11,940 new computational predicted DTIs as described in our recent study (Fang et al., 2017c). The global DTI network (Table 1) was consisted of 17,223 DTIs connecting 2,349 unique natural products and 732 targets. The average experimental target degree (connectivity) of a natural product is 2.97, which is significantly stronger than the average degree 2.22 of non-natural product drugs in DrugBank database ($P = 6.81 \times 10^{-72}$, one-side

TABLE 1 | The statistics of global drug-target interactions (DTI) network and local DTI network for natural products.

Data set	N_D	$N_T(N_{AT})$	N_{DTI}	Sparsity (%)
Global DTI network	2,349	732 (101)	17,223	1.00
Local DTI network	224	494 (70)	2408	2.17

Local DTI network: a specific drug-target network by focusing on FDA-approved or clinically investigational natural products, N_D , the number of natural products; N_T , the number of targets; N_{AT} , the number of aging-associated targets; N_{DTI} , the number of DTIs; Sparsity, the ratio of N_{DTI} to the number of all possible DTIs.

Wilcoxon test). The detailed DTI pairs are provided in **Table S4**. We further built a specific drug-target network by focusing on FDA-approved or clinically investigational natural products (**Table S4**). **Figure 3** displays a bipartite drug-target network of 2,408 DTIs connecting 224 FDA-approved or clinically investigational natural products and 494 targets encoded by 70 AAGs and 424 non-AAGs. Network analysis shows that the average connectivity of experimentally known targets for each natural product in this network is 6.26, which is significantly stronger than that (average degree = 2.22) of non-natural products drugs in DrugBank ($P = 4.34 \times 10^{-50}$, one-side Wilcoxon test, **Table S5**). Among 224 FDA-approved or clinically investigational natural products, eight natural products have connectivity ($K > 25$): quercetin ($K = 73$), ellagic acid ($K = 56$), apigenin ($K = 43$), haloperidol ($K = 32$), myricetin ($K = 32$), resveratrol ($K = 30$), genistein ($K = 26$), and dopamine ($K = 25$). Meanwhile, among 70 targets encoded by AAGs, 6 are targeted by over 15 natural products (D): LMNA ($D = 79$), MAPT ($D = 33$), BLM ($D = 22$), HIF1A ($D = 22$), TP53 ($D = 20$), and NFKB1 ($D = 16$), based on current available experimental data. The targets encoded by these AAGs play essential roles in aging-associated diseases. For example, products encoded by LMNA are primarily lamin A and C. Alterations in lamin A and C were reported to accelerate physiological aging via nuclear envelope budding (Li Y. et al., 2016). A recent study also showed that nuclear factor-kappa B (NF- κ B) inhibition could delay the onset of aging symptoms in mice via reducing DNA damage (Tilstra et al., 2012).

Chemical Diversity Analysis of Natural Products Targeting Aging-Associated Proteins

We extracted 1,877 natural products targeting AAP via mapping 411 high-quality human or human-orthologous AAGs into the global drug-target network of natural products. Clustering analysis was performed to examine chemical scaffolds of 1,877 natural products by measuring the root-mean-square value of the Tanimoto distance based on FCFP₆ fingerprint implemented in Discovery Studio 4.0 (version 4.0, Accelrys Inc.). The 1,887 natural products are clustered into 10 groups with cluster centers: 1,2-propanediol, luteolin, tetrahydroalstoin, ZINC03870415, chryseriol, benzamide, p-toluidine, L-His, cis-10-octadecenoic acid, and 3-epioleanolic acid, respectively (**Figure 4A**). The structures of each cluster center are shown in **Figure 4B**.

Among them, cluster 5 (Cluster center: Chryseriol) and cluster 2 (Cluster center: Luteolin) are grouped as flavonoids, with the largest number of natural products. The structures in cluster 3 and cluster 9 are represented as alkaloids, while the structures in cluster 8 are represented as unsaturated aliphatic hydrocarbon or unsaturated fatty acid. Overall, 1887 natural products share diverse chemical scaffolds (**Figure 4**), providing a valuable resource for systems pharmacology-based anti-aging drug discovery.

Mechanism-of-Action of Anti-aging Indications by Natural Products

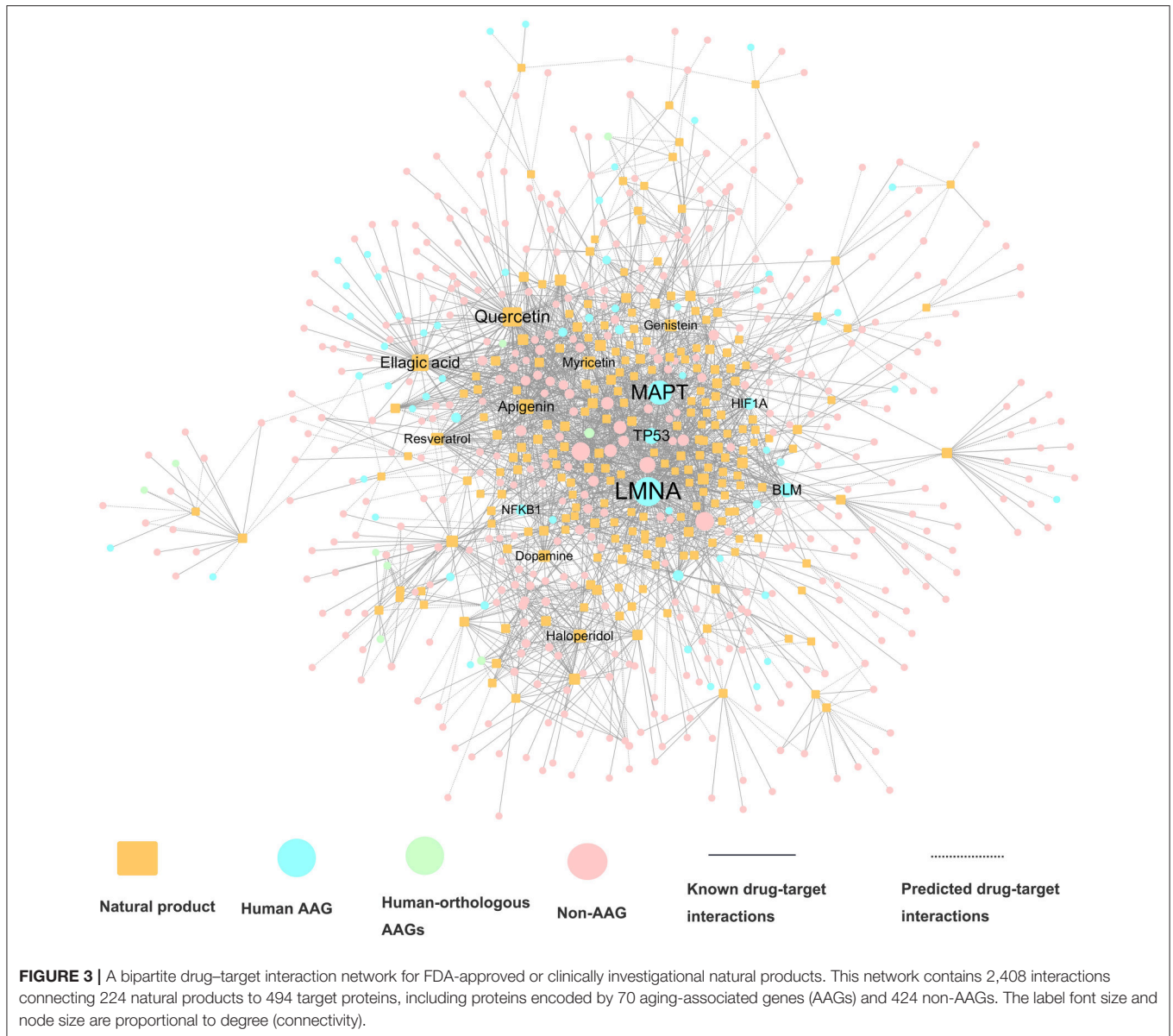
To investigate the anti-aging mechanism-of-action (MOA) of natural products, we performed KEGG pathway, molecular function, and biological process enrichment analysis using ClueGO (Bindea et al., 2009). Here, we focused on 54 AAPs with connectivity larger than 10 in the global drug-target network of natural products (**Table S6**). **Figure S1** showed that 54 anti-aging targets are significantly enriched in several aging-associated pathways: longevity regulating pathway (adjusted- $P = 1.9 \times 10^{-5}$), MAPK signaling pathway (adjusted- $P = 1.6 \times 10^{-5}$), ERBB signaling pathway (adjusted- $P = 7.8 \times 10^{-7}$), estrogen signaling pathway (adjusted- $P = 3.3 \times 10^{-4}$), and insulin signaling pathway (adjusted- $P = 2.1 \times 10^{-3}$) (Hall et al., 2017). Similar trends were observed for molecular function and biological process enrichment analyses (**Table S7**). To further showcase the aging-associated mechanisms, we selected four typical natural products: caffeic acid, hesperetin, myricetin and resveratrol.

Caffeic Acid

Caffeic acid is a natural phenol found in fruits, tea and wine (Magnani et al., 2014), with a wide range of aging-associated pharmacological activities, such as antioxidant (Deshmukh et al., 2016), anti-inflammatory (da Cunha et al., 2004), and neuroprotective (Pereira et al., 2006). For example, caffeic acid phenethyl ester (CAPE) was reported to extend lifespan in CE via regulation of the insulin-like IGF-1 signaling pathway (Havermann et al., 2014). The detailed molecular mechanisms of anti-aging effects by caffeic acid remain unclear. **Figure 5** shows that caffeic acid interacts with 5 AAPs (LMNA, MAPT, NFKB1, PTPN1 and MAPK1) and 22 non-AAPs, consisting of 23 experimentally validated and 4 computationally predicted ones. Protein tyrosine phosphatase 1B (PTP1B), encoded by *PTPN1*, is a potential target for treatment of type-2 diabetes (Gonzalez-Rodriguez et al., 2012) and Alzheimer's disease (Vieira et al., 2017). A recent study showed that caffeic acid is a moderate inhibitor of PTP1B with an IC_{50} value of $3.06 \mu\text{M}$ (He et al., 2009).

Hesperetin

Hesperetin is flavanone abundant in citrus fruits with a wide range of biological activities. Recent studies revealed the potential antioxidant, neuroprotective, and anti-inflammatory properties (Parhiz et al., 2015; Miler et al., 2016), by hesperetin. Furthermore, a recent clinical trial (NCT02095873) has reported that hesperetin in combination with trans-resveratrol can



prevent and alleviate early-stage of aging-associated disorders (Xue et al., 2016). Network analysis reveals that hesperetin binds with 9 targets (6 AAPs and 3 non-AAPs), including 4 computationally predicted targets and 5 experimentally reported ones. Interestingly, 4 predicted anti-aging targets (MAPT, LMNA, TP53, and NFKB1) suggest potential underlying anti-aging mechanisms by hesperetin. For example, a previous study revealed that hesperetin modulated the aging-associated NF- κ B pathway in the kidney of rats (Kim et al., 2006).

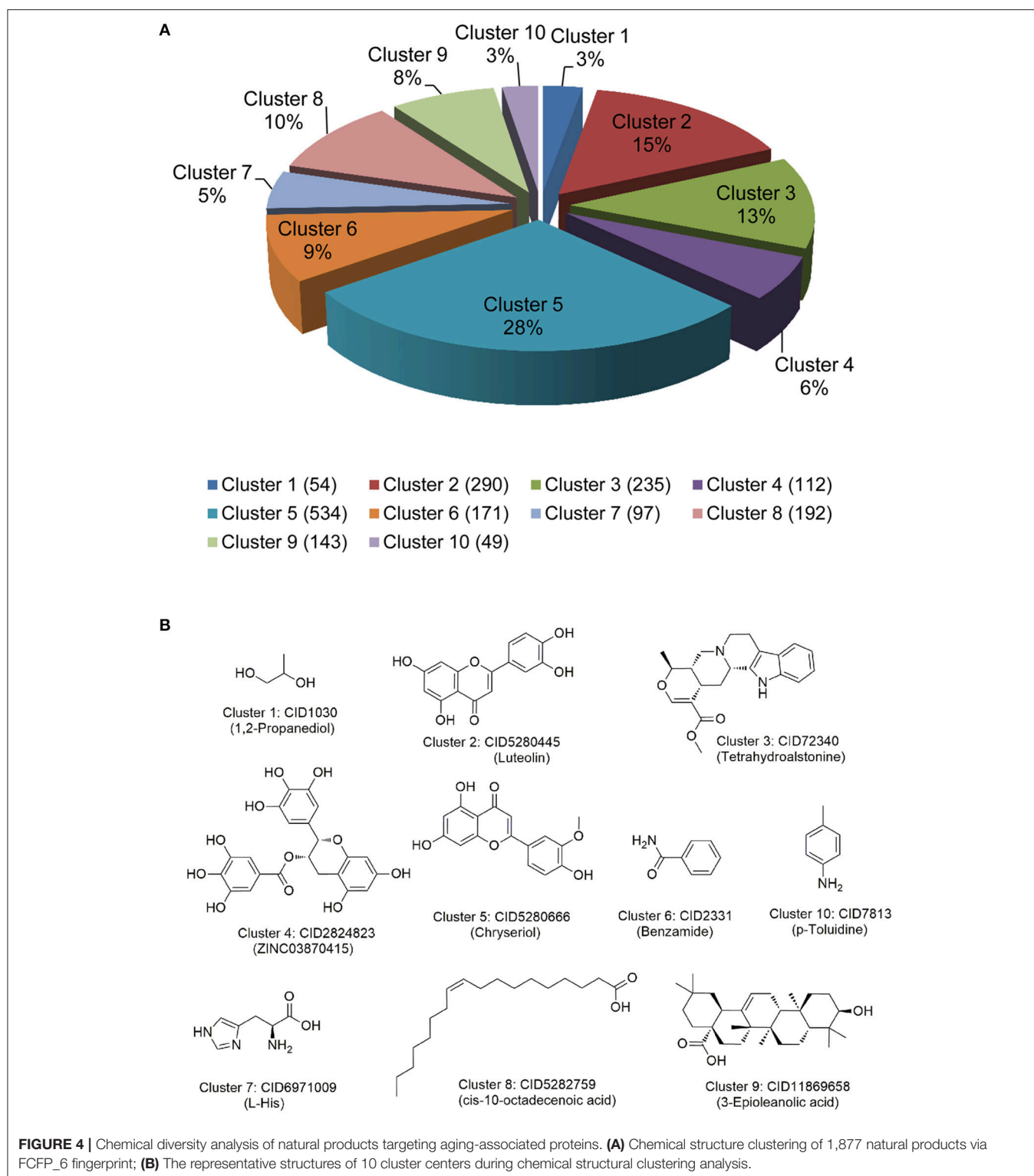
Myricetin

Myricetin, a common plant-derived flavonoid, displays several pharmacological activities against aging-associated indications, such as anti-aging (Aliper et al., 2016), antioxidant (Wang et al., 2010), anti-inflammatory (Lee et al., 2007), and

immunomodulatory (Fu et al., 2013) effects. **Figure 5** shows that myricetin binds with 11 AAPs and 25 non-AAPs, consisting of 4 computationally predicted targets (TP53, LMNA, ELAVL1, and KMT2A) and 32 experimentally reported ones. A recent study has suggested that myricetin can extend lifespan in *Caenorhabditis elegans* via modulating aging-related transcription factors (Buchter et al., 2013).

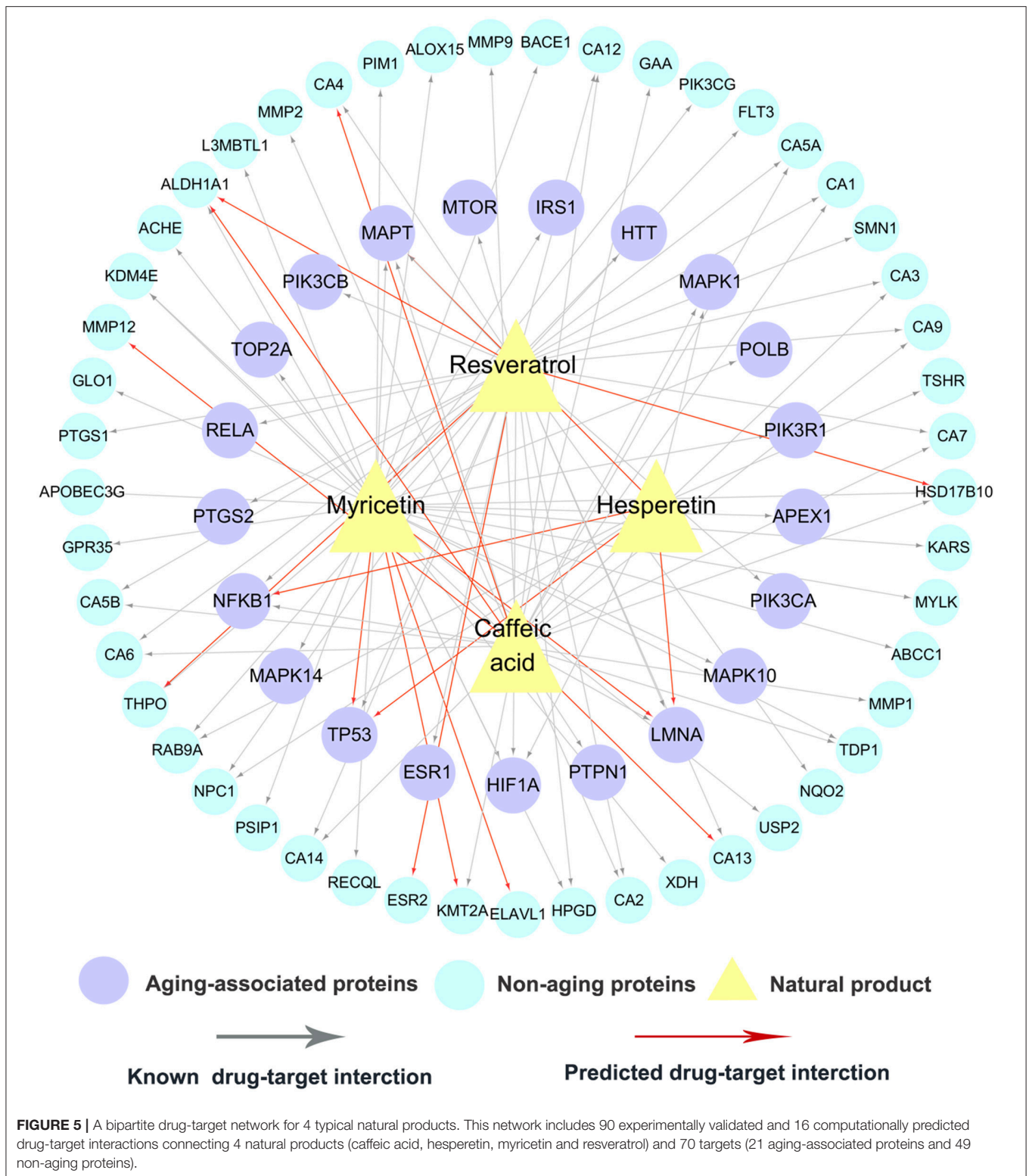
Resveratrol

Resveratrol, a non-flavonoid polyphenol abundant in the skin of grapes, displays a broad spectrum of anti-aging effects (Gines et al., 2017). Currently, over 20 clinical trials (<http://clinicaltrials.gov/>) are being conducted or completed to treat aging or aging-associated disorders by resveratrol, such as anti-aging (NCT02523274 and NCT02909699), aging-associated



macular degeneration (NCT02625376), and Alzheimer's disease (NCT01504854). **Figure 5** indicates that resveratrol interacts with 12 AAPs: ESR1, HIF1A, HTT, LMNA, MAPT, MTOR, NFKB1, PIK3CA, PIK3CB, PTGS2, RELA, and TP53, suggesting

new potential anti-aging mechanisms of resveratrol. For example, two AAPs: estrogen receptor alpha (ER-alpha) and cyclooxygenase-2 (COX-2), play crucial role on the pathogenesis of several aging-associated diseases, such as Alzheimer's disease



and osteoporosis (Kermath et al., 2014; Kim et al., 2016). Resveratrol was reported to bind to ER-alpha with a K_i value of $0.78 \mu\text{M}$ (de Medina et al., 2005) and inhibit COX-2 with an IC_{50} value of $0.99 \mu\text{M}$ (Kang et al., 2009).

Taken together, aforementioned examples demonstrated that network analysis could assist to identify new potential anti-aging mechanisms of natural products. Systems pharmacology-based integration of drug-target networks and known AAPs would

enable to identify new natural products for treatment of aging-associated diseases.

Discovery of Potential Anti-aging Indications for Natural Products with Novel Mechanism-of-Action

We further built statistical network models for comprehensive identification of new anti-aging indications of natural products through integrating both experimentally reported and computationally predicted drug-target network into the curated APPs (see section Materials and Methods). Here, we focused on 224 FDA-approved or clinical investigational natural products annotated in DrugBank database (Law et al., 2014). **Table 2** summarizes number of the predicted anti-aging indications for the experimentally reported drug-target network only and the pooled data from both experimentally reported and computationally predicted drug-network, respectively. We only identified 56 natural products with significantly predicted anti-aging indications ($q < 0.05$) using the experimentally reported drug-target network, while we identified 143 natural products with significantly predicted anti-aging indications ($q < 0.05$) via integration of both experimentally reported and computationally predicted drug-target networks (**Table S8**). Interestingly, among 143 natural products, 92 natural products cannot be identified to have significant anti-aging indications using experimentally reported drug-target network only, including some well-known anti-aging natural products (e.g., metformin, vitamin E, and huperzine A). We systematically retrieved previously anti-aging reported data from PubMed for 73 FDA-approved natural products out of 143 ones. The detailed experimental evidences are provided in **Table S9**. Then we found 23 natural products [with a success rate of 31.5% (23/73)] with reported experimental data. This suggests a reliable accuracy of our proposed network model. The remaining 50 natural products without experimental data provide potential anti-aging candidates that deserve to be validated by various experimental assays in the future.

In summary, we showed that integration of computationally predicted drug-target network could improve the chance to identify new anti-aging indications of natural products via increasing completeness of current drug-target network. We next chose three typical natural products (metformin, vitamin E, and

huperzine A) as case studies to illustrate the predicted anti-aging indications with new mechanism-of-actions.

Metformin

Metformin, originating from *Galega officinalis*, is a biguanide drug widely used in clinical practice for treating type-2 diabetes. Nowadays, metformin is currently being tested as an anti-aging drug in several clinical trials, such as NCT02432287 and NCT02308228 (Barzilai et al., 2016). **Figure 6** shows that metformin binds with 3 AAPs (BLM, HTT, and LMNA) and 3 non-APPs. In our network model, metformin was predicted to have significant anti-aging indication ($Z = 8.42$, $q < 10^{-5}$) via integration of one experimentally validated target and five predicted ones. There is no significant anti-aging indication for metformin based on experimentally validated DTI only. Previous studies have shown that metformin extended lifespan in several model organisms (Anisimov, 2013; Cabreiro et al., 2013; Martin-Montalvo et al., 2013). **Figure 6** shows several potential anti-aging mechanisms of metformin, including inhibition of the inflammatory pathway, activation of AMP-activated kinase (AMPK), and inducing autophagy (Moiseeva et al., 2013; Foretz et al., 2014; Song et al., 2015).

Vitamin E

Vitamin E, the most potent antioxidant, protects cells from damage related to oxidative stress (La Fata et al., 2014). Vitamin E supplementation has been reported to delay or prevent aging and inflammatory aging-associated diseases via prolonging the life span in several model organisms (Navarro et al., 2005; Mocchegiani et al., 2014). However, mechanism-of-action of anti-aging effects by vitamin E remains unclear. **Figure 6** shows that vitamin E interacts with 2 known and 4 predicted targets, consisted of 3 AAPs (TP53, LMNA, and MAPT) as well as 3 non-AAPs. In our network model, vitamin E was predicted to show potential for anti-aging indication ($Z = 8.32$, $q < 10^{-5}$) based on the pooled data of experimentally validated and computationally predicted DTIs. However, there is no significance based on experimentally validated DTIs only. Among 4 predicted targets, TP53, a well-known AAP, regulates cell cycle progression, apoptosis, and cellular senescence. A recent study reported that vitamin E significantly down-regulated TP53 expression in senescent cells, indicating a potential anti-aging mechanism of vitamin E (Durani et al., 2015).

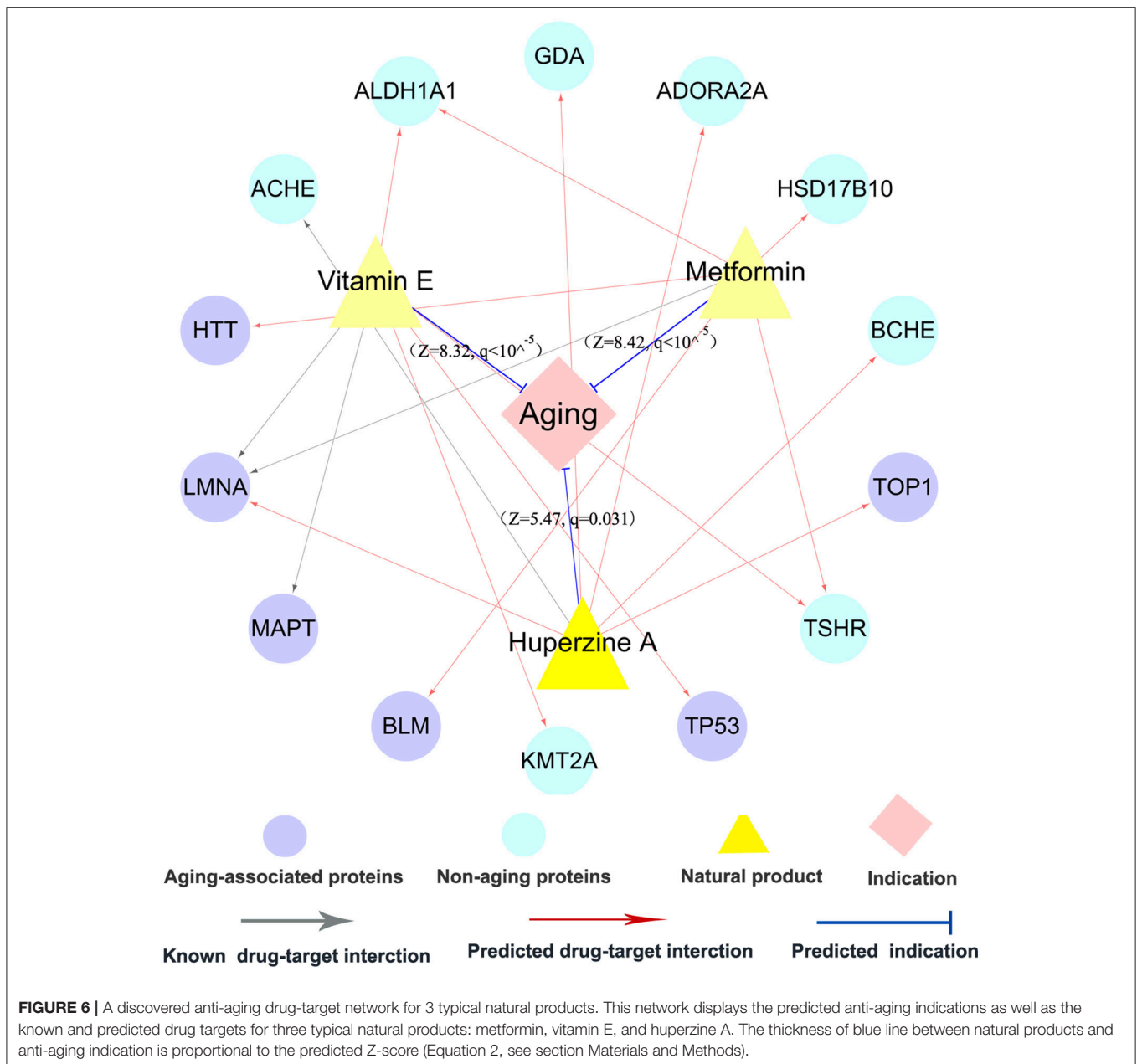
Huperzine A

Huperzine A (HupA), a natural acetylcholinesterase (ACHE) inhibitor derived from *Huperzia serrate*, is a licensed anti-Alzheimer drug in China (Qian and Ke, 2014). HupA was reported to show various anti-inflammatory, neuroprotective, and anti-aging properties (Ruan et al., 2013; Damar et al., 2016). **Figure 6** reveals that HupA binds with one experimentally reported target (ACHE) and 5 computationally predicted targets (BCHE, GDA, LMNA, TOP1, and ADORA2A). Among five predicted targets, LMNA and TOP1 are experimentally reported AAPs (Li Y. et al., 2016). Here, HupA was predicted to have significant anti-aging indication ($Z = 5.47$, $q = 0.031$) via the integration of both experimentally reported and computationally

TABLE 2 | Summary of the newly predicted anti-aging indications of natural products based on the experimentally reported drug-target network only (ExpNet) and the combination of the experimentally reported and computationally predicted (ExpNet&ComNet) drug-target networks, respectively.

Data source	Number of DTIs (number of targets, number of drugs)	# N_{sal} ($q < 0.05$)	# N_{sal} ($q < 1/10^{-5}$)
ExpNet	1,163 (361, 113)	56	28
ExpNet&ComNet	2,408 (494, 224)	143	87

N_{sal} denotes to the number of natural products with significantly predicted anti-aging indication.



predicted targets, while no significance using the experimentally reported targets alone. Oxidative stress accelerates the chronic inflammatory process during aging and aging-associated diseases (Cannizzo et al., 2011). A previous study showed that HupA alleviated oxidative stress-induced inflammatory damage in aging rat (Ruan et al., 2014).

Put together, we have suggested that our network model provided a useful tool for systematic identification of natural products for treatment of aging-associated disorders with novel molecular mechanisms. Some newly predicted anti-aging indications of natural products and the according mechanisms are suggested to be experimentally validated before clinical uses, which we hope to be promoted by findings shown here.

DISCUSSION

Natural products are valuable pharmaceutical wealth and show great promise for developing anti-aging agents (Ding et al., 2017). In this study, we developed an integrated systems pharmacology infrastructure to identify new targets of natural products for treatment of aging-associated diseases. This computational infrastructure is consisted of three key components: (i) reconstructing DTI networks of natural products via integrating known and computationally predicted DTIs; (ii) curation of high-quality aging-associated human or orthologous genes from various aging-related bioinformatics sources; (iii) building statistical network models

to prioritize new aging-associated indications of natural products through integrating data from aforementioned two steps. Overall, this framework has several advantages. First, we found that assembling computationally predicted drug-target network could identify more significant anti-aging indications for natural products by increasing completeness of currently known drug-target network. Second, our systems pharmacology-based approach is independent of three-dimensional (3D) structure of targets, which can be applied in human targets without known 3D structures (e.g., membrane proteins).

There are still several potential limitations in the current systems pharmacology model. First, antagonistic or agonistic effects of drug-target pairs have not been considered. Drug-induced gene expression database, such as the Connectivity Map (CMap), has provided specific biological functions (upregulation or downregulation) (Lamb et al., 2006). Integration of large-scale gene expression profiles of natural products may help improve performance of our network model (Cheng et al., 2016). In addition, current approach can only predict the potential aging-associated indications of natural products targeting known or predicted AAPs. Integrating systems biology resources may assist on identifying the growing potential AAPs by indirectly targeting their neighbors in the human protein-protein interaction network, gene regulatory network, or biological pathways (Li et al., 2014; Li J. et al., 2016). Finally, we only focused on three well-known natural products (metformin, vitamin E, and huperzine A) with more available literature-reported data for validation. Further *in vitro* or *in vivo* experimental assays should be performed to validate the predicted DTIs and anti-aging effects of natural products before preclinical and clinical studies.

AUTHOR CONTRIBUTIONS

JF and FC conceived the project. FC and QWa provided supervision. JF and LG performed the research. JF, HM, QWu, TW, JW, and FC analyzed the data. JF and FC wrote the article.

REFERENCES

- Aliper, A., Belikov, A. V., Garazha, A., Jellen, L., Artemov, A., Sunstova, M., et al. (2016). In search for geroprotectors: *in silico* screening and *in vitro* validation of signalome-level mimetics of young healthy state. *Aging (Albany, NY)* 8, 2127–2152. doi: 10.18632/aging.101047
- Anisimov, V. N. (2013). Metformin: do we finally have an anti-aging drug? *Cell Cycle* 12, 3483–3489. doi: 10.4161/cc.26928
- Banerjee, P., Erehman, J., Gohlke, B. O., Wilhelm, T., Preissner, R., and Dunkel, M. (2015). Super natural II—a database of natural products. *Nucleic Acids Res.* 43, D935–D939. doi: 10.1093/nar/gku886
- Barzilai, N., Crandall, J. P., Kritchevsky, S. B., and Espeland, M. A. (2016). Metformin as a tool to target aging. *Cell Metab.* 23, 1060–1065. doi: 10.1016/j.cmet.2016.05.011
- Benjamini, Y., and Hochberg, Y. (1995). Controlling the false discovery rate: a practical and powerful approach to multiple testing. *J. R. Stat. Soc. B* 57, 289–300.
- Bento, A. P., Gaulton, A., Hersey, A., Bellis, L. J., Chambers, J., Davies, M., et al. (2014). The ChEMBL bioactivity database: an update. *Nucleic Acids Res.* 42, D1083–D1090. doi: 10.1093/nar/gkt1031

ACKNOWLEDGMENTS

This work was supported by the National Natural Science Foundation of China (Grants 81603318), Guangzhou Science Technology and Innovation Commission Technology Research Projects, and the National Heart, Lung, and Blood Institute of the National Institutes of Health under Award Number K99HL138272 to FC.

SUPPLEMENTARY MATERIAL

The Supplementary Material for this article can be found online at: <https://www.frontiersin.org/articles/10.3389/fphar.2017.00747/full#supplementary-material>

Figure S1 | Pathway, biological, functional enrichment analyses of 54 aging-associated targets in global drug-target network of natural products. **(A)** KEGG pathway enrichment analysis; **(B)** Biological process enrichment analysis; **(C)** Molecular function enrichment analysis.

Table S1 | List of 1,460 curated aging-associated genes (AAGs) across five organisms.

Table S2 | List of 20,462 human protein-coding genes from the NCBI database.

Table S3 | List of 411 essential human or human-orthologous aging-associated genes (AAGs).

Table S4 | The detailed information of two drug-target interaction (DTI) networks (a global DTI network and a specific DTI network for FDA-approved or clinically investigational natural products).

Table S5 | The detailed information of known experimental targets for both natural products and non-natural products collected from DrugBank for Wilcoxon test.

Table S6 | List of 54 aging-associated proteins of which degree (connectivity) were higher than 10.

Table S7 | The detailed information for ClueGO analysis.

Table S8 | List of predicted indications of natural products based on experimental drug-target network only and the pooled drug-target network from both computationally predicted and experimentally validated drug-target interactions.

Table S9 | The anti-aging reported data in PubMed for 73 FDA-approved natural products.

- Bindea, G., Mlecnik, B., Hackl, H., Charoentong, P., Tosolini, M., Kirilovsky, A., et al. (2009). ClueGO: a Cytoscape plug-in to decipher functionally grouped gene ontology and pathway annotation networks. *Bioinformatics* 25, 1091–1093. doi: 10.1093/bioinformatics/btp101
- Buchter, C., Ackermann, D., Havermann, S., Honnen, S., Chovolou, Y., Fritz, G., et al. (2013). Myricetin-mediated lifespan extension in *Caenorhabditis elegans* is modulated by DAF-16. *Int. J. Mol. Sci.* 14, 11895–11914. doi: 10.3390/ijms140611895
- Cabreiro, F., Au, C., Leung, K. Y., Vergara-Irigaray, N., Cocheme, H. M., Noori, T., et al. (2013). Metformin retards aging in *C. elegans* by altering microbial folate and methionine metabolism. *Cell* 153, 228–239. doi: 10.1016/j.cell.2013.02.035
- Cannizzo, E. S., Clement, C. C., Sahu, R., Follo, C., and Santambrogio, L. (2011). Oxidative stress, inflamm-aging and immunosenescence. *J. Proteomics* 74, 2313–2323. doi: 10.1016/j.jprot.2011.06.005
- Chen, C. Y. (2011). TCM Database@Taiwan: the world's largest traditional Chinese medicine database for drug screening in silico. *PLoS ONE* 6:e15939. doi: 10.1371/journal.pone.0015939
- Cheng, F., Liu, C., Jiang, J., Lu, W., Li, W., Liu, G., et al. (2012a). Prediction of drug-target interactions and drug repositioning via network-based inference. *PLoS Comput. Biol.* 8:e1002503. doi: 10.1371/journal.pcbi.1002503

- Cheng, F., Zhao, J., Fooksa, M., and Zhao, Z. (2016). A network-based drug repositioning infrastructure for precision cancer medicine through targeting significantly mutated genes in the human cancer genomes. *J. Am. Med. Inform. Assoc.* 23, 681–691. doi: 10.1093/jamia/ocw007
- Cheng, F., Zhou, Y., Li, W., Liu, G., and Tang, Y. (2012b). Prediction of chemical-protein interactions network with weighted network-based inference method. *PLoS ONE* 7:e41064. doi: 10.1371/journal.pone.0041064
- Coordinators, N. R. (2017). Database resources of the National Center for Biotechnology Information. *Nucleic Acids Res.* 45, D12–D17. doi: 10.1093/nar/gkw1071
- Correa, R. C., Peralta, R. M., Haminiuk, C. W., Maciel, G. M., Bracht, A., and Ferreira, I. C. (2016). New phytochemicals as potential human anti-aging compounds: reality, promise, and challenges. *Crit. Rev. Food Sci. Nutr.* doi: 10.1080/10408398.2016.1233860. [Epub ahead of print].
- da Cunha, F. M., Duma, D., Assrey, J., Buzzi, F. C., Niero, R., Campos, M. M., et al. (2004). Caffeic acid derivatives: *in vitro* and *in vivo* anti-inflammatory properties. *Free Radic. Res.* 38, 1241–1253. doi: 10.1080/10715760400016139
- Damar, U., Gersner, R., Johnstone, J. T., Schachter, S., and Rotenberg, A. (2016). Huperzine A as a neuroprotective and antiepileptic drug: a review of preclinical research. *Expert Rev. Neurother.* 16, 671–680. doi: 10.1080/14737175.2016.1175303
- de Medina, P., Casper, R., Savouret, J. F., and Poirot, M. (2005). Synthesis and biological properties of new stilbene derivatives of resveratrol as new selective aryl hydrocarbon modulators. *J. Med. Chem.* 48, 287–291. doi: 10.1021/jm0498194
- Deshmukh, R., Kaundal, M., Bansal, V., and Samardeep (2016). Caffeic acid attenuates oxidative stress, learning and memory deficit in intracerebroventricular streptozotocin induced experimental dementia in rats. *Biomed. Pharmacother.* 81, 56–62. doi: 10.1016/j.biopha.2016.03.017
- Ding, A. J., Zheng, S. Q., Huang, X. B., Xing, T. K., Wu, G. S., Sun, H. Y., et al. (2017). Current perspective in the discovery of anti-aging agents from natural products. *Nat. Prod. Bioprospect.* doi: 10.1007/s13659-017-0135-9. [Epub ahead of print].
- Durani, L. W., Jaafar, F., Tan, J. K., Tajul Arifin, K., Mohd Yusof, Y. A., Wan Ngah, W. Z., et al. (2015). Targeting genes in insulin-associated signalling pathway, DNA damage, cell proliferation and cell differentiation pathways by tocotrienol-rich fraction in preventing cellular senescence of human diploid fibroblasts. *Clin. Ter.* 166, e365–e373. doi: 10.7417/T.2015.1902
- Fang, J., Cai, C., Wang, Q., Lin, P., Zhao, Z., and Cheng, F. (2017a). Systems pharmacology-based discovery of natural products for precision oncology through targeting cancer mutated genes. *CPT Pharmacometrics Syst. Pharmacol.* 6, 177–187. doi: 10.1002/psp4.12172
- Fang, J., Liu, C., Wang, Q., Lin, P., and Cheng, F. (2017b). *In silico* polypharmacology of natural products. *Brief. Bioinformatics.* doi: 10.1093/bib/bbx045. [Epub ahead of print].
- Fang, J., Wu, Z., Cai, C., Wang, Q., Tang, Y., and Cheng, F. (2017c). Quantitative and systems pharmacology. *1. in silico* prediction of drug-target interaction of natural products enables new targeted cancer therapy. *J. Chem. Inf. Model.* doi: 10.1021/acs.jcim.7b00216. [Epub ahead of print].
- Fang, J., Yang, R., Gao, L., Zhou, D., Yang, S., Liu, A. L., et al. (2013). Predictions of BuChE inhibitors using support vector machine and naive Bayesian classification techniques in drug discovery. *J. Chem. Inf. Model.* 53, 3009–3020. doi: 10.1021/ci400331p
- Fontana, L., Partridge, L., and Longo, V. D. (2010). Extending healthy life span—from yeast to humans. *Science* 328, 321–326. doi: 10.1126/science.1172539
- Foretz, M., Guigas, B., Bertrand, L., Pollak, M., and Viollet, B. (2014). Metformin: from mechanisms of action to therapies. *Cell Metab.* 20, 953–966. doi: 10.1016/j.cmet.2014.09.018
- Fu, R. H., Liu, S. P., Chu, C. L., Lin, Y. H., Ho, Y. C., Chiu, S. C., et al. (2013). Myricetin attenuates lipopolysaccharide-stimulated activation of mouse bone marrow-derived dendritic cells through suppression of IKK/NF-kappaB and MAPK signalling pathways. *J. Sci. Food Agric.* 93, 76–84. doi: 10.1002/jsfa.5733
- Gilson, M. K., Liu, T., Baitaluk, M., Nicola, G., Hwang, L., and Chong, J. (2016). BindingDB in 2015: a public database for medicinal chemistry, computational chemistry and systems pharmacology. *Nucleic Acids Res.* 44, D1045–D1053. doi: 10.1093/nar/gkv1072
- Gines, C., Cuesta, S., Kireev, R., Garcia, C., Rancan, L., Paredes, S. D., et al. (2017). Protective effect of resveratrol against inflammation, oxidative stress and apoptosis in pancreas of aged SAMP8 mice. *Exp. Gerontol.* 90, 61–70. doi: 10.1016/j.exger.2017.01.021
- Gonzalez-Rodriguez, A., Mas-Gutierrez, J. A., Mirasierra, M., Fernandez-Perez, A., Lee, Y. J., Ko, H. J., et al. (2012). Essential role of protein tyrosine phosphatase 1B in obesity-induced inflammation and peripheral insulin resistance during aging. *Aging Cell* 11, 284–296. doi: 10.1111/j.1474-9726.2011.00786.x
- Gu, J., Gui, Y., Chen, L., Yuan, G., Lu, H. Z., and Xu, X. (2013). Use of natural products as chemical library for drug discovery and network pharmacology. *PLoS ONE* 8:e62839. doi: 10.1371/journal.pone.0062839
- Hall, J. A., McElwee, M. K., and Freedman, J. H. (2017). Identification of ATF-7 and the insulin signaling pathway in the regulation of metallothionein in *C. elegans* suggests roles in aging and reactive oxygen species. *PLoS ONE* 12:e0177432. doi: 10.1371/journal.pone.0177432
- Havermann, S., Chovolou, Y., Humpf, H. U., and Watjen, W. (2014). Caffeic acid phenethyl ester increases stress resistance and enhances lifespan in *Caenorhabditis elegans* by modulation of the insulin-like DAF-16 signalling pathway. *PLoS ONE* 9:e100256. doi: 10.1371/journal.pone.0100256
- He, M., Yan, X., Zhou, J., and Xie, G. (2001). Traditional Chinese medicine database and application on the Web. *J. Chem. Inf. Comput. Sci.* 41, 273–277. doi: 10.1021/ci0003101
- He, Z. Z., Yan, J. F., Song, Z. J., Ye, F., Liao, X., Peng, S. L., et al. (2009). Chemical constituents from the aerial parts of *Artemisia minor*. *J. Nat. Prod.* 72, 1198–1201. doi: 10.1021/np800643n
- Huhne, R., Thalheim, T., and Suhnel, J. (2014). AgeFactDB—the JenAge Ageing Factor Database—towards data integration in ageing research. *Nucleic Acids Res.* 42, D892–D896. doi: 10.1093/nar/gkt1073
- Kaerberlein, M., Rabinovitch, P. S., and Martin, G. M. (2015). Healthy aging: the ultimate preventative medicine. *Science* 350, 1191–1193. doi: 10.1126/science.aad3267
- Kang, S. S., Cuendet, M., Endringer, D. C., Croy, V. L., Pezzuto, J. M., and Lipton, M. A. (2009). Synthesis and biological evaluation of a library of resveratrol analogues as inhibitors of COX-1, COX-2 and NF-kappaB. *Bioorg. Med. Chem.* 17, 1044–1054. doi: 10.1016/j.bmc.2008.04.031
- Kermath, B. A., Riha, P. D., Woller, M. J., Wolfe, A., and Gore, A. C. (2014). Hypothalamic molecular changes underlying natural reproductive senescence in the female rat. *Endocrinology* 155, 3597–3609. doi: 10.1210/en.2014-1017
- Kim, J., Vaish, V., Feng, M., Field, K., Chatzistamou, I., and Shim, M. (2016). Transgenic expression of cyclooxygenase-2 (COX2) causes premature aging phenotypes in mice. *Aging (Albany, NY)* 8, 2392–2406. doi: 10.18632/aging.101060
- Kim, J. Y., Jung, K. J., Choi, J. S., and Chung, H. Y. (2006). Modulation of the age-related nuclear factor-kappaB (NF-kappaB) pathway by hesperetin. *Aging Cell* 5, 401–411. doi: 10.1111/j.1474-9726.2006.00233.x
- La Fata, G., Weber, P., and Mohajeri, M. H. (2014). Effects of vitamin E on cognitive performance during aging and in Alzheimer's disease. *Nutrients* 6, 5453–5472. doi: 10.3390/nu6125453
- Lamb, J., Crawford, E. D., Peck, D., Modell, J. W., Blat, I. C., Wrobel, M. J., et al. (2006). The Connectivity Map: using gene-expression signatures to connect small molecules, genes, and disease. *Science* 313, 1929–1935. doi: 10.1126/science.1132939
- Law, V., Knox, C., Djoumbou, Y., Jewison, T., Guo, A. C., Liu, Y., et al. (2014). DrugBank 4.0: shedding new light on drug metabolism. *Nucleic Acids Res.* 42, D1091–D1097. doi: 10.1093/nar/gkt1068
- Lee, K. M., Kang, N. J., Han, J. H., Lee, K. W., and Lee, H. J. (2007). Myricetin down-regulates phorbol ester-induced cyclooxygenase-2 expression in mouse epidermal cells by blocking activation of nuclear factor kappa B. *J. Agric. Food Chem.* 55, 9678–9684. doi: 10.1021/jf0717945
- Li, J., Lei, K., Wu, Z., Li, W., Liu, G., Liu, J., et al. (2016). Network-based identification of microRNAs as potential pharmacogenomic biomarkers for anticancer drugs. *Oncotarget* 7, 45584–45596. doi: 10.18632/oncotarget.10052
- Li, J., Wu, Z., Cheng, F., Li, W., Liu, G., and Tang, Y. (2014). Computational prediction of microRNA networks incorporating environmental toxicity and disease etiology. *Sci. Rep.* 4:5576. doi: 10.1038/srep05576
- Li, Y., Hassinger, L., Thomson, T., Ding, B., Ashley, J., Hassinger, W., et al. (2016). Lamin mutations accelerate aging via defective export of mitochondrial mRNAs through nuclear envelope budding. *Curr. Biol.* 26, 2052–2059. doi: 10.1016/j.cub.2016.06.007

- Lopez-Otin, C., Blasco, M. A., Partridge, L., Serrano, M., and Kroemer, G. (2013). The hallmarks of aging. *Cell* 153, 1194–1217. doi: 10.1016/j.cell.2013.05.039
- Lu, W., Cheng, F., Jiang, J., Zhang, C., Deng, X., Xu, Z., et al. (2015). FXR antagonism of NSAIDs contributes to drug-induced liver injury identified by systems pharmacology approach. *Sci. Rep.* 5:8114. doi: 10.1038/srep08114
- Magnani, C., Isaac, V. L. B., Correa, M. A., and Salgado, H. R. N. (2014). Caffeic acid: a review of its potential use in medications and cosmetics. *Anal. Methods* 6, 3203–3210. doi: 10.1039/C3AY41807C
- Martin-Montalvo, A., Mercken, E. M., Mitchell, S. J., Palacios, H. H., Mote, P. L., Scheibye-Knudsen, M., et al. (2013). Metformin improves healthspan and lifespan in mice. *Nat. Commun.* 4:2192. doi: 10.1038/ncomms3192
- Miler, M., Zivanovic, J., Ajdzanovic, V., Orescanin-Dusic, Z., Milenkovic, D., Konic-Ristic, A., et al. (2016). Citrus flavanones naringenin and hesperetin improve antioxidant status and membrane lipid compositions in the liver of old-aged Wistar rats. *Exp. Gerontol.* 84, 49–60. doi: 10.1016/j.exger.2016.08.014
- Mocchegiani, E., Costarelli, L., Giacconi, R., Malavolta, M., Basso, A., Piacenza, F., et al. (2014). Vitamin E-gene interactions in aging and inflammatory age-related diseases: implications for treatment. A systematic review. *Ageing Res. Rev.* 14, 81–101. doi: 10.1016/j.arr.2014.01.001
- Moiseeva, O., Deschenes-Simard, X., St-Germain, E., Igelmann, S., Huot, G., Cadar, A. E., et al. (2013). Metformin inhibits the senescence-associated secretory phenotype by interfering with IKK/NF- κ B activation. *Ageing Cell* 12, 489–498. doi: 10.1111/ace1.12075
- Navarro, A., Gomez, C., Sanchez-Pino, M. J., Gonzalez, H., Bandez, M. J., Boveris, A. D., et al. (2005). Vitamin E at high doses improves survival, neurological performance, and brain mitochondrial function in aging male mice. *Am. J. Physiol. Regul. Integr. Comp. Physiol.* 289, R1392–R1399. doi: 10.1152/ajpregu.00834.2004
- O'Boyle, N. M., Banck, M., James, C. A., Morley, C., Vandermeersch, T., and Hutchison, G. R. (2011). Open Babel: an open chemical toolbox. *J. Cheminform.* 3:33. doi: 10.1186/1758-2946-3-33
- Pan, M. H., Lai, C. S., Tsai, M. L., Wu, J. C., and Ho, C. T. (2012). Molecular mechanisms for anti-aging by natural dietary compounds. *Mol. Nutr. Food Res.* 56, 88–115. doi: 10.1002/mnfr.201100509
- Parhiz, H., Roohbakhsh, A., Soltani, F., Rezaee, R., and Iranshahi, M. (2015). Antioxidant and anti-inflammatory properties of the citrus flavonoids hesperidin and hesperetin: an updated review of their molecular mechanisms and experimental models. *Phytother. Res.* 29, 323–331. doi: 10.1002/ptr.5256
- Patridge, E., Gareiss, P., Kinch, M. S., and Hoyer, D. (2016). An analysis of FDA-approved drugs: natural products and their derivatives. *Drug Discov. Today* 21, 204–207. doi: 10.1016/j.drudis.2015.01.009
- Pereira, P., de Oliveira, P. A., Ardenghi, P., Rotta, L., Henriques, J. A., and Picada, J. N. (2006). Neuropharmacological analysis of caffeic acid in rats. *Basic Clin. Pharmacol. Toxicol.* 99, 374–378. doi: 10.1111/j.1742-7843.2006.pto_533.x
- Qian, Z. M., and Ke, Y. (2014). Huperzine A: is it an effective disease-modifying drug for Alzheimer's disease? *Front. Aging Neurosci.* 6:216. doi: 10.3389/fnagi.2014.00216
- Ru, J., Li, P., Wang, J., Zhou, W., Li, B., Huang, C., et al. (2014). TCMSP: a database of systems pharmacology for drug discovery from herbal medicines. *J. Cheminform.* 6:13. doi: 10.1186/1758-2946-6-13
- Ruan, Q., Hu, X., Ao, H., Ma, H., Gao, Z., Liu, F., et al. (2014). The neurovascular protective effects of huperzine A on D-galactose-induced inflammatory damage in the rat hippocampus. *Gerontology* 60, 424–439. doi: 10.1159/000358235
- Ruan, Q., Liu, F., Gao, Z., Kong, D., Hu, X., Shi, D., et al. (2013). The anti-inflammatory and hepatoprotective effects of huperzine A in D-galactose-treated rats. *Mech. Ageing Dev.* 134, 89–97. doi: 10.1016/j.mad.2012.12.005
- Shen, J., Xu, X., Cheng, F., Liu, H., Luo, X., Shen, J., et al. (2003). Virtual screening on natural products for discovering active compounds and target information. *Curr. Med. Chem.* 10, 2327–2342. doi: 10.2174/0929867033456729
- Song, Y. M., Lee, Y. H., Kim, J. W., Ham, D. S., Kang, E. S., Cha, B. S., et al. (2015). Metformin alleviates hepatosteatosis by restoring SIRT1-mediated autophagy induction via an AMP-activated protein kinase-independent pathway. *Autophagy* 11, 46–59. doi: 10.4161/15548627.2014.984271
- Tacutu, R., Craig, T., Budovsky, A., Wuttke, D., Lehmann, G., Taranukha, D., et al. (2013). Human Ageing genomic resources: integrated databases and tools for the biology and genetics of ageing. *Nucleic Acids Res.* 41, D1027–D1033. doi: 10.1093/nar/gks1155
- Tilstra, J. S., Robinson, A. R., Wang, J., Gregg, S. Q., Clauson, C. L., Reay, D. P., et al. (2012). NF- κ B inhibition delays DNA damage-induced senescence and aging in mice. *J. Clin. Invest.* 122, 2601–2612. doi: 10.1172/JCI45785
- Vaiserman, A. M., Lushchak, O. V., and Koliada, A. K. (2016). Anti-aging pharmacology: promises and pitfalls. *Ageing Res. Rev.* 31, 9–35. doi: 10.1016/j.arr.2016.08.004
- Vaiserman, A. M., and Marotta, F. (2016). Longevity-promoting pharmaceuticals: is it a time for implementation? *Trends Pharmacol. Sci.* 37, 331–333. doi: 10.1016/j.tips.2016.02.003
- Vicini, P., and van der Graaf, P. H. (2013). Systems pharmacology for drug discovery and development: paradigm shift or flash in the pan? *Clin. Pharmacol. Ther.* 93, 379–381. doi: 10.1038/clpt.2013.40
- Vieira, M. N., Lyra, E. S. N. M., Ferreira, S. T., and De Felice, F. G. (2017). Protein tyrosine phosphatase 1B (PTP1B): a potential target for Alzheimer's therapy? *Front. Aging Neurosci.* 9:7. doi: 10.3389/fnagi.2017.00007
- Wang, Z. H., Ah Kang, K., Zhang, R., Piao, M. J., Jo, S. H., Kim, J. S., et al. (2010). Myricetin suppresses oxidative stress-induced cell damage via both direct and indirect antioxidant action. *Environ. Toxicol. Pharmacol.* 29, 12–18. doi: 10.1016/j.etap.2009.08.007
- Wu, Z., Cheng, F., Li, J., Li, W., Liu, G., and Tang, Y. (2017). SDTNBI: an integrated network and chemoinformatics tool for systematic prediction of drug-target interactions and drug repositioning. *Brief. Bioinform.* 18, 333–347. doi: 10.1093/bib/bbw012
- Wu, Z., Lu, W., Wu, D., Luo, A., Bian, H., Li, J., et al. (2016). *In silico* prediction of chemical mechanism of action via an improved network-based inference method. *Br. J. Pharmacol.* 173, 3372–3385. doi: 10.1111/bph.13629
- Xue, M., Weickert, M. O., Qureshi, S., Kandala, N. B., Anwar, A., Waldron, M., et al. (2016). Improved glycemic control and vascular function in overweight and obese subjects by glyoxalase 1 inducer formulation. *Diabetes* 65, 2282–2294. doi: 10.2337/db16-0153
- Xue, R., Fang, Z., Zhang, M., Yi, Z., Wen, C., and Shi, T. (2013). TCMID: Traditional Chinese Medicine integrative database for herb molecular mechanism analysis. *Nucleic Acids Res.* 41, D1089–D1095. doi: 10.1093/nar/gks1100

Conflict of Interest Statement: The authors declare that the research was conducted in the absence of any commercial or financial relationships that could be construed as a potential conflict of interest.

Copyright © 2017 Fang, Gao, Ma, Wu, Wu, Wang and Cheng. This is an open-access article distributed under the terms of the Creative Commons Attribution License (CC BY). The use, distribution or reproduction in other forums is permitted, provided the original author(s) or licensor are credited and that the original publication in this journal is cited, in accordance with accepted academic practice. No use, distribution or reproduction is permitted which does not comply with these terms.



Ginkgolide C Alleviates Myocardial Ischemia/Reperfusion-Induced Inflammatory Injury via Inhibition of CD40-NF- κ B Pathway

Rui Zhang¹, Dan Han², Zhenyu Li¹, Chengwu Shen¹, Yahui Zhang¹, Jun Li¹, Genquan Yan¹, Shasha Li¹, Bo Hu³, Jiangbing Li⁴ and Ping Liu^{1*}

OPEN ACCESS

Edited by:

Yuhei Nishimura,
Mie University Graduate School
of Medicine, Japan

Reviewed by:

Sang-Bing Ong,
National University of Singapore,
Singapore
Jason N. Peart,
Griffith University, Australia
Lewis J. Watson,
University of Pikeville, United States

*Correspondence:

Ping Liu
330632664@qq.com

Specialty section:

This article was submitted to
Experimental Pharmacology and Drug
Discovery,
a section of the journal
Frontiers in Pharmacology

Received: 07 November 2017

Accepted: 31 January 2018

Published: 21 February 2018

Citation:

Zhang R, Han D, Li Z, Shen C,
Zhang Y, Li J, Yan G, Li S, Hu B,
Li J and Liu P (2018) Ginkgolide C
Alleviates Myocardial
Ischemia/Reperfusion-Induced
Inflammatory Injury via Inhibition
of CD40-NF- κ B Pathway.
Front. Pharmacol. 9:109.
doi: 10.3389/fphar.2018.00109

¹ Department of Pharmacy, Shandong Provincial Hospital Affiliated to Shandong University, Jinan, China, ² Department of Pharmacy, Nanjing Drum Tower Hospital, The Affiliated Hospital of Nanjing University Medical School, Nanjing, China, ³ Minimally Invasive Urology Center, Shandong Provincial Hospital Affiliated to Shandong University, Jinan, China, ⁴ Department of Cardiology, Shandong Provincial Hospital Affiliated to Shandong University, Jinan, China

Increasing evidence shows that inflammation plays a vital role in the occurrence and development of ischemia/reperfusion (I/R). Suppression of excessive inflammation can ameliorate impaired cardiac function, which shows therapeutic potential for clinical treatment of myocardial ischemia/reperfusion (MI/R) diseases. In this study, we investigated whether Ginkgolide C (GC), a potent anti-inflammatory flavone, extenuated MI/R injury through inhibition of inflammation. *In vivo*, rats with the occlusion of the left anterior descending (LAD) coronary artery were applied to mimic MI/R injury. *In vitro*, primary cultured neonatal ventricular myocytes exposed to hypoxia/reoxygenation (H/R) were applied to further discuss the anti-H/R injury property of GC. The results revealed that GC significantly improved the symptoms of MI/R injury, as evidenced by reducing infarct size, preventing myofibrillar degeneration and reversing the mitochondria dysfunction. Moreover, histological analysis and Myeloperoxidase (MPO) activity measurement showed that GC remarkably suppressed Polymorphonuclears (PMNs) infiltration and ameliorated the histopathological damage. Furthermore, GC pretreatment was shown to improve H/R-induced ventricular myocytes viability and enhance tolerance of inflammatory insult, as evidenced by suppressing expression of CD40, translocation of NF- κ B p65 subunit, phosphorylation of I κ B- α , as well as the activity of IKK- β . In addition, downstream inflammatory cytokines modulated by NF- κ B signaling were effectively down-regulated both *in vivo* and *in vitro*, as determined by immunohistochemistry and ELISA. In conclusion, these results indicate that GC possesses a beneficial effect against MI/R injury via inflammation inhibition that may involve suppression of CD40-NF- κ B signal pathway and downstream inflammatory cytokines expression, which may offer an alternative medication for MI/R diseases.

Keywords: ginkgolide C, myocardial ischemia/reperfusion injury, inflammation, CD40, NF- κ B

INTRODUCTION

Nowadays, cardiovascular disease becomes one of the leading cause of disability and death worldwide, and one of the most popular and dangerous cardiovascular diseases is myocardial ischemia/reperfusion (MI/R) injury (Anzell et al., 2017; de Waha et al., 2017). While prompt reperfusion is favorable for myocardial salvage, ischemia/reperfusion (I/R) injury which involved a strong inflammatory response may often present itself as an adverse consequence (Liebert et al., 2017). According to the recent researches, an inflammatory response severely ignites the whole process of MI/R injury by accelerating generation of inflammatory factors and by boosting inflammatory eruption simultaneously (Montecucco et al., 2017). A disturbed inflammatory stimuli is associated with poor prognosis and increased tissue damage, may aggravate the degree of I/R injury and it may seriously delay the recovery procedures (Pantazi et al., 2016; Yarijani et al., 2017). Therefore, restoration of cardiac dysfunction through modulation of inflammatory pathways is a favorable therapeutic strategy against MI/R diseases superimposed on other cardiovascular disease risk factors.

CD40, one member of tumor necrosis factor receptor (TNFR) family, serves as a transmembrane type I receptor (Clark, 2014). Except for immune cells, CD40 has been similarly found on endothelial cells, myocytes, epithelial cells, fibroblasts, and monocytes (Senhaji et al., 2015). Tumor necrosis factor (TNF)- α , Interleukin (IL)-1, Interferon (IFN)- γ , CD40 ligand (CD40L) and others inflammatory factors can regulate the expression of CD40. Then, the abundant expression of CD40 in the cytoplasmic domain will tend to TNF receptor-associated factors (TRAFs), which consequently activates different signal pathways, such as nuclear factor- κ B (NF- κ B), phosphoinositide 3-kinase (PI3K) and MAPKs, in different stages of MI/R injury process (Jansen et al., 2016). Researches for near years have indicated that CD40 was closely related to the occurrence and development of many diseases, including lung ailments, inflammatory kidney disease, diabetes, coronary artery disease and arteriosclerosis disease (Aloui et al., 2014; Mansouri et al., 2016; Michel et al., 2017). However, few studies investigated the role of CD40 in the whole inflammatory process induced by MI/R injury.

Increasing evidence suggested that NF- κ B activation elevated in the MI/R-related infarct area, inflammation was suppressed when NF- κ B activation was inhibited, and cardiac preservation was provided (Zhang et al., 2017). I κ B- α , which binds to NF- κ B p65/p50 heterodimer in the cytoplasm under the rest state, serves as an inhibitor of NF- κ B. Subsequently, I κ B kinase β (IKK- β) activation induces the phosphorylation and degradation of I κ B- α resulting in the translocation of NF- κ B from cytoplasm to nucleus, which will enhance synthesis of various inflammatory cytokines, such as TNF- α , IL-1 β , IL-6, vascular cell adhesion molecule-1 (VCAM-1), intracellular adhesion molecule-1 (ICAM-1) and inducible nitric oxide synthase (iNOS), that act directly or indirectly to depress cardiac function (Durand and Baldwin, 2017; Nennig and Schank, 2017). However, many studies have reported that aspirin possesses the strong anti-inflammatory properties through inhibiting the transcription factor such as NF- κ B (He et al.,

2012). Moreover, neutrophils infiltration into the post-ischemic myocardium has previously been related to the pathogenesis of I/R injury. Reperfusion accelerates the recruitment of neutrophils into the ischemic myocardium (Sivalingam et al., 2017). Thus, suppressing neutrophils infiltration and NF- κ B pathway activation can diminish MI/R damage and possibly improve myocardial function. From this evidence, it was reasonable to speculate that NF- κ B signal pathway played a key role throughout the whole course of MI/R injury. Therefore, potent new agents for treatment of MI/R injury via anti-inflammatory effect become an imperative requirement.

Ginkgolide C (GC, **Figure 1**), isolated from *Ginkgo biloba* leaves, is a flavone with multiple biological functions and has a long application history in clinical therapy in Asia (Huang et al., 2014). It was reported that GC exerted protection of ischemic diseases, inhibition of platelet aggregation, prevention of thrombus, anti-inflammation, and anti-allergy (Lau et al., 2013; Liou et al., 2015). However, up to now, there is little research on the relations between GC and MI/R injury, and the exact mechanism of its anti-inflammatory protective effects is still obscure to us.

Thus, taking into account activation of inflammatory response during MI/R injury, we have not only investigated the protective effect of GC both *in vivo* and *in vitro*, but also made great efforts to clarify the potential mechanism. Considering the supposed signal pathway of GC, aspirin which represents the prototype of anti-inflammatory and MI/R protective effects was selected as the positive control in this study. Left anterior descending (LAD)-occlusion-induced myocardial infarction rat model was established to imitate MI/R *in vivo*. Moreover, ventricular myocytes treatment with hypoxia/reoxygenation (H/R) were used to mimic I/R injury *in vitro*. To further explore the mechanism, we also explored the role of CD40-NF- κ B signal pathway in the protection of ventricular myocytes treated with H/R.

MATERIALS AND METHODS

Materials and Reagents

GC (PubChem CID: 161120), Aspirin (PubChem CID: 2244), 2, 3, 5-Triphenyltetrazolium chloride (TTC), 3-(4, 5-dimethylthiazol-2-yl)-2, 5-diphenyltetrazolium bromide (MTT) and chloral hydrate were bought from Sigma (St. Louis, MO, United States). DMEM medium (high glucose) and newborn calf serum were products of Gibco (Grand Island,

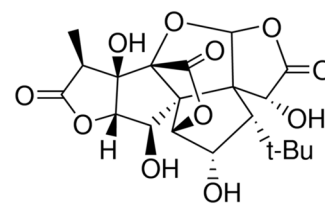


FIGURE 1 | Chemical structure of GC.

NY, United States). Trypsin was purchased from Amresco (Solon, OH, United States). TNF- α , IL-1 β and IL-6 ELISA kits were bought from Sigma (St. Louis, MO, United States). Anti-ICAM-1, anti-VCAM-1, anti-iNOS, anti-CD40, anti-NF- κ B p65, anti-p-I κ B- α , anti-IKK- β , anti- β -actin, anti-Histone, goat anti-rabbit and anti-mouse IgG antibodies were purchased from Santa Cruz (Santa Cruz, CA, United States). Nuclear-Cytosol Extraction Kit and ECL plus kit was purchased from Jiancheng (Nanjing Jiancheng Bioengineering Inc., Nanjing, China)

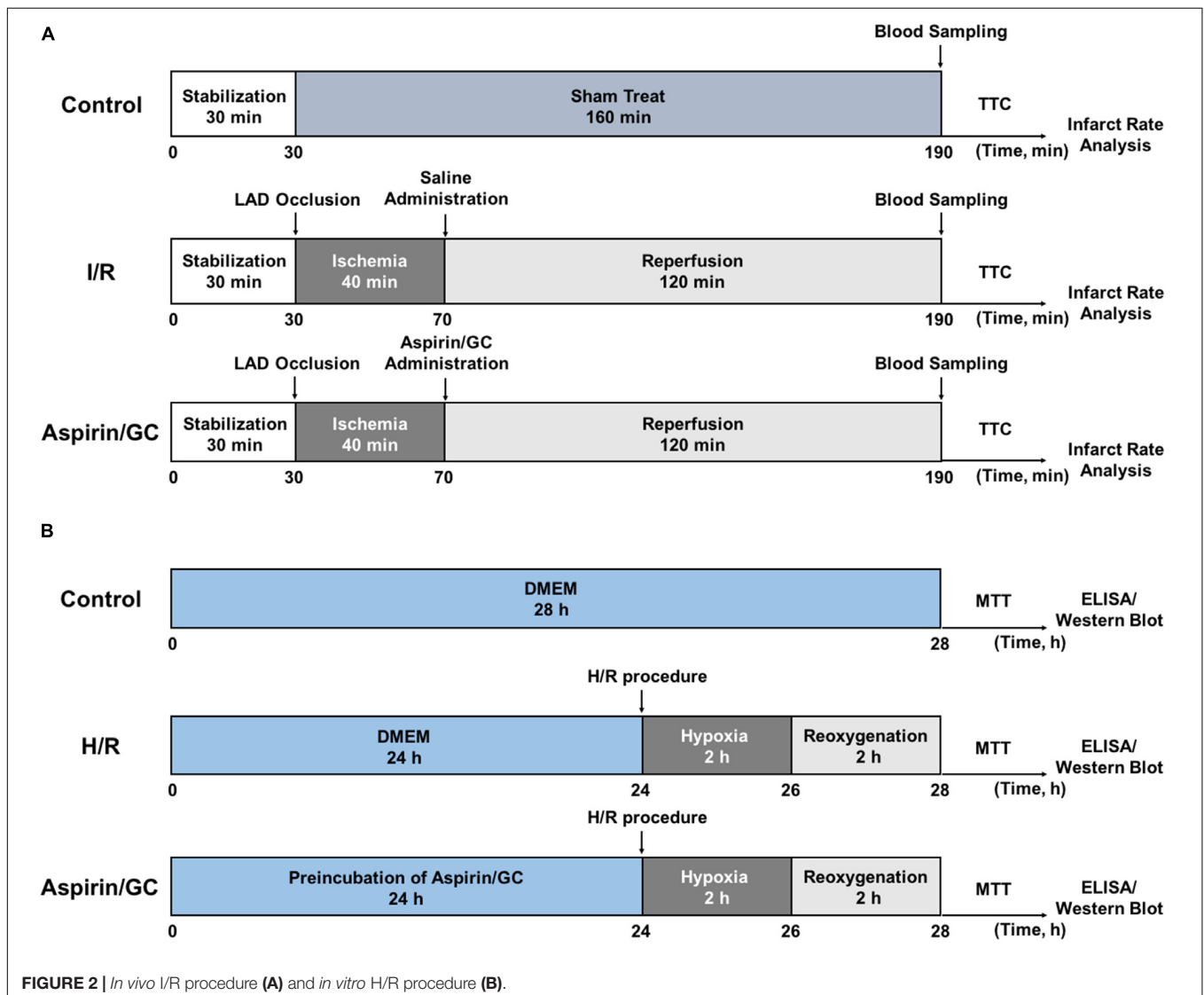
Animals

Adult male Sprague-Dawley rats (250 \pm 20 g) were provided by Experimental Animal Center of Shandong University. Rats were raised in a controlled environment (temperature 18–22°C, humidity 40–70%) with a 12 h light-dark cycle and allowed to eat and drink freely until the experiment. All the experiments were approved by the ethics committee of the Shandong University (Permission No. 2013-092).

In Vivo I/R Procedure to Induce MI/R Injury in Rats

MI/R surgery was precisely implemented according to the procedure in **Figure 2A**. The rats were anesthetized with 3% sodium pentobarbital (40 mg/kg, i.p.) and mechanically ventilated the lung with a rodent respirator. Holter monitoring electrocardiogram was continuously used to monitor the changes of S-T segment in order to estimate the success of surgery. After a left thoracotomy, a suture tied with a plastic tube was twined round the LAD coronary artery to form a snare for reversible LAD occlusion. According to procedure, transient regional myocardial ischemia for 40 min was realized by straining the suture, and reperfusion for 120 min was initiated by releasing the suture and removing the tension. The blood samples were collected before the rats were sacrificed.

Rats were randomly divided into 6 groups as follows ($n = 8$ per group): Control group, non-I/R rats received saline; I/R group, I/R rats received saline; Aspirin group, I/R rats



received 16 mg/kg of Aspirin; 8, 16, 32 mg/kg GC group, I/R rats received 8, 16, 32 mg/kg of GC. Saline, Aspirin and GC were administered intraperitoneally for 7 days before I/R procedure.

Measurement of Infarct Size

Infarct size was assessed by TTC staining technique in accordance with a previous study report (Panda et al., 2017). After the completion of the experimental protocols, the hearts were removed. The left ventricle area was sectioned into five 2–3 mm-thick slices from the apex to the base. The third slice was incubated in pH 7.4, 2% TTC at 37°C for 15 min. Viable tissue was stained to dark red while the infarct area remained pale. Then, the area of the infarcted tissues was demarcated and measured digitally using Image-Pro Plus software (version 6.0, Media Cybernetic, United States) by computerized planimetry. Infarct size was calculated as the ratio of infarcted myocardium to the risk region \times 100%.

Transmission Electron Microscope (TEM) Observation

The third heart slice was fixed in 3.0% glutaraldehyde buffered fixative (pH 7.2) for 2–3 days. After being rinsed in PBS, the specimens were embedded in Polybed 812. Then, 90 nm-thick specimens were made and observed under electron microscope (JEM-2000EX).

Histopathological Analysis and Qualitative Observation of PMNs Infiltration

The third heart slice was stained with hematoxylin and eosin (HE) after fixation. The degree of histopathological damage was assessed with pathological scores according to the criteria reported by the previous study (Jiang et al., 2012). Scores from 0 to 5 represented no damage, mild damage, moderate damage, severe damage and highly severe damage, respectively. The total number of PMNs was also recorded simultaneously. The degree of PMNs infiltration of the area at risk was determined in three random high-power fields (HPF).

Immunohistochemistry

The expressions of ICAM-1, VCAM-1 and iNOS were examined by immunohistochemistry. In brief, the third frozen heart slice incubated with anti-ICAM-1, anti-VCAM-1, and anti-iNOS antibodies overnight at 4°C after being blocked by 10% normal serum. Then, anti-rabbit IgG was applied to incubate the heart slices combined with primary antibody for 30 min. Consequently, immunohistochemical staining protocol was applied to heart slice in accordance with the instructions. Images were obtained using fluorescence microscope. The optical density of positive staining area was quantified by Image-Pro Plus software (version 6.0, Media Cybernetic, United States) and the results were expressed as mean optical density mean \pm SD.

Quantitative Determination of MPO Activity

The homogenized tissue samples were sonicated to release the MPO from tissue into the supernatant. Then, *o*-dianisidine hydrochloride and hydrogen peroxide were added, after that, MPO activity was tested at 460 nm according to spectrophotometer method during a period of 3 min. The number of PMNs was counted in three random high power fields.

In Vitro H/R Procedure to Induce H/R Injury in Ventricular Myocytes

Ventricular myocytes isolated from 1 to 4-day-old Sprague-Dawley rats were treated with H/R injury according to the procedure in **Figure 2B**. Trypsin enzymic digestion and differential attachment methods were applied to separate and purify the primary cultures of neonatal ventricular myocytes. The cells at a final density of 1×10^5 /mL were cultured in a humidified incubator (95% air/5% CO₂ at 37°C) in DMEM supplement with 10% fetal calf serum, streptomycin (100 μ g/mL), penicillin (100 μ g/mL) and 0.5 mM L-glutamine. Three days later, the cells were incubated with DMEM (low glucose) in an oxygen-free condition (95% N₂/5% CO₂) for 2 h (hypoxia). And then, the cells were incubated with DMEM-F12 in a well-oxygenated condition (95% air/5% CO₂) for 2 h (reoxygenation).

The cells were randomly divided into 6 groups as follows ($n = 8$ per group): Control group, non-H/R cells cultured in DMEM medium; H/R group, cells treated with H/R procedure; Aspirin group, H/R cells preincubated with Aspirin (10 μ M) for 24 h; 1, 10, 100 μ M GC group, H/R cells preincubated with GC (1, 10, 100 μ M) for 24 h.

Reconstruction of CD40-Silencing Ventricular Myocytes

When ventricular myocytes reached 80–85% confluence, the cells in control group were transfected with pGPU6/Hygro while other groups' cells were transfected with pGPU6/Hygro-CD40. The transfection should take 24 h using the GenePharma Transfection Reagent before the pretreatment of GC, Aspirin and H/R procedure.

Analysis of Cell Vitality

Cell survival of ventricular myocytes was determined by MTT assay. After H/R procedure, 5 mg/mL MTT was added to the medium to incubate the cells for 4 h at 37°C. MTT was then removed, and cells were lysed with DMSO for 15 min. Absorbance was tested at wavelength of 490 nm by a microplate reader. Results were expressed as the percent of the optical density (OD) of control cells.

Detections of TNF- α , IL-1 β , and IL-6

Following 120 min reperfusion, all rats were deeply anesthetized, and blood samples were obtained. Cell supernatant was collected from medium after H/R procedure. The concentrations of TNF- α , IL-1 β and IL-6 were detected by ELISA kits.

Isolation of Cytoplasmic and Nuclear Protein

Cytoplasmic and nuclear proteins from cells were extracted by Nuclear-Cytosol Extraction Kit (Applygen Technologies Inc, Beijing, China). Cultured medium from plates was removed and astrocytes were detached with cold PBS and centrifuged at 1000 rpm for 5 min at 4°C. Pellets were resuspended in 200 μ L of cytosol extraction buffer A and incubated on ice for 10 min. Then, 10 μ L cytosol extraction buffer B was added, incubated on ice for 1 min and centrifuged at 1000 \times g for 5 min at 4°C. The pellet contains crude nuclei. The supernatant was transferred to a new tube and further centrifuged at 12,000 \times g for 5 min at 4°C. The supernatant is cytoplasmic proteins. The crude pellet was washed once with 100 μ L cytosol extraction buffer A, spined for 5 min at 1000 \times g and the supernatant was discarded. Fifty microliter of cold nuclear extraction buffer was added and incubated on ice for 30 min. Finally, samples were centrifuged at 12,000 \times g for 5 min at 4°C and supernatants were collected as nuclear proteins.

Western Blot for ICAM-1, VCAM-1, iNOS, CD40, NF- κ B p65, p-I κ B- α , and IKK- β Expression in Ventricular Myocytes

The quantity of total protein was assessed by BCA assay. Fifty microgram of protein was loaded to SDS-PAGE gel and then, transferred to a PVDF membrane. After being blocked with 5% skim milk, the membrane was incubated with primary antibody (1:800) that recognized ICAM-1, VCAM-1, iNOS, CD40, NF- κ B p65, p-I κ B- α and IKK- β proteins. After incubation for 4 h at 37°C, horseradish peroxidase-conjugated secondary antibody (1:1000) was added to the membrane and the immune complexes was determined using an ECL plus kit. Images were taken using the Gel Imaging System with Quantity One software.

Statistical Analysis

All data values were expressed as the mean \pm standard deviation (SD). *Post hoc* tests were used to assess the statistical significance among means. Significance of difference between groups was determined by ANOVA followed by Bonferroni correction for multiple comparisons. Results were considered to be statistically significant when $P < 0.05$. All statistical figures were performed using Graph Pad Prism software (Version 5.0).

RESULTS

GC Relieved the Outcomes of MI/R-Induced Inflammatory Injury GC Reduced Infarct Size in MI/R Rats

As shown in **Figure 3**, infarct size as a percentage of area at risk was $44.1 \pm 5.5\%$ ($P < 0.01$ vs. control group) in the I/R group, whereas administration with 8, 16, 32 mg/kg GC dose-dependently decreased infarct size to $37.1 \pm 4.9\%$

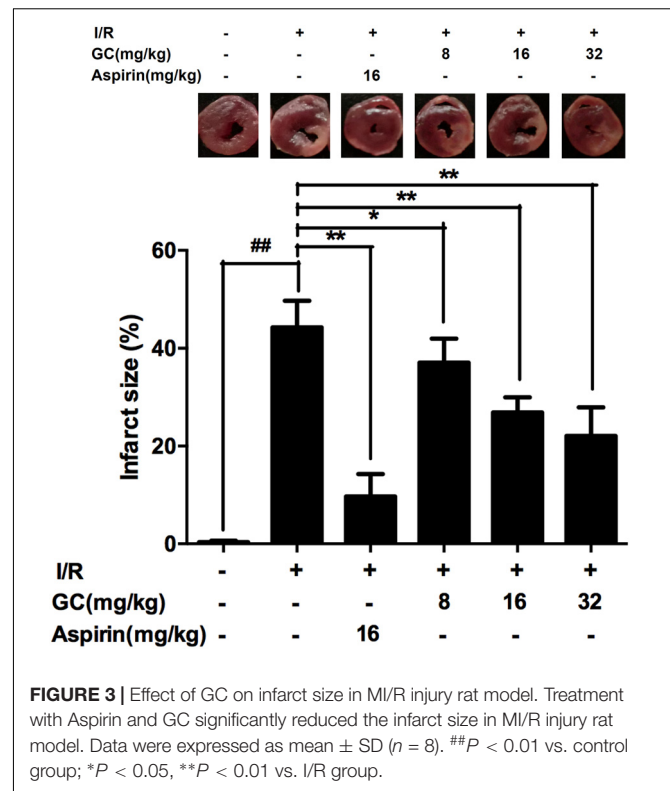


FIGURE 3 | Effect of GC on infarct size in MI/R injury rat model. Treatment with Aspirin and GC significantly reduced the infarct size in MI/R injury rat model. Data were expressed as mean \pm SD ($n = 8$). ## $P < 0.01$ vs. control group; * $P < 0.05$, ** $P < 0.01$ vs. I/R group.

($P < 0.05$), $26.9 \pm 3.1\%$ ($P < 0.01$), and $22.1 \pm 5.8\%$ ($P < 0.01$), respectively, compared with the I/R group. The infarct size of rats after administrated with 16 mg/kg Aspirin decreased to $9.7 \pm 4.6\%$ ($P < 0.01$) compared with I/R group. These findings strongly suggested that GC was effective at ameliorating MI/R injury.

GC Improved Cardiac Ultrastructural Characterization in MI/R Rats

In the present study, mitochondrial alignment and myofibrillar banding appeared normal in the control group (**Figure 4A1**). However, in I/R group (**Figure 4A2**), mitochondria became swelling and degeneration, crista fragmentation and nuclear stained deeper. Z-band disalignment and myofibrillar degeneration occurred. There was no significant change of mitochondria and myofibrillar in Aspirin group (**Figure 4A3**). In 8 mg/kg GC group (**Figure 4A4**), damages on mitochondria and formation vacuoles alleviated. In 16 mg/kg GC group (**Figure 4A5**), mitochondria showed mild separation of cristae without swelling and vacuolation. In 32 mg/kg GC group (**Figure 4A6**), only a few mitochondria showed swelling and vacuolation.

GC Inhibited PMNs Infiltration in MI/R Rats

Pathological changes were applied to further evaluate the protective effect of GC on MI/R injury. After I/R occurred, the tissue in I/R injured area became necrotic, and the structure of intercalated disk and gap junction was severely impaired. However, treatment with GC and Aspirin could largely improve the histological features caused by I/R injury, characterized by

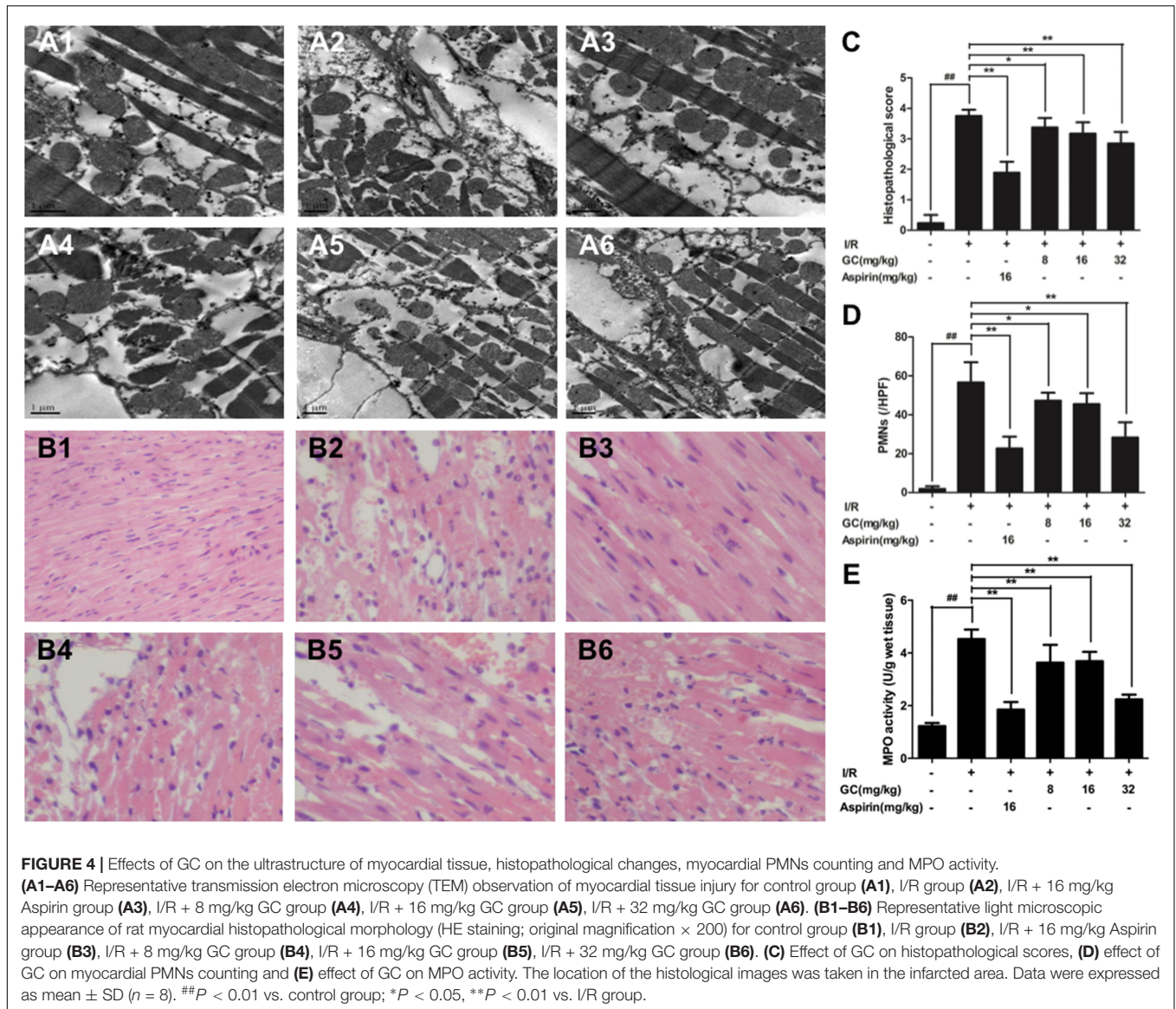


TABLE 1 | Effects of GC on serum inflammatory cytokines after I/R in rats.

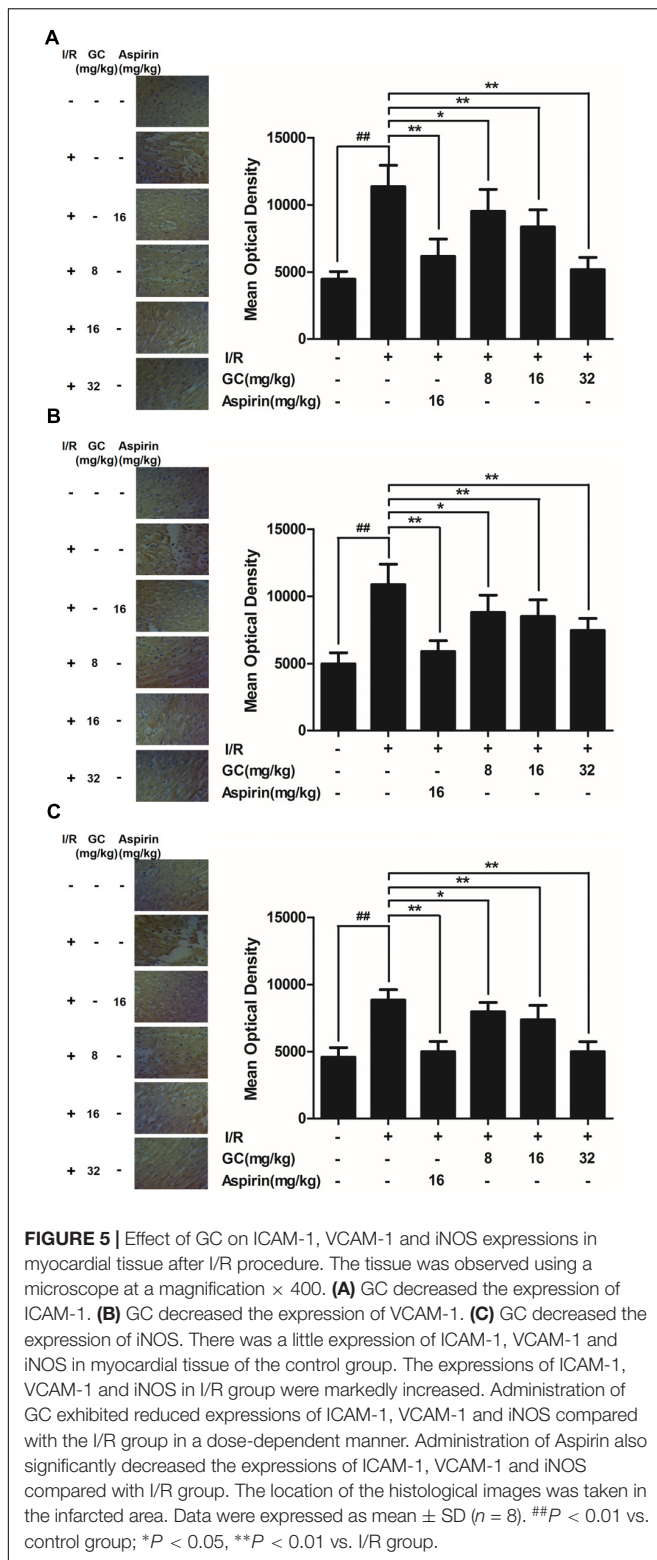
Group	Dose (mg/kg)	TNF- α (pg/mL)	IL-1 β (pg/mL)	IL-6 (pg/mL)
Control		25.50 \pm 6.91	86.63 \pm 12.52	29.74 \pm 5.07
I/R		76.10 \pm 12.91 $##$	257.23 \pm 18.69 $##$	95.87 \pm 4.80 $##$
I/R + Aspirin	16	31.41 \pm 6.99 $**$	102.92 \pm 7.31 $**$	40.87 \pm 5.29 $**$
I/R + GC	8	63.01 \pm 6.93 $*$	200.96 \pm 8.71 $**$	87.55 \pm 4.50 $*$
	16	49.23 \pm 7.68 $**$	156.96 \pm 13.88 $**$	67.53 \pm 5.34 $**$
	32	35.79 \pm 7.23 $**$	129.58 \pm 7.05 $**$	53.58 \pm 6.01 $**$

Values were expressed as mean \pm SD ($n = 8$). $##P < 0.01$ vs. control group; $*P < 0.05$, $**P < 0.01$ vs. I/R group.

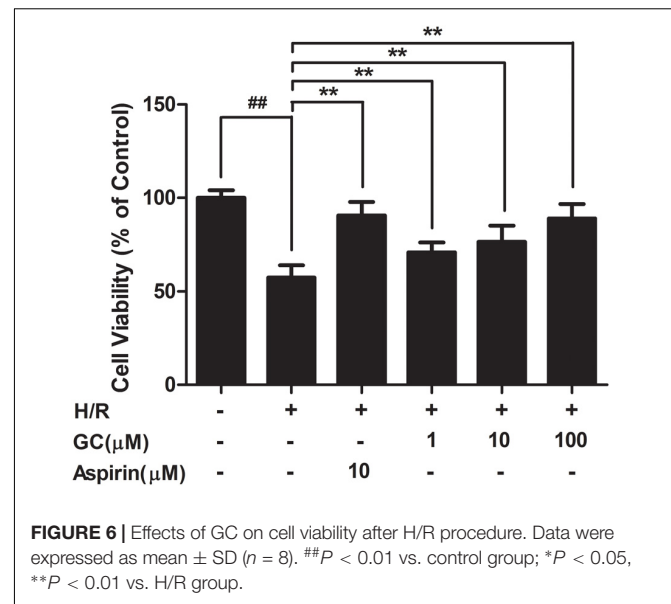
alleviative inflammatory infiltration and recoverable structure of ischemic myocardial tissue (Figures 4B1–B6). As shown in Figure 4C, the histopathological scores were also decreased significantly by 8, 16, 32 mg/kg GC group compared with I/R group ($P < 0.05$, $P < 0.01$, $P < 0.01$). Above all, the total numbers of infiltrated and adherent PMNs in GC

and Aspirin groups were remarkably less compared with that of the I/R group, as well as the histopathological score (Figures 4C,D).

To quantify neutrophilic infiltration, myocardial MPO activity was subsequently investigated. Very low MPO activity (1.21 ± 0.05 U/g protein) was tested in control group (Figure 4E).



On the contrary, elevated MPO activity was found in I/R injured group, indicating that remarkable neutrophil accumulation appeared in the I/R area of the left ventricle (4.45 ± 0.23 U/g protein) ($P < 0.01$ vs. control group). However, compared with



the I/R group, pretreatment with GC 8 mg/kg (4.20 ± 0.22 U/g protein, $P < 0.05$), 16 mg/kg (3.75 ± 0.30 U/g protein, $P < 0.01$), 32 mg/kg (2.22 ± 0.20 U/g protein, $P < 0.01$) and Aspirin 16 mg/kg (1.80 ± 0.25 U/g protein, $P < 0.01$) could prevent excessive MPO activity in myocardial tissue after I/R injury.

GC Inhibited Inflammatory Cytokines Overproduction in Serum of MI/R Rats

The concentration of inflammatory cytokines following I/R procedure in serum were detected by ELISA. **Table 1** showed that I/R injury elevated the levels of TNF- α by 2.98-fold ($P < 0.01$), IL-1 β by 2.97-fold ($P < 0.01$), and IL-6 by 3.22-fold ($P < 0.01$), respectively, compared to control group. GC (8, 16, 32 mg/kg) dose-dependently decreased the levels of TNF- α by 17.2% ($P < 0.05$), 35.3% ($P < 0.01$) and 53.0% ($P < 0.01$), respectively, IL-1 β by 21.9% ($P < 0.01$), 39.0% ($P < 0.01$) and 49.6% ($P < 0.01$), respectively, and IL-6 by 8.7% ($P < 0.05$), 29.6% ($P < 0.01$) and 44.1% ($P < 0.01$), respectively, compared with I/R group. In Aspirin group, the levels of TNF- α , IL-1 β and IL-6 were decreased by 58.7% ($P < 0.01$), 60.0% ($P < 0.01$) and 57.4% ($P < 0.01$), respectively, compared with I/R group.

GC Downregulated Overexpressions of ICAM-1, VCAM-1, and iNOS in Myocardial Tissue of MI/R Rats

Immunostaining was used to visualize the expressions of ICAM-1, VCAM-1 and iNOS in myocardial tissue. Compared with the control group, I/R procedure significantly increased the expressions of ICAM-1, VCAM-1 and iNOS (**Figure 5**). However, the administration of Aspirin remarkably reduced the damage to myocardium and decreased the expressions of ICAM-1, VCAM-1 and iNOS compared with I/R group. Furthermore, pretreatment with 8, 16, 32 mg/kg GC remarkably reduced the expressions of ICAM-1, VCAM-1 and iNOS in contrast with I/R group. These results indicated that GC could protect against I/R injury

through inhibiting expressions of key inflammatory factors and thus inhibiting inflammation.

GC Protected Ventricular Myocytes against H/R-Induced Inflammatory Injury GC Protected against Cell Insult after H/R Procedure in Ventricular Myocytes

As shown in **Figure 6**, exposure of ventricular myocytes to H/R procedure resulted in a markedly reduce in cell viability ($57.4 \pm 5.0\%$, $P < 0.01$ vs. control group) as assessed by MTT assay. Pretreatment with 1, 10, 100 μM GC significantly increased the viability of ventricular myocytes in a concentration dependent manner ($77.3 \pm 6.9\%$, $83.5 \pm 9.6\%$, $94.2 \pm 5.0\%$, $P < 0.01$ vs. H/R group). Compared with H/R group, pretreatment with Aspirin also significantly increased the cell viability ($93.3 \pm 6.7\%$, $P < 0.01$).

GC Inhibited Inflammatory Cytokines Overreleasing after H/R Procedure in Ventricular Myocytes

As shown in **Table 2**, the production of TNF- α in H/R group were markedly increased by 8.47-fold ($P < 0.01$ vs. control group). Pretreatment with 10 μM Aspirin and 1, 10, 100 μM GC could significantly reduce the levels of TNF- α by 68.3% ($P < 0.01$), 15.1% ($P < 0.05$), 22.4% ($P < 0.01$) and 71.0% ($P < 0.01$), respectively, compared with H/R group. After treatment with H/R procedure, the levels of IL-1 β and IL-6 in H/R group remarkably increased by 26.69-fold ($P < 0.01$) and 12.51-fold ($P < 0.01$) compared with control group. Pretreatment with GC at the concentration of 1, 10, and 100 μM dose-dependently decreased the levels of IL-1 β by 41.5% ($P < 0.01$), 52.9% ($P < 0.01$), and 69.6% ($P < 0.01$), respectively, and IL-6 by 6.1% ($P < 0.01$), 30.1% ($P < 0.01$), and 57.0% ($P < 0.01$), respectively, compared with H/R group. In addition, 10 μM Aspirin reduced the levels of IL-1 β and IL-6 by 77.2% ($P < 0.01$) and 74.0% ($P < 0.01$) in contrast with H/R group.

GC Inhibited the Expression Level of CD40

As shown in **Figure 7A**, H/R group revealed apparently higher level of CD40 compared with control group. There was no significant difference between H/R group and Aspirin group in CD40 expression level. Nevertheless, 1, 10, 100 μM GC groups significantly decreased CD40 level in response to H/R injury ($P < 0.05$, $P < 0.01$, $P < 0.01$ vs. H/R group).

GC Inhibited Overexpressions of ICAM-1, VCAM-1, and iNOS after H/R Procedure in Ventricular Myocytes

As shown in **Figures 7B–D**, the expressions of ICAM-1, VCAM-1, and iNOS in ventricular myocytes significantly elevated to about 8.16-fold ($P < 0.01$), 3.06-fold ($P < 0.01$), and 6.74-fold ($P < 0.01$) after H/R procedure, compared with control group. While pretreated with GC (1, 10, 100 μM) exhibited reduced expressions of ICAM-1 by 19.1% ($P < 0.05$), 41.3% ($P < 0.01$) and 85.5% ($P < 0.01$), VCAM-1 by 27.2% ($P < 0.05$), 46.1% ($P < 0.01$) and 54.3% ($P < 0.01$) and iNOS by 11.8% ($P > 0.05$), 43.8% ($P < 0.01$) and 60.0% ($P < 0.01$) compared with H/R group in a concentration-dependent manner. In addition, 10 μM Aspirin reduced the levels of ICAM-1, VCAM-1 and iNOS by 82.4% ($P < 0.01$), 59.3% ($P < 0.01$) and 70.1% ($P < 0.01$), respectively, compared with H/R group.

GC Inhibited NF- κB p65 Translocation from Cytosol to Nucleus

Activation of NF- κB pathway is thought to be a key signaling event involved in the pathogenesis of MI/R. To determine whether GC inhibited H/R-induced cardiac NF- κB activation, we first examined the translocation of NF- κB p65 from cytoplasm to the nucleus by western blot. As shown in **Figures 7E,F**, a relatively high level of NF- κB p65 appeared in the cytoplasm of cells but low levels in nucleus in control group. Translocation of p65 from the cytosol into nucleus was evident in H/R group, whereas 10 μM Aspirin blocked this effect. As expected, such nuclear translocation was also concentration-dependently decreased by pretreatment of GC (1, 10, 100 μM). These results confirmed our hypothesis that GC was able to inhibit the translocation of p65 subunit to nucleus upon an inflammatory stimulus such as H/R injury.

GC Inhibited I κB - α Phosphorylation and IKK- β Activity

NF- κB translocation is preceded by the phosphorylation and ubiquitination of I κB - α , we then studied whether I κB - α was also in relation to the effect of GC on NF- κB pathway activation. First, we checked whether the total I κB - α had degraded. The results showed that the total I κB - α in each group was not different (**Figure 7G**). However, the level of p-I κB - α in H/R group remarkably increased by 4.08-fold ($P < 0.01$ vs. control group). In our study, we found a notably inhibitory effect on the H/R-induced I κB - α phosphorylation in the presence of Aspirin

TABLE 2 | Effects of GC on the supernatant inflammatory cytokines of ventricular myocytes.

Group	Concentration (μM)	TNF- α (pg/mL)	IL-1 β (pg/mL)	IL-6 (pg/mL)
Control		6.45 \pm 1.41	34.02 \pm 8.85	48.94 \pm 6.82
H/R		54.61 \pm 9.36 ^{##}	907.96 \pm 32.08 ^{##}	612.16 \pm 41.17 ^{##}
H/R + Aspirin	10	17.33 \pm 3.92 ^{**}	207.46 \pm 81.12 ^{**}	159.03 \pm 9.08 ^{**}
H/R + GC	1	46.38 \pm 4.08 [*]	531.29 \pm 54.70 ^{**}	574.98 \pm 48.95 ^{**}
	10	42.35 \pm 4.47 ^{**}	427.73 \pm 43.31 ^{**}	427.75 \pm 42.88 ^{**}
	100	15.86 \pm 2.91 ^{**}	275.89 \pm 78.23 ^{**}	263.16 \pm 15.52 ^{**}

Values were expressed as mean \pm SD ($n = 8$). ^{##} $P < 0.01$ vs. control group; ^{*} $P < 0.05$, ^{**} $P < 0.01$ vs. H/R group.

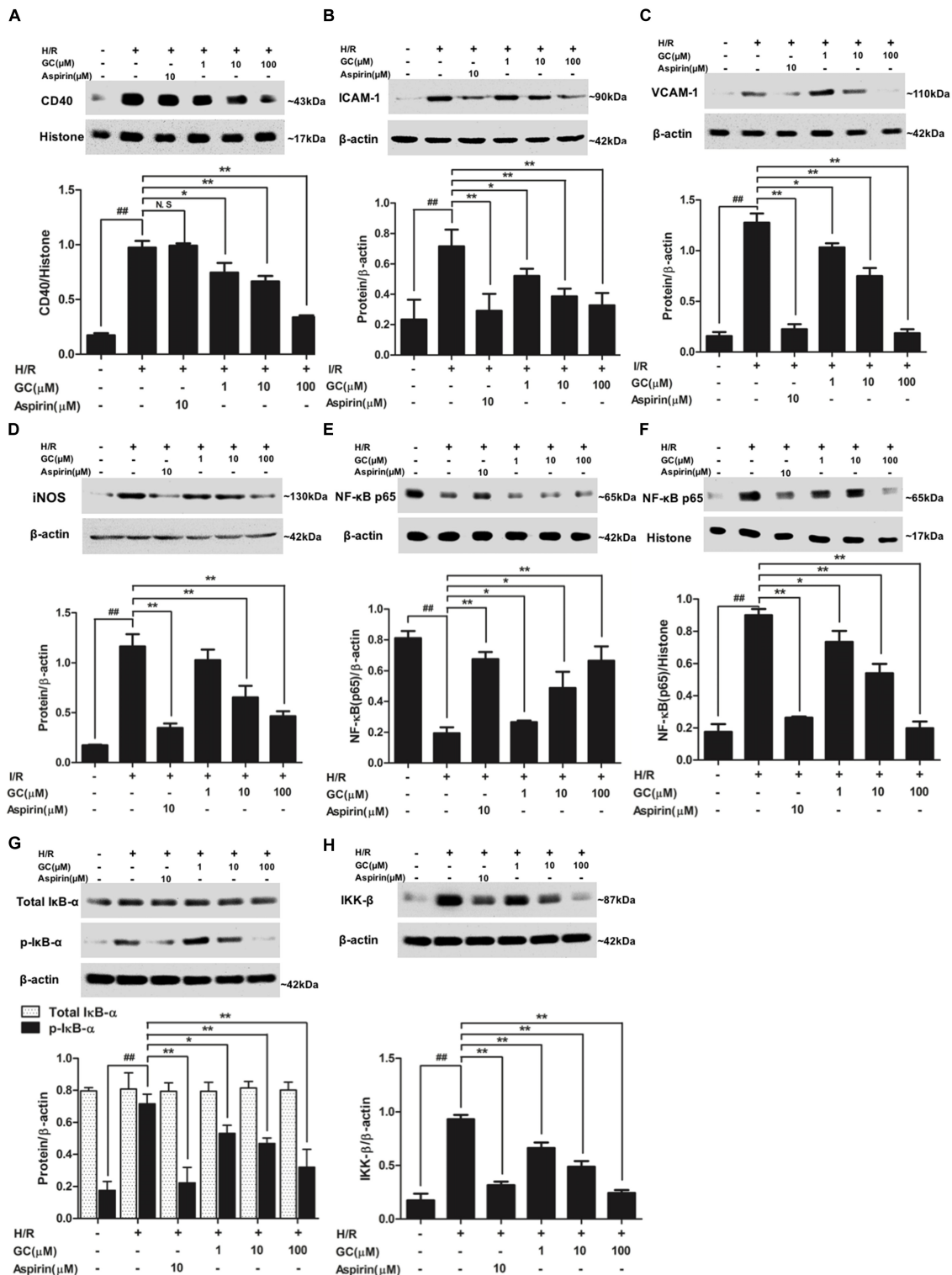


FIGURE 7 | Effects of GC on the expressions of CD40, ICAM-1, VCAM-1, iNOS, NF-κB p65, p-IκB-α and IKK-β by Western blot after H/R procedure.

(A) GC decreased the expression of CD40. (B) GC decreased the expression of ICAM-1. (C) GC decreased the expression of VCAM-1. (D) GC decreased the expression of iNOS. GC blocked the translocation of NF-κB p65 from cytosolic (E) to nuclear (F). (G) GC down-regulated the expression of p-IκB-α. (H) GC decreased the expression of IKK-β. CD40, ICAM-1, VCAM-1, iNOS, p-IκB-α and IKK-β proteins were measured in cytosolic extract. The NF-κB p65 protein levels were assayed separately in cytosolic and nuclear extracts. Results were expressed as Protein/reference protein ratio. Data were expressed as mean ± SD of three independent experiments. ## $P < 0.01$ vs. control group; * $P < 0.05$, ** $P < 0.01$ vs. H/R group.

and GC. The results showed that Aspirin (10 μ M) and GC (1, 10, 100 μ M) all reduced the expressions of p-I κ B- α by 68.9% ($P < 0.01$), 25.8% ($P < 0.01$), 34.7% ($P < 0.01$) and 55.2% ($P < 0.01$) compared with H/R group. These results indicated that GC could produce suppressive effect on NF- κ B by disturbing the phosphorylation of I κ B- α .

Substantial evidence unequivocally shows that a wide variety of influential factors regulate the activity of NF- κ B, especially IKK- β . Then, we investigated the effect of GC on IKK- β activity. The results revealed a significant inhibitory effect on the H/R-induced IKK- β activation in the presence of GC (**Figure 7H**). The level of IKK- β in H/R group remarkably increased by 5.34-fold ($P < 0.01$ vs. control group). In contrast, pretreated with Aspirin (10 μ M) and GC (1, 10, 100 μ M) reduced the expressions of IKK- β (by 66.1, 28.9, 47.6, and 73.8%) ($P < 0.01$) compared with H/R group. These findings indicate that GC could mediate IKK- β activity.

GC Failed to Alleviate H/R-Induced Ventricular Myocytes Inflammatory Injury in the Presence of CD40 Gene Silencing **GC Could Not Elevate Cell Viability in the Presence of CD40 Gene Silence**

The cell viability in H/R + CD40 silencing group was significantly lower than that in control group ($P < 0.01$). After the procedure of CD40 gene silence, GC could not increase the cell viability against to H/R injury (**Figure 8A**).

Successful and Stable CD40 Gene Silencing in Ventricular Myocytes

The ventricular myocytes preincubated with pGPU6/Hygro expressed little CD40 after transfection in control group, and preincubation of pGPU6/Hygro-CD40 successfully and stably inhibited CD40 expression in all groups (**Figure 8B**).

GC Could Not Inhibit Inflammatory Factors Expression in the Presence of CD40 Gene Silence

The expressions of TNF- α , IL-1 β , IL-6, ICAM-1, VCAM-1 and iNOS in H/R + CD40 silencing group were significantly elevated compared with control group. After the procedure of CD40 gene silencing, GC could not regulate the expressions of TNF- α , IL-1 β , IL-6, ICAM-1, VCAM-1 and iNOS (shown in **Figure 8** and **Table 3**).

GC Had No Effect on NF- κ B p65 Translocation, I κ B- α Phosphorylation and IKK- β Activity in the Presence of CD40 Gene Silence

H/R + CD40 silencing group procedure significantly affected the translocation level of NF- κ B, activation of I κ B- α phosphorylation and up-regulation of IKK- β activity. Nonetheless, all GC groups showed no difference in NF- κ B p65 translocation, I κ B- α phosphorylation and IKK- β activity compared with H/R + CD40 silencing group (shown in **Figure 8**).

DISCUSSION

This is the first investigation studied on I/R rats subjected to GC to examine whether GC exerts significant protective effect against MI/R injury *in vivo*, whether CD40 is down-regulated by GC on ventricular myocytes in response to H/R injury *in vitro*, and whether NF- κ B signal pathway plays a considerable role in the whole pathogenesis.

It has been broadly illuminated that inflammation played a vital role in the entire process of MI/R injury, and its effects refer to myocytes dysfunction, inflammatory cytokines overexpression, neutrophil accumulation and myocardium ischemia (Mohanta et al., 2014; Gragnano et al., 2017; Ma et al., 2017). Knowledge of the molecular mechanism underlying the proinflammatory processes of MI/R injury outlined above remains incomplete. However, information does exist regarding distinct signal pathways affected, including the activation of NF- κ B signal pathway.

Ginkgo biloba is a unique tree species with no close living relatives and extracts of its leaves contain anti-inflammatory compounds including glycosides and terpenoids known as ginkgolides and bilobalides which have been reported to possess the properties of anti-cerebrovascular and anti-cardiovascular diseases (Ran et al., 2014). And, the different types of ginkgolides (A, B, C, J, and M) are the main pharmaceutical effective ingredients playing major part in the established medicinal functions of *G. biloba* extracts (Li et al., 2017b). Among them, the pharmacologic effects of GA and GB have been studied deeply now, especially focusing on their anti-inflammatory effects applied to treatment of vascular diseases (Yao et al., 2015; Anderson and Morrow, 2017; Li et al., 2017a). Nevertheless, GC which possesses the similarity chemical structure to GA and GB has not attracted the attention of us so far. Here, GC is investigated whether it possessed a strong anti-inflammatory property, which may be one of its molecular mechanisms of how GC exerts a protective effect in the pretreatment of MI/R injury.

It is clear that lack of blood to heart results in insufficient blood and oxygen transmitted to the beat of the heart muscle, named ischemia, following by damage or dysfunction of the cardiac tissue (Hansen, 1995). In addition, in this study we investigated the effect of GC in a rat model of MI/R injury in a prophylactic approach. Here, we uncovered that pretreatment with GC at 8, 16, 32 mg/kg per day for 7 days protected rat from I/R insult by occlusion of LAD coronary artery, through reduction of infarct size and improvement of myocardium damage. One of the most critical and accepted indicators reflecting therapeutic effect of MI/R injury is reduction of infarct size. In this study, our findings certified that GC was an efficient and promising target drug for prevention of MI/R injury via significant reduction of infarct size. GC also improves the ischemic myocytes damage and inhibits reperfusion-induced energy metabolism dysfunction, at least to a certain extent via suppression of myofibrillar degeneration and restoration of myocardial ultrastructure. Moreover, our recent research clearly provides additional and strong support that *G. biloba* has an irreplaceable role in the therapy of diseases as a valuable herb.

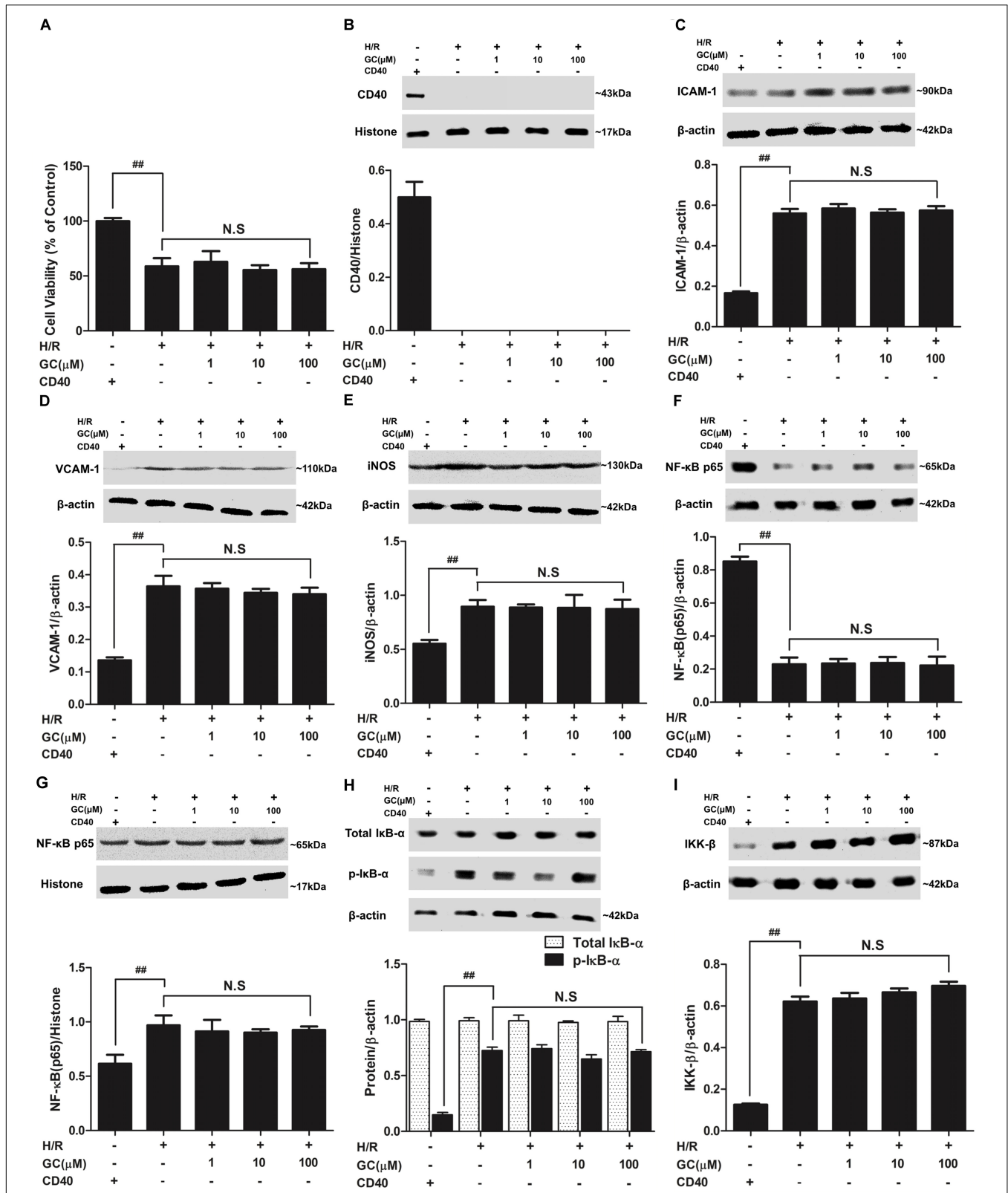


FIGURE 8 | Effects of GC on cell viability (A) and the expressions of (B) CD40, (C) ICAM-1, (D) VCAM-1, (E) iNOS, (F) cytoplasm NF-κB p65, (G) nucleus NF-κB p65, (H) p-IκB-α and (I) IKK-β by Western blot after CD40 silencing procedure. Results were expressed as Protein/reference protein ratio. Data were expressed as mean ± SD of three independent experiments. ##*P* < 0.01 vs. control group; **P* < 0.05, ***P* < 0.01 vs. H/R group.

TABLE 3 | Effects of GC on the supernatant inflammatory cytokines of ventricular myocytes under the condition of CD40 gene silencing.

Group	Concentration (μM)	TNF- α (pg/mL)	IL-1 β (pg/mL)	IL-6 (pg/mL)
Control		6.64 \pm 0.94	35.40 \pm 7.11	48.42 \pm 9.09
H/R + CD40 ⁻		70.08 \pm 11.39 ^{##}	1036.01 \pm 105.01 ^{##}	603.53 \pm 59.57 ^{##}
H/R + GC + CD40 ⁻	1	69.27 \pm 5.88	1041.32 \pm 62.15	600.48 \pm 107.81
	10	68.88 \pm 7.47	1037.66 \pm 52.72	601.44 \pm 80.31
	100	68.56 \pm 4.19	1023.08 \pm 72.66	598.30 \pm 60.98

Values were expressed as mean \pm SD ($n = 8$). ^{##} $P < 0.01$ vs. control group.

Importantly, neutrophils “shoot at first sight,” releasing reactive oxygen species and proteases, thereby causing extensive collateral damage to the ischemic myocardium and increasing infarct size (Stakos et al., 2015). Therefore, adherence of PMNs is identified as the beginning of a series of chain reaction after I/R injury. What is more, a large extent by PMNs infiltrating is a main inflammation response after MI/R. Activated PMNs will lead to a mass of inflammatory mediators’ release, which may directly result in the necrosis and apoptosis of myocytes (Hiroi et al., 2013; Xiao et al., 2017). Suppression of PMNs infiltration diminishes MI/R damage and potentially offers myocardial protection. In the present study, we found a significant aggravation of histopathological damage in *in vivo* model, indicating that there was a definite relationship between PMNs infiltration and MI/R injury. Whereas, administration with GC to rats could remarkably alleviate this situation that leukocyte infiltration was effectively attenuated, as determined by histopathological scores and the counting of PMNs. In addition, MPO activity which correlates closely with the number of neutrophils present in the heart was also evaluated. This result corresponds with respective histopathological scores data. Our investigation may provide a new insight: the potential use of GC as a cardio protective strategy to attenuate PMNs infiltration is clinically feasible for the prevention of MI/R injury.

Moreover, *in vitro*, we further applied H/R-treated ventricular myocytes to stimulate I/R injury *in vivo* thereby confirming the cardioprotective property of GC. Primary cultured neonatal ventricular myocytes stimulated by H/R were further applied to explore the anti-I/R injury property of GC *in vitro*. Increasing evidence suggests that inflammatory and immune responses have a profound impact on the damage process of myocytes directly exposed to H/R which had a strong influence on MI/R injury (Jin et al., 2017). Thus, based on the above reasons, H/R-induced ventricular myocytes *in vitro* model was applied to explore whether GC had protected cells from inflammatory damage caused by MI/R injury. In this study, we stated for the first time that GC increased cell viability after I/R-like insult, suggesting GC can elicit anti-MI/R injury effects by promoting tolerance and viability of cells injured by H/R-induced inflammation.

NF- κB could induce the transcription and expression of multiple cytokines related to immunity and inflammation and other relative gene so as to cause heart damage following pathologic process of I/R injury (Gao et al., 2016). However, there is some evidence that inhibition of NF- κB improves left ventricle (LV) remodeling and contributes to a decrease in cardiac dysfunction after MI/R injury (Lu et al., 2016). Moreover, an

extensive body of research has demonstrated that inhibition of the indirect signal pathways mediated by NF- κB signaling can sharply suppress the inflammation after MI/R injury (Hayden and Ghosh, 2014; Xie et al., 2015). Furthermore, there is the certainty that phosphorylation of I κB - α acts as the trigger of NF- κB p50/p65 heterodimers’ translocation from cytoplasm to the nucleus (Mitchell and Vargas, 2016). Many studies have shown that aspirin treatment caused a strong decrease in NF- κB activation, inhibitor of I κB - α phosphorylation together with translocation of NF- κB p65 to nucleus and IKK- β activation (Shi et al., 2017). And many studies have shown that aspirin could improve I/R injury indexes as a positive and meaningful drug in the treatment of cardiovascular and cerebrovascular diseases (Basili et al., 2014). So we chose aspirin as the positive control to compare with the effect of GC in order to elucidate the exact mechanism. These conclusions are supported by our studies, where H/R group obviously elevated translocation of NF- κB p65, indicating an increased transcriptional activity of p65, whereas GC and aspirin effectively reversed this activated effect. In addition, stimulation with H/R procedure resulted in I κB - α phosphorylation and degradation, which was blocked by pretreatment with GC and aspirin. These results demonstrate that the molecular regulation of GC for I/R-induced inflammation involves in the inhibition of the NF- κB signal pathway, as shown by the reduction in phosphorylation of I κB - α and translocation of NF- κB p65.

It is now clear that NF- κB signaling is tightly regulated at the level of I κB phosphorylation. The IKK complex, composed of IKK (α , β , and γ), is activated by phosphorylation of IKK- α or IKK- β on serine residues within their activation loops either by upstream kinases or through autophosphorylation (Kondylis et al., 2017). The activated complex goes on to phosphorylate I κB - α , causing its ubiquitin-mediated degradation and release of the NF- κB subunits (Yang et al., 2017). And lots of evidence has shown that aspirin’s inhibitory effect of NF- κB has a close relationship with downregulation of IKK- β activity (Gao et al., 2014). Then, we detected whether GC has the similar impact like aspirin on IKK- β activity. Interestingly, IKK- β could also be inhibited by GC in H/R-induced intact ventricular myocytes. Therefore, we concluded that one of the anti-inflammatory targets of GC was IKK- β /NF- κB signaling.

Indeed, much evidence was given that activation of NF- κB occurred at the very early stages of I/R process and then sequentially modulated the occurrence of downstream inflammatory factors (Hostager, 2007). Therefore, we performed immunostaining and ELISA analyses to check whether GC

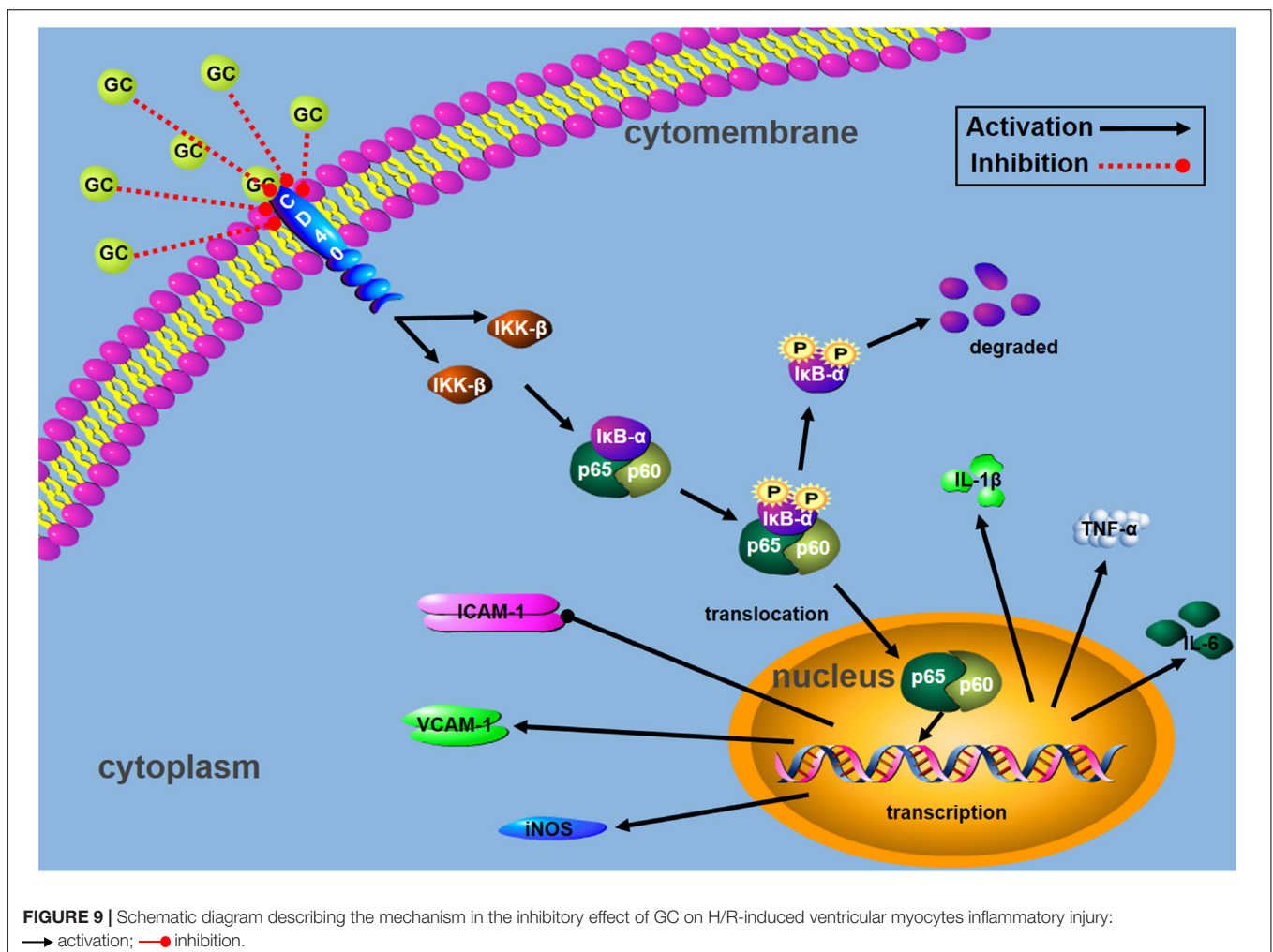
could inhibit the inflammatory chain reaction caused by NF- κ B-dependent gene transcription after I/R procedure. Our findings revealed that GC exerted its cardioprotective effects by an inhibitory mechanism that acted on excretion of pro-inflammatory mediators (TNF- α , IL-1 β and IL-6) and expression of inflammatory proteins (ICAM-1, VCAM-1 and iNOS) through the NF- κ B dependent pathway of inflammation. This is in accord with the investigation that studies the effects of GC on H/R-induced ventricular myocytes model *in vitro*. It means that, GC plays a protective role in the management of MI/R injury by blocking NF- κ B pathway.

CD40 signaling is now widely accepted as a model of the non-canonical NF- κ B pathway, which will strongly trigger its downstream signaling events (Jiang et al., 2011). More importantly, the expression of myocardial CD40 could significantly increase in the whole progression of inflammatory cardiovascular diseases (Hostager and Bishop, 2013). Therefore, CD40-mediated NF- κ B activation is thought to be responsible for the massive inflammation and tissue damage after MI/R injury, and considered to be a valuable and promising therapeutic target against MI/R injury. Interestingly, we found that GC

significantly down-regulated the expression of CD40 compared with H/R group.

According to the fact, we concluded that CD40 played the vital role in regulating inflammation for ventricular myocytes in response to H/R injury. Therefore, we silence the CD40 gene in ventricular myocytes stimulated by H/R to verify our hypothesis. As we expected, the cardioprotective effect of GC disappeared after CD40 gene was silenced. Consequently, it was evident that GC protected heart from MI/R injury through inhibiting NF- κ B pathway via CD40. It is also consistent with other investigations reporting that inhibition of CD40 reduces the activation of NF- κ B.

Taken together, our results obtained from this work demonstrated that GC protected rat from inflammatory insult by occlusion of LAD coronary artery and inhibited H/R-induced inflammatory damage to ventricular myocytes through blocking CD40 dependent NF- κ B signal pathway on the basis of following evidence: (1) GC improved cardiac outcomes of MI/R injury and alleviated PMNs infiltration in rats, (2) GC inhibited overproduction of inflammatory factors (TNF- α , IL-1 β and IL-6) and overexpression of inflammatory proteins (ICAM-1, VCAM-1



and iNOS) both *in vivo* and *in vitro*, (3) CD40 was down-regulated in ventricular myocytes in response to H/R injury, and (4) such effects were dependent on regulating CD40-NF- κ B pathway (Figure 9).

CONCLUSION

GC can exhibit significant cardioprotective effects through reducing infarct size, inhibiting inflammatory response, improving myocardial histological structure and alleviating PMNs infiltration during I/R injury. Inhibition of excessive inflammation via suppressing CD40/NF- κ B signal pathway should be the key mechanism of GC in the protective of MI/R injury. Thus, GC will be a prospective and preventive agent in the management of MI/R injury.

ETHICS STATEMENT

Animal experiments were carried out in accordance with the National Institutes of Health Guide for the Care and

Use of Laboratory Animals. All procedures involved in the use of the laboratory animals were approved by the ethics committee of Shandong University (Permission No. 2013-092).

AUTHOR CONTRIBUTIONS

RZ, DH, ZL, YZ, and PL performed the research. JL, GY, SL, BH, and JbL designed the research study. RZ and CS analyzed the data. RZ wrote and edited the paper.

FUNDING

This study was supported by grants from the National Natural Science Foundation of China (Program No. 81300964), China Postdoctoral Science Foundation (Program Nos. 2013M531611 and 2014T70648), Natural Science Foundation of Shandong Province (Program No. ZR2011HM054), and Science and Technology Development Plan Project of Shandong Province (Program No. 2014GSF118092).

REFERENCES

- Aloui, C., Prigent, A., Sut, C., Tariket, S., Hamzeh-Cognasse, H., Pozzetto, B., et al. (2014). The signaling role of CD40 ligand in platelet biology and in platelet component transfusion. *Int. J. Mol. Sci.* 15, 22342–22364. doi: 10.3390/ijms151222342
- Anderson, J. L., and Morrow, D. A. (2017). Acute myocardial infarction. *N. Engl. J. Med.* 376, 2053–2064. doi: 10.1056/NEJMra1606915
- Anzell, A. R., Maizy, R., Przyklenk, K., and Sanderson, T. H. (2017). Mitochondrial quality control and disease: insights into ischemia-reperfusion injury. *Mol. Neurobiol.* doi: 10.1007/s12035-017-0503-9 [Epub ahead of print].
- Basili, S., Tanzilli, G., Raparelli, V., Calvieri, C., Pignatelli, P., Carnevale, R., et al. (2014). Aspirin reload before elective percutaneous coronary intervention: impact on serum thromboxane b2 and myocardial reperfusion indexes. *Circ. Cardiovasc. Interv.* 7, 577–584. doi: 10.1161/CIRCINTERVENTIONS.113.001197
- Clark, E. A. (2014). A short history of the B-Cell-associated surface molecule CD40. *Front. Immunol.* 5:472. doi: 10.3389/fimmu.2014.00472
- de Waha, S., Jobs, A., Eitel, I., Poss, J., Stiermaier, T., Meyer-Saraei, R., et al. (2017). Multivessel versus culprit lesion only percutaneous coronary intervention in cardiogenic shock complicating acute myocardial infarction: a systematic review and meta-analysis. *Eur. Heart J. Acute Cardiovasc. Care* doi: 10.1177/2048872617719640 [Epub ahead of print].
- Durand, J. K., and Baldwin, A. S. (2017). Targeting IKK and NF-kappaB for therapy. *Adv. Protein Chem. Struct. Biol.* 107, 77–115. doi: 10.1016/bs.apcsb.2016.11.006
- Gao, F., Si, F., Feng, S., and Yi, Q. (2016). Resistin enhances inflammatory cytokine production in coronary artery tissues by activating the NF-kappaB signaling. *Biomed Res. Int.* 2016:3296437. doi: 10.1155/2016/3296437
- Gao, Y., Masoudi, F. A., Hu, S., Li, J., Zhang, H., Li, X., et al. (2014). Trends in early aspirin use among patients with acute myocardial infarction in China, 2001–2011: the China PEACE-Retrospective AMI study. *J. Am. Heart Assoc.* 3:e001250. doi: 10.1161/JAHA.114.001250
- Gragnano, F., Sperlongano, S., Golia, E., and Natale, F. (2017). The role of von willebrand factor in vascular inflammation: from pathogenesis to targeted therapy. *Mediators Inflamm.* 2017:5620314. doi: 10.1155/2017/5620314
- Hansen, P. R. (1995). Role of neutrophils in myocardial ischemia and reperfusion. *Circulation* 91, 1872–1885. doi: 10.1161/01.CIR.91.6.1872
- Hayden, M. S., and Ghosh, S. (2014). Regulation of NF-kappaB by TNF family cytokines. *Semin. Immunol.* 26, 253–266. doi: 10.1016/j.smim.2014.05.004
- He, F., Qu, F., and Song, F. (2012). Aspirin upregulates the expression of neuregulin 1 and survivin after focal cerebral ischemia/reperfusion in rats. *Exp. Ther. Med.* 3, 613–616. doi: 10.3892/etm.2012.450
- Hiroi, T., Wajima, T., Negoro, T., Ishii, M., Nakano, Y., Kiuchi, Y., et al. (2013). Neutrophil TRPM2 channels are implicated in the exacerbation of myocardial ischaemia/reperfusion injury. *Cardiovasc. Res.* 97, 271–281. doi: 10.1093/cvr/cvs332
- Hostager, B. S. (2007). Roles of TRAF6 in CD40 signaling. *Immunol. Res.* 39, 105–114. doi: 10.1007/s12026-007-0082-3
- Hostager, B. S., and Bishop, G. A. (2013). CD40-mediated activation of the NF-kappaB2 pathway. *Front. Immunol.* 4:376. doi: 10.3389/fimmu.2013.00376
- Huang, P., Zhang, L., Chai, C., Qian, X. C., Li, W., Li, J. S., et al. (2014). Effects of food and gender on the pharmacokinetics of ginkgolides A, B, C and bilobalide in rats after oral dosing with ginkgo terpene lactones extract. *J. Pharm. Biomed. Anal.* 100, 138–144. doi: 10.1016/j.jpba.2014.07.030
- Jansen, M. F., Hollander, M. R., Van Royen, N., Horrevoets, A. J., and Lutgens, E. (2016). CD40 in coronary artery disease: a matter of macrophages? *Basic Res. Cardiol.* 111:38. doi: 10.1007/s00395-016-0554-5
- Jiang, W. L., Zhang, S. M., Tang, X. X., and Liu, H. Z. (2011). Protective roles of cornuside in acute myocardial ischemia and reperfusion injury in rats. *Phytomedicine* 18, 266–271. doi: 10.1016/j.phymed.2010.07.009
- Jiang, W. L., Zhang, S. P., Zhu, H. B., and Hou, J. (2012). Cardioprotection of Asperosaponin X on experimental myocardial ischemia injury. *Int. J. Cardiol.* 155, 430–436. doi: 10.1016/j.ijcard.2011.06.010
- Jin, J. L., Deng, Z. T., Lyu, R. G., Liu, X. H., and Wei, J. R. (2017). Expression changes of Notch and nuclear factor-kappaB signaling pathways in the rat heart with myocardial infarction. *Zhonghua Xin Xue Guan Bing Za Zhi* 45, 507–512. doi: 10.3760/cma.j.issn.0253-3758.2017.06.013
- Kondylis, V., Kumari, S., Vlantis, K., and Pasparakis, M. (2017). The interplay of IKK, NF-kappaB and RIPK1 signaling in the regulation of cell death, tissue homeostasis and inflammation. *Immunol. Rev.* 277, 113–127. doi: 10.1111/imr.12550
- Lau, A. J., Yang, G., Rajaraman, G., Baucom, C. C., and Chang, T. K. (2013). Evaluation of *Ginkgo biloba* extract as an activator of human glucocorticoid receptor. *J. Ethnopharmacol.* 145, 670–675. doi: 10.1016/j.jep.2012.11.038
- Li, Y., Wu, Y., Yao, X., Hao, F., Yu, C., Bao, Y., et al. (2017a). Ginkgolide A ameliorates LPS-induced inflammatory responses in vitro and in vivo. *Int. J. Mol. Sci.* 18:E794. doi: 10.3390/ijms18040794
- Li, Y., Zhang, Y., Wen, M., Zhang, J., Zhao, X., Zhao, Y., et al. (2017b). *Ginkgo biloba* extract prevents acute myocardial infarction and suppresses

- the inflammation and apoptosis-regulating p38 mitogen-activated protein kinases, nuclear factor-kappaB and B-cell lymphoma 2 signaling pathways. *Mol. Med. Rep.* 16, 3657–3663. doi: 10.3892/mmr.2017.6999
- Liebert, A., Krause, A., Goonetilke, N., Bicknell, B., and Kiat, H. (2017). A role for photobiomodulation in the prevention of myocardial ischemic reperfusion injury: a systematic review and potential molecular mechanisms. *Sci. Rep.* 7:42386. doi: 10.1038/srep42386
- Liou, C. J., Lai, X. Y., Chen, Y. L., Wang, C. L., Wei, C. H., and Huang, W. C. (2015). Ginkgolide C suppresses adipogenesis in 3T3-L1 adipocytes via the AMPK signaling pathway. *Evid. Based Complement. Alternat. Med.* 2015:298635. doi: 10.1155/2015/298635
- Liu, L., Wei, P., Cao, Y., Zhang, Q., Liu, M., Liu, X. D., et al. (2016). Effect of total peony glucoside pretreatment on NF- κ B and ICAM-1 expression in myocardial tissue of rat with myocardial ischemia-reperfusion injury. *Genet. Mol. Res.* 15, 1–10. doi: 10.4238/gmr15048978
- Ma, Y., Iyer, R. P., Jung, M., Czubyrt, M. P., and Lindsey, M. L. (2017). Cardiac fibroblast activation post-myocardial infarction: current knowledge gaps. *Trends Pharmacol. Sci.* 38, 448–458. doi: 10.1016/j.tips.2017.03.001
- Mansouri, L., Papakonstantinou, N., Ntoufa, S., Stamatopoulos, K., and Rosenquist, R. (2016). NF-kappaB activation in chronic lymphocytic leukemia: a point of convergence of external triggers and intrinsic lesions. *Semin. Cancer Biol.* 39, 40–48. doi: 10.1016/j.semcancer.2016.07.005
- Michel, N. A., Zirluk, A., and Wolf, D. (2017). CD40L and its receptors in atherothrombosis—an update. *Front. Cardiovasc. Med.* 4:40. doi: 10.3389/fcvm.2017.00040
- Mitchell, S., and Vargas, J. (2016). Signaling via the NFkappaB system. *Wiley Interdiscip. Rev. Syst. Biol. Med.* 8, 227–241. doi: 10.1002/wsbm.1331
- Mohanta, T. K., Tamboli, Y., and Zubaidha, P. K. (2014). Phytochemical and medicinal importance of *Ginkgo biloba* L. *Nat. Prod. Res.* 28, 746–752. doi: 10.1080/14786419.2013.879303
- Montecucco, F., Liberale, L., Bonaventura, A., Vecchie, A., Dallegri, F., and Carbone, F. (2017). The role of inflammation in cardiovascular outcome. *Curr. Atheroscler. Rep.* 19:11.
- Nennig, S. E., and Schank, J. R. (2017). The role of NFkB in drug addiction: beyond inflammation. *Alcohol Alcohol.* 52, 172–179. doi: 10.1093/alcac/agw098
- Panda, S., Kar, A., and Biswas, S. (2017). Preventive effect of agnucastolide C against isoproterenol-induced myocardial injury. *Sci. Rep.* 7:16146. doi: 10.1038/s41598-017-16075-0
- Pantazi, E., Bejaoui, M., Folch-Puy, E., Adam, R., and Rosello-Catafau, J. (2016). Advances in treatment strategies for ischemia reperfusion injury. *Expert Opin. Pharmacother.* 17, 169–179. doi: 10.1517/14656566.2016.1115015
- Ran, K., Yang, D. L., Chang, Y. T., Duan, K. M., Ou, Y. W., Wang, H. P., et al. (2014). *Ginkgo biloba* extract postconditioning reduces myocardial ischemia reperfusion injury. *Genet. Mol. Res.* 13, 2703–2708. doi: 10.4238/2014.April.8.14
- Senhaji, N., Kojok, K., Darif, Y., Fadainia, C., and Zaid, Y. (2015). The contribution of CD40/CD40L axis in inflammatory bowel disease: an update. *Front. Immunol.* 6:529. doi: 10.3389/fimmu.2015.00529
- Shi, C., Zhang, N., Feng, Y., Cao, J., Chen, X., and Liu, B. (2017). Aspirin inhibits IKK-beta-mediated prostate cancer cell invasion by targeting matrix metalloproteinase-9 and urokinase-type plasminogen activator. *Cell Physiol. Biochem.* 41, 1313–1324. doi: 10.1159/000464434
- Sivalingam, Z., Larsen, S. B., Grove, E. L., Hvas, A. M., Kristensen, S. D., and Magnusson, N. E. (2017). Neutrophil gelatinase-associated lipocalin as a risk marker in cardiovascular disease. *Clin. Chem. Lab. Med.* 56, 5–18. doi: 10.1515/cclm-2017-0120
- Stakos, D. A., Kambas, K., Konstantinidis, T., Mitroulis, I., Apostolidou, E., Arelaki, S., et al. (2015). Expression of functional tissue factor by neutrophil extracellular traps in culprit artery of acute myocardial infarction. *Eur. Heart J.* 36, 1405–1414. doi: 10.1093/eurheartj/ehv007
- Xiao, R., Xiang, A. L., Pang, H. B., and Liu, K. Q. (2017). Hyperoside protects against hypoxia/reoxygenation induced injury in cardiomyocytes by suppressing the Bnip3 expression. *Gene* 629, 86–91. doi: 10.1016/j.gene.2017.07.063
- Xie, Y., Xie, K., Gou, Q., and Chen, N. (2015). IkappaB kinase alpha functions as a tumor suppressor in epithelial-derived tumors through an NF-kappaB-independent pathway (Review). *Oncol. Rep.* 34, 2225–2232. doi: 10.3892/or.2015.4229
- Yang, C. H., Yen, T. L., Hsu, C. Y., Thomas, P. A., Sheu, J. R., and Jayakumar, T. (2017). Multi-targeting andrographolide, a novel NF-kappaB inhibitor, as a potential therapeutic agent for stroke. *Int. J. Mol. Sci.* 18:E1638. doi: 10.3390/ijms18081638
- Yao, X., Chen, N., Ma, C. H., Tao, J., Bao, J. A., Zong-Qi, C., et al. (2015). *Ginkgo biloba* extracts attenuate lipopolysaccharide-induced inflammatory responses in acute lung injury by inhibiting the COX-2 and NF-kappaB pathways. *Chin. J. Nat. Med.* 13, 52–58. doi: 10.1016/S1875-5364(15)60006-1
- Yarjani, Z. M., Pourmotabbed, A., Pourmotabbed, T., and Najafi, H. (2017). Crocin has anti-inflammatory and protective effects in ischemia-reperfusion induced renal injuries. *Iran. J. Basic Med. Sci.* 20, 753–759. doi: 10.22038/IJBMS.2017.9005
- Zhang, Q., Lenardo, M. J., and Baltimore, D. (2017). 30 years of NF-kappaB: a blossoming of relevance to human pathobiology. *Cell* 168, 37–57. doi: 10.1016/j.cell.2016.12.012

Conflict of Interest Statement: The authors declare that the research was conducted in the absence of any commercial or financial relationships that could be construed as a potential conflict of interest.

Copyright © 2018 Zhang, Han, Li, Shen, Zhang, Li, Yan, Li, Hu, Li and Liu. This is an open-access article distributed under the terms of the Creative Commons Attribution License (CC BY). The use, distribution or reproduction in other forums is permitted, provided the original author(s) and the copyright owner are credited and that the original publication in this journal is cited, in accordance with accepted academic practice. No use, distribution or reproduction is permitted which does not comply with these terms.



Halofuginone Attenuates Osteoarthritis by Rescuing Bone Remodeling in Subchondral Bone Through Oral Gavage

Wenbo Mu¹, Boyong Xu¹, Hairong Ma², Jiao Li¹, Baochao Ji¹, Zhendong Zhang¹, Abdusami Amat¹ and Li Cao^{1*}

¹ Orthopaedics, First Affiliated Hospital of Xinjiang Medical University, Ürümqi, China, ² State Key Laboratory of Pathogenesis, Prevention and Treatment of High Incidence Diseases in Central Asian Xinjiang Key Laboratory of Echinococcosis, Clinical Medical Research Institute, First Affiliated Hospital of Xinjiang Medical University, Ürümqi, China

OPEN ACCESS

Edited by:

Yuhei Nishimura,
Mie University Graduate School of
Medicine, Japan

Reviewed by:

Cleo Selina Bonnet,
Cardiff University, United Kingdom
Chaozong Liu,
University College London,
United Kingdom

*Correspondence:

Li Cao
xjbone@21cn.com

Specialty section:

This article was submitted to
Experimental Pharmacology and Drug
Discovery,
a section of the journal
Frontiers in Pharmacology

Received: 08 September 2017

Accepted: 09 March 2018

Published: 27 March 2018

Citation:

Mu W, Xu B, Ma H, Li J, Ji B, Zhang Z,
Amat A and Cao L (2018)
Halofuginone Attenuates Osteoarthritis
by Rescuing Bone Remodeling in
Subchondral Bone Through Oral
Gavage. *Front. Pharmacol.* 9:269.
doi: 10.3389/fphar.2018.00269

Osteoarthritis (OA) is a common debilitating joint disorder worldwide without effective medical therapy. Articular cartilage and subchondral bone act in concert as a functional unit with the onset of OA. Halofuginone is an analog of the alkaloid febrifugine extracted from the plant *Dichroa febrifuga*, which has been demonstrated to exert inhibition of SMAD 2/3 phosphorylation downstream of the TGF- β signaling pathway and osteoclastogenesis. To investigate whether halofuginone (HF) alleviates OA after administration by oral gavage, 3-month-old male mice were allocated to the Sham group, vehicle-treated anterior cruciate ligament transection (ACLT) group, and HF-treated ACLT group. The immunostaining analysis indicated that HF reduced the number of matrix metalloproteinase 13 (MMP-13) and collagen X (Col X) positive cells in the articular cartilage. Moreover, HF lowered histologic OA score and prevented articular cartilage degeneration. The micro-computed tomography (μ CT) scan showed that HF maintained the subchondral bone microarchitecture, demonstrated by the restoration of bone volume fraction (BV/TV), subchondral bone plate thickness (SBP.Th.), and trabecular pattern factor (Tb.Pf) to a level comparable to that of the Sham group. Immunostaining for CD31 and μ CT based angiography showed that the number and volume of vessels in subchondral bone was restored by HF. HF administered by oral gavage recoupled bone remodeling and inhibited aberrant angiogenesis in the subchondral bone, further slowed the progression of OA. Therefore, HF administered by oral gavage could be a potential therapy for OA.

Keywords: osteoarthritis, articular cartilage, subchondral bone, TGF- β 1, halofuginone

INTRODUCTION

Osteoarthritis (OA) is the most common degenerative condition of the weight-bearing joints, characterized by pain and loss of function (McAlindon et al., 2014). Data from the Third National Health and Nutrition Examination Survey in USA showed that the prevalence of knee joint OA was 12.1% (Pereira et al., 2011). In Asia, knee joint OA affects an estimated 5.7 and 4.4% of men and 10.3 and 19.2% of women in China and Korea respectively (Tang et al., 2015; Lee and Kim, 2017). It's been estimated that the cost of OA treatment is up to 25–50% of a country's GDP

(Puig-Junoy and Ruiz Zamora, 2015). The annual average direct cost of OA management varies from \$1,442 to \$21,335 per person (Xie et al., 2016). Currently, effective disease-modifying therapy for OA is still lacking, leaving pain management and joint replacement as the last option for end-stage OA (Bijlsma et al., 2011; Carr et al., 2012). The pathogenesis of OA is not well understood (van den Berg, 2011), and an improved understanding is greatly needed to develop preventative and effective therapeutic interventions for early-stage OA.

Although maintenance of the articular cartilage is the primary concern of OA treatment, this disease affects the entire joint (Loeser et al., 2012; Findlay and Kuliwaba, 2016). The characteristic pathological changes in OA include articular cartilage degeneration, subchondral bone sclerosis, inflammation, and osteophyte formation (Goldring and Goldring, 2016; Robinson et al., 2016). The articular cartilage and subchondral bone act as a functional unit that transfers the load during weight-bearing and joint motion (Madry et al., 2010; Lories and Luyten, 2011). The subchondral bone, which plays a pivotal role in the initiation and progression of OA, exhibits changes prior to those seen in the articular cartilage (Goldring and Goldring, 2007; Loeser et al., 2012). The subchondral bone is located immediately beneath the CC and can adapt its structural and functional property during modeling and remodeling in response to mechanical stress (Burr and Gallant, 2012).

The temporally and spatially regulated osteoclast and osteoblast activity guarantee the integrity of the subchondral bone (Cao, 2011). Osteoclasts remove bone and, thereby, form the bone marrow microenvironment, which is followed by targeted osteogenesis and angiogenesis for subsequent osteoblast bone formation (Tang et al., 2009). Alterations in the underlying subchondral bone that eventually affect the overlying articular cartilage occur under certain conditions such as ligament injury, overweight individuals, and age-related weakening of muscle strength (Burr and Radin, 2003).

Transforming growth factor $\beta 1$ (TGF- $\beta 1$) is a polypeptide member of the TGF superfamily of cytokines and (de Caestecker, 2004) high levels have detrimental effects on adult joints. Itayem et al. (1999) reported that injecting TGF- $\beta 1$ into the knee joints of adult rats resulted in the onset of OA. Maeda et al. (2011) found that elevated TGF- $\beta 1$ levels were harmful to the tendon. Therefore, maintaining physiological levels of TGF- $\beta 1$ in the subchondral bone is crucial. TGF- $\beta 1$ has been noted to be an important coupling factor of bone resorption and formation and is activated unduly by elevated osteoclast bone resorption when mechanical loading is altered. High levels of active TGF- $\beta 1$ in subchondral bone uncouples bone remodeling, which further adversely affects the overlying articular cartilage (Zhen et al., 2013). Besides, elevated TGF- $\beta 1$ activity has been shown to promote angiogenesis and abnormal angiogenesis in subchondral bone is a known pathological feature of OA (Arnoldi et al., 1972; Cunha and Pietras, 2011). Therefore, targeting excessively elevated TGF- $\beta 1$ signaling in the subchondral bone attenuates the progression of OA (Xie et al., 2016).

Halofuginone (HF) is an analog of the alkaloid febrifugine, which was originally isolated from the plant *Dichroa febrifuga* (Pines and Nagler, 1998) and it is used in commercial poultry production worldwide (Pinion et al., 1995). Increasing attention has been focused on this small molecule because of its beneficial biological activity. HF has been shown effective in treating fibrotic disease, e.g., chronic graft-vs.-host disease and AIDS-related Kaposi sarcoma in human clinical trials (Pines et al., 2003; Koon et al., 2011). It is reported to play an important role in inhibiting fibrosis and the transition of fibroblasts to myofibroblasts by inhibiting SMAD 2/3 phosphorylation downstream of the TGF- β signaling pathway (Pines, 2008, 2014). Besides, HF has been shown to exhibit antiangiogenesis effect from *in vivo* and *in vitro* study through inhibiting sequential events involved in the angiogenic cascade, such as MMP-2 expression, basement membrane invasion, capillary tube formation and deposition of sub-endothelial ECM (Abramovitch et al., 1999; Elkin et al., 2000; Spector et al., 2010). Moreover, HF has also been demonstrated to inhibit TH17 cell differentiation by activating the Amino Acid Starvation Response (Sundrud et al., 2009). The intraperitoneal administration of HF has been shown to attenuate OA progression in one instance by targeting elevated subchondral bone TGF- $\beta 1$ activity in a rodent OA model (Cui et al., 2016). The oral route of administration is a common, convenient, and noninvasive treatment procedure used in scientific experimentation, although it is not always as efficient as other more invasive ways. The aim of the present study is to investigate the potential attenuation of OA progression by HF following administration by oral gavage in a rodent anterior cruciate ligament transection (ACLT) model, which may provide evidence to support the oral route as an alternative route of HF administration for potential clinical application.

MATERIALS AND METHODS

Mice

Three-month-old male C57BL/6 mice were purchased from Vital River and maintained in an animal room on a 12-h light/dark cycle with a temperature and humidity of $25 \pm 2^\circ\text{C}$ and 55%, respectively. The mice were provided with food and water *ad libitum* and subsequently divided into the Sham group, vehicle-, and HF-treated OA groups ($n = 6-8$ per group). Before the surgery to establish the OA model, the mice were anesthetized using a combination of ketamine and xylazine (80/10 mg/kg) administered intraperitoneally. Following a parapatellar incision, the anterior cruciate ligament (ACL) of the right knee was transected using a pair of microscissors to establish the OA model. Then, the joint capsule and skin were sutured separately. For the Sham group, after anesthesia, a sham operation was performed on each mouse, which is, making the parapatellar incision in the right knee joint to expose the ACL, followed by the joint capsule and skin sutured separately without transecting the ACL. After the surgery, the mice were exposed to heat and were monitored until they recovered from the anesthesia. The mice were checked daily postoperatively to monitor their

general health, pain, discomfort, and development of infections. To select the HF dose, a single-dose acute toxicity test was performed in C57BL/6 male mice of 3-month-old and the median lethal dose (LD₅₀) was calculated by the method of Bliss (Pinion et al., 1995). HF hydrobromide (17395-31-2, Watson & Noke) was administered at single doses of 1.068, 1.424, 1.898, 2.531, 3.375, 4.5, and 6 mg/kg body weight by oral gavage, followed by a 14-day observation ($n = 13/\text{group}$). After the dose range selection, HF hydrobromide at three different doses or an equivalent volume of distilled water was administered by oral gavage every other day for 30 days after postoperative day 2. The mice were euthanized 30 and 60 days postoperatively. All the animal experiment protocols were reviewed and approved by the Institutional Animal Care and Use Committee of First Affiliated Hospital of Xinjiang Medical University.

Histochemistry, Immunohistochemistry, and Histomorphometry

Following euthanasia, the right knee joints of the mice were harvested, fixed in 10% buffered formalin for 24 h, and then the specimens were decalcified in 10% ethylene diamine tetraacetic acid (EDTA, pH 7.3) for 21 days, followed by embedment in paraffin (Leica), sagittally. Then, 4- μm -thick serial sections of the medial compartment of the right knee joint were processed for Safranin O—Fast Green, and hematoxylin and eosin (H&E) staining. The tidemark was defined as the boundary between the non-calcified and calcified cartilage (CC). The distance between the surface of the articular cartilage and the tidemark was defined as the thickness of the hyaline cartilage (HC), whereas the thickness of the CC was defined as the distance between the tidemark and the subchondral bone plate (SBP). The thickness parameters mentioned above was measured under $10 \times$ magnification. Tartrate-resistant acid phosphatase (TRAP) staining was also performed following a standard protocol (Sigma-Aldrich). A standard protocol was used to perform the immunohistochemical analysis. The sections were incubated with primary antibodies against matrix metalloproteinase 13 (MMP-13) (Abcam, ab39012, 1:100), collagen X (Col X, Abcam, ab58632, 1:100), phosphorylated Smad2/3 (pSmad2/3, Santa Cruz Biotechnology Inc., 1:40), osterix (Abcam, 22552, 1:500), and CD31 (Abcam, ab28364, 1:100) overnight at 4°C. Subsequently, a horseradish peroxidase-streptavidin detection system (ZSGB BIO) was used to detect the immunoactivity, followed by counterstaining with hematoxylin (ZSGB BIO). A histomorphometric measurement was performed on the entire tibial subchondral bone using an Olympus DP26 microscope, and the quantitative analysis was conducted in a blinded way using cellSens software (Olympus, Int.). The total and positively stained chondrocyte numbers were calculated in the entire articular cartilage for MMP-13 and Col X analysis, whereas the pSmad2/3- and osterix-positive cells in the subchondral bone were counted in three views per specimen for the analysis. The histologic score of OA in medial tibial plateau was calculated as described by Glasson et al. (2010).

Micro-Computed Tomography (μCT) Analysis

The entire right knee joint of the mice was dissected with the soft tissue removed, and then fixed in 10% buffered formalin overnight. Then, the specimen were scanned by micro-computed (μCT , Skyscan 1176). The images were reconstructed (NRecon, v1.6), analyzed (CTAn, v1.9), and the data were analyzed further using three-dimensional (3D) model visualization (CTVol, v2.0). The micro-CT scanner was set at a voltage of 50 kVp, filter of 0.5 mm Al, and resolution of 9 $\mu\text{m}/\text{pixel}$. The sagittal view of the entire medial compartment of the tibial subchondral bone was used for the 3D histomorphometric analysis and the structural parameters analyzed were the trabecular thickness (Tb.Th), bone volume/total tissue volume (BV/TV), and Tb. pattern factor (Tb.Pf).

μCT Based Microangiography

After the mice were euthanized, the thoracic cavity of the mice was opened and a needle was inserted into the left ventricle, through which the vascular circulation system was flushed with 0.9% normal saline containing heparin sodium of 100 $\mu\text{m}/\text{ml}$. Then the vascular circulation system was flushed with 10% neutral buffered formalin, followed by the radiopaque silicone rubber compound containing lead chromate (Microphil MV-122, Flow Tech). The mice were stored at 4°C overnight and then the knee joints were harvested and fixed in 10% neutral buffered formalin for 4 d. Then the specimen were decalcified in a rapid acid decalcifier solution (Rapid Cal Immuno, ZSGB-BIO) for 3 d in order to facilitate image thresholding of the vasculature from the surrounding tissues. μCT imaging system (μCT , Skyscan 1176) were used to obtain images and the μCT scanner was set at a voltage of 45 kVp, filter of 0.2 mm Al, and resolution of 9 $\mu\text{m}/\text{pixel}$.

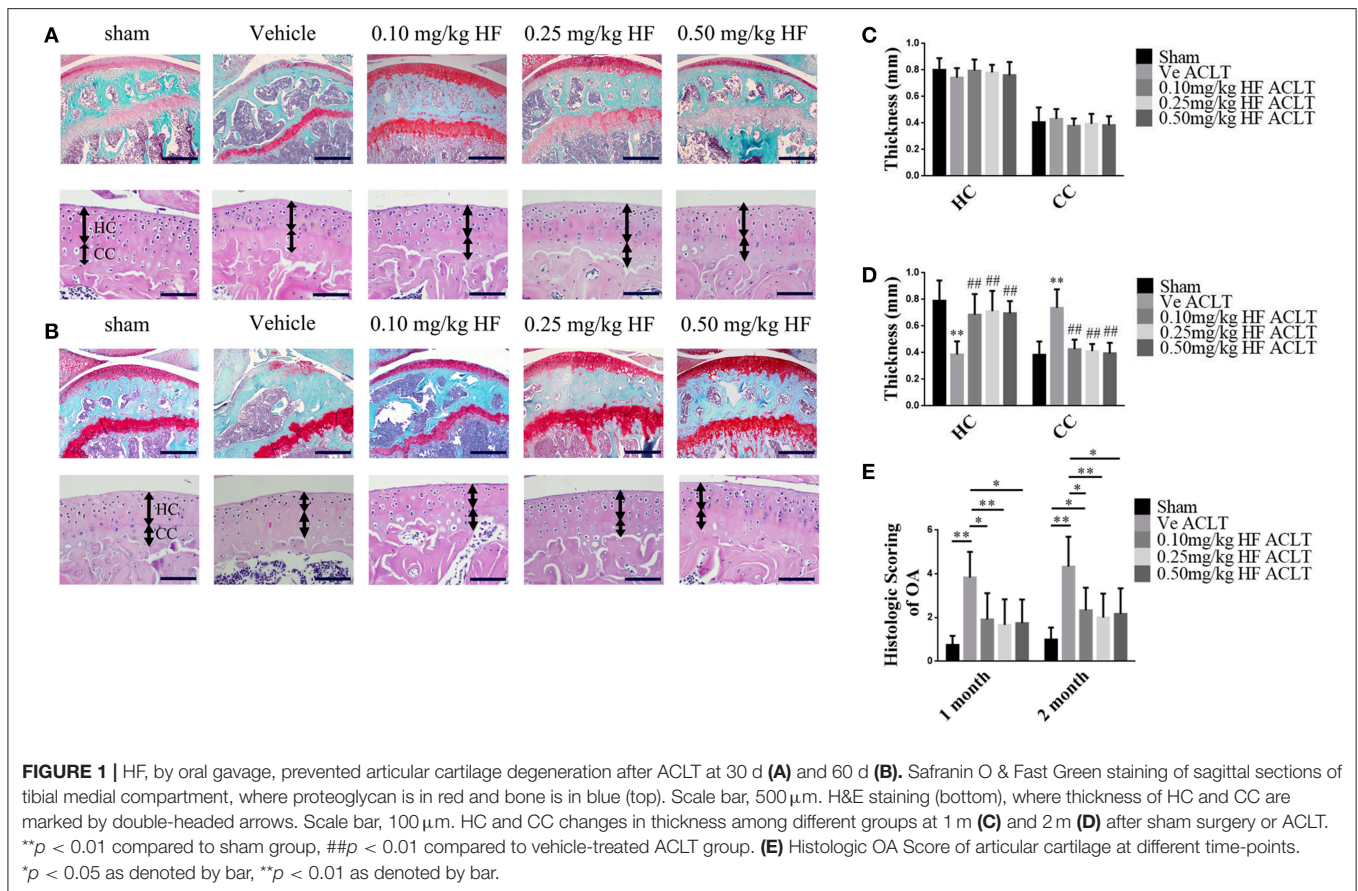
Statistics

The data are presented as the mean \pm standard deviation (*SD*). One-way analysis of variance (ANOVA) with a significance level of 0.05 was used to determine whether the difference among different groups was statistically significant. The statistical package for the social sciences (SPSS) 22.0 (SPSS Inc.) was used for all the data analysis.

RESULTS

HF Preserved Articular Cartilage Following Oral Gavage Administration

The LD₅₀ of HF was calculated as 3.7514 mg/kg, and the test doses used were 0.1, 0.25, and 0.5 mg/kg to investigate whether HF attenuated OA progression following oral gavage. An ACLT-induced OA mouse model was established and HF, which was administered at different doses every other day, protected the articular cartilage. Specifically, the Safranin O and Fast Green staining indicated that the proteoglycan loss in the HF-treated group was comparable to that of the Sham group (**Figures 1A,B**). Histologic score of OA in medial tibial

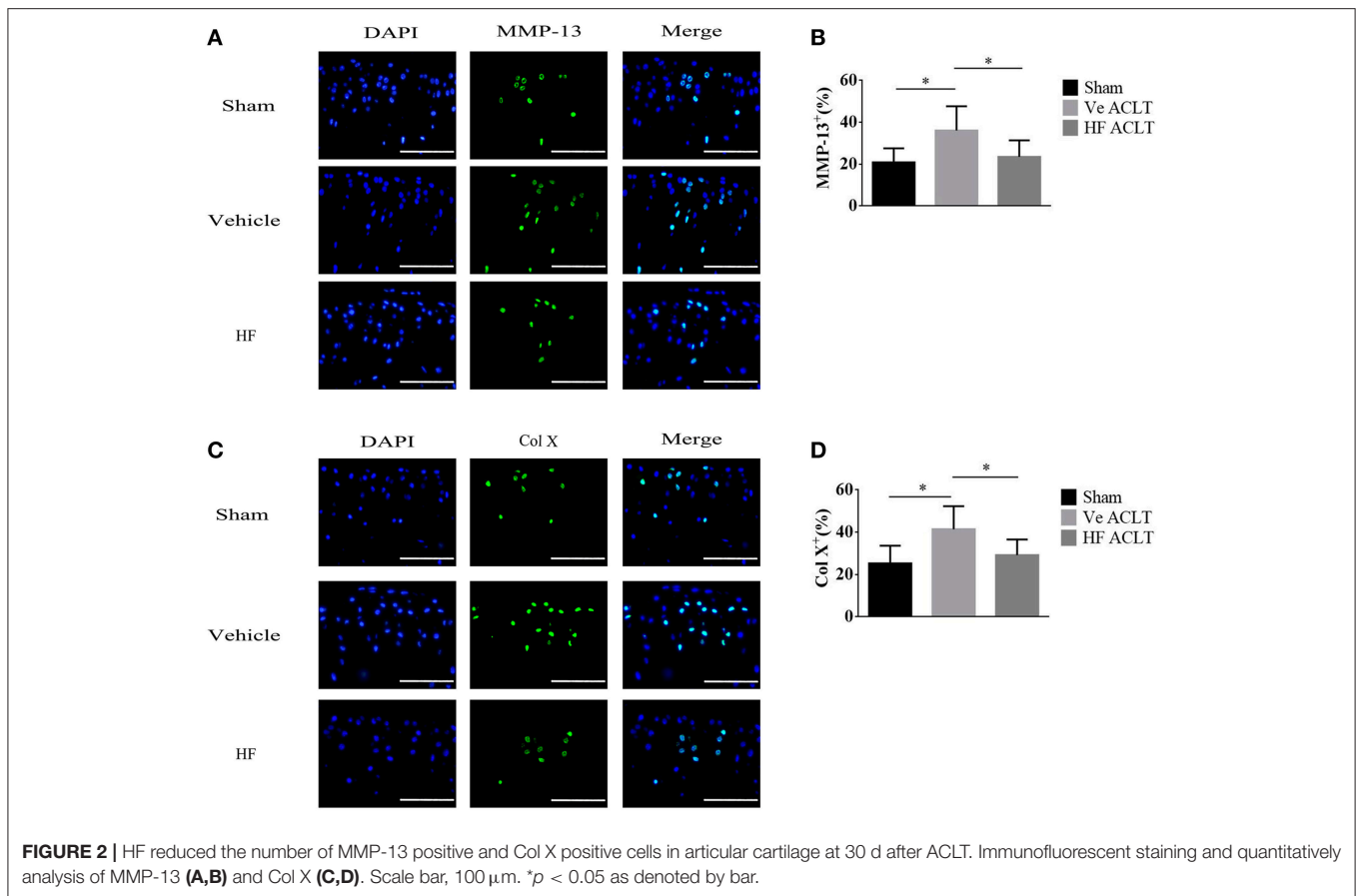


plateau was performed to quantitatively assess the severity of cartilage degeneration. The vehicle-treated ACLT group showed almost twice the score of HF-treated ACLT groups at 1 and 2 months post-operatively (Figure 1E). Similarly, H&E staining showed that the thickness of the CC in vehicle-treated ACLT group was 1.91 times the thickness in sham group at 2 months post-operatively. However, no statistically significance was found in the thickness of HC and CC among sham group and HF-treated ACLT groups ($p > 0.05$) (Figures 1C,D). These results indicate that the three different dosages of HF also attenuated OA progression. HF of 0.25 mg/kg showed maximal effects, although the difference among the three dosage groups was not statistically significant. To validate whether HF itself would cause detrimental effect to the joint, the histologic score was compared and the thickness of HC and CC between sham group and sham + 0.25 mg/kg HF group was assessed. The sham + 0.50 mg/kg HF group was added to further investigate whether higher dosage of HF would harm the joint. As a result, the difference in the histologic score and thickness of HC and CC was not statistically significant among the three groups ($p > 0.05$) (Supplementary Figure 1). Therefore, HF of 0.25 mg/kg was used in the further analysis. The immunostaining results revealed that the number of MMP-13 positive cells was higher after ACLT ($36.10 \pm 11.53\%$) when compared with Sham group ($20.88 \pm 6.69\%$). After transecting the ACL, the number of MMP-13

positive cells was comparable to that of Sham group with use of HF ($23.54 \pm 7.82\%$) (Figure 2). The number of Col X positive cells increased following transecting the ACL ($41.41 \pm 10.89\%$). However, HF abrogated this phenomenon ($29.25 \pm 7.33\%$) to the level comparable to Sham group ($25.26 \pm 8.37\%$) ($p > 0.05$) (Figure 2). These results suggest that HF played a protective role against articular cartilage degeneration.

HF Maintained Subchondral Bone Microarchitecture

This study further investigated whether the protective effect of HF on the articular cartilage is associated with its potential effects on the subchondral bone. Micro-CT was used to analyze the subchondral bone structure. HF improved the subchondral bone microarchitecture (Figure 3A). The ratio of BV to TV was 55.34 ± 5.78 in the Sham group and it decreased substantially to 46.22 ± 4.58 in the vehicle-treated ACLT group. The effect of decreased BV/TV after ACLT was abrogated in the HF-treated group with the BV/TV of 52.99 ± 5.59 at 1 month post-operatively. Similar findings were also noticed at 2 months post-operatively, where BV/TV were decreased from 60.61 ± 3.93 in Sham group to 54.03 ± 3.87 in the vehicle-treated ACLT group and HF maintained it to 59.21 ± 3.75 (Figure 3B). The SBP and articular cartilage interact. Compared with the Sham group, the SBP thickness (SBP.Th.)



was decreased from 0.0762 ± 0.0026 and 0.0784 ± 0.0039 mm to 0.0640 ± 0.0093 and 0.0728 ± 0.0034 mm in the vehicle-treated ACLT group at 1 and 2 months post-operatively. HF maintained the thickness of SBP to 0.0739 ± 0.0088 and 0.0774 ± 0.0023 mm with ACLT at 1 and 2 months post-operatively (**Figure 3C**). The Tb.Pf, with higher value indicating disruption of the connectivity and microarchitecture of the subchondral trabecular bone, was increased from -1.81 ± 0.72 and -1.83 ± 0.62 mm^{-1} in sham group to 1.63 ± 0.78 and 1.30 ± 0.69 mm^{-1} in the vehicle-treated ACLT group at 1 and 2 months post-operatively. Application of HF orally maintained the value of Tb.Pf to -1.17 ± 0.87 and -1.42 ± 0.79 mm^{-1} at 1 and 2 months respectively (**Figure 3D**). These results showed that in the vehicle-treated ACLT group, BV/TV and SBP.Th. was decreased while Tb.Pf was increased when compared with sham group and these effects were abrogated by using HF. Together, these data suggest that de novo aberrant bone formation of subchondral bone after ACLT could be prevented by the administration of HF via oral gavage.

HF Coupled Subchondral Bone Remodeling and Inhibited Aberrant Angiogenesis

The immunohistochemistry analysis was performed to investigate the potential mechanism underlying the effect

of HF on the subchondral bone microarchitecture. It was found that the number of p-Smad2/3 positive cells was increased to $232.32 \pm 27.61/\text{mm}^2$ significantly in the vehicle-treated ACLT group, whereas the difference in the number of p-Smad2/3-positive cells between Sham group ($33.87 \pm 19.29/\text{mm}^2$) and HF-treated ACLT group ($61.62 \pm 29.15/\text{mm}^2$) was not statistically significant ($p > 0.05$) (**Figures 4A,E**). Moreover, the number of TRAP-positive osteoclasts, which indicate the severity of bone resorption, was higher in the vehicle-treated ACLT group ($27.67 \pm 12.14/\text{mm}^2$) than Sham group ($9.00 \pm 4.19/\text{mm}^2$) and this effect was abrogated by HF to a level of $17.00 \pm 7.48/\text{mm}^2$ (**Figures 4B,F**). Furthermore, HF not only affected the number of osterix-positive osteoprogenitors, but also maintained its location. Specifically, the number of osterix-positive osteoprogenitors was increased in the vehicle-treated ACLT group ($91.75 \pm 33.94/\text{mm}^2$) when compared with sham group ($38.79 \pm 24.09/\text{mm}^2$), and this effect was attenuated by HF to a level of $54.55 \pm 19.51/\text{mm}^2$. Furthermore, HF also maintained the location of most osterix-positive cells to the bone surface, instead of the bone marrow, as was observed in the vehicle-treated ACLT group (**Figures 4C,G**). These results suggest that HF restored bone remodeling by inducing coupling bone resorption and formation. The effect of HF on vessel formation in subchondral bone was also investigated in this study. The results showed that the number of CD31 positive endothelial cells were more than three times

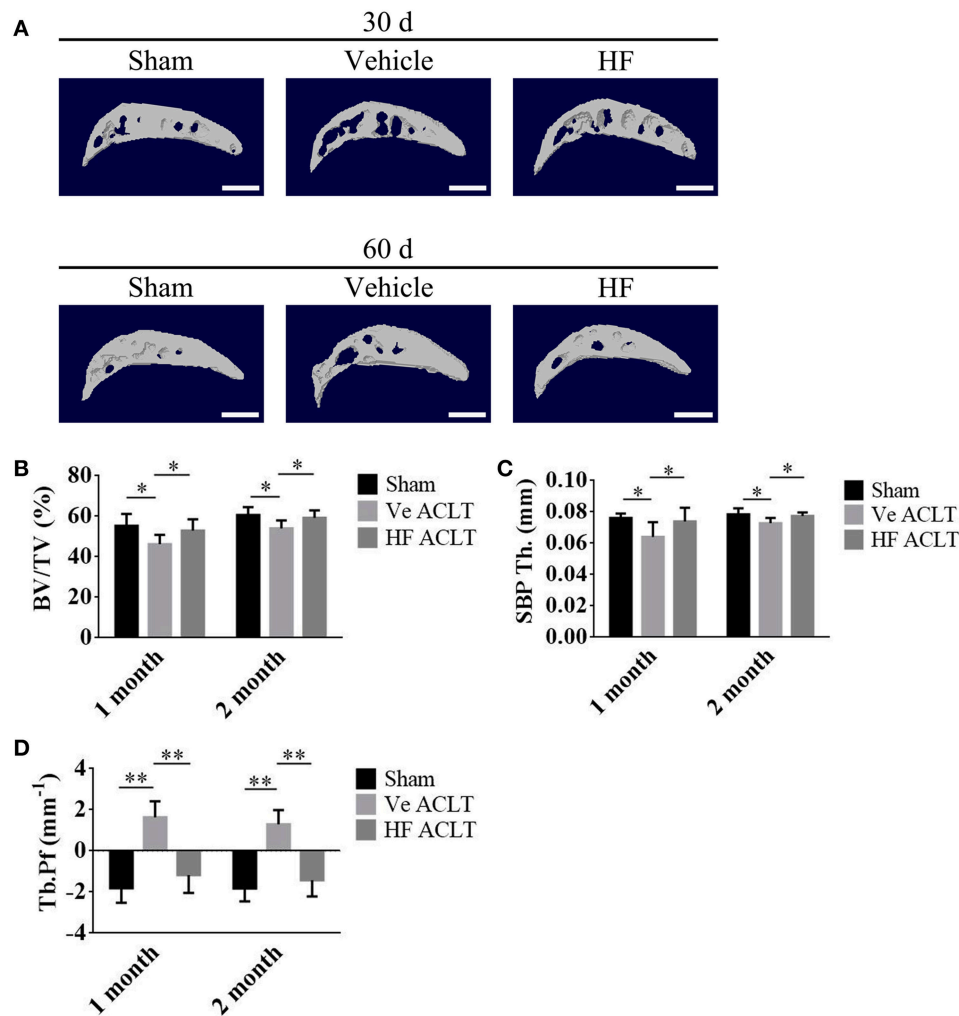


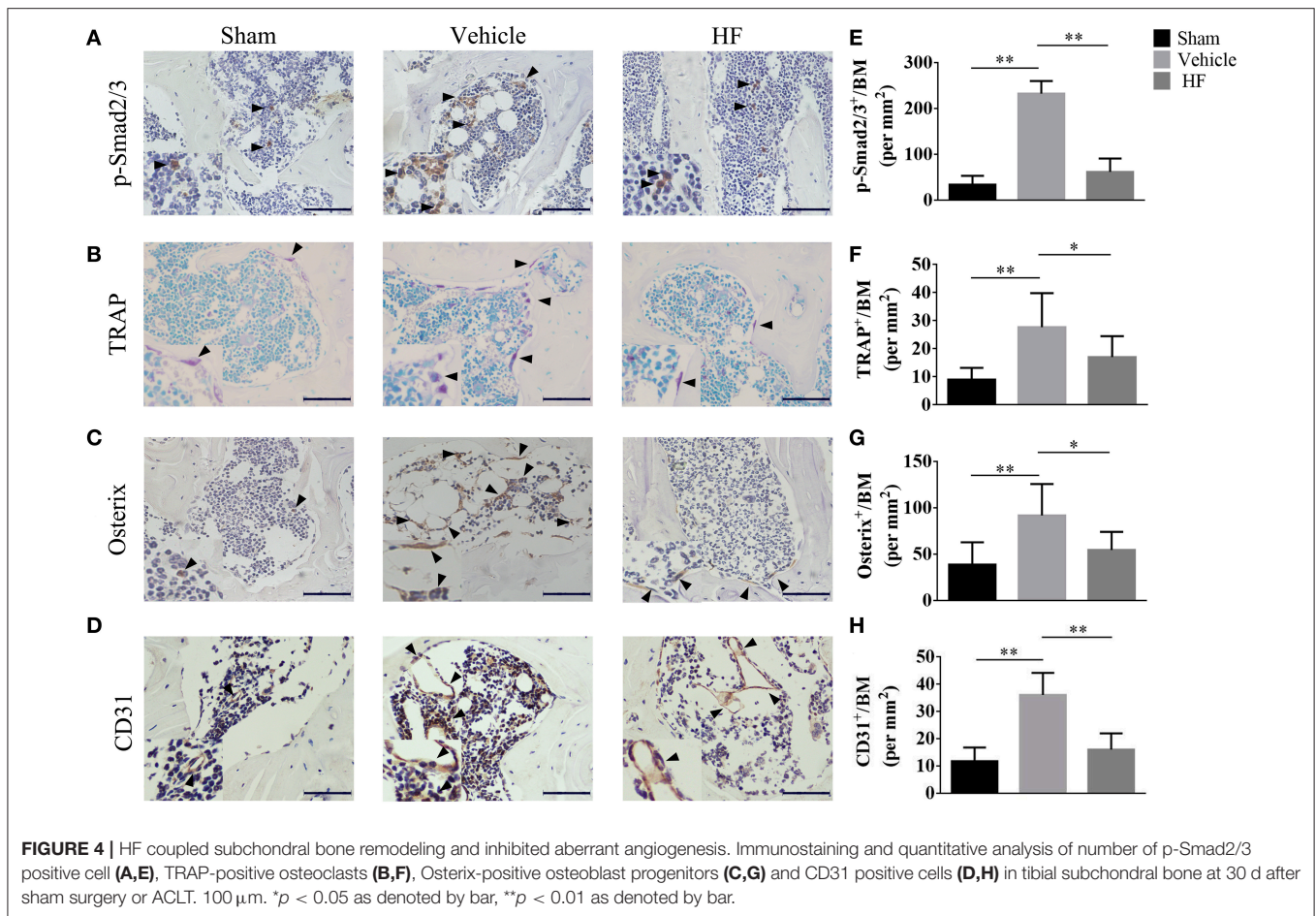
FIGURE 3 | HF maintained normal subchondral bone microarchitecture after ACLT. **(A)** 3D micro-CT image of tibial subchondral bone medial compartment in sagittal view at 30 and 60 d after sham surgery or ACLT. Scale bar, 500 μ m. **(B–D)** Quantitative analysis of micro-CT parameters of tibial subchondral bone: bone volume fraction (BV/TV) **(B)**, thickness of subchondral bone plate (SBP.Th.) **(C)** and trabecular pattern factor (Tb.Pf) **(D)**. * $p < 0.05$ as denoted by bar, ** $p < 0.01$ as denoted by bar.

higher in the vehicle-treated ACLT group ($36.15 \pm 8.09/\text{mm}^2$) when compared with sham group ($11.90 \pm 4.99/\text{mm}^2$) and HF downregulated its value ($16.16 \pm 5.92/\text{mm}^2$) to a level comparable to sham group (Figures 4D,H). Moreover, results from μ CT based microangiography showed that the volume of vessels in subchondral bone was bigger than Sham group ($0.0127 \pm 0.0020 \text{ mm}^3$) after ACLT ($0.0166 \pm 0.0042 \text{ mm}^3$). This phenomenon was inhibited in HF ACLT group with the value of VV as ($0.0113 \pm 0.0027 \text{ mm}^3$) (Figure 5B). Not only the volume of vessels in subchondral bone, but also the number of vessels in subchondral bone was increased in the vehicle-treated ACLT group ($0.3860 \pm 0.0601/\text{mm}$) when compared with sham group. However, the difference in the VN between Sham group ($0.3141 \pm 0.0288/\text{mm}$) and HF ACLT group ($0.2874 \pm 0.0377/\text{mm}$) was not statistically significant ($p > 0.05$) (Figure 5C). Altogether, these results showed that HF significantly reduced the number

of p-Smad2/3 positive cells, TRAP-positive osteoclasts and osterix-positive osteoprogenitors when compared with vehicle-treated group. HF also relocated the majority of osterix-positive osteoprogenitors to the bone surface, instead of subchondral bone marrow in the vehicle-treated group. Besides, HF inhibited the aberrant angiogenesis and restored the volume and number of vessels in subchondral bone to a level comparable to that of sham group (Figure 5).

DISCUSSION

Articular cartilage and subchondral bone function as a unit in the joint and homeostasis of the articular cartilage relies on its interplay with the subchondral bone (Burr and Gallant, 2012). In this study, an unstable, mechanical-loading OA model was established by transecting the ACL.

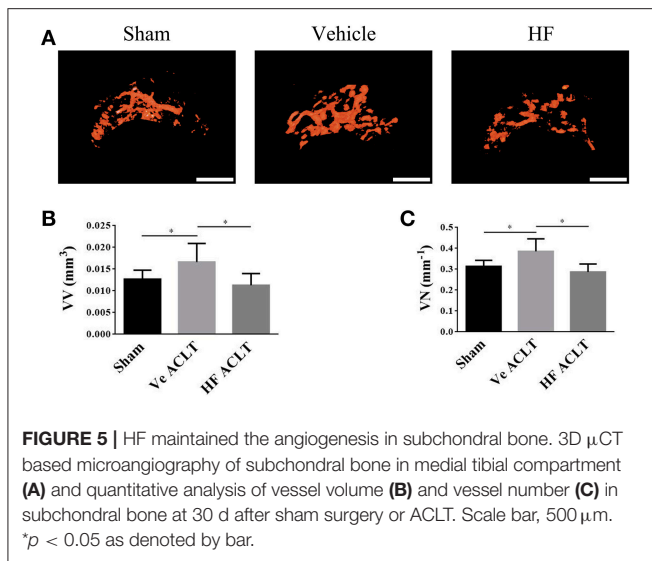


Furthermore, the established model was used to show that HF administered by oral gavage re-established coupled bone remodeling, reduced aberrant angiogenesis, maintained the subchondral bone microarchitecture, preserved the articular cartilage from degeneration and thus slowed OA progression.

The microarchitecture of the subchondral bone changes with the onset of OA, which may precede the articular cartilage degeneration (Zhen et al., 2013). Micro-CT is used to detect subtle changes in subchondral bone. In the present study, it was found that the BV/TV and SBP.Th. were decreased, whereas the Tb.Pf was increased in the vehicle-treated group compared with values in the Sham group. These findings are in agreement with those of previous studies (Botter et al., 2006; Sniekers et al., 2008; Xie et al., 2016). However, the value of these parameters was comparable between the Sham group and HF-treated ACLT groups, indicating that HF maintained the properties of the subchondral bone.

Bone remodeling of the subchondral bone is the major step in mechanical loading changes, which involves bone matrix degradation and formation by osteoclast and osteoblast (Castañeda et al., 2012). Bone resorption and formation occur at specific region following well-defined cascades of events. Osteoclasts resorb the bone at the site of the bone surface during normal bone remodeling, followed by bone formation. It

has been reported that TGF- β is an important coupling factor of bone resorption and formation, which were buried in the bone mineral matrix. TGF- β was released and activated from bone mineral matrix following osteoclast bone resorption. The active TGF- β will direct the mesenchymal stem cells (MSCs) to form the new bone exactly where bone resorption occurs. Osterix-positive osteoprogenitor from MSCs are the precursor cells of osteoblasts. Osteoblasts and their progenitor cells are mainly located at the bone resorption site on bone surface during normal physiological bone remodeling process. However, abnormal mechanical loading results in excessive release and activation of TGF- β from bone mineral matrix in subchondral bone owing to increased bone resorption (Zhen et al., 2013; Shen et al., 2014). Dysregulation of TGF- β alters MSCs recruitment and their fate, uncoupling bone remodeling. Specifically, the excessively released TGF- β mediate further differentiation of MSCs into osteoblast precursors and lead to the commitment of osteoprogenitors in-situ in bone marrow cavities instead of bone surface. The clustered bone marrow osteoprogenitors will lead to osteoid islets in the subchondral bone marrow, visualized as bone marrow lesions from MRI and identified as a prognostic factor of OA progression (Suri and Walsh, 2012), further resulting in alteration of SBP.Th. and advancement of CC into the overlying HC (Bullough, 2004; Suri and Walsh, 2012). In this study,



it was found that HF administered by oral gavage, prevented abnormal bone resorption and aberrant bone formation. Besides, the activity TGF- β , which were indicated by the number of p-Smad 2/3 positive cells in subchondral bone was decreased to a level comparable to that in Sham group with HF after ACLT. The possible underlying mechanism of rescuing uncoupled bone remodeling with HF involves a decrease in the release and activation of TGF- β from the bone mineral matrix because HF reduced abnormal bone resorption, thus further inhibited osteoid islets formation.

Adequate blood supply is critical to bone tissues and bone formation is usually coupled with vessel formation (Portal-Núñez et al., 2012). Blood circulation can supply nutrients, oxygen, minerals that required during osteogenesis and it can carry away the metabolic waste (Percival and Richtsmeier, 2013). Aberrant vessel formation in subchondral bone is a known characteristic of OA (Lotz, 2012). Increasing the TGF β signaling in endothelial progenitor cells can enhance vessel formation (Cunha and Pietras, 2011). Besides, TGF β has also been demonstrated to promote angiogenesis via stimulating the paracrine machinery in MSCs (Guiducci et al., 2011). HF has been demonstrated to result in inhibitory effects on representative sequential events in the angiogenic cascade (Pines and Spector, 2015). It inhibits the diameter and length of vessels in tumor tissue (Gavish et al., 2002). CD31 is a classic marker of endothelial cells and it is used for evaluation of angiogenesis (Newman et al., 1990). In the present study, increased CD31 positive staining in subchondral bone was observed in the vehicle-treated ACLT group. Moreover, micro-CT based microangiography analysis showed that both the vessel volume and vessel number was increased after ACLT. These results confirmed the role of aberrant vessel formation in subchondral bone during the progression of OA. By way of oral gavage, HF abrogated the aberrant angiogenesis, maintained both the volume and number of vessels in subchondral bone. Previously it has been demonstrated that abrogation of increased TGF β activity in subchondral bone can normalize the aberrant

angiogenesis in subchondral bone during OA (Zhen et al., 2013). This study showed that HF reduced the number of p-Smad 2/3 positive cells and inhibited aberrant angiogenesis in subchondral bone, contributing to the maintenance of the subchondral bone microarchitecture. It is hypothesized that the profound effect of HF on normalization of angiogenesis in subchondral bone was likely primarily due to the inhibition of elevated TGF β activity in subchondral bone and further *in-vitro* experiment are needed to validate the exact mechanism in the future.

The normalization of bone remodeling and angiogenesis in the subchondral bone preserved the overlying articular cartilage. Cartilage is composed of specialized chondrocyte cells that produce a large amount of collagenous extracellular matrix proteins including proteoglycan and type II collagen (collagen II). Proteoglycan and collagen II maintain the homeostasis of the articular cartilage, which keeps it intact. During the progression of OA, the chondrocytes hypertrophy and synthesized proinflammatory cytokines that contribute to their destruction (Luyten et al., 2006; Goldring and Goldring, 2010). Col X is a classic marker of hypertrophic differentiation of chondrocytes (von der Mark et al., 1992). MMP-13 is the primary collagenase synthesized by chondrocytes, which damages aggrecan and collagen II during OA. The histologic scoring system for OA in mice is used to quantitatively assess the severity of cartilage damage (Glasson et al., 2010). In the present study, it was discovered that advancement of the CC zone was blocked in the HF-treated ACLT group compared with that in the vehicle-treated ACLT group. It was also noticed that treatment with HF reduced the number of Col X and MMP-13 positive cells in the cartilage and lowered the histologic score more than that of the vehicle-treated ACLT group. These results demonstrate that HF rescued the homeostasis and integrity of the articular cartilage.

HF was investigated in clinical trials for the treatment of chronic graft-vs.-host disease and solid tumors and showed safe therapeutic efficacy following oral administration (Nagler and Pines, 1999; De Jonge et al., 2006). The results of this study may contribute to expanding its clinical application. The kinetics of drug uptake and distribution may differ dramatically between the various routes of administration and bioavailability following oral administration may be relatively lower. However, oral administration is a considerably more convenient route that is often more acceptable to patients, especially for those who need to repeatedly administer medications. In the present study, for the first time, it was shown that HF administered by oral gavage recoupled bone remodeling and inhibited aberrant angiogenesis in the subchondral bone in early-stage OA. More importantly, the articular cartilage, which is the primary concern in OA treatment, was preserved. Altogether, these results indicate that HF administered by oral gavage is an effective strategy for preventing OA progression.

AUTHOR CONTRIBUTIONS

WM: Designed, performed the research and wrote the paper; BX: Performed the research and contributed reagents; HM: Designed

the research and edited the paper; JL: Performed the research; BJ and ZZ: Analyzed the data; AA: Coordinated the research process; LC: Revised the paper and guided the research.

ACKNOWLEDGMENTS

We would like to express our sincere thanks to Prof. Xu Cao from the department of orthopedic surgery of Johns Hopkins University for the guidance and support for this study. This study was supported by grants from Major Science and Technology Projects in Xinjiang Uygur Autonomous Region (No. 201430123-3) and Joint Funds of the National Natural Science Foundation of China (No. U1503221).

REFERENCES

- Abramovitch, R., Dafni, H., Neeman, M., Nagler, A., and Pines, M. (1999). Inhibition of neovascularization and tumor growth, and facilitation of wound repair, by halofuginone, an inhibitor of collagen type I synthesis. *Neoplasia* 1, 321–329.
- Arnoldi, C. C., Linderholm, H., and Müssbichler, H. (1972). Venous engorgement and intraosseous hypertension in osteoarthritis of the hip. *J. Bone Joint Surg. Br.* 54, 409–421. doi: 10.1302/0301-620X.54B3.409
- Bijlsma, J. W., Berenbaum, F., and Lefeber, F. P. (2011). Osteoarthritis: an update with relevance for clinical practice. *Lancet* 377, 2115–2126. doi: 10.1016/S0140-6736(11)60243-2
- Botter, S. M., van Osch, G. J., Waarsing, J. H., Day, J. S., Verhaar, J. A., Pols, H. A., et al. (2006). Quantification of subchondral bone changes in a murine osteoarthritis model using micro-CT. *Biorheology* 43, 379–388.
- Bullough, P. G. (2004). The role of joint architecture in the etiology of arthritis. *Osteoarthr. Cartil.* 12, S2–S9. doi: 10.1016/j.joca.2003.09.010
- Burr, D. B., and Gallant, M. A. (2012). Bone remodelling in osteoarthritis. *Nat. Rev. Rheumatol.* 8, 665–673. doi: 10.1038/nrrheum.2012.130
- Burr, D. B., and Radin, E. L. (2003). Microfractures and microcracks in subchondral bone: are they relevant to osteoarthritis? *Rheum. Dis. Clin. North Am.* 29, 675–685. doi: 10.1016/S0889-857X(03)00061-9
- Cao, X. (2011). Targeting osteoclast–osteoblast communication. *Nat. Med.* 17, 1344–1346. doi: 10.1038/nm.2499
- Carr, A. J., Robertsson, O., Graves, S., Price, A. J., Arden, N. K., Judge, A., et al. (2012). Knee replacement. *Lancet* 379, 1331–1340. doi: 10.1016/S0140-6736(11)60752-6
- Castañeda, S., Roman-Blas, J. A., Largo, R., and Herrero-Beaumont, G. (2012). Subchondral bone as a key target for osteoarthritis treatment. *Biochem. Pharmacol.* 83, 315–323. doi: 10.1016/j.bcp.2011.09.018
- Cui, Z., Crane, J., Xie, H., Jin, X., Zhen, G., Li, C., et al. (2016). Halofuginone attenuates osteoarthritis by inhibition of TGF- β activity and H-type vessel formation in subchondral bone. *Ann. Rheum. Dis.* 75, 1714–1721. doi: 10.1136/annrheumdis-2015-207923
- Cunha, S. I., and Pietras, K. (2011). ALK1 as an emerging target for antiangiogenic therapy of cancer. *Blood* 117, 6999–7006. doi: 10.1182/blood-2011-01-330142
- de Caestecker, M. (2004). The transforming growth factor-beta superfamily of receptors. *Cytokine Growth Factor Rev.* 15, 1–11. doi: 10.1016/j.cytogfr.2003.10.004
- De Jonge, M. J., Dumez, H., Verweij, J., Yarkoni, S., Snyder, D., Lacombe, D., et al. (2006). Phase I, and pharmacokinetic study of halofuginone, an oral quinazolinone derivative in patients with advanced solid tumors. *Eur. J. Cancer* 42, 1768–1774. doi: 10.1016/j.ejca.2005.12.027
- Elkin, M., Miao, H. Q., Nagler, A., Aingorn, E., Reich, R., Hemo, I., et al. (2000). Halofuginone: a potent inhibitor of critical steps in angiogenesis progression. *FASEB J.* 14, 2477–2485. doi: 10.1096/fj.00-0292com

SUPPLEMENTARY MATERIAL

The Supplementary Material for this article can be found online at: <https://www.frontiersin.org/articles/10.3389/fphar.2018.00269/full#supplementary-material>

Supplementary Figure 1 | HF, by oral gavage, shows no obvious detrimental effect on the joint after sham operation at 30 d (A) and 60 d (B). Safranin O & Fast Green staining of sagittal sections of tibial medial compartment, where proteoglycan is in red and bone is in blue (top). Scale bar, 500 μ m. H&E staining (A, bottom, B, bottom), where thickness of HC and CC are marked by double-headed arrows at 1 m (A) and 2 m (B) after sham surgery. Scale bar, 100 μ m. Changes of HC and CC in thickness among different groups at 1 m (C) and 2 m (D) after sham surgery. (E) Histologic OA Score of articular cartilage at different time-points.

- Findlay, D. M., and Kuliwaba, J. S. (2016). Bone-cartilage crosstalk: conversation for understanding osteoarthritis. *Bone Res.* 4:16028. doi: 10.1038/boneres.2016.28
- Gavish, Z., Pinthus, J. H., Barak, V., Ramon, J., Nagler, A., Eshhar, Z., et al. (2002). Growth inhibition of prostate cancer xenografts by halofuginone. *Prostate* 51, 73–83. doi: 10.1002/pros.10059
- Glasson, S. S., Chambers, M. G., Van Den Berg, W. B., and Little, C. B. (2010). The OARSI histopathology initiative - recommendations for histological assessments of osteoarthritis in the mouse. *Osteoarthr. Cartil.* 18, 17–23. doi: 10.1016/j.joca.2010.05.025
- Goldring, M. B., and Goldring, S. R. (2007). Osteoarthritis. *J. Cell. Physiol.* 213, 626–634. doi: 10.1002/jcp.21258
- Goldring, M. B., and Goldring, S. R. (2010). Articular cartilage and subchondral bone in the pathogenesis of osteoarthritis. *Ann. N. Y. Acad. Sci.* 1192, 230–237. doi: 10.1111/j.1749-6632.2009.05240.x
- Goldring, S. R., and Goldring, M. B. (2016). Changes in the osteochondral unit during osteoarthritis: structure, function and cartilage-bone crosstalk. *Nat. Rev. Rheumatol.* 12, 632–644. doi: 10.1038/nrrheum.2016.148
- Guiducci, S., Manetti, M., Romano, E., Mazzanti, B., Ceccarelli, C., Dal Pozzo, S., et al. (2011). Bone marrow-derived mesenchymal stem cells from early diffuse systemic sclerosis exhibit a paracrine machinery and stimulate angiogenesis *in vitro*. *Ann. Rheum. Dis.* 70, 2011–2021. doi: 10.1136/ard.2011.150607
- Itayem, R., Mengarelli-Widholm, S., and Reinholt, F. P. (1999). The long-term effect of a short course of transforming growth factor-beta1 on rat articular cartilage. *APMIS* 107, 183–192.
- Koon, H. B., Fingleton, B., Lee, J. Y., Geyer, J. T., Cesarman, E., Parise, R. A., et al. (2011). Phase II AIDS Malignancy Consortium trial of topical halofuginone in AIDS-related Kaposi sarcoma. *J. Acquir. Immune Defic. Syndr.* 56, 64–68. doi: 10.1097/QAI.0b013e3181fc0141
- Lee, S., and Kim, S. J. (2017). Prevalence of knee osteoarthritis, risk factors, and quality of life: the Fifth Korean National Health and Nutrition Examination Survey. *Int. J. Rheum. Dis.* 20, 809–817. doi: 10.1111/1756-185X.12795
- Loeser, R. F., Goldring, S. R., Scanzello, C. R., and Goldring, M. B. (2012). Osteoarthritis: a disease of the joint as an organ. *Arthritis Rheum.* 64, 1697–1707. doi: 10.1002/art.34453
- Lories, R. J., and Luyten, F. P. (2011). The bone-cartilage unit in osteoarthritis. *Nat. Rev. Rheumatol.* 7, 43–49. doi: 10.1038/nrrheum.2010.197
- Lotz, M. (2012). Osteoarthritis year 2011 in review: biology. *Osteoarthritis Cartilage* 20, 192–196. doi: 10.1016/j.joca.2011.11.015
- Luyten, F. P., Lories, R. J., Verschuere, P., de Vlam, K., and Westhovens, R. (2006). Contemporary concepts of inflammation, damage and repair in rheumatic disease. *Best Pract. Res. Clin. Rheumatol.* 20, 829–848. doi: 10.1016/j.berh.2006.06.009
- Madry, H., van Dijk, C. N., and Mueller-Gerbl, M. (2010). The basic science of the subchondral bone. *Knee Surg. Sports Traumatol. Arthrosc.* 18, 419–433. doi: 10.1007/s00167-010-1054-z

- Maeda, T., Sakabe, T., Sunaga, A., Sakai, K., Rivera, A. L., Keene, D. R., et al. (2011). Conversion of mechanical force into TGF- β -mediated biochemical signals. *Curr. Biol.* 21, 933–941. doi: 10.1016/j.cub.2011.04.007
- McAlindon, T. E., Bannuru, R. R., Sullivan, M. C., Arden, N. K., Berenbaum, F., Bierma-Zeinstra, S. M., et al. (2014). OARSI guidelines for the non-surgical management of knee osteoarthritis. *Osteoarthr. Cartil.* 22, 363–388. doi: 10.1016/j.joca.2014.01.003
- Nagler, A., and Pines, M. (1999). Topical treatment of cutaneous chronic graft versus host disease (cGVHD) with halofuginone: a novel inhibitor of collagen type I synthesis. *Transplantation* 68, 1806–1809. doi: 10.1097/00007890-199912150-00027
- Newman, P. J., Berndt, M. C., Gorski, J., White, G. C., Lyman, S., Paddock, C., et al. (1990). PECAM-1(CD31) cloning and relation to adhesion molecules of the immunoglobulin gene superfamily. *Science* 247, 1219–1222. doi: 10.1126/science.1690453
- Percival, C. J., and Richtsmeier, J. T. (2013). Angiogenesis and intramembranous osteogenesis. *Dev. Dyn.* 242, 909–922. doi: 10.1002/dvdy.23992
- Pereira, D., Peleteiro, B., Araujo, J., Branco, J., Santos, R. A., and Ramos, E. (2011). The effect of osteoarthritis definition on prevalence and incidence estimates: a systematic review. *Osteoarthr. Cartil.* 19, 1270–1285. doi: 10.1016/j.joca.2011.08.009
- Pines, M. (2008). Targeting TGF β signaling to inhibit fibroblasts activation as a therapy for fibrosis and cancer. *Expert Opin Drug Dis.* 3, 11–20. doi: 10.1517/17460441.3.1.11
- Pines, M. (2014). Halofuginone for fibrosis, regeneration and cancer in the gastrointestinal tract. *World J. Gastroenterol.* 20, 14778–14786. doi: 10.3748/wjg.v20.i40.14778
- Pines, M., and Nagler, A. (1998). Halofuginone: a novel antifibrotic therapy. *Gen. Pharmacol.* 30, 445–450. doi: 10.1016/S0306-3623(97)00307-8
- Pines, M., and Spector, I. (2015). Halofuginone—the multifaceted molecule. *Molecules* 20, 573–594. doi: 10.3390/molecules20010573
- Pines, M., Snyder, D., Yarkoni, S., and Nagler, A. (2003). Halofuginone to treat fibrosis in chronic graft-versus-host disease and scleroderma. *Biol. Blood Marrow Transplant.* 9, 417–425. doi: 10.1016/S1083-8791(03)00151-4
- Pinion, J. L., Bilgili, S. F., Eckman, M. K., and Hess, J. B. (1995). The effects of halofuginone and salinomycin, alone and in combination, on live performance and skin characteristics of broilers. *Poult. Sci.* 74, 391–397. doi: 10.3382/ps.0740391
- Portal-Núñez, S., Lozano, D., and Esbrit, P. (2012). Role of angiogenesis on bone formation. *Histol. Histopathol.* 27, 559–566. doi: 10.14670/HH-27.559
- Puig-Junoy, J., and Ruiz Zamora, A. (2015). Socio-economic costs of osteoarthritis: a systematic review of cost-of-illness studies. *Semin. Arthritis Rheum.* 44, 531–541. doi: 10.1016/j.semarthrit.2014.10.012
- Robinson, W. H., Lepus, C. M., Wang, Q., Raghu, H., Mao, R., Lindstrom, T. M., et al. (2016). Low-grade inflammation as a key mediator of the pathogenesis of osteoarthritis. *Nat. Rev. Rheumatol.* 12, 580–592. doi: 10.1038/nrrheum.2016.136
- Shen, J., Li, S., and Chen, D. (2014). TGF- β signaling and the development of osteoarthritis. *Bone Res* 2:14002. doi: 10.1038/boneres.2014.2
- Sniekers, Y. H., Intema, F., Lafeber, F. P., van Osch, G. J., van Leeuwen, J. P., Weinans, H., et al. (2008). A role for subchondral bone changes in the process of osteoarthritis: a micro-CT study of two canine models. *BMC Musculoskelet. Disord.* 9:20. doi: 10.1186/1471-2474-9-20
- Spector, I., Honig, H., Kawada, N., Nagler, A., Genin, O., and Pines, M. (2010). Inhibition of pancreatic stellate cell activation by halofuginone prevents pancreatic xenograft tumor development. *Pancreas* 39, 1008–1015. doi: 10.1097/MPA.0b013e3181da8aa3
- Sundrud, M. S., Koralov, S. B., Feuerer, M., Calado, D. P., Kozhaya, A. E., Rhule-Smith, A., et al. (2009). Halofuginone inhibits TH17 cell differentiation by activating the amino acid starvation response. *Science* 324, 1334–1338. doi: 10.1126/science.1172638
- Suri, S., and Walsh, D. A. (2012). Osteochondral alterations in osteoarthritis. *Bone* 51, 204–211. doi: 10.1016/j.bone.2011.10.010
- Tang, X., Wang, S., Zhan, S., Niu, J., Tao, K., Zhang, Y., et al. (2015). The prevalence of symptomatic knee osteoarthritis in China: results from China Health and Retirement Longitudinal Study. *Arthritis Rheumatol.* 68, 648–653. doi: 10.1002/art.39465
- Tang, Y., Wu, X., Lei, W., Pang, L., Wan, C., Shi, Z., et al. (2009). TGF- β 1-induced migration of bone mesenchymal stem cells couples bone resorption with formation. *Nat. Med.* 15, 757–765. doi: 10.1038/nm.1979
- van den Berg, W. B. (2011). Osteoarthritis year 2010 in review: pathomechanisms. *Osteoarthritis Cartilage* 19, 338–341. doi: 10.1016/j.joca.2011.01.022
- von der Mark, K., Kirsch, T., Nerlich, A., Kuss, A., Weseloh, G., Glücker, K., et al. (1992). Type X collagen synthesis in human osteoarthritic cartilage. Indication of chondrocyte hypertrophy. *Arthritis Rheum.* 35, 806–811. doi: 10.1002/art.1780350715
- Xie, F., Kovic, B., Jin, X., He, X., Wang, M., and Silvestre, C. (2016). Economic and humanistic burden of osteoarthritis: a systematic review of large sample studies. *Pharmacoeconomics* 34, 1087–1100. doi: 10.1007/s40273-016-0424-x
- Xie, L., Tintani, F., Wang, X., Li, F., Zhen, G., Qiu, T., et al. (2016). Systemic neutralization of TGF- β attenuates osteoarthritis. *Ann. N.Y. Acad. Sci.* 1376, 53–64. doi: 10.1111/nyas.13000
- Zhen, G., Wen, C., Jia, X., Li, Y., Crane, J. L., Mears, S. C., et al. (2013). Inhibition of TGF- β signaling in mesenchymal stem cells of subchondral bone attenuates osteoarthritis. *Nat. Med.* 19, 704–712. doi: 10.1038/nm.3143

Conflict of Interest Statement: The authors declare that the research was conducted in the absence of any commercial or financial relationships that could be construed as a potential conflict of interest.

Copyright © 2018 Mu, Xu, Ma, Li, Ji, Zhang, Amat and Cao. This is an open-access article distributed under the terms of the Creative Commons Attribution License (CC BY). The use, distribution or reproduction in other forums is permitted, provided the original author(s) and the copyright owner are credited and that the original publication in this journal is cited, in accordance with accepted academic practice. No use, distribution or reproduction is permitted which does not comply with these terms.



Nardosinone Suppresses RANKL-Induced Osteoclastogenesis and Attenuates Lipopolysaccharide-Induced Alveolar Bone Resorption

Chenguang Niu^{1†}, Fei Xiao^{2†}, Keyong Yuan¹, XuChen Hu¹, Wenzhen Lin¹, Rui Ma¹, Xiaoling Zhang^{2*} and Zhengwei Huang^{1*}

¹ Shanghai Key Laboratory of Stomatology, Department of Endodontics, Ninth People's Hospital, Shanghai Jiao Tong University School of Medicine, Shanghai, China, ² Department of Orthopedic Surgery, Xin Hua Hospital Affiliated to Shanghai Jiao Tong University School of Medicine, Shanghai, China

OPEN ACCESS

Edited by:

Yuhei Nishimura,
Mie University, Japan

Reviewed by:

Diego Maria Michele Fornasari,
Università degli Studi di Milano, Italy
Yoshito Zamami,
Tokushima University Graduate
School of Medical Sciences, Japan

*Correspondence:

Zhengwei Huang
huangzhengwei@shsmu.edu.cn
Xiaoling Zhang
xlzhang@sibs.ac.cn

[†]These authors have contributed
equally to this work.

Specialty section:

This article was submitted to
Experimental Pharmacology and Drug
Discovery,
a section of the journal
Frontiers in Pharmacology

Received: 26 June 2017

Accepted: 25 August 2017

Published: 12 September 2017

Citation:

Niu C, Xiao F, Yuan K, Hu X, Lin W,
Ma R, Zhang X and Huang Z (2017)
Nardosinone Suppresses
RANKL-Induced Osteoclastogenesis
and Attenuates
Lipopolysaccharide-Induced Alveolar
Bone Resorption.
Front. Pharmacol. 8:626.
doi: 10.3389/fphar.2017.00626

Periodontitis is a chronic inflammatory disease that damages the integrity of the tooth-supporting tissues, known as the periodontium, and comprising the gingiva, periodontal ligament and alveolar bone. In this study, the effects of nardosinone (Nd) on bone were tested in a model of lipopolysaccharide (LPS)-induced alveolar bone loss, and the associated mechanisms were elucidated. Nd effectively suppressed LPS-induced alveolar bone loss and reduced osteoclast (OC) numbers *in vivo*. Nd suppressed receptor activator of nuclear factor- κ B ligand (RANKL)-mediated OC differentiation, bone resorption, and F-actin ring formation in a dose-dependent manner. Further investigation revealed that Nd suppressed osteoclastogenesis by suppressing the ERK and JNK signaling pathways, scavenging reactive oxygen species, and suppressing the activation of PLC γ 2 that consequently affects the expression and/or activity of the OC-specific transcription factors, c-Fos and nuclear factor of activated T-cells cytoplasmic 1 (NFATc1). In addition, Nd significantly reduced the expression of OC-specific markers in mouse bone marrow-derived pre-OCs, including *c-Fos*, cathepsin K (*Ctsk*), *VATPase d2*, and *Nfatc1*. Collectively, these findings suggest that Nd has beneficial effects on bone, and the suppression of OC number implies that the effect is exerted directly on osteoclastogenesis.

Keywords: nardosinone, RANKL, osteoclastogenesis, alveolar bone resorption, MAPKs

INTRODUCTION

Periodontitis is a chronic inflammatory disease that damages the integrity of the tooth-supporting tissues, known as the periodontium, and comprising the gingiva, periodontal ligament and alveolar bone (Hajishengallis, 2015). Oral bacteria in subgingival plaque have been identified as the primary etiological agent (Madianos et al., 2005), with *Porphyromonas gingivalis* lipopolysaccharide (LPS) (*P. gingivalis* LPS) identified as a key stimulus (Holt et al., 1988). Not only is periodontitis instigated by local dysbiotic microbial communities, but it is also the host inflammatory response to this microbial challenge that in the long run causes tissue damage, including pathologic activation of

osteoclast cells (OCs) to resorb bone (Lamont and Hajishengallis, 2015). Normally, alveolar bone is constantly reconstructed by means of the balanced activities of OCs and osteoblasts (Hadjidakis and Androulakis, 2006). However, in periodontitis, OC activity is increased in the presence of pro-inflammatory cytokines produced by inflammatory cells and LPS produced by bacteria. This leads to alveolar bone loss, resulting in early tooth loss (Pihlstrom et al., 2005).

Osteoclast cells are best known as multinucleated giant cells derived from the monocyte/macrophage lineage. Their exclusive function is to resorb bone in response to macrophage colony-stimulating factor (M-CSF) and RANKL signaling generated from the bone microenvironment (Boyle et al., 2003; Asagiri and Takayanagi, 2007). The cytokine M-CSF is a prerequisite for providing proliferation and survival signals to OC precursor cells and increasing expression of receptor activator of nuclear factor kappa B (RANK), which is essential for OC differentiation (Boyle et al., 2003). Upon the binding of RANKL to RANK, tumor necrosis factor receptor-associated factor 6 (TRAF6) is invoked, resulting in a long series of downstream signaling cascades, including activation of the NF- κ B signaling pathway and the mitogen-activated protein kinase (MAPK) signaling pathways. The signaling cascades conclude with the activation of c-Fos and nuclear factor of activated T cells cytoplasmic 1 (NFATc1), which are vital for osteoclastogenesis (Udagawa et al., 1999; Teitelbaum, 2000; Asagiri and Takayanagi, 2007). During RANKL-mediated osteoclastogenesis, it has been revealed that reactive oxygen species (ROS) play important roles in the differentiation, survival, activation, and bone resorptive activities of OCs (Garrett et al., 1990; Bhatt et al., 2002; Ha et al., 2004; Lee et al., 2005). In addition, excessive ROS generation has been associated with estrogen-deficient osteoporosis (Lean et al., 2003; Manolagas, 2010). The Ca^{2+} -NFATc1 signaling pathway plays an important role in osteoclastogenesis, namely, the upregulation of intracellular Ca^{2+} , which is dependent on the phosphorylation of phospholipase C γ (PLC γ). PLC γ is essential for the activation of NFATc1 (Negishi-Koga and Takayanagi, 2009; Kim et al., 2014; Kim J.Y. et al., 2015). Intracellular Ca^{2+} and ROS have been revealed to upregulate and auto-amplify NFATc1, the master regulator of osteoclastogenesis, through the CaMKIV/CREB pathway (Hwang and Putney, 2011; Li P. et al., 2014). Accordingly, numerous biological compounds targeting modulation of the above signaling pathways involved in OC differentiation have been found to have the ability to ameliorate periodontal damage, especially alveolar bone loss (Kim Y.G. et al., 2015; Bhattarai et al., 2016). Therefore, screening active compounds which can promote the healing and regeneration of periodontal tissues or attenuate the injury of periodontitis is an effective strategy for the treatment of OC-related periodontal diseases.

Nardosinone (Nd), isolated from *Nardostachys* root, an important Chinese herbal medicine, has been reported to be an enhancer of nerve growth factor (Li et al., 1999). Several studies have proven that Nd possesses a wide range of pharmacological effects, including sedative, adaptogen-like, anti-depressive, anti-leukemic, anti-tumorous, and anti-trypanosomal activities (Otoguro et al., 2011; Li Z.H. et al., 2014; Ju et al.,

2015; Kapoor et al., 2017). Interestingly, Nd was found to effectively suppress osteoclastogenesis in our previous screening work of single compounds extracted from Chinese herbs. However, the role of Nd on OC differentiation, as well as the underlying mechanisms through which osteoclastogenesis is regulated, have not been fully examined so far. In the present study, we confirmed that Nd can suppress the generation and differentiation of OCs from mouse bone marrow macrophages (BMMs) through JNK, ERK, PLC γ 2, c-Fos, and NFATc1 signaling pathways in association with scavenging the RANKL-induced ROS. Furthermore, the defensive effect of Nd on *P. gingivalis* LPS-induced alveolar bone loss was evaluated in a mouse periodontitis model. These data add substance to the suggestion that Nd can help prevent inflammatory bone loss.

MATERIALS AND METHODS

Reagents and Antibodies

Nardosinone (Figure 1A), purchased from Must Biotechnology (Chengdu, China), was dissolved in dimethyl sulfoxide (DMSO). Alpha modification of Eagle's minimum essential medium (α -MEM), fetal bovine serum (FBS), and penicillin/streptomycin were purchased from Gibco BRL (Gaithersburg, MD, United States). Recombinant murine M-CSF and RANKL were purchased from R&D Systems (Minneapolis, MN, United States). Tartrate-resistant acid phosphatase (TRAP) staining solution, Triton X-100, and 4',6-diamidino-2'-phenylindole dihydrochloride (DAPI) were obtained from Sigma-Aldrich (St. Louis, MO, United States). FITC phalloidin was obtained from Yeasen biotech Co., Ltd (Chengdu, China). Primary antibodies targeting GAPDH, I κ B α , phospho-Akt, Akt, phospho-ERK1/2, ERK1/2, phospho-JNK1/2, JNK1/2, phospho-p38, p38, phospho-PLC γ 2, PLC γ 2, c-Fos and NFATc1 were purchased from Cell Signaling Technology (Danvers, MA, United States). Dichlorofluorescein diacetate (DCFDA) cellular ROS detection assay kits were obtained from Beyotime Institute of Biotechnology (Jiangsu, China). LPS from *P. gingivalis* was purchased from InvivoGen (San Diego, CA, United States).

Cell Culture

Bone marrow macrophages were prepared as previously described (Xiao et al., 2015). Briefly, monocyte/macrophage precursors were prepared by flushing the marrow from the long bones of 6-week-old C57BL/6 mice and differentiated into BMMs in α -MEM containing 10% FBS, 100 U/mL penicillin/streptomycin (complete α -MEM) and 30 ng/mL M-CSF. The OC-like RAW264.7 cell line (TIB-71, ATCC, Manassas, VA, United States) was cultured in complete α -MEM. All cell cultures were maintained in a humidified environment of 95% air/5% CO $_2$ at 37°C.

Cell Viability Assay

The anti-proliferative effect of Nd on BMMs was measured with a CCK-8 kit (Dojindo Molecular Technology, Kumamoto, Japan) according to the manufacturer's instructions. In brief, BMMs plated into 96-well plates at a density of 1×10^4 cells/well were

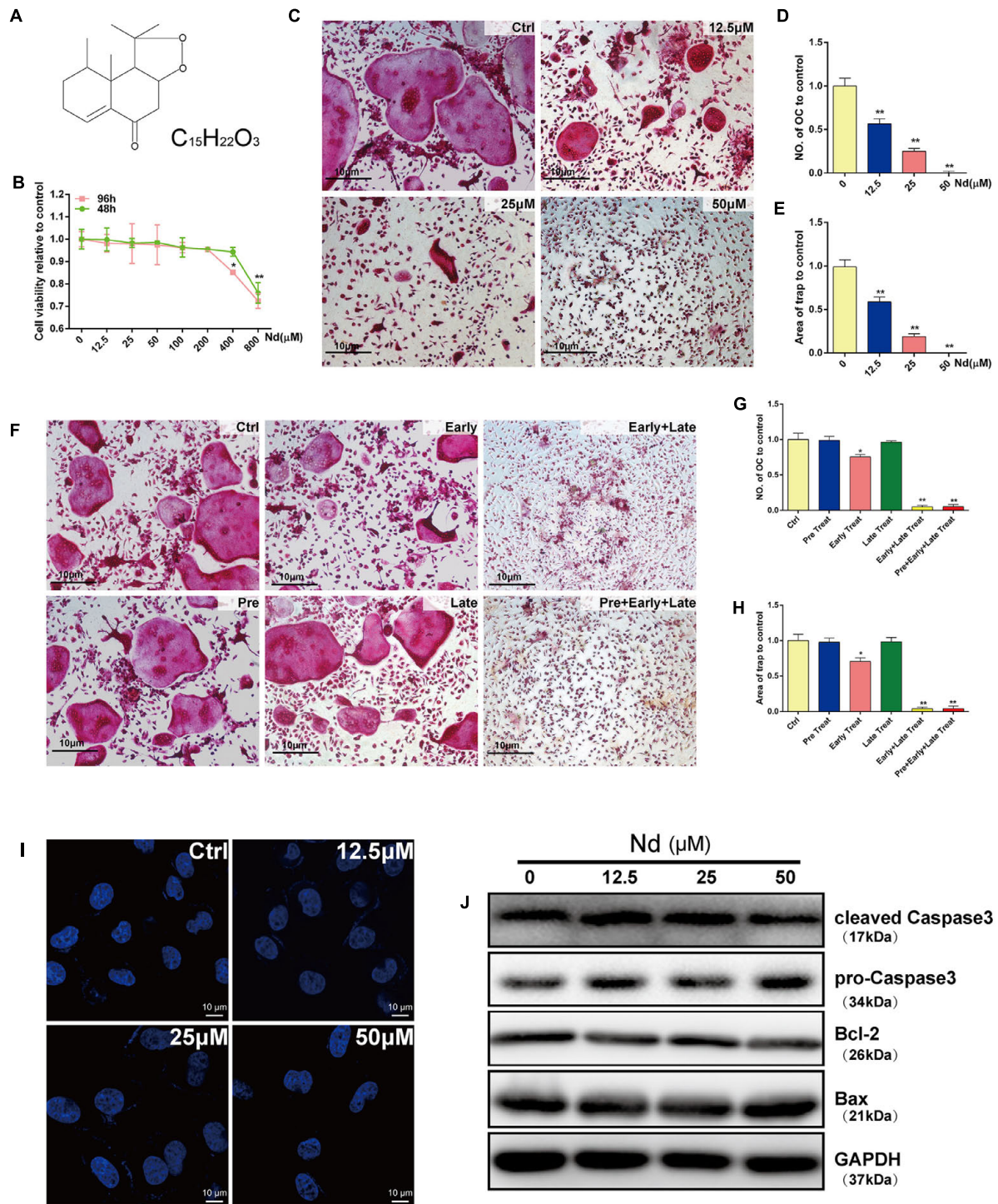


FIGURE 1 | Evaluation of Nardosinone (Nd) toxicity and its effects on RANKL-induced osteoclastogenesis and apoptosis *in vitro*. **(A)** Chemical formula of Nd. **(B)** Cell viability of mouse bone marrow macrophages (BMMs) treated with varying doses of Nd (0, 12.5, 25, or 50 μM) for 48 or 96 h. **(C)** Typical images of BMMs stained for TRAP (red) after treatment with different concentration of Nd. **(D)** The number of TRAP⁺ve multinucleated osteoclasts (≥ 3 nuclei) and the area **(E)** of TRAP compared to control were quantified. **(F)** The effect of time of addition of Nd on osteoclast formation. BMMs were stimulated with RANKL (100 ng/mL) alone or together with Nd (50 μM) at different stages of the 5-day osteoclast culture as described in Section “Materials and Methods.” **(G)** The number of TRAP⁺ve multinucleated osteoclasts (≥ 3 nuclei) and the area **(H)** of TRAP compared to control were quantified. **(I)** The nuclear size and shape of BMMs at concentrations that affect OC formation and activity. Nd did not induce nuclear fragmentation. OCs cultured on glass coverslips were incubated with Nd at different doses (0, 12.5, 25, or 50 μM) for 48 h then fixed and stained with DAPI and examined by fluorescence microscopy. **(J)** Western blotting to check whether Nd induces apoptosis at concentrations that affect OC formation and activity. Values are expressed as mean \pm SD; * $P < 0.05$, ** $P < 0.01$ compared to control.

treated for 48 or 96 h with serial dilutions of Nd (0–800 μM). Next, 10 μL CCK-8 mixed with 90 μL complete α -MEM was added to each well. After incubation for 2 h, the optical density (OD) was measured with an ELX800 absorbance microplate reader (Bio-Tek Instruments, Inc., Winooski, VT, United States) at a wavelength of 450 nm (650 nm reference).

Analysis of DAPI Staining

Bone marrow macrophages were treated with Nd (0, 12.5, 25, or 50 μM) for 48 h. The cells were washed three times with PBS, then treated for 15 min with Triton X-100 to disrupt the cell membrane integrity. Nuclei were stained with 0.1 $\mu\text{g}/\text{mL}$ DAPI in PBS at 37°C for 10 min in the dark. The cell nuclei were observed and photographed using an LSM5 confocal microscope (Carl Zeiss, Oberkochen, Germany).

In Vitro Osteoclastogenesis Assay

Bone marrow macrophages were seeded into 96-well plates at a density of 8×10^3 cells/well, in triplicate, in complete α -MEM containing M-CSF (30 ng/mL), and allowed to adhere overnight. Next day BMMs were treated with RANKL (50 ng/mL) and various concentrations of Nd (0, 12.5, 25, or 50 μM) over a 5 day period. Conversely, to investigate Nd addition-dependent effects on osteoclastogenesis at a particular stage, Nd (50 μM) was added to BMMs cultured with M-CSF and RANKL at different stages of the 5 day culture period as follows: pre-treatment (12 h before RANKL); early treatment (day 1); late treatment (day 3), early + late treatment (days 1 and 3); and pre + early + late treatment (12 h before RANKL, then days 1 and 3). After 5 days, cells were fixed with 4% paraformaldehyde and stained for TRAP activity. TRAP⁺ve cells that contained three or more nuclei were counted as mature OCs, and their cell spread areas were measured.

Quantitative Polymerase Chain Reaction (PCR) Analysis

For real-time polymerase chain reaction (PCR), 2×10^5 BMMs were plated into each well of a 12-well plate and cultured in complete α -MEM containing M-CSF (30 ng/mL), and RANKL (50 ng/mL). Cells were then treated with or without Nd at a range of concentrations (0, 12.5, 25, or 50 μM). Total RNA was extracted from cultured cells using an RNeasy Mini kit (Qiagen, Valencia, CA, United States) according to the manufacturer's instructions, and cDNA was synthesized from 1 μg of total RNA using reverse transcriptase (TaKaRa Biotechnology, Otsu, Japan). Real-time PCR was performed using a SYBR Premix Ex Taq kit (TaKaRa Biotechnology) and an ABI 7500 Sequencing Detection System (Applied Biosystems, Foster City, CA, United States). PCR was performed under the following conditions: 40 cycles each involving 5 s of denaturation at 95°C and 34 s of amplification at 60°C. All PCRs were performed in triplicate and levels were normalized to those of the gene *Gapdh*. The following primer sets were used as previously described: mouse *Gapdh*: forward, 5'-ACC CAG AAG ACT GTG GAT GG-3' and reverse, 5'-CAC ATT GGG GGT AGG AAC AC-3'; mouse *Nfatc1*: forward, 5'-CCG TTG CTT CCA GAA AAT AAC A-3' and reverse, 5'-TGT GGG ATG TGA ACT CGG AA-3'; mouse

cathepsin K: forward, 5'-CTT CCA ATA CGT GCA GCA GA-3' and reverse, 5'-TCT TCA GGG CTT TCT CGT TC-3'; mouse *c-Fos*: forward, 5'-CCA GTC AAG AGC ATC AGC AA-3', reverse, 5'-AAG TAG TGC AGC CCG GAG TA-3'; and mouse *V-ATPase d2*: forward, 5'-AAG CCT TTG TTT GAC GCT GT-3' reverse, 5'-TTC GAT GCC TCT GTG AGA TG-3'.

Western Blot Analysis

RAW264.7 cells were seeded into 6-well plates at a density of 6×10^5 cells/well. When the cells were confluent, they were pretreated with or without Nd for 4 h. Cells were then stimulated with 50 ng/mL RANKL for 0, 5, 10, 20, 30, and 60 min. Cellular proteins were extracted from cultured BMMs or RAW264.7 cells using RIPA lysis buffer (Thermo Fisher Scientific, Waltham, MA, United States) supplemented with 10 mg/mL phenylmethylsulfonyl fluoride (PMSF), and the protein concentration was determined using a BCA protein assay (Thermo Fisher Scientific). Lysate proteins (25 μg) were separated by 10% SDS-PAGE and transferred to polyvinylidene difluoride membranes. Membranes were then blocked with 5% skimmed milk in TBS-Tween (TBS: 0.05 M Tris, 0.15 M NaCl pH 7.5; with 0.2% Tween-20) for 1 h, and incubated with primary antibodies diluted in 1% (w/v) skimmed milk powder in TBS-Tween overnight at 4°C. Experiments were repeated independently at least three times.

Bone Resorption Pit Assay

Equivalent amounts of BMM-derived pre-OCs (after 4 days of RANKL stimulation) were seeded onto 100-mm bovine bone disks, treated with Nd (0, 12.5, 25, or 50 μM) for 48 h and then fixed and stained for TRAP activity. Resorption pits were visualized under a scanning electron microscope (FEI Quanta 250), and the bone resorption area was quantified using Image J software (National Institutes of Health, Bethesda, MD, United States).

Immunofluorescence Confocal Microscopy

Osteoclast cells differentiated from BMMs were cultured on glass coverslips and fixed for 15 min at RT with 4% paraformaldehyde, permeabilized for 5 min with 0.1% Triton X-100 in PBS, and non-specific antibody binding was blocked by incubating for 30 min in 5% skimmed milk in PBS. F-actin was stained with FITC-conjugated phalloidin and nuclei were stained with DAPI. Actin ring distribution was visualized using an LSM5 confocal microscope (Carl Zeiss, Oberkochen, Germany).

Intracellular ROS Detection

The DCFDA cellular ROS detection assay kit was used to detect intracellular ROS levels. BMMs (8×10^3 cells/well in 96-well plates) were treated with RANKL (50 ng/mL), M-CSF (30 ng/mL), and Nd (25 or 50 μM) for 72 h. Intracellular ROS levels were determined using 2',7'-dichlorofluorescein diacetate (DCFH), which oxidizes into fluorescent DCF in the presence of ROS. Cells were washed in PBS and incubated in the dark for

60 min with 10 μM DCFH-DA. Images were obtained using a fluorescence microscope (Carl Zeiss, Oberkochen, Germany).

Alveolar Bone Resorption Experiments

Animal studies were conducted in accordance with the principles and procedures approved by the Animal Care Committee of Shanghai Jiao Tong University, China. Twenty specific-pathogen-free 8-week-old male C57BL/6J mice were randomly divided into four groups: phosphate-buffered saline (PBS; control), LPS (1 mg/kg body weight; Sigma-Aldrich), LPS + Nd (5 mg/kg body weight, low dose group), and LPS + Nd (15 mg/kg body weight, high dose group). Nd was given by intraperitoneal injection on days 1, 4, and 7. On days 4 and 7, mice were sedated via light anesthesia and injected with 1 mg/kg of *P. gingivalis* LPS at the gingiva of the second molar in the lower left and right jaw (Kim Y.G. et al., 2015). Mice were sacrificed on day 10 and their jaws were collected for further analysis. Left jaws were dissected for micro-CT analysis and right jaws for bone histology and histomorphometry.

MicroCT Analysis of Jaws

Left jaws were fixed in 4% paraformaldehyde for 1 day at 4°C and stored in 70% ethanol at 4°C. They were then scanned using high-resolution micro-computed tomography (μCT) (Scanco microCT100, Brüttisellen, Switzerland). Each jaw was then imaged with the following instrument settings: 70 kV, 200 μA , 0.5 mm Al filter, 300 ms exposure, pixel size 5 μm . After scanning, the data were reconstructed using Scanco μCT Evaluation software V6.5-3 with a constant threshold value. An image of a precise ruler was captured at the same magnification and used for calibration area measurements, which were performed with Olympus Microsuite 3.2 imaging software. A volume of interest was generated covering the first to third molars and the relevant alveolar bone. The volume of alveolar bone included in the region of interest (bone volume/total volume) (ROI [BV/TV]) was measured for each sample, and comparisons were made among different groups. The polygonal area enclosed by the cemento-enamel junction (CEJ), the lateral margins of the exposed tooth root, and the alveolar bone crest (ABC) were also measured, and results are expressed in millimeters squared (mm^2).

Histological and Histomorphometric Analysis

Right jaws were fixed in 4% paraformaldehyde for 1 day at 4°C, subsequently decalcified in 10% EDTA for approximately 1 month, and then embedded in paraffin. Histological sections (7 μm thick) were prepared for hematoxylin and eosin as well as TRAP staining. The specimens were then examined and photographed using a high quality microscope. The number of TRAP⁺ multi-nucleated OCs (N.Oc/BS, 1/mm) and the percentage of OC surface per bone surface (OcS/BS, %) were assessed for each sample.

Statistical Analysis

Data are shown as mean \pm standard deviation (SD) from at least three independent experiments. Student's *t*-test was used

to determine statistical significance between the results of test and control groups, with **P* < 0.05 and ***P* < 0.01 considered statistically significant.

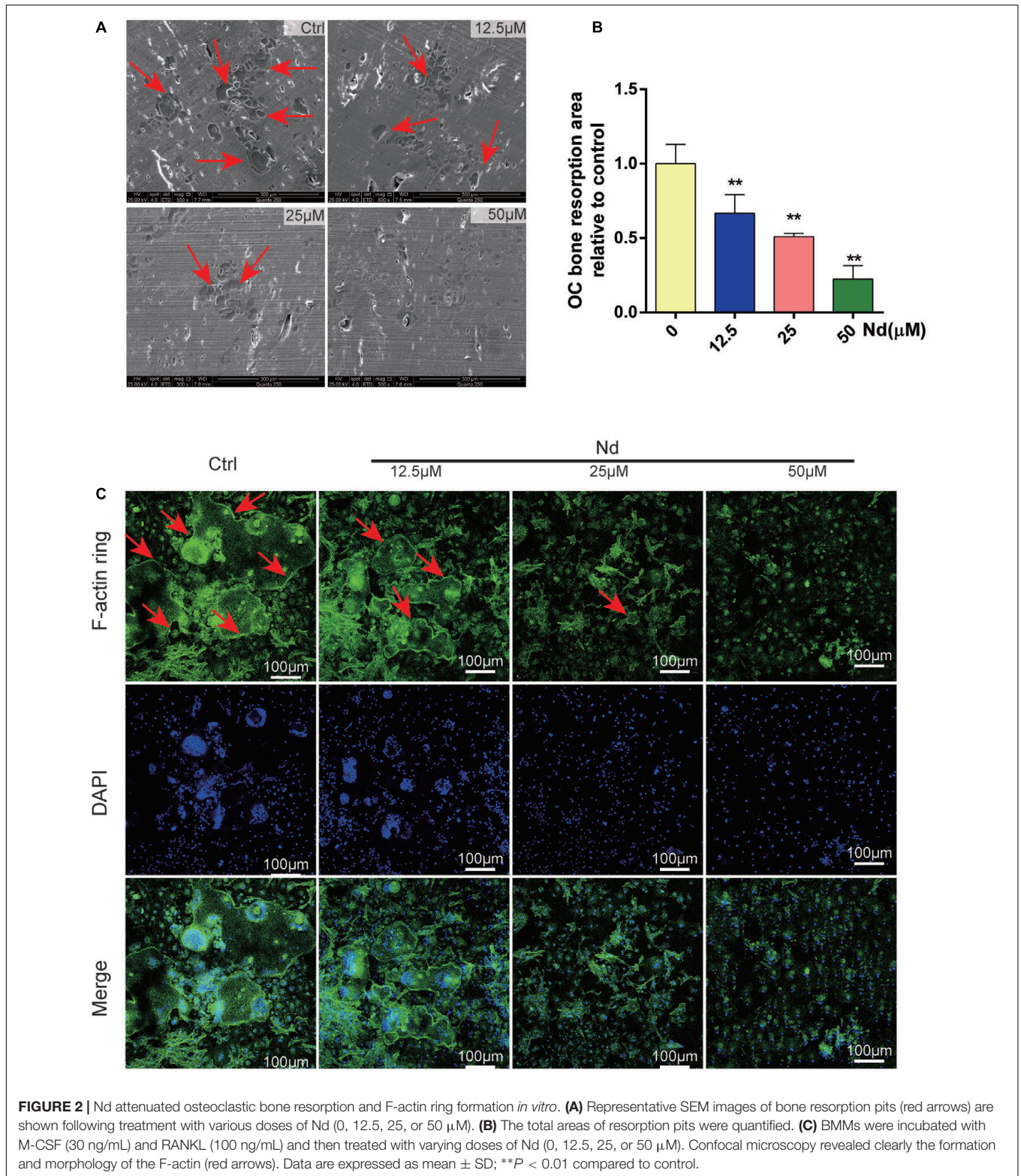
RESULTS

Nd Suppressed RANKL-Induced Osteoclastogenesis without Cytotoxic Effects

The CCK-8 assay was used to examine the potential cytotoxicity of Nd on BMMs. Treatment with Nd for 48 or 96 h at concentrations less than 400 μM did not induce cytotoxicity (Figure 1B). BMMs were exposed to M-CSF and RANKL in the absence or presence of different concentrations of Nd for 5 days. The formation of TRAP⁺ OCs was suppressed by Nd (Figure 1C) and the number of OCs and the area of TRAP-positive staining were reduced to approximately 9% of control levels by treatment with 50 μM Nd (Figures 1D,E). To determine the stage at which Nd suppressed osteoclastogenesis, BMMs were treated with 50 μM Nd at several time points. Neither treatment for 12 h prior to RANKL stimulation (pre-treatment) nor on the third day of RANKL stimulation (late treatment) altered the number or size of TRAP⁺ OCs induced after 5 days of culture, whereas treatment on the first day of RANKL stimulation (early treatment) led to an almost 35% reduction in OC number and area of TRAP (Figures 1F-H). Continuous exposure to early and late treatment or pre-, early and late treatment potently suppressed OC formation (Figures 1F-H). To exclude the possibility that Nd induced BMM apoptosis during the course of differentiation, BMMs were stained with DAPI following Nd treatment (Figure 1I), and were found to exhibit normal intact nuclei, confirming that the suppressory effects of Nd on osteoclastogenesis were not attributable to the induction of BMM apoptosis. Furthermore, western blotting was carried out to examine whether the apoptotic cell death pathways were activated after Nd treatment. There was no alteration in the levels of the anti-apoptotic protein Bcl-2, nor any activation of the Bax and caspase-3 apoptotic pathways following treatment with up to 50 μM of Nd (Figure 1J).

Nd Decreased Osteoclastic Bone Resorption and F-Actin Ring Formation

Next, the effects of Nd on OC bone resorption were assessed. SEM results verified the bone resorptive ability of OCs differentiated from BMMs on the bone surface (Figure 2A). Meanwhile, most of the bone resorption activity was suppressed and was almost completely blocked at the higher concentration of Nd (≥ 50 μM) (Figures 2A,B). The establishment of F-actin-rich podosomes-polarized cytoskeletal structures known as F-actin rings-indicates the maturity of OCs and is also essential for OC bone resorption (Wu et al., 2015; Zhu et al., 2016). The results showed that osteoclastic bone resorption is suppressed by Nd; further experimentation to verify whether Nd suppresses F-actin ring formation was carried out. Confocal



microscopy revealed clearly the formation and morphology of the F-actin ring of mature OCs stained with phalloidin in the control group (Figure 2C). However, in the group treated with Nd the size and morphology of the F-actin

ring were reduced, with dose-dependent reductions. Together, these findings clearly indicate that the application of Nd reduced osteoclastic bone resorption and formation of OCs *in vitro*.

Nd Eliminated ROS Production and Suppressed Activation of PLC γ 2

To elucidate the inhibitory effects of Nd on OC formation, intracellular ROS was semi-quantitatively measured using DCFDA. As shown in **Figure 3A**, intracellular ROS was at a low level before RANKL stimulation but increased sharply to a high level when BMMs were treated with RANKL. This effect could be markedly attenuated by Nd. Both the number of ROS (+) cells and the level of ROS were decreased by Nd (**Figures 3B,C**). Ca²⁺ signaling is indispensable for osteoclastogenesis and its trigger is the phosphorylation of PLC γ 2. Thus, we investigated the inhibitory effects of Nd on the phosphorylation of PLC γ 2. As expected, the phosphorylation of PLC γ 2 was clearly blocked compared with the control group (**Figures 3D,E**).

Nd Inhibited RANKL-Induced ERK and JNK1/2 Activation

To detect the underlying mechanisms by which Nd mediated OC formation, the bearing of RANKL-induced signaling pathways on osteoclastogenesis were examined. The phosphorylation of MAPK family members (ERK, JNK, and p38) and Akt occurred within 10 min of RANKL stimulation, and continued for 30 min in the control group (**Figures 4A–C**). In the meantime, by comparison, Nd attenuated the phosphorylation of ERK and JNK, without affecting that of p38 (**Figure 4A**). The results also showed that Nd did not reduce phosphorylation of Akt or of I κ B α , an inhibitory subunit of NF κ B, indicating that it does not influence the Akt and NF κ B signaling pathway (**Figure 4A**). Overall, these data suggest that the suppressive influence of Nd on osteoclastogenesis could be put down to the attenuation of RANKL-induced JNK and ERK signaling cascades.

Nd Suppressed the Activation of c-Fos and NFATc1

It has been shown that activation of NFATc1, the master regulator of osteoclastogenesis which relies on c-Fos, results from phosphorylation of the MAPK signaling pathway (Nakashima et al., 2012). BMMs were stimulated with RANKL in the absence or presence of Nd for 0, 24, 48, or 72 h. As shown in **Figures 4D–F**, c-Fos protein expression increased after 24, 48, and 72 h, and NFATc1, the downstream transcriptional targets of c-Fos, showed steep increases at 48 and 72 h. By comparison, the situation was potently suppressed by Nd at various time-points. (**Figures 4G–J**) On the other hand, Nd also suppressed the expression of OC marker genes including *c-Fos*, *VATPase d2*, *ctsk*, and *Nfatc1*, shown by quantitative PCR.

Nd Attenuated LPS-Stimulated Bone Loss

To evaluate the role of Nd in bone resorption *in vivo*, we created the LPS-induced mouse alveolar-bone-loss model. No fatalities were recorded after LPS and Nd administration, and all the animals maintained normal activity throughout the experiment. Micro-CT, morphometric and histomorphometric analyses were performed. Micro-CT confirmed that LPS-injected mice exhibited significantly greater areas of exposed roots than

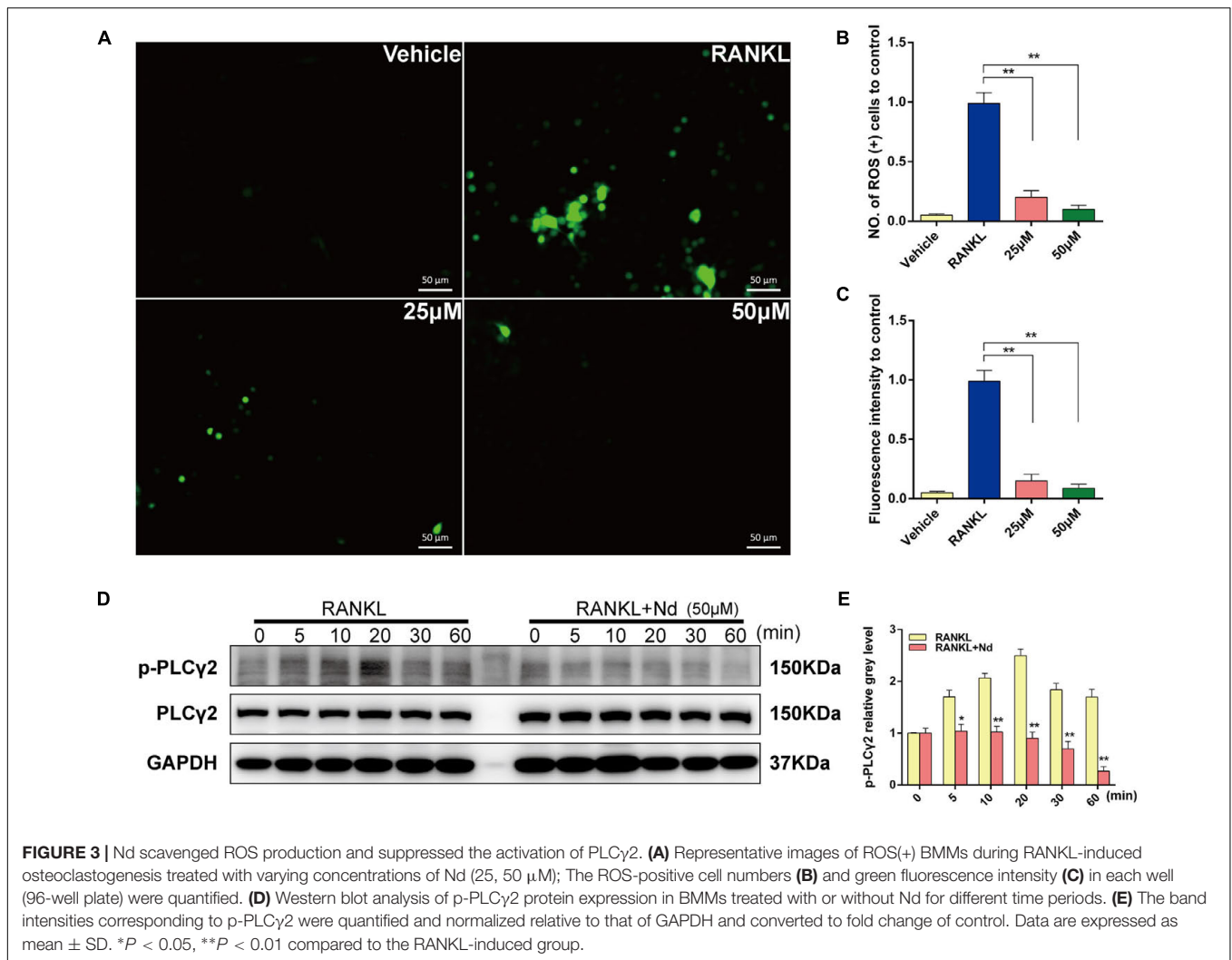
the control and Nd groups (**Figures 5A,B**). No significant differences in areas of exposed roots were observed among control, low dose, and high dose groups (**Figures 5A,B**). A volumetric quantitative analysis of alveolar bone loss with micro-CT verified the results obtained by macroscopic analysis. BV/TV in the LPS group was also significantly lower than those of the control or Nd groups (**Figure 5C**). The LPS-mediated decrease in BV/TV values was restored up to a level similar to the control group by treatment with Nd at 5 or 15 mg/kg (**Figure 5C**).

To further explore whether OCs were involved in the inhibitory effects of Nd on LPS-induced alveolar bone loss, TRAP staining was performed to calculate the number of OCs in tissue sections. TRAP-positive multinucleated cells lining the alveolar bone surface were visually enumerated (black arrows in **Figure 5D**) in a specific AOI with standardized dimensions and surfaces. The LPS group showed the highest number of OCs compared with the control group. However, the administration of 5 mg/kg of Nd significantly reduced OC number. Furthermore, the administration of 15 mg/kg of Nd almost completely prevented an LPS-induced increase in OC number and bone erosion (**Figure 5D**). Histomorphometric analysis of Oc.S/BS and OC number confirmed that Nd treatment attenuated LPS-induced alveolar bone loss and reduced OC numbers (**Figures 5E,F**). Collectively, these results indicated that Nd effectively prevented LPS-induced alveolar bone loss *in vivo*. Tissue toxicities of Nd on the liver and kidney were confirmed by histological analyses (**Supplementary Figure S1**). Compared to control animals, administration of Nd at 5 or 15 mg/kg body weight/day for 10 days did not induce visible hepatotoxicity or nephrotoxicity.

DISCUSSION

Bone resorption is a major pathological factor in periodontitis and it is now clear that deregulation of immune and inflammatory responses is crucial in initiating the bone destruction associated with these conditions (Jimi et al., 2004). In the present study, our data show that Nd efficiently suppresses *P. gingivalis* LPS-induced alveolar bone loss, demonstrated by direct microCT analyses and histology *in vivo*, and suppressed osteoclastogenesis *in vitro*. To our knowledge, this is the first study to explore the effects of Nd on bone metabolism. At the molecular level, Nd profoundly suppressed multiple pathways downstream of RANK, including ROS, PLC γ 2, MAPKs, c-Fos, and NFATc1.

In the present study, the inhibitory effect of Nd on RANKL-induced OC formation from BMMs with RANKL and M-CSF was first explored *in vitro* and *in vivo*. It is well-known that RANKL, together with M-CSF, is a prerequisite for osteoclastogenesis (Boyle et al., 2003) and OCs are differentiated from hematopoietic cells through a multi-step process, including proliferation, expression of TRAP, and fusion of cells, and are TRAP⁺ve multinucleated cells with bone resorbing activity (Takahashi et al., 1999). Then, based on these theories, the results in **Figures 1C–H** suggest that the effects of Nd do not last long, and treatment at the early stages and during

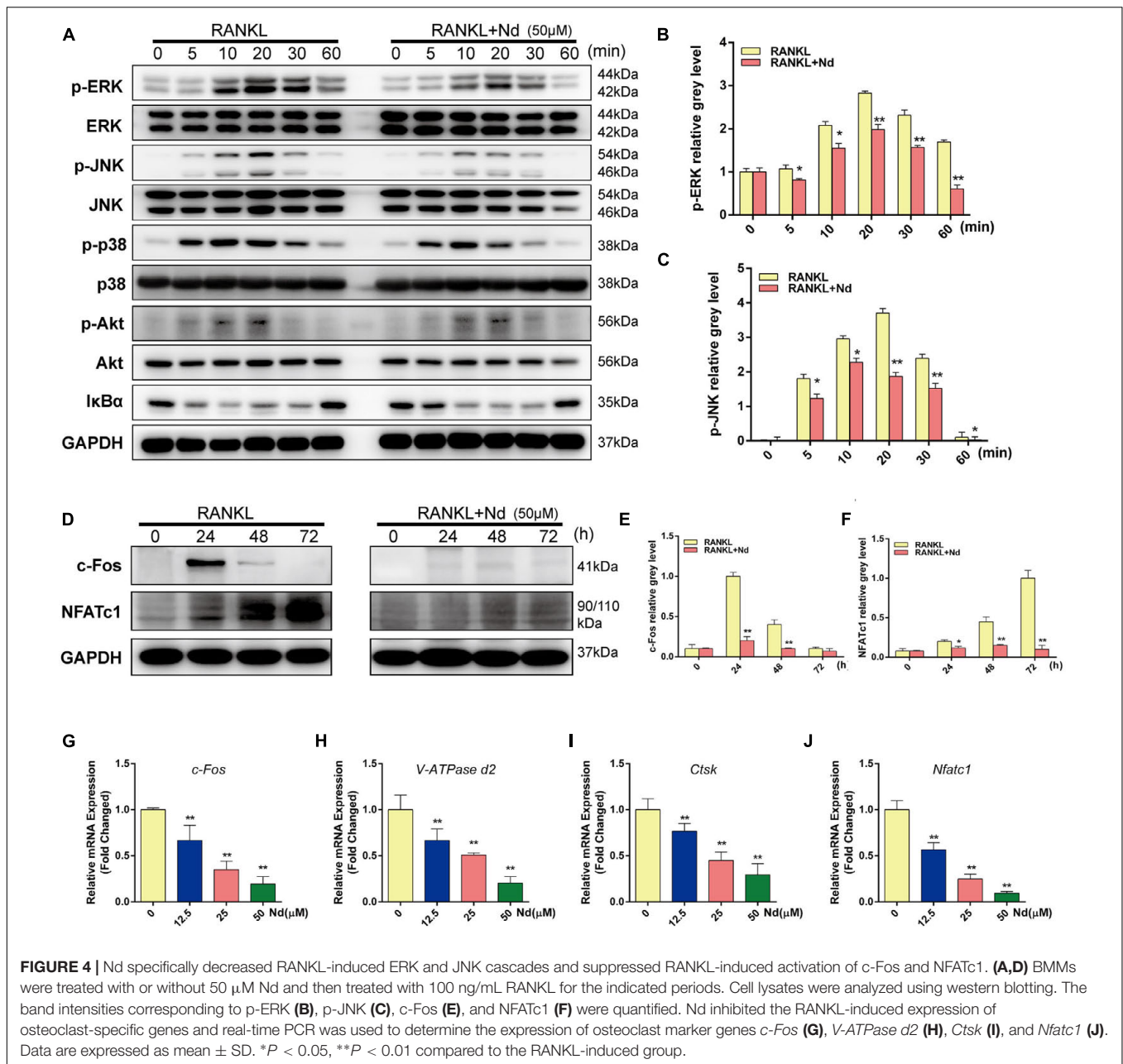


the course of RANKL-induced differentiation could produce a more effective inhibition of OC formation. The dose-dependent effect is transient since the removal of Nd in the early stage of osteoclastogenesis largely restored OC formation. A well-polarized F-actin ring is the most distinct characteristic of mature OCs and it is also essential for osteoclastic bone resorption (Wilson et al., 2009). The effect of Nd on F-actin ring formation and bone resorption ability are verified in our study.

Stimulation with RANKL has been shown to transiently increase the intracellular levels of ROS, which regulates RANK signaling pathways including Akt, MAPKs, and NF κ B, thereby promoting osteoclastogenesis, while osteoclastogenesis is blocked entirely when ROS production is prevented (Lee et al., 2005). Our results described here show that Nd is more effective at inhibiting the generation and accumulation of ROS, indicating that Nd may also suppress osteoclastogenesis through antioxidation. ROS acts as a second messenger in signal transduction and gene regulation in a variety of cell types, and under the influence of several biological factors such as cytokine, growth factor, or hormone treatments (Lander, 1997; Hensley et al., 2000; Hadjidakis and

Androulakis, 2006). Cells are capable of defending themselves against ROS damage with enzymes such as catalases, superoxide dismutases, glutathione peroxidases, glutathione reductase, and peroxiredoxins under normal circumstances (Finkel, 2003; Moon et al., 2006; Wauquier et al., 2009). The induction of oxidative stress is a potential mechanism by which periodontitis manifests its systemic effects (D'Aiuto et al., 2010). Previous studies point to the association of ROS with the pathogenesis of periodontitis (Waddington et al., 2000). Cellular ROS accumulation occurs during OC formation and, if it is prolonged and persistent, brings about the destruction of periodontal tissue and oxidative damage (Bhatt et al., 2002; Bhattarai et al., 2016). In addition, Altindag *et al.* reported that an accumulation of ROS and a lessened anti-oxidative status have been observed in osteoporosis patients (Altindag et al., 2008).

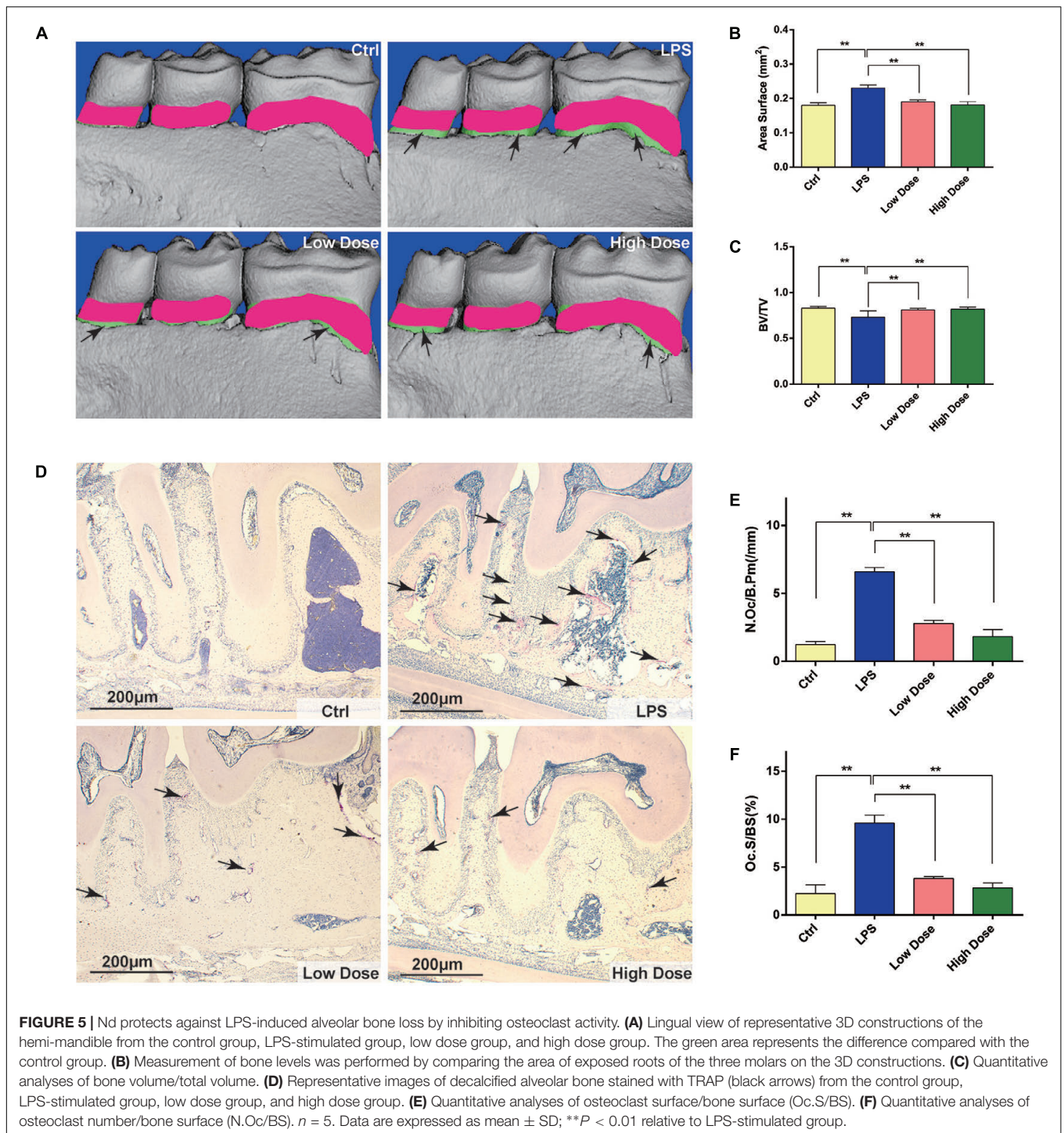
RANKL also triggers the phosphorylation of PLC γ 2, which subsequently leads to Ca²⁺ mobilization in the process of OC formation (Negishi-Koga and Takayanagi, 2009). Ca²⁺ signaling is crucial for osteoclastogenesis. The transient initial release of Ca²⁺ from intracellular stores and the influx through



specialized Ca^{2+} channels controls the dephosphorylation of NFATc1 protein, and leads to its nuclear localization, which is followed by the activation of OC-specific genes (Yeon et al., 2015). PLC γ 2 phosphorylation is directly and closely coupled with Ca^{2+} oscillations and the Ca^{2+} -dependent translocation of NFATc1 induced by RANKL (Takayanagi, 2007). In addition, it has been suggested that it is the phosphorylation of PLC γ 2 rather than PLC γ 1 that is required for RANKL-mediated Ca^{2+} signaling in OC differentiation (Mao et al., 2006). In light of the above, we speculated that the inhibitory effect of Nd on the phosphorylation of PLC γ 2 is likely to suppress the RANKL- Ca^{2+} -oscillation-NFATc1 activation signaling axis during OC differentiation. Further study is required to investigate whether

Nd treatment reduces the amplitude and frequency of Ca^{2+} oscillations in the OC differentiation process.

One of the most important downstream pathways mediating the effects of Nd on osteoclastogenesis could be components of MAPK signaling, namely ERK and JNK. RANKL invokes the rapid phosphorylation and activation of MAPKs and AKT, which consequently stimulates the activation of transcription factors such as c-Fos and NFATc1 to regulate the expression of genes required for OC differentiation (Stevenson et al., 2011; Yeon et al., 2014). Increasing evidence shows that the RANKL-induced ERK signaling pathway plays an important role in osteoclastogenesis (Tsai et al., 2008; Tang et al., 2009). When ERK signaling is still active, c-Fos is phosphorylated by



sustained ERK (Okawa et al., 2009). It is well-known that c-Fos is a member of the AP-1 transcription factor family and is required for the differentiation of OC precursors into bone-resorbing OCs. c-Fos-deficient mice suffer from osteopetrosis because of a block of OC differentiation. At the same time, by means of ectopic c-Fos expression, impaired osteoclastogenesis in BMMs is completely rescued (Grigoriadis et al., 1994).

c-Fos regulates expression of NFATc1, which is critical for the differentiation of OCs. NFATc1-deficient mice have defects of osteoclastogenesis and also show symptoms of osteopetrosis (Winslow et al., 2006). Similarly, activated JNK phosphorylates downstream factors, including c-Fos, which is required for NFATc1 induction (Jimi et al., 1999; Takayanagi et al., 2000). Our data (Figure 4) suggest that Nd may act on ERK and JNK

signaling pathways along the c-Fos/NFATc1 axis to interfere with osteoclastogenesis.

Erosion of alveolar bone is one of the grave consequences of periodontitis which is an inflammatory disease. For the moment, antiresorptive agent available for periodontitis is in urgent need, since bisphosphonates and anti-RANKL antibodies have the risk of increasing osteonecrosis of the jaw. In an LPS-induced mouse periodontitis model, the administration of Nd meaningfully reduced the number of osteoclasts as well as alveolar bone erosion (**Figure 5**) and this suggests Nd suppresses osteoclastogenesis and could play an effective role in depressing bone resorption *in vivo*. It is important to note the limitations within the present study that represent the future direction of our research. Firstly, whether Nd correlates negatively with these inflammatory cytokines should be explored in future studies, since IL-1, IL-6, IL-8, and TNF- α promote osteoclastogenesis and bone resorption through multiple mechanisms, such as increasing the production of M-CSF and RANKL (Koerner et al., 2008; Xu et al., 2011). Secondly, further study should focus on identifying the target binding molecules of Nd, and the mechanism via which Nd suppresses the fusion of pre-OCs and the pit formation of mature OCs might be elucidated.

Collectively, our data demonstrate that Nd can suppress osteoclastogenesis and periodontal bone loss. This effect is mediated by scavenging RANKL-induced ROS activity and the suppression of RANKL-stimulated activation of JNK, ERK, PLC γ 2, c-Fos, and NFATc1 signaling pathways during OC formation and bone resorption. Taken together, our data suggest that Nd may represent a potential agent for

the treatment of periodontitis or other OC-related osteolytic diseases.

AUTHOR CONTRIBUTIONS

All authors listed have made a substantial, direct and intellectual contribution to the work, and approved it for publication.

ACKNOWLEDGMENTS

This work was supported by grants from the National Natural Science Foundation of China (NSFC) (No. 81570964/81371143/81190133/81401844/81572123/81772347), Chinese Academy of Sciences (No. XDA01030502), Science and Technology Commission of Shanghai Municipality (No. 14431900900/16430723500), Shanghai Municipal Education Commission-Gaofeng Clinical Medicine Grant Support (No. 20161314) and was partly supported by Shanghai Summit & Plateau Disciplines.

SUPPLEMENTARY MATERIAL

The Supplementary Material for this article can be found online at: <http://journal.frontiersin.org/article/10.3389/fphar.2017.00626/full#supplementary-material>

FIGURE S1 | Nd toxicity on mouse liver and kidney.

REFERENCES

- Altindag, O., Erel, O., Soran, N., Celik, H., and Selek, S. (2008). Total oxidative/anti-oxidative status and relation to bone mineral density in osteoporosis. *Rheumatol. Int.* 28, 317–321. doi: 10.1007/s00296-007-0452-0
- Asagiri, M., and Takayanagi, H. (2007). The molecular understanding of osteoclast differentiation. *Bone* 40, 251–264. doi: 10.1016/j.bone.2006.09.023
- Bhatt, N. Y., Kelley, T. W., Khramtsov, V. V., Wang, Y., Lam, G. K., Clanton, T. L., et al. (2002). Macrophage-colony-stimulating factor-induced activation of extracellular-regulated kinase involves phosphatidylinositol 3-kinase and reactive oxygen species in human monocytes. *J. Immunol.* 169, 6427–6434. doi: 10.4049/jimmunol.169.11.6427
- Bhattacharj, G., Poudel, S. B., Kook, S., and Lee, J. (2016). Resveratrol prevents alveolar bone loss in an experimental rat model of periodontitis. *Acta Biomater.* 29, 398–408. doi: 10.1016/j.actbio.2015.10.031
- Boyle, W. J., Simonet, W. S., and Lacey, D. L. (2003). Osteoclast differentiation and activation. *Nature* 423, 337–342. doi: 10.1038/nature01658
- D'Aiuto, F., Nibali, L., Parkar, M., Patel, K., Suvan, J., and Donos, N. (2010). Oxidative stress, systemic inflammation, and severe periodontitis. *J. Dent. Res.* 89, 1241–1246. doi: 10.1177/0022034510375830
- Finkel, T. (2003). Oxidant signals and oxidative stress. *Curr. Opin. Cell Biol.* 15, 247–254. doi: 10.1016/S0955-0674(03)00002-4
- Garrett, I. R., Boyce, B. F., Oreffo, R. O., Bonewald, L., Poser, J., and Mundy, G. R. (1990). Oxygen-derived free radicals stimulate osteoclastic bone resorption in rodent bone in vitro and in vivo. *J. Clin. Invest.* 85, 632–639. doi: 10.1172/JCI114485
- Grigoriadis, A. E., Wang, Z. Q., Cecchini, M. G., Hofstetter, W., Felix, R., Fleisch, H. A., et al. (1994). c-Fos: a key regulator of osteoclast-macrophage lineage determination and bone remodeling. *Science* 266, 443–448. doi: 10.1126/science.7939685
- Ha, H., Kwak, H. B., Lee, S. W., Jin, H. M., Kim, H. M., Kim, H. H., et al. (2004). Reactive oxygen species mediate RANK signaling in osteoclasts. *Exp. Cell Res.* 301, 119–127. doi: 10.1016/j.yexcr.2004.07.035
- Hadjidakis, D. J., and Androulakis, I. I. (2006). Bone remodeling. *Ann. N. Y. Acad. Sci.* 1092, 385–396. doi: 10.1196/annals.1365.035
- Hajishengallis, G. (2015). Periodontitis: from microbial immune subversion to systemic inflammation. *Nat. Rev. Immunol.* 15, 30–44. doi: 10.1038/nri3785
- Hensley, K., Robinson, K. A., Gabbita, S. P., Salsman, S., and Floyd, R. A. (2000). Reactive oxygen species, cell signaling, and cell injury. *Free Radic. Biol. Med.* 28, 1456–1462. doi: 10.1016/S0891-5849(00)00252-5
- Holt, S. C., Ebersole, J., Felton, J., Brunsvold, M., and Kornman, K. S. (1988). Implantation of *Bacteroides gingivalis* in nonhuman primates initiates progression of periodontitis. *Science* 239, 55–57. doi: 10.1126/science.3336774
- Hwang, S. Y., and Putney, J. J. (2011). Calcium signaling in osteoclasts. *Biochim. Biophys. Acta* 1813, 979–983. doi: 10.1016/j.bbamcr.2010.11.002
- Jimi, E., Akiyama, S., Tsurukai, T., Okahashi, N., Kobayashi, K., Udagawa, N., et al. (1999). Osteoclast differentiation factor acts as a multifunctional regulator in murine osteoclast differentiation and function. *J. Immunol.* 163, 434–442.
- Jimi, E., Aoki, K., Saito, H., D'Acquisto, F., May, M. J., Nakamura, I., et al. (2004). Selective inhibition of NF- κ B blocks osteoclastogenesis and prevents inflammatory bone destruction in vivo. *Nat. Med.* 10, 617–624. doi: 10.1038/nm1054
- Ju, S. M., Lee, J., Kang, J. G., Jeong, S. O., Park, J. H., Pae, H. O., et al. (2015). Nardostachys chinensis induces granulocytic differentiation with the

- suppression of cell growth through p27(Kip1) protein-related G0/G1 phase arrest in human promyelocytic leukemic cells. *Pharm. Biol.* 53, 1002–1009. doi: 10.3109/13880209.2014.952834
- Kapoor, H., Yadav, N., Chopra, M., Mahapatra, S. C., and Agrawal, V. (2017). Strong anti-tumorous potential of nardostachys jatamansi rhizome extract on glioblastoma and in silico analysis of its molecular drug targets. *Curr. Cancer Drug Targets* 17, 74–88. doi: 10.2174/1570163813666161019143740
- Kim, J. Y., Cheon, Y. H., Oh, H. M., Rho, M. C., Erkhembaatar, M., Kim, M. S., et al. (2014). Oleanolic acid acetate inhibits osteoclast differentiation by downregulating PLCgamma2-Ca²⁺-NFATc1 signaling, and suppresses bone loss in mice. *Bone* 60, 104–111. doi: 10.1016/j.bone.2013.12.013
- Kim, J. Y., Park, S. H., Baek, J. M., Erkhembaatar, M., Kim, M. S., Yoon, K. H., et al. (2015). Harpagoside inhibits RANKL-induced osteoclastogenesis via Syk-Btk-PLCgamma2-Ca²⁺ signaling pathway and prevents inflammation-mediated bone loss. *J. Nat. Prod.* 78, 2167–2174. doi: 10.1021/acs.jnatprod.5b00233
- Kim, Y. G., Kang, J. H., Kim, H. J., Kim, H. J., Kim, H. H., Kim, J. Y., et al. (2015). Bortezomib inhibits osteoclastogenesis and porphyromonas gingivalis lipopolysaccharide-induced alveolar bone resorption. *J. Dent. Res.* 94, 1243–1250. doi: 10.1177/0022034515592592
- Koerner, I. P., Zhang, W., Cheng, J., Parker, S., Hurn, P. D., and Alkayed, N. J. (2008). Soluble epoxide hydrolase: regulation by estrogen and role in the inflammatory response to cerebral ischemia. *Front. Biosci.* 13, 2833–2841. doi: 10.2741/2889
- Lamont, R. J., and Hajishengallis, G. (2015). Polymicrobial synergy and dysbiosis in inflammatory disease. *Trends Mol. Med.* 21, 172–183. doi: 10.1016/j.molmed.2014.11.004
- Lander, H. M. (1997). An essential role for free radicals and derived species in signal transduction. *FASEB J.* 11, 118–124.
- Lean, J. M., Davies, J. T., Fuller, K., Jagger, C. J., Kirstein, B., Partington, G. A., et al. (2003). A crucial role for thiol antioxidants in estrogen-deficiency bone loss. *J. Clin. Invest.* 112, 915–923. doi: 10.1172/JCI200318859
- Lee, N. K., Choi, Y. G., Baik, J. Y., Han, S. Y., Jeong, D. W., Bae, Y. S., et al. (2005). A crucial role for reactive oxygen species in RANKL-induced osteoclast differentiation. *Blood* 106, 852–859. doi: 10.1182/blood-2004-09-3662
- Li, P., Liu, C., Hu, M., Long, M., Zhang, D., and Huo, B. (2014). Fluid flow-induced calcium response in osteoclasts: signaling pathways. *Ann. Biomed. Eng.* 42, 1250–1260. doi: 10.1007/s10439-014-0984-x
- Li, P., Matsunaga, K., Yamamoto, K., Yoshikawa, R., Kawashima, K., and Ohizumi, Y. (1999). Nardosinone, a novel enhancer of nerve growth factor in neurite outgrowth from PC12D cells. *Neurosci. Lett.* 273, 53–56. doi: 10.1016/S0304-3940(99)00629-1
- Li, Z. H., Li, W., Shi, J. L., and Tang, M. K. (2014). Nardosinone improves the proliferation, migration and selective differentiation of mouse embryonic neural stem cells. *PLOS ONE* 9:e91260. doi: 10.1371/journal.pone.0091260
- Madianos, P. N., Bobetsis, Y. A., and Kinane, D. F. (2005). Generation of inflammatory stimuli: how bacteria set up inflammatory responses in the gingiva. *J. Clin. Periodontol.* 32(Suppl. 6), 57–71. doi: 10.1111/j.1600-051X.2005.00821.x
- Manolagas, S. C. (2010). From estrogen-centric to aging and oxidative stress: a revised perspective of the pathogenesis of osteoporosis. *Endocr. Rev.* 31, 266–300. doi: 10.1210/er.2009-0024
- Mao, D., Eppler, H., Uthgenannt, B., Novack, D. V., and Faccio, R. (2006). PLCgamma2 regulates osteoclastogenesis via its interaction with ITAM proteins and GAB2. *J. Clin. Invest.* 116, 2869–2879. doi: 10.1172/JCI28775
- Moon, E. Y., Noh, Y. W., Han, Y. H., Kim, S. U., Kim, J. M., Yu, D. Y., et al. (2006). T lymphocytes and dendritic cells are activated by the deletion of peroxiredoxin II (Prx II) gene. *Immunol. Lett.* 102, 184–190. doi: 10.1016/j.imlet.2005.09.003
- Nakashima, T., Hayashi, M., and Takayanagi, H. (2012). New insights into osteoclastogenic signaling mechanisms. *Trends Endocrinol. Metab.* 23, 582–590. doi: 10.1016/j.tem.2012.05.005
- Negishi-Koga, T., and Takayanagi, H. (2009). Ca²⁺-NFATc1 signaling is an essential axis of osteoclast differentiation. *Immunol. Rev.* 231, 241–256. doi: 10.1111/j.1600-065X.2009.00821.x
- Okawa, Y., Hideshima, T., Steed, P., Vallet, S., Hall, S., Huang, K., et al. (2009). SNX-2112, a selective Hsp90 inhibitor, potently inhibits tumor cell growth, angiogenesis, and osteoclastogenesis in multiple myeloma and other hematologic tumors by abrogating signaling via Akt and ERK. *Blood* 113, 846–855. doi: 10.1182/blood-2008-04-151928
- Otoguro, K., Iwatsuki, M., Ishiyama, A., Namatame, M., Nishihara-Tukashima, A., Kiyohara, H., et al. (2011). *In vitro* antitrypanosomal activity of plant terpenes against *Trypanosoma brucei*. *Phytochemistry* 72, 2024–2030. doi: 10.1016/j.phytochem.2011.07.015
- Pihlstrom, B. L., Michalowicz, B. S., and Johnson, N. W. (2005). Periodontal diseases. *Lancet* 366, 1809–1820. doi: 10.1016/S0140-6736(05)67728-8
- Stevenson, D. A., Schwarz, E. L., Carey, J. C., Viskochil, D. H., Hanson, H., Bauer, S., et al. (2011). Bone resorption in syndromes of the Ras/MAPK pathway. *Clin. Genet.* 80, 566–573. doi: 10.1111/j.1399-0004.2010.01619.x
- Takahashi, N., Udagawa, N., and Suda, T. (1999). A new member of tumor necrosis factor ligand family, ODF/OPGL/TRANCE/RANKL, regulates osteoclast differentiation and function. *Biochem. Biophys. Res. Commun.* 256, 449–455. doi: 10.1006/bbrc.1999.0252
- Takayanagi, H. (2007). Osteoimmunology: shared mechanisms and crosstalk between the immune and bone systems. *Nat. Rev. Immunol.* 7, 292–304. doi: 10.1038/nri2062
- Takayanagi, H., Ogasawara, K., Hida, S., Chiba, T., Murata, S., Sato, K., et al. (2000). T-cell-mediated regulation of osteoclastogenesis by signalling crosstalk between RANKL and IFN-gamma. *Nature* 408, 600–605. doi: 10.1038/35046102
- Tang, C. H., Huang, T. H., Chang, C. S., Fu, W. M., and Yang, R. S. (2009). Water solution of onion crude powder inhibits RANKL-induced osteoclastogenesis through ERK, p38 and NF-kappaB pathways. *Osteoporos. Int.* 20, 93–103. doi: 10.1007/s00198-008-0630-2
- Teitelbaum, S. L. (2000). Bone resorption by osteoclasts. *Science* 289, 1504–1508. doi: 10.1126/science.289.5484.1504
- Tsai, H. Y., Lin, H. Y., Fong, Y. C., Wu, J. B., Chen, Y. F., Tsuzuki, M., et al. (2008). Paeonol inhibits RANKL-induced osteoclastogenesis by inhibiting ERK, p38 and NF-kappaB pathway. *Eur. J. Pharmacol.* 588, 124–133. doi: 10.1016/j.ejphar.2008.04.024
- Udagawa, N., Takahashi, N., Jimi, E., Matsuzaki, K., Tsurukai, T., Itoh, K., et al. (1999). Osteoblasts/stromal cells stimulate osteoclast activation through expression of osteoclast differentiation factor/RANKL but not macrophage colony-stimulating factor: receptor activator of NF-kappa B ligand. *Bone* 25, 517–523. doi: 10.1016/S8756-3282(99)00210-0
- Waddington, R. J., Moseley, R., and Embery, G. (2000). Reactive oxygen species: a potential role in the pathogenesis of periodontal diseases. *Oral Dis.* 6, 138–151. doi: 10.1111/j.1601-0825.2000.tb00325.x
- Wauquier, F., Leotoing, L., Coxam, V., Guicheux, J., and Wittrant, Y. (2009). Oxidative stress in bone remodelling and disease. *Trends Mol. Med.* 15, 468–477. doi: 10.1016/j.molmed.2009.08.004
- Wilson, S. R., Peters, C., Saftig, P., and Bromme, D. (2009). Cathepsin K activity-dependent regulation of osteoclast actin ring formation and bone resorption. *J. Biol. Chem.* 284, 2584–2592. doi: 10.1074/jbc.M805280200
- Winslow, M. M., Pan, M., Starbuck, M., Gallo, E. M., Deng, L., Karsenty, G., et al. (2006). Calcineurin/NFAT signaling in osteoblasts regulates bone mass. *Dev. Cell* 10, 771–782. doi: 10.1016/j.devcel.2006.04.006
- Wu, C., Wang, W., Tian, B., Liu, X., Qu, X., Zhai, Z., et al. (2015). Myricetin prevents titanium particle-induced osteolysis in vivo and inhibits RANKL-induced osteoclastogenesis in vitro. *Biochem. Pharmacol.* 93, 59–71. doi: 10.1016/j.bcp.2014.10.019
- Xiao, F., Zhai, Z., Jiang, C., Liu, X., Li, H., Qu, X., et al. (2015). Geraniin suppresses RANKL-induced osteoclastogenesis in vitro and ameliorates wear particle-induced osteolysis in mouse model. *Exp. Cell Res.* 330, 91–101. doi: 10.1016/j.yexcr.2014.07.005
- Xu, X., Zhang, X. A., and Wang, D. W. (2011). The roles of CYP450 epoxygenases and metabolites, epoxyeicosatrienoic acids, in cardiovascular and malignant diseases. *Adv. Drug Deliv. Rev.* 63, 597–609. doi: 10.1016/j.addr.2011.03.006

- Yeon, J. T., Kim, K. J., Choi, S. W., Moon, S. H., Park, Y. S., Ryu, B. J., et al. (2014). Anti-osteoclastogenic activity of praeruptorin A via inhibition of p38/Akt-c-Fos-NFATc1 signaling and PLCgamma-independent Ca^{2+} oscillation. *PLoS ONE* 9:e88974. doi: 10.1371/journal.pone.0088974
- Yeon, J. T., Kim, K. J., Chun, S. W., Lee, H. I., Lim, J. Y., Son, Y. J., et al. (2015). KCNK1 inhibits osteoclastogenesis by blocking the Ca^{2+} oscillation and JNK-NFATc1 signaling axis. *J. Cell Sci.* 128, 3411–3419. doi: 10.1242/jcs.170738
- Zhu, X., Gao, J., Ng, P. Y., Qin, A., Steer, J. H., Pavlos, N. J., et al. (2016). Alexidine dihydrochloride attenuates osteoclast formation and bone resorption and protects against LPS-induced osteolysis. *J. Bone Miner. Res.* 31, 560–572. doi: 10.1002/jbmr.2710

Conflict of Interest Statement: The authors declare that the research was conducted in the absence of any commercial or financial relationships that could be construed as a potential conflict of interest.

Copyright © 2017 Niu, Xiao, Yuan, Hu, Lin, Ma, Zhang and Huang. This is an open-access article distributed under the terms of the Creative Commons Attribution License (CC BY). The use, distribution or reproduction in other forums is permitted, provided the original author(s) or licensor are credited and that the original publication in this journal is cited, in accordance with accepted academic practice. No use, distribution or reproduction is permitted which does not comply with these terms.



Synergistic Effect of Pleuromutilins with Other Antimicrobial Agents against *Staphylococcus aureus* *In Vitro* and in an Experimental *Galleria mellonella* Model

Chun-Liu Dong^{1,2}, Lin-Xiong Li^{1,2}, Ze-Hua Cui^{1,2}, Shu-Wen Chen^{1,2}, Yan Q. Xiong³, Jia-Qi Lu^{1,2}, Xiao-Ping Liao^{1,2}, Yuan Gao^{1,2}, Jian Sun^{1,2,4*} and Ya-Hong Liu^{1,2,4,5*}

¹ National Risk Assessment Laboratory for Antimicrobial Resistance of Animal Original Bacteria, South China Agricultural University, Guangzhou, China, ² Guangdong Provincial Key Laboratory of Veterinary Pharmaceutics Development and Safety Evaluation, South China Agricultural University, Guangzhou, China, ³ David Geffen School of Medicine, University of California, Los Angeles, Los Angeles, CA, United States, ⁴ Laboratory of Veterinary Pharmacology, College of Veterinary Medicine, South China Agricultural University, Guangzhou, China, ⁵ Jiangsu Co-Innovation Center for Prevention and Control of Important Animal Infectious Diseases and Zoonoses, Yangzhou, China

OPEN ACCESS

Edited by:

Yuhei Nishimura,
Mie University, Japan

Reviewed by:

Nadezhda A. German,
Texas Tech University Health
Sciences Center, United States
Yoshito Zamami,
Tokushima University Graduate
School of Medical Sciences, Japan

*Correspondence:

Ya-Hong Liu
lyh@scau.edu.cn
Jian Sun
jjiansun@scau.edu.cn

Specialty section:

This article was submitted to
Experimental Pharmacology and Drug
Discovery,
a section of the journal
Frontiers in Pharmacology

Received: 10 June 2017

Accepted: 07 August 2017

Published: 22 August 2017

Citation:

Dong C-L, Li L-X, Cui Z-H,
Chen S-W, Xiong YQ, Lu J-Q,
Liao X-P, Gao Y, Sun J and Liu Y-H
(2017) Synergistic Effect
of Pleuromutilins with Other
Antimicrobial Agents against
Staphylococcus aureus *In Vitro*
and in an Experimental *Galleria*
mellonella Model.
Front. Pharmacol. 8:553.
doi: 10.3389/fphar.2017.00553

Invasive infections due to *Staphylococcus aureus*, including methicillin-resistant *S. aureus* are prevalent and life-threatening. Combinations of antibiotic therapy have been employed in many clinical settings for improving therapeutic efficacy, reducing side effects of drugs, and development of antibiotic resistance. Pleuromutilins have a potential to be developed as a new class of antibiotics for systemic use in humans. In the current study, we investigated the relationship between pleuromutilins, including valnemulin, tiamulin, and retapamulin, and 13 other antibiotics representing different mechanisms of action, against methicillin-susceptible and -resistant *S. aureus* both *in vitro* and in an experimental *Galleria mellonella* model. *In vitro* synergistic effects were observed in combination of all three study pleuromutilins with tetracycline (TET) by standard checkerboard and/or time-kill assays. In addition, the combination of pleuromutilins with ciprofloxacin or enrofloxacin showed antagonistic effects, while the rest combinations presented indifferent effects. Importantly, all study pleuromutilins in combination with TET significantly enhanced survival rates as compared to the single drug treatment in the *G. mellonella* model caused by *S. aureus* strains. Taken together, these results demonstrated synergy effects between pleuromutilins and TET against *S. aureus* both *in vitro* and *in vivo*.

Keywords: pleuromutilins, other antibiotics, antibiotic combination, *Staphylococcus aureus*, *Galleria mellonella* model

INTRODUCTION

Staphylococcus aureus is a predominant cause of community-acquired and healthcare-associated infection in human (VanEperen and Segreti, 2016). In particular, it is the most common cause of life-threatening endovascular infections. Despite modern antibiotic treatment, morbidity and mortality with such syndromes remain unacceptably high (Boucher and Sakoulas, 2007; Boucher et al., 2010). In addition, the growing population in

methicillin-resistant *S. aureus* (MRSA) infections and the dwindling industry investment in anti-infective development further portend a looming threat of untreatable infections (Deng et al., 2017). Therefore, there is a great need to find novel strategies for the treatment of these invasive infections. One of important approaches is the combinations of preexisting antibiotics which has been addressed by our current studies.

Pleuromutilins were discovered as natural-product antibiotics in 1950s (Kavanagh et al., 1951). Tiamulin (TIA) was the first pleuromutilin compound to be approved for veterinary use in 1979, followed by valnemulin (VAL) in 1999 (Sader et al., 2012). Retapamulin (RET) became the first pleuromutilin approved for use in humans, only topical application in 2007. Recently, synthesized pleuromutilins, which combine potent antibacterial activity with favorable pharmaceutical properties, make these compounds suitable for systemic administration in humans (Zeitlinger et al., 2016). Pleuromutilins inhibit bacterial growth via a specific interaction with the 23S rRNA of the 50S bacterial ribosome subunit that is responsible for bacterial protein synthesis (Davidovich et al., 2007). Their unique mechanism of action implies a broad antibacterial spectrum against a wide range of both Gram-positive and Gram-negative bacteria (Paukner et al., 2013), including MRSA, as well a low probability of cross resistance with other antibiotics and development of resistance.

Although pleuromutilins have been used in clinical settings for almost 40 years, very little is known about their interaction with other antibiotics. Therefore, in the current study, we tested the combination of pleuromutilins with other antibiotics representing diverse mechanisms of action, including targeting protein, cell wall, DNA gyrase and folic acid syntheses against methicillin-susceptible *S. aureus* (MSSA) and MRSA *in vitro* and in an experimental *Galleria mellonella* model.

MATERIALS AND METHODS

Antimicrobial Agents, Bacterial Strains, and Growth Conditions

Three pleuromutilins, including TIA, VAL, and RET, and 13 other antimicrobial agents were selected for our studies based on their mechanism of action (Table 1). All study antibiotics were purchased from Guangzhou Xiang Bo Biological Technology Co., Ltd. (Guangzhou, China). Antibiotic stocks solutions were prepared according to the manufacturer's recommendations.

Two standard *S. aureus* strains (MSSA ATCC 29213 and MRSA ATCC 43300) and two *S. aureus* clinical strains (MSSA N54 and MRSA N9) were used in this study. All strains were incubated overnight at 37°C in brain heart infusion (BHI). Mueller-Hinton broth (MHB) was used for all *in vitro* susceptibility assays.

Determination of MICs

Determination of the study antibiotic MICs was conducted by broth microdilution as recommended by the CLSI guidelines (CLSI, 2013).

Determination of Fractional Inhibitory Concentration Index (FICI) by a Checkerboard Method

A checkerboard technique was employed to delineate the Fractional Inhibitory Concentration Index (FICI) of pleuromutilins plus antibiotic combinations (White et al., 1996). Briefly, 96 well plates containing serial dilutions of pleuromutilins + antibiotic (range, 0.125 × MIC to 4 × MIC) were inoculated with 5×10^5 of *S. aureus* and incubated for 18 h. Control wells were free of pleuromutilins or antibiotic. After incubation, plates were screened for visual growth. The FICI were then calculated as previously described (≤ 0.5 , synergy; 0.6–1.0, additivity; 1.1–4.0, indifference; > 4.0 , antagonism) (White et al., 1996; Odds, 2003).

In Vitro Time-Kill Curves

Time-kill curves of pleuromutilins (VAL, TIA, and RET at 0.5 × MIC) and tetracycline (TET) (0.5 × MIC) alone, and in combination were carried in glass flasks containing a final inoculum of 5×10^5 CFU/mL of the study *S. aureus* strain at 37°C with shaking for 24 h. At 0, 3, 6, 9, and 24 h of incubation, 0.1 mL aliquots were taken from each group, serially diluted in sterile saline, plated onto MH agar plates, and incubated at 37°C for 24 h for a viable count enumeration. All experiments were performed at least three times on different days.

Galleria mellonella Model

A well-characterized *G. mellonella* model was used in this study based on previous publication (Desbois and Coote, 2011). Larvae of *G. mellonella* were obtained from Kaide Ruixin Co., Ltd. (Tianjin, China). In order to determine the optimal infection doses of the study *S. aureus* strains, *G. mellonella* larvae (~250 mg with a creamy color) were randomly distributed in six experimental groups ($n = 10$ /group), and were then infected

TABLE 1 | Antibiotics used in this study.

Antibiotics	Abbreviation	Classification	Primary target
Cefotaxime	CTX	Cephalosporins	Cell wall
Erythromycin	ERY	Macrolides	Protein synthesis 50S
Florfenicol	FFC	Phenicol	Protein synthesis 50S
Clindamycin	CLI	Lincosamides	Protein synthesis 50S
Ciprofloxacin	CIP	Fluoroquinolones	DNA gyrase
Enrofloxacin	ENR	Fluoroquinolones	DNA gyrase
Gentamicin	GEN	Aminoglycosides	Protein synthesis 30S
Amikacin	AMK	Aminoglycosides	Protein synthesis 30S
Tetracycline	TET	Tetracyclines	Protein synthesis 30S
Valnemulin	VAL	Pleuromutilins	Protein synthesis 50S
Tiamulin	TIA	Pleuromutilins	Protein synthesis 50S
Retapamulin	RET	Pleuromutilins	Protein synthesis 50S
Vancomycin	VAN	Glycopeptides	Cell wall
Bacitracin	BCR	Polypeptides	Cell wall
Sulfamethoxazole	SMZ	Sulfonamides	Folic acid
Trimethoprim	TMP	Diaminopyrimidines	Folic acid

TABLE 2 | The minimum inhibitory concentrations (MICs) of antibiotics against *Staphylococcus aureus* strains.

Antibiotics	MICs (mg/L)			
	ATCC 29213	ATCC 43300	N54	N9
CTX	4	16	4	16
ERY	0.25	0.25	0.25	0.25
FFC	8	8	8	8
CLI	0.25	0.125	0.125	1
CIP	0.25	0.5	0.5	0.5
ENR	0.125	0.125	0.25	0.25
GEN	0.5	1	0.5	0.5
AMK	1	4	1	4
TET	0.5	0.5	64	64
VAL	0.0625	0.0625	0.0625	0.0625
TIA	0.5	0.5	0.5	0.5
RET	0.0625	0.03125	0.0625	0.0625
VAN	1	1	1	1
BCR	64	64	32	64
SMZ	128	>256	>256	>256
TMP	4	>256	>256	>256

CTX, cefotaxime; ERY, erythromycin; FFC, florfenicol; CLI, clindamycin; CIP, ciprofloxacin; ENR, enrofloxacin; GEN, gentamicin; AMK, amikacin; TET, tetracycline; VAL, valnemulin; TIA, tiamulin; RET, retapamulin; VAN, vancomycin; BCR, bacitracin; SMZ, sulfamethoxazole; TMP, trimethoprim; ATCC 29213 and N54: MSSA; ATCC 4330 and N9: MRSA.

by injection of 10 μ L of logarithmic phase *S. aureus* cells (10^3 – 10^9 CFU/larval) into the last left proleg. After injection, the larvae were incubated in plastic Petri dishes at 37°C for 5 days and scored for survival daily. In all experiments, two controls were included: (1) PBS injections and (2) without any injection.

The *in vivo* efficacy of VAL, TIA, and RET alone, and in combination with TET or CIP was assessed in the same *G. mellonella* model caused by study *S. aureus* strains using the optimal infection doses as determined above ($\sim 10^6$ CFU/larva). At 2 h post-infection, animals were randomized to receive no therapy or VAL, TIA, RET, TET, CIP alone, or VAL+TET, TIA+TET, RET+TET, VAL+CIP, TIA+CIP, or RET+CIP ($n = 16$ /group). The antibiotics were administered only once (10 μ L) into the last right proleg at doses of VAL, 10 mg/kg; TIA, 10 mg/kg; RET, 10 mg/kg; TET, 20 mg/kg; or CIP, 20 mg/kg. Larvae were observed daily for 5 days and percent of survival was calculated for each group.

Statistical Analyses

Statistical tests were performed using GraphPad Prism v.5.04 (GraphPad Software Inc., San Diego, CA, United States). The *in vivo* survival data were plotted using the log rank test. *P*-value of ≤ 0.05 was considered significant.

RESULTS

MICs of Antimicrobials against *S. aureus*

The MICs of study antibiotics against *S. aureus* strains are showed in Table 2. The MICs VAL, TIA, and RET on ATCC 29213, ATCC

43300, N9, and N54 were ranged from 0.03125 to 0.5 mg/L. The MICs of TET against the two ATCC strains were 0.5 mg/L which are considered susceptible by CLSI guidance. However, the two study clinical *S. aureus* strains were resistant to TET with MICs of 64 mg/L based on the CLSI break point (CLSI, 2015).

FICI Determination

The FICI of study antibiotic combinations are shown in Table 3. For all study strains, the FICI of the VAL/TET and RET/TET combinations were 0.375–0.5 indicating synergy effects. Tiamulin/tetracycline combination showed synergistic action against *S. aureus* ATCC 29213 strain, but additivity effect on ATCC 43300 and the two clinical strains with FICI of 0.75. While the FICI of VAL, TIA, RET in combination with CIP, or ENR were 4 or 5 that demonstrate antagonistic effects. Moreover, the interactions of other antibiotic combinations with pleuromutilins resulted in indifference with the FICI of 1.5 or 2 (data not shown for TIA and RET in combination with the other antibiotics).

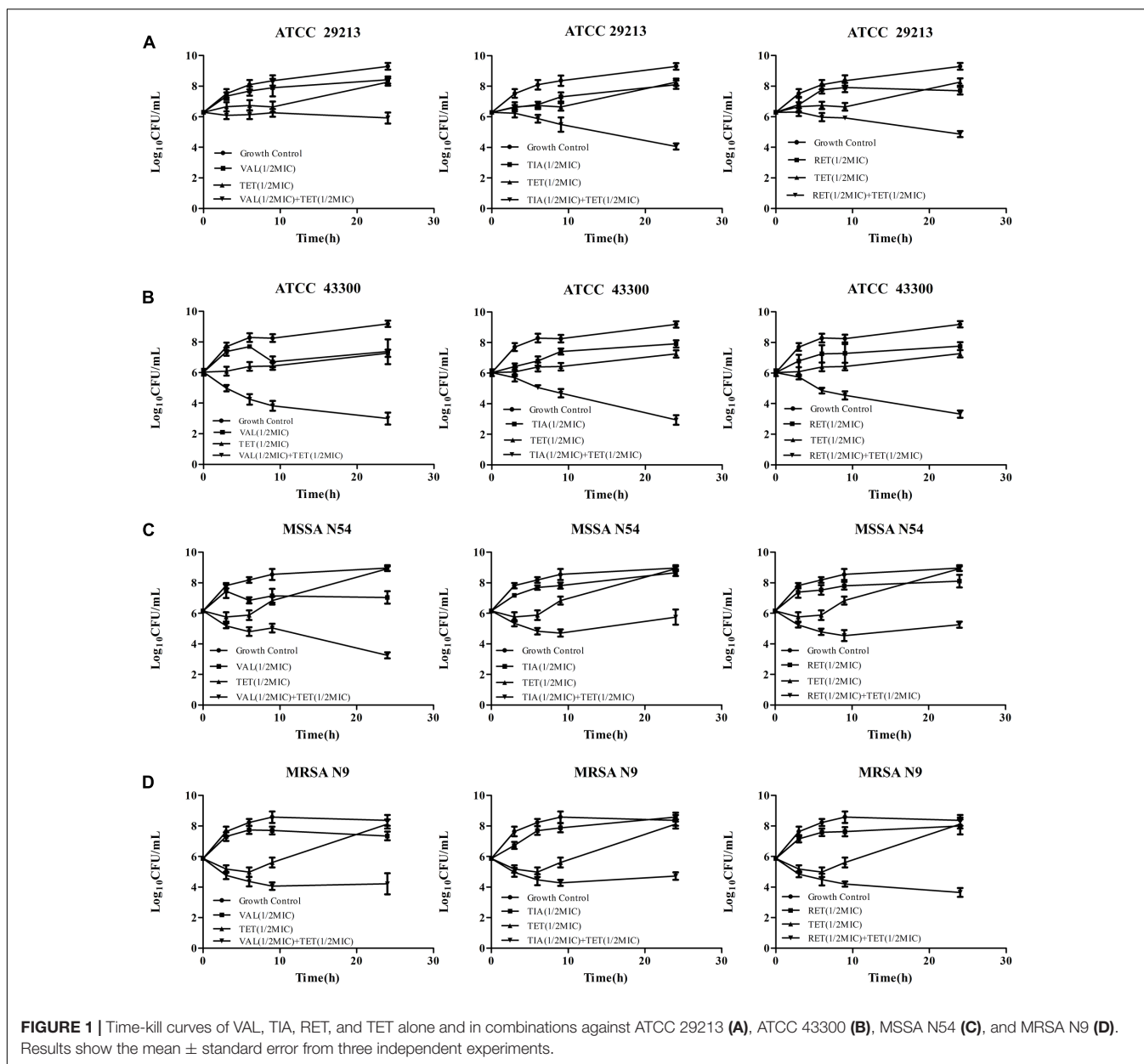
In Vitro Time-Killing Curves

The *in vitro* time-kill activities of the combination of pleuromutilins with TET at concentrations of $0.5 \times \text{MIC}$ against study *S. aureus* strains are shown in Figure 1 and specific \log_{10} CFU/mL changes are shown in Table 4. All three

TABLE 3 | The fractional inhibitory concentrations index (FICI) of the combinations of antimicrobial agents against *Staphylococcus aureus*.

Antibiotics combination	FICI				Interaction
	ATCC 29213	ATCC 43300	N54	N9	
VAL+CTX	2	2	2	2	Indifferent
VAL+ERY	2	2	2	2	Indifferent
VAL+FFC	1.5	1.5	2	2	Indifferent
VAL+CLI	2	2	2	2	Indifferent
VAL+CIP	5	5	4	5	Antagonistic
VAL+ENR	5	5	4	5	Antagonistic
VAL+GEN	2	2	2	2	Indifferent
VAL+AMK	2	2	2	2	Indifferent
VAL+TET	0.375	0.5	0.5	0.5	Synergistic
VAL+VAN	2	2	2	2	Indifferent
VAL+BCR	1.5	2	2	2	Indifferent
VAL+SMZ	2	2	2	2	Indifferent
VAL+TMP	2	2	2	2	Indifferent
TIA+TET	0.5	0.75	0.75	0.75	Synergistic or additivity
RET+TET	0.5	0.5	0.5	0.5	Synergistic
TIA+CIP	4	4	4	4	Antagonistic
TIA+ENR	4	4	4	4	Antagonistic
RET+CIP	4	4	4	4	Antagonistic
RET+ENR	4	5	5	5	Antagonistic

CTX, cefotaxime; ERY, erythromycin; FFC, florfenicol; CLI, clindamycin; CIP, ciprofloxacin; ENR, enrofloxacin; GEN, gentamicin; AMK, amikacin; TET, tetracycline; VAL, valnemulin; TIA, tiamulin; RET, retapamulin; VAN, vancomycin; BCR, bacitracin; SMZ, sulfamethoxazole; TMP, trimethoprim; ATCC 29213 and N54: MSSA; ATCC 4330 and N9: MRSA.



study pleuromutilins in combination with TET had synergy effects against all study ATCC and clinical *S. aureus* strains. For instance, the combination of VAN with TET caused more than 2 log₁₀ CFU/mL reductions on both MSSA and MRSA strains as compared with the most active antibiotic alone (Figure 1 and Table 4).

Optimal Inoculum Dose in the *G. mellonella* Model

A good infective dose-dependent survival rate was observed during 5 days post-infection time period in the *G. mellonella* model caused by the study *S. aureus* strains (Supplementary Figures S1A–D represent ATCC 29213, ATCC 43300, N54, and N9, respectively). At approximate 10⁶ CFU/larval infection

dose, infected larval had 20–60% survival rates during experimental time period. At 10³–10⁴ CFU/larval infection doses, larval survival rates were 70–100% during the 5 days, while at approximate 10⁸ CFU/larval for ATCC 43300, and 10⁹ CFU/larval for other three *S. aureus* strains, animals dead within 24 h post-infection. Therefore, 10⁶ CFU/larval challenge dose was selected for the efficacy experiments in the model.

Efficacy of Antibiotics for *G. mellonella*

The efficacies of pleuromutilins alone and in combination with TET against the four study *S. aureus* strains in the *G. mellonella* model were presented in Figures 2–4 for VAL, TIA, and RET, respectively. In this study, VAL and TET monotherapy increased *G. mellonella* survival from infections caused by all

TABLE 4 | The log change (\log_{10} CFU/mL) between the combinations vs. initial inoculum and the most active single agent after 24 h of incubation.

		Colony changes (\log_{10} CFU/mL) at 24 h			
		ATCC 29213	ATCC 43300	N54	N9
VAL+TET	vs. initial inoculum	-3.37	-6.19	-5.71	-4.15
	vs. most active drug	-2.35	-4.26	-3.78	-3.13
TIA+TET	vs. initial inoculum	-5.24	-6.30	-3.21	-3.65
	vs. most active drug	-4.04	-5.03	-2.91	-3.41
RET+TET	vs. initial inoculum	-4.44	-5.87	-3.71	-4.72
	vs. most active drug	-2.84	-3.94	-2.85	-4.35

Valnemulin (VAL), tiamulin (TIA), retapamulin (RET), and tetracycline (TET). $1/2 \times$ MICs of all antibiotics were used in this assay.

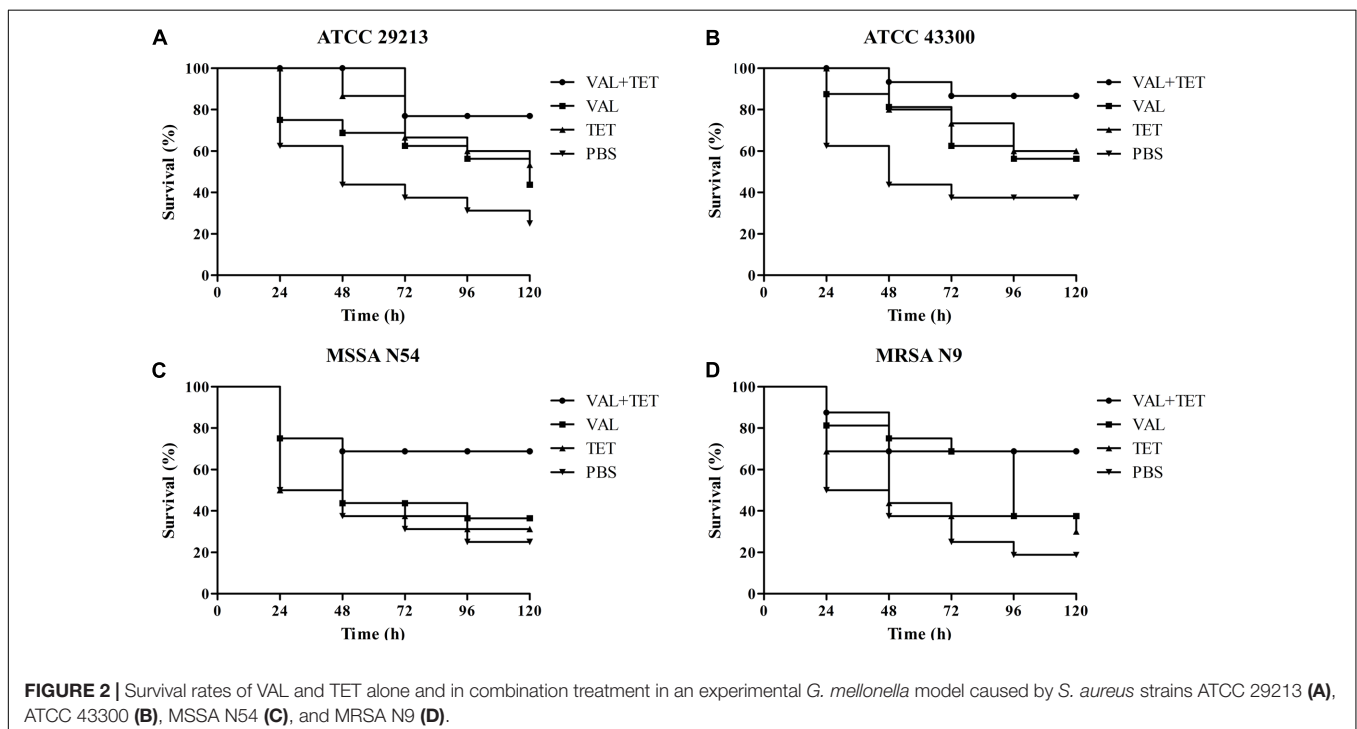
study *S. aureus* strains. Importantly, the combination of VAL with TET significantly increased survival as compared with VAL and TET treatment alone in the model (Figure 2; $p < 0.05$). Similarly, the combinations of TIA/TET and RET/TET also significantly improved animal survival rates as compared with monotherapy (Figures 3, 4, respectively; $p < 0.05$). The efficacies of pleuromutilins alone and in combination with CIP against the four study *S. aureus* strains in the *G. mellonella* model were presented in Figure 5. The combinations of VAL/CIP, TIA/CIP, and RET/CIP did not improve the larvae survival rates as compared with monotherapy.

DISCUSSION

The emergence of multiple drug-resistant bacteria is a great threat to public health. Antibiotics combinations offer potential

strategies to increase the therapeutic efficacy of antibiotics against infections caused by drug-resistant microorganism. Some recent studies have demonstrated that the combination of pleuromutilins derivative with doxycycline had synergy effect against multidrug-resistant *Acinetobacter baumannii* *in vitro* (Siricilla et al., 2017). Another investigation showed that TIA had a synergistic antimicrobial effect when in combination with chlortetracycline against *Mycoplasma* infection in birds (Islam et al., 2008). The present study was designed to study the anti-*S. aureus* activity of pleuromutilins (VAL, TIA, and RET) alone and in combination with other antibiotics with different mechanism of action both *in vitro* and *in vivo*.

We demonstrated that all study *S. aureus* strains, including MSSA and MRSA, had very low pleuromutilins MICs ranged from 0.03125 to 0.5 mg/L. In addition, the two study ATCC *S. aureus* strains are susceptible to TET, while the two clinical *S. aureus* strains were resistant to TET. Interestingly, synergistic effects of all study pleuromutilins, VAL, TIA, and RET, in combinations with TET were observed *in vitro* by a standard checkerboard methods and/or time-kill curves. However, antagonistic effects were exhibited in the combinations of pleuromutilins with two study fluoroquinolones (CIP and ENR). The exact mechanisms of these different interactions between pleuromutilins with other classes of antibiotic are not well identified. It is known that both pleuromutilins and TET belong to bacteriostatic agents. However, pleuromutilins and TET bind to bacterial 50S and 30S subunit of microbial ribosomes, respectively. Thus, the synergy effects between these two antibiotics might be due to their different bacterial targets and/or more complex relationships when they combined (Bollenbach, 2015). In consistence with other studies, we demonstrated

**FIGURE 2** | Survival rates of VAL and TET alone and in combination treatment in an experimental *G. mellonella* model caused by *S. aureus* strains ATCC 29213 (A), ATCC 43300 (B), MSSA N54 (C), and MRSA N9 (D).

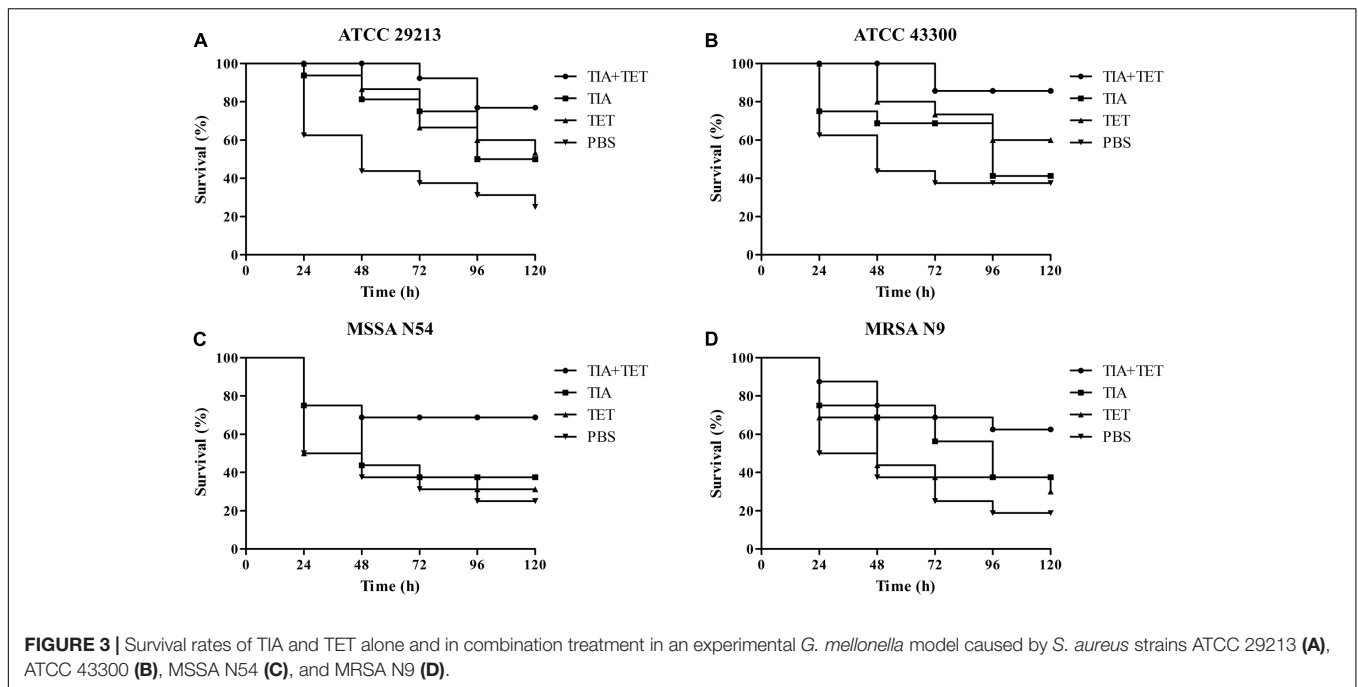


FIGURE 3 | Survival rates of TIA and TET alone and in combination treatment in an experimental *G. mellonella* model caused by *S. aureus* strains ATCC 29213 (A), ATCC 43300 (B), MSSA N54 (C), and MRSA N9 (D).

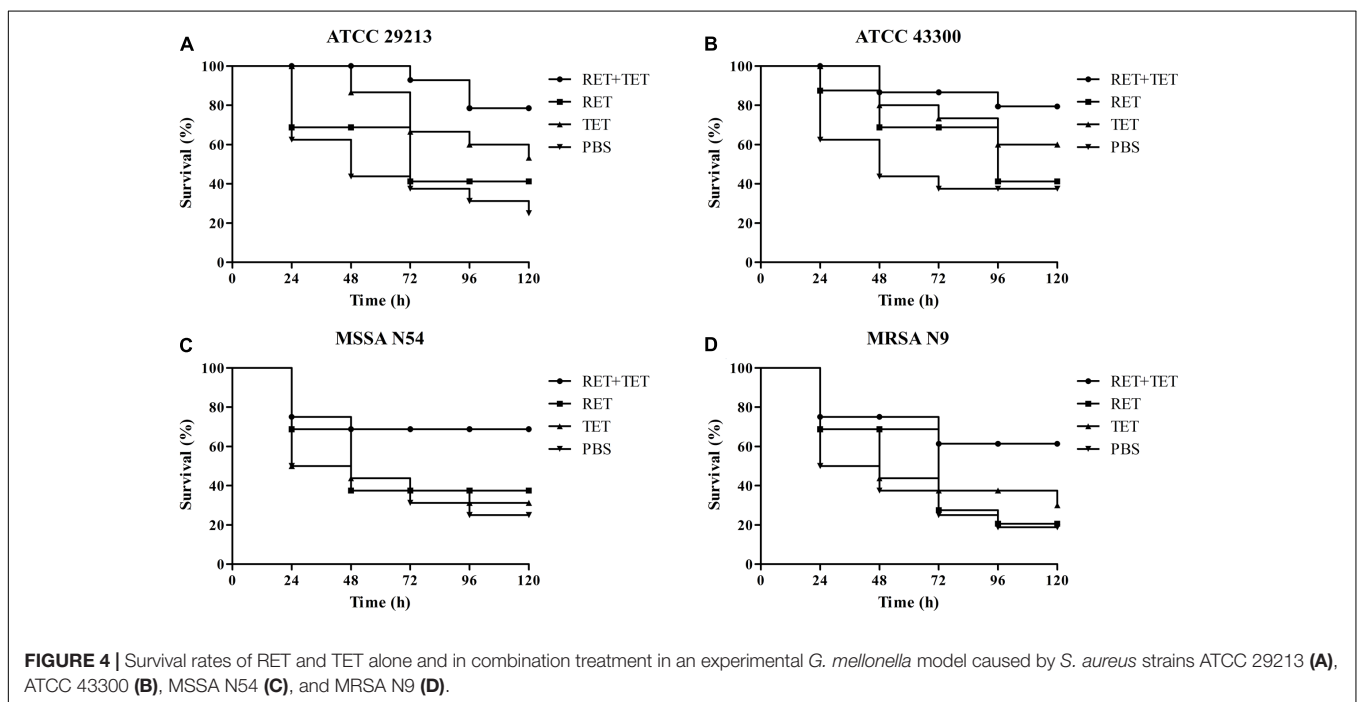
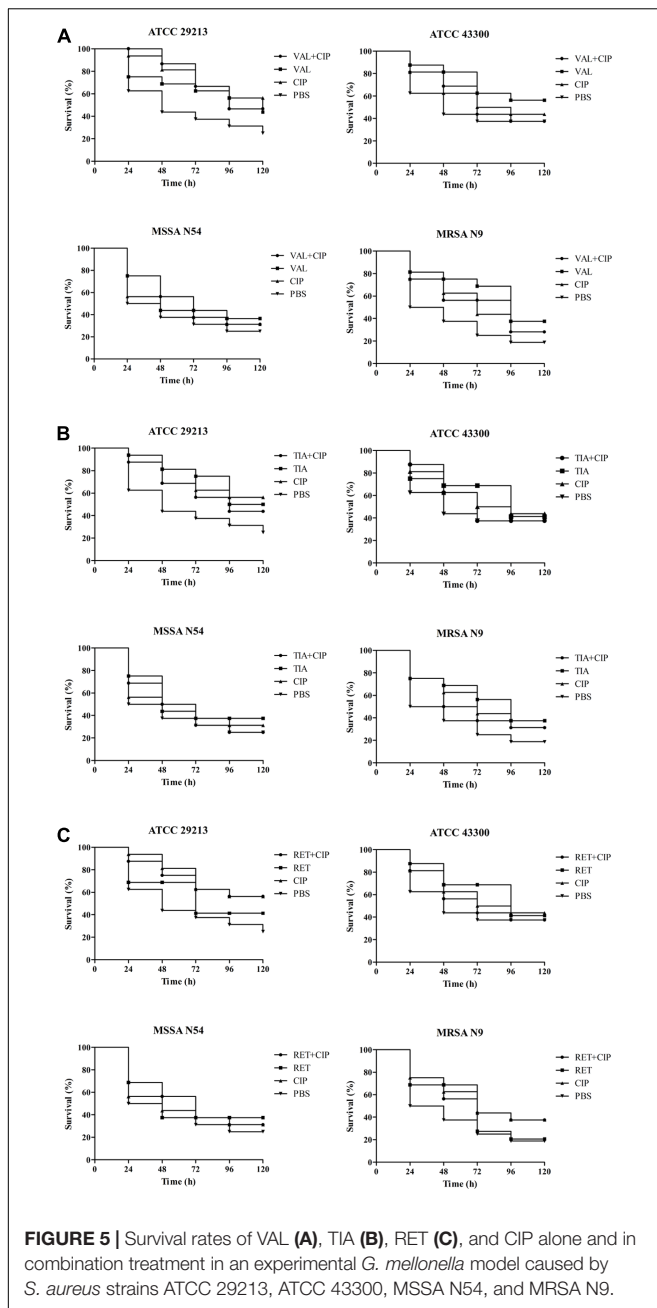


FIGURE 4 | Survival rates of RET and TET alone and in combination treatment in an experimental *G. mellonella* model caused by *S. aureus* strains ATCC 29213 (A), ATCC 43300 (B), MSSA N54 (C), and MRSA N9 (D).

that the combination of bacteriostatic with bactericidal antibiotics exhibited antagonism (e.g., pleuromutilins plus fluoroquinolones) or indifference effects (e.g., pleuromutilins in combination with most study bactericidal antibiotics) (Yeh et al., 2006; Ocampo et al., 2014). The mechanism of fluoroquinolones is to inhibit bacterial replication by blocking their DNA replication pathway (Bollenbach et al., 2009). On the other hand, pleuromutilins inhibit protein synthesis. Therefore, these different mechanisms of action might contribute to the

antagonism effects between pleuromutilins and fluoroquinolones. However, the exact mechanism of these phenotypes is not clear up to date. In addition, it has been reported that these antagonism and indifference effects were antibiotics and/or organisms dependent (Pankey and Sabath, 2004; Ocampo et al., 2014).

Importantly, to the best of our knowledge, this is the first study demonstrated the synergy effects between pleuromutilins and TET in the experiment of *G. mellonella* infection model



caused by MSSA and MRSA strains. Our results showed that the combination of VAL with TET significantly increased survival rates of animals infected by all study *S. aureus* strains as compared to the single treatment, with increased percent of survival from 30 to 90%. However, the combination of pleuromutilins with CIP do not increase survival rates of animals infected by all study *S. aureus* strains as compared to the single treatment, which is similar to the *in vitro* antagonistic effects by the checkerboard test. Recently, Desbois et al. used the same *G. mellonella* infection model due to *S. aureus* and demonstrated that anti-staphylococcal antibiotics, such as daptomycin and vancomycin, could increase larval survival (Desbois and Coote,

2011). In addition, penicillin improved survival of larvae infected with a penicillin-susceptible MRSA strain, but was ineffective with penicillin-resistant MRSA (Desbois and Coote, 2011). These results indicated that the *G. mellonella* model is useful for assessing the *in vivo* efficacy of anti-*S. aureus* agents.

CONCLUSION

In the current studies, synergistic effects between pleuromutilins and TET were demonstrated both *in vitro* and in an experimental *G. mellonella* model caused by all four study MSSA and MRSA strains. There were no significant differences among the three pleuromutilins observed in *in vitro* assays, as well as in the *in vivo* animal mode. These findings provided important information that anti-staphylococcal effect of pleuromutilins is increased when it combined with TET. In addition, our study confirmed that the *G. mellonella* mode is a useful tool to investigate the *in vivo* efficacy of antimicrobial agents against *S. aureus* infections. We realized that our studies have some limitations. For instance, we only studied two ATCC and two clinical *S. aureus* strains. Future studies will include more MSSA and MRSA isolates. In addition, other animal models (e.g., murine bacteremia, skin and soft tissues infections) are needed to confirm the *in vivo* efficacy between pleuromutilins and other antibiotics. Moreover, we are interested in defining the mechanism of the antibiotic combined actions against *S. aureus*.

AUTHOR CONTRIBUTIONS

Y-HL and JS conceived this study and participated in its design and coordination. C-LD and YX designed the experiment and drafted the manuscript. C-LD, L-XL, and J-QL carried out the *G. mellonella* model experiments. S-WC, Z-HC, and YG carried out the time-kill curve studies and the checkerboard method. X-PL participated in the data analysis and revision of manuscript. All authors read and approved the final manuscript.

FUNDING

This work was supported by the National Key Research and Development Program (2016YFD0501300), Program for Changjiang Scholars and Innovative Research Team in University of Ministry of Education of China (IRT13063), and Science and Technology Program of Guangzhou, China (2012A020800004).

SUPPLEMENTARY MATERIAL

The Supplementary Material for this article can be found online at: <http://journal.frontiersin.org/article/10.3389/fphar.2017.00553/full#supplementary-material>

FIGURE S1 | Kill kinetics of strains: ATCC 29213 (A); ATCC 43300 (B); MSSA N54 (C); and MRSA N9 (D) at various numbers of CFU/mL in *Galleria mellonella* over 120 h.

REFERENCES

- Bollenbach, T. (2015). Antimicrobial interactions: mechanisms and implications for drug discovery and resistance evolution. *Curr. Opin. Microbiol.* 27, 1–9. doi: 10.1016/j.mib.2015.05.008
- Bollenbach, T., Quan, S., Chait, R., and Kishony, R. (2009). Nonoptimal microbial response to antibiotics underlies suppressive drug interactions. *Cell* 139, 707–718. doi: 10.1016/j.cell.2009.10.025
- Boucher, H., Miller, L. G., and Razonable, R. R. (2010). Serious infections caused by methicillin-resistant *Staphylococcus aureus*. *Clin. Infect. Dis.* 51(Suppl. 2), S183–S197. doi: 10.1086/653519
- Boucher, H. W., and Sakoulas, G. (2007). Perspectives on Daptomycin resistance, with emphasis on resistance in *Staphylococcus aureus*. *Clin. Infect. Dis.* 45, 601–608. doi: 10.1086/520655
- CLSI. (2013). *Performance Standards for Antimicrobial Disk and Dilution Susceptibility Tests for Bacteria Isolated From Animals CLSI Document VET01-A4*, 4th Edn. Wayne, PA: Clinical and Laboratory Standard Institute.
- CLSI. (2015). *Performance Standards for Antimicrobial Susceptibility Testing CLSI M100-S25*. Wayne, PA: Clinical and Laboratory Standards Institute.
- Davidovich, C., Bashan, A., Auerbach-Nevo, T., Yaggie, R. D., Gontarek, R. R., and Yonath, A. (2007). Induced-fit tightens pleuromutilins binding to ribosomes and remote interactions enable their selectivity. *Proc. Natl. Acad. Sci. U.S.A.* 104, 4291–4296. doi: 10.1073/pnas.0700041104
- Deng, F., Wang, H., Liao, Y., Li, J., Fessler, A. T., Michael, G. B., et al. (2017). Detection and genetic environment of pleuromutilin-lincosamide-streptogramin a resistance genes in staphylococci isolated from pets. *Front. Microbiol.* 8:234. doi: 10.3389/fmicb.2017.00234
- Desbois, A. P., and Coote, P. J. (2011). Wax moth larva (*Galleria mellonella*): an in vivo model for assessing the efficacy of antistaphylococcal agents. *J. Antimicrob. Chemother.* 66, 1785–1790. doi: 10.1093/jac/dkr198
- Islam, K. M., Afrin, S., Khan, M. J., Das, P. M., Hassan, M. M., Valks, M., et al. (2008). Compatibility of a combination of tiamulin plus chlortetracycline with salinomycin in feed during a long-term co-administration in broilers. *Poult. Sci.* 87, 1565–1568. doi: 10.3382/ps.2008-00071
- Kavanagh, F., Herve, A., and Robbins, W. J. (1951). Antibiotic substances from basidiomycetes VIII. *Pleurotus Multilus* (Fr.) Sacc. and *Pleurotus passeckerianus* Pilat. *Proc. Natl. Acad. Sci. U.S.A.* 37, 570–574. doi: 10.1073/pnas.37.9.570
- Ocampo, P. S., Lázár, V., Papp, B., Arnoldini, M., Abel zur Wiesch, P., Busa-Fekete, R., et al. (2014). Antagonism between bacteriostatic and bactericidal antibiotics is prevalent. *Antimicrob. Agents Chemother.* 58, 4573–4582. doi: 10.1128/AAC.02463-14
- Odds, F. C. (2003). Synergy, antagonism, and what the checkerboard puts between them. *J. Antimicrob. Chemother.* 52:1. doi: 10.1093/jac/dkg301
- Pankey, G. A., and Sabath, L. D. (2004). Clinical relevance of bacteriostatic versus bactericidal mechanisms of action in the treatment of gram-positive bacterial infections. *Clin. Infect. Dis.* 38, 864–870. doi: 10.1086/381972
- Paukner, S., Sader, H. S., Ivezic-Schoenfeld, Z., and Jones, R. N. (2013). Antimicrobial activity of the pleuromutilin antibiotic BC-3781 against bacterial pathogens isolated in the SENTRY antimicrobial surveillance program in 2010. *Antimicrob. Agents Chemother.* 57, 4489–4495. doi: 10.1128/AAC.00358-13
- Sader, H. S., Biedenbach, D. J., Paukner, S., Ivezic-Schoenfeld, Z., and Jones, R. N. (2012). Antimicrobial activity of the investigational pleuromutilin compound BC-3781 tested against Gram-positive organisms commonly associated with acute bacterial skin and skin structure infections. *Antimicrob. Agents Chemother.* 56, 1619–1623. doi: 10.1128/AAC.05789-11
- Sircilla, S., Mitachi, K., Yang, J., Eslamimehr, S., Lemieux, M. R., Meibohm, B., et al. (2017). A new combination of a pleuromutilin derivative and doxycycline for treatment of multidrug-resistant *Acinetobacter baumannii*. *J. Med. Chem.* 60, 2869–2878. doi: 10.1021/acs.jmedchem.6b01805
- VanEperen, A. S., and Segreti, J. (2016). Empirical therapy in methicillin-resistant *Staphylococcus aureus* infections: an up-to-date approach. *J. Infect. Chemother.* 22, 351–359. doi: 10.1016/j.jiac.2016.02.012
- White, R. L., Burgess, D. S., Manduru, M., and Bosso, J. A. (1996). Comparison of three different in vitro methods of detecting synergy: time-kill, checkerboard, and E test. *Antimicrob. Agents Chemother.* 40, 1914–1918.
- Yeh, P., Tschumi, A. I., and Kishony, R. (2006). Functional classification of drugs by properties of their pairwise interactions. *Nat. Genet.* 38, 489–494. doi: 10.1038/ng1755
- Zeitlinger, M., Schwameis, R., Burian, A., Burian, B., Matzneller, P., Muller, M., et al. (2016). Simultaneous assessment of the pharmacokinetics of a pleuromutilin, lefamulin, in plasma, soft tissues and pulmonary epithelial lining fluid. *J. Antimicrob. Chemother.* 71, 1022–1026. doi: 10.1093/jac/dkv442

Conflict of Interest Statement: The authors declare that the research was conducted in the absence of any commercial or financial relationships that could be construed as a potential conflict of interest.

Copyright © 2017 Dong, Li, Cui, Chen, Xiong, Lu, Liao, Gao, Sun and Liu. This is an open-access article distributed under the terms of the Creative Commons Attribution License (CC BY). The use, distribution or reproduction in other forums is permitted, provided the original author(s) or licensor are credited and that the original publication in this journal is cited, in accordance with accepted academic practice. No use, distribution or reproduction is permitted which does not comply with these terms.



Chymase Inhibitor as a Novel Therapeutic Agent for Non-alcoholic Steatohepatitis

Shinji Takai* and Denan Jin

Department of Innovative Medicine, Graduate School of Medicine, Osaka Medical College, Takatsuki, Japan

OPEN ACCESS

Edited by:

Yuhei Nishimura,
Mie University Graduate School
of Medicine, Japan

Reviewed by:

Claudio Sorio,
University of Verona, Italy
Cesario Bianchi,
University of Mogi das Cruzes, Brazil
Tetsuo Nakata,
Kyoto Pharmaceutical University,
Japan

*Correspondence:

Shinji Takai
pha010@art.osaka-med.ac.jp

Specialty section:

This article was submitted to
Experimental Pharmacology and Drug
Discovery,
a section of the journal
Frontiers in Pharmacology

Received: 27 September 2017

Accepted: 09 February 2018

Published: 21 February 2018

Citation:

Takai S and Jin D (2018) Chymase
Inhibitor as a Novel Therapeutic Agent
for Non-alcoholic Steatohepatitis.
Front. Pharmacol. 9:144.
doi: 10.3389/fphar.2018.00144

Non-alcoholic steatohepatitis (NASH) is characterized by inflammation and fibrosis, in addition to steatosis, of the liver, but no therapeutic agents have yet been established. The mast cell protease chymase can generate angiotensin II, matrix metalloproteinase-9 and transforming growth factor- β , all of which are associated with liver inflammation or fibrosis. In animal models of NASH, augmented chymase has been observed in the liver. In histological analysis, chymase inhibitor prevented hepatic steatosis, inflammation, and fibrosis. Chymase inhibitor also attenuated the augmentation of angiotensin II, matrix metalloproteinase-9, and transforming growth factor- β observed in the liver of NASH. Oxidative stress, inflammatory markers, and collagen were attenuated by chymase inhibition. Moreover, chymase inhibitor showed a mitigating effect on established NASH, and survival rates were significantly increased by treatment with chymase inhibitor. In this review, we propose that chymase inhibitor has potential as a novel therapy for NASH.

Keywords: angiotensin II, chymase, fibrosis, inflammation, inhibitor, matrix metalloproteinase-9, non-alcoholic steatohepatitis, transforming growth factor- β

INTRODUCTION

Non-alcoholic fatty liver disease (NAFLD) has been recognized as the most common form of liver disease (Angulo, 2002; Clark et al., 2002). Non-alcoholic steatohepatitis (NASH) mimics alcoholic hepatitis despite the absence of a history of drinking (Ludwig et al., 1980). NAFLD and NASH are associated with metabolic syndrome resulting from obesity, insulin resistance, hyperlipidemia, and hypertension. NAFLD is considered to be the most common liver disease and typically presents as simple hepatic steatosis (Tiniakos et al., 2010). In contrast, NASH is characterized by severe steatosis, lobular inflammation, and fibrosis of the liver (Powell et al., 1990; Bertot and Adams, 2016). Although the mechanism responsible for the development of NASH remains unclear, NASH is proposed to be caused by a 'multiple-hit' process, with hepatic steatosis as the 'first hit' and subsequent hits such as inflammation, oxidative stress, and endotoxins (Tilg and Moschen, 2010). NASH is closely related to metabolic syndrome, and several clinical studies have investigated the therapeutic treatment of NASH by focusing on the symptoms of diabetes, hyperlipidemia, and hypertension (Georgescu et al., 2009; Park et al., 2010; Mahady et al., 2011). However, no commonly accepted therapeutic agents have been established.

Chymase may be involved in the pathogenesis of hepatic fibrosis. Chymase activity was significantly increased in the livers of patients with fibrosis or cirrhosis and there was a significant correlation between chymase level and degree of fibrosis (Komeda et al., 2008). Although increased chymase activity has not been reported in patients with NASH, it has been observed in animal

models of NASH (Tashiro et al., 2010; Masubuchi et al., 2013; Miyaoka et al., 2017). In contrast, the inhibition of chymase using low molecule inhibitors resulted in a significant reduction of inflammation, steatosis, and fibrosis in rat and hamster NASH models (Tashiro et al., 2010; Masubuchi et al., 2013; Miyaoka et al., 2017). These findings indicate that chymase may be involved in inflammation, steatosis, and fibrosis during the development and progression of NASH (Figure 1).

MULTIPLE FUNCTIONS OF CHYMASE

Chymase in Mast Cells

Chymase (EC 3.4.21.39) is expressed in the secretory granules of mast cells. Chymase is produced as an inactive prochymase within secretory granules, and requires dipeptidyl peptidase I (DPPI) for activation. DPPI is a thiol proteinase and its optimum pH is 6.0. The optimal pH value is consistent with the proposed function of DPPI to activate prochymase, since the pH within secretory granules is regulated at pH 5.5 (De Young et al., 1987) (Figure 2). However, chymase has no enzymatic activity within mast cells at this pH, because the optimal pH for chymase is between 7 and 9 (Takai et al., 1996, 1997). Following activation of mast cell granules by stimuli such as inflammation and injury, chymase is released and exhibits enzymatic function at its optimal pH 7.4 (Figure 2).

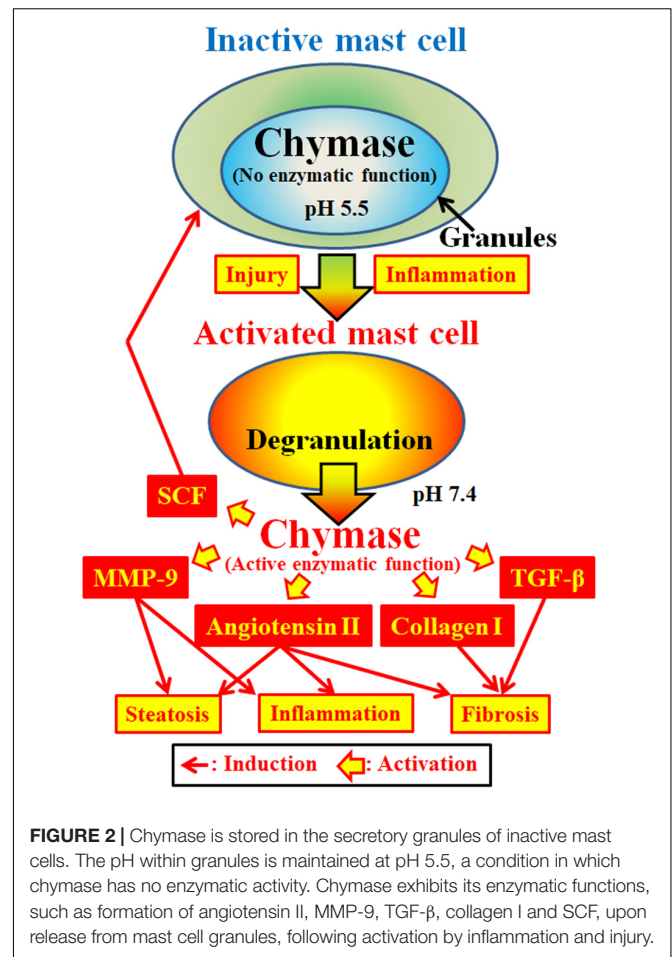


FIGURE 2 | Chymase is stored in the secretory granules of inactive mast cells. The pH within granules is maintained at pH 5.5, a condition in which chymase has no enzymatic activity. Chymase exhibits its enzymatic functions, such as formation of angiotensin II, MMP-9, TGF- β , collagen I and SCF, upon release from mast cell granules, following activation by inflammation and injury.

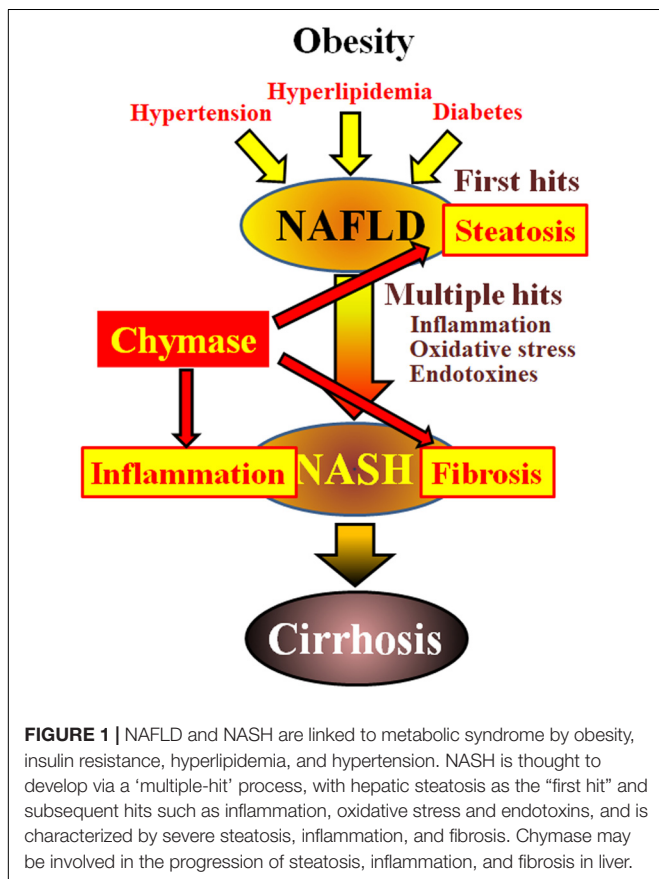


FIGURE 1 | NAFLD and NASH are linked to metabolic syndrome by obesity, insulin resistance, hyperlipidemia, and hypertension. NASH is thought to develop via a ‘multiple-hit’ process, with hepatic steatosis as the “first hit” and subsequent hits such as inflammation, oxidative stress and endotoxins, and is characterized by severe steatosis, inflammation, and fibrosis. Chymase may be involved in the progression of steatosis, inflammation, and fibrosis in liver.

Multiple Enzymatic Functions of Chymase

Chymase is a serine protease and cleaves the C-terminal side of proteins after aromatic amino acids such as Phe, Tyr, and Trp in general. Chymase can cleave the Phe⁸-His⁹ bond of the non-bioactive peptide angiotensin I and form its bioactive peptide angiotensin II in mammalian tissues including human (Urata et al., 1990; Takai et al., 1996, 1997). In addition, chymase enzymatically cleaves the precursors of matrix metalloproteinase (MMP)-9, transforming growth factor (TGF)- β and collagen I to their active forms (Kofford et al., 1997; Takai et al., 2003; Furubayashi et al., 2008). Furthermore, enzymatic function of chymase can produce stem cell factor (SCF) by enzymatic cleavage of the inactive membrane-bound form of SCF, which induces the formation of mature mast cells from immature mast cells via the stimulation of c-kit receptor (Longley et al., 1997). Thus, chymase has multiple enzymatic functions, including activation of angiotensin II, MMP-9, TGF- β , collagen I, and SCF (Figure 2).

Enzymatic Function of Chymase in NASH

Angiotensin II may promote hepatic steatosis and inflammation by increasing reactive oxygen species (ROS) following

stimulation of angiotensin II receptors in animal NASH models (Hirose et al., 2007; Nabeshima et al., 2009). Angiotensin II also induced hepatic fibrosis via induction of α -smooth muscle actin (SMA) in hepatic stellate cells (HSCs) (Yoshiji et al., 2001). MMP-9 has been reported to induce the infiltration of neutrophils and macrophages via degradation of intercellular matrixes such as vitronectin and fibronectin, resulting in augmentation of inflammation (Medina et al., 2006). In NASH patients, a significant increase of MMP-9 gene expression was observed in the liver compared to normal controls (Ljumovic et al., 2004). Hepatic overexpression of TGF- β in transgenic mice produced severe hepatic fibrosis via augmentation of procollagen I gene expression (Casini et al., 1993). Both TGF- β formation and collagen I accumulation are known to induce hepatic fibrosis. Activation of SCF induces increases in mast cell number, and its enzymatic function may result in an increase of chymase activity in fibrotic tissues (Maruichi et al., 2004). These enzymatic functions of chymase may be involved in steatosis, inflammation and fibrosis, all of which are observed in the livers of NASH patients and animal models (Figure 2).

Involvement of Chymase in NASH Animal Models

The methionine- and choline-deficient (MCD) diet has been widely used to induce a typical NASH model. In hamsters fed the MCD diet, significant increases in total bilirubin, triglyceride, and hyaluronic acid were observed in plasma (Tashiro et al., 2010). Moreover, accumulation of inflammatory cells and increases of lipid deposit area and fibrotic area were observed in the liver. In this MCD diet-induced NASH model, hepatic chymase activity and related factors, such as angiotensin II, MMP-9 and collagen I, were significantly increased (Tashiro et al., 2010; Masubuchi et al., 2013). Recently, a new NASH model was developed in which stroke-prone spontaneously hypertensive 5/Dmcr (SHRSP5/Dmcr) rats were fed a high-fat and -cholesterol (HFC) diet (Kitamori et al., 2012). This model showed symptoms of metabolic syndrome thought to clinically resemble those of NASH patients (Kitamori et al., 2012). In the HFC diet-induced NASH model, hypertension and hyperlipidemia were observed, and severe steatosis, fibrosis, and inflammatory cell accumulation were detected in the liver (Miyaoaka et al., 2017). Further, a significant augmentation of chymase activity was observed along with MMP-9, TGF- β , and collagen I in the liver (Miyaoaka et al., 2017). Thus, there appears to be a close relationship between chymase and NASH pathogenesis in animal models of NASH.

EFFECT OF CHYMASE INHIBITOR IN NASH ANIMAL MODELS

Effect of Chymase Inhibitor in NASH Animal Models

A low molecule chymase inhibitor significantly attenuated chymase activity and decreased angiotensin II, MMP-9 and collagen I levels in the liver in an MCD diet-fed NASH hamster model, when administration of the inhibitor was initiated at the

same time as the MCD diet (Tashiro et al., 2010; Masubuchi et al., 2013). The chymase inhibitor significantly prevented hepatic steatosis, fibrosis, and inflammatory cell accumulation in this NASH model (Tashiro et al., 2010; Masubuchi et al., 2013). Oxidative stress is thought to play a role in the 'multiple-hit' theory of NASH development, and augmentation of the oxidative stress marker malondialdehyde was significantly attenuated in the liver by the chymase inhibitor (Masubuchi et al., 2013). In a hamster MCD diet-induced NASH model, the chymase inhibitor showed an ameliorative effect when administered in established NASH (Masubuchi et al., 2013). The degrees of both steatosis and fibrosis in the liver were reduced compared to before administration of the chymase inhibitor (Masubuchi et al., 2013).

In the liver of a hypertensive rat HFC diet-induced NASH model, a low molecule chymase inhibitor attenuated the levels of chymase as well as MMP-9, TGF- β and collagen I, which are all chymase-associated factors (Miyaoaka et al., 2017). The chymase inhibitor significantly attenuated hepatic steatosis and fibrosis, and reduced myeloperoxidase as a marker of inflammation, particularly of neutrophil infiltration (Miyaoaka et al., 2017). In this HFC diet-induced model, survival of the placebo-treated group was 0% at 14 weeks following the start of the HFC diet, and resulted from severe liver failure (Miyaoaka et al., 2017). However, the chymase inhibitor-treated group, in which the rats were treated with the chymase inhibitor immediately following the start of the HFC diet, showed 100% survival at 14 weeks. Moreover, a 50% survival rate was reported for rats treated with the chymase inhibitor beginning 8 weeks after the start of HFC diet feeding, at which point NASH was established (Miyaoaka et al., 2017).

Therefore, chymase inhibitors could be useful agents for the prevention and improvement of NASH in animal models. On the other hand, angiotensin II also indirectly promotes hepatic inflammation, steatosis, and fibrosis via increases of MMP-9 and TGF- β gene expression. Both MMP-9 and TGF- β are closely involved in the pathogenesis of NASH, but these factors are not necessarily induced only by angiotensin II (Takai et al., 2010). Factors other than angiotensin II stimulation contribute to the increases of MMP-9 and TGF- β gene expression (Takai et al., 2010). In such cases, angiotensin II receptor blocker (ARB) is not able to attenuate MMP-9 and TGF- β actions; however, a chymase inhibitor could have attenuating effects via inhibition of MMP-9 and TGF- β activation, indicating a potential treatment course for the prevention of NASH progression.

Mechanism of Hepatic Inflammation Attenuated by Chymase Inhibitor

Chymase inhibitor was able to reduce inflammation in hamster MCD diet- and rat HFC diet-induced NASH models (Tashiro et al., 2010; Masubuchi et al., 2013; Miyaoaka et al., 2017). Chymase inhibitor treatment significantly attenuated chymase activity in the liver as well as reduced angiotensin II and MMP-9 levels (Tashiro et al., 2010; Masubuchi et al., 2013; Miyaoaka et al., 2017). In HSC, angiotensin II induces ROS generation such as hydrogen peroxide and superoxide through the activation of nicotinamide adenine dinucleotide phosphate

(NADPH) oxidase (De Minicis and Brenner, 2007). Chymase inhibitor resulted in reductions in the gene expression of the NADPH oxidase component Rac-1 and the oxidative stress marker malondialdehyde in addition to a reduction of angiotensin II levels in a hamster MCD-induced NASH model (Masubuchi et al., 2013). Angiotensin II-induced augmentation of ROS promoted MMP-9 gene expression in neutrophils and macrophages (Yaghooti et al., 2011; Kurihara et al., 2012). Therefore, chymase inhibitor directly inhibits the activation of proMMP-9 to MMP-9 and indirectly reduces MMP-9 gene expression via decreased angiotensin II. MMP-9 cleaves extracellular matrix constituents, such as vitronectin and fibronectin, leads to the disintegration of hepatic integrity and induces the infiltration of macrophages and neutrophils (Medina et al., 2006). In a HFC diet-induced NASH model, a significant increase in myeloperoxidase expression in macrophages and neutrophils was observed in the liver, and was reduced by chymase inhibitor (Miyaoaka et al., 2017). Therefore, the mechanism of inflammation attenuated by chymase inhibitor may be dependent on the reduction of angiotensin II and MMP-9 levels in the liver.

Mechanism of Hepatic Steatosis Attenuated by Chymase Inhibitor

Angiotensin II may influence hepatic steatosis via ROS production. In murine HSC, an inhibitor of NADPH oxidase significantly decreased ROS production and an ARB slowed the development of hepatic steatosis via attenuation of ROS production (Hirose et al., 2007; Guimarães et al., 2010). In a MCD diet-induced NASH mouse model, a significant attenuation of steatosis was observed in angiotensin II receptor-deficient mice (Nabeshima et al., 2009). Both *in vivo* and *in vitro* experiments showed that angiotensin II upregulated sterol regulatory element-binding protein (SREBP)-1c and fatty acid synthase (FAS) gene expression, both of which are important factors in the regulation of lipogenesis, following ROS augmentation (Kim et al., 2001; Hongo et al., 2009). In contrast, ARB attenuated hepatic steatosis along with downregulating the gene expression of SREBP-1c and FAS via ROS attenuation in a mouse NASH model (Kato et al., 2012). In a hamster MCD diet-induced NASH model, significant attenuation of SREBP-1c and FAS gene expression was observed following treatment with a low molecule chymase inhibitor (Masubuchi et al., 2013). Therefore, the ameliorative mechanism of hepatic steatosis by chymase inhibitor may be dependent on the reduction of ROS production via reduced angiotensin II generation in the liver.

Mechanism of Hepatic Fibrosis Attenuated by Chymase Inhibitor

Chymase may be closely associated with the progression of tissue fibrosis, since it contributes to the formation of TGF- β from the non-bioactive precursor TGF- β , and TGF- β is known to strongly induce the growth of fibroblasts (Takai et al., 2003; Oyamada et al., 2011). TGF- β is known to play a

central role in the progression of fibrosis in NASH patients via activated HSC (Williams et al., 2000). Inhibition of TGF- β function via gene expression and signaling resulted in improved hepatic fibrosis in experimental models (George et al., 1999; Arias et al., 2003). In a rat HFC diet-induced NASH model, attenuation of chymase activity by chymase inhibitor resulted in reductions in TGF- β level and fibrotic area in the liver (Miyaoaka et al., 2017). Thus, the reduction in TGF- β by chymase inhibitor may contribute to the prevention of hepatic fibrosis.

Angiotensin II may also be involved in the induction of hepatic fibrosis. Angiotensin II induces contraction and proliferation of HSC, and also induces the gene expression of TGF- β in fibroblasts *in vitro* (Kagami et al., 1994; Bataller et al., 2000). Both TGF- β levels and the degree of collagen accumulation and fibrotic lesions were observed by bile duct ligation in wild-type mice, however, these were attenuated in angiotensin II receptor-deficient mice (Yang et al., 2005). In a rat NASH model, ARB also attenuated hepatic fibrosis via the reduction of TGF- β gene expression (Hirose et al., 2007). There may also be a relationship between angiotensin II and hepatic fibrosis other than angiotensin II-induced TGF- β gene expression. In patients with chronic hepatitis C, ARB reduced collagen gene expression via Rac-1 gene expression (Colmenero et al., 2009). HSC are recognized as the main producing cells of collagen in the liver, and augmentation in the expression of α -smooth muscle actin (SMA) in HSC strongly induces extracellular matrix deposition, including collagen I (De Minicis and Brenner, 2007). Angiotensin II can induce α -SMA gene expression in rat HSC. In contrast, angiotensin II blockade results in the attenuation of hepatic fibrosis along with reduction of α -SMA (Yoshiji et al., 2001). Although not evaluated in patients with NASH, both chymase and angiotensin II-forming activities were significantly augmented in fibrotic regions of livers from patients with cirrhosis, and significant correlations among chymase, angiotensin II-forming activity and hepatic fibrosis were observed (Komeda et al., 2008). In a hamster tetrachloride-induced hepatic cirrhosis model, significant increases in chymase and angiotensin II-forming activity were observed, which were significantly attenuated along with hepatic cirrhosis following treatment with a low molecule chymase inhibitor (Komeda et al., 2010).

The mast cell stabilizer tranilast could inhibit the activation of mast cells, blocking the release of chymase and thereby preventing the development of hepatic fibrosis in a rat diabetes and HFC diet-induced NASH model (Uno et al., 2008). Chymase promotes the proliferation of mast cells via SCF activation by its enzymatic function (Longley et al., 1997). In NASH animal models, chymase inhibitor reduced the increase in mast cell number in the liver, resulting in reduced chymase activity following direct inhibition by chymase inhibitor and an indirect reduction of chymase expression in mast cells (Masubuchi et al., 2013; Miyaoaka et al., 2017).

Therefore, chymase inhibitor may contribute to the prevention of hepatic fibrosis via inhibition of TGF- β activation by chymase inhibition and/or attenuation of TGF- β level via reduction of angiotensin II and mast cell proliferation.

CONCLUSION

Metabolic syndrome comprising obesity, insulin resistance, hyperlipidemia, and hypertension is closely related to the development of NASH, and trials of anti-diabetic, anti-hyperlipidemic, and anti-hypertensive agents have been conducted for the treatment of NASH. The concept behind these agents is to attenuate the symptoms of metabolic syndrome (Georgescu et al., 2009; Park et al., 2010; Mahady et al., 2011). Previous reports have demonstrated that chymase inhibitor attenuates inflammation and fibrosis without influencing blood glucose and lipid levels and blood pressure in animal models of

diabetes, hyperlipidemia, and hypertension, respectively (Inoue et al., 2009; Takai et al., 2014; Zhang et al., 2016). Therefore, the concept behind chymase inhibition is to attenuate hepatic inflammation and fibrosis of NASH directly. We propose that chymase inhibitor targeting metabolic syndrome is a potentially powerful strategy for the attenuation of NASH progression.

AUTHOR CONTRIBUTIONS

ST and DJ: wrote the manuscript. Both authors read and approved the final manuscript.

REFERENCES

- Angulo, P. (2002). Nonalcoholic fatty liver disease. *N. Engl. J. Med.* 346, 1221–1231. doi: 10.1056/NEJMra011775
- Arias, M., Sauer-Lehnen, S., Treptau, J., Janoschek, N., Theuerkauf, I., Buettner, R., et al. (2003). Adenoviral expression of a transforming growth factor-beta1 antisense mRNA is effective in preventing liver fibrosis in bile-duct ligated rats. *BMC Gastroenterol.* 3:29. doi: 10.1186/1471-230X-3-29
- Bataller, R., Ginès, P., Nicolás, J. M., Görbig, M. N., Garcia-Ramallo, E., Gasull, X., et al. (2000). Angiotensin II induces contraction and proliferation of human hepatic stellate cells. *Gastroenterology* 118, 1149–1156. doi: 10.1016/S0016-5085(00)70368-4
- Bertot, L. C., and Adams, L. A. (2016). The natural course of non-alcoholic fatty liver disease. *Int. J. Mol. Sci.* 17:774. doi: 10.3390/ijms17050774
- Casini, A., Pinzani, M., Milani, S., Grappone, C., Galli, G., Jezequel, A. M., et al. (1993). Regulation of extracellular matrix synthesis by transforming growth factor β 1 in human fat-storing cells. *Gastroenterology* 105, 245–253. doi: 10.1016/0016-5085(93)90033-9
- Clark, J. M., Brancati, F. L., and Diehl, A. M. (2002). Nonalcoholic fatty liver disease. *Gastroenterology* 122, 1649–1657. doi: 10.1053/gast.2002.33573
- Colmenero, J., Bataller, R., Sancho-Bru, P., Dominguez, M., Moreno, M., Forns, X., et al. (2009). Effects of losartan on hepatic expression of nonphagocytic NADPH oxidase and fibrogenic genes in patients with chronic hepatitis C. *Am. J. Physiol. Gastrointest. Liver Physiol.* 297, G726–G734. doi: 10.1152/ajpgi.00162.2009
- De Minicis, S., and Brenner, D. A. (2007). NOX in liver fibrosis. *Arch. Biochem. Biophys.* 462, 266–272. doi: 10.1016/j.abb.2007.04.016
- De Young, M. B., Nemeth, E. F., and Scarpa, A. (1987). Measurement of the internal pH of mast cell granules using microvolumetric fluorescence and isotopic techniques. *Arch. Biochem. Biophys.* 254, 222–233. doi: 10.1016/0003-9861(87)90098-1
- Furubayashi, K., Takai, S., Jin, D., Miyazaki, M., Katsumata, T., Inagaki, S., et al. (2008). Chymase activates promatrix metalloproteinase-9 in human abdominal aortic aneurysm. *Clin. Chim. Acta* 388, 214–216. doi: 10.1016/j.cca.2007.10.004
- George, J., Roulot, D., Koteliensky, V. E., and Bissell, D. M. (1999). *In vivo* inhibition of rat stellate cell activation by soluble transforming growth factor beta type II receptor: a potential new therapy for hepatic fibrosis. *Proc. Natl. Acad. Sci. U.S.A.* 96, 12719–12724. doi: 10.1073/pnas.96.22.12719
- Georgescu, E. F., Ionescu, R., Niculescu, M., Mogoanta, L., and Vancica, L. (2009). Angiotensin receptor blockers as therapy for mild-to-moderate hypertension-associated non-alcoholic steatohepatitis. *World J. Gastroenterol.* 15, 942–954. doi: 10.3748/wjg.15.942
- Guimarães, E. L., Empsen, C., Geerts, A., and van Grunsven, L. A. (2010). Advanced glycation end products induce production of reactive oxygen species via the activation of NADPH oxidase in murine hepatic stellate cells. *J. Hepatol.* 52, 389–397. doi: 10.1016/j.jhep.2009.12.007
- Hirose, A., Ono, M., Saibara, T., Nozaki, Y., Masuda, K., Yoshioka, A., et al. (2007). Angiotensin II type 1 receptor blocker inhibits fibrosis in rat nonalcoholic steatohepatitis. *Hepatology* 45, 1375–1381. doi: 10.1002/hep.21638
- Hongo, M., Ishizaka, N., Furuta, K., Yahagi, N., Saito, K., Sakurai, R., et al. (2009). Administration of angiotensin II, but not catecholamines, induces accumulation of lipids in the rat heart. *Eur. J. Pharmacol.* 604, 87–92. doi: 10.1016/j.ejphar.2008.12.006
- Inoue, N., Muramatsu, M., Jin, D., Takai, S., Hayashi, T., Katayama, H., et al. (2009). Effects of chymase inhibitor on angiotensin II-induced abdominal aortic aneurysm development in apolipoprotein E-deficient mice. *Atherosclerosis* 204, 359–364. doi: 10.1016/j.atherosclerosis.2008.09.032
- Kagami, S., Border, W. A., Miller, D. E., and Noble, N. A. (1994). Angiotensin II stimulates extracellular matrix protein synthesis through induction of transforming growth factor- β expression in rat glomerular mesangial cells. *J. Clin. Invest.* 93, 2431–2437. doi: 10.1172/JCI117251
- Kato, J., Koda, M., Kishina, M., Tokunaga, S., Matono, T., Sugihara, T., et al. (2012). Therapeutic effects of angiotensin II type 1 receptor blocker, irbesartan, on nonalcoholic steatohepatitis using FLS-ob/ob male mice. *Int. J. Mol. Med.* 30, 107–113. doi: 10.3892/ijmm.2012.958
- Kim, S., Dugail, I., Standridge, M., Claycombe, K., Chun, J., and Moustaid-Moussa, N. (2001). Angiotensin II-responsive element is the insulin-responsive element in the adipocyte fatty acid synthase gene: role of adipocyte determination and differentiation factor 1/sterol-regulatory-element-binding protein 1c. *Biochem. J.* 357(Pt 3), 899–904. doi: 10.1042/bj3570899
- Kitamori, K., Naito, H., Tamada, H., Kobayashi, M., Miyazawa, D., Yasui, Y., et al. (2012). Development of novel rat model for high-fat and high-cholesterol diet-induced steatohepatitis and severe fibrosis progression in SHRSP5/Dmcr. *Environ. Health Prev. Med.* 17, 173–182. doi: 10.1007/s12199-011-0235-9
- Kofford, M. W., Schwartz, L. B., Schechter, N. M., Yager, D. R., Diegelmann, R. F., and Graham, M. F. (1997). Cleavage of type I procollagen by human mast cell chymase initiates collagen fibril formation and generates a unique carboxyl-terminal propeptide. *J. Biol. Chem.* 272, 7127–7131. doi: 10.1074/jbc.272.11.7127
- Komeda, K., Jin, D., Takai, S., Hayashi, M., Takeshita, A., Shibayama, Y., et al. (2008). Significance of chymase-dependent angiotensin II formation in the progression of human liver fibrosis. *Hepatol. Res.* 38, 501–510. doi: 10.1111/j.1872-034X.2007.00271.x
- Komeda, K., Takai, S., Jin, D., Tashiro, K., Hayashi, M., Tanigawa, N., et al. (2010). Chymase inhibition attenuates tetrachloride-induced liver fibrosis in hamsters. *Hepatol. Res.* 40, 832–840. doi: 10.1111/j.1872-034X.2010.00672.x
- Kurihara, T., Shimizu-Hirota, R., Shimoda, M., Adachi, T., Shimizu, H., Weiss, S. J., et al. (2012). Neutrophil-derived matrix metalloproteinase 9 triggers acute aortic dissection. *Circulation* 126, 3070–3080. doi: 10.1161/CIRCULATIONAHA.112.097097
- Ljumovic, D., Diamantis, I., Alegakis, A. K., and Kouroumalis, E. A. (2004). Differential expression of matrix metalloproteinases in viral and non-viral chronic liver diseases. *Clin. Chim. Acta* 349, 203–211. doi: 10.1016/j.cccn.2004.06.028
- Longley, B. J., Tyrrell, L., Ma, Y., Williams, D. A., Halaban, R., Langley, K., et al. (1997). Chymase cleavage of stem cell factor yields a bioactive, soluble product. *Proc. Natl. Acad. Sci. U.S.A.* 94, 9017–9021. doi: 10.1073/pnas.94.17.9017
- Ludwig, J., Viggiano, T. R., McGill, D. B., and Oh, B. J. (1980). Nonalcoholic steatohepatitis: mayo clinic experiences with a hitherto unnamed disease. *Mayo Clin. Proc.* 55, 434–438.
- Mahady, S. E., Webster, A. C., Walker, S., Sanyal, A., and George, J. (2011). The role of thiazolidinediones in non-alcoholic steatohepatitis: a systematic review and meta analysis. *J. Hepatol.* 55, 1383–1390. doi: 10.1016/j.jhep.2011.03.016
- Maruichi, M., Takai, S., Sugiyama, T., Ueki, M., Oku, H., Sakaguchi, M., et al. (2004). Role of chymase on growth of cultured canine Tenon's capsule

- fibroblasts and scarring in a canine conjunctival flap model. *Exp. Eye Res.* 79, 111–118. doi: 10.1016/j.exer.2004.02.009
- Masubuchi, S., Takai, S., Jin, D., Tashiro, K., Komeda, K., Li, Z. L., et al. (2013). Chymase inhibitor ameliorates hepatic steatosis and fibrosis on established non-alcoholic steatohepatitis in hamsters fed a methionine- and choline-deficient diet. *Hepatol. Res.* 43, 970–998. doi: 10.1111/hepr.12042
- Medina, C., Santana, A., Paz, M. C., Diaz-Gonzalez, F., Farre, E., Salas, A., et al. (2006). Matrix metalloproteinase-9 modulates intestinal injury in rats with transmural colitis. *J. Leukoc. Biol.* 79, 954–962. doi: 10.1189/jlb.1005544
- Miyaoka, Y., Jin, D., Tashiro, K., Komeda, K., Masubuchi, S., Hirokawa, F., et al. (2017). Chymase inhibitor prevents the development and progression of non-alcoholic steatohepatitis in rats fed a high-fat and high-cholesterol diet. *J. Pharmacol. Sci.* 134, 139–146. doi: 10.1016/j.jpsh.2017.04.005
- Nabeshima, Y., Tazuma, S., Kanno, K., Hyogo, H., and Chayama, K. (2009). Deletion of angiotensin II type I receptor reduces hepatic steatosis. *J. Hepatol.* 50, 1226–1235. doi: 10.1016/j.jhep.2009.01.018
- Oyamada, S., Bianchi, C., Takai, S., Chu, L. M., and Sellke, F. W. (2011). Chymase inhibition reduces infarction and matrix metalloproteinase-9 activation and attenuates inflammation and fibrosis after acute myocardial ischemia/reperfusion. *J. Pharmacol. Exp. Ther.* 339, 143–151. doi: 10.1124/jpet.111.179697
- Park, H., Hasegawa, G., Shima, T., Fukui, M., Nakamura, N., Yamaguchi, K., et al. (2010). The fatty acid composition of plasma cholesteryl esters and estimated desaturase activities in patients with nonalcoholic fatty liver disease and the effect of long-term ezetimibe therapy on these levels. *Clin. Chim. Acta* 411, 1735–1740. doi: 10.1016/j.cca.2010.07.012
- Powell, E. E., Cooksley, W. G., Hanson, R., Searle, J., Halliday, J. W., and Powell, L. W. (1990). The natural history of nonalcoholic steatohepatitis: a follow-up study of forty-two patients for up to 21 years. *Hepatology* 11, 74–80. doi: 10.1002/hep.1840110114
- Takai, S., Jin, D., Chen, H., Li, W., Yamamoto, H., Yamanishi, K., et al. (2014). Chymase inhibition improves vascular dysfunction and survival in stroke-prone spontaneously hypertensive rats. *J. Hypertens.* 32, 1637–1648. doi: 10.1097/HJH.0000000000000231
- Takai, S., Jin, D., and Miyazaki, M. (2010). New approaches to blockade of the renin-angiotensin-aldosterone system: chymase as an important target to prevent organ damage. *J. Pharmacol. Sci.* 113, 301–309. doi: 10.1254/jphs.10R05FM
- Takai, S., Jin, D., Sakaguchi, M., Katayama, S., Muramatsu, M., Sakaguchi, M., et al. (2003). A novel chymase inhibitor, 4-[1-([bis-(4-methyl-phenyl)-methyl]-carbonyl)3-(2-ethoxy-benzyl)-4-oxo-azetidine-2-yloxy]-benzoic acid (BCEAB), suppressed cardiac fibrosis in cardiomyopathic hamsters. *J. Pharmacol. Exp. Ther.* 305, 17–23. doi: 10.1124/jpet.102.045179
- Takai, S., Shiota, N., Sakaguchi, M., Muraguchi, H., Matsumura, E., and Miyazaki, M. (1997). Characterization of chymase from human vascular tissues. *Clin. Chim. Acta* 265, 13–20. doi: 10.1016/S0009-8981(97)00114-9
- Takai, S., Shiota, N., Yamamoto, D., Okunishi, H., and Miyazaki, M. (1996). Purification and characterization of angiotensin II-generating chymase from hamster cheek pouch. *Life Sci.* 58, 591–597. doi: 10.1016/0024-3205(95)02328-3
- Tashiro, K., Takai, S., Jin, D., Yamamoto, H., Komeda, K., Hayashi, M., et al. (2010). Chymase inhibitor prevents the nonalcoholic steatohepatitis in hamsters fed a methionine- and choline-deficient diet. *Hepatol. Res.* 40, 514–523. doi: 10.1111/j.1872-034X.2010.00627.x
- Tilg, H., and Moschen, A. R. (2010). Evolution of inflammation in nonalcoholic fatty liver disease: the multiple parallel hits hypothesis. *Hepatology* 52, 1836–1846. doi: 10.1002/hep.24001
- Tiniakos, D. G., Vos, M. B., and Brunt, E. M. (2010). Nonalcoholic fatty liver disease: pathology and pathogenesis. *Annu. Rev. Pathol.* 5, 145–171. doi: 10.1146/annurev-pathol-121808-102132
- Uno, M., Kurita, S., Misu, H., Ando, H., Ota, T., Matsuzawa-Nagata, N., et al. (2008). Tranilast, an antifibrogenic agent, ameliorates a dietary rat model of nonalcoholic steatohepatitis. *Hepatology* 48, 109–118. doi: 10.1002/hep.22338
- Urata, H., Kinoshita, A., Misono, K. S., Bumpus, F. M., and Husain, A. (1990). Identification of a highly specific chymase as the major angiotensin II-forming enzyme in the human heart. *J. Biol. Chem.* 265, 22348–22357.
- Williams, E. J., Gaça, M. D., Brigstock, D. R., Arthur, M. J., and Benyon, R. C. (2000). Increased expression of connective tissue growth factor in fibrotic human liver and in activated hepatic stellate cells. *J. Hepatol.* 32, 754–761. doi: 10.1016/S0168-8278(00)80244-5
- Yaghoobi, H., Firoozrai, M., Fallah, S., and Khorramizadeh, M. R. (2011). Angiotensin II induces NF- κ B, JNK and p38 MAPK activation in monocytic cells and increases matrix metalloproteinase-9 expression in a PKC- and Rho kinase-dependent manner. *Braz. J. Med. Biol. Res.* 44, 193–199. doi: 10.1590/S0100-879X2011007500008
- Yang, L., Bataller, R., Dulyx, J., Coffman, T. M., Ginès, P., Rippe, R. A., et al. (2005). Attenuated hepatic inflammation and fibrosis in angiotensin type 1a receptor deficient mice. *J. Hepatol.* 43, 317–323. doi: 10.1016/j.jhep.2005.02.034
- Yoshiji, H., Kuriyama, S., Yoshii, J., Ikenaka, Y., Noguchi, R., Nakatani, T., et al. (2001). Angiotensin-II type 1 receptor interaction is a major regulator for liver fibrosis development in rats. *Hepatology* 34, 745–750. doi: 10.1053/jhep.2001.28231
- Zhang, M., Huang, W., Bai, J., Nie, X., and Wang, W. (2016). Chymase inhibition protects diabetic rats from renal lesions. *Mol. Med. Rep.* 14, 121–128. doi: 10.3892/mmr.2016.5234

Conflict of Interest Statement: The authors declare that the research was conducted in the absence of any commercial or financial relationships that could be construed as a potential conflict of interest.

Copyright © 2018 Takai and Jin. This is an open-access article distributed under the terms of the Creative Commons Attribution License (CC BY). The use, distribution or reproduction in other forums is permitted, provided the original author(s) and the copyright owner are credited and that the original publication in this journal is cited, in accordance with accepted academic practice. No use, distribution or reproduction is permitted which does not comply with these terms.



Drug Repositioning of Proton Pump Inhibitors for Enhanced Efficacy and Safety of Cancer Chemotherapy

Kenji Ikemura^{1,2}, Shunichi Hiramatsu² and Masahiro Okuda^{1,2*}

¹ Department of Pharmacy, Mie University Hospital, Tsu, Japan, ² Department of Clinical Pharmacy and Biopharmaceutics, Mie University Graduate School of Medicine, Tsu, Japan

OPEN ACCESS

Edited by:

Hideaki Hara,
Gifu Pharmaceutical University, Japan

Reviewed by:

Tomohiro Mizuno,
Meijo University, Japan
Ge-Hong Sun-Wada,
Doshisha Women's College of Liberal
Arts, Japan

*Correspondence:

Masahiro Okuda
okudam@clin.medic.mie-u.ac.jp

Specialty section:

This article was submitted to
Experimental Pharmacology and Drug
Discovery,
a section of the journal
Frontiers in Pharmacology

Received: 27 October 2017

Accepted: 29 November 2017

Published: 12 December 2017

Citation:

Ikemura K, Hiramatsu S and
Okuda M (2017) Drug Repositioning
of Proton Pump Inhibitors
for Enhanced Efficacy and Safety
of Cancer Chemotherapy.
Front. Pharmacol. 8:911.
doi: 10.3389/fphar.2017.00911

Proton pump inhibitors (PPIs), H⁺/K⁺-ATPase inhibitors, are the most commonly prescribed drugs for the treatment of gastroesophageal reflux and peptic ulcer diseases; they are highly safe and tolerable. Since PPIs are frequently used in cancer patients, studies investigating interactions between PPIs and anticancer agents are of particular importance to achieving effective and safe cancer chemotherapy. Several studies have revealed that PPIs inhibit not only the H⁺/K⁺-ATPase in gastric parietal cells, but also the vacuolar H⁺-ATPase (V-ATPase) overexpressed in tumor cells, as well as the renal basolateral organic cation transporter 2 (OCT2) associated with pharmacokinetics and/or renal accumulation of various drugs, including anticancer agents. In this mini-review, we summarize the current knowledge regarding the impact of PPIs on the efficacy and safety of cancer chemotherapeutics via inhibition of targets other than the H⁺/K⁺-ATPase. Co-administration of clinical doses of PPIs protected kidney function in patients receiving cisplatin and fluorouracil, presumably by decreasing accumulation of cisplatin in the kidney via OCT2 inhibition. In addition, co-administration or pretreatment with PPIs could inhibit H⁺ transport via the V-ATPase in tumor cells, resulting in lower extracellular acidification and intracellular acidic vesicles to enhance the sensitivity of the tumor cells to the anticancer agents. In the present mini-review, we suggest that PPIs enhance the efficacy and safety of anticancer agents via off-target inhibition (e.g., of OCT2 and V-ATPase), rather than on-target inhibition of the H⁺/K⁺-ATPase. The present findings should provide important information to establish novel supportive therapy with PPIs during cancer chemotherapy.

Keywords: proton pump inhibitor, drug repositioning, drug interaction, organic cation transporter 2, vacuolar H⁺-ATPase

INTRODUCTION

Proton pump inhibitors (PPIs) inhibit gastric acid secretion by interaction with the H⁺/K⁺-ATPase in gastric parietal cells. Because PPIs have high safety and tolerability, they are the most commonly prescribed drugs for the treatment of gastroesophageal reflux disease and peptic ulcer disease (Zimmermann and Katona, 1997; Sachs et al., 2006; Shin and Kim, 2013). Interestingly, it has been estimated that approximately 20% of cancer patients are treated with PPIs to alleviate the symptoms of gastroesophageal reflux (Smelick et al., 2013). In clinical studies, many investigators have reported that co-administration of PPIs affect the development of side effect and the efficacy

of anticancer agents (Suzuki et al., 2009; Santucci et al., 2010; Reeves et al., 2014; Ikemura et al., 2016, 2017). Therefore, the effect of PPIs on the efficacy and safety of anticancer agents needs to be investigated thoroughly.

Drug repositioning, the process of finding novel indications of previously approved drugs, is of growing interest to academia and industry because it reduces the time and costs associated with drug development (Ashburn and Thor, 2004). Several reports revealed that PPIs inhibited not only the H^+/K^+ -ATPase in gastric parietal cells, but also the vacuolar H^+ -ATPase (V-ATPase) overexpressed in tumor cells (Luciani et al., 2004; De Milito and Fais, 2005; Lee et al., 2015). In addition, very recent evidence has indicated that PPIs are potent inhibitors of renal drug transporters, including human organic anion transporters (hOATs) and human organic cation transporters (hOCTs) that are associated with pharmacokinetics and/or renal accumulation of various drugs, including anticancer agents (Nies et al., 2011; Chioukh et al., 2014; Hacker et al., 2015; Ikemura et al., 2016). Therefore, co-administration of PPIs could represent novel supportive therapies during cancer chemotherapy to improve the efficacy and safety of anticancer agents via inhibition of targets other than the H^+/K^+ -ATPase.

In this mini-review, we summarize the current knowledge regarding the impact of PPIs on the efficacy and safety of cancer chemotherapeutic drugs.

PROTECTIVE EFFECT OF PPIs ON CISPLATIN-INDUCED NEPHROTOXICITY BY INHIBITION OF OCT2

In the renal proximal tubules, membrane transport proteins expressed in the apical or basolateral membranes are responsible for the urinary secretion of diverse drugs. The structures and functions of hOATs and hOCTs encoded by *SLC22A* genes have been characterized (Sweet and Pritchard, 1999; Inui et al., 2000; Sekine et al., 2000). OAT1 (*SLC22A6*) and OAT3 (*SLC22A8*) expressed in the basolateral membrane of the proximal tubules, transport various organic anions using opposite α -ketoglutarate as a driving force (Sweet and Pritchard, 1999). In contrast, OCT1 (*SLC22A1*) and OCT2 (*SLC22A2*) were reported to be driven by inside-negative membrane potentials (Busch et al., 1996; Okuda et al., 1996), mediating basolateral uptake of diverse organic cations. Moreover, at the brush-border membranes, multidrug and toxin extrusion 1 (MATE1/*SLC47A1*) mediates the extrusion of organic cations from the cells into the tubular lumen using the transmembrane H^+ gradient as a driving force (Yonezawa and Inui, 2011a), and is considered to be responsible for the final step of urinary excretion of cationic drugs.

Cisplatin (CDDP) is a chemotherapeutic drug widely used for the treatment of various solid tumors, including lung, ovarian, and esophageal cancers (Go and Adjei, 1999). The major side effects of CDDP include nephrotoxicity, ototoxicity, myelosuppression, and peripheral neuropathy (Arany and Safirstein, 2003). Because CDDP-induced nephrotoxicity is a dose-limiting side effect that restricts its clinical application

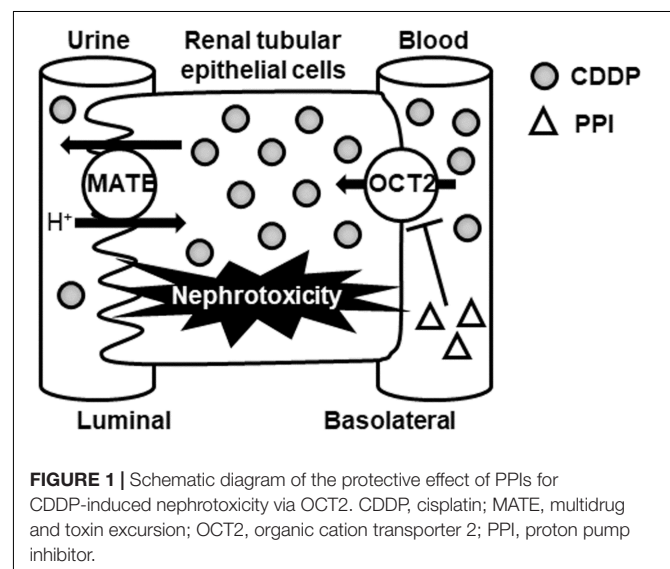
(Pabla and Dong, 2008), the development of renal protective strategies for CDDP chemotherapy is an urgent matter that requires a solution.

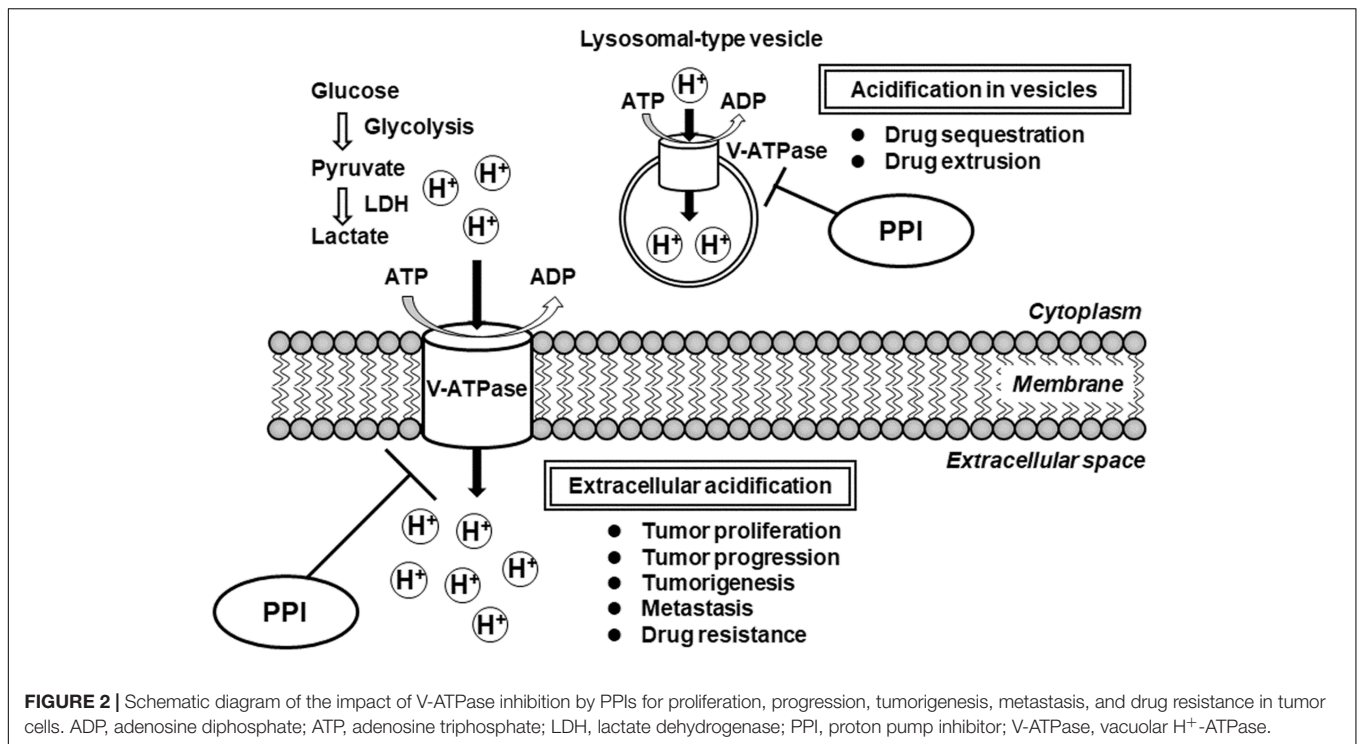
Cisplatin is known to accumulate specifically in the kidney compared to its accumulation in other organs or in plasma (Litterst et al., 1976). As shown in **Figure 1**, OCT2 is predominantly responsible for the accumulation of CDDP in the kidney (Yonezawa and Inui, 2011b). Therefore, CDDP-induced nephrotoxicity is expected to be ameliorated by reduction or inhibition of OCT2 activity in the kidney.

Hacker et al. (2015) demonstrated that PPIs (lansoprazole and pantoprazole) inhibited OCT2-mediated transport of metformin (a typical substrate of OCT2) at a clinical dose. In addition, these PPIs were tested for clinical drug interactions with metformin in patients and healthy subjects (Ding et al., 2014; Kim et al., 2014). Therefore, co-administration of PPI may inhibit the renal accumulation of CDDP via OCT2 (**Figure 1**).

Recently, we retrospectively investigated the effect of co-administration of PPI on nephrotoxicity in 133 patients who received CDDP and fluorouracil (5-FU) therapy for the treatment of esophageal or head and neck cancer (Ikemura et al., 2017). The rate of nephrotoxicity in patients receiving PPI (12%, $n = 33$) was significantly lower than that in patients not receiving PPI (30%, $n = 100$). Severe nephrotoxicity was not observed in patients receiving PPI, whereas the rate of hematological toxicity was comparable between patients with and without PPI treatment. These findings indicate that co-administration of clinical doses of PPI ameliorates nephrotoxicity without exacerbation of hematological toxicity in patients receiving CDDP and 5-FU therapy. Although it remains unclear whether PPI directly inhibits OCT2-mediated uptake of CDDP in the kidney, co-administration of PPI during CDDP chemotherapy should be a novel approach to minimize the nephrotoxicity of CDDP using OCT2 drug interactions.

On the other hand, MATE1 is also responsible for CDDP-induced nephrotoxicity (Nakamura et al., 2010; Oda et al.,





2014) as shown in **Figure 1**. Many OCT2 inhibitors also inhibit MATE1, which may increase intracellular CDDP accumulation and nephrotoxicity. Because there have been no reports regarding the effect of PPI on MATE1 activity, further study is needed to clarify the effect of PPI against MATE1-mediated transport of CDDP.

PPIs ENHANCE THE ANTITUMOR EFFECTS AND SENSITIVITIES OF ANTICANCER AGENTS BY TARGETING V-ATPase IN TUMOR CELLS

As shown in **Figure 2**, the V-ATPase is an ATP-dependent proton pump that transports H⁺ across both intracellular and plasma membranes to regulate intracellular and extracellular pH (Forgac, 2007). In tumor cells, increased glucose consumption via glycolysis leads to the production of lactic acid and H⁺ ions (Warburg, 1956). Because this cytoplasmic acidification is detrimental to the cells, overexpression of V-ATPase maintains an appropriate neutral cytoplasmic pH in the tumor cells, and consequently causes extracellular acidification (Nelson and Harvey, 1999). Lee et al. (2015) found that elevated expression of V-ATPase mRNA was significantly associated with poor survival in ovarian cancer patients. Extracellular acidification in tumor cells is known to be involved in proliferation, tumorigenesis, drug resistance, metastasis, and tumor progression (Fais et al., 2007). Inhibition of V-ATPase causes loss of the pH gradient across the plasma membranes, increasing the extracellular pH and decrease the intracellular

pH, leading to slowed growth and increased cell death (De Milito et al., 2010). Furthermore, some human tumor cells exhibit elevated V-ATPase activity in intracellular lysosomal-type vesicles, leading to drug sequestration in intracellular acidic vesicles and drug extrusion from the cells through the secretory pathway (Altan et al., 1998; Raghunand et al., 1999). The acidification in intracellular vesicles is also involved in resistance to cancer chemotherapeutic drugs. Therefore, V-ATPase should be considered a promising target in the development of anticancer therapeutics.

Various prior studies have reported inhibitory effects of V-ATPase against cancer growth and metastasis in *in vivo* animal models. In mice implanted with human hepatocellular carcinoma cells, the knockdown of V-ATPase by siRNA markedly decreased primary tumor growth and suppressed intrahepatic and pulmonary metastases (Lu et al., 2005). Furthermore, the knockdown of V-ATPase by lentivirus-mediated shRNA in a 4T1 mouse model of metastatic breast cancer reduced tumor formation and decreased metastasis to the lung, liver, and bone, and consequently improved survival (Feng et al., 2013).

Interestingly, inhibition of V-ATPase could also lead to the activation of protective cellular responses (Stransky et al., 2016). Graham et al. (2014) demonstrated that bafilomycin A1, a selective V-ATPase inhibitor, upregulated mitogen-activated protein (MAP) kinases and significantly reduced tumor growth in MCF7 and MDA-MB-231 mouse xenografts. In addition, the inhibitory effect of combination treatment of bafilomycin A1 and sorafenib [an extracellular signal-regulated kinase 1/2 (ERK1/2) inhibitor] for breast tumor growth and metastasis in mice was higher than that of single administration

of bafilomycin A1 or sorafenib. Thus, these findings suggest that the co-treatment of V-ATPase inhibitor with anticancer agents has synergistic antitumor effects.

Although PPIs are clinically used as H⁺/K⁺-ATPase inhibitors for the treatment of gastroesophageal reflux and peptic ulcer diseases, several *in vitro* and *in vivo* studies have addressed that PPIs also inhibit V-ATPase. Luciani et al. (2004) demonstrated that pretreatment with PPIs (omeprazole and esomeprazole) enhanced the effects of various anticancer agents (CDDP, 5-FU, and vinblastine) via inhibition of V-ATPase in cell lines derived from human melanoma, adenocarcinoma, and lymphoma. Moreover, an *in vivo* study demonstrated that oral pretreatment with omeprazole enhanced sensitivity against CDDP in mice engrafted with melanoma cells (Luciani et al., 2004). Furthermore, *in vivo* experiments were performed to confirm the synergistic effects of omeprazole and paclitaxel on tumors in orthotopic and patient-derived xenograft mouse models (Luciani et al., 2004). Interestingly, they demonstrated that PPI treatment in tumor cells increased both the extracellular pH and pH of intracellular vesicles, consistent with the inhibition of V-ATPase activity. Their evidences indicated that pretreatment with PPIs enhanced the antitumor effect through the inhibition of acidification in extracellular environment and/or in intracellular vesicles. Therefore, these findings suggest that co-administration or pretreatment with PPIs enhances the antitumor effect and sensitivity of anticancer agents by targeting V-ATPase in tumor cells.

REFERENCES

- Altan, N., Chen, Y., Schindler, M., and Simon, S. M. (1998). Defective acidification in human breast tumor cells and implications for chemotherapy. *J. Exp. Med.* 187, 1583–1598. doi: 10.1084/jem.187.10.1583
- Arany, I., and Safirstein, R. L. (2003). Cisplatin nephrotoxicity. *Semin. Nephrol.* 23, 460–464. doi: 10.1016/S0270-9295(03)00089-5
- Ashburn, T. T., and Thor, K. B. (2004). Drug repositioning: identifying and developing new uses for existing drugs. *Nat. Rev. Drug Discov.* 3, 673–683. doi: 10.1038/nrd1468
- Busch, A. E., Quester, S., Ulzheimer, J. C., Waldegger, S., Gorboulev, V., Arndt, P., et al. (1996). Electrogenic properties and substrate specificity of the polyspecific rat cation transporter rOCT1. *J. Biol. Chem.* 271, 32599–32604. doi: 10.1074/jbc.271.51.32599
- Chioukh, R., Noel-Hudson, M. S., Ribes, S., Fournier, N., Becquemont, L., and Verstuyft, C. (2014). Proton pump inhibitors inhibit methotrexate transport by renal basolateral organic anion transporter hOAT3. *Drug Metab. Dispos.* 42, 2041–2048. doi: 10.1124/dmd.114.058529
- De Milito, A., Canese, R., Marino, M. L., Borghi, M., Iero, M., Villa, A., et al. (2010). pH-dependent antitumor activity of proton pump inhibitors against human melanoma is mediated by inhibition of tumor acidity. *Int. J. Cancer* 127, 207–219. doi: 10.1002/ijc.25009
- De Milito, A., and Fais, S. (2005). Proton pump inhibitors may reduce tumour resistance. *Expert Opin. Pharmacother.* 6, 1049–1054. doi: 10.1517/14656566.6.7.1049
- Ding, Y., Jia, Y., Song, Y., Lu, C., Li, Y., Chen, M., et al. (2014). The effect of lansoprazole, an OCT inhibitor, on metformin pharmacokinetics in healthy subjects. *Eur. J. Clin. Pharmacol.* 70, 141–146. doi: 10.1007/s00228-013-1604-7
- Fais, S., De Milito, A., You, H., and Qin, W. (2007). Targeting vacuolar H⁺-ATPases as a new strategy against cancer. *Cancer Res.* 67, 10627–10630. doi: 10.1158/0008-5472.CAN-07-1805
- Feng, S., Zhu, G., McConnell, M., Deng, L., Zhao, Q., Wu, M., et al. (2013). Silencing of atp6v1c1 prevents breast cancer growth and bone metastasis. *Int. J. Biol. Sci.* 9, 853–862. doi: 10.7150/ijbs.6030

CONCLUSION

This mini-review suggests that PPIs enhance the efficacy and safety of cancer chemotherapy via off-target inhibition (i.e., of OCT2 and V-ATPase), rather than on-target inhibition (i.e., of H⁺/K⁺-ATPase). The present findings should provide important information for the establishment of novel supportive therapy during cancer chemotherapy.

AUTHOR CONTRIBUTIONS

KI and MO performed the literature searches. All authors contributed to the writing and final approval of the manuscript.

FUNDING

This work was supported by a Grant-in-Aid for Scientific Research (C) (17K08411 and 17K08412) from the Japan Society for the Promotion of Science.

ACKNOWLEDGMENT

The authors would like to thank Editage (www.editage.jp) for English language editing.

- Forgac, M. (2007). Vacuolar ATPases: rotary proton pumps in physiology and pathophysiology. *Nat. Rev. Mol. Cell Biol.* 8, 917–929. doi: 10.1038/nrm2272
- Go, R. S., and Adjei, A. A. (1999). Review of the comparative pharmacology and clinical activity of cisplatin and carboplatin. *J. Clin. Oncol.* 17, 409–422. doi: 10.1200/jco.1999.17.1.409
- Graham, R. M., Thompson, J. W., and Webster, K. A. (2014). Inhibition of the vacuolar ATPase induces Bnip3-dependent death of cancer cells and a reduction in tumor burden and metastasis. *Oncotarget* 5, 1162–1173. doi: 10.18632/oncotarget.1699
- Hacker, K., Maas, R., Kornhuber, J., Fromm, M. F., and Zolk, O. (2015). Substrate-dependent inhibition of the human organic cation transporter OCT2: a comparison of metformin with experimental substrates. *PLOS ONE* 10:e0136451. doi: 10.1371/journal.pone.0136451
- Ikemura, K., Hamada, Y., Kaya, C., Enokiya, T., Muraki, Y., Nakahara, H., et al. (2016). Lansoprazole exacerbates pemetrexed-mediated hematologic toxicity by competitive inhibition of renal basolateral human organic anion transporter 3. *Drug Metab. Dispos.* 44, 1543–1549. doi: 10.1124/dmd.116.070722
- Ikemura, K., Oshima, K., Enokiya, T., Okamoto, A., Oda, H., Mizuno, T., et al. (2017). Co-administration of proton pump inhibitors ameliorates nephrotoxicity in patients receiving chemotherapy with cisplatin and fluorouracil: a retrospective cohort study. *Cancer Chemother. Pharmacol.* 79, 943–949. doi: 10.1007/s00280-017-3296-7
- Inui, K. I., Masuda, S., and Saito, H. (2000). Cellular and molecular aspects of drug transport in the kidney. *Kidney Int.* 58, 944–958. doi: 10.1046/j.1523-1755.2000.00251.x
- Kim, A., Chung, I., Yoon, S. H., Yu, K. S., Lim, K. S., Cho, J. Y., et al. (2014). Effects of proton pump inhibitors on metformin pharmacokinetics and pharmacodynamics. *Drug Metab. Dispos.* 42, 1174–1179. doi: 10.1124/dmd.113.055616
- Lee, Y. Y., Jeon, H. K., Hong, J. E., Cho, Y. J., Ryu, J. Y., Choi, J. J., et al. (2015). Proton pump inhibitors enhance the effects of cytotoxic agents in chemoresistant epithelial ovarian carcinoma. *Oncotarget* 6, 35040–35050. doi: 10.18632/oncotarget.5319

- Litterst, C. L., Gram, T. E., Dedrick, R. L., Leroy, A. F., and Guarino, A. M. (1976). Distribution and disposition of platinum following intravenous administration of cis-diamminedichloroplatinum(II) (NSC 119875) to dogs. *Cancer Res.* 36, 2340–2344.
- Lu, X., Qin, W., Li, J., Tan, N., Pan, D., Zhang, H., et al. (2005). The growth and metastasis of human hepatocellular carcinoma xenografts are inhibited by small interfering RNA targeting to the subunit ATP6L of proton pump. *Cancer Res.* 65, 6843–6849. doi: 10.1158/0008-5472.CAN-04-3822
- Luciani, F., Spada, M., De Milito, A., Molinari, A., Rivoltini, L., Montinaro, A., et al. (2004). Effect of proton pump inhibitor pretreatment on resistance of solid tumors to cytotoxic drugs. *J. Natl. Cancer Inst.* 96, 1702–1713. doi: 10.1093/jnci/djh305
- Nakamura, T., Yonezawa, A., Hashimoto, S., Katsura, T., and Inui, K. (2010). Disruption of multidrug and toxin extrusion MATE1 potentiates cisplatin-induced nephrotoxicity. *Biochem. Pharmacol.* 80, 1762–1767. doi: 10.1016/j.bcp.2010.08.019
- Nelson, N., and Harvey, W. R. (1999). Vacuolar and plasma membrane proton-adenosinetriphosphatases. *Physiol. Rev.* 79, 361–385.
- Nies, A. T., Hofmann, U., Resch, C., Schaeffeler, E., Rius, M., and Schwab, M. (2011). Proton pump inhibitors inhibit metformin uptake by organic cation transporters (OCTs). *PLOS ONE* 6:e22163. doi: 10.1371/journal.pone.0022163
- Oda, M., Koyanagi, S., Tsurudome, Y., Kanemitsu, T., Matsunaga, N., and Ohdo, S. (2014). Renal circadian clock regulates the dosing-time dependency of cisplatin-induced nephrotoxicity in mice. *Mol. Pharmacol.* 85, 715–722. doi: 10.1124/mol.113.089805
- Okuda, M., Saito, H., Urakami, Y., Takano, M., and Inui, K. (1996). cDNA cloning and functional expression of a novel rat kidney organic cation transporter, OCT2. *Biochem. Biophys. Res. Commun.* 224, 500–507. doi: 10.1006/bbrc.1996.1056
- Pabla, N., and Dong, Z. (2008). Cisplatin nephrotoxicity: mechanisms and renoprotective strategies. *Kidney Int.* 73, 994–1007. doi: 10.1038/sj.ki.5002786
- Raghunand, N., Martinez-Zaguilan, R., Wright, S. H., and Gillies, R. J. (1999). pH and drug resistance. II. turnover of acidic vesicles and resistance to weakly basic chemotherapeutic drugs. *Biochem. Pharmacol.* 57, 1047–1058. doi: 10.1016/S0006-2952(99)00021-0
- Reeves, D. J., Moore, E. S., Bascom, D., and Rensing, B. (2014). Retrospective evaluation of methotrexate elimination when co-administered with proton pump inhibitors. *Br. J. Clin. Pharmacol.* 78, 565–571. doi: 10.1111/bcp.12384
- Sachs, G., Shin, J. M., and Howden, C. W. (2006). Review article: the clinical pharmacology of proton pump inhibitors. *Aliment. Pharmacol. Ther.* 23 (Suppl. 2), 2–8. doi: 10.1111/j.1365-2036.2006.02943.x
- Santucci, R., Leveque, D., Lescoute, A., Kemmel, V., and Herbrecht, R. (2010). Delayed elimination of methotrexate associated with co-administration of proton pump inhibitors. *Anticancer Res.* 30, 3807–3810.
- Sekine, T., Cha, S. H., and Endou, H. (2000). The multispecific organic anion transporter (OAT) family. *Pflugers Arch.* 440, 337–350. doi: 10.1007/s004240000297
- Shin, J. M., and Kim, N. (2013). Pharmacokinetics and pharmacodynamics of the proton pump inhibitors. *J. Neurogastroenterol. Motil.* 19, 25–35. doi: 10.5056/jnm.2013.19.1.25
- Smelick, G. S., Heffron, T. P., Chu, L., Dean, B., West, D. A., Duvall, S. L., et al. (2013). Prevalence of acid-reducing agents (ARA) in cancer populations and ARA drug-drug interaction potential for molecular targeted agents in clinical development. *Mol. Pharm.* 10, 4055–4062. doi: 10.1021/mp400403s
- Stransky, L., Cotter, K., and Forgac, M. (2016). The function of V-ATPases in cancer. *Physiol. Rev.* 96, 1071–1091. doi: 10.1152/physrev.00035.2015
- Suzuki, K., Doki, K., Homma, M., Tamaki, H., Hori, S., Ohtani, H., et al. (2009). Co-administration of proton pump inhibitors delays elimination of plasma methotrexate in high-dose methotrexate therapy. *Br. J. Clin. Pharmacol.* 67, 44–49. doi: 10.1111/j.1365-2125.2008.03303.x
- Sweet, D. H., and Pritchard, J. B. (1999). The molecular biology of renal organic anion and organic cation transporters. *Cell Biochem. Biophys.* 31, 89–118. doi: 10.1007/BF02738157
- Warburg, O. (1956). On the origin of cancer cells. *Science* 123, 309–314. doi: 10.1126/science.123.3191.309
- Yonezawa, A., and Inui, K. (2011a). Importance of the multidrug and toxin extrusion MATE/SLC47A family to pharmacokinetics, pharmacodynamics/toxicodynamics and pharmacogenomics. *Br. J. Pharmacol.* 164, 1817–1825. doi: 10.1111/j.1476-5381.2011.01394.x
- Yonezawa, A., and Inui, K. (2011b). Organic cation transporter OCT/SLC22A and H(+)/organic cation antiporter MATE/SLC47A are key molecules for nephrotoxicity of platinum agents. *Biochem. Pharmacol.* 81, 563–568. doi: 10.1016/j.bcp.2010.11.016
- Zimmermann, A. E., and Katona, B. G. (1997). Lansoprazole: a comprehensive review. *Pharmacotherapy* 17, 308–326. doi: 10.1002/j.1875-9114.1997.tb03714.x

Conflict of Interest Statement: The authors declare that the research was conducted in the absence of any commercial or financial relationships that could be construed as a potential conflict of interest.

Copyright © 2017 Ikemura, Hiramatsu and Okuda. This is an open-access article distributed under the terms of the Creative Commons Attribution License (CC BY). The use, distribution or reproduction in other forums is permitted, provided the original author(s) or licensor are credited and that the original publication in this journal is cited, in accordance with accepted academic practice. No use, distribution or reproduction is permitted which does not comply with these terms.



Simvastatin Therapy for Drug Repositioning to Reduce the Risk of Prostate Cancer Mortality in Patients With Hyperlipidemia

Yu-An Chen^{1†}, Ying-Ju Lin^{2†}, Cheng-Li Lin^{1,3}, Hwai-Jeng Lin^{4,5†}, Hua-Shan Wu^{2,6}, Hui-Ying Hsu¹, Yu-Chen Sun⁷, Hui-Yu Wu⁸, Chih-Ho Lai^{1,6,8,9*} and Chia-Hung Kao^{1,10,11*}

OPEN ACCESS

Edited by:

Yuhei Nishimura,
Mie University Graduate
School of Medicine, Japan

Reviewed by:

William B. Grant,
Sunlight Nutrition and Health
Research Center, United States
Chia-Yang Li,
Kaohsiung Medical University, Taiwan
Muhammad Imran Qadir,
Bahauddin Zakariya University,
Pakistan

*Correspondence:

Chih-Ho Lai
chlai@mail.cgu.edu.tw
Chia-Hung Kao
d10040@mail.cmu.edu.tw

†These authors have contributed
equally to this work.

Specialty section:

This article was submitted to
Experimental Pharmacology
and Drug Discovery,
a section of the journal
Frontiers in Pharmacology

Received: 27 October 2017

Accepted: 27 February 2018

Published: 22 March 2018

Citation:

Chen Y-A, Lin Y-J, Lin C-L, Lin H-J,
Wu H-S, Hsu H-Y, Sun Y-C, Wu H-Y,
Lai C-H and Kao C-H (2018)
Simvastatin Therapy for Drug
Repositioning to Reduce the Risk
of Prostate Cancer Mortality
in Patients With Hyperlipidemia.
Front. Pharmacol. 9:225.
doi: 10.3389/fphar.2018.00225

¹ Graduate Institute of Basic Medical Science, School of Medicine, College of Medicine, China Medical University, Taichung, Taiwan, ² Department of Medical Research, School of Chinese Medicine, China Medical University and Hospital, Taichung, Taiwan, ³ Management Office for Health Data, China Medical University Hospital, Taichung, Taiwan, ⁴ Division of Gastroenterology and Hepatology, Department of Internal Medicine, School of Medicine, College of Medicine, Taipei Medical University, Taipei, Taiwan, ⁵ Division of Gastroenterology and Hepatology, Department of Internal Medicine, Shuang-Ho Hospital, New Taipei City, Taiwan, ⁶ Department of Nursing, Asia University, Taichung, Taiwan, ⁷ Department of Laboratory Medicine, Chang Gung Memorial Hospital, Linkou, Taiwan, ⁸ Department of Microbiology and Immunology, Graduate Institute of Biomedical Sciences, College of Medicine, Chang Gung University, Taoyuan, Taiwan, ⁹ Molecular Infectious Disease Research Center, Chang Gung Memorial Hospital, Linkou, Taiwan, ¹⁰ Department of Bioinformatics and Medical Engineering, Asia University, Taichung, Taiwan, ¹¹ Department of Nuclear Medicine, PET Center, China Medical University Hospital, Taichung, Taiwan

Prostate cancer (PCa) is one of the most commonly diagnosed cancers in the western world, and the mortality rate from PCa in Asia has been increasing recently. Statins are potent inhibitors of 3-hydroxy-3-methyl glutaryl coenzyme A (HMG-CoA) reductase and are commonly used for treating hyperlipidemia, with beneficial effects for cardiovascular disease and they also exhibit anti-cancer activity. However, the protective effects of statins against PCa are controversial. In this study, we investigated the effect of two types of statins (simvastatin and lovastatin) and the mortality rate of PCa patients by using the Taiwan National Health Insurance Research Database (NHIRD). A total of 15,264 PCa patients with hyperlipidemia records and medical claims from the Registry of Catastrophic Illness were enrolled. The patients were divided into two cohorts based on their statin use before the diagnosis of PCa: statin users ($n = 1,827$) and non-statin users ($n = 1,826$). The results showed that patients who used statins exhibited a significantly reduced risk of mortality from PCa [adjusted hazard ratio (HR) = 0.84, 95% CI = 0.73–0.97]. Analysis of the cumulative defined daily dose (DDD) indicated that patients who were prescribed simvastatin ≥ 180 DDD had a dramatically decreased risk of death from PCa (adjusted HR = 0.63; 95% CI = 0.51–0.77). This population-based cohort study demonstrated that statin use significantly decreased the mortality of PCa patients, and that this risk was inversely associated with the cumulative DDD of simvastatin therapy. The results of this study revealed that statins may be used for drug repositioning and in the development of a feasible approach to prevent death from PCa.

Keywords: hyperlipidemia, HMG-CoA reductase, prostate cancer, statin, cohort study

INTRODUCTION

Prostate cancer (PCa) is one of the most prevalent male cancers in western developed countries, and its incidence is increasing in the Asia-Pacific region (Global Burden of Disease Cancer et al., 2017). Although recent advances in surgical techniques and radiotherapy have improved the disease-free survival rates of men with localized PCa, the recurrence rate after radical prostatectomy, chemotherapy, or radiotherapy is still high (Trock et al., 2008). Men are at higher risk for developing PCa, while the risk factors include having a family history of PCa along with environmental and lifestyle-related factors, such as physical inactivity, obesity, and a high-fat diet (Barnard, 2007; Meyerhardt et al., 2010).

Statins, inhibitors of 3-hydroxy-3-methyl glutaryl coenzyme A (HMG-CoA) reductase, the rate-limiting enzyme in cholesterol biosynthesis, are widely used for treating high levels of serum cholesterol (Hebert et al., 1997). The activity of HMG-CoA reductase may be increased due to the activation of transcriptional regulation mediated by sterol regulatory element binding proteins (SREBPs) (Chen et al., 1978). In LNCaP and PC-3 PCa cells, inhibition of SREBP2 activity reduced cell viability (Krycer et al., 2012). Recent studies indicated that statins possess the potential to prevent and treat several types of cancers, including PCa (Hindler et al., 2006; Bonovas et al., 2008; Yu et al., 2014). The protective functions of statins are included reducing the risk of PCa through arrest cell cycle, inducing apoptosis, and inhibiting tumor metastasis (Papadopoulos et al., 2011; Sun Q. et al., 2015). However, some conflicting results about the protective effects of statins against PCa have not been clearly clarified (Moon et al., 2014; Alfaqih et al., 2017).

Although previous studies indicated that statins may decrease the incidence of PCa (Shannon et al., 2005; Flick et al., 2007), there have been no large-scale epidemiologic studies on the effects of statins for treating PCa patients with hyperlipidemia who received different therapeutic modalities including radical prostatectomy, chemotherapy, or radiotherapy. In this study, we conducted a nationwide population-based cohort study to analyze the mortality in PCa patients with hyperlipidemia who were prescribed either simvastatin or lovastatin. The association between the cumulative defined daily dose (DDD) of two types of statins and the risk of PCa mortality was also investigated. Our results showed that statin prescriptions effectively reduced the risk of death from PCa. This study also revealed that cholesterol-lowering agents, such as statins, may be used for drug repurposing to help prevent death in PCa patients who also have hyperlipidemia.

MATERIALS AND METHODS

Data Source

To examine whether statin use is associated with risk of PCa, a nationwide cohort study was conducted. Data were obtained from the Registry of Catastrophic Illness and Taiwan National Health Insurance Research Database (NHIRD). The National Health Research Institutes (NHRI) in Taiwan is responsible for

managing the insurance claims data reported to the Bureau of Health Insurance. For research purposes, the NHRI compiles all medical claims in the National Health Insurance (NHI) program and releases the database annually to the public. Patient consent is not required to access the NHIRD. This study was approved by the Institutional Review Board of China Medical University in Taiwan (CMUH104-REC2-115-CR2).

Population-Based Cohort Study

A total of 15,264 PCa patients with hyperlipidemia (ICD-9-CM 272) were included in this study (Figure 1). The patients were divided into two cohorts, the statin users (either simvastatin or lovastatin) and non-statin users before the diagnosis of PCa. Patients under 20 years old were excluded. In the statin use cohort, 1,827 PCa patients prescribed statins for at least 6 months during January 1, 1998 to December 31, 2010. The non-statin cohort ($n = 1,826$) was randomly selected from 12,111 PCa patients without receiving statin therapy. Comparison group was established by 1:1 randomly frequency matching (according to age and index year) with PCa patients who did not use any types of statin-based drugs during the study period. The study endpoint was mortality.

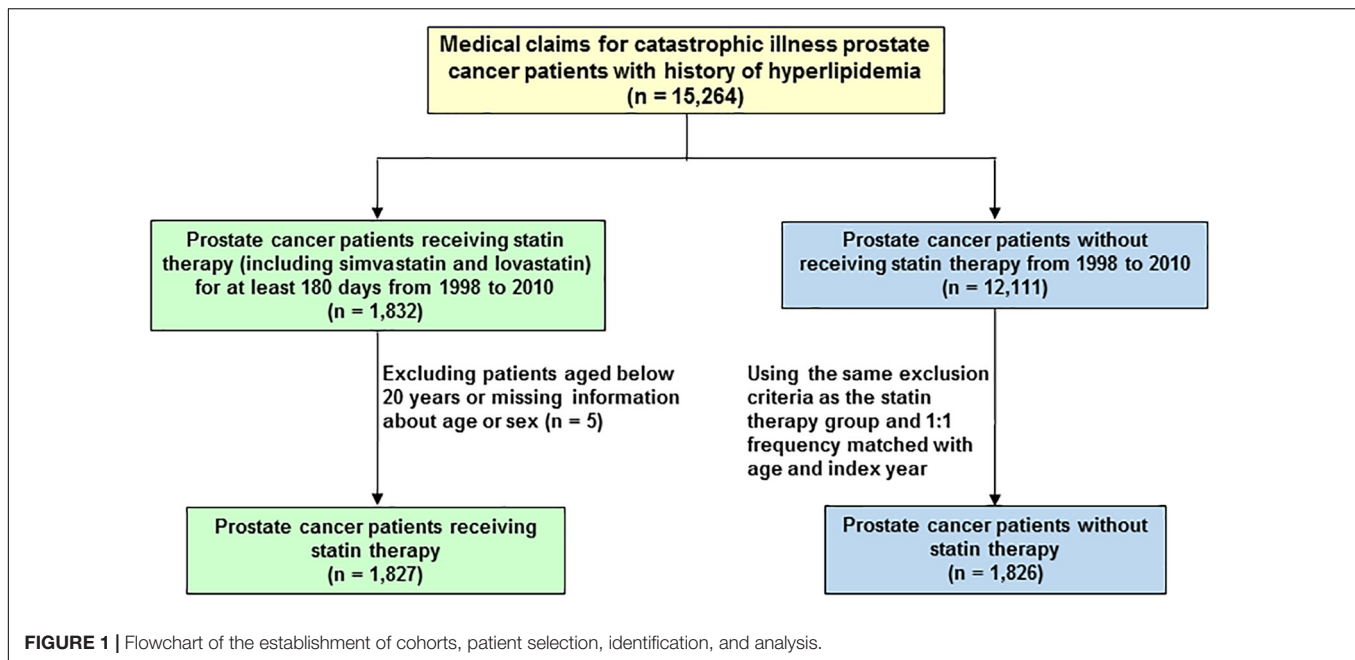
Medication and Analysis of Statin Prescription

Hazard ratio (HR) and 95% confidence interval (CI) were adjusted for age, treatment of hormone therapy (including oral and injection), radical prostatectomy, radiotherapy, chemotherapy, and the comorbidities of diabetes (ICD-9-CM codes 250), hypertension (ICD-9-CM codes 401-405), stroke (ICD-9-CM codes 430-438), cardiovascular disease (CAD; ICD-9-CM codes 410-414) and chronic obstructive pulmonary disease (COPD; ICD-9-CM codes 490-496).

The DDD, recommended by the World Health Organization (WHO), was assumed to be the average maintenance dose per day of a drug and analyzed as described previously (Lin et al., 2017). The cumulative DDD was calculated by deriving the total prescribed DDD of each type of statin, namely simvastatin (ATC C10AA01) and lovastatin (ATC C10AA02), for statin users. For each statin type, the cumulative DDD was partitioned into two levels by setting the cutoff value in the median.

Statistical Analysis

The distributions of demographic characteristics were compared between the statin and non-statin cohorts, and the differences were examined using the Chi-squared test for categorical variables and the Student's *t*-test for continuous variables. The multivariate analysis of the mortality rates associated with statin use was performed using the cox proportional hazard regressions. Furthermore, we divided each statin type into two groups according to the quartile of cumulative DDD. Cox proportional hazard regression was used to assess how the statin dose affected the relative risk of mortality. A *P*-value of < 0.05 indicated statistical significance. All analyses were conducted using SAS statistical software (Version 9.3 for Windows; SAS Institute, Inc., Cary, NC, United States).



RESULTS

Demographic Characteristics of Study Patients

A total of 15,264 PCa patients with hyperlipidemia were enrolled in this study and analyzed. In the population-based cohort study, we first evaluated 3,653 patients with PCa, aged ≥ 20 years (Figure 1). There were 1,827 patients using statin-based drugs (either simvastatin or lovastatin) and 1,826 patients who did not. Table 1 shows the age, comorbidities, hormone therapy, and treatments of the cohorts. Among the patients with PCa, 85.4% of the patients were older than 60 years of age. Compared with non-statin users (Group 1), the statin users (Group 2) were more likely to have coronary artery disease (CAD) (41.2% vs. 52.2%, $P < 0.0001$), diabetes mellitus (20.2% vs. 32.3%, $P < 0.0001$), hypertension (68.9% vs. 81.3%, $P < 0.0001$), and stroke (5.37% vs. 7.88%, $P < 0.0001$). In the treatments used for PCa including hormone therapy, radical prostatectomy, chemotherapy, and radiotherapy, the statin users and non-statin users did not show statistically significant differences.

Comparison of Incidence and Hazard Ratio (HR) of Mortality in PCa Patients

The person-years (PY), incidence (age, comorbidity, hormone therapy, and treatments), and HR for the risk of mortality among the cohorts were then analyzed. As shown in Table 2, statin users had a significantly lower HR of mortality (adjusted HR = 0.84, 95% CI = 0.73–0.97, $P < 0.05$) compared with the non-statin users. Among patients who had no comorbidities, statin users exhibited the lowest HR of mortality (adjusted HR = 0.55, 95% CI = 0.31–0.99, $P < 0.05$). A significantly reduced adjusted HR of mortality was also found in the following groups

for patients prescribed statins: treatment with chemotherapy (adjusted HR = 0.60, 95% CI = 0.41–0.87, $P < 0.01$), non-oral hormone therapy (adjusted HR = 0.81, 95% CI = 0.68–0.98, $P < 0.05$), and non-prostatectomy (adjusted HR = 0.86, 95% CI = 0.74–0.99, $P < 0.05$).

TABLE 1 | Demographic characteristics of PCa patients with hyperlipidemia by medications.

Parameter	Group 1 ^a	Group 2	P-value ^b
Age, years, n (%)			0.99
≤59	266 (14.6%)	267 (14.6%)	
60–69	747 (40.9%)	747 (40.9%)	
70–79	712 (39.0%)	712 (39.0%)	
≥80	101 (5.5%)	101 (5.5%)	
Mean (SD)	68.3 (8.1%)	68.3 (7.8%)	0.68
Comorbidity^c, n (%)			
CAD	753 (41.2%)	954 (52.2%)	<0.0001
Diabetes mellitus	368 (20.2%)	590 (32.3%)	<0.0001
Hypertension	1258 (68.9%)	1486 (81.3%)	<0.0001
Stroke	98 (5.4%)	144 (7.9%)	<0.0001
COPD	675 (37.0%)	661 (36.2%)	0.62
Hormone therapy, n (%)			
Oral	780 (42.7%)	825 (45.2%)	0.14
Injection	215 (11.8%)	193 (10.6%)	0.25
Treatment, n (%)			
Radical prostatectomy	355 (19.4%)	379 (20.7%)	0.33
Chemotherapy	121 (6.6%)	100 (5.5%)	0.14
Radiotherapy	591 (32.4%)	609 (33.3%)	0.53

^aGroup 1, non-statin users (n = 1826); group 2, statin users (n = 1827);

^bChi-square test and Student's t-test were used to compare the statin user and non-statin user groups; ^cCAD, coronary artery disease; COPD, chronic obstructive pulmonary disease.

TABLE 2 | Hazard ratios and 95% confidence intervals of PCa mortality in statin user and non-statin user groups.

Variable	Group 1 ^a			Group 2			Hazard ratio	
	Event	PY ^b	Rate	Event	PY	Rate	Crude	Adjusted HR ^c (95% confidence interval)
All	402	14902	27.0	377	15119	24.9	0.91	0.84 (0.73–0.97)*
Age, years								
≤59	22	2480	8.87	18	2516	7.15	0.80	0.83 (0.43–1.60)
60–69	123	6516	18.9	111	6584	16.9	0.88	0.90 (0.69–1.17)
70–79	217	5415	40.1	220	5508	40.0	0.98	0.88 (0.73–1.06)
≥80	40	492	81.3	28	512	54.7	0.63	0.67 (0.41–1.12)
Comorbidity^d								
No	50	2494	20.0	16	1199	13.4	0.61	0.55 (0.31–0.99)*
Yes	352	12408	28.4	316	13920	25.9	0.90	0.91 (0.79–1.05)
Hormone therapy (Oral)								
No	264	8437	31.3	227	8136	27.9	0.88	0.81 (0.68–0.98)*
Yes	138	6465	21.3	150	6983	21.5	0.99	0.92 (0.72–1.16)
Hormone therapy (Injection)								
No	342	13156	26.0	331	13556	24.4	0.93	0.86 (0.74–1.01)
Yes	60	1747	34.4	46	1564	29.4	0.85	0.75 (0.50–1.12)
Treatment								
Radical prostatectomy								
No	363	11983	30.3	340	11871	28.6	0.94	0.86 (0.74–0.99)*
Yes	39	2919	13.4	37	3249	11.4	0.82	0.67 (0.42–1.08)
Chemotherapy								
No	325	13942	23.3	328	14313	22.9	0.97	0.95 (0.81–1.11)
Yes	77	960	80.2	49	806	60.8	0.73	0.60 (0.41–0.87)**
Radiotherapy								
No	260	9969	26.1	236	9971	23.7	0.90	0.84 (0.70–1.00)
Yes	142	4933	28.8	141	5148	27.4	0.93	0.88 (0.70–1.12)

^aGroup 1, non-statin users; group 2, statin users; ^bPY, per 1000 person-years; Rate, incidence rate; ^cAdjusted HR, multivariable analysis including age, sex, hormone therapy, treatment and comorbidities of coronary artery disease (CAD), diabetes, hypertension, stroke, and chronic obstructive pulmonary disease (COPD); * $P < 0.05$; ** $P < 0.01$; ^dComorbidity: only to have one of comorbidities classified as the comorbidity group.

TABLE 3 | Prescribed statins reduce the mortality of PCa patients.

	Event/Total number	Crude HR ^a (95% confidence interval)	Adjusted HR ^b (95% confidence interval)
Non-use of statins	402/1826	1 (Reference)	1 (Reference)
Use of statin^c			
Simvastatin			
<180 DDD	263/1101	1.11 (0.95–1.29)	0.99 (0.85–1.16)
≥180 DDD	114/726	0.65 (0.53–0.80)***	0.63 (0.51–0.77)***
Lovastatin			
< 115 DDD	259/1314	0.91 (0.78–1.06)	0.83 (0.71–0.97)*
≥ 115 DDD	118/513	0.93 (0.76–1.14)	0.87 (0.71–1.07)

^aCrude HR, relative hazard ratio; ^bAdjusted HR, multivariable analysis including age, sex, hormone therapy, treatment and comorbidities of coronary artery disease (CAD), diabetes, hypertension, stroke, and chronic obstructive pulmonary disease (COPD); ^cThe cumulative defined daily dose (DDD) is partitioned in to 2 segments by median; * $P < 0.05$; *** $P < 0.001$.

Statin Use Reduces the Risk of PCa Mortality

The association between the cumulative DDD of two types of statins and the risk of PCa mortality was further analyzed. Compared with non-statin users, patients who were prescribed simvastatin at a DDD ≥ 180 (adjusted HR = 0.63, 95% CI = 0.51–0.77) exhibited the lowest risk of mortality, which

was associated with the high cumulative DDD of prescribed simvastatin (Table 3). Patients who received lovastatin at a DDD < 115 (adjusted HR = 0.83, 95% CI = 0.71–0.97) had a lower adjusted HR of mortality compared with the non-statin user group. The results from these analyses demonstrate that statin use effectively reduced the mortality of PCa patients, and that this risk was associated with a high cumulative DDD of prescribed simvastatin.

DISCUSSION

Prostate cancer is a commonly diagnosed cancer and the second leading cause of cancer-related deaths in US men (Wadajkar et al., 2013). In Taiwan, the prevalence of PCa has gradually increased in recent years (Chiang et al., 2016; Hung et al., 2016). Based on a statistical report from the Ministry of Health and Welfare [MOHW] (2016) of Taiwan in 2016, PCa has become the fifth most prevalent cancer and the seventh leading cause of cancer-related death, indicating that the threat of PCa to men has become severe. Therefore, it is important to pay more attention to the diagnosis and treatment of patients with PCa.

The regulation of lipid rafts (also referred to cholesterol-rich microdomains) is critical for PCa cell survival and growth (Zhuang et al., 2002). PCa cells harbored the activity to synthesize dihydrotestosterone (DHT) from acetic acid, indicating that the entire mevalonate-steroidogenic pathway was functionally intact (Locke et al., 2008). In addition, all enzymes contributed to testosterone and DHT synthesis are presented in many human primary and metastatic PCa (Montgomery et al., 2008). Therefore, new therapeutic agents with lesser toxicity and higher selectivity for preventing recurrence and progression of PCa are urgently required. This population-based cohort analysis revealed that statin therapy significantly decreased the mortality of PCa patients treated with chemotherapy. In addition, the reduced risk was correlated with the high cumulative DDD of prescribed simvastatin. This nationwide population-based study provides evidence that statin therapy not only reduced the risk of cardiovascular disease but may also be used for drug repurposing to prevent death of PCa patients who also have hyperlipidemia.

It has been demonstrated that simvastatin inhibits the proliferation, migration, and invasion of PCa cells via the up-regulation of ANXA10 and inactivation of the AKT/PI3K pathway (Miyazawa et al., 2017). Simvastatin can arrest the cell cycle at G1 in PC-3 cells through the AMPK pathway (Karlic et al., 2017). In addition, lovastatin was found to enhance the efficacy of PRRA-TRAIL via the promotion of tumor suppression and induction of apoptosis (Liu et al., 2015). A recent study also indicated that the induction of the LDL receptor is a possible mechanism of resistance that prostate tumors use to counteract the therapeutic effects of reducing serum cholesterol (Masko et al., 2017). Therefore, statins can be used to delay PCa progression by reducing LDL levels (Murtola et al., 2012).

Clinical studies have been reported that statins significantly reduced the incidence of advanced PCa (Bonovas et al., 2008). A 10-year retrospective cohort study indicated that statin users had a 31% lower risk of PCa (Farwell et al., 2011). The mechanism for statins was the indirect reduction in cellular cholesterol levels in multiple cell types through the lowering of circulating cholesterol, which impacts the membrane microdomains and steroidogenesis (Moon et al., 2014). In addition, statin can prevent against PCa by inhibiting the proliferation and inducing apoptosis of PCa cells, which inhibits angiogenesis, inflammation, and metastasis (Papadopoulos et al., 2011). A recent clinical analysis demonstrated that statin users had a significantly longer median time to progression during

androgen deprivation therapy than non-users (Harshman et al., 2015).

Both *in vitro* and *in vivo* studies have demonstrated that statins inhibited cancer cell growth and induced apoptosis in a variety of tumor cell types, including PCa, colon adenocarcinoma, pancreatic carcinoma, and gastric cancer cells (Lochhead and Chan, 2013; Babcook et al., 2016; Lin et al., 2016; Gong et al., 2017). A population-based cohort study revealed that not all types of statin were associated with a decreased incidence of PCa, except for simvastatin, atorvastatin, and rosuvastatin (Lustman et al., 2014). Simvastatin was identified to inhibit the migration and invasion of PCa cells (Shah et al., 2016). The inhibitory effect of statin-derivatives on tumorigenicity of castrate-resistant prostate cancer (CRPC) may be mediated via concurrent inhibition of both androgen receptor and AKT signaling pathways, and membrane destabilization (Ingersoll et al., 2016). Furthermore, the mechanism for inhibition of CRPC growth by statins suppressed nuclear factor- κ B pathway to induce apoptosis and prevent CRPC development (Park et al., 2013; Kang et al., 2017). Our current study also revealed that statins can function as a radiosensitizer in PCa cells for triggering the CHK1 checkpoint response and promoting DNA double-strand breaks (unpublish data). Together, these findings demonstrated the potential mechanism of statins in the treatment of PCa.

Although we recently reported the protective effects of statins against PCa (Sun L.M. et al., 2015), certain limitations and confounding factors of previous studies are still emerging. In the current study, we further selected patients with hyperlipidemia and divided them into two cohorts based on the prescription of statins. Because statin users may have other comorbidities, several treatments and comorbidities were adjusted for, including hormone therapy, diabetes, hypertension, stroke, CAD, and COPD. In addition, the cause of death among patients with PCa was documented in the Registry of Catastrophic Illness, and thus, mortality from PCa can be precisely analyzed. Therefore, our current findings have been thoroughly investigated and are based on rigorous and valid methods.

Some limitations exist in the current studies, including potential confounders, concomitant use of other chemopreventive drugs, short enrollment periods, and small sample sizes. A social gradient in statin use may reflect social inequalities in health care use or health care quality, as well as systematic differences in factors such as smoking, nutrition, physical activity, and obesity (Bonovas and Sitaras, 2009). Patients with cardiovascular disease prescribed statins may also take non-steroidal anti-inflammatory drugs (NSAIDs), which have been reported to reduce the risk of PCa (Papadopoulos et al., 2011). Although current studies using population-based analysis consistently report an inverse association between statin use and PCa risk, the detailed mechanism of statins for the primary prevention of PCa requires further investigation.

The Taiwan government has launched an NHI program that has provided citizens with comprehensive coverage since 1995. All insurance claims are scrutinized by medical reimbursement specialists and recorded in the database. The NHIRD enabled appropriately selecting matched patients to represent the underlying population. In addition, we have analyzed data in the

NHIRD to perform several studies and have evaluated statin-based drugs for protection against several diseases (Peng et al., 2015; Sun L.M. et al., 2015; Lin et al., 2016). Therefore, these results obtained by using a nationwide cohort study regarding statin use and diagnoses for patients with PCa mortality are reliable.

CONCLUSION

This study demonstrated that statin prescription has effectively reduced the deaths of PCa patients with hyperlipidemia. The mortality risk of patients with PCa is inversely associated with a high cumulative DDD of simvastatin. Therefore, statins, cholesterol-lowering agents, can be drug repurposed and used in a preventive application for protecting against death from PCa. However, large, long-term clinical analysis and experimental studies on the biological mechanisms of statin therapy are required to further validate statins as a means of reducing PCa mortality.

AUTHOR CONTRIBUTIONS

C-HL and C-HK: conceived and designed the experiments. Y-AC, Y-JL, C-LL, H-JL, H-YH, Y-CS, and H-YW: performed the

experiments and analyzed the data. Y-AC, Y-JL, C-LL, and H-JL: wrote the manuscript. All authors reviewed the final version of the manuscript.

FUNDING

This work was supported by grants from the Ministry of Health and Welfare, Taiwan (MOHW107-TDU-B-212-123004), China Medical University Hospital, Academia Sinica Stroke Biosignature Project (BM10701010021), MOST Clinical Trial Consortium for Stroke (MOST 106-2321-B-039-005), Tseng-Lien Lin Foundation, Taichung, Taiwan, and Katsuzo and Kiyo Aoshima Memorial Funds, Japan, Taiwan Ministry of Science and Technology (105-2313-B-182-001 and 106-2320-B-182-012-MY3), Chang Gung Memorial Hospital (CMRPD1F0011-3, CMRPD1F0431-3, and BMRPE90), and Tomorrow Medical Foundation.

ACKNOWLEDGMENTS

The authors would like to thank the editor and the reviewers for the editorial assistance and their valuable comments. The authors sincerely appreciate the Bureau of National Health Insurance for providing the NHIRD.

REFERENCES

- Alfaqih, M. A., Allott, E. H., Hamilton, R. J., Freeman, M. R., and Freedland, S. J. (2017). The current evidence on statin use and prostate cancer prevention: are we there yet? *Nat. Rev. Urol.* 14, 107–119. doi: 10.1038/nrurol.2016.199
- Babcook, M. A., Joshi, A., Montellano, J. A., Shankar, E., and Gupta, S. (2016). Statin use in prostate cancer: an update. *Nutr. Metab. Insights* 9, 43–50. doi: 10.4137/NMI.S38362
- Barnard, R. J. (2007). Prostate cancer prevention by nutritional means to alleviate metabolic syndrome. *Am. J. Clin. Nutr.* 86, s889–s893. doi: 10.1093/ajcn/86.3.889S
- Bonovas, S., Filioussi, K., and Sitaras, N. M. (2008). Statin use and the risk of prostate cancer: a metaanalysis of 6 randomized clinical trials and 13 observational studies. *Int. J. Cancer* 123, 899–904. doi: 10.1002/ijc.23550
- Bonovas, S., and Sitaras, N. M. (2009). Statins and cancer risk: a confounded association. *Gastroenterology* 137, 740; author reply 740–741. doi: 10.1053/j.gastro.2009.02.088
- Chen, H. W., Kandutsch, A. A., and Heiniger, H. J. (1978). The role of cholesterol in malignancy. *Prog. Exp. Tumor Res.* 22, 275–316. doi: 10.1159/000401203
- Chiang, C. J., Lo, W. C., Yang, Y. W., You, S. L., Chen, C. J., and Lai, M. S. (2016). Incidence and survival of adult cancer patients in Taiwan, 2002–2012. *J. Formos. Med. Assoc.* 115, 1076–1088. doi: 10.1016/j.jfma.2015.10.011
- Farwell, W. R., D'Avolio, L. W., Scranton, R. E., Lawler, E. V., and Gaziano, J. M. (2011). Statins and prostate cancer diagnosis and grade in a veterans population. *J. Natl. Cancer Inst.* 103, 885–892. doi: 10.1093/jnci/djr108
- Flick, E. D., Habel, L. A., Chan, K. A., Van Den Eeden, S. K., Quinn, V. P., Haque, R., et al. (2007). Statin use and risk of prostate cancer in the California Men's Health Study cohort. *Cancer Epidemiol. Biomarkers Prev.* 16, 2218–2225. doi: 10.1158/1055-9965.EPI-07-0197
- Global Burden of Disease Cancer, Collaboration, Fitzmaurice, C., Allen, C., Barber, R. M., Barregard, L., Bhutta, Z. A., et al. (2017). Global, regional, and national cancer incidence, mortality, years of life lost, years lived with disability, and disability-adjusted life-years for 32 cancer groups, 1990 to 2015: a systematic analysis for the Global Burden of Disease Study. *JAMA Oncol.* 3, 524–548. doi: 10.1001/jamaoncol.2016.5688
- Gong, J., Sachdev, E., Robbins, L. A., Lin, E., Hendifar, A. E., and Mita, M. M. (2017). Statins and pancreatic cancer. *Oncol. Lett.* 13, 1035–1040. doi: 10.3892/ol.2017.5572
- Harshman, L. C., Wang, X., Nakabayashi, M., Xie, W., Valenca, L., Werner, L., et al. (2015). Statin use at the time of initiation of androgen deprivation therapy and time to progression in patients with hormone-sensitive prostate cancer. *JAMA Oncol.* 1, 495–504. doi: 10.1001/jamaoncol.2015.0829
- Hebert, P. R., Gaziano, J., Chan, K., and Hennekens, C. H. (1997). Cholesterol lowering with statin drugs, risk of stroke, and total mortality: an overview of randomized trials. *JAMA* 278, 313–321. doi: 10.1001/jama.1997.03550040069040
- Hindler, K., Cleeland, C. S., Rivera, E., and Collard, C. D. (2006). The role of statins in cancer therapy. *Oncologist* 11, 306–315. doi: 10.1634/theoncologist.11-3-306
- Hung, C. F., Yang, C. K., and Ou, Y. C. (2016). Urologic cancer in Taiwan. *Jpn. J. Clin. Oncol.* 46, 605–609. doi: 10.1093/jcco/hyw038
- Ingersoll, M. A., Miller, D. R., Martinez, O., Wakefield, C. B., Hsieh, K. C., Simha, M. V., et al. (2016). Statin derivatives as therapeutic agents for castration-resistant prostate cancer. *Cancer Lett.* 383, 94–105. doi: 10.1016/j.canlet.2016.09.008
- Kang, M., Lee, K. H., Lee, H. S., Jeong, C. W., Ku, J. H., Kim, H. H., et al. (2017). Concurrent treatment with simvastatin and NF-kappaB inhibitor in human castration-resistant prostate cancer cells exerts synergistic anti-cancer effects via control of the NF-kappaB/LIN28/let-7 miRNA signaling pathway. *PLoS One* 12:e0184644. doi: 10.1371/journal.pone.0184644
- Karlic, H., Haider, F., Thaler, R., Spitzer, S., Klaushofer, K., and Varga, F. (2017). Statin and bisphosphonate induce starvation in fast-growing cancer cell lines. *Int. J. Mol. Sci.* 18:e1982. doi: 10.3390/ijms18091982
- Krycer, J. R., Phan, L., and Brown, A. J. (2012). A key regulator of cholesterol homeostasis, SREBP-2, can be targeted in prostate cancer cells with natural products. *Biochem. J.* 446, 191–201. doi: 10.1042/BJ20120545
- Lin, C. J., Liao, W. C., Chen, Y. A., Lin, H. J., Feng, C. L., Lin, C. L., et al. (2017). statin therapy is associated with reduced risk of peptic ulcer disease

- in the Taiwanese population. *Front. Pharmacol.* 8:210. doi: 10.3389/fphar.2017.00210
- Lin, C. J., Liao, W. C., Lin, H. J., Hsu, Y. M., Lin, C. L., Chen, Y. A., et al. (2016). Statins Attenuate *Helicobacter pylori* CagA translocation and reduce incidence of gastric cancer: *In Vitro* and population-based case-control studies. *PLoS One* 11:e0146432. doi: 10.1371/journal.pone.0146432
- Liu, Y., Chen, L., Gong, Z., Shen, L., Kao, C., Hock, J. M., et al. (2015). Lovastatin enhances adenovirus-mediated TRAIL induced apoptosis by depleting cholesterol of lipid rafts and affecting CAR and death receptor expression of prostate cancer cells. *Oncotarget* 6, 3055–3070. doi: 10.18632/oncotarget.3073
- Lochhead, P., and Chan, A. T. (2013). Statins and colorectal cancer. *Clin. Gastroenterol. Hepatol.* 11, 109–118; quiz e13–e14. doi: 10.1016/j.cgh.2012.08.037
- Locke, J. A., Guns, E. S., Lubik, A. A., Adomat, H. H., Hendy, S. C., Wood, C. A., et al. (2008). Androgen levels increase by intratumoral *De novo* steroidogenesis during progression of castration-resistant prostate cancer. *Cancer Res.* 68, 6407–6415. doi: 10.1158/0008-5472.CAN-07-5997
- Lustman, A., Nakar, S., Cohen, A. D., and Vinker, S. (2014). Statin use and incident prostate cancer risk: does the statin brand matter? A population-based cohort study. *Prostate Cancer Prostatic Dis.* 17, 6–9. doi: 10.1038/pcan.2013.34
- Masko, E. M., Alfaqih, M. A., Solomon, K. R., Barry, W. T., Newgard, C. B., Muehlbauer, M. J., et al. (2017). Evidence for feedback regulation following cholesterol lowering therapy in a prostate cancer xenograft model. *Prostate* 77, 446–457. doi: 10.1002/pros.23282
- Meyerhardt, J. A., Ma, J., and Courneya, K. S. (2010). Energetics in colorectal and prostate cancer. *J. Clin. Oncol.* 28, 4066–4073. doi: 10.1200/JCO.2009.26.8797
- Ministry of Health and Welfare [MOHW]. (2016). *Taiwan Statistics of Causes of Death 2016*. Available at: <http://www.mohw.gov.tw/lp-3327-2.html> [accessed March 6, 2018].
- Miyazawa, Y., Sekine, Y., Kato, H., Furuya, Y., Koike, H., and Suzuki, K. (2017). Simvastatin up-regulates annexin A10 that can inhibit the proliferation, migration, and invasion in androgen-independent human prostate cancer cells. *Prostate* 77, 337–349. doi: 10.1002/pros.23273
- Montgomery, R. B., Mostaghel, E. A., Vessella, R., Hess, D. L., Kalthorn, T. F., Higano, C. S., et al. (2008). Maintenance of intratumoral androgens in metastatic prostate cancer: a mechanism for castration-resistant tumor growth. *Cancer Res.* 68, 4447–4454. doi: 10.1158/0008-5472.CAN-08-0249
- Moon, H., Hill, M. M., Roberts, M. J., Gardiner, R. A., and Brown, A. J. (2014). Statins: protectors or pretenders in prostate cancer? *Trends Endocrinol. Metab.* 25, 188–196. doi: 10.1016/j.tem.2013.12.007
- Murtola, T. J., Syvala, H., Pennanen, P., Blauer, M., Solakivi, T., Ylikomi, T., et al. (2012). The importance of LDL and cholesterol metabolism for prostate epithelial cell growth. *PLoS One* 7:e39445. doi: 10.1371/journal.pone.0039445
- Papadopoulos, G., Delakas, D., Nakopoulou, L., and Kassimatis, T. (2011). Statins and prostate cancer: molecular and clinical aspects. *Eur. J. Cancer* 47, 819–830. doi: 10.1016/j.ejca.2011.01.005
- Park, Y. H., Seo, S. Y., Lee, E., Ku, J. H., Kim, H. H., and Kwak, C. (2013). Simvastatin induces apoptosis in castrate resistant prostate cancer cells by deregulating nuclear factor-kappaB pathway. *J. Urol.* 189, 1547–1552. doi: 10.1016/j.juro.2012.10.030
- Peng, Y. C., Lin, C. L., Hsu, W. Y., Chang, C. S., Yeh, H. Z., Tung, C. F., et al. (2015). Statins are associated with a reduced risk of cholangiocarcinoma: a population-based case-control study. *Br. J. Clin. Pharmacol.* 80, 755–761. doi: 10.1111/bcp.12641
- Shah, E. T., Upadhyaya, A., Philp, L. K., Tang, T., Skalamera, D., Gunter, J., et al. (2015). Repositioning "old" drugs for new causes: identifying new inhibitors of prostate cancer cell migration and invasion. *Clin. Exp. Metastasis* 33, 385–399. doi: 10.1007/s10585-016-9785-y
- Shannon, J., Tewoderos, S., Garzotto, M., Beer, T. M., Derenick, R., Palma, A., et al. (2005). Statins and prostate cancer risk: a case-control study. *Am. J. Epidemiol.* 162, 318–325. doi: 10.1093/aje/kwi203
- Sun, L. M., Lin, M. C., Lin, C. L., Chang, S. N., Liang, J. A., Lin, I. C., et al. (2015). Statin use reduces prostate cancer all-cause mortality: a nationwide population-based cohort study. *Medicine* 94:e1644. doi: 10.1097/MD.0000000000001644
- Sun, Q., Arnold, R. S., Sun, C. Q., and Petros, J. A. (2015). A mitochondrial DNA mutation influences the apoptotic effect of statins on prostate cancer. *Prostate* 75, 1916–1925. doi: 10.1002/pros.23089
- Trock, B. J., Han, M., Freedland, S. J., Humphreys, E. B., DeWeese, T. L., Partin, A. W., et al. (2008). Prostate cancer-specific survival following salvage radiotherapy vs observation in men with biochemical recurrence after radical prostatectomy. *JAMA* 299, 2760–2769. doi: 10.1001/jama.299.23.2760
- Wadajkar, A. S., Menon, J. U., Tsai, Y. S., Gore, C., Dobin, T., Gandee, L., et al. (2013). Prostate cancer-specific thermo-responsive polymer-coated iron oxide nanoparticles. *Biomaterials* 34, 3618–3625. doi: 10.1016/j.biomaterials.2013.01.062
- Yu, O., Eberg, M., Benayoun, S., Aprikian, A., Batist, G., Suissa, S., et al. (2014). Use of statins and the risk of death in patients with prostate cancer. *J. Clin. Oncol.* 32, 5–11. doi: 10.1200/JCO.2013.49.4757
- Zhuang, L., Lin, J., Lu, M. L., Solomon, K. R., and Freeman, M. R. (2002). Cholesterol-rich lipid rafts mediate akt-regulated survival in prostate cancer cells. *Cancer Res.* 62, 2227–2231.

Conflict of Interest Statement: The authors declare that the research was conducted in the absence of any commercial or financial relationships that could be construed as a potential conflict of interest.

Copyright © 2018 Chen, Lin, Lin, Lin, Wu, Hsu, Sun, Wu, Lai and Kao. This is an open-access article distributed under the terms of the Creative Commons Attribution License (CC BY). The use, distribution or reproduction in other forums is permitted, provided the original author(s) and the copyright owner are credited and that the original publication in this journal is cited, in accordance with accepted academic practice. No use, distribution or reproduction is permitted which does not comply with these terms.



Three-Dimensional *in Vitro* Cell Culture Models in Drug Discovery and Drug Repositioning

Sigrid A. Langhans*

Nemours Center for Childhood Cancer Research and Nemours Center for Neuroscience Research, Alfred I. duPont Hospital for Children, Wilmington, DE, United States

OPEN ACCESS

Edited by:

Yuhei Nishimura,
Mie University Graduate School of
Medicine, Japan

Reviewed by:

Franz Rödel,
Universitätsklinikum Frankfurt,
Germany
Johannes F. W. Greiner,
Bielefeld University, Germany

*Correspondence:

Sigrid A. Langhans
sigrid.langhans@nemours.org

Specialty section:

This article was submitted to
Experimental Pharmacology and Drug
Discovery,
a section of the journal
Frontiers in Pharmacology

Received: 27 November 2017

Accepted: 03 January 2018

Published: 23 January 2018

Citation:

Langhans SA (2018)
Three-Dimensional *in Vitro* Cell Culture
Models in Drug Discovery and Drug
Repositioning. *Front. Pharmacol.* 9:6.
doi: 10.3389/fphar.2018.00006

Drug development is a lengthy and costly process that proceeds through several stages from target identification to lead discovery and optimization, preclinical validation and clinical trials culminating in approval for clinical use. An important step in this process is high-throughput screening (HTS) of small compound libraries for lead identification. Currently, the majority of cell-based HTS is being carried out on cultured cells propagated in two-dimensions (2D) on plastic surfaces optimized for tissue culture. At the same time, compelling evidence suggests that cells cultured in these non-physiological conditions are not representative of cells residing in the complex microenvironment of a tissue. This discrepancy is thought to be a significant contributor to the high failure rate in drug discovery, where only a low percentage of drugs investigated ever make it through the gamut of testing and approval to the market. Thus, three-dimensional (3D) cell culture technologies that more closely resemble *in vivo* cell environments are now being pursued with intensity as they are expected to accommodate better precision in drug discovery. Here we will review common approaches to 3D culture, discuss the significance of 3D cultures in drug resistance and drug repositioning and address some of the challenges of applying 3D cell cultures to high-throughput drug discovery.

Keywords: three-dimensional cell culture, hydrogel, spheroid, high-throughput screening, extracellular matrix

INTRODUCTION

With low success rates in clinical trials, drug discovery remains a slow and costly business. Currently, more than half of all drugs fail in Phase II and Phase III clinical trials due to a lack of efficacy and about another third of drugs fail due to safety issues including an insufficient therapeutic index (Arrowsmith and Miller, 2013). As attrition rates in drug discovery remain high, there is an urgent need for new technologies that accommodate better precision in drug discovery. Two of the most promising areas expected to improve the success rates in drug development are the advance of precision medicine with the prospect of new biomarkers and more precise drug targets and the availability of new preclinical models that better recapitulate *in vivo* biology and microenvironmental factors. Pioneered in the 1980's by Mina Bissell and her team performing studies on the importance of the extracellular matrix (ECM) in cell behavior, it is now well-accepted that culturing cells in three-dimensional (3D) systems that mimic key factors of tissue is much more representative of the *in vivo* environment than simple two-dimensional (2D) monolayers (Pampaloni et al., 2007; Ravi et al., 2015). While traditional monolayer cultures still are predominant in cellular assays used for high-throughput screening (HTS), 3D cell cultures

techniques for applications in drug discovery are making rapid progress (Edmondson et al., 2014; Montanez-Sauri et al., 2015; Sittampalam et al., 2015; Ryan et al., 2016). In this review, we will provide an overview on the most common 3D cell culture techniques, address the opportunities they provide for both drug repurposing and the discovery of new drugs, and discuss the challenges in moving those techniques into mainstream drug discovery.

THE EXTRACELLULAR MATRIX (ECM) AND OTHER MICROENVIRONMENTAL FACTORS INFLUENCING THE CELL PHENOTYPE AND DRUG RESPONSE

Extracellular Matrix Composition

Cell-based assays are a crucial element of the drug discovery process. Compared to cost-intensive animal models, assays using cultured cells are simple, fast and cost-effective as well as versatile and easily reproducible. To date, the majority of cell cultures used in drug discovery are 2D monolayers of cells grown on planar, rigid plastic surfaces optimized for cell attachment and growth. Over the past decades, such 2D cultures have provided a wealth of information on fundamental biological and disease processes. Nevertheless, it has become clear that 2D cultures do not necessarily reflect the complex microenvironment cells encounter in a tissue (**Figure 1**). One of the biggest influences shaping our understanding of the limited physiological relevance of 2D cultures is the growing awareness of the interconnections between cells and the extracellular matrix (ECM) surrounding them. Earlier thought to mostly provide structural support, ECM components (for a comprehensive review of ECM constituents see Hynes and Naba, 2012) are now known to actively affect most aspects of cellular behavior in a tissue-specific manner. ECM molecules include matrix proteins (e.g., collagens, elastin), glycoproteins (e.g., fibronectin), glycosaminoglycans [e.g., heparan sulfate, hyaluronan (HA)], proteoglycans (e.g., perlecan, syndecan), ECM-sequestered growth factors [e.g., transforming growth factor- β (TGF- β), vascular endothelial growth factor (VEGF), platelet-derived growth factor (PDGF), hepatocyte growth factor (HGF)] and other secreted proteins (e.g., proteolytic enzymes and protease inhibitors). Dynamic changes in these components regulate cell proliferation, differentiation, migration, survival, adhesion, as well as cytoskeletal organization and cell signaling in normal physiology and development and in many diseases such as fibrosis, cancer and genetic disorders (Bonnans et al., 2014; Mouw et al., 2014). Thus, it is not surprising that the composition of the ECM along with its physical properties can also influence a

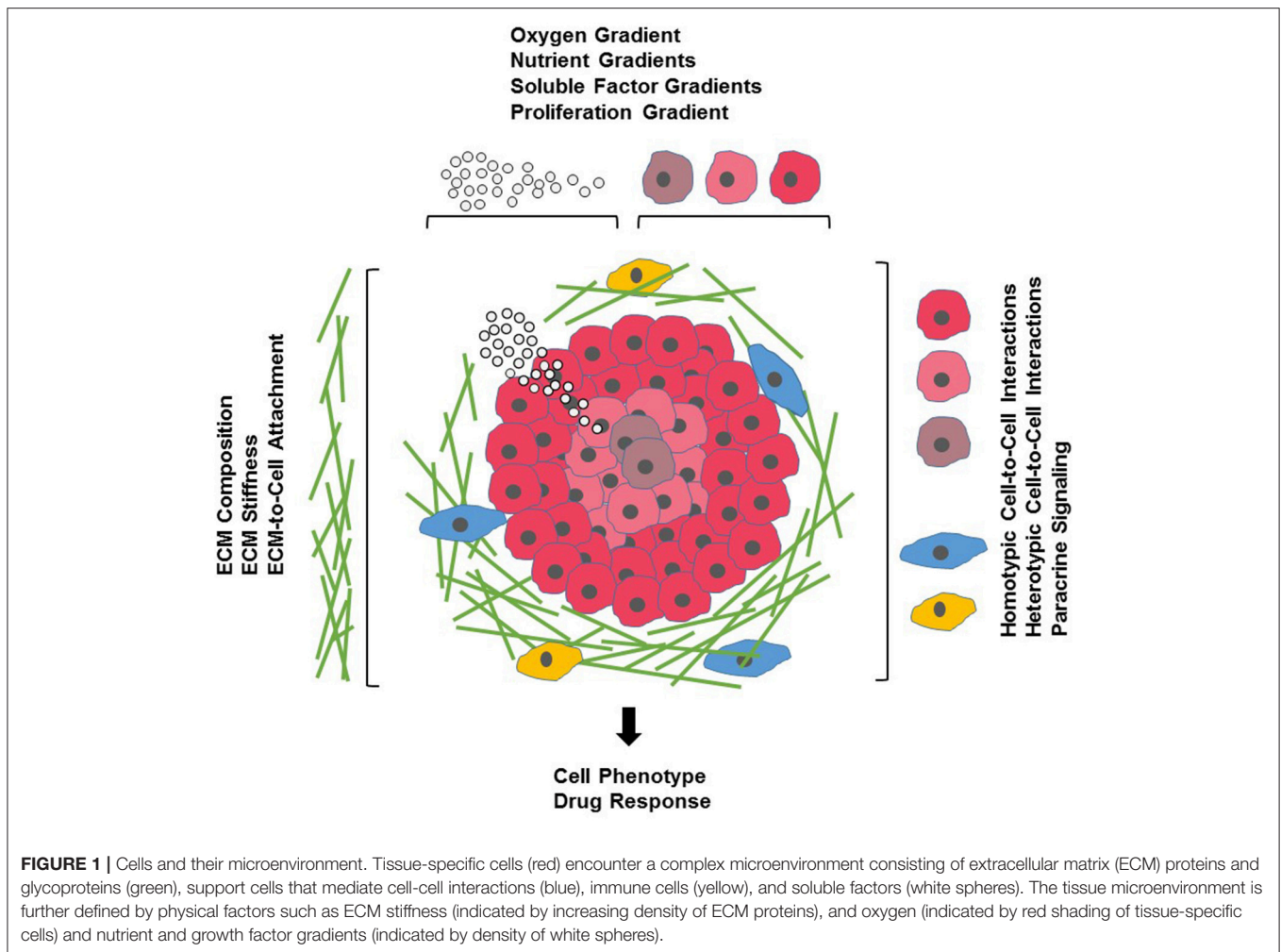
cell's response to drugs by either enhancing drug efficacy, altering a drug's mechanism of action (MOA) or by promoting drug resistance (Sebens and Schafer, 2012; Bonnans et al., 2014).

Much of our knowledge on how the ECM can affect drug response and contributes to drug resistance comes from studies on the interaction of cancer cells and the tumor stroma in hematological malignancies and solid tumors. The microenvironment of a tumor, comprised of non-tumor cells (such as fibroblasts, endothelial cells, adipocytes, and immune cells) and ECM, is highly variable and depends on tumor type and location. Changes in ECM composition may influence drug response through altered local drug availability, by affecting expression of drug targets, or by changing intrinsic cellular defense mechanisms such as increased repair upon DNA damage or evasion of apoptosis (Sebens and Schafer, 2012; Junttila and de Sauvage, 2013; McMillin et al., 2013; Holle et al., 2016). Interactions between cells and ECM can also lead to a heterogeneous drug response with matrix-attached outer cells being drug resistant and matrix-deprived cells in the core of the tumor being sensitive (Muranen et al., 2012). It is well documented that the adhesion between cells and ECM proteins, mediated mainly by the integrin system of transmembrane receptors, is an important factor modulating the response to chemotherapeutics and targeted therapies in oncology or to other therapeutic approaches such as immunotherapy, radiation or radiochemotherapy (Holohan et al., 2013; Holle et al., 2016; Dickreuter and Cordes, 2017; Jiang et al., 2017). Other ECM components such as heparan sulfate (Lanzi et al., 2017), hyaluronic acid (a physiological ligand for the cell surface receptor CD44 often found in cancer stem cell niches) (Bourguignon, 2016), soluble factors such as matrix metalloproteinases (MMPs) (Candido et al., 2016), tissue inhibitors of metalloproteinases (TIMPs) (DeClerck, 2000) and various cytokines and growth factors (Holohan et al., 2013), all have been shown to alter drug response and mediate drug resistance in cancer. For this reason, modern drug strategies take advantage of targeting the interactions between tumor cells and tumor-promoting microenvironmental factors. Such an approach requires cancer models that more faithfully mimic a tumor's microenvironment and makes cancer drug discovery the fastest growing application for 3D cell cultures. However, changes in drug response in response to ECM remodeling are not limited to tumors. For example, insulin resistance in obesity is known to be affected by EMC remodeling in adipose tissue (Williams et al., 2015; Lin et al., 2016) and cytokines, growth factors and ECM proteins play significant roles in the development of fibrotic diseases in many tissues including liver, lung and kidney (Wynn and Ramalingam, 2012; Bonnans et al., 2014; Handorf et al., 2015), requiring genuine culture models that can mimic *in vivo* conditions for such diseases.

Matrix Stiffness

The ECM is characterized by its biochemical composition and its physical and mechanical properties with tissue stiffness being important for the maintenance of homeostasis (Handorf et al., 2015). Changes in ECM composition are often accompanied by changes in physical cues such as rigidity, leading to

Abbreviations: 2D, Two-dimensional; 3D, Three-dimensional; bFGF, Basic fibroblast growth factor; CNS, Central nervous system; ECM, Extracellular matrix; EGF, Epidermal growth factor; HA, Hyaluronan/hyaluronic acid; HCS, High-content screening; HDP, Hanging drop plate; HGF, Hepatocyte growth factor; HTS, High-throughput screening; IGF-1, Insulin-like growth factor 1; iPSC, Induced pluripotent stem cell; MMP, Matrix metalloproteinase; NGF, Nerve growth factor; PDGF, platelet-derived growth factor; PEG, Polyethylene glycol; TGF- β , Transforming growth factor- β ; TIMP, Tissue inhibitor of metalloproteinase; VEGF, Vascular endothelial growth factor.



bidirectional changes in cells and the ECM (Hynes, 2014; Alcaraz et al., 2017; Zollinger and Smith, 2017). Cells can respond to mechanical forces through changes in cell division, morphogenesis, migration, signaling, gene expression, ion channel gating, or vesicle formation and by further remodeling of the ECM (Hamill and Martinac, 2001; Eyckmans et al., 2011; Tyler, 2012). The relationship between tissue stiffness and cell phenotype and cell function has been well described in tumors and in the brain. Tumors are usually stiffer than surrounding healthy tissue and tissue stiffness can contribute to drug resistance (Holle et al., 2016; Bordeleau et al., 2017; Lin et al., 2017). In the brain, tissue stiffness is a major factor in development and brain plasticity (Tyler, 2012; Barnes et al., 2017). With brain being one of the softest tissues in the body, its ECM is characterized by a relative low abundance of matrix proteins and a high prevalence of glycosaminoglycans, proteoglycans and glycoproteins, some of which are brain-specific. This leads to cell-ECM interactions that are not only mediated by integrins, but also by a variety of tissue-specific non-integrin receptors predominantly found in neurons and glial cells (Barros et al., 2011). The stiffness of brain regions varies in normal brain and mechanical properties change with

age (Happel and Frischknecht, 2016) and in a wide range of neurological disorders, including multiple sclerosis, Alzheimer's disease, epilepsy and schizophrenia (Tyler, 2012; Murphy et al., 2016). The unique composition of brain ECM together with its well-established roles in neurotransmitter function and receptor turnover, ion channel activity, synaptic plasticity and dendritic spine formation (Frischknecht and Gundelfinger, 2012) gives rise to the need of cell culture models that reflect the complexity of the brain ECM surrounding neurons and glial cells such as astrocytes, oligodendrocytes and microglia. With drug failure in neurological disorders exceeding that in many other diseases, 3D culture models are promising technologies to meet the challenge of developing more realistic *in vitro* disease models for CNS drug discovery.

Concentration Gradients

Within a tissue, concentration gradients exist for oxygen, pH and soluble components such as nutrients and effector molecules as well as cellular metabolites. These natural gradients are influenced by the proximity to blood vessels, by the diffusion of molecules through the ECM, and thus, the composition of the ECM, and by the extent of cellular metabolism that regulates

oxygen and nutrient consumption and the production of cellular waste products. Molecular concentration gradients affect various cell behavior, including cell motility, cell migration, and cell signaling and are important in chemotaxis and morphogenesis in normal development and in wound healing. Depending on the proximity to a blood vessel, small, avascular tumors or metastasis often display a gradient in oxygen levels leading to a proliferative zone and a hypoxic core with quiescent cells that are more resistant to chemotherapy, immunotherapy and radiation therapy (Herrmann et al., 2008; Carrera et al., 2010; Chouaib et al., 2017). Traditional monolayer cultures are not amenable to studies of oxygen or nutrient gradients as all cells are homogeneously exposed to the tissue culture medium. In *in vivo* models, hypoxia occurs naturally or can be induced. However, these are complex models and are associated with high cost and variability. Thus, 3D cultures such as spheroids, cells encapsulated into 3D matrices and microdevice platforms provide opportunities to understand oxygen, growth factor and nutrient-mediated mechanisms leading to changes in cell phenotype and alterations in drug response.

Stromal Cells

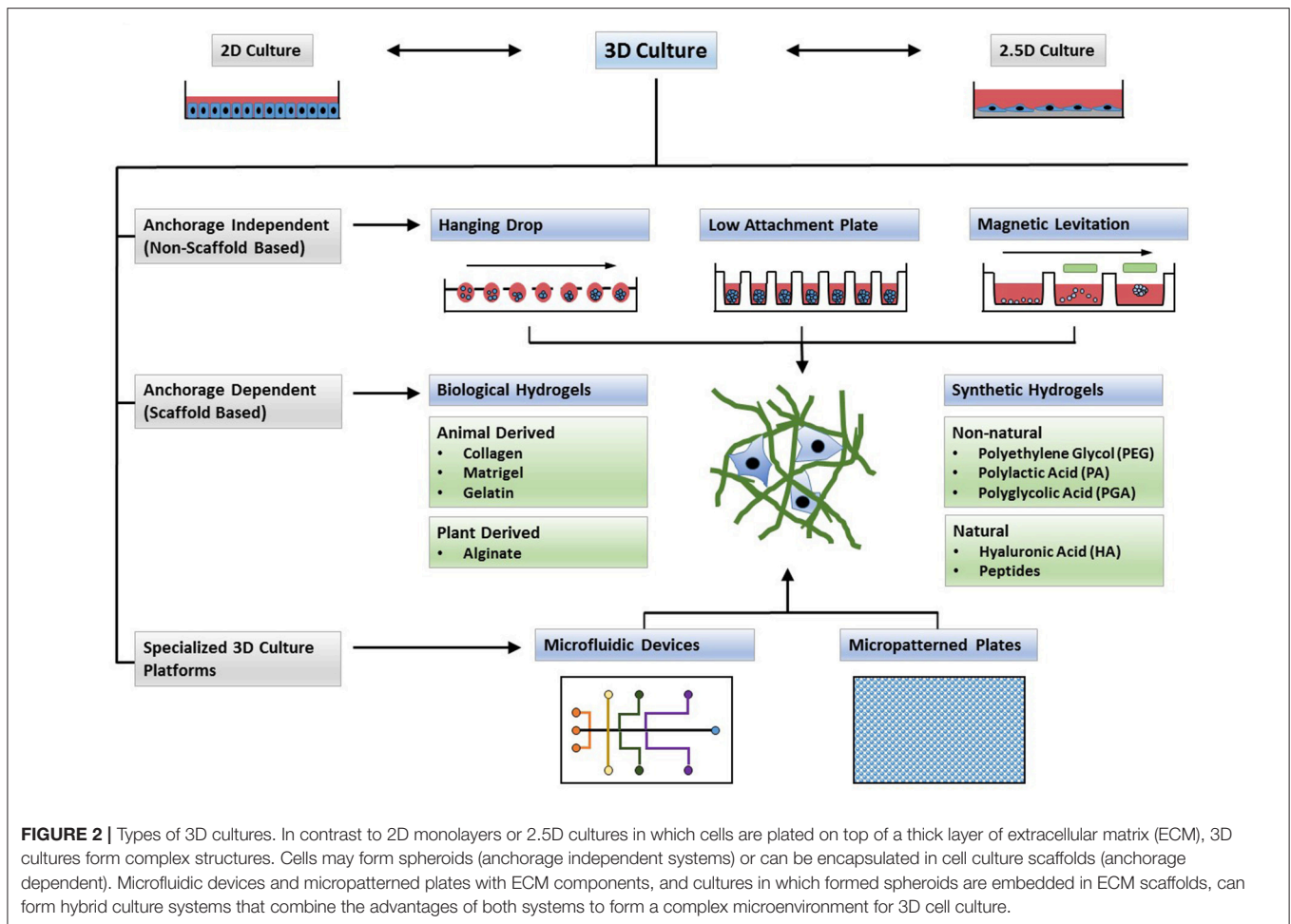
In vivo, cells are not only surrounded by ECM and ECM-associated signaling molecules, but connective tissue also contains stromal cells, including mesenchymal supporting cells such as fibroblasts or adipocytes in epithelial tissue, glial cells in neuronal tissue, cells of the surrounding vasculature and cells of the immune system. Interactions with stromal cells can regulate surrounding epithelial and neuronal tissue, contribute to disease progression and influence the therapeutic response of cells. In tumors, carcinoma-associated fibroblasts can stimulate tumor cell growth, induce angiogenesis and promote inflammation and stromal cells within cancer stem cell niches drive drug resistance (Egeblad et al., 2010; Jones et al., 2016; Prieto-Vila et al., 2017). During the angiogenic switch of tumors, vasculogenesis involves the recruitment of endothelial cells, perivascular cells and bone marrow-derived cells, a process that cannot only be exploited for cancer therapy but for which the stromal environment is an important factor in regulating drug response (Crawford and Ferrara, 2009; Egeblad et al., 2010; Gacche, 2015; Lopes-Bastos et al., 2016; De Palma et al., 2017). Inflammatory cells are components of normal tissue and play an important role during normal development. At the same time, stromal immune cells contribute to a variety of diseases ranging from diabetes to atherosclerosis, fibrosis, cancer and neurodegeneration (Wynn et al., 2013). While targeting stromal immune cells is a promising strategy for the development of novel therapeutics for a wide range of diseases (Kersh et al., 2018) and recently has gained wide attention in cancer drug discovery and for the therapy of neurological diseases (Villoslada et al., 2008; Pitt et al., 2016; Alsaab et al., 2017; Chitnis and Weiner, 2017; Kabba et al., 2017; Pogge von Strandmann et al., 2017), immune cells also modulate therapeutic response to drugs not directly targeting the immune system (Kersh et al., 2018). In drug discovery, *in vitro* modeling of such complex interactions will require multicellular 3D tissue models with organoids currently being at the forefront for disease modeling, drug screening and drug development.

3D Cell Culture Models

An ideal 3D culture model would simulate a tissue-specific physiological or pathophysiological disease-specific microenvironment where cells can proliferate, aggregate and differentiate. Such a model would include cell-to-cell and cell-to-ECM interactions, tissue-specific stiffness, oxygen, nutrient and metabolic waste gradients, and a combination of tissue-specific scaffolding cells (Griffith and Swartz, 2006). Most 3D culture techniques, often categorized into non-scaffold, anchorage-independent and scaffold-based 3D culture systems as well as hybrid 3D culture models in which formed spheroids are incorporated into a 3D polymeric scaffold (Ho et al., 2010), currently do not meet all of the above criteria but rather have their own strengths and limitations. Thus, one will need to choose the most appropriate 3D cell culture model for a specific application. For example, scaffold-based models more readily mimic cell-to-ECM interactions while non-scaffold based spheres of certain size are more amenable to cellular and physiological gradients. Traditional 3D cell culture models such as spinner flasks (Sutherland et al., 1970) or gyratory rotation devices (Goodwin et al., 1993; Breslin and O'Driscoll, 2013) provide large-scale methods to generate 3D spheres but lack the possibility for miniaturization and are not compatible with HTS methods. Many of the newer 3D culture systems (Figure 2) allow for microscale 3D cultures and provide a first step toward developing technologies for 3D cultures that are compatible with automated high-throughput screening allowing for the discovery of new drug candidates or repositioning of known drugs in physiologically more relevant cell cultures.

Anchorage-Independent Technologies

Scaffold-free 3D culture methods rely on the self-aggregation of cells in specialized culture plates, such as hanging drop microplates, low adhesion plates with ultra-low attachment coating that promotes spheroid formation and micropatterned plates that allow for microfluidic cell culture. Spheroids, and in particular multicellular spheroids (Mueller-Klieser, 1987; Sutherland, 1988), recapitulate physiological characteristics of tissues and tumors with regard to cell-cell contact, and if synthesizing their own ECM, allow for natural cell-matrix interactions. Spheroid size depends on the initial number of cells seeded and spheroids can be grown to a size where they display oxygen and nutrient gradients similar to tissue (Cukierman et al., 2001; Doublier et al., 2012; Ekert et al., 2014). Neurospheres are spheres of mixed cultures of progenitors, neuronal and glial cells. While they consist mostly of poorly differentiated cells, neurospheres allow for interactions between different cell types of the CNS. These interactions play important roles in neuronal differentiation, in the conversion of toxic compounds into active metabolites, and in the secretion of apoptotic factors upon drug treatment; thus neurospheres allow for CNS drug discovery in a physiologically more relevant culture system (Campos, 2004; Moors et al., 2009). Tumor spheroid models derived from established cell lines or obtained through *ex vivo* propagation of tumors from individual patients (tumor organoids) have been established for a variety of tumor types. Tumor spheroids from patients retain their genome over time and can be used



to perform drug screens and facilitate drug development in a patient-centered manner (Stadler et al., 2015; Nath and Devi, 2016; Pauli et al., 2017; Weeber et al., 2017). The disadvantage of spheroid cultures, whether tumor spheroids or neurospheres, however, is the need for much optimization of culture conditions to obtain uniform spheroids to enhance reproducibility and of size not too large to prevent insufficient nutrient supply and necrosis.

Hanging Drop Microplates

Hanging drop cultures are a well-known 3D culture technology taking advantage of self-aggregation of cells into spheroids when a surface is not available for cell attachment. Hanging drops can be created in specialized plates with open, bottom-less wells that are designed for the formation of a small droplet of media. The droplet is big enough for cells suspended in the medium to aggregate but small enough to prevent it from being dislodged during manipulation. Cultured for several days, cells in hanging drop plates (HDP) can form spheres that may represent tumor layers in the vicinity of a capillary—a peripheral layer with proliferating cells due to the closeness to the supply of oxygen and nutrients, underlaid by an intermediate layer with quiescent cells and an inner necrotic core. With this, spheres can mimic

inward diffusion to form oxygen and nutrient gradients, model in- and outward diffusion of regulatory molecules, and provide a reservoir for the accumulation of waste, accompanied by low pH. The spheroid size can be controlled by the initial number of cells suspended in the drops but may require transfer from an HDP plate to a second non-attachment propagation plate with higher media volume to ensure suitable culture conditions with adequate nutrient supply and pH over longer times and to allow for the formation of bigger spheres. Multi-cellular spheres may be created by co-suspending several cell types or by consecutive addition of different cell types to promote the formation of separate cell layers. Embedding of formed spheres into ECM-like scaffolds allows for the modeling of cell adhesion of the outer layers of the spheres with ECM components surrounding tumor tissues. Spheroids formed in HDP plates as well as in low adhesion plates described below have evolved into a common 3D cell culture technology in cancer research, examples of which are described in a comprehensive review by Stadler et al. (2015). Hanging drop cultures have also found applications in toxicity testing in hepatocytes (Shri et al., 2017) or in engineering cardiac spheroids (Chitnis and Weiner, 2017). In a recent study, human primary or induced pluripotent stem cell (iPSC)-derived cardiomyocytes were co-cultured with endothelial cells

and fibroblasts in a ratio similar to that found *in vivo*. The cardiac spheroids mimicked important *in vivo* features of the human heart biochemically and pharmacologically offering a 3D cell culture model to study toxic effects in human heart tissue (Polonchuk et al., 2017).

Spheroid Microplates with Ultra-Low Attachment Coating (Low Adhesion Plates)

Similar to HDP cultures, spheroid microplates with round, tapered or v-shaped bottoms, take advantage of the lack of cell attachment surfaces to promote aggregation of cells and spheroid formation. In contrast to HDP cultures, however, a transfer of spheroids to a different plate for prolonged culture or experimental procedures is often not necessary. 96- or 384-well plates have an initial higher volume capacity than droplets and eliminate steps that would involve the need for manipulating spheroids. Low adhesion plates are often made of polystyrene and treated with hydrophilic or hydrophobic coatings like the non-adherent polymer poly-HEMA (Ivascu and Kubbies, 2006) or natural polymers such as agarose (Friedrich et al., 2009; Li et al., 2011). The coating reduces the attachment of cells to the point that they preferably aggregate with each other to form spheroids. Because of their larger volume, low adhesion plates are well suited for multicellular culture and are frequently used for studies in tumor cells. For example, when grown on chitosan-hyaluronan substrates, multicellular spheres formed from two non-small cell lung cancer (NSCLC) cells exhibited more stem-cell like characteristics, an increase in cell motility and expression of markers for epithelial-to-mesenchymal transition (EMT), and the stem-cell like cells displayed multidrug resistance when compared to 2D cell cultures (Huang and Hsu, 2014). Spheroids, but not 2D cultures, of patient-derived breast cancer cells simulated tumor characteristics *in vivo* such as hypoxia, dormancy, anti-apoptotic features and drug resistance (Imamura et al., 2015). Another recent study took advantage of forming brain tumor spheres in a mixed-neuronal culture environment by co-culturing brain tumor cells with human fetal brain tissue to develop an *in vitro* model for drug delivery assessments in pediatric medulloblastoma (Iskandar et al., 2015).

Magnetic Levitation

Magnetic cell levitation is an emerging technique for the formation of spheroids. To generate spheroids, cells are preloaded with magnetic nanoparticles and then, using an externally applied magnetic field, are floated toward the air/liquid interface within a low adhesion plate to promote cell-cell aggregation and spheroid formation. Magnetic levitation has been used to generate spheroids from cells of various tissue, to form multicellular mesenchymal stem cells spheroids and for tissue engineering (Souza et al., 2010; Haisler et al., 2013; Tseng et al., 2013; Lewis et al., 2016, 2017). Magnetically levitated human glioblastoma cells closely recapitulated *in vivo* protein expression observed in human glioblastoma tumor xenografts (Souza et al., 2010) and recently, a high-throughput assay for toxicity screening in 3D cell cultures using magnetic levitation was described, making this a promising new technique in drug discovery (Timm et al., 2013).

Scaffold-Based Technologies

Scaffold-based culture technologies provide physical support, ranging from simple mechanical structures to ECM-like matrices, on which cells can aggregate, proliferate and migrate. In 2.5D cultures, cells are grown on top of a thick layer of ECM proteins that allows for tissue-specific differentiation of a variety of cells. Nevertheless, such cultures do not necessarily represent an *in vivo* environment as cells are still exposed to tissue culture medium and lack ECM contact on the surface (Shamir and Ewald, 2014). In scaffold-based 3D cultures, cells are embedded into the matrix and the chemical and physical properties of the scaffold material will influence cell characteristics. Scaffolds can be of biological origin or they can be synthetic engineered to mimic key properties of ECM such as stiffness, charge or adhesive moieties. In some synthetic scaffolds, growth factors, hormones or other biologically active molecules can be encapsulated to enhance cell proliferation or to promote a specific cell phenotype. Thus, when selecting a 3D cell culture scaffold for a certain application, one will need to consider properties of the material that define physical factors such as porosity, stiffness and stability in culture as well as biological properties such as cell compatibility or adhesiveness (Caliari and Burdick, 2016). Hard polymers can provide the physical support found in a specialized tissue, such as skin, tendons or bone and micropatterned surface microplates can be designed for specific applications such as support of cell networking.

Hydrogel Scaffolds of Biological Origin

Hydrogels are networks formed from dilute polymer chains with given structure and properties, obtained either by intermolecular (polymer network) or by interfibrillar crosslinks (supramolecular fibrillary hydrogel network) (Tibbitt and Anseth, 2009; Li and Deming, 2010; Yan and Pochan, 2010; Worthington et al., 2015). Although hydrogels display solid-like material properties in the quiescent state, with over 95% of water by volume, they can indeed provide a cell-liquid interface (Sathaye et al., 2015). Hydrogels may come from natural sources or can be synthetic, with the possibility of mixing different hydrogel materials to obtain hybrid hydrogels possessing new physical and biological properties. Hydrogels from natural sources such as collagen, fibrin or Matrigel are biocompatible, have natural adhesive properties and sustain many physiological cell functions—resulting in high cell viability, controlled proliferation or controlled differentiation, and often a cell phenotype typically observed *in vivo*. Collagen, with type I collagen being the most abundant form, is the most widely used ECM protein for 3D cell culture (Glowacki and Mizuno, 2008; Pathak and Kumar, 2011; Orgel et al., 2014). Altering collagen concentrations or gelation temperature leads to changes in collagen hydrogel stiffness allowing for controlled changes in cell proliferation (Kutschka et al., 2006; Doyle et al., 2015) and, depending on collagen stiffness, pancreatic cancer cells respond differently to gemcitabine (Puls et al., 2017). Collagen, as well as Matrigel, facilitate cell attachment through integrin receptors which leads to activation of cell signaling pathways that control cell survival, growth and differentiation (Yang et al., 2004; Kutschka et al., 2006) and can modulate the response to therapeutic approaches,

including chemotherapy, immunotherapy and radiation (Holle et al., 2016; Dickreuter and Cordes, 2017). For example, comparison of drug response profiles of breast, prostate and lung cancer cell lines revealed clear differences in dose response curves to docetaxel and fulvestrant when cells were grown in collagen and compared to 2D cultures or other 3D culture systems such as low attachment plates and other natural scaffolds, including alginate and Matrigel (Stock et al., 2016). Multiple myeloma cells cultured in a Matrigel-based human bone marrow-like microenvironment provide a system for preclinical testing of chemotherapeutics that take into account adhesion-mediated mechanisms of drug resistance (Kirshner et al., 2008) and Matrigel-embedded 3D-tumoroids derived from tissue of patients with colorectal cancer and lung cancer can provide a 3D culture system for drug testing that contains not only tumor cells but also immune cells from surrounding tissues (Finnberg et al., 2017). Matrigel and similar products are a gelatinous mixture of proteins and growth factors secreted by Engelbreth-Holm-Swarm mouse sarcoma cells (Kleinman and Martin, 2005). Since Matrigel is minimally processed, it provides a good mimic of *in vivo* ECM (Poincloux et al., 2011; Wong et al., 2011). Matrigel consists mostly of laminin and collagen as well as a small fraction of entactin (a basement membrane glycoprotein) and contains several growth factors, including EGF (epidermal growth factor), bFGF (basic fibroblast growth factor), NGF (nerve growth factor), PDGF, IGF-1 (insulin-like growth factor 1) and TGF- β (Hughes et al., 2010). Since Matrigel is processed from natural sources, batch-to-batch variability of the purified scaffold may interfere with pharmacological studies of drug response. A growth-factor reduced formulation of Matrigel is available, allowing for a 3D culture setup with more defined properties (Wallace and Rosenblatt, 2003). Nevertheless, due to the natural origin and manufacture from live tissue, collagen and Matrigel are complex scaffolds that contain besides their major constituents many other components and are therefore chemically not well defined (Hughes et al., 2010; Gill and West, 2014). While collagen and Matrigel both support enhanced interaction of cells with ECM proteins, due to their different composition, cells embedded into collagen or Matrigel can display different phenotypes (Borlak et al., 2015). Collagen and Matrigel are available in liquid form and require handling at cold temperatures to avoid premature gelation. The need for handling these hydrogels at low temperatures makes them unsuitable for common liquid handling equipment used for high-throughput screens in drug discovery (Ryan et al., 2016; Worthington et al., 2017). Fibrin is obtained through polymerization of fibrinogen, a plasma protein, and is a natural polymer formed during wound coagulation. While it has been used for *in vitro* cultures, including angiogenesis studies, biomechanical studies and mesenchymal stem cell culture, its high susceptibility to protease-mediated degradation limits its use in long-term cultures (Ahmed et al., 2008; Anitua et al., 2013; Kural and Billiar, 2013; Brown and Barker, 2014; Caliarì and Burdick, 2016). Gelatin is a partial thermally and chemically degraded product of collagen and can be stabilized by covalent modification. The possibility of covalent linking of functional groups also allows for the production of specialized gelatin gels, that for

example can be photoreactive (Banks et al., 2015) or oxygen-controllable to form hypoxic gradients in 3D cultures (Lewis et al., 2017). Another natural hydrogel is alginate that is isolated from the cell walls of brown algae. The mechanical properties and rapid degradation of the alginate hydrogel somewhat limits its application for 3D cultures but alginate hydrogels have found their use as 3D-printed scaffolds for specialized tissue such as vascular tissue, bone and cartilage (Axpe and Oyen, 2016; Joddar et al., 2016; Silva et al., 2017).

Synthetic Hydrogels

When well-designed, synthetic hydrogels are ideal materials to use as 3D cell culture scaffolds as they can mimic biological properties of ECM, be functionalized with defined adhesive moieties, include proteolytic sites and encapsulate growth factors. At the same time, they are chemically and physically well-defined and often have tunable mechanical properties to achieve a desired stiffness or porosity (Worthington et al., 2015; Zhang and Khademhosseini, 2017). Synthetic hydrogels can be categorized into non-natural and natural polymers. Polyethylene glycol (PEG), polylactic acid (PA), polyglycolic acid (PGA) and other unnatural polymer hydrogels (Raeber et al., 2005; Zhang and Khademhosseini, 2017) have the advantage of being comparatively inexpensive, are relatively inert, have reproducible material properties that are usually easy to tune through synthesis or crosslinking, and are reproducible, thereby supporting the acquisition of consistent results. On the other side, however, unnatural polymers lack adhesive moieties found in natural ECM and require crosslinking of biological peptides to the scaffold to improve functionality (Weber et al., 2007; Kraehenbuehl et al., 2008). PEG gels and their derivatives have been used in a variety of 3D cell culture applications including stem cell differentiation, cell invasion and angiogenesis (Lutolf et al., 2003; Moon et al., 2010; Zhu, 2010; Caiazzo et al., 2016). Synthetic natural polymers share with non-natural polymers the advantage of consistent and tunable material properties for reproducible results. Due to the biological nature of their naturally occurring moieties, natural synthesized hydrogels are highly compatible with encapsulation of cells for 3D cell culture. However, material cost can be high due to complex chemical synthesis requirements. One of the best characterized natural hydrogels is hyaluronic acid (HA)—a glycosaminoglycan that can be modified with functional groups, allowing for the formation of hydrogels with diverse properties for a wide range of applications (Burdick and Prestwich, 2011; Baeva et al., 2014; Goubko et al., 2014). Small peptide-based hydrogel materials are an evolving field in materials science and provide a new 3D cell culture technology that is amenable to drug discovery studies. Recently, a peptide-based 3D mesenchymal stem cell co-culture model of the multiple myeloma bone marrow niche has been described where patient-derived tumor cells displayed resistance to chemotherapeutics that was reflective of clinical resistance and thus, may provide a technology platform for drug testing and precision medicine in multiple myeloma patients (Jakubikova et al., 2016). While diverse in primary structure, the peptides have a similar overall ability to form nanofibrillar structures with

intramolecular folding and intermolecular assembly triggered by physical or chemical cues. Peptide hydrogels are highly versatile and material properties can be modulated by substituting amino acids, extending or shortening the peptide sequence, or by the addition of functional epitopes (Branco et al., 2011; Yang and Zhao, 2011; Li et al., 2013; Wang et al., 2013; Worthington et al., 2015). Current peptide hydrogels that are most successfully used for 3D culture (reviewed in Worthington et al., 2015) are: the yeast-derived peptides EAK16 and RADA16 (Zhang et al., 1992, 2005); the peptides Fmoc-FF (Fluorenylmethoxycarbonyl-diphenylalanine) and Fmoc-RGD (Fluorenylmethoxycarbonyl-arginine-glycine-aspartic acid) (Jayawarna et al., 2006; Mahler et al., 2006; Smith et al., 2008; Orbach et al., 2009; Zhou et al., 2009); the peptide hydrogel h9e that is based on the fusion of functional domains from a silk protein and a human calcium channel (Huang and Sun, 2010; Huang et al., 2011, 2013); FEFK and FEFKEFK, which form hydrogels in the presence of a metalloprotease (Toledano et al., 2006; Guilbaud et al., 2010); and the MAX1 peptide that gels under physiological conditions, and like h9e, has shear-thinning properties (Schneider et al., 2002; Haines-Butterick et al., 2007). A single acid substitution derivative of the MAX1 peptide, MAX8 (Haines-Butterick et al., 2007), with reduced gelation times has recently been reported to be compatible with liquid handling equipment making it suitable for high-throughput drug discovery (Worthington et al., 2017).

Polymeric Hard Scaffolds, Micropatterned Surface Microplates, and Microfluidic Devices

Microfabrication technology allows for the fabrication of an endless array of imprinted micropatterns on the surface of plates. Coated for low adhesion, the micro-patterned plates can be designed to promote cell-to-cell adhesion for scaffold-free microsphere formation within the confinement of a microspace. Micropatterned plates can also be manufactured to provide a scaffold-based 3D culture environment to promote cell attachment for the formation of contiguous networks along surfaces and organoids. Polymeric pre-fabricated scaffolds, such as porous discs, electrospun scaffolds or orthogonally layered polymers, are physical supports that can be an inert matrix or designed to mimic *in vivo* ECM on which cells can attach, migrate or fill scaffold compartments to form 3D cultures carrying a geometric configuration (Knight et al., 2011). Currently, the most common applications for such scaffolds are for tissue regeneration recreating the natural physical and structural environment of bone, ligaments and cartilage, for skin, vascular, skeletal muscle or CNS tissue and for preclinical *in vitro* 3D culture testing of tumoroids or engineered tissues (organoids). In particular, tumoroids derived from patient samples are promising techniques for drug screening and drug development in precision medicine (Stadler et al., 2015; Nath and Devi, 2016; Pauli et al., 2017; Weeber et al., 2017). Recently, a microspun 3D fibrous scaffold for tumoroid formation was developed as a platform for anticancer drug development (Girard et al., 2013). When compared to 2D monolayers, HepG2 liver cells

grown on 3D porous polystyrene scaffolds had greater cell viability and formed bile canaliculi, and at the same time were less susceptible to cytotoxic compounds (Bokhari et al., 2007). Microfluidic devices are designed for cell cultures under perfusion and allow for steady supplies of oxygen and nutrients while at the same time removing waste. Microfluidic devices can be built to mimic shear forces found *in vivo* in cells that are exposed to blood flow like endothelial cells. A barrier between compartments can be physically incorporated into the device or it can consist of a non-physical barrier such as a supporting matrix mimicking ECM. Microfluidic devices allow for the continued application of drugs or other soluble molecules such as growth factors, or the exchange of fluid between different compartments that may harbor different types of cells. Microfluidic devices can be used for long-term tumoroid cultures (Aw Yong et al., 2017) and Montanez-Sauri, et al recently described an automated microfluidic ECM screening platform with the capability for small molecule screening (Montanez-Sauri et al., 2013). Microengineering of microfluidic devices also allows for the development of organ-on-a-chip platforms with 3D tissue models having been described for a variety of organs including skin, muscle, liver and neural tissue, bridging *in vitro* cell culture and *in vivo* animal models. With the advancement of these 3D culture technologies, organs-on-a-chip are poised to provide advanced tools for drug development and high-throughput screening in the future (Alépée et al., 2014; Pamies et al., 2014; Abaci et al., 2017).

Organoids

Originally, the term organoid referred to primary cultures of tissue fragments separated from the stroma within 3D gels to form organ-like structures (Simian and Bissell, 2017). Over the past decade, the term organoid has broadened and now encompasses a variety of tissue culture techniques that result in self-organizing, self-renewing 3D cultures derived from primary tissue, embryonic stem cells, or induced pluripotent stem cells that have a similar functionality as the tissue from which the cells originate (Lancaster and Knoblich, 2014; Shamir and Ewald, 2014; Clevers, 2016; Fatehullah et al., 2016; Kretzschmar and Clevers, 2016; Simian and Bissell, 2017). While current organoid cultures often still face limitations, such as the lack of a native microenvironment (e.g., ECM composition, growth factor gradients) or the lack of interactions with immune cells and, consequently, the inability to model immune responses, organoids derived from human cells have the potential to provide near-physiological models to study human development and human diseases. With this, more advanced organoid cultures will allow for developing screening platforms for drug discovery that are more cost-effective than animal models and can provide precise models of human diseases that cannot be recapitulated in animals. Organoid cultures have been described for a variety of organs, including various normal tissue and disease models of the digestive tract, prostate, lung, kidney and the brain (Clevers, 2016; Fatehullah et al., 2016; Dutta et al., 2017). Currently, transcriptome profiling is one of the most common downstream applications of organoids but applications in drug discovery and precision therapy are evolving

(Fatehullah et al., 2016; Liu et al., 2016). For example, kidney organoids have been used for toxicity screening in response to cisplatin (Takasato et al., 2015), an organoid model of cystic fibrosis for drug screening has been described (Dekkers et al., 2013) and a high-throughput platform for intestinal stem cell niche co-cultures has been developed (Gracz et al., 2015). Beyond such organoids, tumoroids derived from patient cancer tissues that contain tumor cells and stroma cells of the tumor microenvironment are poised to provide advanced and more realistic 3D culture platforms for personalized drug evaluation and development (Xu et al., 2014; Stadler et al., 2015; Pauli et al., 2017). Further, tumoroids that retain tissue identity, paired with organoids of adjacent healthy tissue, can lay the foundation to construct tumor organoid biobanks as repository for drug screening and development (van de Wetering et al., 2015).

Applications of 3D Cultures in Drug Discovery and Drug Repositioning

In the past, cell-based drug discovery emphasized chemical screens in well-characterized cell monolayers, and mostly in cancer drug discovery, in large panels of authenticated cell lines (Smith et al., 2010; Barretina et al., 2012). However, in recent years, 3D cell culture systems that model *in vivo* microenvironmental aspects, and are therefore expected to yield results with higher predictive value for clinical outcome, are becoming more prominent in drug discovery. In addition, authentic 3D cell culture models using human cells can circumvent drawbacks of mouse models that, aside from the high cost and ethical considerations, are not always able to accurately recapitulate human diseases or capture side effects of drugs such as liver toxicity (Sivaraman et al., 2005; Aparicio et al., 2015). In order to enhance the drug discovery process, aid in the development of new pharmacological approaches or to be useful *in vitro* toxicity screens, 3D cell culture models will need take into account that the response to a broad spectrum of drugs varies not only with a particular cell line or tumor type, but also with its surrounding stroma. The response to therapeutic compounds may range from drug resistance to enhanced sensitivity based on tissue-specific composition of the ECM, the interaction with stromal cells and the presence of immunomodulatory molecules (Turley et al., 2015; Johansson et al., 2016; Stock et al., 2016). While research into new 3D culture technologies that take into account the functional unit of tissues such as organoids has gained great momentum (Lancaster and Knoblich, 2014; Shamir and Ewald, 2014; Clevers, 2016; Kretzschmar and Clevers, 2016; Simian and Bissell, 2017), much work remains to be done to develop systems that accurately represent *in vivo* conditions and disease pathology. At the same time, 3D cell cultures open up the door to model the cell culture environment to promote a desired cell behavior. Models focused on enhanced cell motility, induction of cell dormancy, promotion of cell differentiation in epithelial cells and neurons, the support of stem cell-like properties or a desired microenvironment like that of a metastatic niche (Valastyan and Weinberg, 2011; Sleeman, 2012), enable the possibility

of more specifically targeting certain cell behavior in drug discovery. In addition, cancer drug discovery combining 3D cell culture technology with primary patient-derived tumor cells (Ma et al., 2015), and molecular profiling data or the formation of 3D organoid banks of tumor cells that are representative of molecular tumor subtypes (van de Wetering et al., 2015), may open the door for preclinical screening of a personalized panel of drug candidates to improve outcome and reduce side effects of cancer therapy.

Limitations of 3D Cell Culture Technologies in Drug Discovery

High-throughput screening (HTS) to determine the biological or biochemical activity of chemically diverse small compound libraries or high-content screening (HCS) used to identify compounds that alter a cell's phenotype is an integral part of drug discovery. Application of 3D cell culture in HTS and HCS, however, remains a challenge (Rimann and Graf-Hausner, 2012; Edmondson et al., 2014; Montanez-Sauri et al., 2015; Ryan et al., 2016). Aside from the question of biological and disease relevance, labor intensiveness and material cost, scalability to 384- and 1,536-well plates, reproducibility, incorporation into an automated screening setup and compatibility with currently available assay and detection methods are areas of concern (Janzen, 2014). In HCS, one of the biggest challenges to overcome will be the visualization of 3D structures with automated imaging systems. Optical light scattering, light absorption and poor light penetration with prolonged imaging acquisition times, and imaging of multicellular cultures and cells grown within complex geometrical structures, currently limit the applications of 3D cultures in HCS. One of the biggest challenges of incorporating 3D cultures into HTS will be to design systems that are compatible with liquid handling equipment. The hanging drop culture is the spheroid technology that has most advanced toward use in HTS. HDPs are available in 96- and 384-well formats but they require significant expertise in the use of the technology within a HTS setup. Collagen and Matrigel are commonly used hydrogels, but their natural origin limits the possibility of mimicking different tissue environments, the variations of different preparations impacts reproducibility, and their gelation properties prevent the handling at ambient temperature. Despite these challenges, HTS-compatible screening platforms are emerging. Synthetic matrices, while costly, have the advantages of providing defined, designed, and tunable material properties and allow for the controlled inclusion of biochemical cues. Self-assembling peptide hydrogels do not require covalent crosslinking reactions and can assemble into a defined hydrogel at physiological conditions. We have recently described an injectable hydrogel that flows under shear and is compatible with standard liquid automated handling equipment to form reproducible 3D cultures in 384-well plates (Worthington et al., 2017). The next step will be to build a 3D culture system that is versatile enough to enter mainstream drug discovery but can easily be fine-tuned to meet the tissue-specific characteristics of an *in vivo*-like microenvironment.

CONCLUSIONS

The field of 3D cultures has grown exponentially in the past few years and offers considerable promise with broad applications in drug development and toxicity testing for a wide variety of diseases ranging from cancer to fibrosis to cardiac and neurological disorders. The major challenge will remain the creation of 3D cultures which are biologically relevant and recapitulate microenvironmental factors that resemble *in vivo* tissue and disease pathology. Given that the ECM alone has more than 300 biochemical constituents not including cellular components, this remains a daunting task. Nevertheless, with an increasing list of available 3D cell culture methods, we can take advantage of technologies that are most appropriate for a particular purpose such as mimicking a tumor environment or brain-specific matrix with appropriate tissue stiffness, recreation of a tissue barrier, or other specialized technical application. By combining biomedical engineering knowledge in the design

of 3D scaffolds with knowledge of disease mechanism and biomarkers and genomic data, informed decisions can be made for the specific design of biomimetic scaffolds that most closely recapitulate factors promoting a particular disease phenotype, moving 3D drug discovery into the age of precision medicine.

AUTHOR CONTRIBUTIONS

The author confirms being the sole contributor of this work and approved it for publication.

ACKNOWLEDGMENTS

Support was provided by the National Institute of General Medical Sciences of the National Institutes of Health (NIGMS-P20GM103464 and U54GM104941), The Do Believe Foundation and The Nemours Foundation.

REFERENCES

- Abaci, H. E., Guo, Z., Doucet, Y., Jackow, J., and Christiano, A. (2017). Next generation human skin constructs as advanced tools for drug development. *Exp. Biol. Med.* 242, 1657–1668. doi: 10.1177/1535370217712690
- Ahmed, T. A., Dare, E. V., and Hincke, M. (2008). Fibrin: a versatile scaffold for tissue engineering applications. *Tissue Eng. B Rev.* 14, 199–215. doi: 10.1089/ten.teb.2007.0435
- Alcaraz, J., Otero, J., Jorba, I., and Navajas, D. (2017). Bidirectional mechanobiology between cells and their local extracellular matrix probed by atomic force microscopy. *Semin. Cell Dev. Biol.* 73, 71–81. doi: 10.1016/j.semcdb.2017.07.020
- Alépée, N., Bahinski, A., Daneshian, M., De Wever, B., Fritsche, E., Goldberg, A., et al. (2014). State-of-the-art of 3D cultures (organs-on-a-chip) in safety testing and pathophysiology. *ALTEX* 31, 441–477. doi: 10.14573/altex1406111
- Alsaab, H. O., Sau, S., Alzhrani, R., Tatiparti, K., Bhise, K., Kashaw, S. K., et al. (2017). PD-1 and PD-L1 Checkpoint signaling inhibition for cancer immunotherapy: mechanism, combinations, and clinical outcome. *Front. Pharmacol.* 8:561. doi: 10.3389/fphar.2017.00561
- Anitua, E., Prado, R., and Orive, G. (2013). Endogenous morphogens and fibrin bioscaffolds for stem cell therapeutics. *Trends Biotechnol.* 31, 364–374. doi: 10.1016/j.tibtech.2013.04.003
- Aparicio, S., Hidalgo, M., and Kung, A. L. (2015). Examining the utility of patient-derived xenograft mouse models. *Nat. Rev. Cancer* 15, 311–316. doi: 10.1038/nrc3944
- Arrowsmith, J., and Miller, P. (2013). Trial watch: phase II and phase III attrition rates 2011–2012. *Nat. Rev. Drug Discov.* 12:569. doi: 10.1038/nrd4090
- Aw Yong, K. M., Li, Z., Merajver, S. D., and Fu, J. (2017). Tracking the tumor invasion front using long-term fluidic tumoroid culture. *Sci. Rep.* 7:10784. doi: 10.1038/s41598-017-10874-1
- Axpe, E., and Oyen, M. L. (2016). Applications of alginate-based bioinks in 3D bioprinting. *Int. J. Mol. Sci.* 17:E1976. doi: 10.3390/ijms17121976
- Baeva, L. F., Lyle, D. B., Rios, M., Langone, J. J., and Lightfoote, M. M. (2014). Different molecular weight hyaluronic acid effects on human macrophage interleukin 1beta production. *J. Biomed. Mater. Res. A* 102, 305–314. doi: 10.1002/jbm.a.34704
- Banks, J. M., Harley, B. A. C., and Bailey, R. C. (2015). Tunable, photoreactive hydrogel system to probe synergies between mechanical and biomolecular cues on adipose-derived mesenchymal stem cell differentiation. *ACS Biomater. Sci. Engineer.* 1, 718–725. doi: 10.1021/acsbiomaterials.5b00196
- Barnes, J. M., Przybyla, L., and Weaver, V. M. (2017). Tissue mechanics regulate brain development, homeostasis and disease. *J. Cell Sci.* 130, 71–82. doi: 10.1242/jcs.191742
- Barretina, J., Caponigro, G., Stransky, N., Venkatesan, K., Margolin, A. A., Kim, S., et al. (2012). The cancer cell line encyclopedia enables predictive modelling of anticancer drug sensitivity. *Nature* 483, 603–607. doi: 10.1038/nature11003
- Barros, C. S., Franco, S. J., and Müller, U. (2011). Extracellular matrix: functions in the nervous system. *Cold Spring Harb. Perspect. Biol.* 3:a005108. doi: 10.1101/cshperspect.a005108
- Bokhari, M., Carnachan, R. J., Cameron, N. R., and Przyborski, S. A. (2007). Culture of HepG2 liver cells on three dimensional polystyrene scaffolds enhances cell structure and function during toxicological challenge. *J. Anat.* 211, 567–576. doi: 10.1111/j.1469-7580.2007.00778.x
- Bonnans, C., Chou, J., and Werb, Z. (2014). Remodelling the extracellular matrix in development and disease. *Nat. Rev. Mol. Cell Biol.* 15, 786–801. doi: 10.1038/nrm3904
- Bordeleau, F., Mason, B. N., Lollis, E. M., Mazzola, M., Zanotelli, M. R., Somasegar, S., et al. (2017). Matrix stiffening promotes a tumor vasculature phenotype. *Proc. Natl. Acad. Sci. U.S.A.* 114, 492–497. doi: 10.1073/pnas.1613855114
- Borlak, J., Singh, P. K., and Rittelmeyer, I. (2015). Regulation of liver enriched transcription factors in rat hepatocytes cultures on collagen and EHS sarcoma matrices. *PLoS ONE* 10:e0124867. doi: 10.1371/journal.pone.0124867
- Bourguignon, L. Y. (2016). Matrix hyaluronan promotes specific MicroRNA upregulation leading to drug resistance and tumor progression. *Int. J. Mol. Sci.* 17:517. doi: 10.3390/ijms17040517
- Branco, M. C., Sigano, D. M., and Schneider, J. P. (2011). Materials from peptide assembly: towards the treatment of cancer and transmittable disease. *Curr. Opin. Chem. Biol.* 15, 427–434. doi: 10.1016/j.cbpa.2011.03.021
- Breslin, S., and O'Driscoll, L. (2013). Three-dimensional cell culture: the missing link in drug discovery. *Drug Discov. To.* 18, 240–249. doi: 10.1016/j.drudis.2012.10.003
- Brown, A. C., and Barker, T. H. (2014). Fibrin-based biomaterials: modulation of macroscopic properties through rational design at the molecular level. *Acta Biomater.* 10, 1502–1514. doi: 10.1016/j.actbio.2013.09.008
- Burdick, J. A., and Prestwich, G. D. (2011). Hyaluronic acid hydrogels for biomedical applications. *Adv. Mater. Weinheim.* 23, H41–H56. doi: 10.1002/adma.201003963
- Caiazzo, M., Okawa, Y., Ranga, A., Piersigilli, A., Tabata, Y., and Lutolf, M. P. (2016). Defined three-dimensional microenvironments boost induction of pluripotency. *Nat. Mater.* 15, 344–352. doi: 10.1038/nmat4536
- Caliari, S. R., and Burdick, J. A. (2016). A practical guide to hydrogels for cell culture. *Nat. Methods* 13, 405–414. doi: 10.1038/nmeth.3839
- Campos, L. S. (2004). Neurospheres: insights into neural stem cell biology. *J. Neurosci. Res.* 78, 761–769. doi: 10.1002/jnr.20333
- Candido, S., Abrams, S. L., Steelman, L. S., Lertpiriyapong, K., Fitzgerald, T. L., Martelli, A. M., et al. (2016). Roles of NGAL and MMP-9 in the tumor

- microenvironment and sensitivity to targeted therapy. *Biochim. Biophys. Acta* 1863, 438–448. doi: 10.1016/j.bbamcr.2015.08.010
- Carrera, S., de Verdier, P. J., Khan, Z., Zhao, B., Mahale, A., Bowman, K. J., et al. (2010). Protection of cells in physiological oxygen tensions against DNA damage-induced apoptosis. *J. Biol. Chem.* 285, 13658–13665. doi: 10.1074/jbc.M109.062562
- Chitnis, T., and Weiner, H. L. (2017). CNS inflammation and neurodegeneration. *J. Clin. Invest.* 127, 3577–3587. doi: 10.1172/JCI90609
- Chouaib, S., Noman, M. Z., Kosmatopoulos, K., and Curran, M. A. (2017). Hypoxic stress: obstacles and opportunities for innovative immunotherapy of cancer. *Oncogene* 36, 439–445. doi: 10.1038/ncr.2016.225
- Clevers, H. (2016). Modeling development and disease with organoids. *Cell* 165, 1586–1597. doi: 10.1016/j.cell.2016.05.082
- Crawford, Y., and Ferrara, N. (2009). Tumor and stromal pathways mediating refractoriness/resistance to anti-angiogenic therapies. *Trends Pharmacol. Sci.* 30, 624–630. doi: 10.1016/j.tips.2009.09.004
- Cukierman, E., Pankov, R., Stevens, D. R., and Yamada, K. M. (2001). Taking cell-matrix adhesions to the third dimension. *Science* 294, 1708–1712. doi: 10.1126/science.1064829
- DeClerck, Y. A. (2000). Interactions between tumour cells and stromal cells and proteolytic modification of the extracellular matrix by metalloproteinases in cancer. *Eur. J. Cancer* 36, 1258–1268. doi: 10.1016/S0959-8049(00)00094-0
- Dekkers, J. F., Wiegerinck, C. L., de Jonge, H. R., Bronsveld, I., Janssens, H. M., de Winter-de Groot, K. M., et al. (2013). A functional CFTR assay using primary cystic fibrosis intestinal organoids. *Nat. Med.* 19, 939–945. doi: 10.1038/nm.3201
- De Palma, M., Biziato, D., and Petrova, T. V. (2017). Microenvironmental regulation of tumour angiogenesis. *Nat. Rev. Cancer* 17, 457–474. doi: 10.1038/nrc.2017.51
- Dickreuter, E., and Cordes, N. (2017). The cancer cell adhesion resistome: mechanisms, targeting and translational approaches. *Biol. Chem.* 398, 721–735. doi: 10.1515/hsz-2016-0326
- Doublier, S., Belisario, D. C., Polimeni, M., Annaratone, L., Riganti, C., Allia, E., et al. (2012). HIF-1 activation induces doxorubicin resistance in MCF7 3-D spheroids via P-glycoprotein expression: a potential model of the chemoresistance of invasive micropapillary carcinoma of the breast. *BMC Cancer* 12:4. doi: 10.1186/1471-2407-12-4
- Doyle, A. D., Carvajal, N., Jin, A., Matsumoto, K., and Yamada, K. M. (2015). Local 3D matrix microenvironment regulates cell migration through spatiotemporal dynamics of contractility-dependent adhesions. *Nat. Commun.* 6:8720. doi: 10.1038/ncomms9720
- Dutta, D., Heo, I., and Clevers, H. (2017). Disease modeling in stem cell-derived 3D organoid systems. *Trends Mol. Med.* 23, 393–410. doi: 10.1016/j.molmed.2017.02.007
- Edmondson, R., Broglie, J. J., Adcock, A. F., and Yang, L. (2014). Three-dimensional cell culture systems and their applications in drug discovery and cell-based biosensors. *Assay Drug Dev. Technol.* 12, 207–218. doi: 10.1089/adt.2014.573
- Egeblad, M., Nakasone, E. S., and Werb, Z. (2010). Tumors as organs: complex tissues that interface with the entire organism. *Dev. Cell* 18, 884–901. doi: 10.1016/j.devcel.2010.05.012
- Ekert, J. E., Johnson, K., Strake, B., Pardinas, J., Jarantow, S., Perkinson, R., et al. (2014). Three-dimensional lung tumor microenvironment modulates therapeutic compound responsiveness *in vitro*—implication for drug development. *PLoS ONE* 9:e92248. doi: 10.1371/journal.pone.0092248
- Eyckmans, J., Boudou, T., Yu, X., and Chen, C. S. (2011). A hitchhiker's guide to mechanobiology. *Dev. Cell* 21, 35–47. doi: 10.1016/j.devcel.2011.06.015
- Fatehullah, A., Tan, S. H., and Barker, N. (2016). Organoids as an *in vitro* model of human development and disease. *Nat. Cell Biol.* 18, 246–254. doi: 10.1038/ncb3312
- Finnberg, N. K., Gokare, P., Lev, A., Grivennikov, S. I., MacFarlane, A. W., Campbell, K. S., et al. (2017). Application of 3D tumoroid systems to define immune and cytotoxic therapeutic responses based on tumoroid and tissue slice culture molecular signatures. *Oncotarget* 8, 66747–66757. doi: 10.18632/oncotarget.19965
- Friedrich, J., Seidel, C., Ebner, R., and Kunz-Schughart, L. A. (2009). Spheroid-based drug screen: considerations and practical approach. *Nat. Protoc.* 4, 309–324. doi: 10.1038/nprot.2008.226
- Frischknecht, R., and Gundelfinger, E. D. (2012). The brain's extracellular matrix and its role in synaptic plasticity. *Adv. Exp. Med. Biol.* 970, 153–171. doi: 10.1007/978-3-7091-0932-8_7
- Gacche, R. N. (2015). Compensatory angiogenesis and tumor refractoriness. *Oncogenesis* 4:e153. doi: 10.1038/oncsis.2015.14
- Gill, B. J., and West, J. L. (2014). Modeling the tumor extracellular matrix: Tissue engineering tools repurposed towards new frontiers in cancer biology. *J. Biomech.* 47, 1969–1978. doi: 10.1016/j.jbiomech.2013.09.029
- Girard, Y. K., Wang, C., Ravi, S., Howell, M. C., Mallela, J., Alibrahim, M., et al. (2013). A 3D fibrous scaffold inducing tumoroids: a platform for anticancer drug development. *PLoS ONE* 8:e75345. doi: 10.1371/journal.pone.0075345
- Glowacki, J., and Mizuno, S. (2008). Collagen scaffolds for tissue engineering. *Biopolymers* 89, 338–344. doi: 10.1002/bip.20871
- Goodwin, T. J., Prewett, T. L., Wolf, D. A., and Spaulding, G. F. (1993). Reduced shear stress: a major component in the ability of mammalian tissues to form three-dimensional assemblies in simulated microgravity. *J. Cell. Biochem.* 51, 301–311. doi: 10.1002/jcb.240510309
- Goubko, C. A., Basak, A., Majumdar, S., and Cao, X. (2014). Dynamic cell patterning of photoresponsive hyaluronic acid hydrogels. *J. Biomed. Mater. Res. A* 102, 381–391. doi: 10.1002/jbm.a.34712
- Gracz, A. D., Williamson, I. A., Roche, K. C., Johnston, M. J., Wang, F., Wang, Y., et al. (2015). A high-throughput platform for stem cell niche co-cultures and downstream gene expression analysis. *Nat. Cell Biol.* 17:340. doi: 10.1038/ncb3104
- Griffith, L. G., and Swartz, M. A. (2006). Capturing complex 3D tissue physiology *in vitro*. *Nat. Rev. Mol. Cell Biol.* 7, 211–224. doi: 10.1038/nrm1858
- Guilbaud, J. B., Vey, E., Boothroyd, S., Smith, A. M., Ulijn, R. V., Saiani, A., et al. (2010). Enzymatic catalyzed synthesis and triggered gelation of ionic peptides. *Langmuir* 26, 11297–11303. doi: 10.1021/la100623y
- Haines-Butterick, L., Rajagopal, K., Branco, M., Salick, D., Rughani, R., Pilarz, M., et al. (2007). Controlling hydrogelation kinetics by peptide design for three-dimensional encapsulation and injectable delivery of cells. *Proc. Natl. Acad. Sci. U.S.A.* 104, 7791–7796. doi: 10.1073/pnas.0701980104
- Haisler, W. L., Timm, D. M., Gage, J. A., Tseng, H., Killian, T. C., and Souza, G. R. (2013). Three-dimensional cell culturing by magnetic levitation. *Nat. Protoc.* 8, 1940–1949. doi: 10.1038/nprot.2013.125
- Hamill, O. P., and Martinac, B. (2001). Molecular basis of mechanotransduction in living cells. *Physiol. Rev.* 81, 685–740. doi: 10.1152/physrev.2001.81.2.685
- Handorf, A. M., Zhou, Y., Halanski, M. A., and Li, W. J. (2015). Tissue stiffness dictates development, homeostasis, and disease progression. *Organogenesis* 11, 1–15. doi: 10.1080/15476278.2015.1019687
- Happel, M. F. K., and Frischknecht, R. (2016). “Neuronal plasticity in the juvenile and adult brain regulated by the extracellular matrix,” in *Composition and Function of the Extracellular Matrix in the Human Body [Internet]*, 143–158.
- Herrmann, R., Fayad, W., Schwarz, S., Berndtsson, M., and Linder, S. (2008). Screening for compounds that induce apoptosis of cancer cells grown as multicellular spheroids. *J. Biomol. Screen.* 13, 1–8. doi: 10.1177/1087057107310442
- Ho, W. J., Pham, E. A., Kim, J. W., Ng, C. W., Kim, J. H., Kamei, D. T., et al. (2010). Incorporation of multicellular spheroids into 3-D polymeric scaffolds provides an improved tumor model for screening anticancer drugs. *Cancer Sci.* 101, 2637–2643. doi: 10.1111/j.1349-7006.2010.01723.x
- Holle, A. W., Young, J. L., and Spatz, J. P. (2016). *In vitro* cancer cell-ECM interactions inform *in vivo* cancer treatment. *Adv. Drug Deliv. Rev.* 97:270–279. doi: 10.1016/j.addr.2015.10.007
- Holohan, C., Van Schaeuybroeck, S., Longley, D. B., and Johnston, P. G. (2013). Cancer drug resistance: an evolving paradigm. *Nat. Rev. Cancer* 13, 714–726. doi: 10.1038/nrc3599
- Huang, H., Ding, Y., Sun, X. S., and Nguyen, T. A. (2013). Peptide hydrogelation and cell encapsulation for 3D culture of MCF-7 breast cancer cells. *PLoS ONE* 8:e59482. doi: 10.1371/journal.pone.0059482
- Huang, H., Shi, J., Laskin, J., Liu, Z., McVey, D. S., and Sun, X. S. (2011). Design of a shear-thinning recoverable peptide hydrogel from native sequences and application for influenza H1N1 vaccine adjuvant. *Soft Matter* 7, 8905–8912. doi: 10.1039/c1sm05157a
- Huang, H., and Sun, X. S. (2010). Rational design of responsive self-assembling peptides from native protein sequences. *Biomacromolecules* 11, 3390–3394. doi: 10.1021/bm100894j

- Huang, Y. J., and Hsu, S. H. (2014). Acquisition of epithelial-mesenchymal transition and cancer stem-like phenotypes within chitosan-hyaluronan membrane-derived 3D tumor spheroids. *Biomaterials* 35, 10070–10079. doi: 10.1016/j.biomaterials.2014.09.010
- Hughes, C. S., Postovit, L. M., and Lajoie, G. A. (2010). Matrigel: a complex protein mixture required for optimal growth of cell culture. *Proteomics* 10, 1886–1890. doi: 10.1002/pmic.200900758
- Hynes, R. O. (2014). Stretching the boundaries of extracellular matrix research. *Nat. Rev. Mol. Cell Biol.* 15, 761–763. doi: 10.1038/nrm3908
- Hynes, R. O., and Naba, A. (2012). Overview of the matrisome—an inventory of extracellular matrix constituents and functions. *Cold Spring Harb. Perspect. Biol.* 4:a004903. doi: 10.1101/cshperspect.a004903
- Imamura, Y., Mukohara, T., Shimono, Y., Funakoshi, Y., Chayahara, N., Toyoda, M., et al. (2015). Comparison of 2D- and 3D-culture models as drug-testing platforms in breast cancer. *Oncol. Rep.* 33, 1837–1843. doi: 10.3892/or.2015.3767
- Iskandar, A. R., Xiang, Y., Frentzel, S., Talikka, M., Leroy, P., Kuehn, D., et al. (2015). Impact assessment of cigarette smoke exposure on organotypic bronchial epithelial tissue cultures: a comparison of monoculture and coculture model containing fibroblasts. *Toxicol. Sci.* 147, 207–221. doi: 10.1093/toxsci/kfv122
- Ivascu, A., and Kubbies, M. (2006). Rapid generation of single-tumor spheroids for high-throughput cell function and toxicity analysis. *J. Biomol. Screen.* 11, 922–932. doi: 10.1177/1087057106292763
- Jakubikova, J., Cholujova, D., Hideshima, T., Gronosova, P., Soltysova, A., Harada, T., et al. (2016). A novel 3D mesenchymal stem cell model of the multiple myeloma bone marrow niche: biologic and clinical applications. *Oncotarget* 7, 77326–77341. doi: 10.18632/oncotarget.12643
- Janzen, W. P. (2014). Screening technologies for small molecule discovery: the state of the art. *Chem. Biol.* 21, 1162–1170. doi: 10.1016/j.chembiol.2014.07.015
- Jayawarna, V., Ali, M., Jowitt, T. A., Miller, A. F., Saiani, A., Gough, J. E., et al. (2006). Nanostructured hydrogels for three-dimensional cell culture through self-assembly of fluorenylmethoxycarbonyl-dipeptides. *Adv. Mater.* 18, 611–614. doi: 10.1002/adma.200501522
- Jiang, H., Hegde, S., and DeNardo, D. G. (2017). Tumor-associated fibrosis as a regulator of tumor immunity and response to immunotherapy. *Cancer Immunol. Immunother.* 66, 1037–1048. doi: 10.1007/s00262-017-2003-1
- Jodder, B., Garcia, E., Casas, A., and Stewart, C. M. (2016). Development of functionalized multi-walled carbon-nanotube-based alginate hydrogels for enabling biomimetic technologies. *Sci. Rep.* 6:32456. doi: 10.1038/srep32456
- Johansson, A., Hamzah, J., and Ganss, R. (2016). More than a scaffold: stromal modulation of tumor immunity. *Biochim. Biophys. Acta* 1865, 3–13. doi: 10.1016/j.bbcan.2015.06.001
- Jones, V. S., Huang, R. Y., Chen, L. P., Chen, Z. S., Fu, L., and Huang, R. P. (2016). Cytokines in cancer drug resistance: cues to new therapeutic strategies. *Biochim. Biophys. Acta* 1865, 255–265. doi: 10.1016/j.bbcan.2016.03.005
- Junttila, M. R., and de Sauvage, F. J. (2013). Influence of tumour micro-environment heterogeneity on therapeutic response. *Nature* 501, 346–354. doi: 10.1038/nature12626
- Kabba, J. A., Xu, Y., Christian, H., Ruan, W., Chenai, K., Xiang, Y., et al. (2017). Microglia: housekeeper of the central nervous system. *Cell. Mol. Neurobiol.* doi: 10.1007/s10571-017-0504-2. [Epub ahead of print].
- Kersh, A. E., Ng, S., Chang, Y. M., Sasaki, M., Thomas, S. N., Kissick, H. T., et al. (2018). Targeted therapies: immunologic effects and potential applications outside of cancer. *J. Clin. Pharmacol.* 58, 7–24. doi: 10.1002/jcph.1028
- Kirshner, J., Thulien, K. J., Martin, L. D., Debes Marun, C., Reiman, T., Belch, A. R., et al. (2008). A unique three-dimensional model for evaluating the impact of therapy on multiple myeloma. *Blood* 112, 2935–2945. doi: 10.1182/blood-2008-02-142430
- Kleinman, H. K., and Martin, G. R. (2005). Matrigel: basement membrane matrix with biological activity. *Semin. Cancer Biol.* 15, 378–386. doi: 10.1016/j.semcancer.2005.05.004
- Knight, E., Murray, B., Carnachan, R., and Przyborski, S. (2011). Alvetex(R): polystyrene scaffold technology for routine three dimensional cell culture. *Methods Mol. Biol.* 695, 323–340. doi: 10.1007/978-1-60761-984-0_20
- Kraehenbuehl, T. P., Zammaretti, P., Van der Vlies, A. J., Schoenmakers, R. G., Lutolf, M. P., Jaconi, M. E., et al. (2008). Three-dimensional extracellular matrix-directed cardioprogenitor differentiation: systematic modulation of a synthetic cell-responsive PEG-hydrogel. *Biomaterials* 29, 2757–2766. doi: 10.1016/j.biomaterials.2008.03.016
- Kretzschmar, K., and Clevers, H. (2016). Organoids: modeling development and the stem cell niche in a dish. *Dev. Cell* 38, 590–600. doi: 10.1016/j.devcel.2016.08.014
- Kural, M. H., and Billiar, K. L. (2013). Regulating tension in three-dimensional culture environments. *Exp. Cell Res.* 319, 2447–2459. doi: 10.1016/j.yexcr.2013.06.019
- Kutschka, I., Chen, I. Y., Kofidis, T., Arai, T., von Degenfeld, G., Sheikh, A. Y., et al. (2006). Collagen matrices enhance survival of transplanted cardiomyoblasts and contribute to functional improvement of ischemic rat hearts. *Circulation* 114(1 Suppl.), I167–I173. doi: 10.1161/CIRCULATIONAHA.105.001297
- Lancaster, M. A., and Knoblich, J. A. (2014). Organogenesis in a dish: modeling development and disease using organoid technologies. *Science* 345:1247125. doi: 10.1126/science.1247125
- Lanzi, C., Zaffaroni, N., and Cassinelli, G. (2017). Targeting heparan sulfate proteoglycans and their modifying enzymes to enhance anticancer chemotherapy efficacy and overcome drug resistance. *Curr. Med. Chem.* 24, 2860–2886. doi: 10.2174/0929867324666170216114248
- Lewis, D. M., Blatchley, M. R., Park, K. M., and Gerecht, S. (2017). O2-controllable hydrogels for studying cellular responses to hypoxic gradients in three dimensions *in vitro* and *in vivo*. *Nat. Protoc.* 12, 1620–1638. doi: 10.1038/nprot.2017.059
- Lewis, E. E., Wheadon, H., Lewis, N., Yang, J., Mullin, M., Hursthouse, A., et al. (2016). A quiescent, regeneration-responsive tissue engineered mesenchymal stem cell bone marrow niche model via magnetic levitation. *ACS Nano* 10, 8346–8354. doi: 10.1021/acsnano.6b02841
- Lewis, N. S., Lewis, E. E., Mullin, M., Wheadon, H., Dalby, M. J., and Berry, C. C. (2017). Magnetically levitated mesenchymal stem cell spheroids cultured with a collagen gel maintain phenotype and quiescence. *J. Tissue Eng.* 8:2041731417704428. doi: 10.1177/2041731417704428
- Li, J., Gao, Y., Kuang, Y., Shi, J., Du, X., Zhou, J., et al. (2013). Dephosphorylation of D-peptide derivatives to form biofunctional, supramolecular nanofibers/hydrogels and their potential applications for intracellular imaging and intratumoral chemotherapy. *J. Am. Chem. Soc.* 135, 9907–9914. doi: 10.1021/ja404215g
- Li, Q., Chen, C., Kapadia, A., Zhou, Q., Harper, M. K., Schaack, J., et al. (2011). 3D models of epithelial-mesenchymal transition in breast cancer metastasis: high-throughput screening assay development, validation, and pilot screen. *J. Biomol. Screen.* 16, 141–154. doi: 10.1177/1087057110392995
- Li, Z., and Deming, T. J. (2010). Tunable hydrogel morphology via self-assembly of amphiphilic pentablock copolypeptides. *Soft Matter* 6, 2546–2551. doi: 10.1039/b927137f
- Lin, C. H., Jokela, T., Gray, J., and LaBarge, M. A. (2017). Combinatorial microenvironments impose a continuum of cellular responses to a single pathway-targeted anti-cancer compound. *Cell Rep.* 21, 533–545. doi: 10.1016/j.celrep.2017.09.058
- Lin, Chun, T. H., and Kang, L. (2016). Adipose extracellular matrix remodelling in obesity and insulin resistance. *Biochem. Pharmacol.* 119, 8–16. doi: 10.1016/j.bcp.2016.05.005
- Liu, F., Huang, J., Ning, B., Liu, Z., Chen, S., and Zhao, W. (2016). Drug discovery via human-derived stem cell organoids. *Front. Pharmacol.* 7:334. doi: 10.3389/fphar.2016.00334
- Lopes-Bastos, B. M., Jiang, W. G., and Cai, J. (2016). Tumour-endothelial cell communications: important and indispensable mediators of tumour angiogenesis. *Anticancer Res.* 36, 1119–1126.
- Lutolf, M. P., Lauer-Fields, J. L., Schmoekel, H. G., Metters, A. T., Weber, F. E., Fields, G. B., et al. (2003). Synthetic matrix metalloproteinase-sensitive hydrogels for the conduction of tissue regeneration: engineering cell-invasion characteristics. *Proc. Natl. Acad. Sci. U.S.A.* 100, 5413–5418. doi: 10.1073/pnas.0737381100
- Ma, W. Y., Hsiung, L. C., Wang, C. H., Chiang, C. L., Lin, C. H., Huang, C. S., et al. (2015). A novel 96well-formatted micro-gap plate enabling drug response profiling on primary tumour samples. *Sci. Rep.* 5:9656. doi: 10.1038/srep09656
- Mahler, A., Reches, M., Rechter, M., Cohen, S., and Gazit, E. (2006). Rigid, self-assembled hydrogel composed of a modified aromatic dipeptide. *Adv. Mater.* 18, 1365–1370. doi: 10.1002/adma.200501765

- McMillin, D. W., Negri, J. M., and Mitsiades, C. S. (2013). The role of tumour-stromal interactions in modifying drug response: challenges and opportunities. *Nat. Rev. Drug Discov.* 12, 217–228. doi: 10.1038/nrd3870
- Montanez-Sauri, S. I., Beebe, D. J., and Sung, K. E. (2015). Microscale screening systems for 3D cellular microenvironments: platforms, advances, and challenges. *Cell. Mol. Life Sci.* 72, 237–249. doi: 10.1007/s00018-014-1738-5
- Montanez-Sauri, S. I., Sung, K. E., Berthier, E., and Beebe, D. J. (2013). Enabling screening in 3D microenvironments: probing matrix and stromal effects on the morphology and proliferation of T47D breast carcinoma cells. *Integr. Biol.* 5, 631–640. doi: 10.1039/c3ib20225a
- Moon, J. J., Saik, J. E., Poche, R. A., Leslie-Barbick, J. E., Lee, S. H., Smith, A. A., et al. (2010). Biomimetic hydrogels with pro-angiogenic properties. *Biomaterials* 31, 3840–3847. doi: 10.1016/j.biomaterials.2010.01.104
- Moors, M., Rockel, T. D., Abel, J., Cline, J. E., Gassmann, K., Schreiber, T., et al. (2009). Human neurospheres as three-dimensional cellular systems for developmental neurotoxicity testing. *Environ. Health Perspect.* 117, 1131–1138. doi: 10.1289/ehp.0800207
- Mouw, J. K., Ou, G., and Weaver, V. M. (2014). Extracellular matrix assembly: a multiscale deconstruction. *Nat. Rev. Mol. Cell Biol.* 15, 771–785. doi: 10.1038/nrm3902
- Mueller-Klieser, W. (1987). Multicellular spheroids. A review on cellular aggregates in cancer research. *J. Cancer Res. Clin. Oncol.* 113, 101–122. doi: 10.1007/BF00391431
- Muranen, T., Selfors, L. M., Worster, D. T., Iwanicki, M. P., Song, L., Morales, F. C., et al. (2012). Inhibition of PI3K/mTOR leads to adaptive resistance in matrix-attached cancer cells. *Cancer Cell* 21, 227–239. doi: 10.1016/j.ccr.2011.12.024
- Murphy, M. C., Jones, D. T., Jack, C. R. Jr., Glaser, K. J., Senjem, M. L., Manduca, A., et al. (2016). Regional brain stiffness changes across the Alzheimer's disease spectrum. *Neuroimage Clin.* 10, 283–290. doi: 10.1016/j.nicl.2015.12.007
- Nath, S., and Devi, G. R. (2016). Three-dimensional culture systems in cancer research: focus on tumor spheroid model. *Pharmacol. Ther.* 163, 94–108. doi: 10.1016/j.pharmthera.2016.03.013
- Orbach, R., Adler-Abramovich, L., Zigerson, S., Mironi-Harpaz, I., Seliktar, D., and Gazit, E. (2009). Self-assembled Fmoc-peptides as a platform for the formation of nanostructures and hydrogels. *Biomacromolecules* 10, 2646–2651. doi: 10.1021/bm900584m
- Orgel, J. P., Persikov, A. V., and Antipova, O. (2014). Variation in the helical structure of native collagen. *PLoS ONE* 9:e89519. doi: 10.1371/journal.pone.0089519
- Pamies, D., Hartung, T., and Hogberg, H. T. (2014). Biological and medical applications of a brain-on-a-chip. *Exp. Biol. Med.* 239, 1096–1107. doi: 10.1177/1535370214537738
- Pampaloni, F., Reynaud, E. G., and Stelzer, E. H. (2007). The third dimension bridges the gap between cell culture and live tissue. *Nat. Rev. Mol. Cell Biol.* 8, 839–845. doi: 10.1038/nrm2236
- Pathak, A., and Kumar, S. (2011). Biophysical regulation of tumor cell invasion: moving beyond matrix stiffness. *Integr. Biol.* 3, 267–278. doi: 10.1039/c0ib00095g
- Pauli, C., Hopkins, B. D., Prandi, D., Shaw, R., Fedrizzi, T., Sboner, A., et al. (2017). Personalized *in vitro* and *in vivo* cancer models to guide precision medicine. *Cancer Discov.* 7, 462–477. doi: 10.1158/2159-8290.CD-16-1154
- Pitt, J. M., Marabelle, A., Eggermont, A., Soria, J. C., Kroemer, G., and Zitvogel, L. (2016). Targeting the tumor microenvironment: removing obstruction to anticancer immune responses and immunotherapy. *Ann. Oncol.* 27, 1482–1492. doi: 10.1093/annonc/mdw168
- Pogge von Strandmann, E., Reinartz, S., Wager, U., and Muller, R. (2017). Tumor-host cell interactions in ovarian cancer: pathways to therapy failure. *Trends Cancer* 3, 137–148. doi: 10.1016/j.trecan.2016.12.005
- Poincloux, R., Collin, O., Lizarraga, F., Romao, M., Debray, M., Piel, M., et al. (2011). Contractility of the cell rear drives invasion of breast tumor cells in 3D Matrigel. *Proc. Natl. Acad. Sci. U.S.A.* 108, 1943–1948. doi: 10.1073/pnas.1010396108
- Polonchuk, L., Chabria, M., Badi, L., Hoflack, J. C., Figtree, G., Davies, M. J., et al. (2017). Cardiac spheroids as promising *in vitro* models to study the human heart microenvironment. *Sci. Rep.* 7:7005. doi: 10.1038/s41598-017-06385-8
- Prieto-Vila, M., Takahashi, R. U., Usaba, W., Kohama, I., and Ochiya, T. (2017). Drug resistance driven by cancer stem cells and their niche. *Int. J. Mol. Sci.* 18:E2574. doi: 10.3390/ijms18122574
- Puls, T. J., Tan, X., Whittington, C. F., and Voytik-Harbin, S. L. (2017). 3D collagen fibrillar microstructure guides pancreatic cancer cell phenotype and serves as a critical design parameter for phenotypic models of EMT. *PLoS ONE* 12:e0188870. doi: 10.1371/journal.pone.0188870
- Raeber, G. P., Lutolf, M. P., and Hubbell, J. A. (2005). Molecularly engineered PEG hydrogels: a novel model system for proteolytically mediated cell migration. *Biophys. J.* 89, 1374–1388. doi: 10.1529/biophysj.104.050682
- Ravi, M., Paramesh, V., Kaviya, S. R., Anuradha, E., and Solomon, F. D. (2015). 3D cell culture systems: advantages and applications. *J. Cell. Physiol.* 230, 16–26. doi: 10.1002/jcp.24683
- Rimann, M., and Graf-Hausner, U. (2012). Synthetic 3D multicellular systems for drug development. *Curr. Opin. Biotechnol.* 23, 803–809. doi: 10.1016/j.copbio.2012.01.011
- Ryan, S. L., Baird, A. M., Vaz, G., Urquhart, A. J., Senge, M., Richard, D. J., et al. (2016). Drug discovery approaches utilizing three-dimensional cell culture. *Assay Drug Dev. Technol.* 14, 19–28. doi: 10.1089/adt.2015.670
- Sathaye, S., Mbi, A., Sonmez, C., Chen, Y., Blair, D. L., Schneider, J. P., et al. (2015). Rheology of peptide- and protein-based physical hydrogels: are everyday measurements just scratching the surface? *Wiley Interdiscip. Rev. Nanomed. Nanobiotechnol.* 7, 34–68. doi: 10.1002/wnan.1299
- Schneider, J. P., Pochan, D. J., Ozbas, B., Rajagopal, K., Pakstis, L., and Kretsinger, J. (2002). Responsive hydrogels from the intramolecular folding and self-assembly of a designed peptide. *J. Am. Chem. Soc.* 124, 15030–15037. doi: 10.1021/ja027993g
- Sebens, S., and Schafer, H. (2012). The tumor stroma as mediator of drug resistance—a potential target to improve cancer therapy? *Curr. Pharm. Biotechnol.* 13, 2259–2272. doi: 10.2174/138920112802501999
- Shamir, E. R., and Ewald, A. J. (2014). Three-dimensional organotypic culture: experimental models of mammalian biology and disease. *Nat. Rev. Mol. Cell Biol.* 15, 647–664. doi: 10.1038/nrm3873
- Shri, M., Agrawal, H., Rani, P., Singh, D., and Onteru, S. K. (2017). Hanging drop, a best three-dimensional (3D) culture method for primary buffalo and sheep hepatocytes. *Sci. Rep.* 7:1203. doi: 10.1038/s41598-017-01355-6
- Silva, J. M., Garcia, J. R., Reis, R. L., Garcia, A. J., and Mano, J. F. (2017). Tuning cell adhesive properties via layer-by-layer assembly of chitosan and alginate. *Acta Biomater.* 51, 279–293. doi: 10.1016/j.actbio.2017.01.058
- Simian, M., and Bissell, M. J. (2017). Organoids: a historical perspective of thinking in three dimensions. *J. Cell Biol.* 216, 31–40. doi: 10.1083/jcb.2016.10056
- Sittampalam, S., Eglén, R., Ferguson, S., Maynes, J. T., Olden, K., Schrader, L., et al. (2015). Three-dimensional cell culture assays: are they more predictive of *in vivo* efficacy than 2D monolayer cell-based assays? *Assay Drug Dev. Technol.* 13, 254–261. doi: 10.1089/adt.2015.29001.rtd
- Sivaraman, A., Leach, J. K., Townsend, S., Iida, T., Hogan, B. J., Stolz, D. B., et al. (2005). A microscale *in vitro* physiological model of the liver: predictive screens for drug metabolism and enzyme induction. *Curr. Drug Metab.* 6, 569–591. doi: 10.2174/138920005774832632
- Sleeman, J. P. (2012). The metastatic niche and stromal progression. *Cancer Metastasis Rev.* 31, 429–440. doi: 10.1007/s10555-012-9373-9
- Smith, A. M., Williams, R. J., Tang, C., Coppo, P., Collins, R. F., Turner, M. L., et al. (2008). Fmoc-diphenylalanine self assembles to a hydrogel via a novel architecture based on π - π interlocked β -sheets. *Adv. Mater.* 20, 37–41. doi: 10.1002/adma.200701221
- Smith, S. C., Baras, A. S., Lee, J. K., and Theodorescu, D. (2010). The COXEN principle: translating signatures of *in vitro* chemosensitivity into tools for clinical outcome prediction and drug discovery in cancer. *Cancer Res.* 70, 1753–1758. doi: 10.1158/0008-5472.CAN-09-3562
- Souza, G. R., Molina, J. R., Raphael, R. M., Ozawa, M. G., Stark, D. J., Levin, C. S., et al. (2010). Three-dimensional tissue culture based on magnetic cell levitation. *Nat. Nanotechnol.* 5, 291–296. doi: 10.1038/nnano.2010.23
- Stadler, M., Walter, S., Walzl, A., Kramer, N., Unger, C., Scherzer, M., et al. (2015). Increased complexity in carcinomas: analyzing and modeling the interaction of human cancer cells with their microenvironment. *Semin. Cancer Biol.* 35:107–124. doi: 10.1016/j.semcancer.2015.08.007
- Stock, K., Estrada, M. F., Vidic, S., Gjerde, K., Rudisch, A., Santo, V. E., et al. (2016). Capturing tumor complexity *in vitro*: comparative analysis of 2D and 3D tumor models for drug discovery. *Sci. Rep.* 6:28951. doi: 10.1038/srep28951

- Sutherland, R. M. (1988). Cell and environment interactions in tumor microregions: the multicell spheroid model. *Science* 240, 177–184. doi: 10.1126/science.2451290
- Sutherland, R. M., Inch, W. R., McCredie, J. A., and Kruuv, J. (1970). A multi-component radiation survival curve using an *in vitro* tumour model. *Int. J. Radiat. Biol. Relat. Stud. Phys. Chem. Med.* 18, 491–495. doi: 10.1080/09553007014551401
- Takasato, M., Er, P. X., Chiu, H. S., Maier, B., Baillie, G. J., Ferguson, C., et al. (2015). Kidney organoids from human iPS cells contain multiple lineages and model human nephrogenesis. *Nature* 526, 564–568. doi: 10.1038/nature15695
- Tibbitt, M. W., and Anseth, K. S. (2009). Hydrogels as extracellular matrix mimics for 3D cell culture. *Biotechnol. Bioeng.* 103, 655–663. doi: 10.1002/bit.22361
- Timm, D. M., Chen, J., Sing, D., Gage, J. A., Haisler, W. L., Neeley, S. K., et al. (2013). A high-throughput three-dimensional cell migration assay for toxicity screening with mobile device-based macroscopic image analysis. *Sci. Rep.* 3:3000. doi: 10.1038/srep03000
- Toledano, S., Williams, R. J., Jayawarna, V., and Ulijn, R. V. (2006). Enzyme-triggered self-assembly of peptide hydrogels via reversed hydrolysis. *J. Am. Chem. Soc.* 128, 1070–1071. doi: 10.1021/ja056549l
- Tseng, H., Gage, J. A., Raphael, R. M., Moore, R. H., Killian, T. C., Grande-Allen, K. J., et al. (2013). Assembly of a three-dimensional multitype bronchiole coculture model using magnetic levitation. *Tissue Eng. C Methods* 19, 665–675. doi: 10.1089/ten.tec.2012.0157
- Turley, S. J., Cremasco, V., and Astarita, J. L. (2015). Immunological hallmarks of stromal cells in the tumour microenvironment. *Nat. Rev. Immunol.* 15, 669–682. doi: 10.1038/nri3902
- Tyler, W. J. (2012). The mechanobiology of brain function. *Nat. Rev. Neurosci.* 13, 867–878. doi: 10.1038/nrn3383
- Valastyan, S., and Weinberg, R. A. (2011). Tumor metastasis: molecular insights and evolving paradigms. *Cell* 147, 275–292. doi: 10.1016/j.cell.2011.09.024
- van de Wetering, M., Francies, H. E., Francis, J. M., Bounova, G., Iorio, F., Pronk, A., et al. (2015). Prospective derivation of a living organoid biobank of colorectal cancer patients. *Cell* 161, 933–945. doi: 10.1016/j.cell.2015.03.053
- Villoslada, P., Moreno, B., Melero, I., Pablos, J. L., Martino, G., Uccelli, A., et al. (2008). Immunotherapy for neurological diseases. *Clin. Immunol.* 128, 294–305. doi: 10.1016/j.clim.2008.04.003
- Wallace, D. G., and Rosenblatt, J. (2003). Collagen gel systems for sustained delivery and tissue engineering. *Adv. Drug Deliv. Rev.* 55, 1631–1649. doi: 10.1016/j.addr.2003.08.004
- Wang, Y., Zhang, Z., Xu, L., Li, X., and Chen, H. (2013). Hydrogels of halogenated Fmoc-short peptides for potential application in tissue engineering. *Colloids Surf. B Biointerfaces* 104, 163–168. doi: 10.1016/j.colsurfb.2012.11.038
- Weber, L. M., Hayda, K. N., Haskins, K., and Anseth, K. S. (2007). The effects of cell-matrix interactions on encapsulated beta-cell function within hydrogels functionalized with matrix-derived adhesive peptides. *Biomaterials* 28, 3004–3011. doi: 10.1016/j.biomaterials.2007.03.005
- Weeber, F., Ooft, S. N., Dijkstra, K. K., and Voest, E. E. (2017). Tumor organoids as a pre-clinical cancer model for drug discovery. *Cell Chem. Biol.* 24, 1092–1100. doi: 10.1016/j.chembiol.2017.06.012
- Williams, A. S., Kang, L., and Wasserman, D. H. (2015). The extracellular matrix and insulin resistance. *Trends Endocrinol. Metab.* 26, 357–366. doi: 10.1016/j.tem.2015.05.006
- Wong, C. C., Gilkes, D. M., Zhang, H., Chen, J., Wei, H., Chaturvedi, P., et al. (2011). Hypoxia-inducible factor 1 is a master regulator of breast cancer metastatic niche formation. *Proc. Natl. Acad. Sci. U.S.A.* 108, 16369–16374. doi: 10.1073/pnas.1113483108
- Worthington, P., Drake, K. M., Li, Z., Napper, A. D., Pochan, D. J., and Langhans, S. A. (2017). Beta-hairpin hydrogels as scaffolds for high-throughput drug discovery in three-dimensional cell culture. *Anal. Biochem.* 535, 25–34. doi: 10.1016/j.ab.2017.07.024
- Worthington, P., Pochan, D. J., and Langhans, S. A. (2015). Peptide hydrogels - versatile matrices for 3D cell culture in cancer medicine. *Front. Oncol.* 5:92. doi: 10.3389/fonc.2015.00092
- Wynn, T. A., Chawla, A., and Pollard, J. W. (2013). Macrophage biology in development, homeostasis and disease. *Nature* 496, 445–455. doi: 10.1038/nature12034
- Wynn, T. A., and Ramalingam, T. R. (2012). Mechanisms of fibrosis: therapeutic translation for fibrotic disease. *Nat. Med.* 18, 1028–1040. doi: 10.1038/nm.2807
- Xu, X., Farach-Carson, M. C., and Jia, X. (2014). Three-dimensional *in vitro* tumor models for cancer research and drug evaluation. *Biotechnol. Adv.* 32, 1256–1268. doi: 10.1016/j.biotechadv.2014.07.009
- Yan, C., and Pochan, D. J. (2010). Rheological properties of peptide-based hydrogels for biomedical and other applications. *Chem. Soc. Rev.* 39, 3528–3540. doi: 10.1039/b919449p
- Yang, X. B., Bhatnagar, R. S., Li, S., and Oreffo, R. O. (2004). Biomimetic collagen scaffolds for human bone cell growth and differentiation. *Tissue Eng.* 10, 1148–1159. doi: 10.1089/ten.2004.10.1148
- Yang, Z., and Zhao, X. (2011). A 3D model of ovarian cancer cell lines on peptide nanofiber scaffold to explore the cell-scaffold interaction and chemotherapeutic resistance of anticancer drugs. *Int. J. Nanomed.* 6, 303–310. doi: 10.2147/IJN.S15279
- Zhang, S., Gelain, F., and Zhao, X. (2005). Designer self-assembling peptide nanofiber scaffolds for 3D tissue cell cultures. *Semin. Cancer Biol.* 15, 413–420. doi: 10.1016/j.semcancer.2005.05.007
- Zhang, S., Lockshin, C., Herbert, A., Winter, E., and Rich, A. (1992). Zuotin, a putative Z-DNA binding protein in *Saccharomyces cerevisiae*. *EMBO J.* 11, 3787–3796.
- Zhang, Y. S., and Khademhosseini, A. (2017). Advances in engineering hydrogels. *Science* 356:eaa3627. doi: 10.1126/science.aaf3627
- Zhou, M., Smith, A. M., Das, A. K., Hodson, N. W., Collins, R. F., Ulijn, R. V., et al. (2009). Self-assembled peptide-based hydrogels as scaffolds for anchorage-dependent cells. *Biomaterials* 30, 2523–2530. doi: 10.1016/j.biomaterials.2009.01.010
- Zhu, J. (2010). Bioactive modification of poly(ethylene glycol) hydrogels for tissue engineering. *Biomaterials* 31, 4639–4656. doi: 10.1016/j.biomaterials.2010.02.044
- Zollinger, A. J., and Smith, M. L. (2017). Fibronectin, the extracellular glue. *Matrix Biol.* 60–61, 27–37. doi: 10.1016/j.matbio.2016.07.011

Conflict of Interest Statement: The author declares that the research was conducted in the absence of any commercial or financial relationships that could be construed as a potential conflict of interest.

Copyright © 2018 Langhans. This is an open-access article distributed under the terms of the Creative Commons Attribution License (CC BY). The use, distribution or reproduction in other forums is permitted, provided the original author(s) or licensor are credited and that the original publication in this journal is cited, in accordance with accepted academic practice. No use, distribution or reproduction is permitted which does not comply with these terms.



Is There an Opportunity for Current Chemotherapeutics to Up-regulate MIC-A/B Ligands?

*Kendel Quirk and Shanmugasundaram Ganapathy-Kanniappan**

Division of Interventional Radiology, Russell H. Morgan Department of Radiology and Radiological Science, Johns Hopkins University School of Medicine, Baltimore, MD, United States

OPEN ACCESS

Edited by:

Hideaki Hara,
Gifu Pharmaceutical University, Japan

Reviewed by:

Eric Robinet,
Hôpitaux Universitaires
de Strasbourg, France
Amorette Barber,
Longwood University, United States

*Correspondence:

Shanmugasundaram
Ganapathy-Kanniappan
gshanmu1@jhmi.edu

Specialty section:

This article was submitted to
Experimental Pharmacology and Drug
Discovery,
a section of the journal
Frontiers in Pharmacology

Received: 29 June 2017

Accepted: 28 September 2017

Published: 17 October 2017

Citation:

Quirk K and
Ganapathy-Kanniappan S (2017) Is
There an Opportunity for Current
Chemotherapeutics to Up-regulate
MIC-A/B Ligands?
Front. Pharmacol. 8:732.
doi: 10.3389/fphar.2017.00732

Natural killer (NK) cells are critical effectors of the immune system. NK cells recognize unhealthy cells by specific ligands [e.g., MHC- class I chain related protein A or B (MIC-A/B)] for further elimination by cytotoxicity. Paradoxically, cancer cells down-regulate MIC-A/B and evade NK cell's anticancer activity. Recent data indicate that cellular-stress induces MIC-A/B, leading to enhanced sensitivity of cancer cells to NK cell-mediated cytotoxicity. In this *Perspective* article, we hypothesize that current chemotherapeutics at sub-lethal, non-toxic dose may promote cellular-stress and up-regulate the expression of MIC-A/B ligands to augment cancer's sensitivity to NK cell-mediated cytotoxicity. Preliminary data from two human breast cancer cell lines, MDA-MB-231 and T47D treated with clinically relevant therapeutics such as doxorubicin, paclitaxel and methotrexate support the hypothesis. The goal of this *Perspective* is to underscore the prospects of current chemotherapeutics in NK cell immunotherapy, and discuss potential challenges and opportunities to improve cancer therapy.

Keywords: cancer, natural killer cells, doxorubicin, immunotherapy, MIC-A/B

INTRODUCTION

Cancer continues to be one of the leading causes of death (Global Burden of Disease Cancer Collaboration et al., 2015). Our understanding of carcinogenesis has significantly advanced in the recent decades. Consequently, several novel strategies and potential anticancer therapeutics have emerged, although with limited success in translation. Some of the common challenges that block successful clinical translation of potential therapeutics include resistance to therapy, metastasis, etc. Apart from the biological challenges, the cancer drug development program is also impeded by the high-cost and extensive time incurred for the development of *de novo* drugs (Ishida et al., 2016). Recently, there has been an interest to exploit serendipitous anticancer effects of therapeutics that are indicated for other ailments. This process of recognition of new indications of a clinically approved therapeutic is referred as “drug repositioning” or “drug repurposing” (Ishida et al., 2016). Emerging reports indicate that such drug repositioning and repurposing could have desirable outcome in the management of cancer. For example, compounds of cardiovascular treatments (Ishida et al., 2016), anti-diabetic agents (Gadducci et al., 2016) and HIV therapeutics (Maksimovic-Ivanic et al., 2017) have been found to promote anticancer effects. In this context, extended application of current chemotherapeutics to enhance the efficacy of immunotherapy has also been indicated (Fournier et al., 2017).

Cancer chemotherapeutics at their maximum tolerated dose or the most efficacious dose have long been known to cause undesirable effects, including immune-suppression (Hersh and Oppenheim, 1967). Reports from two independent groups, Browder et al. (2000) and Klement et al. (2000) demonstrated that repeated, low-dose chemotherapy at frequent cycles promote desirable anticancer effects. Interestingly, a decade earlier it was shown that a combinatorial approach using a low-dose of cyclophosphamide with a low-dose of IL-2 had synergistic, improved anticancer effects (Eggermont and Sugarbaker, 1988). However, the inferences were mainly focused on the combination therapy. Nonetheless, these studies provided the foundation for the modern concept of “metronomic therapy.” Consequently, metronomic treatment has gained much attention (Figure 1A) (Romiti et al., 2017), and has been expected to play a significant role in the context of personalized medicine as well (Andre et al., 2014). Concomitantly, data also emerged indicating that conventional maximum tolerated dose of chemotherapeutics affect anticancer immune cells (e.g., NK cells) (Saijo et al., 1982; Sewell et al., 1993). Furthermore, post-chemotherapy though a recovery in total number of immune cells was observed, the functional recovery was not evident indicating loss of immune cell function in breast cancer as well as lung cancer (Saijo et al., 1982; Sewell et al., 1993). On one hand, the anticancer function of immune cells such as NK cells has been known to be affected by high dose chemotherapeutics; on the other hand, low-dose metronomic therapy improves anticancer effects. With this background, emerging concepts point to the optimization of drug regimen that could augment or facilitate anticancer immune activity (Emens et al., 2001; Emens and Middleton, 2015). Yet, there is paucity of data on the immunotherapeutic potential of chemotherapeutics to enhance the efficacy and/or opportunity for natural killer (NK)-cells, a principal component of the immune system. Here, in this *Perspective* in the light of recent research, we discuss the potential of sub-lethal, non-toxic dose of current chemotherapeutics to induce the expression of MIC-A/B to sensitize cancer cells to NK-cell mediated cytotoxicity.

TUMOR CELLS, IMMUNE EVASION, AND NK CELLS

Cancer cells evade immune surveillance, and this “immune evasion” has recently been recognized as one of the hallmarks of cancer (Hanahan and Weinberg, 2011). Though earliest report on the anticancer potential of the immune system dates back to the 19th century (Coley, 1898), only in the past few decades the clinical relevance and plausible outcomes of immunotherapies have been recognized (Burnet, 1957). For example, recent reports on tumor microenvironment (TME) and understanding the impact of cancer metabolism on TME have shed light in deciphering the anti-immune properties of TME (Ganapathy-Kanniappan, 2017a,b). Emerging data indicate that the alteration of TME could impact the antitumor immune response (Husain et al., 2013; Fu et al., 2015). Among immune cells, besides the T cells, studies on NK cells have also gained momentum. NK cells are an integral component of the

immune system and are considered as the “first line” of defense (Lodoen and Lanier, 2006). NK cells detect and target unhealthy or diseased cells including cancer, and induce cytotoxicity. Thus, NK cell-mediated cytotoxicity is an effective anticancer immunotherapeutic approach (Ljunggren and Malmberg, 2007). Mechanistically, cell surface receptors on NK cells recognize specific ligands (commonly known as NK-G2D ligands) on target cells to induce cytolytic processes. Among the NKG2D ligands, MHC- class I chain related protein A or B (MIC-A/B) are known to be up-regulated during cellular pathology. Paradoxically, cancer cells have been known to reduce the surface expression of MIC-A/B ligands through multiple mechanisms such as cleavage/shedding of the extracellular domain of MIC-A/B or down-regulation of expression (Rzymyski et al., 2012; Chitadze et al., 2013). Multiple lines of evidence indicate that restoration of MIC-A/B expression render cancer cells sensitive to NK cell mediated cytotoxicity (de Kruijff et al., 2012; Okita et al., 2012). Thus, interference with cancer’s mechanism of down-regulation of MIC-A/B to up-regulate the expression may be an effective approach to enhance cancer’s sensitivity to NK cells. Akin to this, disruption of energy metabolism of cancer (Fu et al., 2015), induction of thermal stress (Dayanc et al., 2013), exposure to pro-oxidants such as hydrogen peroxide (Yamamoto et al., 2001) and reactive oxygen species (Soriani et al., 2014) have been shown to up-regulate the expression of MIC-A/B in cancer. However, the underlying mechanism of such cellular or metabolic stress-related MIC-A/B up-regulation remains to be known. Nevertheless, the characteristic feature that MIC-A/B are stress-inducible provides a window of opportunity to envisage clinically relevant approaches to induce stress in cancer cells.

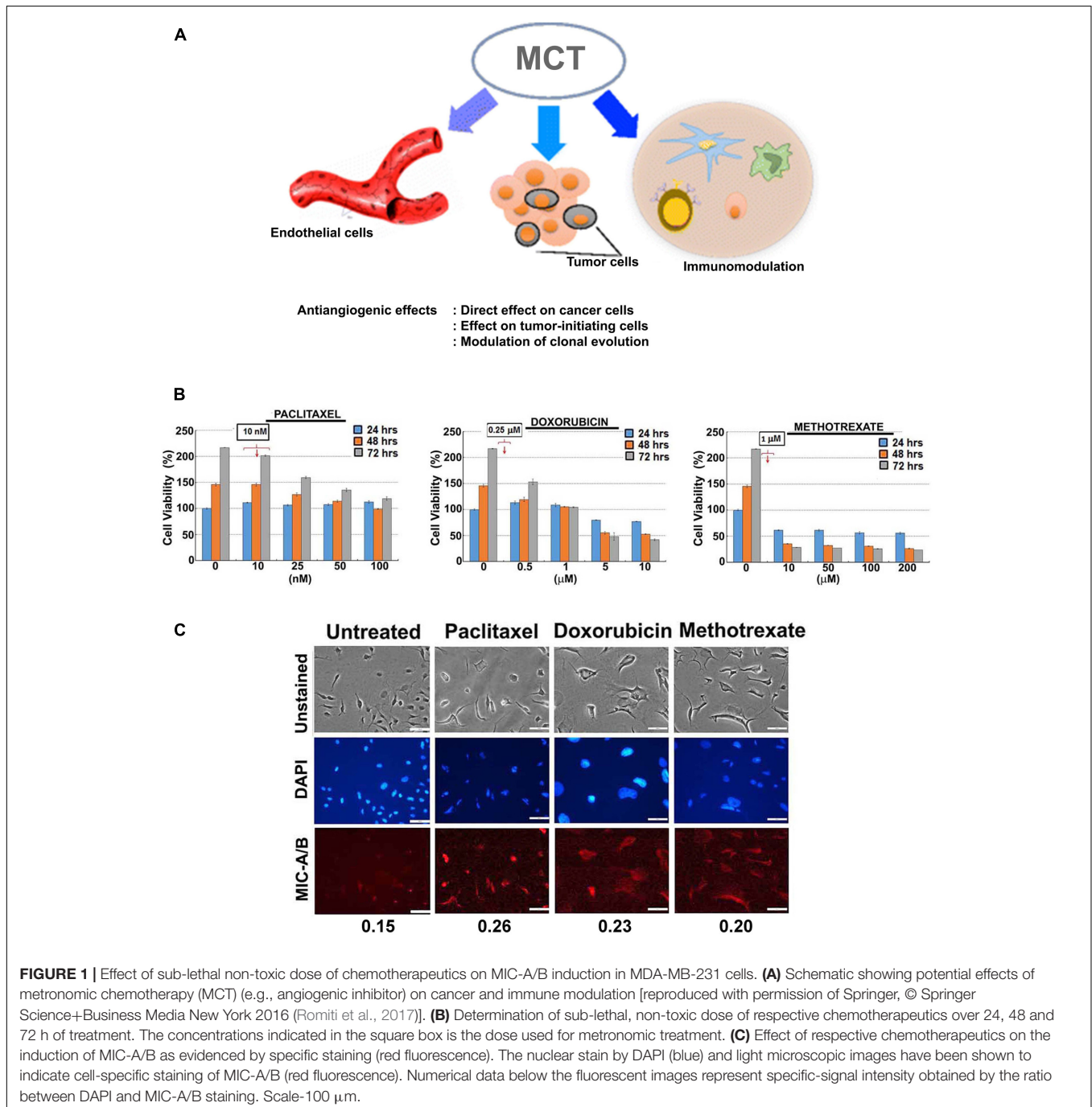
CHEMOTHERAPEUTICS AND THE POTENTIAL FOR SENSITIZATION TO NK CELLS

Current chemotherapeutics play a pivotal role in the management of cancer, especially in advanced stages such as metastatic cancers. Ever since the recognition of chemical agents as potential therapeutics in the dawn of 20th century, the field of chemotherapy has advanced remarkably (refer review by DeVita and Chu, 2008). While some chemotherapeutics have been indicated to interfere with the efficacy of NK cell mediated killing of cancer cells others have proven to be effective in enhancing the outcome of NK cell mediated immunotherapy. Besides, in the presence of natural compounds (e.g., fruit extracts of *Morus alba* L.) chemotherapeutic like 5-fluorouracil demonstrated increased anticancer efficacy which involved enhanced NK cell activity (Markasz et al., 2007). Similarly, inhibitors of histone deacetylases (HDACs) such as Trichostatin A have been shown to sensitize cancer cells to NK cell mediated cytotoxicity (Tiper and Webb, 2016; Shin et al., 2017). Recently, Yang et al. (2015) have documented that the HDAC inhibitor, suberoylanilide hydroxamic acid (SAHA) upregulates MIC-A/B by facilitating gene-specific acetylation. Thus, deregulation of epigenetic mechanisms

have been indicated to up-regulate MIC-A/B based on genetic regulation.

Irrespective of the diverse class of chemotherapeutics such as DNA-damaging agents (e.g., doxorubicin), antimetabolites (e.g., methotrexate), mitotic inhibitors (e.g., paclitaxel), nucleotide analogs (6-mercaptopurine) or inhibitors of topoisomerases (e.g., etoposide), anticancer agents in general mediate their effects by induction of cell death mechanisms (Herr and Debatin, 2001). Noteworthy, a common underlying mechanism is the induction of specific or overall cellular stress, and

the severity of which determines the outcome (i.e.) cell death (Herr and Debatin, 2001). Invariably, the majority of chemotherapeutics implicate the induction of cellular-stress during their anticancer effects (Gewirtz, 1999; Minotti et al., 2004). Since chemotherapeutics could induce cellular-stress and the MIC-A/B ligands required for NK cell recognition are stress-inducible, it is intriguing to verify whether chemotherapeutics could be exploited to up-regulate MIC-A/B. To test this hypothesis it is imperative to include couple of guidelines. (i) The objective of using the chemotherapeutic is not to



achieve cytotoxicity but to induce the expression of MIC-A/B to facilitate NK cell mediated cytotoxicity. This would facilitate effective infiltration and targeting of cancer cells by the NK cell population providing a repertoire of immunological responses against cancer. (ii) The selection of chemotherapeutic dose (sub-lethal, non-toxic low-dose) should be sufficient to cause sustainable cellular stress to allow the induction of MIC-A/B.

For preliminary investigation, two human breast cancer cell lines, MDA-MB-231 and T47D were examined with one or more of the following clinically relevant therapeutics such as doxorubicin, paclitaxel, 4-hydroxy tamoxifen (4-HT) and methotrexate. As indicated in **Figures 1B, 2A**, the sub-lethal, maximum non-toxic dose of respective chemotherapeutics was determined (IC₁₀) and the cells were subjected to treatment at the dose equivalent or lesser than the IC₁₀. The IC₁₀ was determined by Celltiter-Glo Bioluminescent assay (Promega, Co., United States). In brief, a day before the metronomic

treatment, cells growing in log-phase were plated to attain ~60% confluency in 96-well plates (for toxicity assay). The following day, metronomic treatment was initiated with the replacement of complete-growth medium with various concentrations of the drugs to be tested. The drug-containing media was replaced every 48 h, and the viability assay was performed 4-days from the initiation of treatment. For MIC-A/B immunostaining, only the chosen concentration (the dose equivalent or lesser than the IC₁₀) was used, but the cells were plated in 8-well chamber/cover-glass slides (for immunofluorescence imaging). The treatment was performed as described and staining was performed with specific antibodies. Immunofluorescence imaging showed that treatment with sub-lethal, non-toxic dose of chemotherapeutics elevated the expression of MIC-A/B compared to untreated (control) cells (**Figures 1C, 2B**). Quantification of specific signal intensity normalized with nuclear stain (DAPI) signal showed chemotherapy-dependent induction of MIC-A/B (**Figures 1C, 2B**). As discussed earlier,

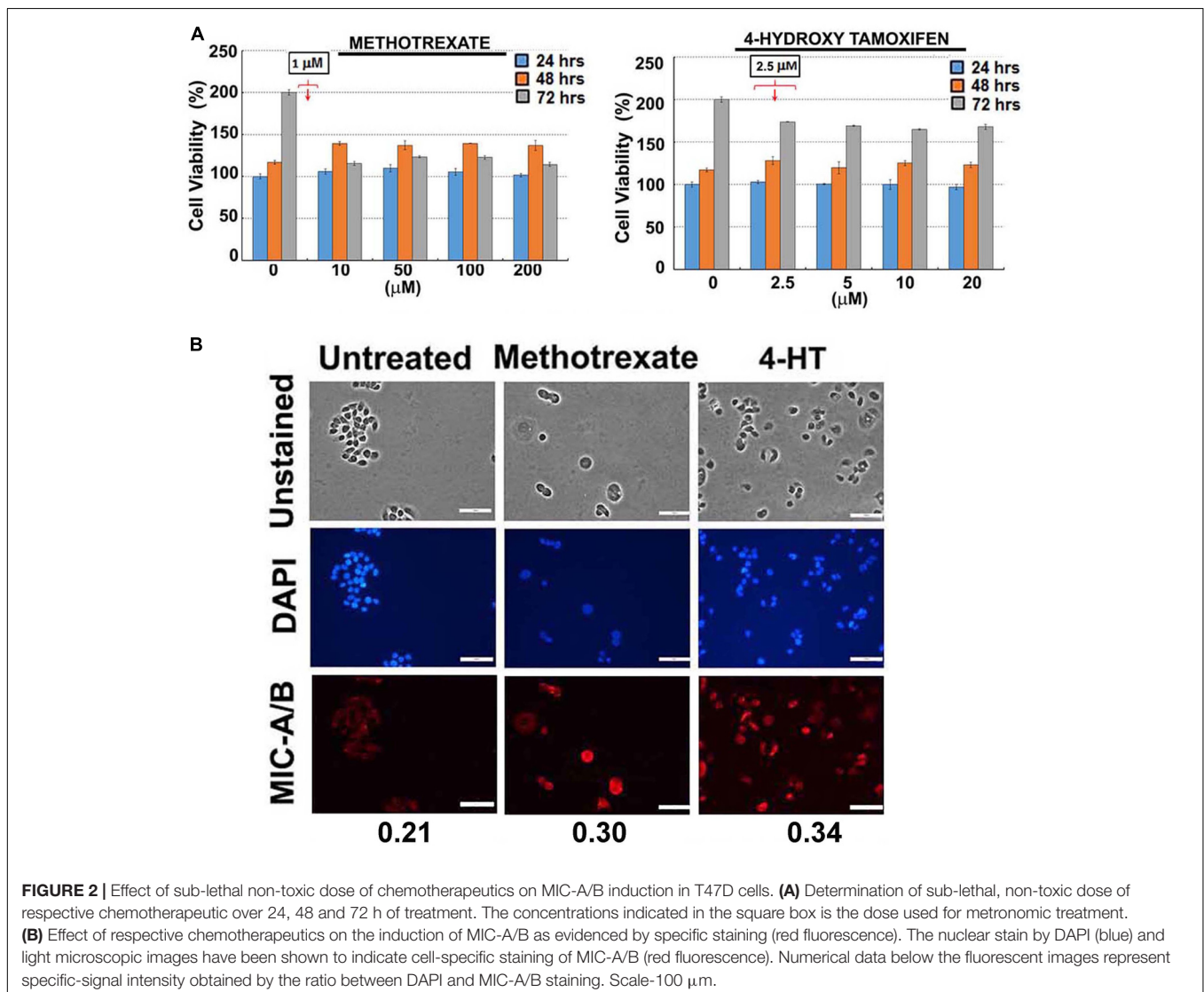


FIGURE 2 | Effect of sub-lethal non-toxic dose of chemotherapeutics on MIC-A/B induction in T47D cells. **(A)** Determination of sub-lethal, non-toxic dose of respective chemotherapeutic over 24, 48 and 72 h of treatment. The concentrations indicated in the square box is the dose used for metronomic treatment. **(B)** Effect of respective chemotherapeutics on the induction of MIC-A/B as evidenced by specific staining (red fluorescence). The nuclear stain by DAPI (blue) and light microscopic images have been shown to indicate cell-specific staining of MIC-A/B (red fluorescence). Numerical data below the fluorescent images represent specific-signal intensity obtained by the ratio between DAPI and MIC-A/B staining. Scale-100 μm.

genetic or epigenetic regulation of MIC-A/B by specific inhibitors like SAHA have already been known (Yang et al., 2015). Yet, the up-regulation of MIC-A/B by clinically relevant chemotherapy-dependent cellular stress remains to be known.

OPPORTUNITIES, CHALLENGES, AND FUTURE DIRECTIONS

Clinical data obtained from 30 patients demonstrated that the functional status of NK cells during or after chemotherapy strongly correlated with the disease-free survival or tumor recurrence (Mackay et al., 1983). Similarly, an overall increase in immune-infiltration of tumors following chemotherapy has also been known (Hernberg et al., 1997). However, due to the lack of mechanistic insights, skepticism overruled the immunotherapeutic potential of chemotherapeutics. Emerging reports unravel the possible mechanisms and provide significant insights on chemotherapy-related sensitivity of cancer to immune cells such as T cells and NK cells. Using clinically relevant chemotherapeutics it has also been demonstrated that induction of cellular stress or genotoxic stress render cancer cells sensitive to NK cells (Fine et al., 2010). Further, it has been shown that chemotherapy-dependent down-regulation of C-type lectin related receptor on cancer cells was coordinated with an up-regulation of NKG2D ligands (Fine et al., 2010). Note, MIC-A/B are also NKG2D ligands that are recognized by NK cells. In fact, in end-stage patients it has been demonstrated that low-dose metronomic treatment with cyclophosphamide depletes the regulatory T cells (T_{reg} - that inhibit the cytotoxic T lymphocytes), and restores the activity of T-cells as well as NK cells (Ghiringhelli et al., 2007). However, a direct molecular link between tumor sensitivity and NK cell efficacy following chemotherapy still remains obscure. Recent data demonstrated that induction cellular stress (e.g., H_2O_2 , thermal stress, metabolic stress) followed by the up-regulation of MIC-A/B is a direct molecular link that sensitizes cancer cells to NK cell mediated cytotoxicity (Yamamoto et al., 2001; Dayanc et al., 2013; Fu et al., 2015). It has also been shown that such stress conditions decrease the rate of shedding or cleavage of the MIC-A/B a mechanism that enables cancer cells to evade NK cell recognition (Chitadze et al., 2013). These reports unequivocally indicate that induction of cellular stress could be pivotal to up-regulate NKG2D ligands (Fine et al., 2010) and sensitize cancer cells to NK cell activity.

The preliminary data shown here certainly necessitates detailed investigation for further validation. Yet, the results provide first indication of the possible application of current chemotherapeutics at non-lethal metronomic doses to induce cellular stress followed by the expression of stress-inducible MIC-A/B. Importantly, as the therapeutics are used at very low, non-toxic doses it is likely to avoid or prevent potential systemic toxicities or undesirable effects that are frequently encountered with conventional chemotherapy. For example, chemotherapy-related complications on gastrointestinal tract (Boussios et al.,

2012) and cardiovascular toxicities (Swain et al., 2003; Jones et al., 2007; Khouri et al., 2012) have already been reported. Furthermore, chemotherapy related toxicities on the central nervous system (e.g., methotrexate) (Cordelli et al., 2017) and cardiomyopathy (e.g., doxorubicin) have also been reported (Chatterjee et al., 2010). Besides toxicities, the undesirable effect of some therapeutics (e.g., tamoxifen) involves impact on patient's face, eyelids, and eyebrows, resulting in frequent visits to the optometrist as well (Omoti and Omoti, 2006).

Paclitaxel, doxorubicin, and methotrexate are common chemotherapeutics approved for the use in the treatment of many cancers. However, using the maximum effective dose with extended periods between treatment cycles has proven to decrease the outcome, with increased systemic toxicity. Recently, metronomic chemotherapy has been suggested as an alternative option to mitigate unwanted side-effects of maximum effective dose (Scharovsky et al., 2009). Thus, by using non-toxic, sub-lethal dose the risk of systemic toxicity is likely to be lowered, if not eliminated. More importantly, such low-dose chemotherapeutics would not hinder or block host immune cells' function.

Arguably, the use of low-dose chemotherapeutics by metronomic treatment may contribute for the emergence of a resistant or "addiction" phenotype. Such cancer cells may become insensitive to any dose escalation if necessary. In principle, cancer cells that are subjected to cellular stress and induction of MIC-A/B would be sensitive to NK cells hence would be eliminated. Thus, cells that are exposed to low-dose metronomic treatment are likely to be eliminated by NK cell mediated cytotoxicity. Furthermore, data also indicate that cancer cells that acquired resistance to low-dose chemotherapy are still sensitive to the maximum tolerated effective dose (Emmenegger et al., 2011). So, it is plausible that despite the low-dose exposure the cancer cells still be responsive to high-dose chemotherapy. Nevertheless, additional pre-clinical as well as clinical investigations are mandatory to verify any potential concerns. Future studies on the stability and half-life of MIC-A/B ligands that are induced by low-dose, non-toxic chemotherapeutic would be critical to ascertain if the MIC-A/B induction will sensitize cancer cells to NK cells. In addition, as cancer cells evade NK cell recognition by shedding or cleavage of the MIC-A/B, it is imperative to determine whether low-dose chemotherapy mitigates or inhibits such shedding of MIC-A/B. Thus, current chemotherapeutics may have an extended application to induce or enhance cancer's sensitivity to NK cell mediated cytotoxicity.

AUTHOR CONTRIBUTIONS

KQ and SG-K designed, discussed, and wrote the manuscript.

ACKNOWLEDGMENT

We gratefully acknowledge the support by Charles Wallace Pratt Research Fund.

REFERENCES

- Andre, N., Carre, M., and Pasquier, E. (2014). Metronomics: towards personalized chemotherapy? *Nat. Rev. Clin. Oncol.* 11, 413–431. doi: 10.1038/nrclinonc.2014.89
- Boussios, S., Penteroudakis, G., Katsanos, K., and Pavlidis, N. (2012). Systemic treatment-induced gastrointestinal toxicity: incidence, clinical presentation and management. *Ann. Gastroenterol.* 25, 106–118.
- Browder, T., Butterfield, C. E., Kraling, B. M., Shi, B., Marshall, B., O'Reilly, M. S., et al. (2000). Antiangiogenic scheduling of chemotherapy improves efficacy against experimental drug-resistant cancer. *Cancer Res.* 60, 1878–1886.
- Burnet, M. (1957). Cancer: a biological approach. I. The processes of control. *Br. Med. J.* 1, 779–786. doi: 10.1136/bmj.1.5022.779
- Chatterjee, K., Zhang, J., Honbo, N., and Karliner, J. S. (2010). Doxorubicin cardiomyopathy. *Cardiology* 115, 155–162. doi: 10.1159/000265166
- Chitadze, G., Lettau, M., Bhat, J., Wesch, D., Steinle, A., Furst, D., et al. (2013). Shedding of endogenous MHC class I-related chain molecules A and B from different human tumor entities: heterogeneous involvement of the “a disintegrin and metalloproteases” 10 and 17. *Int. J. Cancer* 133, 1557–1566. doi: 10.1002/ijc.28174
- Coley, W. B. (1898). The treatment of inoperable sarcoma with the mixed toxins of erysipelas and bacillus prodigiosus: immediate and final results in one hundred and forty cases. *JAMA* 31, 389–395. doi: 10.1001/jama.1898.92450080015001d
- Cordelli, D. M., Masetti, R., Zama, D., Toni, F., Castelli, I., Ricci, E., et al. (2017). Central nervous system complications in children receiving chemotherapy or hematopoietic stem cell transplantation. *Front. Pediatr.* 5:105. doi: 10.3389/fped.2017.00105
- Dayanc, B. E., Bansal, S., Gure, A. O., Gollnick, S. O., and Repasky, E. A. (2013). Enhanced sensitivity of colon tumour cells to natural killer cell cytotoxicity after mild thermal stress is regulated through HSF1-mediated expression of MICA. *Int. J. Hyperthermia* 29, 480–490. doi: 10.3109/02656736.2013.821526
- de Kruif, E. M., Sajet, A., van Nes, J. G., Putter, H., Smit, V. T., Eagle, R. A., et al. (2012). NKG2D ligand tumor expression and association with clinical outcome in early breast cancer patients: an observational study. *BMC Cancer* 12:24. doi: 10.1186/1471-2407-12-24
- DeVita, V. T. Jr., and Chu, E. (2008). A history of cancer chemotherapy. *Cancer Res.* 68, 8643–8653. doi: 10.1158/0008-5472.CAN-07-6611
- Eggermont, A. M., and Sugarbaker, P. H. (1988). Efficacy of chemoimmunotherapy with cyclophosphamide, interleukin-2 and lymphokine activated killer cells in an intraperitoneal murine tumour model. *Br. J. Cancer* 58, 410–414. doi: 10.1038/bjc.1988.231
- Emens, L. A., Machiels, J. P., Reilly, R. T., and Jaffee, E. M. (2001). Chemotherapy: Friend or foe to cancer vaccines? *Curr. Opin. Mol. Ther.* 3, 77–84.
- Emens, L. A., and Middleton, G. (2015). The interplay of immunotherapy and chemotherapy: harnessing potential synergies. *Cancer Immunol. Res.* 3, 436–443. doi: 10.1158/2326-6066.CIR-15-0064
- Emmenegger, U., Francia, G., Chow, A., Shaked, Y., Kouri, A., Man, S., et al. (2011). Tumors that acquire resistance to low-dose metronomic cyclophosphamide retain sensitivity to maximum tolerated dose cyclophosphamide. *Neoplasia* 13, 40–48. doi: 10.1593/neo.101174
- Fine, J. H., Chen, P., Mesci, A., Allan, D. S., Gasser, S., Raulet, D. H., et al. (2010). Chemotherapy-induced genotoxic stress promotes sensitivity to natural killer cell cytotoxicity by enabling missing-self recognition. *Cancer Res.* 70, 7102–7113. doi: 10.1158/0008-5472.CAN-10-1316
- Fournier, C., Rivera Vargas, T., Martin, T., Melis, A., and Apetoh, L. (2017). Immunotherapeutic properties of chemotherapy. *Curr. Opin. Pharmacol.* 35, 1–6. doi: 10.1016/j.coph.2017.05.003
- Fu, D., Geschwind, J. F., Karthikeyan, S., Miller, E., Kunjithapatham, R., Wang, Z., et al. (2015). Metabolic perturbation sensitizes human breast cancer to NK cell-mediated cytotoxicity by increasing the expression of MHC class I chain-related A/B. *Oncoimmunology* 4:e991228. doi: 10.4161/2162402X.2014.991228
- Gadducci, A., Biglia, N., Tana, R., Cosio, S., and Gallo, M. (2016). Metformin use and gynecological cancers: a novel treatment option emerging from drug repositioning. *Crit. Rev. Oncol. Hematol.* 105, 73–83. doi: 10.1016/j.critrevonc.2016.06.006
- Ganapathy-Kanniappan, S. (2017a). Linking tumor glycolysis and immune evasion in cancer: emerging concepts and therapeutic opportunities. *Biochim. Biophys. Acta* 1868, 212–220. doi: 10.1016/j.bbcan.2017.04.002
- Ganapathy-Kanniappan, S. (2017b). Taming tumor glycolysis and potential implications for immunotherapy. *Front. Oncol.* 7:36. doi: 10.3389/fonc.2017.00036
- Gewirtz, D. A. (1999). A critical evaluation of the mechanisms of action proposed for the antitumor effects of the anthracycline antibiotics adriamycin and daunorubicin. *Biochem. Pharmacol.* 57, 727–741. doi: 10.1016/S0006-2952(98)00307-4
- Ghiringhelli, F., Menard, C., Puig, P. E., Ladoire, S., Roux, S., Martin, F., et al. (2007). Metronomic cyclophosphamide regimen selectively depletes CD4+CD25+ regulatory T cells and restores T and NK effector functions in end stage cancer patients. *Cancer Immunol. Immunother.* 56, 641–648. doi: 10.1007/s00262-006-0225-8
- Global Burden of Disease Cancer Collaboration, Fitzmaurice, C., Dicker, D., Pain, A., Hamavid, H., Moradi-Lakeh, M., et al. (2015). The global burden of cancer 2013. *JAMA Oncol.* 1, 505–527. doi: 10.1001/jamaoncol.2015.0735
- Hanahan, D., and Weinberg, R. A. (2011). Hallmarks of cancer: the next generation. *Cell* 144, 646–674. doi: 10.1016/j.cell.2011.02.013
- Hernberg, M., Turunen, J. P., Muhonen, T., and Pyrhonen, S. (1997). Tumor-infiltrating lymphocytes in patients with metastatic melanoma receiving chemoimmunotherapy. *J. Immunother.* 20, 488–495. doi: 10.1097/00002371-199711000-00009
- Herr, I., and Debatin, K. M. (2001). Cellular stress response and apoptosis in cancer therapy. *Blood* 98, 2603–2614. doi: 10.1182/blood.V98.9.2603
- Hersh, E. M., and Oppenheim, J. J. (1967). Inhibition of in vitro lymphocyte transformation during chemotherapy in man. *Cancer Res.* 27, 98–105.
- Husain, Z., Seth, P., and Sukhatme, V. P. (2013). Tumor-derived lactate and myeloid-derived suppressor cells: linking metabolism to cancer immunology. *Oncoimmunology* 2:e26383. doi: 10.4161/onci.26383
- Ishida, J., Konishi, M., Ebner, N., and Springer, J. (2016). Repurposing of approved cardiovascular drugs. *J. Transl. Med.* 14:269. doi: 10.1186/s12967-016-1031-5
- Jones, L. W., Haykowsky, M. J., Swartz, J. J., Douglas, P. S., and Mackey, J. R. (2007). Early breast cancer therapy and cardiovascular injury. *J. Am. Coll. Cardiol.* 50, 1435–1441. doi: 10.1016/j.jacc.2007.06.037
- Khoury, M. G., Douglas, P. S., Mackey, J. R., Martin, M., Scott, J. M., Scherrer-Crosbie, M., et al. (2012). Cancer therapy-induced cardiac toxicity in early breast cancer: addressing the unresolved issues. *Circulation* 126, 2749–2763. doi: 10.1161/CIRCULATIONAHA.112.100560
- Klement, G., Baruchel, S., Rak, J., Man, S., Clark, K., Hicklin, D. J., et al. (2000). Continuous low-dose therapy with vinblastine and VEGF receptor-2 antibody induces sustained tumor regression without overt toxicity. *J. Clin. Invest.* 105, R15–R24. doi: 10.1172/JCI8829
- Ljunggren, H. G., and Malmberg, K. J. (2007). Prospects for the use of NK cells in immunotherapy of human cancer. *Nat. Rev. Immunol.* 7, 329–339. doi: 10.1038/nri2073
- Lodoen, M. B., and Lanier, L. L. (2006). Natural killer cells as an initial defense against pathogens. *Curr. Opin. Immunol.* 18, 391–398. doi: 10.1016/j.coi.2006.05.002
- Mackay, I. R., Goodyear, M. D., Riglar, C., and Penschow, J. (1983). Effect on natural killer and antibody-dependent cellular cytotoxicity of adjuvant cytotoxic chemotherapy including melphalan in breast cancer. *Cancer Immunol. Immunother.* 16, 98–100. doi: 10.1007/BF00199239
- Maksimovic-Ivanic, D., Fagone, P., McCubrey, J., Bendtzen, K., Mijatovic, S., and Nicoletti, F. (2017). HIV-protease inhibitors for the treatment of cancer: repositioning HIV protease inhibitors while developing more potent NO-hybridized derivatives? *Int. J. Cancer* 140, 1713–1726. doi: 10.1002/ijc.30529
- Markasz, L., Stuber, G., Vanherberghen, B., Flaberg, E., Olah, E., Carbone, E., et al. (2007). Effect of frequently used chemotherapeutic drugs on the cytotoxic activity of human natural killer cells. *Mol. Cancer Ther.* 6, 644–654. doi: 10.1158/1535-7163.MCT-06-0358
- Minotti, G., Menna, P., Salvatorelli, E., Cairo, G., and Gianni, L. (2004). Anthracyclines: molecular advances and pharmacologic developments in antitumor activity and cardiotoxicity. *Pharmacol. Rev.* 56, 185–229. doi: 10.1124/pr.56.2.6
- Okita, R., Mougialakos, D., Ando, T., Mao, Y., Sarhan, D., Wennerberg, E., et al. (2012). HER2/HER3 signaling regulates NK cell-mediated cytotoxicity via MHC class I chain-related molecule A and B expression in human breast cancer cell lines. *J. Immunol.* 188, 2136–2145. doi: 10.4049/jimmunol.1102237

- Omoti, A. E., and Omoti, C. E. (2006). Ocular toxicity of systemic anticancer chemotherapy. *Pharm. Pract.* 4, 55–59. doi: 10.4321/S1885-642X2006000200001
- Romiti, A., Falcone, R., Roberto, M., and Marchetti, P. (2017). Current achievements and future perspectives of metronomic chemotherapy. *Invest. New Drugs* 35, 359–374. doi: 10.1007/s10637-016-0408-x
- Rzymiski, T., Petry, A., Kracun, D., Riess, F., Pike, L., Harris, A. L., et al. (2012). The unfolded protein response controls induction and activation of ADAM17/TACE by severe hypoxia and ER stress. *Oncogene* 31, 3621–3634. doi: 10.1038/onc.2011.522
- Saijo, N., Shimizu, E., Shibuya, M., Irimajiri, N., Takizawa, T., Eguchi, K., et al. (1982). Effect of chemotherapy on natural-killer activity and antibody-dependent cell-mediated cytotoxicity in carcinoma of the lung. *Br. J. Cancer* 46, 180–189. doi: 10.1038/bjc.1982.182
- Scharovsky, O. G., Mainetti, L. E., and Rozados, V. R. (2009). Metronomic chemotherapy: changing the paradigm that more is better. *Curr Oncol* 16, 7–15. doi: 10.3747/co.v16i2.420
- Sewell, H. F., Halbert, C. F., Robins, R. A., Galvin, A., Chan, S., and Blamey, R. W. (1993). Chemotherapy-induced differential changes in lymphocyte subsets and natural-killer-cell function in patients with advanced breast cancer. *Int. J. Cancer* 55, 735–738. doi: 10.1002/ijc.2910550506
- Shin, S., Kim, M., Lee, S. J., Park, K. S., and Lee, C. H. (2017). Trichostatin A sensitizes hepatocellular carcinoma cells to enhanced NK cell-mediated killing by regulating immune-related genes. *Cancer Genomics Proteomics* 14, 349–362.
- Soriani, A., Iannitto, M. L., Ricci, B., Fionda, C., Malgarini, G., Morrone, S., et al. (2014). Reactive oxygen species- and DNA damage response-dependent NK cell activating ligand upregulation occurs at transcriptional levels and requires the transcriptional factor E2F1. *J. Immunol.* 193, 950–960. doi: 10.4049/jimmunol.1400271
- Swain, S. M., Whaley, F. S., and Ewer, M. S. (2003). Congestive heart failure in patients treated with doxorubicin: a retrospective analysis of three trials. *Cancer* 97, 2869–2879. doi: 10.1002/cncr.11407
- Tiper, I. V., and Webb, T. J. (2016). Histone deacetylase inhibitors enhance CD1d-dependent NKT cell responses to lymphoma. *Cancer Immunol. Immunother.* 65, 1411–1421. doi: 10.1007/s00262-016-1900-z
- Yamamoto, K., Fujiyama, Y., Andoh, A., Bamba, T., and Okabe, H. (2001). Oxidative stress increases MICA and MICB gene expression in the human colon carcinoma cell line (CaCo-2). *Biochim. Biophys. Acta* 1526, 10–12. doi: 10.1016/S0304-4165(01)00099-X
- Yang, H., Lan, P., Hou, Z., Guan, Y., Zhang, J., Xu, W., et al. (2015). Histone deacetylase inhibitor SAHA epigenetically regulates miR-17-92 cluster and MCM7 to upregulate MICA expression in hepatoma. *Br. J. Cancer* 112, 112–121. doi: 10.1038/bjc.2014.547

Conflict of Interest Statement: The authors declare that the research was conducted in the absence of any commercial or financial relationships that could be construed as a potential conflict of interest.

Copyright © 2017 Quirk and Ganapathy-Kanniappan. This is an open-access article distributed under the terms of the Creative Commons Attribution License (CC BY). The use, distribution or reproduction in other forums is permitted, provided the original author(s) or licensor are credited and that the original publication in this journal is cited, in accordance with accepted academic practice. No use, distribution or reproduction is permitted which does not comply with these terms.



Drug Repositioning in the Mirror of Patenting: Surveying and Mining Uncharted Territory

Hermann A. M. Mucke*

H. M. Pharma Consultancy, Wien, Austria

Keywords: chemistry, data mining, drug repositioning, expert systems, patents as topic

A MULTIMODAL APPROACH TO THE RE-DEVELOPMENT OF DRUGS

Drug repositioning—the investigation, development and use of active pharmaceutical ingredients for a therapeutic class that is different from the original one—is much more than a “recycling” of known drugs or drug candidates (Oprea and Mestres, 2012). Quite the opposite, it creates novel insights that are of additional scientific and public health interest. Exploiting the fact that very few compounds act on only one molecular target is just one aspect; drug repositioning can also use drug targets as a starting point to screen compound libraries. Nowadays it goes far beyond serendipity, making use of the newest insights in chemical genomics (Bisson, 2012), computational biology (Hodos et al., 2016; Li et al., 2016), systems medicine (Mei et al., 2016), and text mining (Tari and Patel, 2014) to utilize pharmacological activities (known or newly identified) in more ways than had been originally envisaged. This approach extends to biotechnology products, and even vaccines (Veljkovic and Paessler, 2016).

The constantly growing number of repositioning-related peer review papers in PubMed reflects the growing scientific interest in the subject. For 2016, a search for papers indexed under the MeSH term “drug repositioning” or the keyword “drug repurposing” returned 306 hits. Considering that many relevant contributions are not being indexed in this way, and do not contain “drug repurposing” in their titles or abstracts, this captures only part of the actual publishing activity even as reflected in PubMed-listed journals.

PATENTING IN DRUG REPOSITIONING PROJECTS

Drug repositioning offers more immediate value than developing a new chemical entity. Re-developing an active compound that is already marketed, or at least has some accessible preclinical or clinical data, is associated with a substantially reduced risk of failure that may be due to safety, resulting in improved success rates (Caban et al., 2017). Depending on circumstances, the path toward regulatory approval can be shortened, and savings in terms of time to market and cost can be realized. Although there are many issues to consider in the commercial valuation of a drug re-development project, obtaining intellectual property for the new use (frequently combined with a new formulation, which may involve a different route of administration) will always be a paramount factor (Sternitzke, 2014).

PATENTS AS AN INFORMATION SOURCE FOR DRUG REPOSITIONING R&D

There is more to patenting than just establishing intellectual property. Drug-related patents are a source of pharmacological and developmental information that offers an orthogonal perspective

OPEN ACCESS

Edited by:

Yuhei Nishimura,
Mie University Graduate School of
Medicine, Japan

Reviewed by:

Bruce Bloom,
Cures Within Reach, United States

***Correspondence:**

Hermann A. M. Mucke
h.mucke@hmpharmacon.com

Specialty section:

This article was submitted to
Experimental Pharmacology and Drug
Discovery,
a section of the journal
Frontiers in Pharmacology

Received: 20 November 2017

Accepted: 07 December 2017

Published: 15 December 2017

Citation:

Mucke HAM (2017) Drug
Repositioning in the Mirror of
Patenting: Surveying and Mining
Uncharted Territory.
Front. Pharmacol. 8:927.
doi: 10.3389/fphar.2017.00927

on research and development activity in the field: while peer reviewed journals aim at publishing what has scientific novelty, patenting primarily reflects what inventors and patent assignees deem to be of relatively immediate applicability. Its requirements for novelty and non-obviousness are not academic but practical ones. To obtain a complete perspective of drug repositioning activity, it would be extremely worthwhile to investigate patent documents as a complement to peer reviewed publishing.

This is not a trivial task because no ontology or keyword pattern exists that would allow a targeted search for “novel medical use” patents. In effect, the abstracts of all patents in the pharmaceutical category (and in many cases, the full texts) have to be examined for such content. For international disclosures published under the Patent Convention Treaty, this amounts to 250–300 documents per week that need to be screened.

WHAT STUDYING DRUG REPOSITIONING PATENTS CAN OFFER

We have shown earlier that source and target indications of drug repurposing, as reflected in international patent applications published during the years 2011–2014, are not randomly distributed in therapeutic space but follow preferred vector patterns (Mucke and Mucke, 2015). Unexpected findings included frequent secondary use claims for oncology agents to treat noninfectious respiratory diseases, and for cardiovascular agents to treat neurological conditions.

A superficial look at the most recent 3-year period between October 2014 and September 2017 confirms that patenting activity in this field continues to be substantial, and is growing. In each quarter during this interval, between 17 and 39 international patent applications claiming drug repositioning matters have been published, to a three-year total of 329 documents—on average, about two per week. Just as with the respective counts in PubMed, these are minimum figures because the repositioning-related content of a patent is sometimes not apparent from its title or abstract.

Some of these patents provide extremely interesting insights into drug re-development work in industry and academia that are not published elsewhere, or are published only later. Arbitrarily chosen examples include WO/2014/164667 reporting that entacapone, a COMT inhibitor used in Parkinson's disease, inhibits Dengue and West Nile virus proteases; WO/2015/189650 claiming the antithrombotic clopidogrel for benign prostate hyperplasia; claims for the X-ray contrast agents iopamidol and iohexol for treating influenza (WO/2015/116861) and Ebola virus (WO/2016/054658) infections; and the potential utility of gamma secretase inhibitors, notorious for their efficacy failures in Alzheimer's disease clinical trials, for multiple myeloma and leukemias (WO/2017/019496).

Many of these documents do not provide the reader with the type and extent of data support that would be expected from a peer-reviewed paper. But then full data sharing is not their primary purpose (“just enough” is the rule, so that later work is not preempted), and what they do disclose is sometimes tantalizing.

STRATEGIES FOR REPOSITIONING PATENT IDENTIFICATION AND ANALYSIS

There are few firm rules to define how the descriptive part of a patent document has to be written. Even just to find out if a given pharmaceutical patent has drug repositioning content can seem difficult to the novice if the document uses the legalistic and repetitive language that patent attorneys often impose on its actual content – for good reasons, discussion of which is beyond this article's scope. However, with practice the required information is relatively easily found, and the scientific information extracted, using manual searches.

Algorithmic text mining of patent documents for information relevant for drug repositioning remains an unmet challenge. In principle, most approaches that have been developed for mining the peer reviewed biomedical literature for this purpose should also be applicable to patent documents, with relatively few modifications. Integrated strategies that combine keyword searches with genetic regulation and disease phenotypes (Jang et al., 2017; Sun et al., 2017) seem most promising. However, efficacy and reliability of such approaches have never been systematically evaluated.

Extracting chemical information that is presented as Markush formulas is a much more complicated matter. Academic papers use this mode of summarizing many related molecules sparingly, by showing only their common core moiety and then inserting placeholders for substituents or substructures, whose meaning is verbally or graphically defined in the accompanying text. In contrast, pharmaceutical patenting makes extensive use of Markush structures, which at present cannot be algorithmically parsed for known compounds that might be included in the multitude of possibilities covered by the generic structural formula. Interesting approaches to this challenge exist (Deng et al., 2011) but are rarely found in the biomedical literature. They will need much more development before they can provide more than assistance to the pharmacologist or medicinal chemist who is interested in finding out if a particular new use for known compounds is already patented, or who is searching for new opportunities for a given molecule.

SUMMARY

Drug repositioning researchers are well advised not to ignore what patent documents have to offer, even if their format might be different, but doing so requires some experience. Developing improved expert systems that assist researchers in the identification and extraction of relevant information is an important task that could eventually result in algorithms that can run unattended. However, this needs not only programming but also calibration and validation, which does not seem to have been attempted yet. Systematic collections of drug repositioning patent documents could provide a most valuable reference standard in this context.

AUTHOR CONTRIBUTIONS

The author confirms being the sole contributor of this work and approved it for publication.

REFERENCES

- Bisson, W. H. (2012). Drug repurposing in chemical genomics: can we learn from the past to improve the future? *Curr. Top Med. Chem.* 12, 1883–1888. doi: 10.2174/1568026611209061883
- Caban, A., Pisarczyk, K., Kopacz, K., Kapuśniak, A., Toumi, M., Rémuzat, C., et al. (2017). Filling the gap in CNS drug development: evaluation of the role of drug repurposing. *J. Mark Access Health Policy* 5:1299833. doi: 10.1080/20016689.2017.1299833
- Deng, W., Berthel, S. J., and So, W. V. (2011). Intuitive patent markush structure visualization tool for medicinal chemists. *J. Chem. Inf. Model.* 51, 511–520. doi: 10.1021/ci100261u
- Hodos, R. A., Kidd, B. A., Shameer, K., Readhead, B. P., and Dudley, J. T. (2016). *In silico* methods for drug repurposing and pharmacology. *Wiley Interdiscip. Rev. Syst. Biol. Med.* 8, 186–210. doi: 10.1002/wsbm.1337
- Jang, G., Lee, T., Lee, B. M., and Yoon, Y. (2017). Literature-based prediction of novel drug indications considering relationships between entities. *Mol. Biosyst.* 13, 1399–1405. doi: 10.1039/c7mb00020k
- Li, J., Zheng, S., Chen, B., Butte, A. J., Swamidass, S. J., and Lu, Z. (2016). A survey of current trends in computational drug repositioning. *Brief Bioinform.* 17, 2–12. doi: 10.1093/bib/bbv020
- Mei, H., Feng, G., Zhu, J., Lin, S., Qiu, Y., Wang, Y., et al. (2016). A practical guide for exploring opportunities of repurposing drugs for CNS diseases in systems biology. *Methods Mol. Biol.* 1303, 531–547. doi: 10.1007/978-1-4939-2627-5_33
- Mucke, H. A., and Mucke, E. (2015). Sources and targets for drug repurposing: landscaping transitions in therapeutic space. *Assay Drug Dev Technol.* 13, 319–324. doi: 10.1089/adt.2015.29009.hmedrrr
- Oprea, T. I., and Mestres, J. (2012). Drug repurposing: far beyond new targets for old drugs. *AAPS J.* 14, 759–763. doi: 10.1208/S12248-012-9390-1
- Sternitzke, C. (2014). Drug repurposing and the prior art patents of competitors. *Drug Discov. Today* 19, 1841–1847. doi: 10.1016/j.drudis.2014.09.016
- Sun, P., Guo, J., Winnenburger, R., and Baumbach, J. (2017). Drug repurposing by integrated literature mining and drug-gene-disease triangulation. *Drug Discov. Today* 22, 615–619. doi: 10.1016/j.drudis.2016.10.008
- Tari, L. B., and Patel, J. H. (2014). Systematic drug repurposing through text mining. *Methods Mol. Biol.* 1159, 253–267. doi: 10.1007/978-1-4939-0709-0_14
- Veljkovic, V., and Paessler, S. (2016). Possible repurposing of seasonal influenza vaccine for prevention of Zika virus infection. *Version 2.* 5:190. doi: 10.12688/f1000research.8102.2

Conflict of Interest Statement: The author declares that the research was conducted in the absence of any commercial or financial relationships that could be construed as a potential conflict of interest.

Copyright © 2017 Mucke. This is an open-access article distributed under the terms of the Creative Commons Attribution License (CC BY). The use, distribution or reproduction in other forums is permitted, provided the original author(s) or licensor are credited and that the original publication in this journal is cited, in accordance with accepted academic practice. No use, distribution or reproduction is permitted which does not comply with these terms.



Overcoming Obstacles to Drug Repositioning in Japan

Yuhei Nishimura^{1*}, Masaaki Tagawa², Hideki Ito³, Kazuhiro Tsuruma⁴ and Hideaki Hara⁴

¹ Department of Integrative Pharmacology, Mie University Graduate School of Medicine, Tsu, Japan, ² Medical Affairs, Sumitomo Dainippon Pharma Co., Ltd., Tokyo, Japan, ³ Department of CNS Research, Otsuka Pharmaceutical Co., Ltd., Tokushima, Japan, ⁴ Molecular Pharmacology, Department of Biofunctional Evaluation, Gifu Pharmaceutical University, Gifu, Japan

Drug repositioning (DR) is the process of identifying new indications for existing drugs. DR usually focuses on drugs that have cleared phase-I safety trials but has yet to show efficacy for the intended indication. Therefore, DR can probably skip the preclinical and phase-I study, which can reduce the cost throughout drug development. However, the expensive phase-II/III trials are required to establish efficacy. The obstacles to DR include identification of new indications with a high success rate in clinical studies, obtaining funding for clinical studies, patent protection, and approval systems. To tackle these obstacles, various approaches have been applied to DR worldwide. In this perspective, we provide representative examples of DR and discuss the ongoing efforts to overcome obstacles to DR in Japan.

OPEN ACCESS

Edited by:

Luc Zimmer,
Université Claude Bernard Lyon 1
and Hospices Civils de Lyon, France

Reviewed by:

Afzal Chowdhury,
Perkins Cole, LLP, United States
Aris Persidis,
Biovista, United States

*Correspondence:

Yuhei Nishimura
yuhei@doc.medic.mie-u.ac.jp

Specialty section:

This article was submitted to
Experimental Pharmacology and Drug
Discovery,
a section of the journal
Frontiers in Pharmacology

Received: 26 July 2017

Accepted: 28 September 2017

Published: 11 October 2017

Citation:

Nishimura Y, Tagawa M, Ito H,
Tsuruma K and Hara H (2017)
Overcoming Obstacles to Drug
Repositioning in Japan.
Front. Pharmacol. 8:729.
doi: 10.3389/fphar.2017.00729

Keywords: industry-sponsored clinical trial, investigator-initiated clinical trial, electronic health record, sharing resources, computational drug repositioning

OBSTACLES TO DR IN JAPAN

Drug repositioning (DR), also known as “drug repurposing,” seeks to develop new indications for existing drugs, to change the formulation, the dosage regimen, and the route of administration, and to create new combinations of drugs directed at multiple therapeutic targets. At present, the conventional *de novo* drug discovery process requires an average of about 14 years and US\$2.5 billion to approve and launch a drug (Nosengo, 2016). The average time and costs to launch a drug *de novo* in Japan are 9.2 years and 55 billion yen, respectively (Yagi and Okubo, 2010). For a preclinical and phase-I study, it takes 1.3 and 1.1 billion yen per drug, respectively, in Japan (Yagi and Okubo, 2010). DR usually focuses on drugs that have cleared phase-I safety trials but has yet to show efficacy for the intended indication. Therefore, DR can probably skip the preclinical and phase-I study, thereby reducing the cost throughout drug development. Some estimates suggest that DR requires an average of ≈6.5 years and ≈US\$300 million to approve and launch a drug (Naylor et al., 2015). However, the cost for a phase-III study remains expensive, and DR is not always a smooth and successful process (Nosengo, 2016). Pharmaceutical companies must have a clear path to economic return to justify the expense of a clinical trial for DR, considering the remaining patent life, new use patents, or data exclusivity (Shineman et al., 2014). This creates an opportunity that foundations and bioventures can help DR (Azvolinsky, 2017). Foundations can directly fund smaller proof-of-concept clinical trials for DR, and positive results from such trials may encourage further investment from government and/or industry to fund larger, multicenter trials. Bioventures can provide various pipelines for DR, such as *in silico* and/or *in vitro* screening platforms to identify DR candidates with a high success rate. Bioventures can also provide consultation on intellectual property to differentiate the DR candidates from those already marketed. DR can be

used to obtain patent protection of a class of drugs in an unexpected indication as a method to block competitors from taking advantage of the new finding (e.g., pipeline management protection against competitors) (Mucke and Mucke, 2015). Currently, ≈ 10 patents related to DR are issued per month (Mucke, 2017). In the United States and Europe, there are many foundations and bioventures supporting DR, including Cure Within Reach (Bloom, 2015), Biovista (Deftereos et al., 2012), Insilico Medicine (Vanhaelen et al., 2017), and H.M. Pharma Consultancy (Mucke and Mucke, 2015). The regulatory frameworks in the US have also been changed to support DR. The US Food and Drug Administration Section 505(b)(2) permits the approval of applications for DR and permits reliance for such approvals on the information from previous studies about safety and/or effectiveness for an approved drug product. Applicants have the possibility to submit a 505(b)(2) application for a previously approved drug product (e.g., to support a new claim). These systems can significantly reduce the cost and effort of clinical trials and stimulate DR in various companies. In contrast, few bioventures support DR in Japan. The Ministry of Health, Labour, and Welfare (MHLW) and the Pharmaceuticals and Medical Devices Agency (PMDA), the regulatory agencies responsible for reviewing applications and approving the marketing authorization of drugs in Japan, do not have regulations equivalent to Section 505(b)(2). Much DR, however, has been successfully performed by both pharmaceutical companies and academia. Between 2001 and 2010, the PMDA gave 463 updated approvals, of which $>60\%$ were approvals for new indications of existing drugs (Hashitara et al., 2013). In this perspective, we provide representative examples of DR and the ongoing efforts to stimulate DR in Japan.

Zonisamide

Zonisamide (1,2-benzisoxazole-3-methanesulfonamide) has been developed and marketed in Japan as an anti-epileptic drug by Sumitomo Dainippon Pharma (SDP) since 1989. Murata colleagues used zonisamide to treat epilepsy in a patient with Parkinson's disease (PD) and serendipitously found that not only epilepsy but also symptoms related to PD were improved. They hypothesized that zonisamide could be repositioned for the treatment of PD and subsequently performed investigator-initiated clinical trials (IIT) in nine patients with PD (Murata et al., 2001). Seven patients showed a clear improvement in PD symptoms. Considering the positive finding, the patent life-cycle management, and the market potential, SDP decided to perform industry-sponsored clinical trials (IST) for the repositioning of zonisamide for PD. Phase IIb/III clinical trial were performed in 320 patients with PD, and patients treated with zonisamide again showed an improvement in PD symptoms. SDP then performed a phase III clinical trial on 133 patients with advanced PD, resulting in positive findings. Although the mechanism of action of zonisamide in both epilepsy and PD has not been fully elucidated, it may differ in each condition because of the 10-fold difference in approval therapeutic dose. The anti-epilepsy effect of zonisamide has been related to the inhibition of voltage-dependent sodium

channels and T-type calcium channels (Holder and Wilfong, 2011). The anti-PD effect of zonisamide, however, may be related to the inhibition of dopamine metabolism via inhibition of monoamine oxidase-B (MAO-B), the stimulation of dopamine release from striatum, and the blockade of T-type calcium channels (Shahed and Jankovic, 2007; Sonsalla et al., 2010; Miwa et al., 2011). Based on these data, zonisamide was approved in Japan as an anti-PD drug under the brand name *Trerief*[®] in 2009. The price of *Trerief*[®] was determined by MHLW according to the price of selegiline, another anti-PD drug. This method of comparison based on similar efficacy means that the price of *Trerief*[®] is significantly higher than that of *Excegran*[®], the brand name of zonisamide as an anti-epileptic drug.

Rebamipide

Rebamipide, a quinolinone derivative, has been developed and marketed in Japan for the treatment of peptic ulcer by Otsuka Pharmaceutical (OP) since 1990. The pharmacodynamics of rebamipide as anti-ulcer drug includes the stimulation of mucin secretion from goblet cells, resulting in the protection of gastric cells from various stimuli by coating the cell surface with a mucinous layer. Mucins are also expressed on the membranes of ocular surface epithelia and are secreted by conjunctival goblet cells, and thus play a role in ocular lubrication and defense. Reduced levels of mucins and changes in their distribution and glycosylation have been reported in patients with dry eye (Vickers and Gupta, 2015). However, therapies for dry eye that functioned by increasing mucin secretion in conjunctiva had not previously been developed. About 35% of the global population is affected by dry eye and this proportion is increasing, possibly as a result of lifestyle changes such as frequent computer and visual display usage (Vickers and Gupta, 2015). Considering the pharmacological effect of rebamipide on mucin secretion from goblet cells and the demanding need to develop novel therapies for dry eye, OP decided to reposition rebamipide for the treatment of dry eye. They demonstrated that rebamipide increased the production of mucin-like substances in the cornea and conjunctiva of a rabbit model of dry eye. They subsequently performed phase II and III ISTs and successfully demonstrated that a rebamipide ophthalmic suspension (unit dose 2%) improved both corneal and conjunctival epithelial damage and associated symptoms. Based on these studies, rebamipide was launched in Japan for the treatment of dry eye in 2012 under the brand name *Mucosta*[®] ophthalmic suspension UD2%. The price of this formulation was set at 27 yen per 0.35 ml, based on the price of diquafosol sodium (*Diquas*[®]), which was developed by Santen as a *de novo* treatment for dry eye by increasing mucin secretion via activation of P2Y2 receptors in corneal epithelium (Nakamura et al., 2012). *Diquas*[®] has been approved as a drug for dry eye since 2010 in Japan at a price of 641 yen per 5 ml, 1.6 times higher than that of *Mucosta*. A popular Japanese television program has promoted both *Mucosta*[®] and *Diquas*[®] as effective treatments for dry eye, and *Mucosta*[®] has also been used to treat the condition in a well-known Japanese medical comedy show. These advertisements can have a significant

impact on the public and effectively increase the sales of these drugs.

Carperitide

Carperitide, a recombinant human atrial natriuretic peptide (ANP), has been used to prevent and/or treat cardiac failure. Nojiri et al. (2012) administered carperitide to patients undergoing lung cancer surgery to prevent post-surgical cardiovascular complications, especially in patients with cardiovascular disease risk factors. However, they serendipitously found that carperitide significantly reduced the metastasis of lung cancer after surgery. They studied the anti-cancer mechanism of carperitide using a mouse model of cancer metastasis and found that it inhibits cancer metastasis through suppression of E-selection in vascular endothelial cells, which decreases the attachment of cancer cells to vascular endothelial cells. They subsequently performed a retrospective study of 467 patients who underwent lung cancer surgery and confirmed that the survival ratio of patients treated with carperitide was significantly higher than that of patients without carperitide treatment. These studies strongly suggest that carperitide can be used to prevent lung cancer metastasis and improve the prognosis of patients with lung cancer (Nojiri et al., 2015). However, the patent for carperitide has expired and many generic ANP therapies are currently in clinical use, with the result that pharmaceutical companies have avoided investing in the repositioning of carperitide as an anti-cancer drug. After prolonged negotiations, Nojiri et al. (2017) have formulated a framework for an IIT that will be performed with the support of Shionogi, a pharmaceutical company based in Japan. The IIT, termed the JANP study, is currently recruiting patients.

Thalidomide

Thalidomide was initially developed as a sedative and later repositioned to treat erythema nodosum leprosum and multiple myeloma because of its anti-angiogenic and anti-inflammatory effects. Kuwabara et al. (2008b) found that polyneuropathy, organomegaly, endocrinopathy, M-protein, and skin changes (POEMS) syndrome could be effectively treated with a combination of intensive chemotherapy and autologous peripheral blood cell-derived stem cell transplantation to suppress the proliferation of monoclonal plasma cells. These treatments, however, cannot be administered to patients with multiple organ failure and/or older age. Kuwabara et al. (2008a) hypothesized that thalidomide could be repositioned for the treatment of POEMS syndrome as it inhibits cytokine production and the proliferation of plasma cells. The authors had previously initiated an IIT in 2006 without pharmaceutical industry support and demonstrated a promising outcome in nine POEMS patients treated with thalidomide, later used as phase II data. Since 2010, Kuwabara et al. have performed a phase II/III IIT, the J-POST study, with the support of Fujimoto Pharmaceutical Corporation, the patent holder of thalidomide for multiple myeloma in Japan (Misawa et al., 2016). The IIT demonstrated that thalidomide reduced serum VEGF concentration and thus represents a novel treatment for patients with POEMS (Misawa et al., 2016). Approval for

the use of thalidomide for this indication is pending from the PMDA.

FUTURE DIRECTIONS

The examples of zonisamide and carperitide presented above demonstrate that serendipitous findings by astute clinicians are an important driver of DR and that the retrospective analysis of clinical records can be used to confirm the validity of these findings. Recent developments in electronic health records (EHRs) have made it possible to identify novel effects of clinical drugs in one EHR database and to validate these findings using other EHR databases (Xu et al., 2015). EHR can also be used to analyze similarity between diseases and between drugs without a prior knowledge of those diseases and drugs (Paik et al., 2015). For example, a novel relationship between disease A and B and drug X and Y can be identified using EHR. If a known relationship exists between disease A and drug X, one can hypothesize that there may also be a relationship between disease B and drug Y. Therefore, the sharing of EHR data between hospitals and of various clinical trial data in public databases can represent a powerful approach to computational DR. The PMDA is currently developing a public EHR database, Medical Information Database NETwork (MID-NET) (Noguchi, 2015), to be launched in 2018. Data from clinical trials can also be valuable resources for computational DR. Serious adverse events (SAEs) can be identified from randomized clinical trials. If a treatment arm has fewer predefined SAEs than the control arm, it is plausible that the drug used for the treatment arm is reducing the level of SAEs (Su and Sanger, 2017). Sharing data from clinical trials can increase the success rate of DR. The Study Data Tabulation Model (SDTM) from the Clinical Data Interchange Standards Consortium (CDISC) is a standard for creating a “data warehouse” for sharing the data from clinical research across studies. The PMDA has begun to request that the submission of data from clinical trials in accordance with the guidelines of CDISC (Ando, 2016). Tools that can generate SDTM data from clinical trials undertaken already without using CDISC guidelines have also been developed in Japan (Yamamoto et al., 2017). The PMDA and the Japan Agency of Medical Research and Development (AMED) are also developing the Clinical Innovation Network (CIN), a collaboration scheme with national medical research centers and industries, to share the clinical trials data between academia and industry (Hori, 2016). These frameworks may promote DR undertaken first by *in silico* analyses using big data, such as EHR and clinical-trial data, and then validated in IIT and/or IST.

High throughput screening of chemicals using *in vitro* and/or *in vivo* systems has also strongly driven DR (Nishimura and Hara, 2016; Imamura et al., 2017). The sharing of chemicals among researchers with various assay systems can increase the success rate of DR, as demonstrated by the success of projects supported by the National Center for Advancing Translational Sciences in the US (Azvolinsky, 2017). AMED has developed the Drug-Discovery Innovation and Screening Consortium, from

which over 200,000 chemicals provided by 20 pharmaceutical companies are publicly available. Chemical libraries specialized in DR have also been provided by pharmaceutical companies within open innovation grants. These frameworks may promote DR firstly performed by *in vitro/vivo* screening, and then evaluated in an IST by the company holding the patent.

A machine-learning approach has also been popular in DR (Napolitano et al., 2013; March-Vila et al., 2017). Various algorithms of machine learning, including random forests (Cao and Moulton, 2014), deep neural networks (Aliper et al., 2016), and deep adversarial networks (Kadurin et al., 2017), have been applied to DR combined with various omics databases, such as the Genome Wide Association Study Catalog (MacArthur et al., 2017) and the Library of Integrated Network-based Cellular Signature (LINCS) (Duan et al., 2014). These approaches have also been carried out successfully in Japan. For example, Iwata colleagues undertook an integrative approach using machine learning combined with multiple big data, including LINCS, Connectivity Map (Lamb et al., 2006), a Toxicogenomics Project-Genomics Assisted Toxicity Evaluation System (Igarashi et al., 2015), ChEMBL (Gaulton et al., 2017), Kyoto Encyclopedia of Genes and Genomes (Kotera et al., 2013), SuperTarget (Gunther et al., 2008), and DrugBank (Law et al., 2014) and found novel drug-protein-disease networks (Iwata et al., 2017). Asako and Uesawa (2017) developed a machine-learning model to predict agonists of the human estrogen receptor based on chemical structures.

The regulatory system for approval can affect the stream of DR significantly. A progressive approval system, in which the drug can be approved following proof of safety (Loike and Miller, 2017), may accelerate DR greatly, as suggested for rare diseases (Dunoyer, 2012) and regenerative medicine (Caplan and West, 2014). However, the risk of eliminating phase-II and -III studies should also be considered carefully (Loike and Miller, 2017). Conditional approval in Europe for

orphan drugs (Dunoyer, 2012) and an approval system for off-label use of drugs validated in publicly funded research in Japan (Shimazawa and Ikeda, 2012) might serve as templates to consider the progressive approval system for DR. Lifecycle management, which includes patent protection and contributes to maximizing the return of investment for drug discovery, is another important aspect of DR. Analyses of lifecycle management in the Japanese market are undertaken actively (Hashitera et al., 2013; Yamanaoka and Kano, 2016).

AUTHOR CONTRIBUTIONS

YN conceived and wrote the paper. MT, HI, KT, and HH wrote the paper.

FUNDING

This work was supported in part by the Japan Society for the Promotion of Science KAKENHI (16K08547), the Long-range Research Initiative of the Japan Chemical Industrial Association (13-PT01-01), and Okasan-Kato Foundation.

ACKNOWLEDGMENTS

The authors would like to thank Dr. Kazutaka Ikeda (Tokyo Metropolitan Institute of Medical Science) for his valuable comments and suggestions. We sincerely apologize to all those researchers and stakeholders whose important works are not cited because of space considerations. We also thank Clare Cox, Ph.D., from Edanz Group (www.edanzediting.com/ac) for editing a draft of this manuscript.

REFERENCES

- Aliper, A., Plis, S., Artemov, A., Ulloa, A., Mamoshina, P., and Zhavoronkov, A. (2016). Deep learning applications for predicting pharmacological properties of drugs and drug repurposing using transcriptomic data. *Mol. Pharm.* 13, 2524–2530. doi: 10.1021/acs.molpharmaceut.6b00248
- Ando, Y. (2016). *PMDA Update*. Available at: <https://www.pmda.go.jp/files/000215352.pdf> [accessed September 1, 2017].
- Asako, Y., and Uesawa, Y. (2017). High-performance prediction of human estrogen receptor agonists based on chemical structures. *Molecules* 22:E675. doi: 10.3390/molecules22040675
- Azvolinsky, A. (2017). *Repurposing Existing Drugs for New Indications*. Available at: <http://www.the-scientist.com/?articles.view/articleNo/47744/title/Repurposing-Existing-Drugs-for-New-Indications/> [accessed October 3, 2017].
- Bloom, B. E. (2015). Creating new economic incentives for repurposing generic drugs for unsolved diseases using social finance. *Assay Drug Dev. Technol.* 13, 606–611. doi: 10.1089/adt.2015.29015.beddrrr
- Cao, C., and Moulton, J. (2014). GWAS and drug targets. *BMC Genomics* 15(Suppl. 4):S5. doi: 10.1186/1471-2164-15-S4-S5
- Caplan, A. L., and West, M. D. (2014). Progressive approval: a proposal for a new regulatory pathway for regenerative medicine. *Stem Cells Transl. Med.* 3, 560–563. doi: 10.5966/sctm.2013-0180
- Deftereos, S. N., Dodou, E., Andronis, C., and Persidis, A. (2012). From depression to neurodegeneration and heart failure: re-examining the potential of MAO inhibitors. *Expert Rev. Clin. Pharmacol.* 5, 413–425. doi: 10.1586/ecp.12.29
- Duan, Q., Flynn, C., Niepel, M., Hafner, M., Muhlich, J. L., Fernandez, N. F., et al. (2014). LINCS Canvas Browser: interactive web app to query, browse and interrogate LINCS L1000 gene expression signatures. *Nucleic Acids Res.* 42, W449–W460. doi: 10.1093/nar/gku476
- Dunoyer, M. (2012). *A Modern Progressive Approval System for Rare Diseases*. Available at: www.raps.org/WorkArea/DownloadAsset.aspx?id=4398 [accessed September 1, 2017].
- Gaulton, A., Hersey, A., Nowotka, M., Bento, A. P., Chambers, J., Mendez, D., et al. (2017). The ChEMBL database in 2017. *Nucleic Acids Res.* 45, D945–D954. doi: 10.1093/nar/gkw1074
- Gunther, S., Kuhn, M., Dunkel, M., Campillos, M., Senger, C., Petsalaki, E., et al. (2008). SuperTarget and Matador: resources for exploring drug-target relationships. *Nucleic Acids Res.* 36, D919–D922.
- Hashitera, Y., Saotome, C., and Yamamoto, H. (2013). Analysis of 10 years drug lifecycle management (LCM) activities in the Japanese market. *Drug Discov. Today* 18, 1109–1116. doi: 10.1016/j.drudis.2013.07.004
- Holder, J. L. Jr., and Wilfong, A. A. (2011). Zonisamide in the treatment of epilepsy. *Expert Opin. Pharmacother.* 12, 2573–2581. doi: 10.1517/14656566.2011.622268

- Hori, A. (2016). *PMDA Perspective: Utilization of the Disease Registry Data for Drug Development*. Available at: <https://www.pmda.go.jp/files/000215446.pdf> [assessed September 3, 2017].
- Igarashi, Y., Nakatsu, N., Yamashita, T., Ono, A., Ohno, Y., Urushidani, T., et al. (2015). Open TG-GATES: a large-scale toxicogenomics database. *Nucleic Acids Res.* 43, D921–D927. doi: 10.1093/nar/gku955
- Imamura, K., Izumi, Y., Watanabe, A., Tsukita, K., Woltjen, K., Yamamoto, T., et al. (2017). The Src/c-Abl pathway is a potential therapeutic target in amyotrophic lateral sclerosis. *Sci. Transl. Med.* 9:eaf3962. doi: 10.1126/scitranslmed.aaf3962
- Iwata, M., Sawada, R., Iwata, H., Kotera, M., and Yamanishi, Y. (2017). Elucidating the modes of action for bioactive compounds in a cell-specific manner by large-scale chemically-induced transcriptomics. *Sci. Rep.* 7:40164. doi: 10.1038/srep40164
- Kadurin, A., Nikolenko, S., Khrabrov, K., Aliper, A., and Zhavoronkov, A. (2017). druGAN: an advanced generative adversarial autoencoder model for de novo generation of new molecules with desired molecular properties in silico. *Mol. Pharm.* 14, 3098–3104. doi: 10.1021/acs.molpharmaceut.7b00346
- Kotera, M., Tabei, Y., Yamanishi, Y., Moriya, Y., Tokimatsu, T., Kanehisa, M., et al. (2013). KCF-S: KEGG chemical function and substructure for improved interpretability and prediction in chemical bioinformatics. *BMC Syst. Biol.* 7(Suppl. 6):S2. doi: 10.1186/1752-0509-7-S6-S2
- Kuwabara, S., Misawa, S., Kanai, K., Sawai, S., Hattori, T., Nishimura, M., et al. (2008a). Thalidomide reduces serum VEGF levels and improves peripheral neuropathy in POEMS syndrome. *J. Neurol. Neurosurg. Psychiatry* 79, 1255–1257. doi: 10.1136/jnnp.2008.150177
- Kuwabara, S., Misawa, S., Kanai, K., Suzuki, Y., Kikkawa, Y., Sawai, S., et al. (2008b). Neurologic improvement after peripheral blood stem cell transplantation in POEMS syndrome. *Neurology* 71, 1691–1695. doi: 10.1212/01.wnl.0000323811.42080.a4
- Lamb, J., Crawford, E. D., Peck, D., Modell, J. W., Blat, I. C., Wrobel, M. J., et al. (2006). The connectivity map: using gene-expression signatures to connect small molecules, genes, and disease. *Science* 313, 1929–1935. doi: 10.1126/science.1132939
- Law, V., Knox, C., Djoumbou, Y., Jewison, T., Guo, A. C., Liu, Y., et al. (2014). DrugBank 4.0: shedding new light on drug metabolism. *Nucleic Acids Res.* 42, D1091–D1097. doi: 10.1093/nar/gkt1068
- Loike, J., and Miller, J. (2017). *Improving FDA Evaluations Without Jeopardizing Safety and Efficacy*. Available at: <http://www.the-scientist.com/articles/view/articleNo/48280/title/Opinion-Improving-FDA-Evaluations-Without-Jeopardizing-Safety-and-Efficacy/> [accessed October 3, 2017].
- MacArthur, J., Bowler, E., Cerezo, M., Gil, L., Hall, P., Hastings, E., et al. (2017). The new NHGRI-EBI catalog of published genome-wide association studies (GWAS Catalog). *Nucleic Acids Res.* 45, D896–D901. doi: 10.1093/nar/gkw1133
- March-Vila, E., Pinzi, L., Sturm, N., Tinivella, A., Engkvist, O., Chen, H., et al. (2017). On the integration of in silico drug design methods for drug repurposing. *Front. Pharmacol.* 8:298. doi: 10.3389/fphar.2017.00298
- Misawa, S., Sato, Y., Katayama, K., Nagashima, K., Aoyagi, R., Sekiguchi, Y., et al. (2016). Safety and efficacy of thalidomide in patients with POEMS syndrome: a multicentre, randomised, double-blind, placebo-controlled trial. *Lancet Neurol.* 15, 1129–1137. doi: 10.1016/S1474-4422(16)30157-0
- Miwa, H., Koh, J., Kajimoto, Y., and Kondo, T. (2011). Effects of T-type calcium channel blockers on a parkinsonian tremor model in rats. *Pharmacol. Biochem. Behav.* 97, 656–659. doi: 10.1016/j.pbb.2010.11.014
- Mucke, H. A. (2017). Patent highlights December 2016–January 2017. *Pharm. Pat. Anal.* 6, 97–104. doi: 10.4155/ppa-2017-0007
- Mucke, H. A., and Mucke, E. (2015). Sources and targets for drug repurposing: landscaping transitions in therapeutic space. *ASSAY Drug Dev. Technol.* 13, 319–324. doi: 10.1089/adt.2015.29009.hmedrrr
- Murata, M., Horiuchi, E., and Kanazawa, I. (2001). Zonisamide has beneficial effects on Parkinson's disease patients. *Neurosci. Res.* 41, 397–399. doi: 10.1016/S0168-0102(01)00298-X
- Nakamura, M., Imanaka, T., and Sakamoto, A. (2012). Diquafosol ophthalmic solution for dry eye treatment. *Adv. Ther.* 29, 579–589. doi: 10.1007/s12325-012-0033-9
- Napolitano, F., Zhao, Y., Moreira, V. M., Tagliaferri, R., Kere, J., D'amato, M., et al. (2013). Drug repositioning: a machine-learning approach through data integration. *J. Cheminform.* 5:30. doi: 10.1186/1758-2946-5-30
- Naylor, S., Kauppi, D., and Schonfeld, J. (2015). *Therapeutic Drug Repurposing, Repositioning and Rescue Part III Market Exclusivity Using Intellectual Property and Regulatory Pathways*. Available at: <http://www.ddw-online.com/drug-discovery/p303678-therapeutic-drug-repurposingrepositioning-and-rescue-part-iiimarket-exclusivity-using-intellectual-property-and-regulatory-pathways.html> [accessed September 3, 2017].
- Nishimura, Y., and Hara, H. (2016). Integrated approaches to drug discovery for oxidative stress-related retinal diseases. *Oxid. Med. Cell Longev.* 2016, 1–9. doi: 10.1155/2016/2370252
- Noguchi, A. (2015). *Challenges for Post-marketing Drug Safety Measures Using Electronic Healthcare Database in Japan*. Available at: <https://www.pmda.go.jp/files/000215551.pdf> [assessed September 3, 2017].
- Nojiri, T., Hosoda, H., Tokudome, T., Miura, K., Ishikane, S., Otani, K., et al. (2015). Atrial natriuretic peptide prevents cancer metastasis through vascular endothelial cells. *Proc. Natl. Acad. Sci. U.S.A.* 112, 4086–4091. doi: 10.1073/pnas.1417273112
- Nojiri, T., Inoue, M., Yamamoto, K., Maeda, H., Takeuchi, Y., Funakoshi, Y., et al. (2012). Effects of low-dose human atrial natriuretic peptide for preventing post-operative cardiopulmonary complications in elderly patients undergoing pulmonary resection for lung cancer. *Eur. J. Cardiothorac. Surg.* 41, 1330–1334. doi: 10.1093/ejcts/ezr202
- Nojiri, T., Yamamoto, H., Hamasaki, T., Onda, K., Ohshima, K., Shintani, Y., et al. (2017). A multicenter randomized controlled trial of surgery alone or surgery with atrial natriuretic peptide in lung cancer surgery: study protocol for a randomized controlled trial. *Trials* 18, 183. doi: 10.1186/s13063-017-1928-1
- Nosengo, N. (2016). Can you teach old drugs new tricks? *Nature* 534, 314–316. doi: 10.1038/534314a
- Paik, H., Chung, A. Y., Park, H. C., Park, R. W., Suk, K., Kim, J., et al. (2015). Repurpose terbutaline sulfate for amyotrophic lateral sclerosis using electronic medical records. *Sci. Rep.* 5:8580. doi: 10.1038/srep08580
- Shahed, J., and Jankovic, J. (2007). Exploring the relationship between essential tremor and Parkinson's disease. *Parkinsonism Relat. Disord.* 13, 67–76. doi: 10.1016/j.parkreldis.2006.05.033
- Shimazawa, R., and Ikeda, M. (2012). Japanese regulatory system for approval of off-label drug use: evaluation of safety and effectiveness in literature-based applications. *Clin. Ther.* 34, 2104–2116. doi: 10.1016/j.clinthera.2012.09.004
- Shineman, D. W., Alam, J., Anderson, M., Black, S. E., Carman, A. J., Cummings, J. L., et al. (2014). Overcoming obstacles to repurposing for neurodegenerative disease. *Ann. Clin. Transl. Neurol.* 1, 512–518. doi: 10.1002/acn3.76
- Sonsalla, P. K., Wong, L. Y., Winnik, B., and Buckley, B. (2010). The antiepileptic drug zonisamide inhibits MAO-B and attenuates MPTP toxicity in mice: clinical relevance. *Exp. Neurol.* 221, 329–334. doi: 10.1016/j.expneurol.2009.11.018
- Su, E. W., and Sanger, T. M. (2017). Systematic drug repositioning through mining adverse event data in ClinicalTrials.gov. *PeerJ* 5:e3154. doi: 10.7717/peerj.3154
- Vanhaelen, Q., Mamoshina, P., Aliper, A. M., Artemov, A., Lezhnina, K., Ozerov, I., et al. (2017). Design of efficient computational workflows for in silico drug repurposing. *Drug Discov. Today* 22, 210–222. doi: 10.1016/j.drudis.2016.09.019
- Vickers, L. A., and Gupta, P. K. (2015). The future of dry eye treatment: a glance into the therapeutic pipeline. *Ophthalmol. Ther.* 4, 69–78. doi: 10.1007/s40123-015-0038-y
- Xu, H., Aldrich, M. C., Chen, Q., Liu, H., Peterson, N. B., Dai, Q., et al. (2015). Validating drug repurposing signals using electronic health records: a case study of metformin associated with reduced cancer mortality.

- J. Am. Med. Inform. Assoc.* 22, 179–191. doi: 10.1136/amiajnl-2014-002649
- Yagi, T., and Okubo, M. (2010). *JPMA News Letter*. Available at: http://www.jpma.or.jp/about/issue/gratis/newsletter/archive_until2014/pdf/2010_136_12.pdf [accessed September 3, 2017].
- Yamamoto, K., Ota, K., Akiya, I., and Shintani, A. (2017). A pragmatic method for transforming clinical research data from the research electronic data capture “REDCap” to Clinical Data Interchange Standards Consortium (CDISC) Study Data Tabulation Model (SDTM): Development and evaluation of REDCap2SDTM. *J. Biomed. Inform.* 70, 65–76. doi: 10.1016/j.jbi.2017.05.003
- Yamanaka, T., and Kano, S. (2016). Patent term extension systems differentiate Japanese and US drug lifecycle management. *Drug Discov. Today* 21, 111–117. doi: 10.1016/j.drudis.2015.09.005
- Conflict of Interest Statement:** MT and HI have been employed by Sumitomo Dainippon Pharma and Otsuka Pharmaceutical, respectively.
- The other authors declare that the research was conducted in the absence of any commercial or financial relationships that could be construed as a potential conflict of interest.
- Copyright © 2017 Nishimura, Tagawa, Ito, Tsuruma and Hara. This is an open-access article distributed under the terms of the Creative Commons Attribution License (CC BY). The use, distribution or reproduction in other forums is permitted, provided the original author(s) or licensor are credited and that the original publication in this journal is cited, in accordance with accepted academic practice. No use, distribution or reproduction is permitted which does not comply with these terms.

Advantages of publishing in Frontiers



OPEN ACCESS

Articles are free to read for greatest visibility and readership



FAST PUBLICATION

Around 90 days from submission to decision



HIGH QUALITY PEER-REVIEW

Rigorous, collaborative, and constructive peer-review



TRANSPARENT PEER-REVIEW

Editors and reviewers acknowledged by name on published articles

Frontiers

Avenue du Tribunal-Fédéral 34
1005 Lausanne | Switzerland

Visit us: www.frontiersin.org

Contact us: info@frontiersin.org | +41 21 510 17 00



REPRODUCIBILITY OF RESEARCH

Support open data and methods to enhance research reproducibility



DIGITAL PUBLISHING

Articles designed for optimal readership across devices



FOLLOW US

[@frontiersin](https://twitter.com/frontiersin)



IMPACT METRICS

Advanced article metrics track visibility across digital media



EXTENSIVE PROMOTION

Marketing and promotion of impactful research



LOOP RESEARCH NETWORK

Our network increases your article's readership